

~~SECRET~~

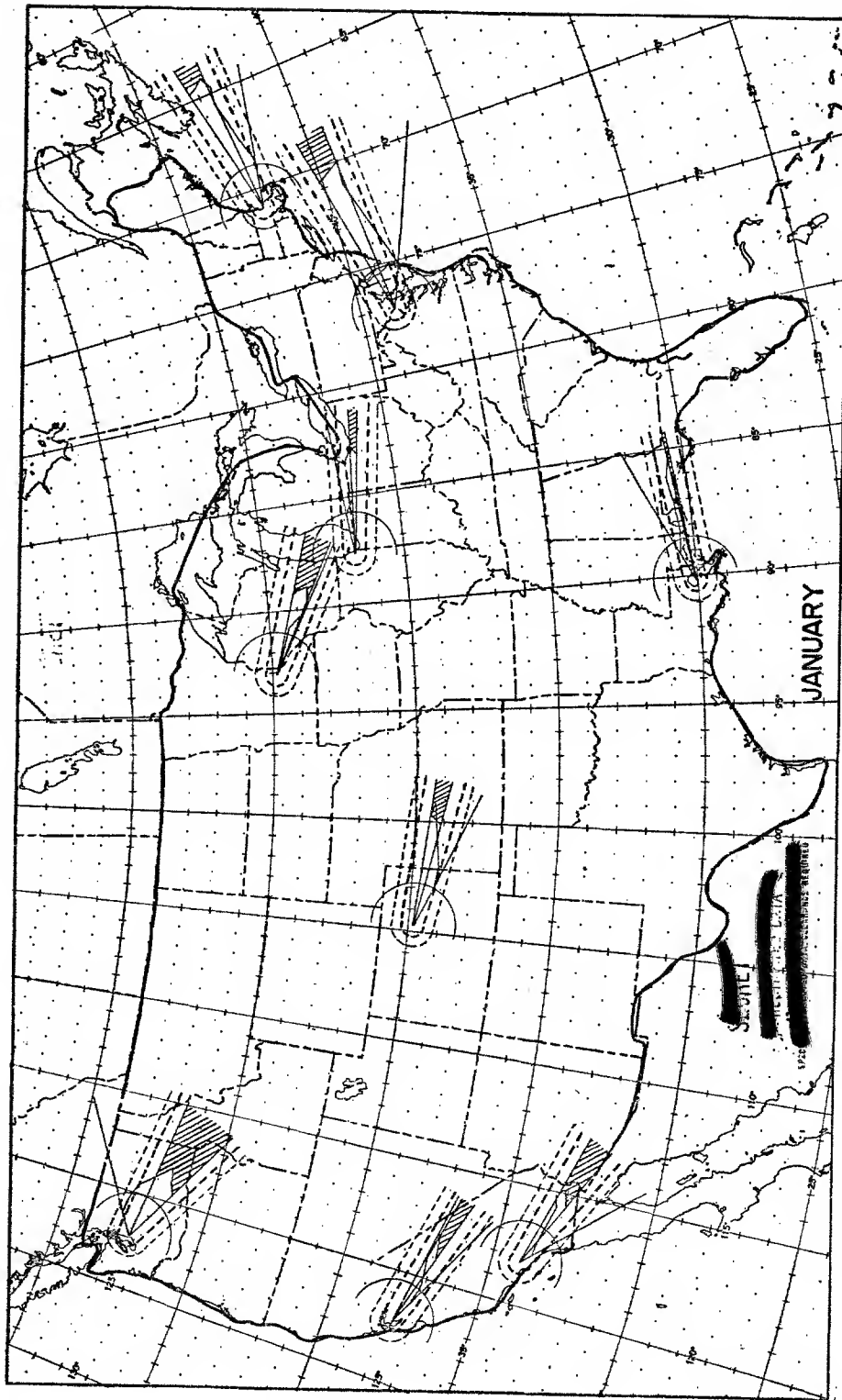


Figure 1
Mean Fall-out Sectors in Winter

DOE ARCHIVES

[REDACTED]

While I feel that the general nature of the picture shown on Figure 1 and Figure 2 is correct, some of the details such as the wider mushroom fallout area at Seattle than Denver, for example, are open to suspicion since the data used to prepare this chart are not homogeneous. That is, at each elevation, we used the best possible average wind, but at, say, 10,000 feet, we used a mean chart based on winds collected from about 10 years of observations, while at 80,000 feet average winds based on records for only 4 years were available. Further, we are always plagued with the fact that high level winds are obtained mainly during periods of fair weather and low wind speeds, while low-level winds are collected more frequently.

Figure 2, the summer patterns, also shows predominant fallout to the east of the burst. The wind speeds become much lighter and the west coast stations actually have a mean northward airflow. The southern tier of States is located in an area of very light winds. Thus, at New Orleans, for example, the mean fallout picture shows no preferential direction. Western Europe would be more like eastern U. S. rather than the U. S. West Coast.

Having viewed the mean picture, we now pass on to the variability of individual cases about this mean. In the troposphere, or up to 30 - 45,000 feet, where one is more familiar with wind patterns, it is well recognized that above the lowest levels (say above 10,000 feet), the prevailing westerly flow is the result of waves or undulations superimposed on a mean zonal flow. At times, the daily picture in the mid-troposphere looks much like the mean with almost straight west-to-east flow, while at other times, we find large amplitude waves or closed centers.

These waves or closed centers most frequently move across the country from west to east, but occasionally, at certain preferred places such as the southwest U. S., remain stationary for many days.

In the winter, in the stratosphere (Figure 3), the winds normally also blow west-to-east over the temperate latitudes. Although this map shows the flow only at 53,000 feet, direction of the airflow is much the same up to 100,000 feet. However, on anomolous occasions, as in Figure 4, which shows the airflow at 67,000 feet in February 1952, large areas of the temperate latitudes possess easterly winds. In this map, northern U. S. and southern Canada is such an area in which the normal wind direction is reversed. Fallout in such a case would probably still be to the east of ground zero in Northern U. S., but not nearly as far away from ground zero as in the average case.

DOE ARCHIVES

However, the typical and almost invariant summer picture above about 60,000 feet (Figure 5 shows east-to-west flow). This will result in many cases of fallout from the stratosphere occurring to the west of ground zero because of light westerly tropospheric winds.

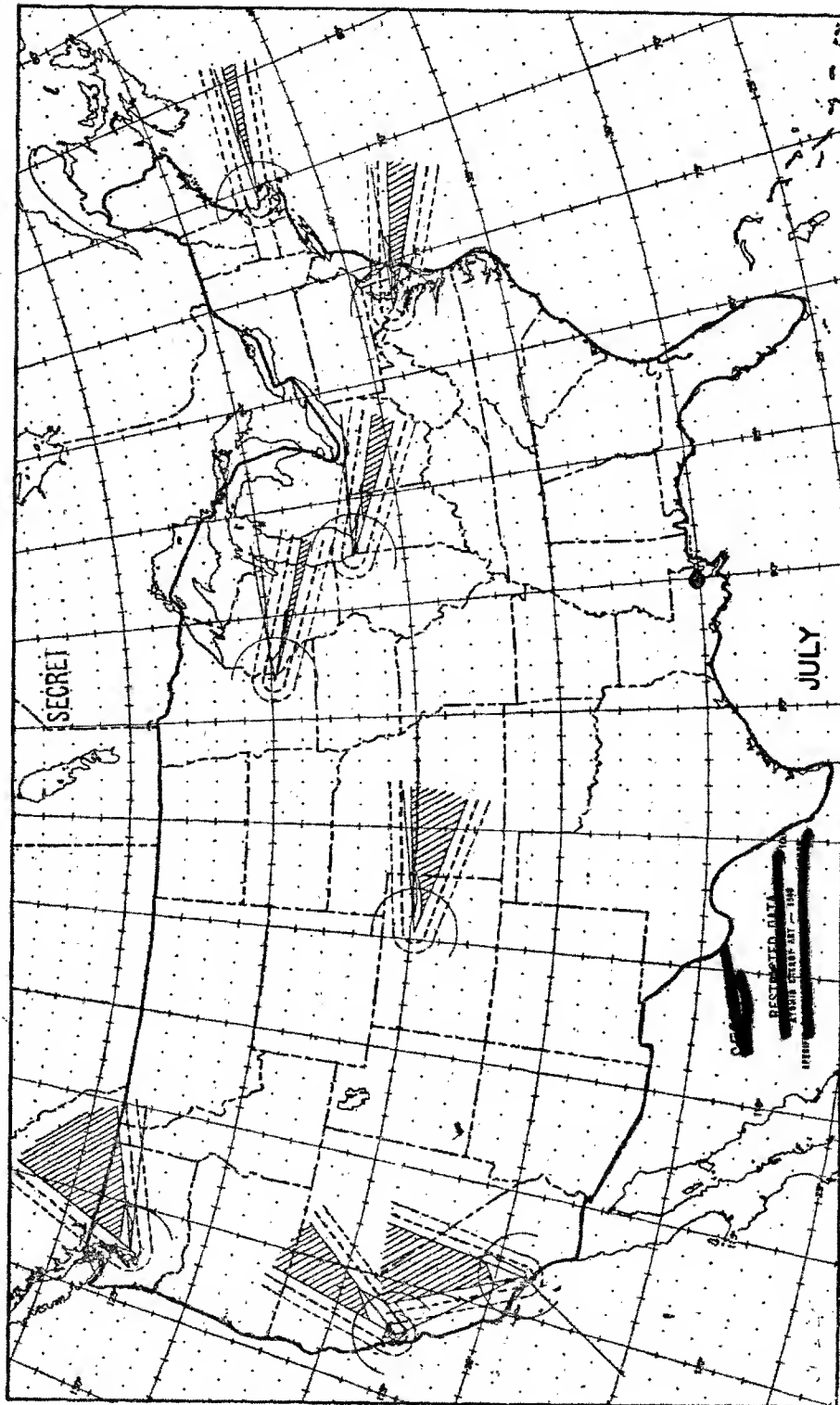


Figure 2
Mean Fall-out Sectors in Summer

DOE ARCHIVES

SECRET

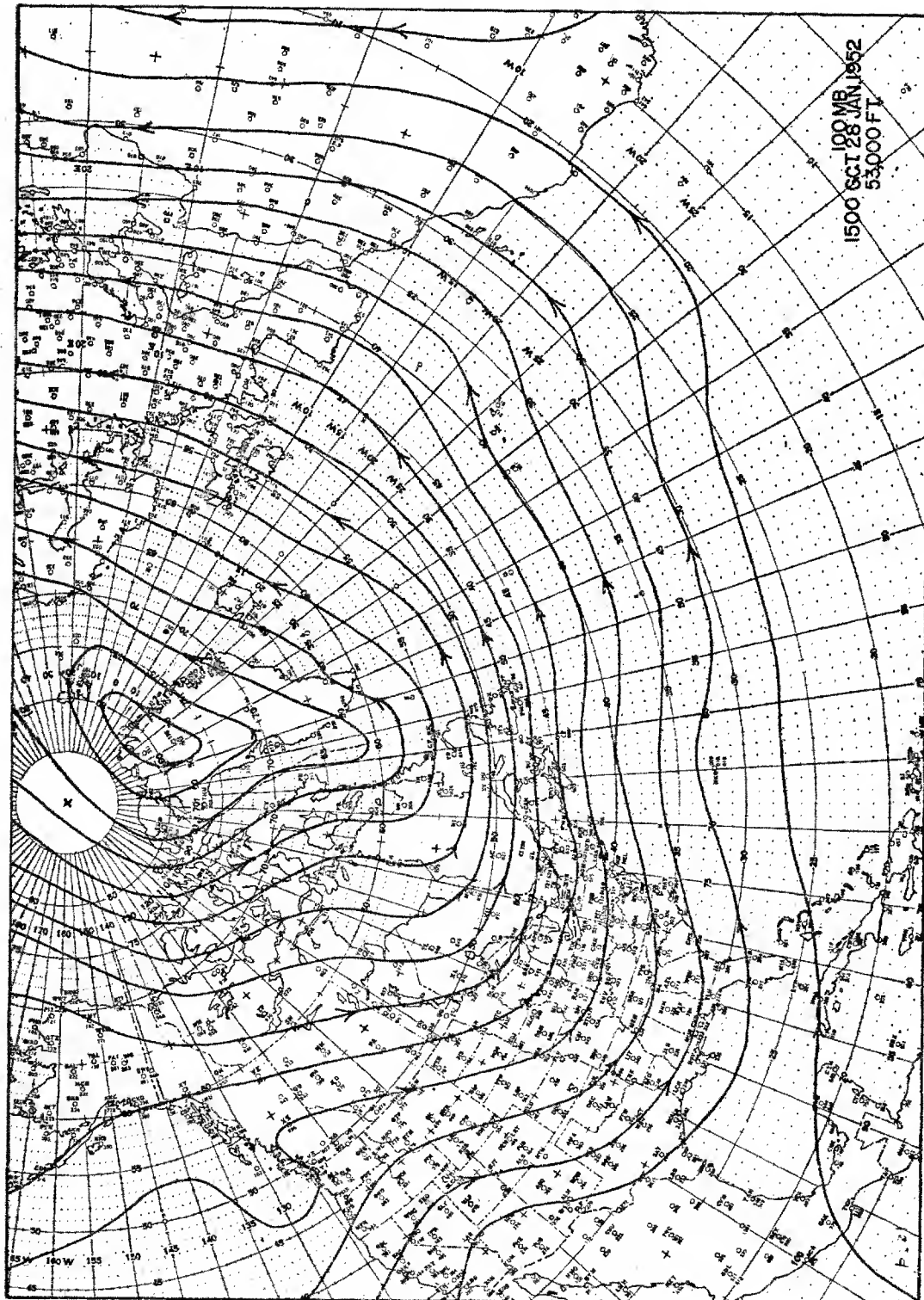


Figure 3
Example of Normal Winter Flow Pattern in the Stratosphere

DOE ARCHIVES

221

SECRET

DATA

ATOMIC ENERGY ACT 1954

225

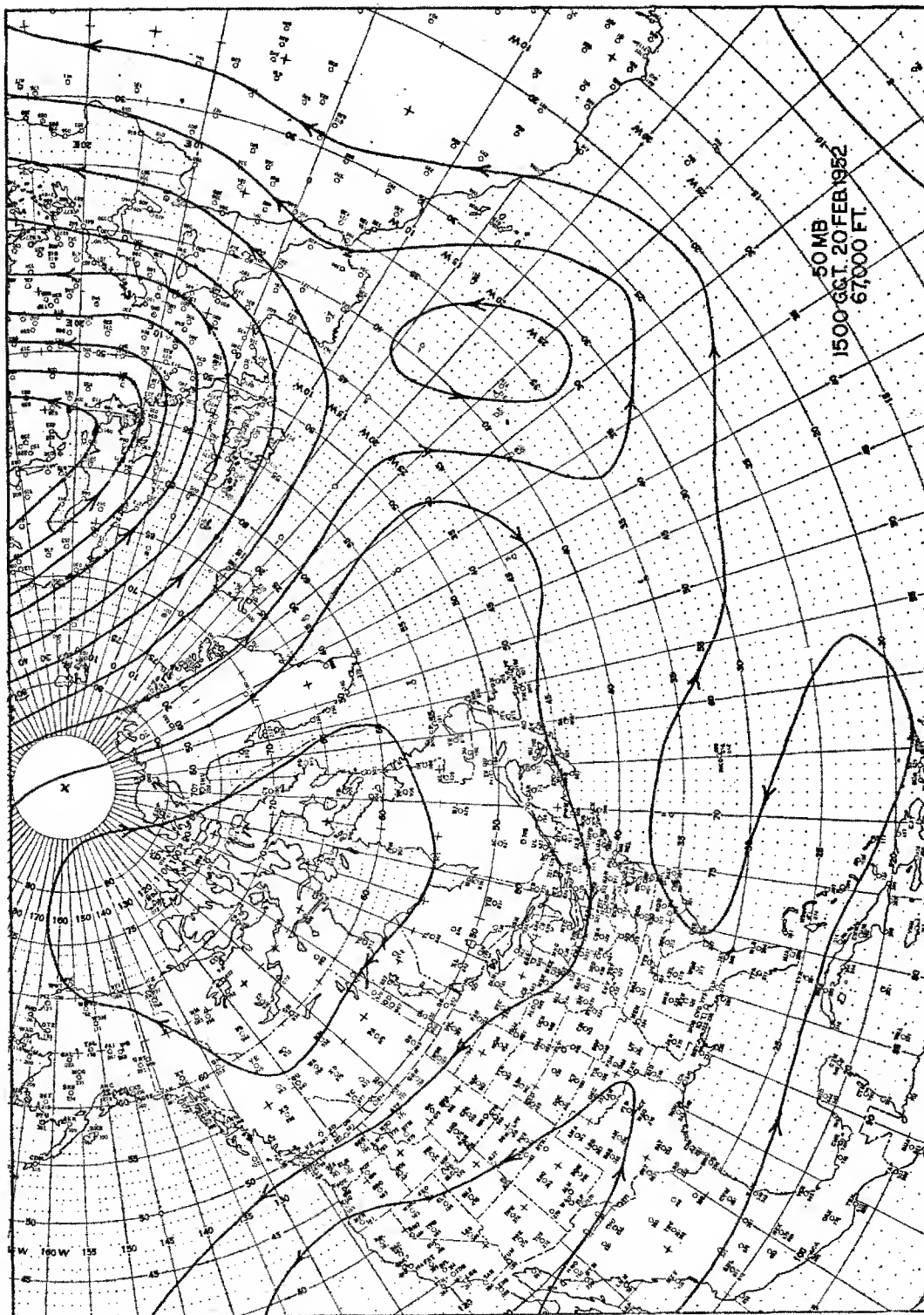


Figure 4
Anomalous Stratospheric Flow Pattern in Winter, with
Easterly Winds over much of the United States and Canada

DOE ARCHIVES



Figure 5
Mean 50-mb. (68,500 ft.) flow for July

DOE ARCHIVES

Figure 6 shows the distribution of points at which fallout will occur for hypothetical bombs detonated at Washington, D. C. (where the lines intersect) for January and July and coming from two elevations; one in the middle or upper troposphere (30,000 feet), and one in the lower stratosphere (60,000 feet). The points actually indicate where a 100 micron particle of 2.5 density would land if started at the indicated height over ground zero. The arcs are at 200-mile intervals. In the winter, while there are pretty wide departures from direct west-to-east fallout, there are no cases of deposition to the west of ground zero during the two Januarys used in this study from either level. During the summer, not only does the 100 micron particle fall much closer to ground zero, but there actually are cases of fallout to the left or the west of ground zero. The filled-in circles show the cases in which it was raining or snowing at the time of the wind observation. In the winter, it is evident that precipitation is far more likely with fallout occurring northeast of the burst. The distribution of the points provides a measure of the scatter of directions of, say, the effective mean winds for the stem in the left side, and lower mushroom on the right side of the figure.

The last bit of climatological statistics appears in Figure 7. Since the distant fallout is felt to come from the mushroom, the size of the area in which potential danger exists depends, in part, on the amount of the directional shear of the winds in the mushroom. Although the climatological data for this figure was taken from Washington, D. C., the results are drawn for Pittsburgh, Pa. We have on this figure the cumulative frequencies of directional shears in the mushroom. Thus, in January, there is almost a 60% likelihood that the directional shear will be no greater than the smallest angle of 5° and almost 90% likelihood that it will be no greater than 10° , etc. The shear is seen to be much greater in summer. For each of the angles, one may get an idea of the fraction of the northeastern U. S. on which fallout would be observed.

The conclusion to be drawn from this figure is the fact that there is only a small likelihood of large directional shear; especially in winter, a saving factor for some Civil Defense considerations. I have no statistics to confirm this state of affairs everywhere in the temperate latitudes, however.

Figures 8 - 13 illustrate actual cases of fallout with typical weather situations. For example, in Figure 8, on the left is the weather situation near Washington, D. C., at 0630 (Greenwich Time) on 10 January 1953 showing the isobars and fronts in the usual fashion and the precipitation area in shading. A storm is approaching Washington from the south with a wide precipitation area to the north and west. To the right of the weather picture, we find the fallout plot in the event of a hypothetical burst at, say, the Pentagon. The radial lines are the lines along

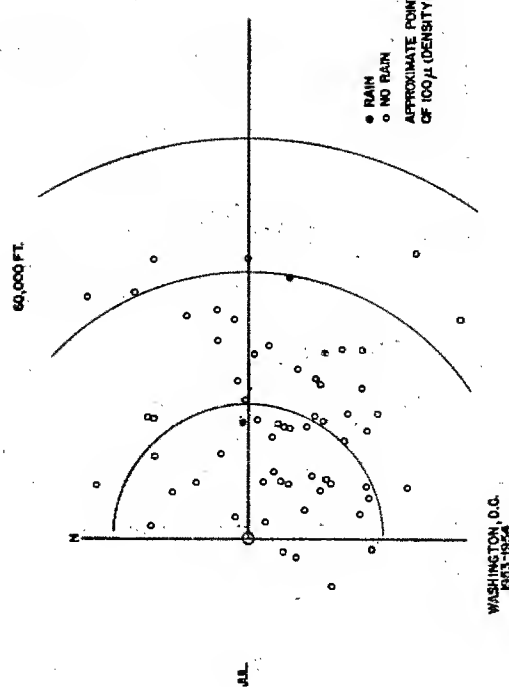
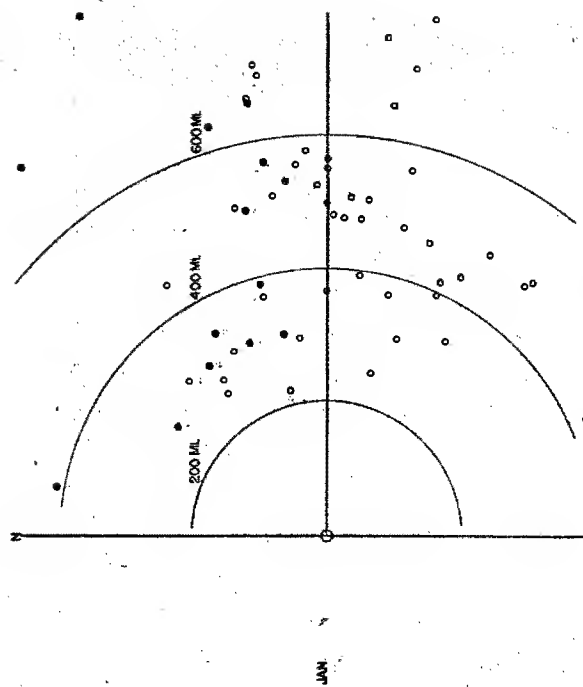


Figure 6
Distribution of Fall-out from 30,000 and 60,000 feet in January and July, Washington, D. C.

DOE ARCHIVES

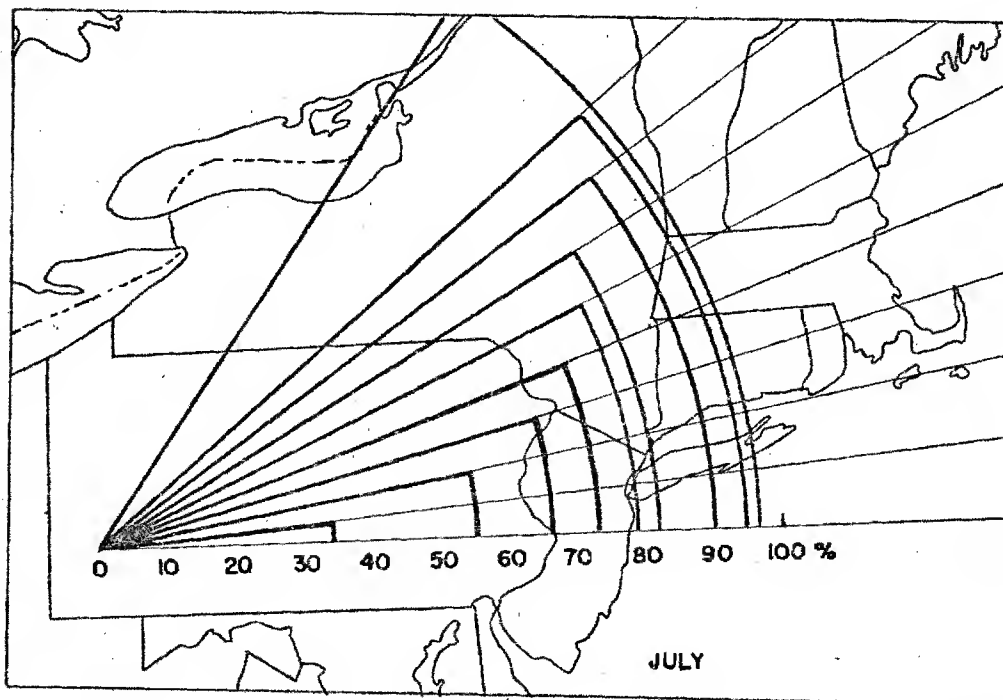
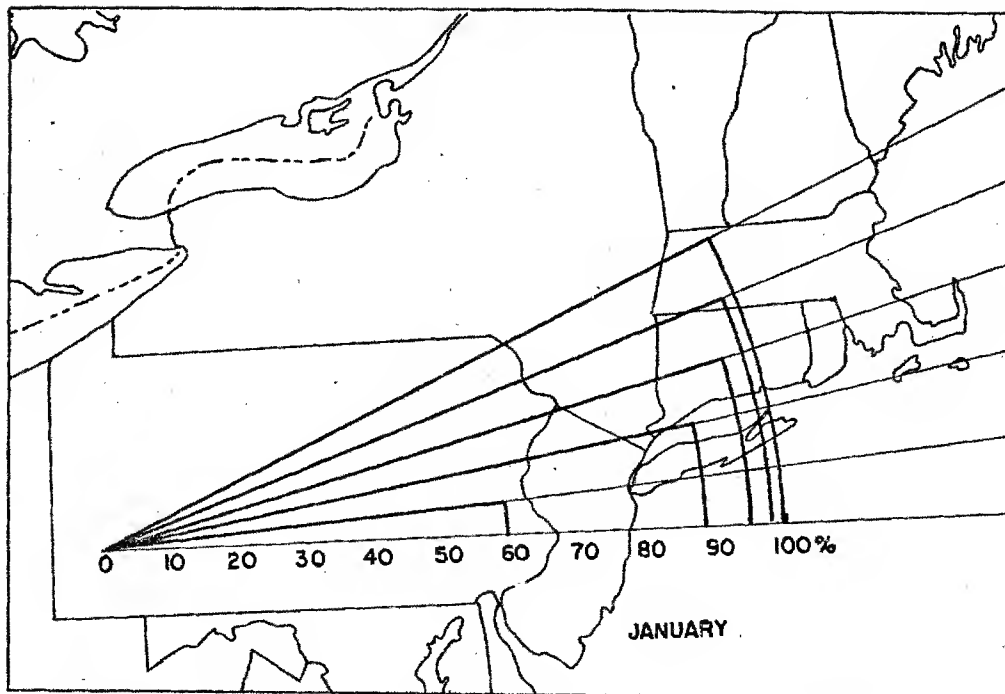


Figure 7
Frequency of Directional Wind Shear in the Mushroom

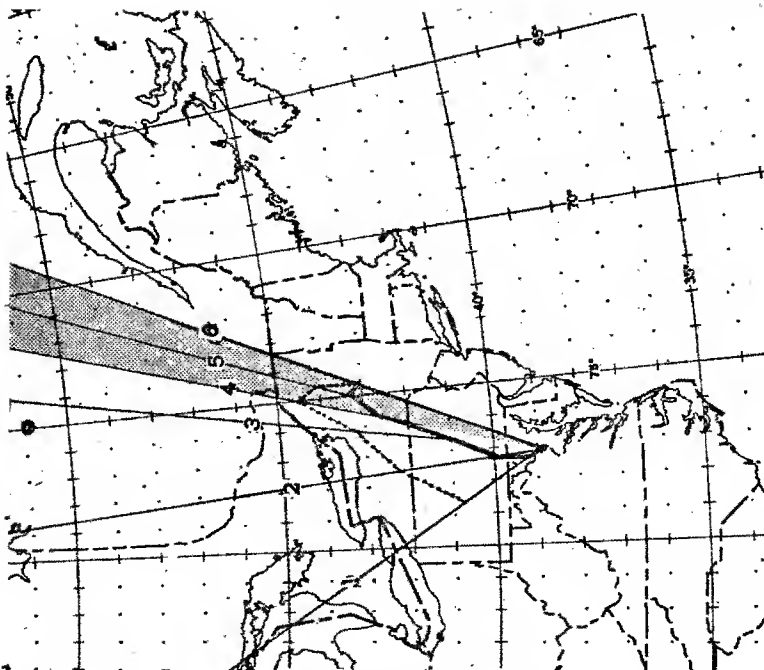
DOE ARCHIVES

which fallout from the indicated height will be deposited. The heavy line shows the places on the ground at which the 100 micron particle of a specific gravity 2.5 will be deposited, while the dotted line shows where fallout will reach at 8 hours after burst. The numbers on the fallout diagram are the heights in tens of thousands of feet: 10,000, 20,000, 30,000 feet and so forth. The direction of motion of the stem below 10,000 feet can be deduced from the surface isobars. No attempt is made to extrapolate beyond the height of observed winds.

It is evident that fallout in Virginia, Maryland, and southern Pennsylvania will be in the rain. No further interpretation of the significance of this fact will be attempted at this time. This is an example of a cyclonic disturbance approaching the target from the south or southwest and shows the fallout to occur typically to the northwest from the lowest levels and the north or northeast from the middle and upper levels.

Other typical winter weather situations are shown in Figures 9 - 11. Figure 9 shows the fallout pattern following the passage of a winter cold front, with fallout occurring to the southeast of Washington. Figure 10 illustrates the conditions well within the cold air, with northwesterly winds in the lowest levels, shifting to southwesterly at the higher levels. Figure 11 typifies conditions after the center of the high has passed Washington and a new low is approaching from the west. Figures 12 and 13 show two examples of summer fallout patterns. Figure 12 illustrates conditions following the passage of a weak summer cold front with northwesterly winds prevailing in the lower levels and very weak easterlies in the stratosphere, while Figure 13 shows a well developed Bermuda high with southerly winds near the surface becoming easterly in the stratosphere resulting in fallout to the northeast of Washington.

I should like to complete the presentation by returning to the role which meteorology plays in fallout and take a look into the future. The two contributions which the meteorologist can make, as mentioned before, are: Collection of climatological fallout data for planning, and operational fallout forecasts for day-to-day use. I feel that the presentation I have made this morning answers only a very limited number of planning questions. The kind of problem it does not answer is: If the Pentagon were the target for an x megaton bomb detonated at the ground, what is the probability that New York or Philadelphia or Boston might be subjected to a dangerous fallout? If this symposium provides a method by which one may either delineate dosages from the wind data or even delineate, say, two kinds of areas showing different dangers, we feel that we can answer the kind of question which Civil Defense or military commanders are prone to ask. The simple plan to be described represents ideas contributed by many groups besides our own and machine methods may be required in its execution.



0630 Z JAN 10, 1953
 WASHINGTON:
 NIMBOSTRATUS OVERCAST
 CONTINUOUS RAIN
 WIND NE 12 KNOTS

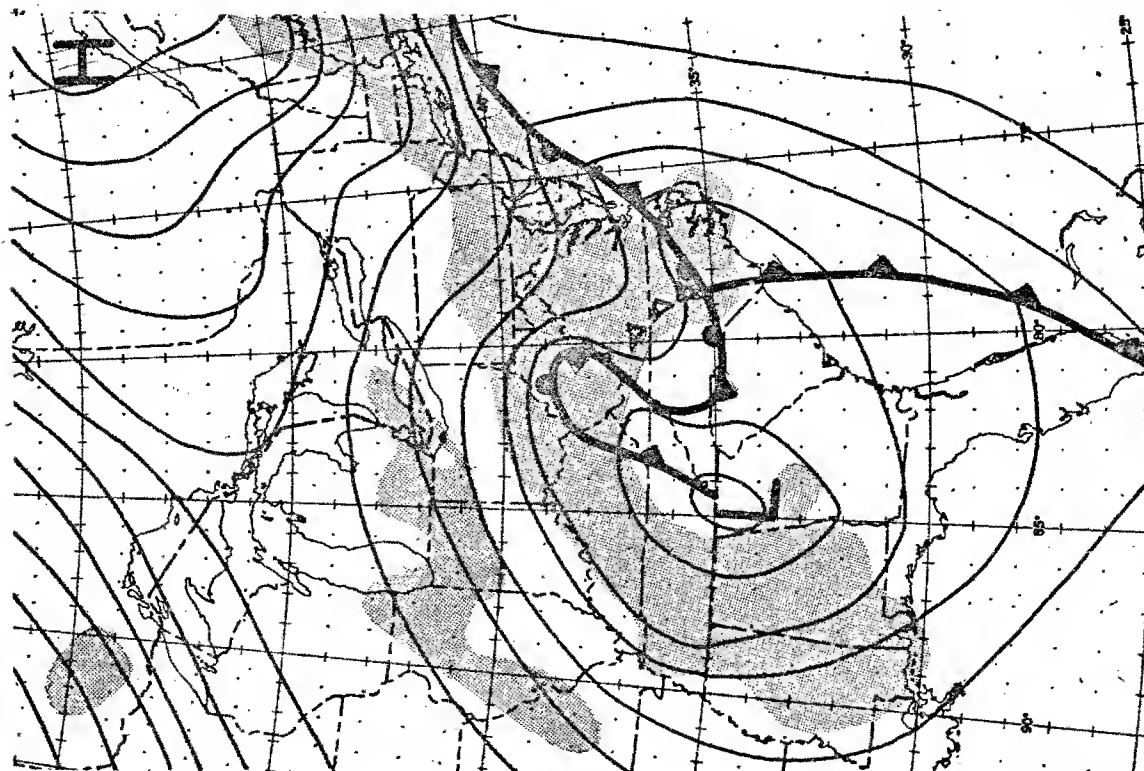
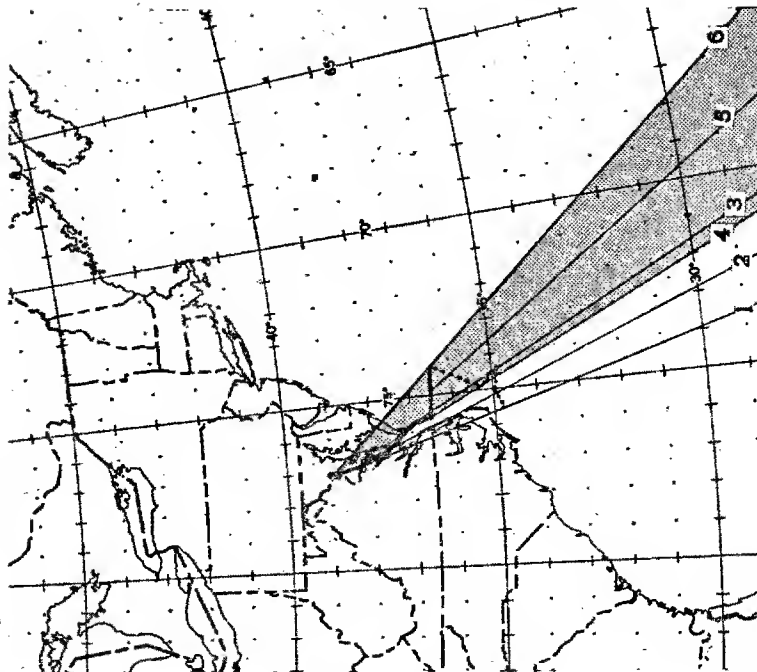
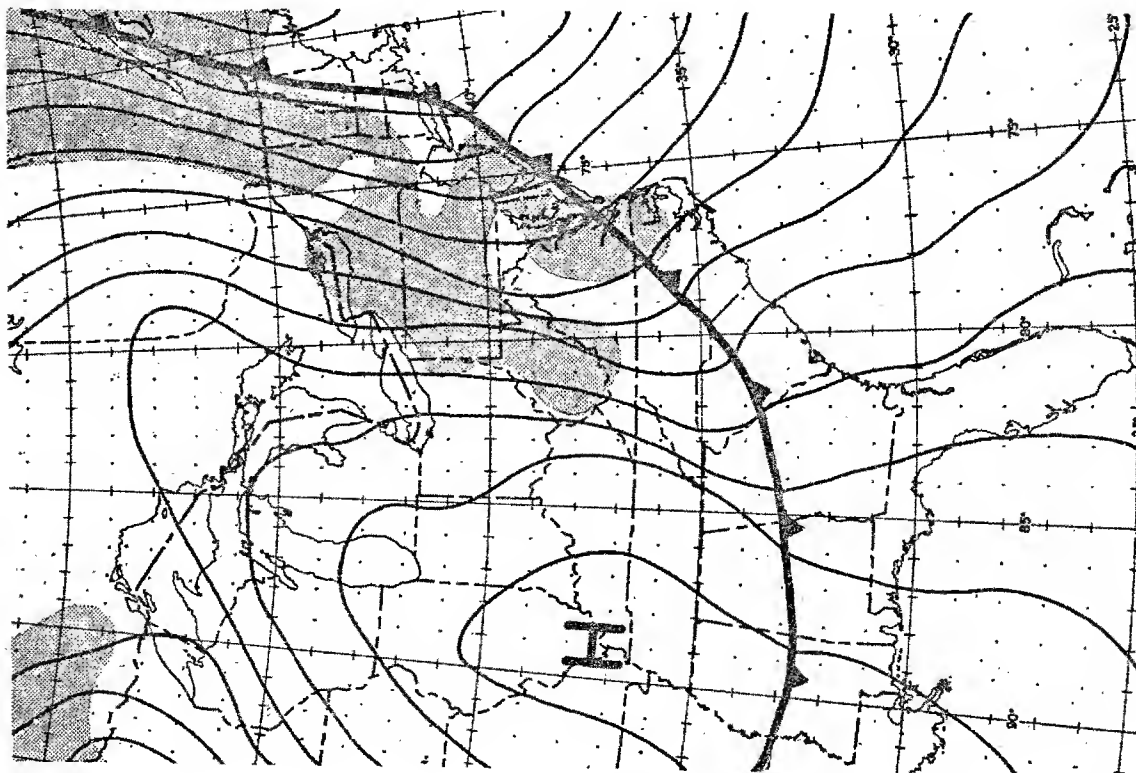


Figure 8
 Surface Weather Map and Associated Fall-out Pattern, January 10, 1953

DOE ARCHIVES



0630 Z JAN 12, 1953

WASHINGTON:

STRATUS OVERCAST

CONTINUOUS RAIN

WIND WNW 12 KNOTS

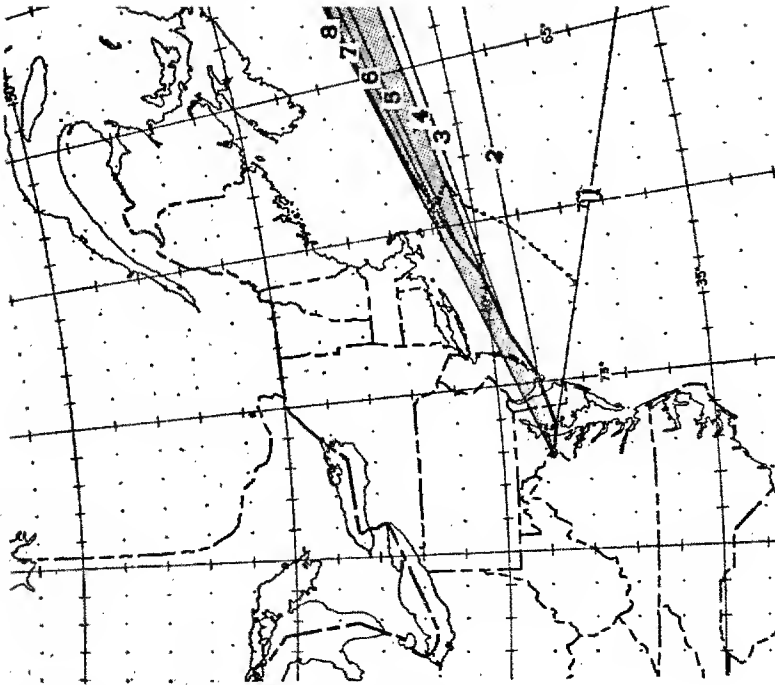
Figure 9
Surface Weather Map and Associated Fall-cut Pattern, January 12, 1953

DOE ARCHIVES

229

ATOMIC ENERGY ACT 1954

233



1830Z JAN 12, 1954
WASHINGTON:
SCATTERED STRATUS
WIND NW 20 KNOTS

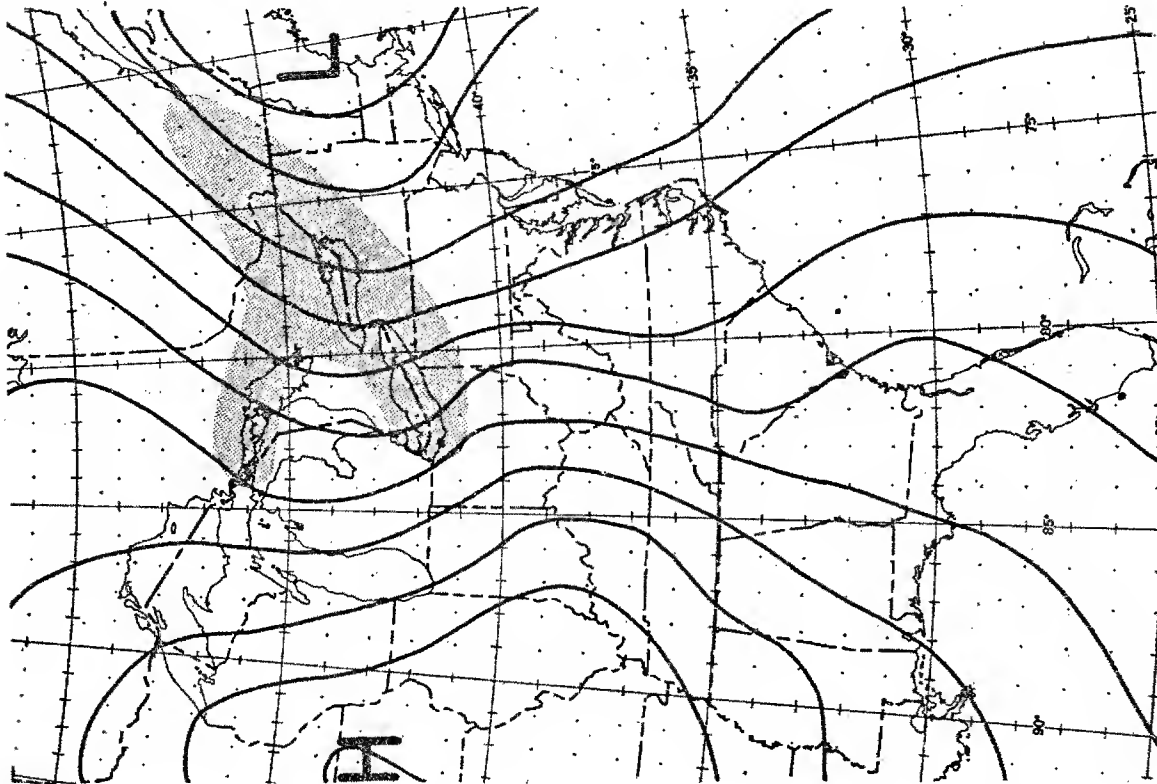
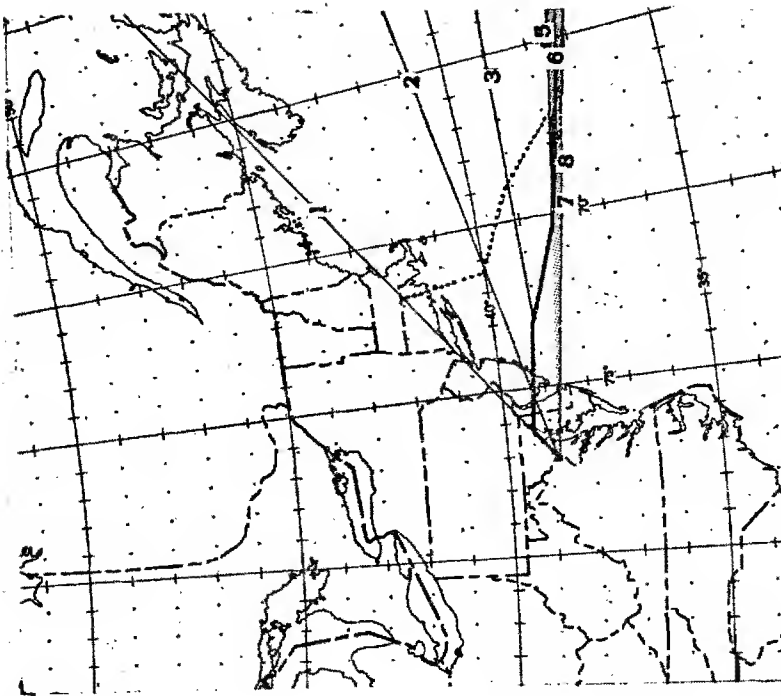


Figure 10
Surface Weather Map and Associated Fall-out Pattern, January 12, 1954



1830Z JAN 14, 1954
 WASHINGTON:
 ALTOCUMULUS OVERCAST
 CONTINUOUS SNOW
 WIND SSW 9 KNOTS

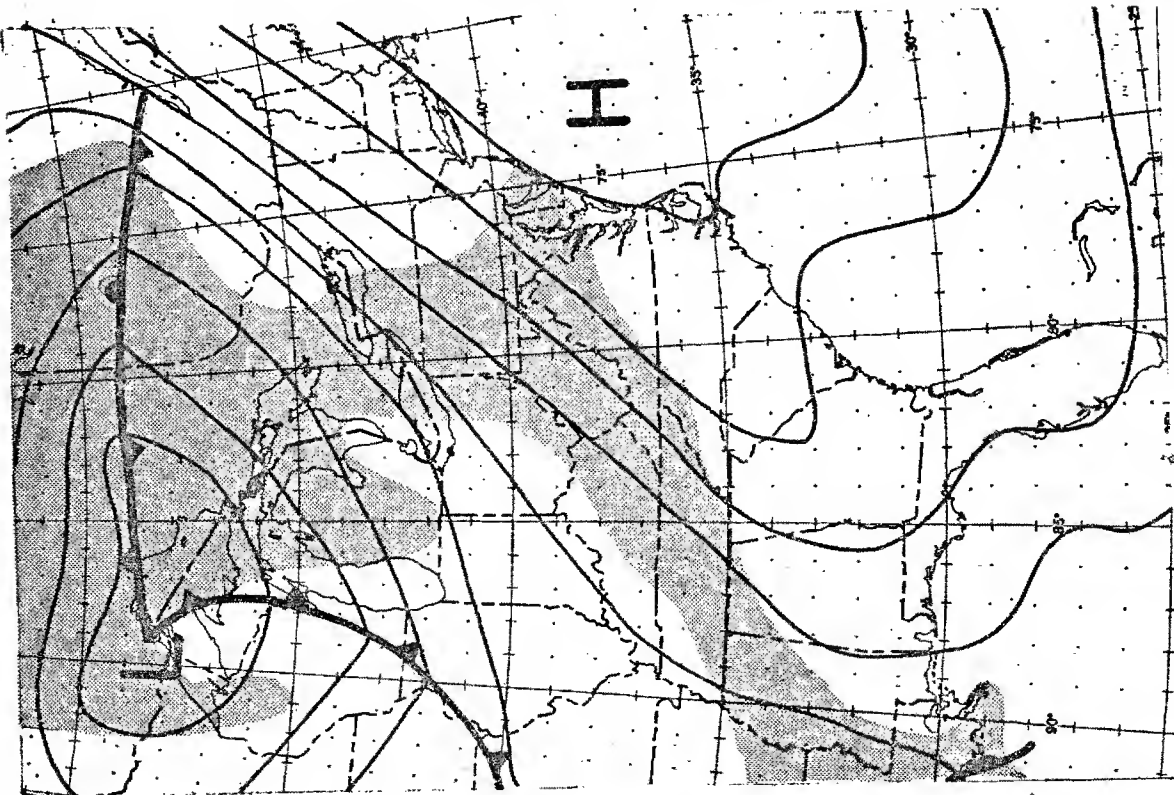
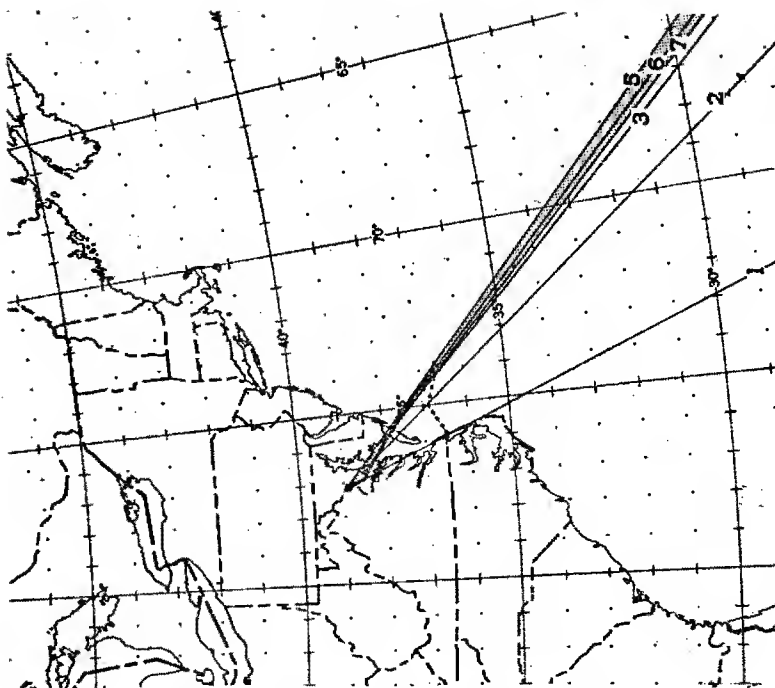


Figure 11
 Surface Weather Map and Associated Fall-out Pattern, January 14, 1954



1830 Z JULY 2, 1954
 WASHINGTON:
 SCATTERED CUMULUS
 AND CIRRUS
 WIND NW 12 KNOTS

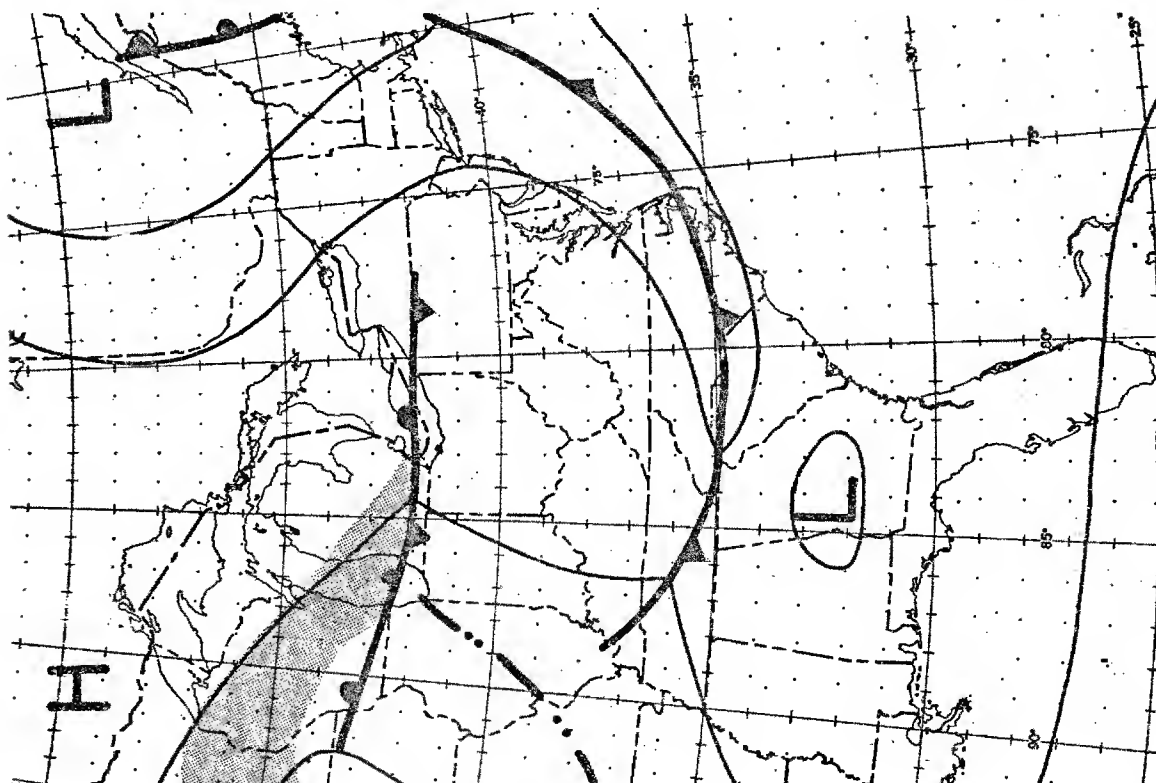
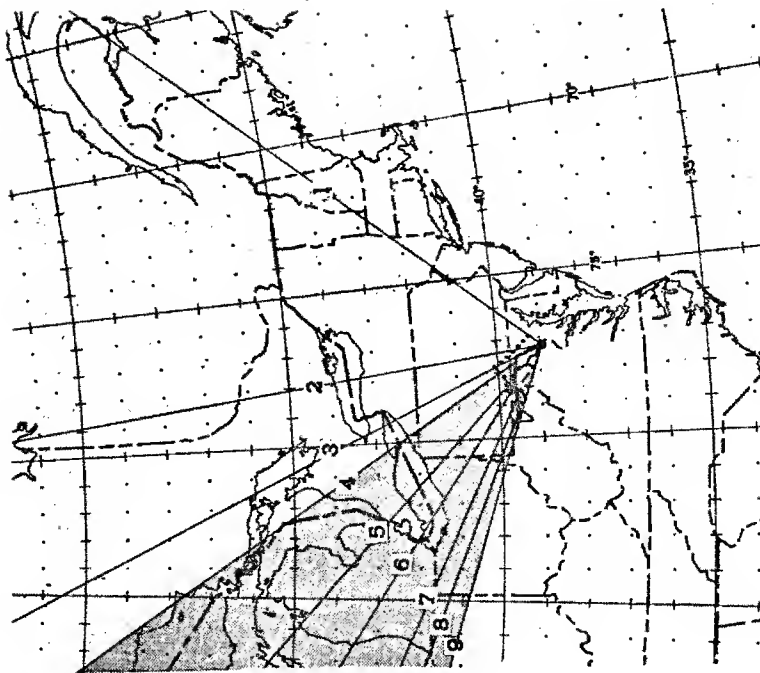


Figure 12
 Surface Weather Map and Associated Fall-out Pattern, July 2, 1954

ATOMIC ENERGY ACT



1830Z JULY 14, 1952
WASHINGTON:
BROKEN STRATUS
WIND S 9 KNOTS

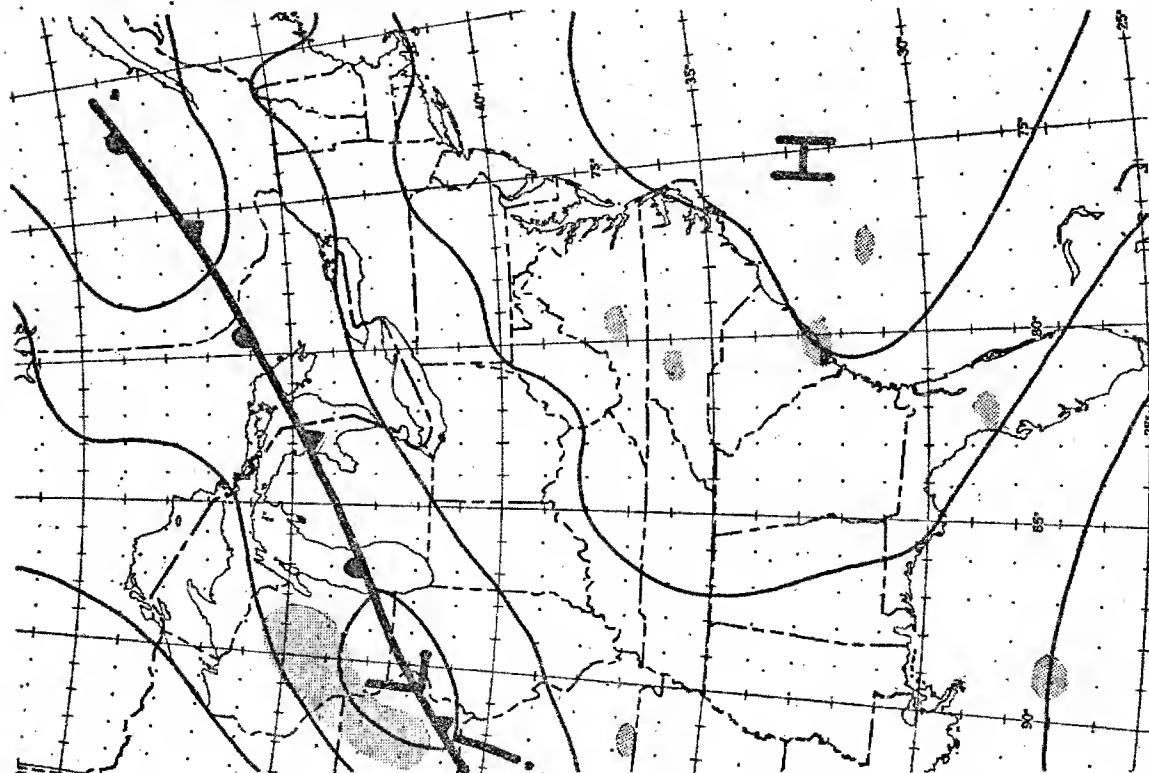


Figure 13
Surface Weather Map and Associates Fall-out Pattern, July 14, 1954

We would first divide the area of interest, for example, the United States, into regions with what we consider to be homogeneous areas of fallout climatology, an example of which is shown in Figure 14. A single upper air wind reporting station would be selected in each region and considered to be representative of the entire region. As we see in Figure 15, fallout diagrams with the areas of, say, dangerous and very dangerous fallout computed from each weather station would then be prepared each day for a number of months of past weather records. For example, the heavy shading might illustrate the very dangerous areas and be surrounded by dangerous areas. On each day, we overlay the same grid of points and then simply count the frequency of occurrence of the point in each area. These may then be tabulated for each season and analyzed to provide probability distributions shown on the right. When the probability distribution for occurrences of very dangerous fallout is superimposed on a potential target, one can readily read off the percentage probability at, say, a nearby city and obtain the likelihood that it would lie within the very dangerous fallout region for the given target.

This, I believe, would satisfy very many planning requirements. A different story must be told for the day-to-day operational capabilities of the meteorologist.

First of all, even if we use persistency as a forecasting tool - that is, take wind observations, say, every 6 hours and use the last observation to transport the fallout debris, I am not even sure our present observational network is adequate. There are two main defects: first, the average height of the wind runs is only 55,000 feet and even at Silver Hill here in the Washington area where ideal operating conditions exist, the average height of the wind runs is only 75,000 feet. Frequently, we do get runs in excess of 100,000 feet, but these are usually in warm climates and with wind speeds which are not excessive. My guess is that, in the winter, with current equipment, the average height of the upper wind observations over northern U. S. is well below 55,000 feet. Second, if the balloon is too near the horizon, it either cannot be tracked at all or the wind data becomes uncertain. Thus, if the speeds are high, making low elevation angles, our wind data becomes much poorer. In addition, the present method of analyzing and reporting upper winds is not particularly suited for fallout computations and certain unnecessary errors are introduced. In Figure 16, we see part of an actual plot of wind speed with height. What is normally used in preparing fallout plots are the winds at 5,000-foot levels rather than vertically integrated winds. The latter would be more desirable from a fallout viewpoint, since winds at all levels transport the particles. Although chosen at random, you can see in Figure 16 that the speed at each 5,000-ft. level is lighter, by chance, than the mean through the layer in which the wind is centered so that the predicted fallout would fall short of where it would actually be.

DOE ARCHIVES

234

~~RESTRICTED DATA~~
ATOMIC ENERGY ACT 1954

~~SECRET~~

238

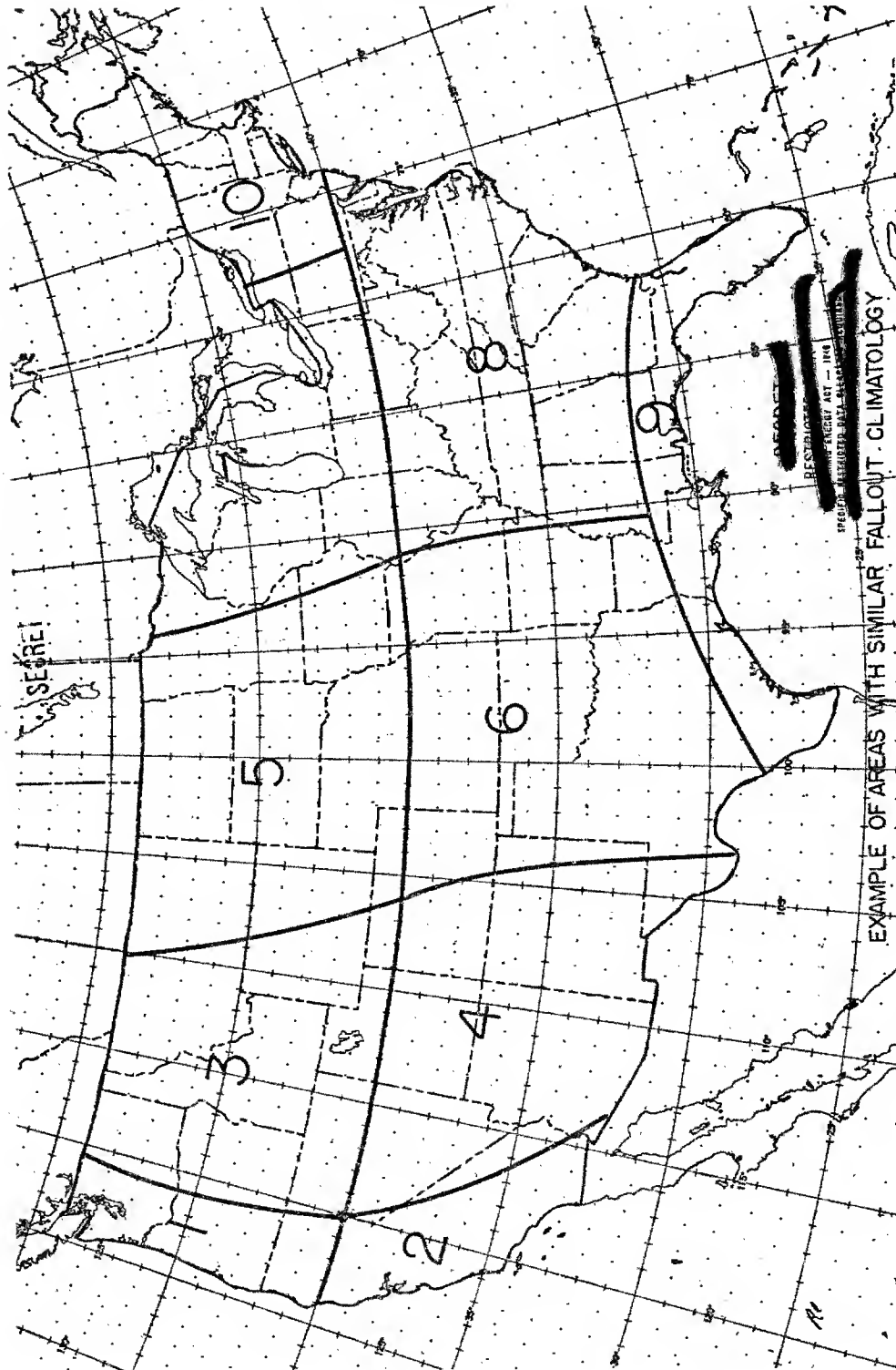


Figure 14
Examples of Areas with Similar Fall-out Climatology

~~RESTRICTED~~
ATOMIC ENERGY ACT 1954

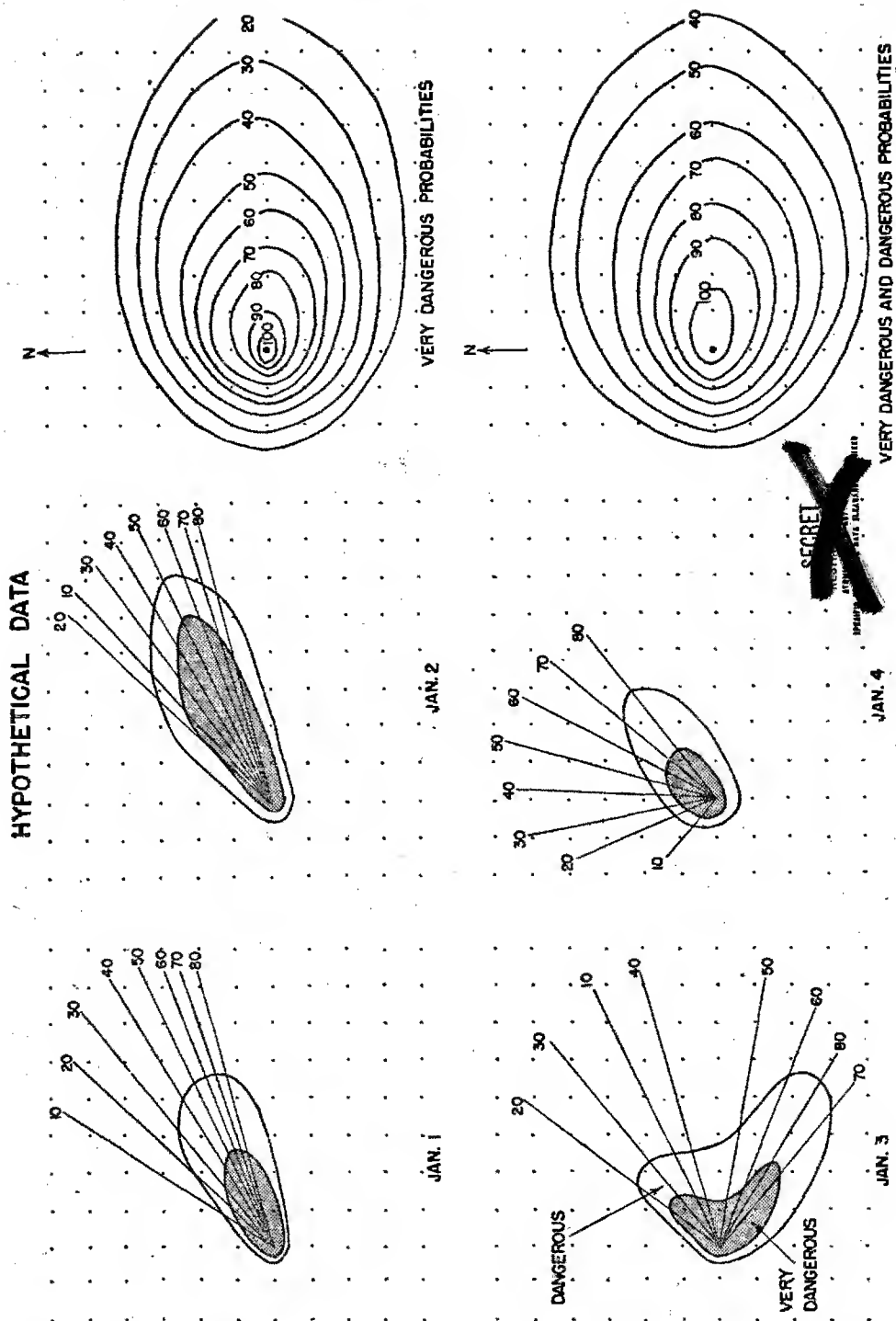


Figure 15
Examples of Fall-out Diagrams and Probability of Occurrence of Very Dangerous and Dangerous Fall-out

~~SECRET~~

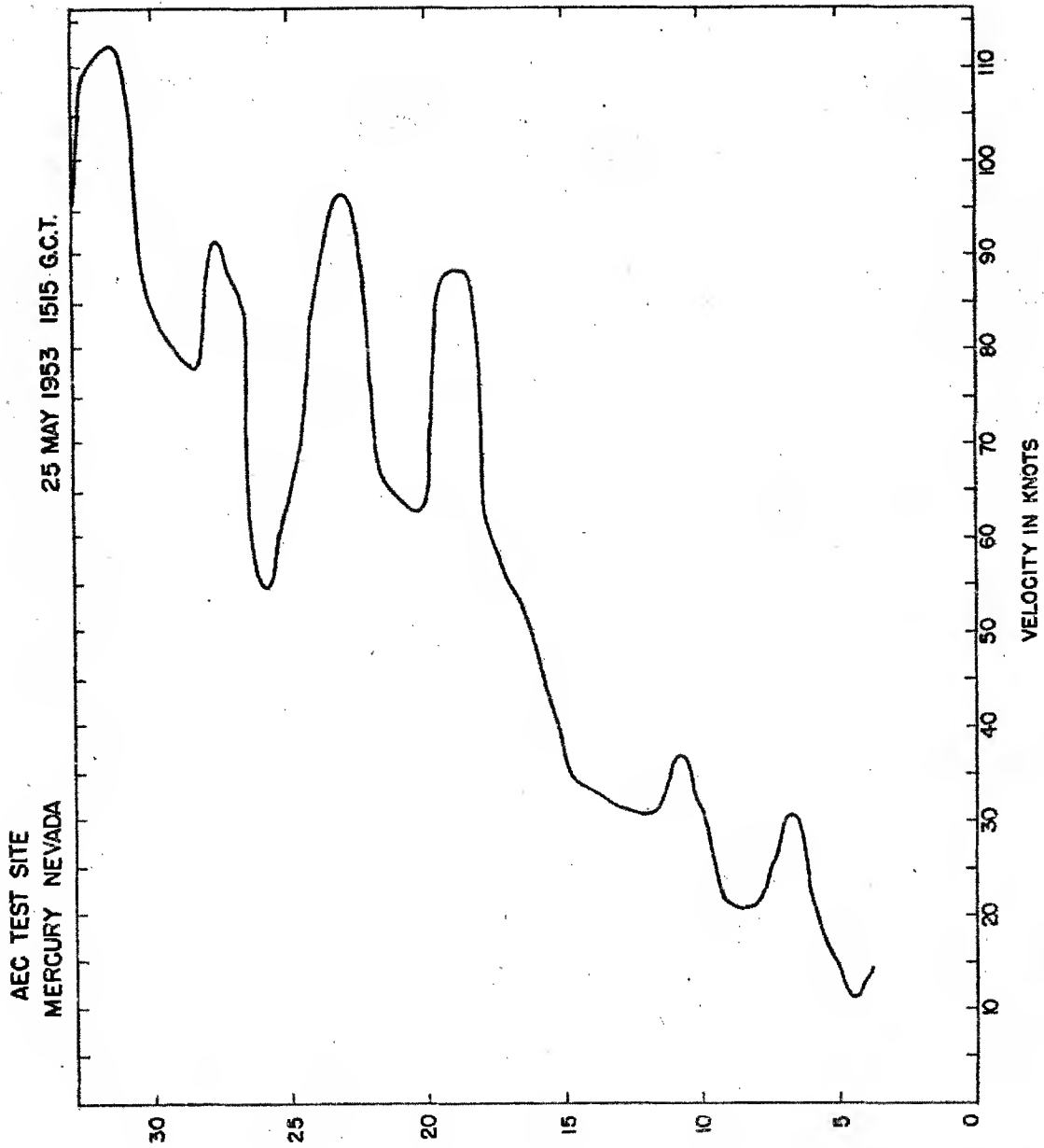


Figure 16
Typical Wind Variation with Altitude

DOE ARCHIVES

237

~~SECRET~~

~~SECRET~~
DATA
NUCLEAR ENERGY ACT

241

It is highly unlikely, if a bomb is actually detonated or we know one will be detonated, that a persistency forecast will be acceptable. Weathermen will be asked to make best possible forecasts where so much is at stake. Unfortunately, we have practically no forecasting experience at levels above about 30,000 feet, and, in fact, do not routinely even draw weather maps above 55,000 feet. Our experience, in fact, is so limited to the lower atmosphere that, at the Nevada Test Site, the absolute wind forecast error doubles from the 20,000 layer to the 40,000-foot layer. Further, time and space variability of the wind can be adequately included only by the meteorologist. Concerning the need to incorporate time and space changes in the wind, I have an interesting case showing a comparison of using point winds with time and space variable winds, in Figure 17. The straight dashed lines are the lines along which fallout occurs from a given height if the test site wind at burst time alone is used at Nevada while the curved solid lines incorporate time and space variability. The numbers are the observed fallout along the roads. It is clear that the time and space variability is superior, although it may not always provide as good a forecast as shown here. The need for time and space variability is much greater in the case of megaton weapons than in Nevada test operations since fallout is important for longer times and to greater distances.

Finally, the meteorologist must be able to provide the Civil Defense official or military commander with a measure of the uncertainty in the forecast. We can all imagine cases in which, if the uncertainty in fallout forecast is too great, it may do more harm than good.

In conclusion, the meteorologist even today can provide certain valuable generalities about the probable areas of radioactive fallout, but much remains yet to be done to answer questions about dosages or dangerous areas and about the details of the fallout probabilities. Finally, the weatherman needs much more development research and training before he can really assist in operational fallout forecasting.

DOE ARCHIVES

~~RESTRICTED DATA~~
~~ENERGY~~

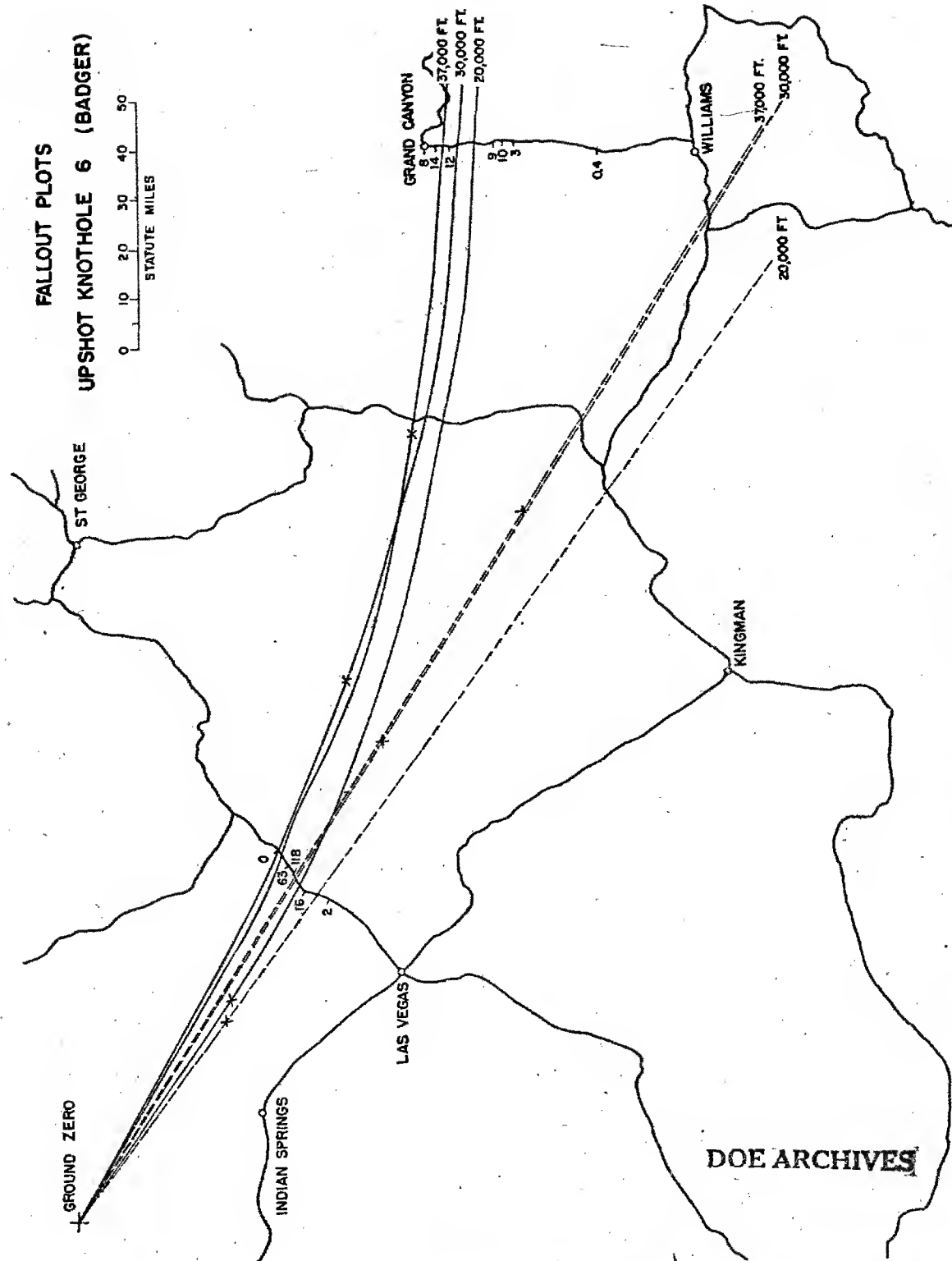


Figure 17
Effect of Time and Space Variability of the Wind on the Location of Fall-out

THIS PAGE IS BLANK

DOE ARCHIVES

240

~~ENERGY ACT~~

244

[REDACTED]

PREDICTION OF DOSE-RATE AND DOSAGE CONTOURS AS
FUNCTIONS OF YIELD AND METEOROLOGICAL CONDITIONS,
AIR WEATHER SERVICE METHOD

Lt. Col. Clifford A. Spohn, USAF
Air Weather Service

My talk today is, in a sense, sailing under false colors. The problem under consideration during this portion of the symposium deals with the determination of ground levels of contamination resulting from fallout, and I am listed in the program as presenting the Air Weather Service method. Actually, the method of fallout prediction used by Air Weather Service does not provide an answer giving ground contamination levels. The technique currently used is concerned only with the meteorological portion of the problem, that is, specifying where and when fallout will occur.

The technique itself is a very simple one, and is based on the following assumptions:

That the point winds near the detonation point (observed or forecast) are representative of the time-space wind field through which fallout takes place.

That winds at successive 10,000-foot layers in the atmosphere are representative of the wind flow through their respective layers.

That the various contaminated particles will have constant fall rates, although the fall rates are unspecified, and need not be related to particle size.

That fallout takes place upon a level surface, i.e. terrain variations are ignored.

Given these assumptions, the fallout plot is easily prepared. The wind sounding, observed or forecast, for the place in question, is used to construct composite wind vectors. The 5000' wind vector (representing flow in the layer from sea level to 10,000') is laid off from the ground zero position. From the end of this vector, the 15,000' wind vector (for the layer 10,000' - 20,000') is next laid off. The 25,000' wind vector is laid off from the end of the 15,000' wind vector, and the process continued to as high a level as desired, or to the end of the wind data. Radial lines are now drawn from ground zero to the ends of the various wind vectors and labeled appropriately. Thus, the radial line to the end of the 15,000' wind vector is labeled 20,000'; to the end of the 25,000' wind vector, 30,000', etc. These radial lines are the resultant

DOE ARCHIVES

wind vectors from the specified level to the ground, and indicate the line away from ground zero along which fallout from the given level will take place. The lengths of these resultant vectors is measured and divided by their labeled heights expressed in tens of thousands of feet (i.e., the length of the resultant vector labeled 20,000' will be divided by "2", the 30,000' vector divided by "3", etc.). The numbers obtained represent the speed at which fallout will progress outward from ground zero along the various radial lines.

The finished plot is prepared by laying off the resultant vectors, and marking off along them successive hourly positions of fallout. By connecting all of the points corresponding to a given time after zero, the line along which fallout will occur at that time is indicated.

The completed plot thus shows three items. First, the general area in which fallout will take place; second, the lines along which fallout from a given level will occur; and, third, the lines along which fallout will occur at particular times.

The validity of the underlying assumptions must certainly be considered. The latter three assumptions, that of a constant fall rate, fallout on a level surface, and using a wind as representative of a 10,000' layer, will not, in general, introduce much error. The first assumption, however, that a spot wind sounding will be representative of the space-time wind field throughout which fallout takes place, is less dependable. On a comparatively small test sample from the Nevada Proving Ground, using wind soundings taken two hours prior to detonation, and for fallout computed out to not more than nine hours after detonation, 75% of the resultant vectors deviated by less than 15° from a post-analyzed position. If the fallout computations are extended considerably beyond nine hours, or if old wind data (i.e., 24-hour forecasts or observations 6 - 12 hours old) are used, this assumption becomes increasingly less reliable, and may lead to quite serious errors in the calculated fallout plot. For this reason, current Air Weather Service practice is to use, if at all possible, observed wind data less than six hours old, and to compute fallout out to 6 - 9 hours from time zero.

DOE ARCHIVES

Note: Examples of problem solutions by the Air Weather Service method are given in the paper, "Comparison of Problem Solutions by Various Methods," by Cdr. R. W. Paine.

[REDACTED]

PREDICTION OF DOSE-RATE AND DOSAGE CONTOURS AS
FUNCTIONS OF YIELD AND METEOROLOGICAL CONDITIONS,
NAVY WEATHER SERVICE METHOD

Dr. F. W. van Straten
Office of the Chief of Naval Operations

The Navy method for predicting the location of potential radioactive areas after a surface burst of an atomic weapon over land or shallow water is designed to permit routine computations in advance of an actual explosion. It is expected that transparent overlays showing potential radioactive areas will be prepared, when necessary, after each wind sounding. These overlays will then be available for superimposition on a map should an atomic explosion occur during the valid time of the wind sounding. Although it is realized that this procedure gives only approximate results, it is felt that immediate operational decisions can be made on the basis of these approximations. Time and data permitting, more refined computations can be made subsequent to the event.

To permit this computation in advance of an explosion - when the height of the explosion is unknown, the size and nature of the bomb is not known and the terrain characteristics are undetermined - a number of assumptions is required. The limitations resulting from these assumptions are acceptable in view of the availability of a rough diagram from which immediate tactical decisions can be made.

It is assumed that the explosion penetrates the tropopause. This assumption is made so that the diagram will show the maximum area which may be affected. If it is determined, subsequently, that the radioactive cloud did not, in fact, penetrate the tropopause, the diagram can later be reduced.

DOE ARCHIVES

Lack of knowledge concerning the nature of the bomb and terrain necessitates assumptions about the distribution of particles in the radioactive cloud and their rate of radioactive decay. It is assumed that any horizontal cross section through the stem is identical with any other horizontal cross section. In other words, it is assumed that all particles sizes are distributed uniformly throughout the cloud. Further, radioactive decay is postulated to occur at a rate proportional to the square of the diameter of the particle and inversely proportional to the square of the time from the explosion.

Although it is recognized that a complete spectrum of particle sizes is probably present, only a size range between 75 and 150

[REDACTED]

microns is considered. It is assumed that particles larger than 150 microns will fall out so close to ground zero as to produce no additional hazard. The smaller size particles, less than 75 microns, are of concern, principally, because of the great distances they can travel in the time it takes them to fall from high altitudes. For particles smaller than 75 microns, this time is so great that considerable modification in the wind field is possible, and a computation based on a current wind sounding may lead to completely erroneous results. Particles of 75-micron size are assumed to fall at a rate of 5,000 feet per hour, while those of 150-micron size fall at a rate of 5,000 feet in 3/10 of an hour.

For the original construction of the potential radioactive area, it is assumed that validity is limited to 6 hours in time, and 250 miles in radius.

It should be noted that provision is made for subsequent extension in time and area. Further, while the diagram plotted in advance is designed to show fall-out on the surface, the method also lends itself to subsequent computations to show radioactive areas at any altitude and time - air radex plots - following the explosion.

In brief, the method used by the Navy consists of the following steps:

Determination of the mean wind vectors between specified levels.

From the mean wind vector and the rate of fall, the position of fall-out and the time taken to fall are computed for each size particle.

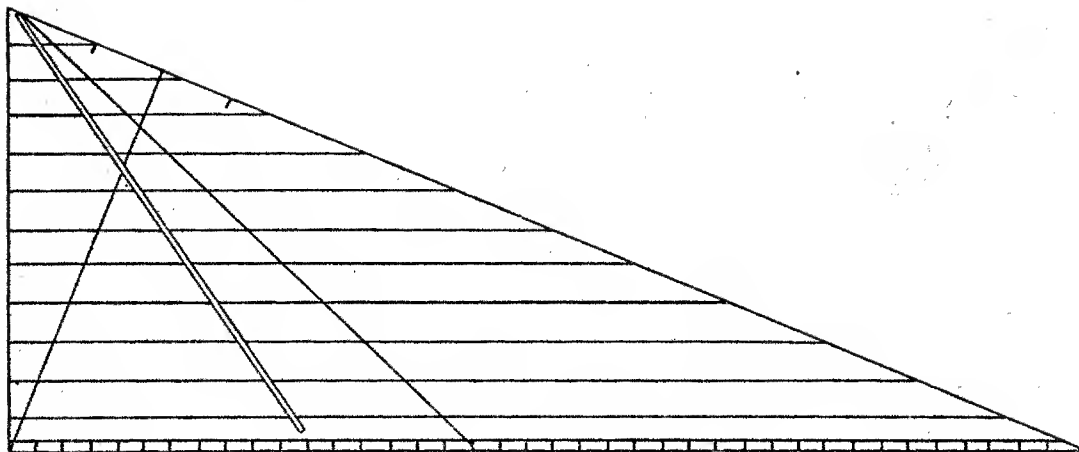
The positions marked along the mean wind vectors permit definition of the area of fall-out.

The time marks can be used to draw lines showing the approximate time at which radioactivity reaches the surface within the affected area.

The degree of radioactive contamination in any given unit area is considered to be proportional to the number of mean vectors traversing that area. From the vector concentration and the time lines, it is possible to compare relative radioactivity from unit area to unit area. A series of lines is drawn on the diagram connecting area of equal radioactivity.

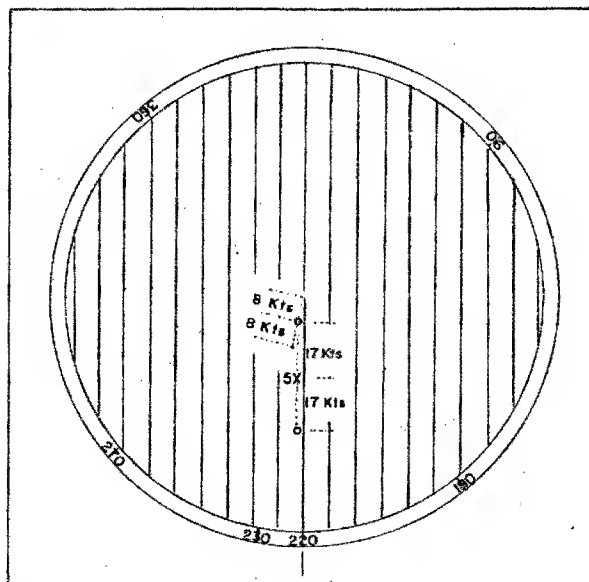
DOE ARCHIVES

In practice a conventional winds aloft plotting board, a transparent plastic sheet and a radex rule are used. Figure 1 is a diagrammatic sketch of the radex rule.



RADEX RULE
ML-502/UM

Figure 1



PLOT OF SURFACE AND 5000'
VECTOR ON PLOTTING BOARD

DOE ARCHIVES

Figure 2
245

~~RESTRICTED DATA~~
ENERGY ACT

249

Across the base of the radex rule is a scale used for plotting wind speeds. When a given mean wind vector is placed under the radex rule in such a way that it is parallel to the horizontal lines on the rule and extends from the vertical side to the dark line hypotenuse, the slot in the radex rule marks the position of fall-out of the 150 micron particles and the outer hypotenuse - edge - marks the position of fall-out of the 75 micron particles. The line extending from zero on the base scale to the hypotenuse, together with the tick marks on either side of this line, is used to expand a plotted diagram by 10° to take care of dispersion and minor errors in wind information.

The following specific steps are followed to produce the Navy diagram:

On the plotting board, add the 5,000 foot wind vector to $1/2$ the surface wind vector. On the end of the 5,000 foot vector add the 10,000 foot vector. Continue this process with each 5,000 foot wind vector to the top of the sounding. The radex rule is used for marking the wind speeds. See figure 2.

Place a transparent, plastic sheet over the plotting board. Mark the center of the plotting board and then mark the 180° position of the plotting board as north. Transcribe the mid point of each wind vector on the plastic sheet. Thus the mid point of the 5,000 foot vector is transcribed and labeled 5. The mid point of the 10,000 foot vector is labeled 10, etc.

Connect the center indicated on the plastic sheet with the points marked 5, 10, 15, etc., extending the line well beyond the marked points.

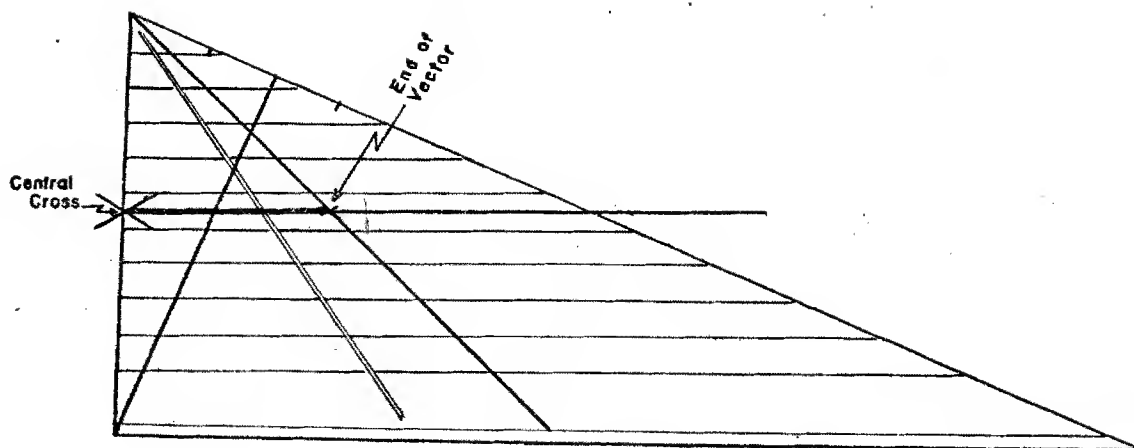
Place the radex rule on each vector in turn so that the center indicated on the plastic sheet is on the vertical edge of the rule, and the numbered point is on the dark line hypotenuse with the vector parallel to the horizontal lines. Mark through the slot on to the vector and mark the edge of the radex rule on the vector. See figure 3.

For the vector labeled 5 the slot marking is labeled 3 indicating $3/10$ of an hour. The outer mark is labeled 10 indicating one hour. On the vector labeled 10 these corresponding points are 6 and 20. The 15 vector shows 9 and 30, etc. See figures 4 and 5.

Using the radex rule, expand the diagram by adding 10° on either side of the outer vectors. See figure 6.

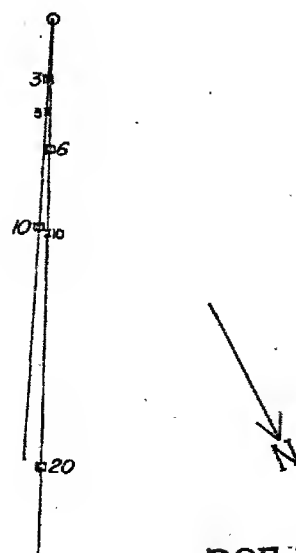
Estimate the position of "10" - the one hour position - on each of the vectors, and draw a line through these points. Repeat for 2 hours, 3 hours, etc.

Enclose an area on the overlay limited by the 10° expansion lines, the vector ends, the 6-hour line and the 250 mile radius arc, whichever is smallest (the scale of the radex rule is such that 20" is equal to 250 miles).



RADEX RULE IN POSITION ON VECTOR

Figure 3



DOE ARCHIVES

Time Marks on first two Vectors

Figure 4
247

~~REDACTED DATA~~
ATOMIC ENERGY ACT 1954

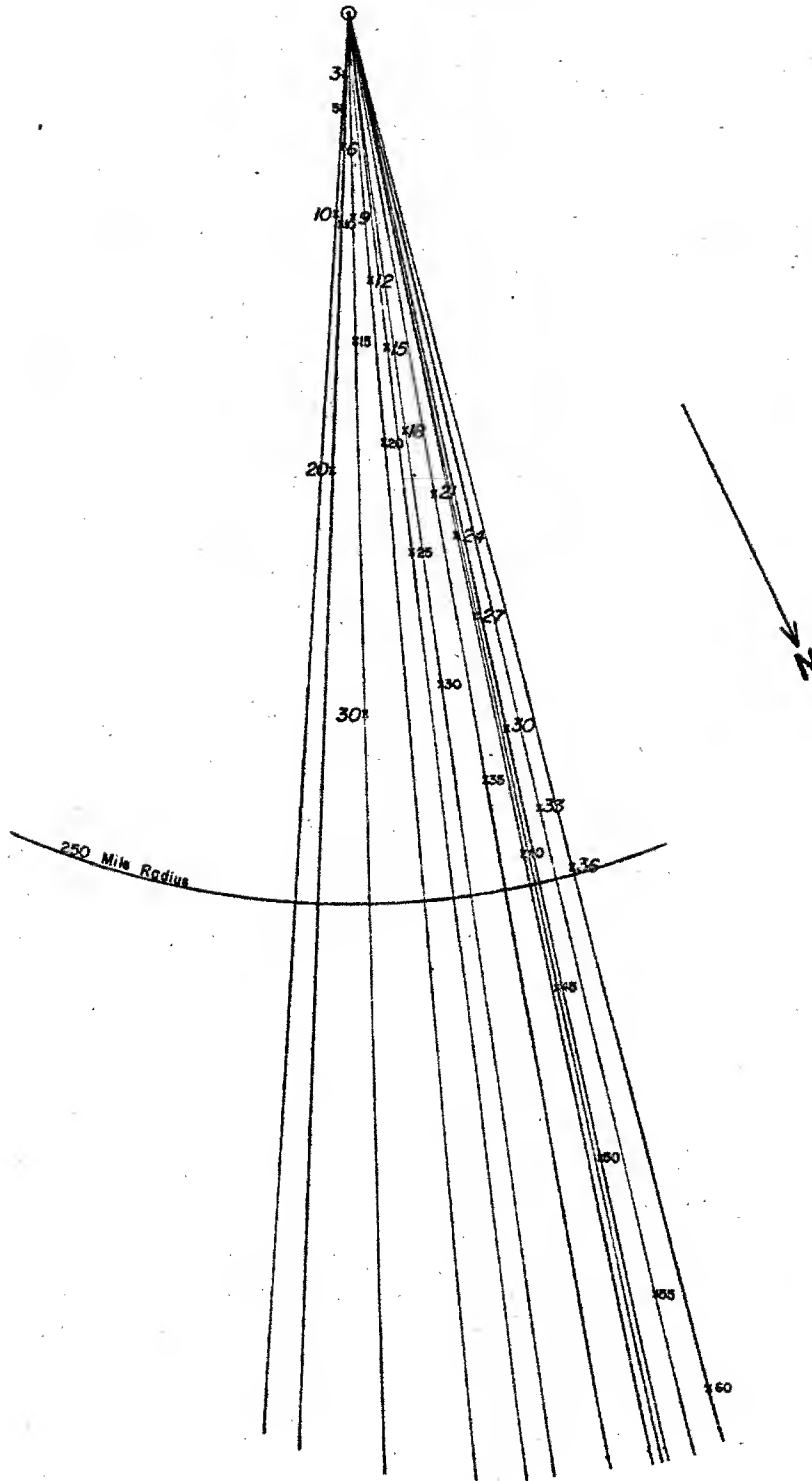


Figure 5
248

DOE ARCHIVES

~~RESTRICTED DATA~~
ATOMIC ENERGY ACT 1954

TABLE I

<u>LARGE</u>		<u>SMALL</u>	
<u>TIME</u>	<u>ACTIVITY</u>	<u>TIME</u>	<u>ACTIVITY</u>
1	1300	1	600
2	600	2	350
3	150	3	60
4	80	4	40
5	60	5	20
6	40	6	16
7	30	7	12
8	20	8	9
9	16	9	7
10	13	10	6
11	12	11	5
12	10	12	4

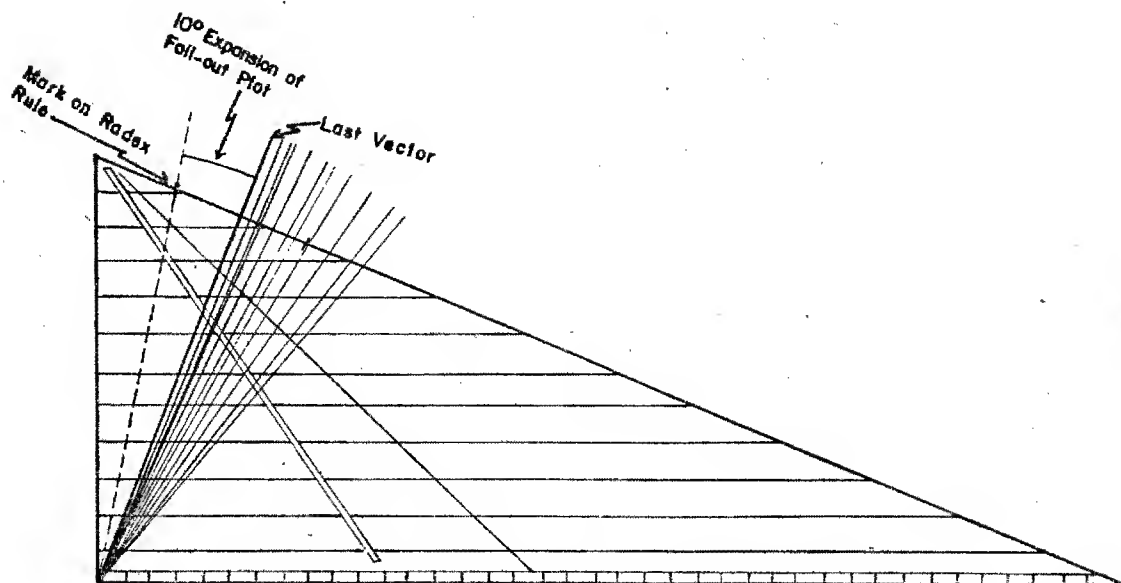


Figure 6
249

DOE ARCHIVES

NUCLEAR ENERGY

Place a rectangular grid over the diagram and count up the number of vectors traversing each grid area. The grid is drawn in squares $8/10$ of an inch from the side. On the grid draw a line connecting the 3, 6, 9, etc., points. Those portions of the vectors which fall closer to the center than this line represent large particle fall-out. The remainder of the vector represents small particle fall-out. Using Table I, the number of vectors and the time lines calculate the relative radioactivity in each area. Connect areas of equal indicated activity. See figures 7 and 8.

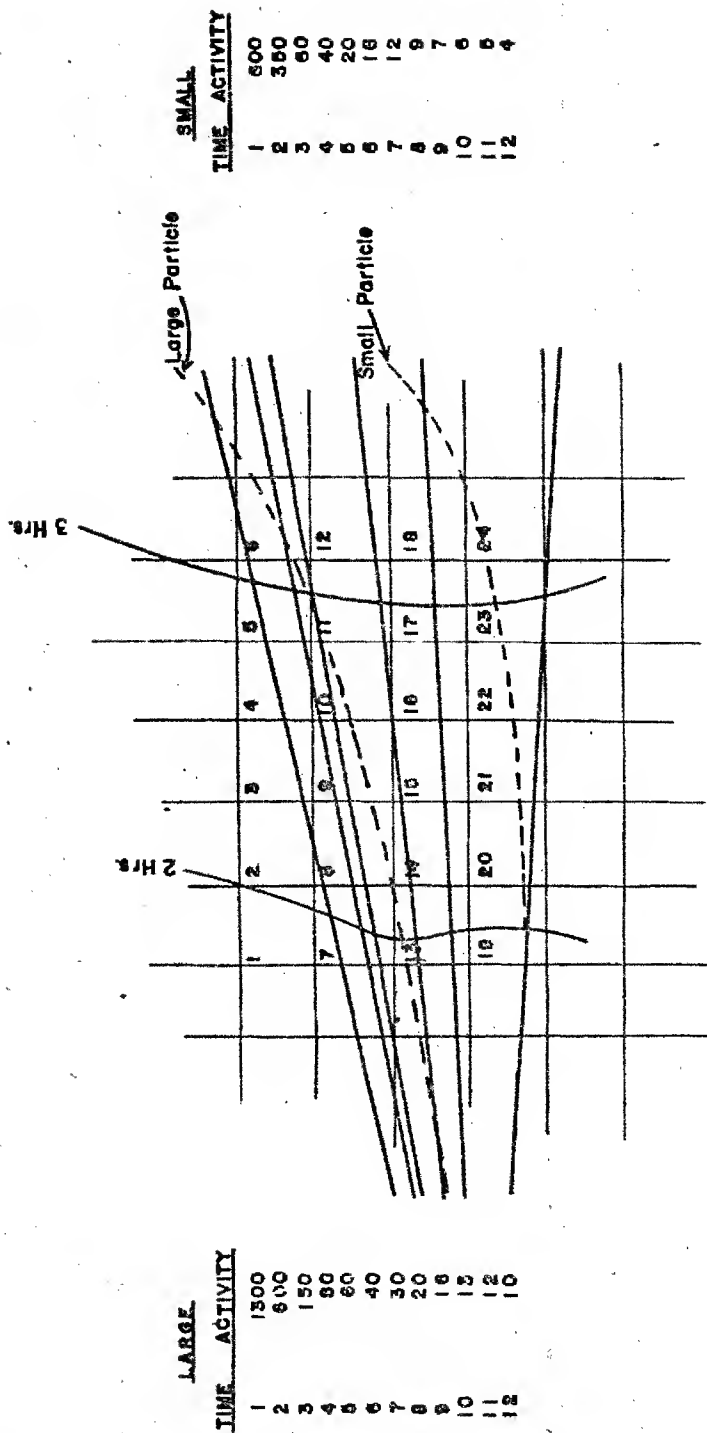
The diagram is now completed since it shows the area of probable fall-out, the time of fall-out and the relative activity.

The steps for preparing an air radex plot will not be outlined in detail. Suffice it to say that appropriate mean wind vectors are selected. For example, if an air radex plot at 5,000 feet and $H + 1$ hours is required, small particle fall-out will originate from the 10,000 foot level and large particle fall-out from the 20,000 foot level. Thus, only vectors between 5,000 and 20,000 feet are used.

To expand the diagram timewise, an appropriate air radex plot is first constructed and then a new wind field used to determine how particles fall from the selected level to the surface.

One final note is required, it is assumed that the intensity of radiation is proportional to the ratio of the square of the diameter of the particle to the square of time. This ratio is given as relative activity. To convert relative activity to actual activity it is necessary to have a proportionality constant. Presumably a single measurement anywhere within the area can provide this constant and will permit conversion of all relative values to actual values.

DOE ARCHIVES



Grid #	Activity	Grid #	Activity	Grid #	Activity	Grid #	Activity
1	0	7	3 x 600=1800	13	2 x 350=700	19	600
2	600	8	3 x 600=1800	14	2 x 350=700	20	0
3	600	9	2 x 600=1200	15	2 x 350=700	21	0
4	2 x 150=300	10	2 x 150+60=360	16	60	22	0
5	2 x 150+60=360	11	150+60=210	17	60	23	0
	2 x 150+60=360	12	60	18	60	24	0

DOE ARCHIVES

~~RESTRICTED DATA~~
ATOMIC ENERGY ACT 1954

Figure 7

SECRET

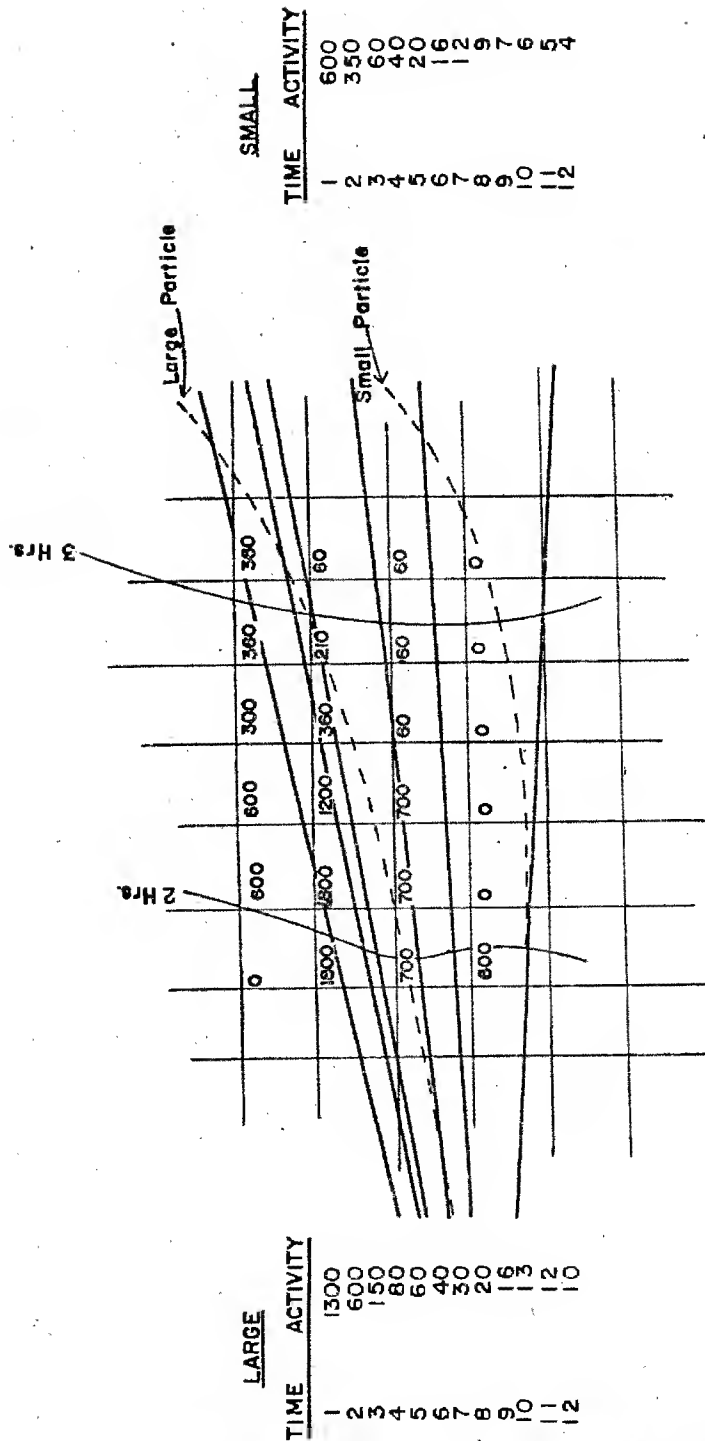


Figure 8

DOE ARCHIVES

SECRET

[REDACTED]

PREDICTION OF DOSE-RATE AND DOSAGE CONTOURS AS
FUNCTIONS OF YIELD AND METEOROLOGICAL CONDITIONS,
ARMY SIGNAL CORPS METHOD

Donald M. Swingle
Signal Corps Engineering Laboratories

The Army Problem

During the latter half of 1954 the Signal Corps received an urgent requirement to provide fall-out computations for a study. The two Signal Corps organizations interested in meteorology, i.e., the Signal Corps Engineering Laboratories and the Army Electronic Proving Ground, united to perform the required job. SCEL was to determine or develop a suitable fall-out computation method and AELCTPG was to apply the method to the computation of the patterns required.

The requirements of the Army problem called for the quantitative computation of radioactive fall-out material and dosage under a number of different meteorological conditions. A survey of existing computation methods revealed none that would obtain the required results. It was, therefore, decided to devise a suitable method subject to the following requirements:

The method must be physically reasonable, starting with a specified initial state of the cloud, accounting for modifying influences occurring during fall-out, and yielding quantitative plots of the amount and times of arrival of fall-out material on the ground. Modifying influences would include the effects of wind, diffusion, varying fall velocities, decay of radioactivity during fall-out, and special effects such as the occurrence of precipitation and cloud and details of the terrain on which the fall-out would occur.

The method must yield quantitative plots of dose rate referred to H plus 1, total dose, time of arrival of fall-out and time of ending of fall-out.

The method must yield results in agreement with the observations made at CASTLE BRAVO.

The method must account for real winds in the atmosphere.

The method should be applicable to 15 MT detonations, any day, anywhere.

DOE ARCHIVES

The method must use the best available background information.

The method must be as simple and fast in its application as possible, consistent with not further degrading the existing sparse data on fall-out from high yield weapons.

[REDACTED]

The method should be amenable to scaling, if possible. The method derived below in this report was based on a 15 MT detonation but may be scaled either by use of the AFSWP scaling laws (which are not based on our cloud model but are convenient) or by the computation of another model of the same nature and having similar treatment but differing in the values utilized.

Sources and Acknowledgements

Since the personnel assigned to this task had not had previous contact with the fall-out problem, arrangements were made to visit all groups active in the field which were located in or near Washington, D. C. Contacts were made with AFSWP, JTF-7, Hq. Air Weather Service, Office of the Chief of Naval Operations, Hq. Air Research and Development Command, and the U.S. Weather Bureau.

Personnel interviewed included the following:

Captain Russell Maynard	Hq. AFSWP
Commander R.W. Paine	Hq. AFSWP
Lt. Col. C.D. Bonnot	JTF-7
Lt. Col. House	JTF-7
Lt. Col. C.A. Spohn	Hq. Air Weather Service
Dr. Florence Van Straten	Office of the Chief of Naval Operations
Lt. Col. N.M. Lulejian	Hq. ARDC
Dr. Lester Machta	U.S. Weather Bureau

Source documents utilized included the following:

AFSWP Report TAR-507 and others issued by AFSWP
RAND Report R-265-AEC
Instruction books of the various services and offices.

Special acknowledgement must be given to the assistance given us by Captain Maynard and for the information contained in the RAND report. Without his extensive knowledge of sources of information and without the full description of the cloud growth and structure contained in the RAND report, it would have been quite difficult, if not impossible to derive the cloud model utilized in this study.

Derivation of the Signal Corps Method

DOE ARCHIVES

The derivation of the computation method used by the Signal Corps is described below in terms of a) basic concepts, b) information on the initial conditions within the cloud structure and related factors, c)

analysis of the basic data, d) derivation of model to obtain the distribution of fall-out material on the ground, and e) the abbreviated method of obtaining total dose.

Concept:

As a result of the understanding which evolved during our inquiry, it was decided to attempt a simple physical model of the cloud and of its fall-out processes. It was conceived that the initial conditions of distribution of radioactivity vs. fall velocity, cloud dimensions, and distribution of cloud radioactivity in height and distance could be specified. This cloud would then be considered as consisting of a number of different "slabs" of suitable thickness. Each slab would be divided into "wafers" representing particles of given size classes located within the slab and each wafer would be followed to the earth from the initial location of the center of the slab in accordance with the fall velocity of the particles and the wind field. The division into slabs and wafers would be so done that each wafer, upon landing on the earth would exert "unit radioactive pressure" URP, i.e., would yield a given unit number of roentgens per hour referred to H plus 1 hour over the area which it covered. The URPs would be tallied over a grid system and summed to indicate the total accumulated radioactivity at that point. This pattern would be analyzed to yield the fall-out pattern. By noting the times of arrival of each wafer, its contribution to total dose could also be evaluated.

Initial Conditions:

It was decided to do the basic analysis in terms of a 15 MT detonation in order to use the relatively good size, shape, and fall-out data obtained from CASTLE BRAVO.

It was assumed that the cloud shape would be as follows: The mushroom top has a radius of 25 miles and extends from 60,000 to 95,000 feet. The stem has a radius of 2.5 miles, extends as a cylinder to 20,000 feet, and then flares out to mushroom diameter. In addition a spike may develop on the top of the mushroom cloud, but is ignored in our analysis since it contains but a small volume of the total cloud.

It was assumed that the particle size distribution and fall velocity curves contained in the RAND report were the best available and sensibly correct. This implied a relationship between radioactivity and fall velocity.

It was assumed that the RAND 9:1 ratio of fall-out activity coming from the mushroom to that coming from the stem was correct.

DOE ARCHIVES

Analysis of Problem:

Having specified the initial data and assumptions we next attempted to obtain as simple a mathematical description of the cloud as possible.

It appeared unreasonable that the radioactivity of the mushroom would be evenly distributed in height but, similar to the distribution of water vapor in turbulent air, it seemed reasonable that the mixing ratio of radioactivity per unit mass of air should be nearly constant within each of the two major regions, mushroom and stem. Uniform height distribution in the mushroom would have placed half the activity in the upper third of the mushroom mass. Any stratification of radioactivity would also tend in the direction of increasing the content of the lower portions of the cloud. It was, therefore, decided to represent the activity in the cloud by a "mixing ratio model." This means that equal pressure thicknesses of cloud contain equal initial radioactivity, subject to the differential of activity between mushroom and stem.

The above decision led to considering all aspects of the problem, including cloud shape and particle fall velocities, in terms of pressure as the vertical coordinate. Pressure has uniformly been related to height through the U.S. Standard Atmosphere.

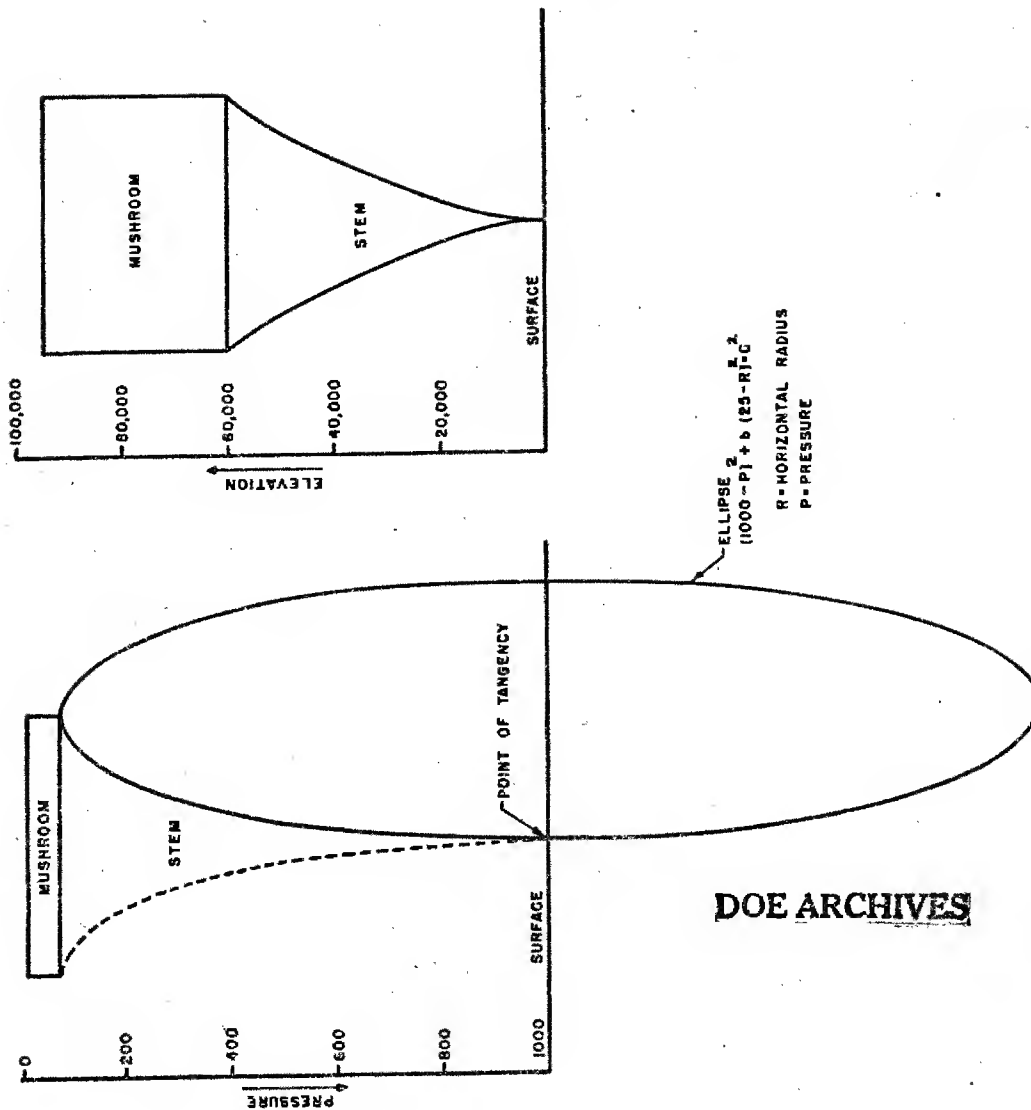
Representation of the flare of the stem was next considered and an effort made to obtain a simple continuous function which would approximate the reported shape. The flare is concave in height coordinates; in pressure coordinates it must therefore be more so. The simple shape chosen was that of an ellipse in pressure-radius coordinates. It was assumed that for our purposes all detonations could be assumed to occur at low elevations. The nominal surface pressure was taken to be 1000 mb. An ellipse having a vertical tangent at 1000 mb and ground zero, and a horizontal tangent at the lower edge of the mushroom was assumed. The equation of this ellipse in miles and millibars is

$$(1000 - p)^2 + b^2(25 - R)^2 = c^2$$

Figure 1 illustrates this in both pressure and height coordinates. It will be noted that the only pertinent parameters here are the height of the mushroom base and its radius. This shape was somewhat large at 20,000 feet but, in agreement with the Rand report, assigned little volume, and hence little activity, below 10,000 feet. DOE ARCHIVES

The volumes of the mushroom and of the stem in pressure-radius space were next computed taking the mushroom as a cylinder and the stem as a figure of revolution bounded by the ellipse. Using the given ratio of total activity led to determining that the "radioactivity mixing ratio" of the mushroom was about 12 times that of the stem.

ATOMIC ENERGY



METHOD OF DETERMINING THE STEM PROFILE

Figure 1

DOE ARCHIVES

SECRET

Using the URP concept introduced above, the mushroom was divided into five "slabs" of about 12 mb thickness, with the consideration that this number of slabs would adequately represent the differences of wind and of particle fall time with height. Each slab was to contain nine "wafers" corresponding to various particle size classes so chosen as to account for all the activity within the mushroom and to adequately represent the differences in fall velocity expected between various sizes of particles. Finally, the largest of the size classes (230 microns) was divided into five classes ranging up to 500 microns in order to better represent the fastest falling particles. The 230 micron class was deleted from all slabs and five wafers having an equal total activity and covering the new large sizes were assigned to the middle slab of the mushroom. Each slab then contained 8 wafers and the central slab was assigned the five additional wafers, thus retaining the total of 45 wafers.

Since the stem contains primarily large particles, four large particle size wafers were determined and a thickness of the stem having the previously calculated stem radioactivity mixing ratio was computed which would yield unit radioactive pressure at the center of stem slabs, i.e., the stem was divided into URP wafers. The volume of each such stem pressure slab was determined and an effective cylindrical radius, defining an equal volume, was computed. The stem cloud is then represented by a series of cylindrical slabs having varying radii. These slabs were about 70 mb thick and were assigned from about 70 to 280 mb. Beyond 280 mb, double thickness slabs and double weight wafers were assigned down to about 700 mb.

To obtain the particle size classes mentioned above, the Rand particle size data were replotted and appropriate fractional portions were scaled off. For the mushroom each slab contains wafers representing the following nominal sizes: 20, 42, 68, 85, 100, 110, 125, and 150 microns. In addition the center slab contains particles of 180, 190, 230, 290, and 500 microns. The stem contains wafers representing particles of 180, 260, 375, and 640 microns. Figure 2 shows how these size classes account for the total cloud fall-out radioactivity.

The result of this breakdown is to yield 69 URP or double URP wafers totaling 81 weights in the initial cloud. To obtain a fall-out pattern, each of the wafers is plotted on an overlay at the point where the winds would move it. This process may be rather burdensome but it can lead to quantitative results depending upon the wind. Calibration to CASTLE BRAVO showed that each wafer "weighed" about 100 roentgens per hour at H+1 hour.

It was noted that the information on which the dimensions of the model cloud was based came entirely from tropical ocean areas. The problem arose of how to account for varying atmospheric conditions. In

DOE ARCHIVES

MUSHROOM

SIZE GROUP IN MICRONS	20	40	68	85	100	110	125	150	180	210	230	290	500
PERCENTAGE OF TOTAL RADIOACTIVITY	10%	10%	10%	10%	10%	10%	10%	10%	2%	2%	2%	2%	2%

TOTAL 90%

STEM

SIZE GROUP IN MICRONS	180	220	290	640
PERCENTAGE OF TOTAL RADIOACTIVITY	2½%	2½%	2½%	2½%

TOTAL 10%

Figure 2

DOE ARCHIVES

~~SECRET~~

the present work no account is being taken of cloud, precipitation, diffusion and terrain effects. The possibilities of major changes in cloud height and shape with changes in the hydrostatic structure of the atmosphere, which might occur from the test condition to perhaps polar continental conditions, appeared important enough for some thought. Based on consideration of the increased buoyancy of cold air at low levels, the effects of entrainment of this colder air, and the relatively warm and low tropopause characteristic of polar air masses, it was estimated that the following table of mushroom top and base height would be expected as the tropopause height varied:

Height in Feet of:			
Tropopause	55,000	45,000	35,000
Mushroom base	60,000	55,000	50,000
Mushroom top	95,000	80,000	65,000

A complete model computation was run on each of these structures. The results of this work are shown in Figure 3, which gives the structures in pressure terms, and in Figure 4, which gives the structures in height terms. It will be noted that the assumed behavior of the mushroom resulted in maintaining the pressure thickness of the mushroom almost constant, resulting in similar mixing ratio ratios between mushroom and stem and in identical numbers of layers having similar radii.

Fall Time and Trajectory Calculations:

In order to determine the point on the earth's surface on which any wafer would be deposited, it was necessary to devise a method which would integrate the effect of the winds through which the particles fall. In principle, this required

$$\bar{S} = \int_p^{1000} \frac{V(p)}{W(p,d)} dp$$

where $V(p)$ is the horizontal wind at pressure p , and $w(p,d)$ is the fall velocity (in millibars per hour), depending on d , the particle size, and on pressure. Precise evaluation of this would be difficult and unwarranted by the available data. The approximation used was

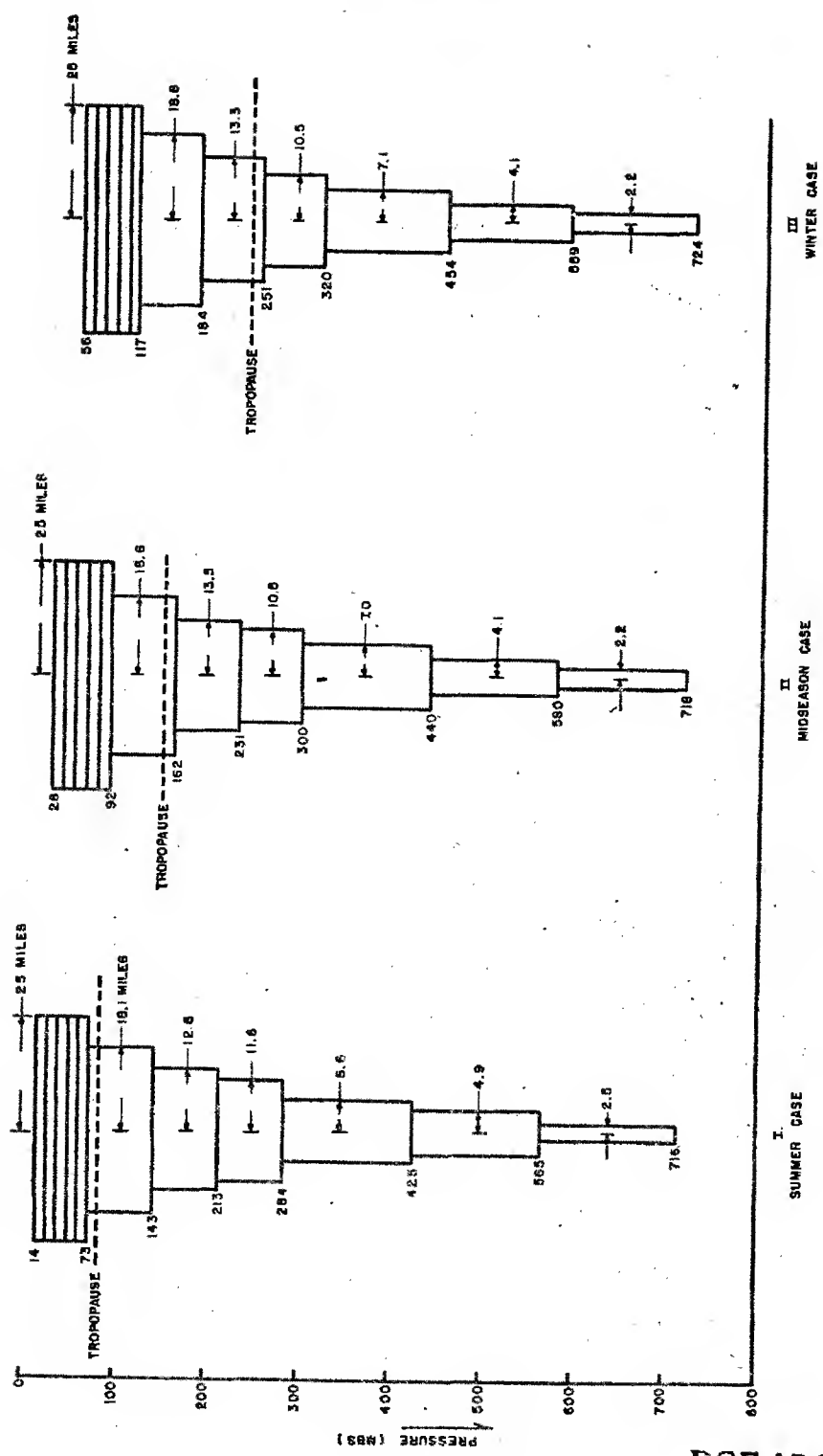
$$\bar{S} \approx \frac{1}{W(d)} \sum_{i=1}^n \frac{\bar{V}_i}{K_i} \Delta p_i$$

DOE ARCHIVES

where i indicates the reported wind level representing a pressure thickness Δp_i , $K_i(p)$ accounts for the deviations of fall velocity from constancy, and $w(d)$ reflects the fall velocity for different particle sizes.

As indicated above, the Rand fall time curves were assumed. These were replotted in pressure terms for the particle sizes used in the model described above. All curves were found to be concave upward, re-

~~SECRET~~



THE THREE MODELS PLOTTED IN PRESSURE-RATIO COORDINATES

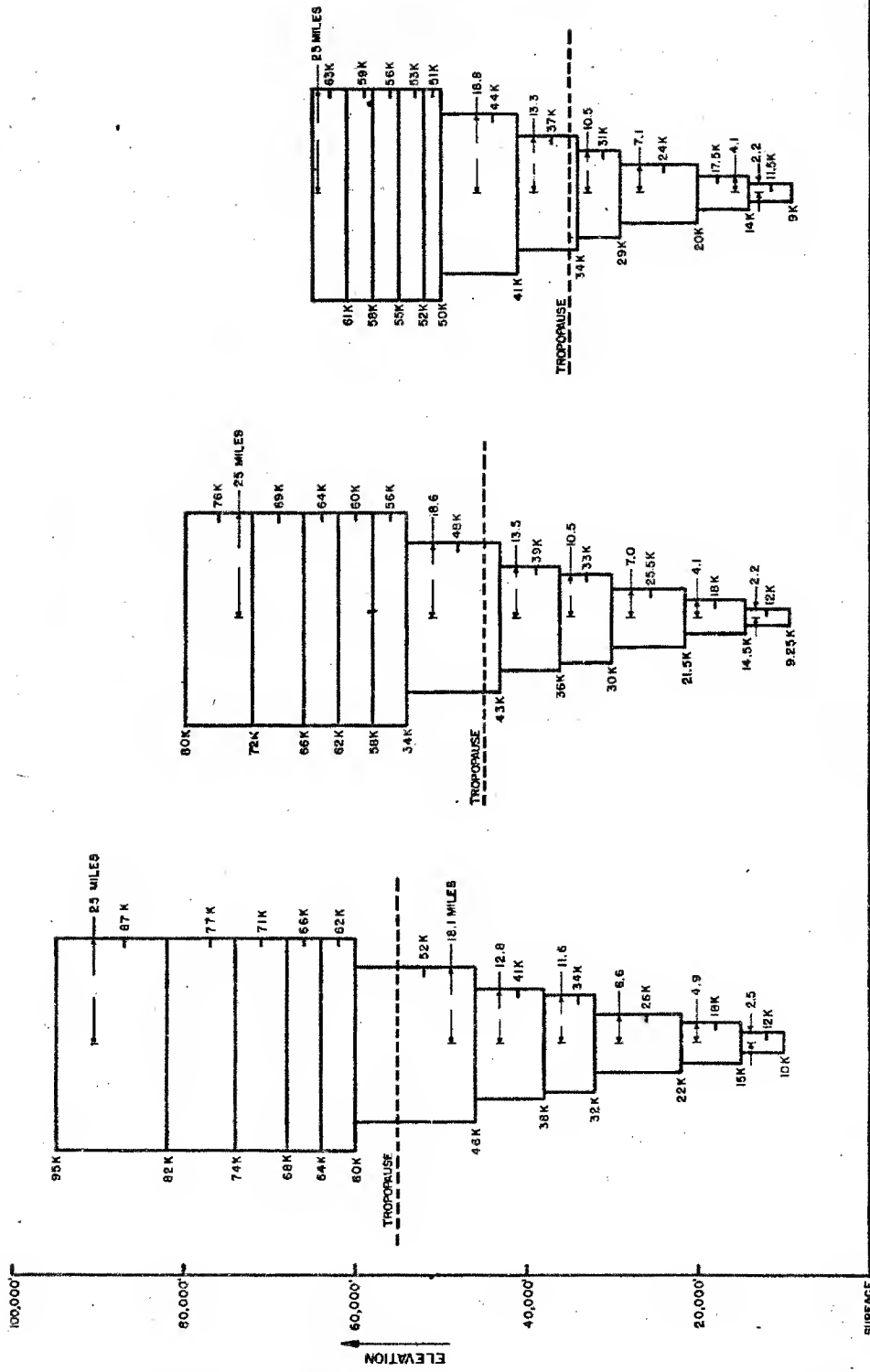
Figure 3

DOE ARCHIVES

261

~~SECRET~~
ATOMIC ENERGY ACT 1954
271

265



THE THREE MODELS PLOTTED IN RADIUS-HEIGHT COORDINATES

Figure 4

DOE ARCHIVES

flecting a greater fall velocity, in millibars per hour, at the lower pressures. Since this effect was about the same amount percentage-wise for all the smaller particle sizes and since the real effect of such a change in fall time was small for the larger sizes, the effect was treated by determining the reduction in time which the 40 micron particles would spend in any given pressure level as a result of the curvature compared to the time they would spend in an equal slice near the surface. This gave the $K(p)$ factors required to weight the winds representing such pressure levels so that 40 micron particles passing through these levels at a fall velocity assumed constant and equal to that found in the lower atmosphere would be appropriately moved by this modified wind. Fall velocities of all other particle size classes were scaled to this 40 micron fall velocity so as to introduce no error in the center of the mushroom region, yielding the $W(d)$ factors. Thus $w(p,d)$ was treated as

$$W(p,d) \doteq K(p)W(d)$$

A continuous estimate of the wind as a function of pressure $V(p)$, is not available to the meteorologist under normal conditions. In practice, he is given a number of winds representing the air velocity at a number of given heights, commonly based upon averages over time intervals of the order of one minute (i.e. average over height intervals of the order of 1000 feet). Climatological data may not include winds except for the "mandatory levels," i.e. 1000, 850, 700, 500, and 300 millibars. In using wind data to compute trajectories, the winds are weighted in proportion to the pressure thickness for which they are (and must be) taken as representative. For example, the 850 mb wind may be used to represent the atmospheric flow between 925 and 775 millibars and is weighted by 1.5 since it represents 150 millibars in our vertical coordinate.

Thus wind data are weighted to account for the deviation of particle fall velocity from constancy and to account for the thickness of the atmosphere which they represent. A single weighting function table is used. True (i.e. Rand) fall times are used, however, for determining the time of first and last arrival of wafers, since the fall time for each particle size from each of the nominal pressure levels is easily tabulated.

Dose Rate and Total Dose:

Since the study for which fall-out computations were required had a number of facets, it was necessary to determine both the dose rate referred to $H+1$ hours, D , and the total dose, D_T , received up to an arbitrary time, T , later than the ending of fall-out.

DOE ARCHIVES

The position of each wafer as it arrived at the surface was noted and the number of URP wafers lying over any required point was noted.

~~SECRET~~
~~DATA~~

For CASTLE BRAVO it was found that each wafer represented about 100 r/hr referred to H+1. This calibration was used for all other calculations, since it was the only good point of contact between wafers on the surface and observed fall-out. Following the approach of AFSWP Report 507, we have assumed a decay rate given by $t^{-1.2}$ for all times of interest, although deviations from this which would be the same for all wafers could be accounted for without producing significant complication of the computational problem.

The requirement for some sort of integrated dose related to human effects at first appeared to be exceedingly difficult to meet. Inquiry relating to the present knowledge of biological recovery, however, revealed that (a) the facts are not too well known, particularly as they relate to human beings, and (b) the recovery within the first few days following beginning of exposure was estimated to be less than 30%. Within the accuracy of our computation method and considering the uncertainties of the recovery problem, it was decided not to allow for recovery but rather to compute the total dose. Since each URP wafer is followed to the surface and its time of arrival determinable, one could sum the total dose which each delivered up to any given time. This, however, with some 69 wafers per problem, would be rather lengthy. It was felt that some mathematically simplifying assumption regarding the rate of accumulation of radioactivity on the ground would be desirable. The assumption made was that all the fall-out arrived at a constant rate from the time of first arrival, a , and the time of ending, e . Assuming total fall-out to be 1 r/hr at H+1, the total dose to time T , where $T > e$, is given by the following simple formula:

$$D_T = 6.25 \frac{e^a - e^e}{e - a} - 5 T^{-0.2}$$

The first term corresponds to the infinity dose delivered by unit dose rate accrued between a and e and the second to the dose which would be delivered between T and infinity. In use, the dose rate D is multiplied by the factor given by the formula above, or determined by entering a chart with a and e , to obtain the total dose to T . D_T so obtained was plotted against coordinates a and e and analyzed as a contour chart.

Application of the Model and Method DOE ARCHIVES

In the practical application of the Signal Corps method devised above, an effective wind trajectory was constructed by connecting the weighted winds corresponding to each interval head to tail. The wind for any given slab was picked off by interpolation along the length of the appropriate vector. These winds were actually plotted on a scale such that the 68 micron particles fell directly along the plotted trajectory. All other particle size destinations, as explained above, then scaled linearly with this wind. In order to simplify the practi-

cal work, a triangle was constructed similar to that described earlier by Dr. Van Straten, except that it accounted for a larger number of particle sizes. When the length of the 68 micron trajectory is laid parallel to the base of the scale, with the origin at the left-hand edge and the end of the vector intersecting the 68 micron line, the destination of all other sizes may be plotted at the intersection of the appropriate sloping lines with the 68 micron vector. Thus, all eight (or thirteen) wafers corresponding to a slab within the mushroom can be plotted with ease, and similarly, the four wafers representing each stem slab can be rapidly laid out. A "poker chip" having a diameter corresponding to the proper radius for the slab which it represents (i.e. on the same scale as the 68 micron trajectory plot) is located at each URP wafer destination point. An overlay, ruled in a suitable grid* is positioned and those grid sections which are at least 50% covered by a poker chip are marked. This is done for each of the eleven slabs corresponding to 11 effective winds, using the same overlay. When all the poker chips have been tallied, the number of URP's lying over each area are summed and the resulting pattern analyzed as a pressure field. Since each URP was determined to represent 100 r/hr at H+1, the fall-out field is readily obtained.

At the same time that the "poker chips" are tallied in the overlay, the leading and trailing edge of the chip are sketched and marked with the appropriate time of arrival. From the field of these values, contours of earliest time of arrival, designated above as a, and of latest time of arrival, designated above as the time of ending, e, are drawn. Using the assumption that fall-out (in units of r/hr at H+1) accumulates linearly between a and e, and the equation for total dose discussed above, total dose to $T = a + 48$ is computed. In our later practice, a contour chart entered in a and e and having contours labeled in terms of total dose to $a + 48$ per unit dose rate is used. The values so obtained are again analyzed to obtain the total dose contours.

Since all three models have the same number of slabs and wafers, there is no modification of the computation method necessary except for the location of the nominal initial pressure of each slab. Having selected the model, the computation procedures may be summarized as follows: (1) The weighted winds to the top of the model are plotted in an effective trajectory, (2) the 68 micron trajectory vectors are drawn for each slab, (3) the wafers are positioned using the scaling triangle, (4) URP contributions are tallied on the overlay along with a and e, (5) the sum of tallies and a and e are contour analyzed, (6) total dose is evaluated for a suitable number of points and (7) a total dose chart prepared.

DOE ARCHIVES

* In practical work a 15 mile square grid was used, while for Mr. Barnett's paper a 3.5 mile square grid was used.

Critique of the Signal Corps Method

A paper of this nature would not be complete without reference to those assumptions which are considered weak and consideration of possible means of improving the method.

Weaknesses:

Weaknesses in the method stem from both inadequate basic data and from deficiencies in the development of the method. In the former class the major deficiencies lie in the fact that useful data on total fall-out, original distribution of radioactivity for successive fractions of this radioactivity (or, alternatively, distribution of activity by particle size and height and fall velocity), biological recovery effects, decay of radioactivity, diffusion, and terrain effects are either sparse or non-existent. The major deficiencies in the model lie in the length of time required to perform a computation, the linear arrival assumption, and the finite number of wafers considered. It will be noted that, without the use of machine computation methods, an increase in the number of wafers (which would yield somewhat smoother patterns) would further aggravate the time problem.

It is assumed that many of the informational deficiencies will be met by future tests and that more certain estimates of those which cannot be completely met will result from the analysis of the data obtained. With regard to the model and method, a number of improvements appear possible:

Increase the number of slabs and wafers per slab--this would produce smoother patterns.

Perfect an alternate method of obtaining a and e based on the determination of the maximum and minimum effective winds in each azimuth, or

Replace the linear accretion assumption with immediate summation of total contribution from arrival time to $a + 48$ hours.

Adapt the method to machine computation methods.

Use time-varying trajectories.

DOE ARCHIVES

Use a better approximation of stem shape.

Incorporate any new test results to refine the model and method.

Provide an improved method of scaling either through alternate models or otherwise.

Modify model to take account of diffusion, especially if smaller yield weapons are to be considered.

Use an overlay grid ruled in coordinates suitable to the problem.

Account for variations in particle size distributions of various soils and targets.

Incorporate biological recovery corrections.

Modify method so as to reduce computation time while retaining quantitative results of reasonable accuracy.

DOE ARCHIVES

THIS PAGE IS BLANK
IN ORIGINAL.

DOE ARCHIVES

QUESTIONS AND ANSWERS FOLLOWING DR. SWINGLE'S PRESENTATION

Question: LTCOL Spohn, AWS

On the last paper, I am curious of the time interval it takes to actually work through a plot - how long does it take to run a plot?

Answer: Dr. Swingle, OCSO

After some experience in a well equipped office, three or four man hours. Most of the work we have done was not for operational use; we set it up on a production line basis and at one time we had as many as 20 men working on it.

Question: FCDA

What typical times between arrival of the smaller particles and larger particles; that is, in your computation to get dosage figure?

Answer: Dr. Swingle, OCSO

I think you will see that in Mr. Barnett's paper tomorrow, but it runs for something like half an hour to a matter of ten hours, or more.

Question: LTCOL Spohn, AWS

In applying wind data to this, do you use the same assumption as we (AWS) do; that is, assuming point winds apply throughout the time of fall-out?

Answer: Dr. Swingle, OCSO

DOE ARCHIVES

Yes, so far. In the study which we have done we have been concerned with getting what fall-out might be. A single sounding might be just as good as changing it. We have not had an occasion to want to.

RESTRICTED DATA
ATOMIC ENERGY

PREDICTION OF DOSE-RATE AND DOSAGE CONTOURS AS FUNCTIONS OF YIELD
AND METEOROLOGICAL CONDITIONS, ARDC METHOD

LtCol N. M. Lulejian, USAF
Air Research and Development Command

I have analyzed the fall-out from the first shot of CASTLE test operation. The method of analysis is based on Stokes Law of fall and upon the following assumptions of particle size distribution and activity with height within the atomic cloud:

<u>h</u>	<u>d_{mean}</u>	<u>A</u>	<u>ΣA</u>
0	140	-	-
5	130	3.3	3.3
10	120	7.5	10.8
15	110	3.8	14.6
20	100	4.6	19.2
25	90	6.8	26.0
30	80	10.0	36.0
35	70	17.0	53.0
40	60	12.7	65.7
45	50	6.0	71.7
50	50	5.1	76.8
55	50	2.5	79.3
60	45 <u>non-scav-</u> <u>engable</u>	1.7	81.0
65	45 1	2.7	83.7
70	40 2	2.8	86.5
75	30 2	2.4	88.9

DOE ARCHIVES

~~SECRET~~

<u>h</u>	<u>d_{mean}</u>	<u>non- scavengable</u>	<u>A</u>	<u>Σ A</u>
80	20	2	2.0	90.9
85	10	2	2.0	92.9
90	< 10	2	2.0	94.9
95	< 10	2	2.0	96.9
100	< 10	2	2.0	98.9
110	< 10		1.0	99.9

where h = Height above target in thousands of feet (or height in cloud)

A = Percentage activity in each 5000 ft slice of the cloud.
Σ A is the cumulative percentage activity.

d_{mean} = Mean particle diameter in microns.

I want to now refer to my earlier talk on the percentage fall-out as a function of scaled height. During this discourse I showed that as the scaled height was reduced the percentage activity in the stem of the cloud increased as compared to the activity in the mushroom. Armed with this fact and also with the analysis of particle size in the tower shots of TUMBLER-SNAPPER and UPSHOT-KNOTHOLE test operations, I arrived at the assumptions made in paragraph 1 above. For greater details in this regard, refer to ARDC Report No. C4-23676.

For the winds we have used the composite winds of Eniwetok, Rongerik, and Bikini for H - hour and H + 2:15 hours. For H + 8 and H + 14 hours we have used the composite winds of Eniwetok and Rongerik weather stations. Figure 2 shows the time variation of the winds, and figures 3 and 4 show the composite wind analysis for different sized particles. Figure 1 gives the names of the islands of interest in the Pacific.

DOE ARCHIVES

The main point of difference between our method of analysis and that of RAND is that their assumptions of particle size and activity distribution within the cloud are radically different from ours. I believe this is only possible because the stratospheric winds had a

~~SECRET~~

~~SECRET~~
DATA
MIC ENE

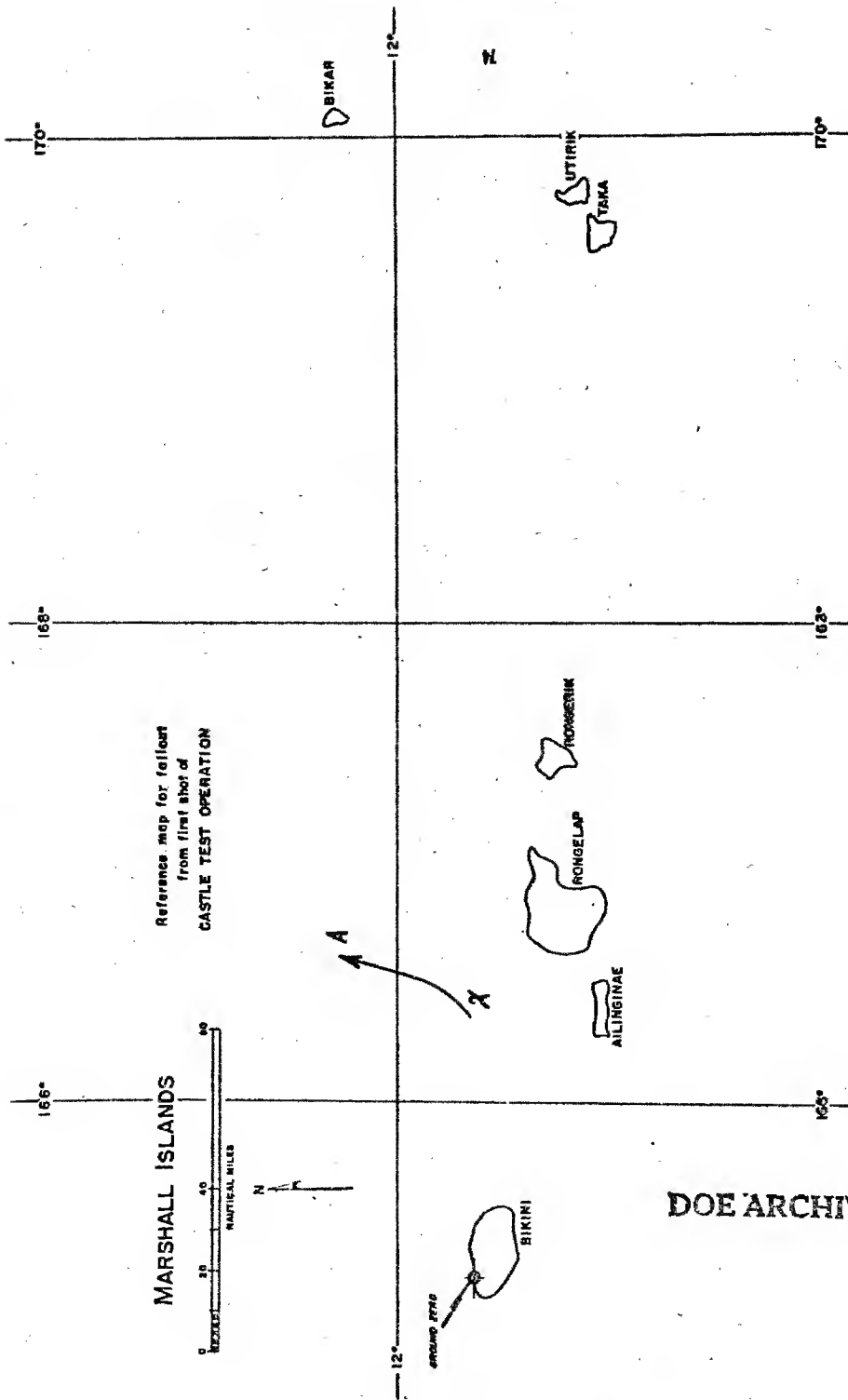


Figure 1

271

DOE ARCHIVES

ATOMIC ENERGY ACT 1954

276

SECRET

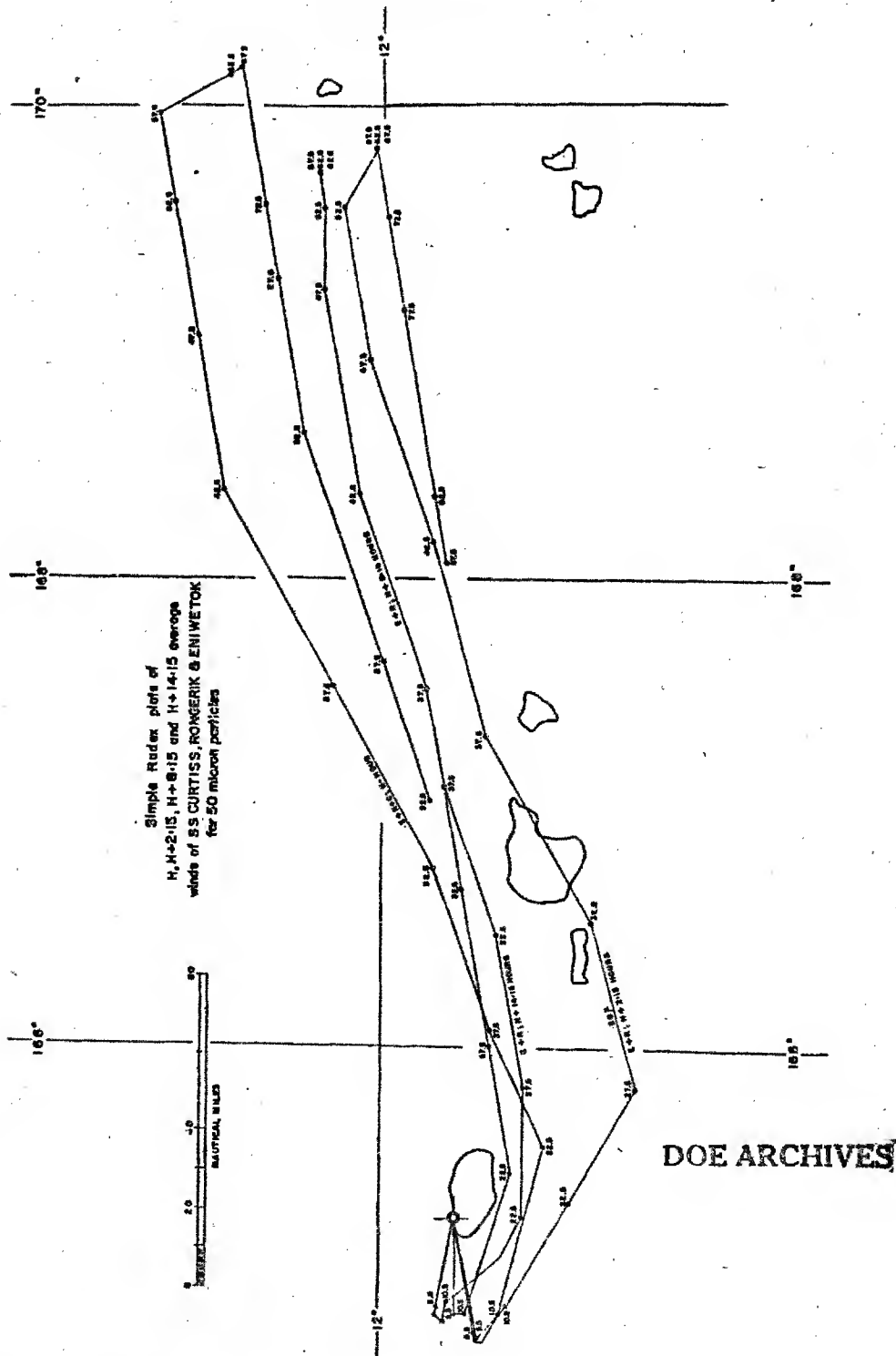


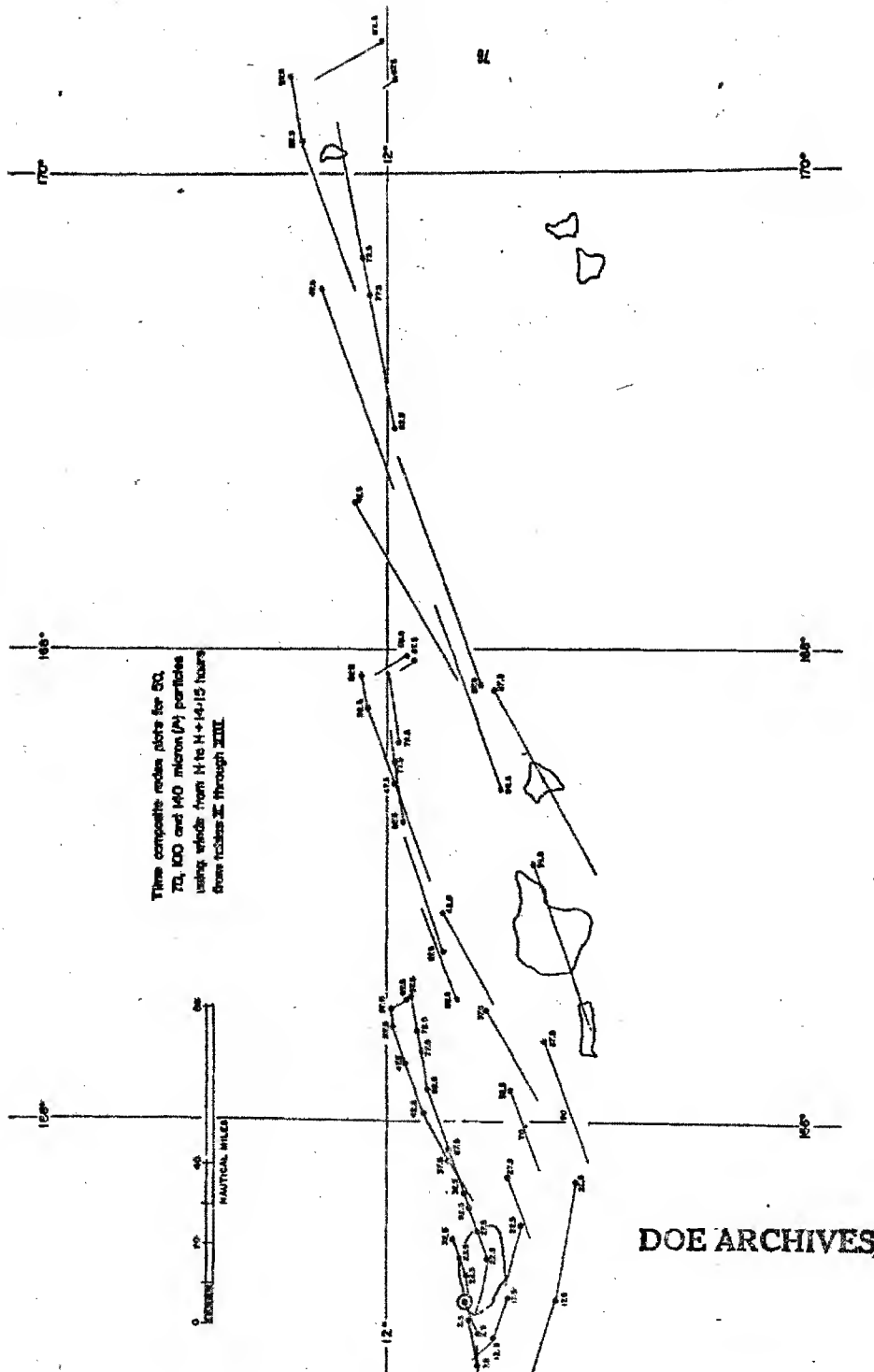
Figure 2

ATOMIC ENERGY

272

277

~~SECRET~~



SECRET

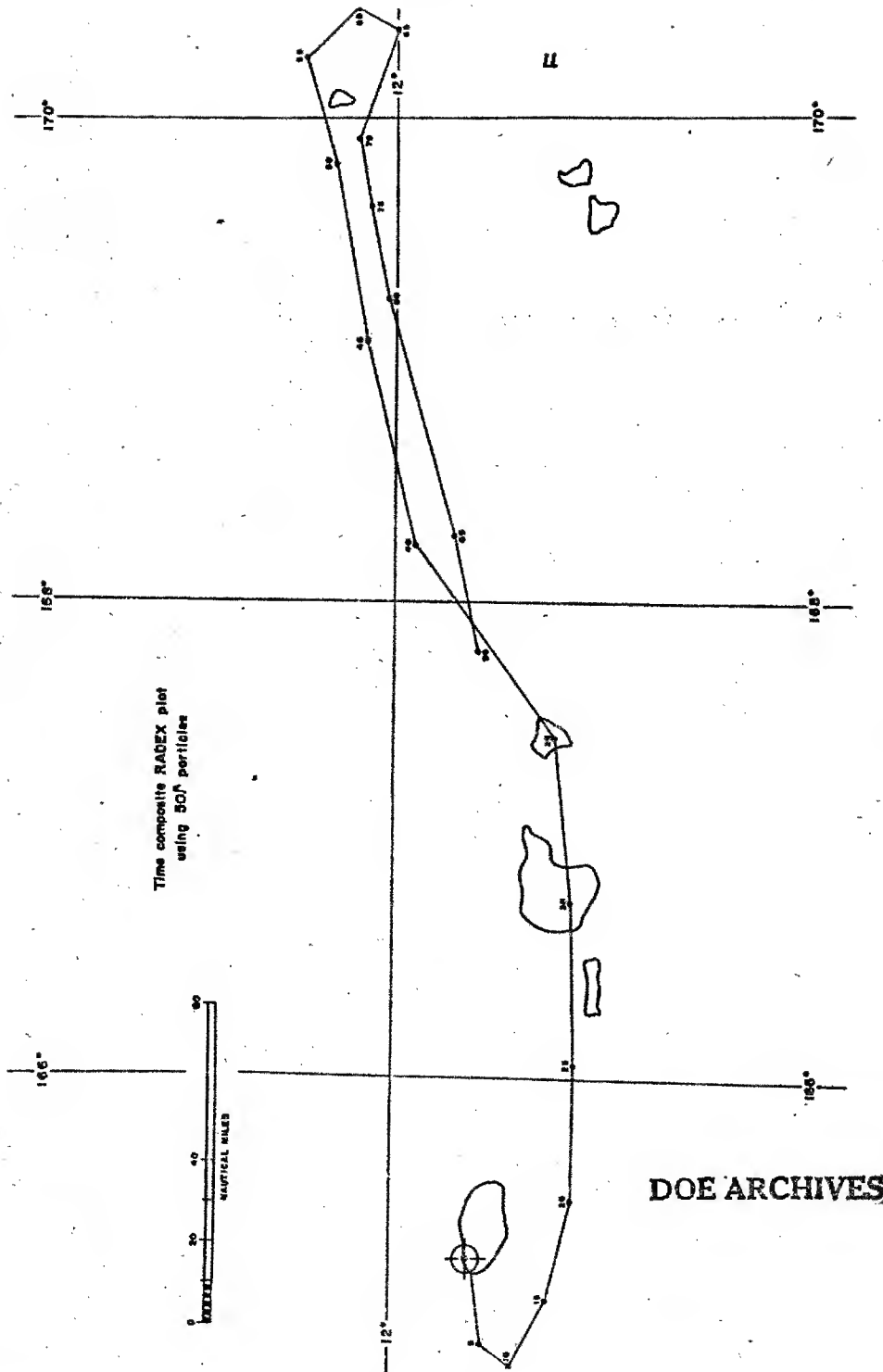


Figure 4

274

RENEWABLE ENERGY ACT 1976

279

SECRET

directional shear of approximately 180° as compared to tropospheric winds during Bravo shot. I say that the fall-out occurred from the stem; RAND says it occurred primarily from the mushroom; but since the ground trajectory of the stem and mushroom actually coincide in many points (see figure 2), the problem cannot be resolved until at some future test when the wind shears between the troposphere and the stratosphere are at approximately 90° . When and if this happens at some future test, we will be able to resolve the problem uniquely, provided we are there to catch the fall-out.

I want to make it clear that my assumptions (given in paragraph 1) apply only to a surface burst on land of an atomic bomb in the range of 10 to 20 MT. It does not apply to a surface burst over water (barge shot). I don't know anything about particle size distribution or activity distribution in a "water" cloud. All I know is that former speakers of this conference (NRDL, Scripps and New York Operations Office of the AEC) have indicated that the total fall-out may be 2 to 5% (Mr. Eisenbud) or it may be 13 to 58% (NRDL-Scripps). All speakers agreed that they make no claim to have caught all of the fall-out. So, as far as I know, fall-out from water shots may be 2 to 58% or more. The activity within a water cloud may be anything. I don't even have a clue as to what it may be.

I have used Stokes Law of fall as compared to aerodynamic fall. The difference between the two rates of fall is relatively small in the size range of 60 to 100 microns, and it is in this very size range that we find most of the activity in the cloud. Therefore, for ARDC method, the use of Stokes Law or aerodynamic fall makes relatively little difference. However, for those other units who assume that particle sizes between 100 and 1000 microns hold most of the cloud activity, the use of aerodynamic fall becomes mandatory. It is my claim that the primary difference in the methods presented is the particle size distribution with activity and height, not the different rates of fall.

DOE ARCHIVES

Figures 5 and 6 show the measured dose rates on the islands in the Pacific for the first shot of Operation CASTLE. These two figures are taken from CASTLE Project 2.5a preliminary report by NRDL. They are shown here as the data that we must try to approximate with our plot of fall-out. Figure 7 is the calculated fall-out area using the assumptions made in paragraph 1. Figure 8 shows the ARDC fall-out plot in isodose contour lines of dosage integrated from time of fall-out to 48 hours after the bomb detonation, using the $t^{-1.2}$ relation. It should be noted that all points on figure 7 are calculated points. They do not show any measured data. All the measured data is in figures 5 and 6.

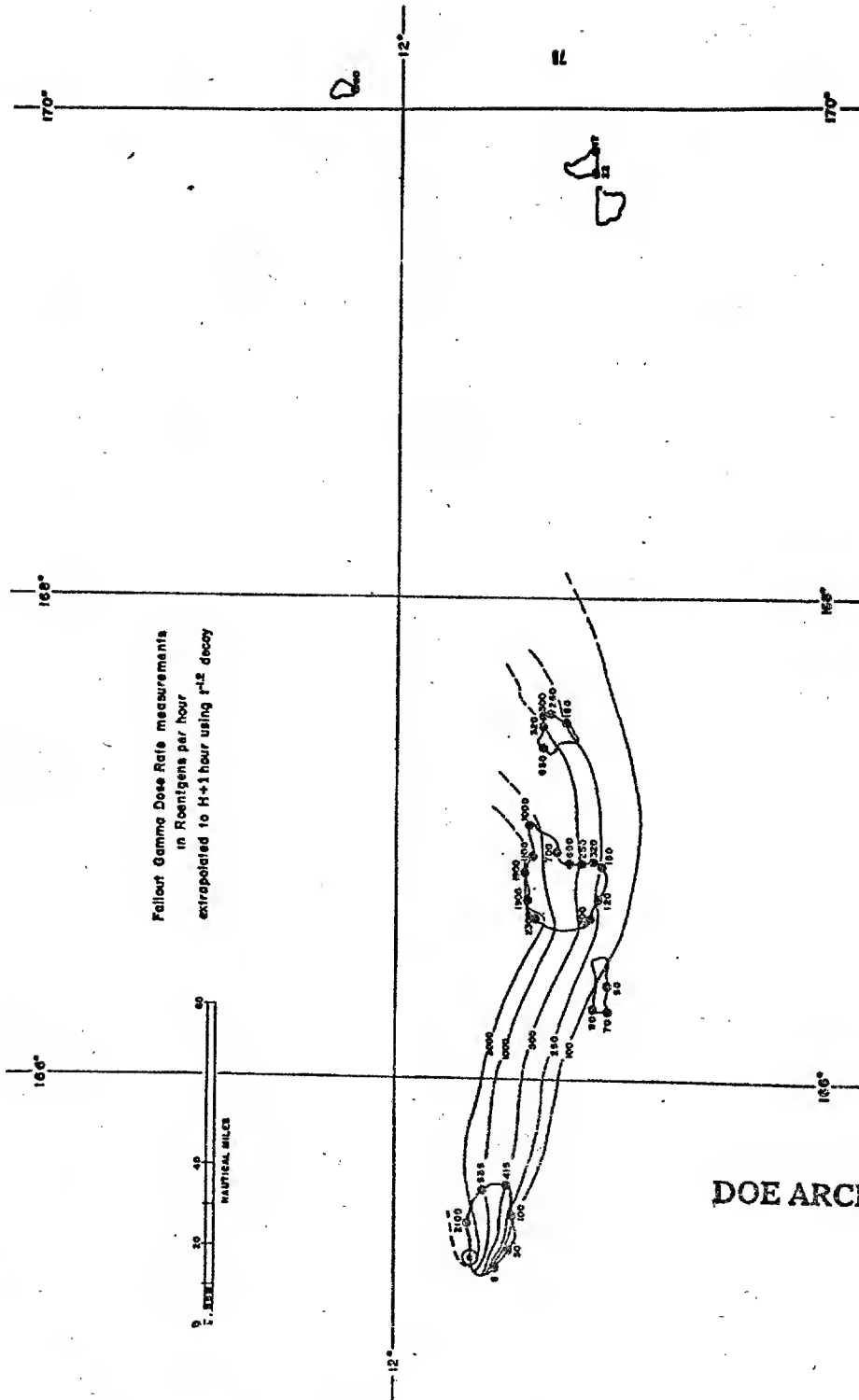


Figure 5

~~RESTRICTED~~
ACT 155

276

Shot I, Fall-out Gamma Pattern
(r/hr at 1 hr)

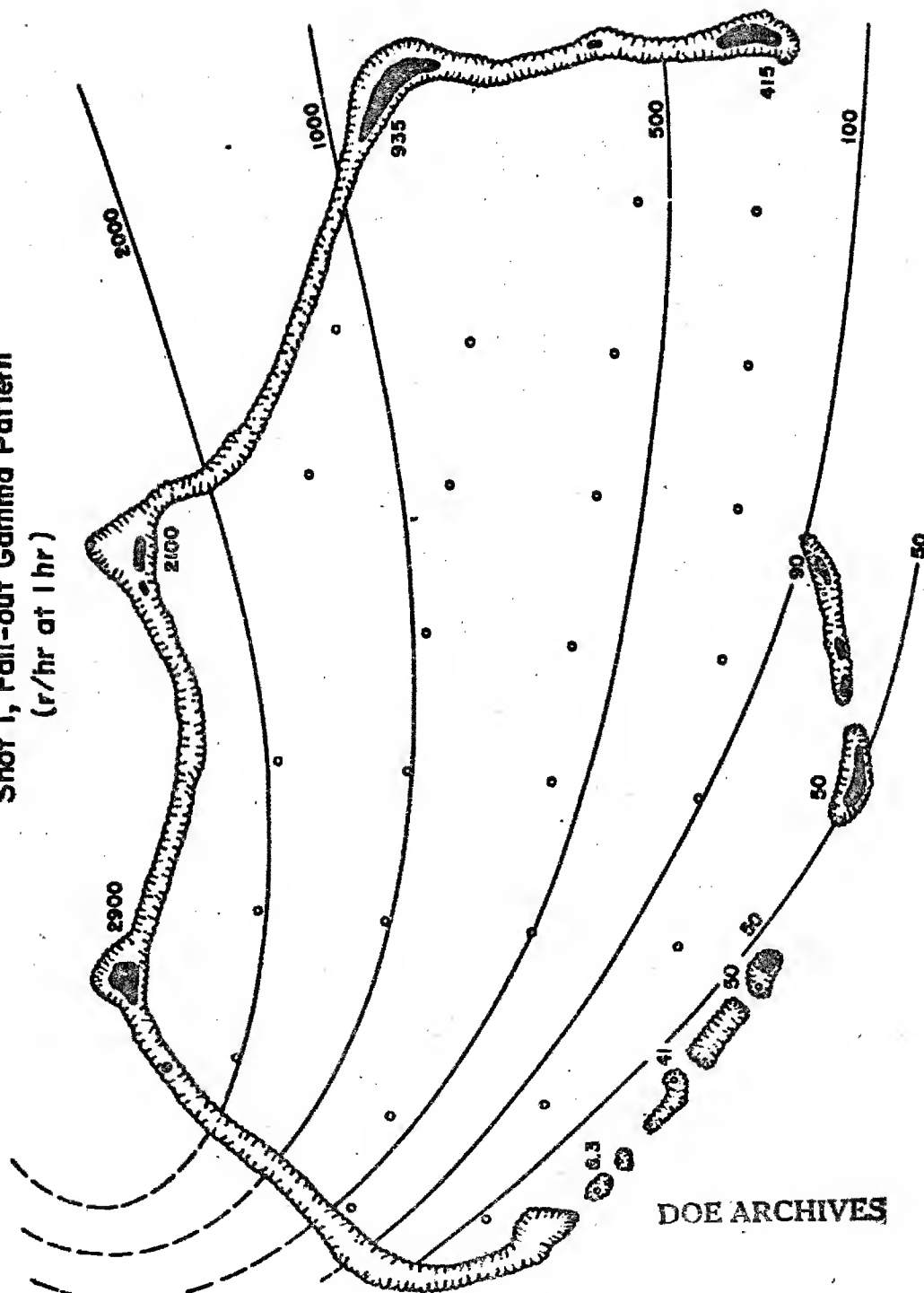
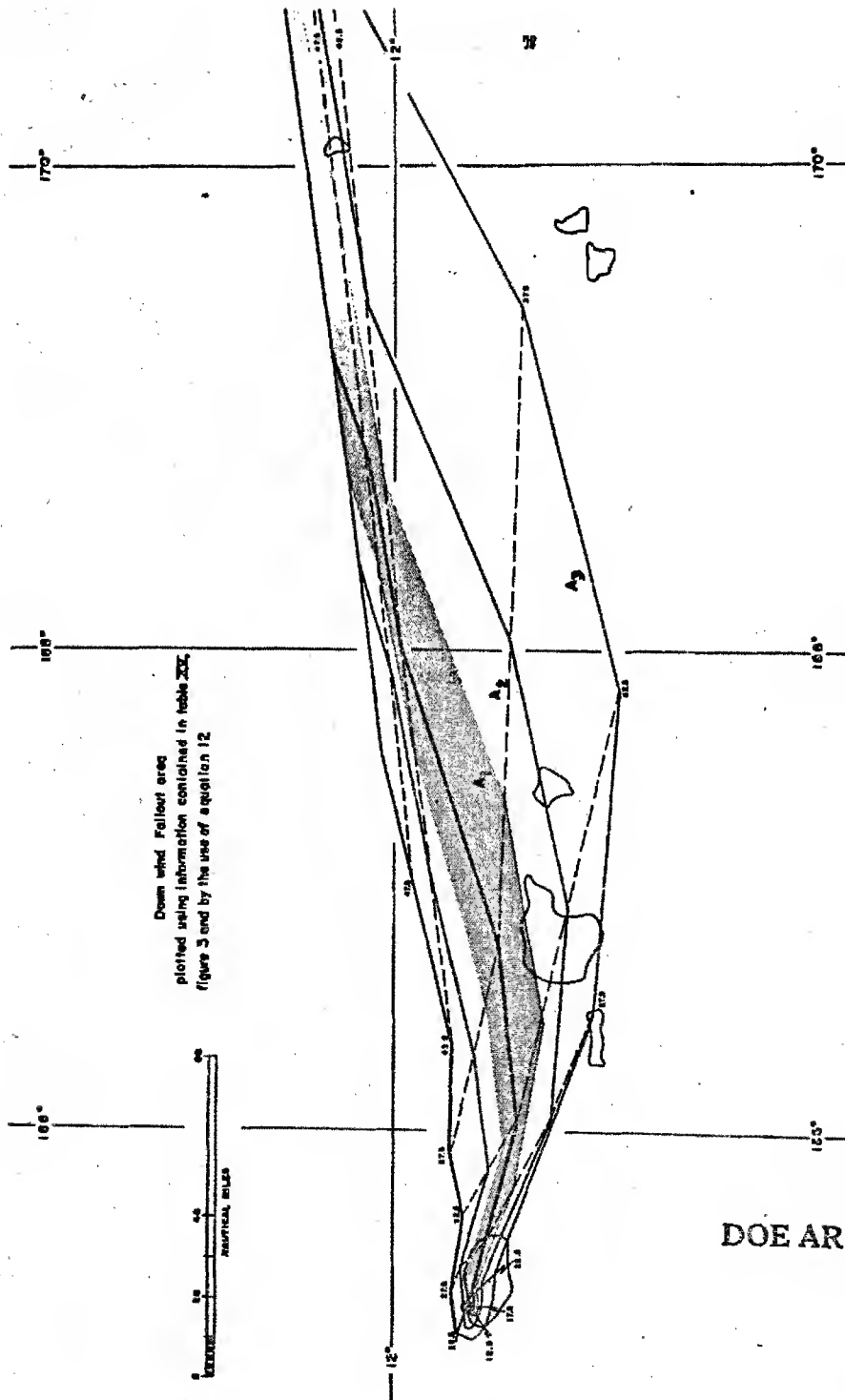


Figure 6

DOE ARCHIVES



Now let me talk to you about what I call the "Volume-Effect" of fall-out which was found during TUMBLER-SNAPPER and UPSHOT-KNOTHOLE test operations in Nevada. In pages 65 to 67 I discuss this matter in greater detail in ARDC Report No. C4-23676. Figure 9, which is taken from AFSWP Report WT-558, shows this "Volume-Effect" at Lincoln Mine (approximately 40 miles north of ground zero) during TUMBLER-SNAPPER Shot No. 5. Similar "Volume-Effects" of fall-out were obtained during TUMBLER-SNAPPER and UPSHOT-KNOTHOLE tower shots. Figure 9 shows that the 48 hour integrated dose calculated by $t^{-1.2}$ relation must be multiplied by 1.67 to account for the "Volume-Effect" of fall-out. In ARDC Report C4-23676, we have indicated what would happen if this same "Volume-Effect" is taken into account for the CASTLE Bravo fall-out. During the evening sessions of this symposium I have been advised by AFSWP and NRDL personnel that the "Volume-Effect" was not observed in and around the Bikini Lagoon. I have been told that there were six continuously recording stations on the islands of Bikini Atoll and that these traces did not show the "Volume-Effect" of the type I found in the desert. It was also conjectured by AFSWP personnel (in night session) that if this "Volume-Effect" occurs at all in fall-out from multi-megaton weapons, it would be observed 500 to 1000 miles downwind (where the total fall-out would be small). It is my opinion that this "Volume-Effect" should have appeared on the northern portions of Rongelap and Rongerik quite strongly. It should also have appeared to a lesser extent on the southern sectors of these two atolls. The fact that they were not observed at Rongerik may be due to the fact that there was very little measured data downwind during the fall-out period. I believe that the distinct possibility exists that Rongelap natives may have received from 1.2 to 1.5 times the 48 hour integrated dose used by the investigators in this field of endeavor. I don't know whether this same "Volume-Effect" would occur from fall-out coming from bombs detonated not on the ground, but on water. As I said earlier, I know nothing about fall-out from "water clouds". However, I believe that this "Volume-Effect" will be observed in future tests for surface burst weapons because I believe these things scale from Nevada to the Pacific.

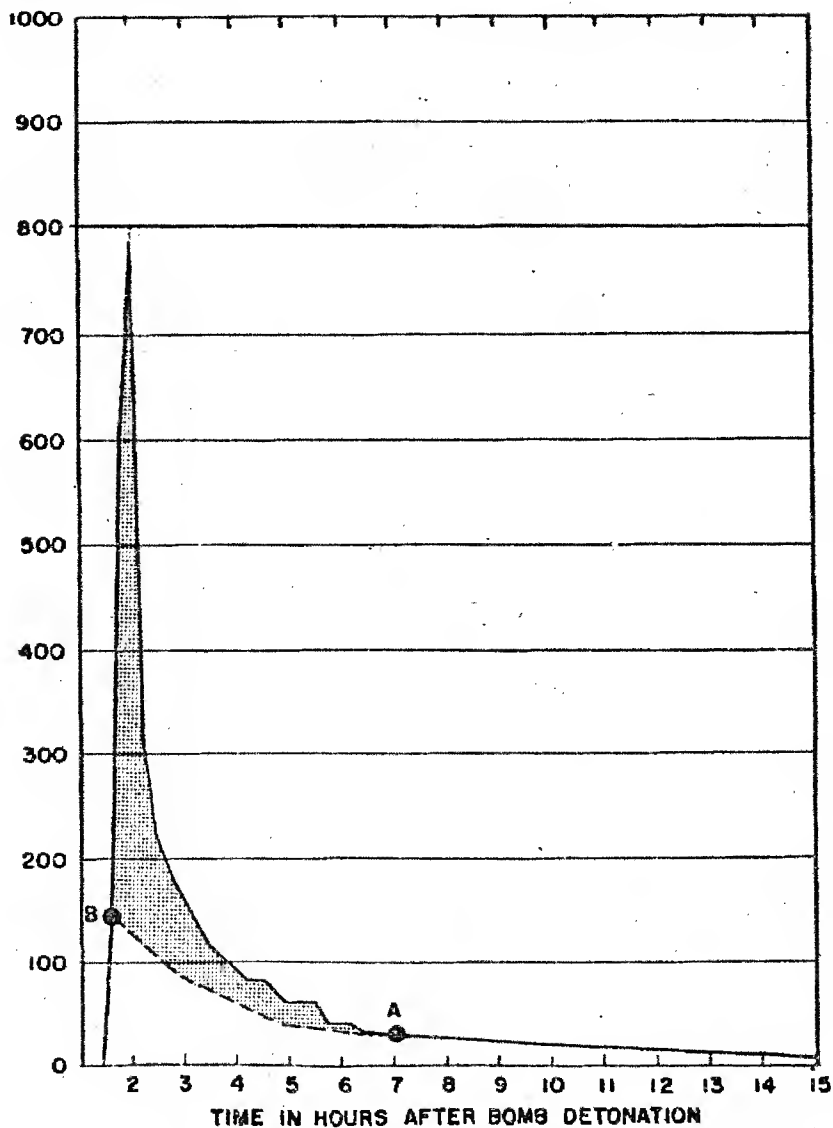
DOE ARCHIVES

It is believed that the ARDC method of fall-out analysis adequately explains the fall-out picture shown in Figures 5 and 6. The important points that must be kept in mind when an attempt is made to fit assumed particle size and activity data to the actual fall-out case are the following:

The time variation of the winds was so great that composite analysis of the winds is required. The winds at ground zero are not valid over the downwind path after the lapse of only one or two hours.

Fallout at Lincoln mine, Nevada
from shot 5 of tumbler/snapper
test operation in 1952.

GAMMA DOSAGE RATE
IN MR/HR



DOE ARCHIVES

Shaded portion shows fallout
in excess of the $t^{-1.2}$ RELATION

Figure 9
281

Any analysis of the fall-out on Bikini Lagoon must take into account the amazing fact that the intensity of fall-out on the lagoon islands to the south and southwest of ground zero is only 8 to 15 r/hr at H+1 hour, even for islands as close as approximately 5 nautical miles from ground zero. On the other islands of Bikini Lagoon, the contamination goes to 1000 to 2100 r/hr at H+1 hour (see figures 5 and 6).

The atoll of Rongelap is contaminated excessively in a steep gradient as shown in figure 5.

The native village on Rongelap Atoll (southern portion of atoll) is in approximately the same radiation intensity field as the weather station on Rongerik.

Ailinginae shows less contamination than Rongelap or Rongerik.

Bikar has less contamination than Rongerik.

Task Force ships 50 miles southeast of ground zero showed less contamination than Ailinginae.

The islands of Taongi and Utirik were least contaminated.

It was later found that the position of the Japanese fishing boat (Fulcuru Maru) was not 10° north of east (80 miles) of ground zero, but thanks to Mr. Eisenbud of NYOO, AEC, the exact position is shown in figures 1 and 8 as point X and the direction of motion of the ship is shown to be from point X to point A. Extrapolation of the Eisenbud data on the Japanese ship shows that it reached the 12° N. latitude line at approximately H+6 to H+8 hours. The fall-out was supposed to have stopped at H+8 hours according to Japanese accounts.

We have kept in mind the measured data mentioned in the paragraph above, and our model fits the above data quite well (see figures 7 and 8). The winds are those obtained from the shot island (Bikini), Rongerik and Eniwetok. Looking over the papers presented by different members of this symposium I note the following:

The RAND Aureole report shows CASTLE Bravo analysis that overestimates the fall-out around ground zero (especially on the southerly islands of the atoll). The downwind fall-out misses Rongerik and Rongelap and if memory serves me right, it also misses Bikar. This model then does not succeed in approximating the measured Bravo fall-out. At this symposium, RAND has presented new and as yet

DOE ARCHIVES

SECRETED DATA

unpublished data which adequately accounts for the fall-out in and around the islands of Bikini Atoll. It also appears to give the correct order of magnitude of the contamination on the northern portion of Rongelap Atoll. The analysis does not go any further than that as far as I can tell.

The NRDL analysis of Bravo event was widened too far to get the fall-out to fall on Rongelap and Rongerik. It is believed that since NRDL used only the ground zero winds (not taking the time variation of winds into account) then they were forced to widen their area of fall-out to account for the observed fall-out.

The particle size and the activity distribution in the cloud shown in paragraph 1 above, was obtained after careful analysis of the TUMBLER-SNAPPER and UPSHOT-KNOTHOLE tower shots and the JANGLE surface shot. Reference is made to ARDC Report C3-36417. On page 40 of this report is shown that the following particle size distribution fits the UPSHOT-KNOTHOLE tower shots (17 to 50 KT from 300 foot towers):

- 125 microns in lower third of stem
- 100 microns in middle third of stem
- 90 microns in upper third of stem
- 80 to 70 microns in mushroom of cloud for a cloud reaching a maximum altitude of 40,000 feet msl

It is assumed that as the cloud height increases the particle size distribution at the higher levels in the cloud decreases. It is from this background of detailed analysis of the tower shots of UPSHOT-KNOTHOLE and TUMBLER-SNAPPER that the assumptions of paragraph 1 were made. So you see, we didn't pick them out of thin air after all! It is unfortunate that most other units have neglected analyses of the Nevada shots as a guide to Bravo fall-out.

DOE ARCHIVES

The next point I want to discuss is my "reasoning" for assuming that the activity in the stem is greater than the activity in the mushroom. During TUMBLER-SNAPPER tower shots (12 to 14 KT from 300 ft towers) the activity in the stem was approximately the same as the activity in the mushroom. However, during the UPSHOT-KNOTHOLE test operation (17 KT to 50 KT from 300 ft towers) the activity in the stem was 2 to 3 times the percentage activity in the mushroom. For the JANGLE surface shot the activity in the stem was approximately thrice times that found in the mushroom. It is for this reason that we assumed in paragraph 1, that approximately 80% of the activity is in the stem and only 20% in the mushroom. This appears to be

~~SECRET~~
DOE ARCHIVES

contrary to common sense, but I can assure you I'm not doing this to be ornery. I am making this assumption because I believe that we can reasonably scale from tower shots to surface shots and we can also scale for increasing yield.

We employ the following scaling law:

$$P_1 = P_2 \text{ for a given scaled height,}$$

where

$$P = \frac{\sum AR}{kWt^{1.2}} \quad \text{Equation 1}$$

P = Percentage fall-out of residual activity

A = Area in square miles

R = Dose rate at time of fall-out in r/hr

W = Bomb yield in kilotons

t = Time in hours after bomb detonation

k = Constant = 12 in our calculations

This means that we assume that the percentage fall-out from a given scaled height is constant. This refers to residual activity deposited on soil debris which falls out within approximately one day due to the gravity of the particle. Equation 1 may be readily written as:

$$\sum A_2 R_2 = \frac{W_2}{W_1} \left[\frac{t_1}{t_2} \right]^{1.2} \sum A_1 R_1 \quad \text{Equation 2}$$

Then for any element of Area, A_1 , inclosed by a contour line R_1 , we may be permitted to write:

DOE ARCHIVES

$$\bar{A}_2 = \bar{A}_1 \left[\frac{W_2}{W_1} \right] \left[\frac{t_1}{t_2} \right]^{1.2} \quad \text{Equation 3}$$

We can also say:

$$\bar{R}_2 = \bar{R}_1 \left[\frac{W_2}{W_1} \right] \left[\frac{t_1}{t_2} \right]^{1.2} \quad \text{Equation 4}$$

We note above that the area scaling with yield depends upon the time.

In the normal formula for scaling it is assumed that

$$A_2 = A_1 \left[\frac{W_2}{W_1} \right]^{2/3} \quad \text{Equation 5}$$

The time variable from Equation 5 may be eliminated by setting $t \sim Z \sim W^{1/3}$, where Z is distance in the vertical direction.

If we do this we get

$$A_2 = A_1 \left[\frac{W_2}{W_1} \right] \left[\frac{W_1}{W_2} \right]^{0.4} = A_1 \left[\frac{W_2}{W_1} \right]^{0.60} \quad \text{Equation 6}$$

It may be argued that Equation 6 and Equation 5 are not too different; and this may be true, except that we have a problem of extrapolating from 1 KT to 15,000 KT, where the use of the 0.60 exponent produces a factor of two differences from the use of the 0.667 exponent. The reason we have gone through the above analysis is to impress the reader with the fact that the time of start of fall-out is very important in any scaling factor for integrated dose. Paradoxically there is least amount of experimental data on this.

Once we have the Bravo model and we try to extrapolate back to 1 KT, we find that we overestimate the problem by a factor of 3 or 4 using Equation 5 and by 6 to 8 when Equation 6 is used. We have applied a correction factor to compensate for this. We believe that by such a procedure we may be able to use the Bravo shot to scale down to 1 MT and up to 60 MT quite adequately. For details see ARDC Report C4-23676.

DOE ARCHIVES

During the conference a number of personnel referred to the ARDC method as implying 90% activity in the stem and 10% activity in the mushroom. Actually in our report (C4-23676) and in the first paragraph above, we showed that our method assumes approximately 80% activity in the stem and 20% in the mushroom, whereas RAND assumed 10% in the stem and 90% in the mushroom. We believe that large particles rise high into the mushroom, immediately as the cloud forms, but it is our opinion that all this falls out fast (within 10 to 30 minutes) and it all lands on or near ground zero or the lagoon. No significant amount of activity falls out downwind in excess of 20% from the mushroom except after 24 hours or so, at which time both dilution and decay would have reduced the radiation intensities to insignificant amounts. For lower yield bombs such as 5 MT, the activity in the mushroom may increase to 30 or 40%, with the stem activity still as high as 60 to 70%. This is because we assume that

~~SECRET~~

the particle size distribution decreases with height, and the 5 MT cloud would not reach as high as the 15 MT cloud of the Bravo shot.

Figure 10 shows what would happen to this country if 111 bombs of 15 MT are detonated over 106 cities whose population is 100,000 or more and over five other selected areas. For details refer to ARDC Report C4-23676. The slide is here shown to illustrate that if 100 or more hydrogen bombs are used, most of the country will be contaminated almost independently of meteorology. For example, if the winds aloft were all easterly, it would not radically change the contamination pattern over the country. Similarly for northerly or southerly winds. The slide also shows that evacuation and dispersal may not be advisable, for it may clearly be a case of evacuating from the frying pan into the fire.

I would like to make a few rather obvious remarks about world-wide contamination that may be derived from our analysis of percentage fall-out for surface burst bombs. It will be assumed that 80% of the residual activity of a bomb is deposited downwind within 15 to 20 hours after bomb detonation. This means that if we need 10,000 bombs, airburst, of a certain yield to uniformly contaminate the world, then we will need only approximately 200 of the same yield bombs to contaminate this country to the same level.

DOE ARCHIVES

This presentation of the ARDC method of prediction of dose rate and dosage contours was not presented in the manner indicated above. However, the ARDC method has not been altered in this presentation. This paper represents rather the many "conferences" within this conference that were held during these three days. Some of the items, notably the scaling method was not presented at the symposium due to shortage of time, but it is included here for sake of completeness. This paper is in effect a condensation of ARDC Report C3-36417 and its supplement, and ARDC Report C4-23676. The illustrations shown here are from the above reports. This paper in substance indicates not only my talks at this symposium, but also my thoughts by the close of the conference after I had seen the presentation by other members of the symposium. My final comment is that it is unfortunate that RAND and other organizations did not utilize the wealth of information available from analysis of TUMBLER-SNAPPER and UPSHOT-KNOTHOLE tower shots. Had they done so, they would not have placed so much scavengable activity in the mushroom.

286

~~SECRET~~
ATOMIC ENERGY

291

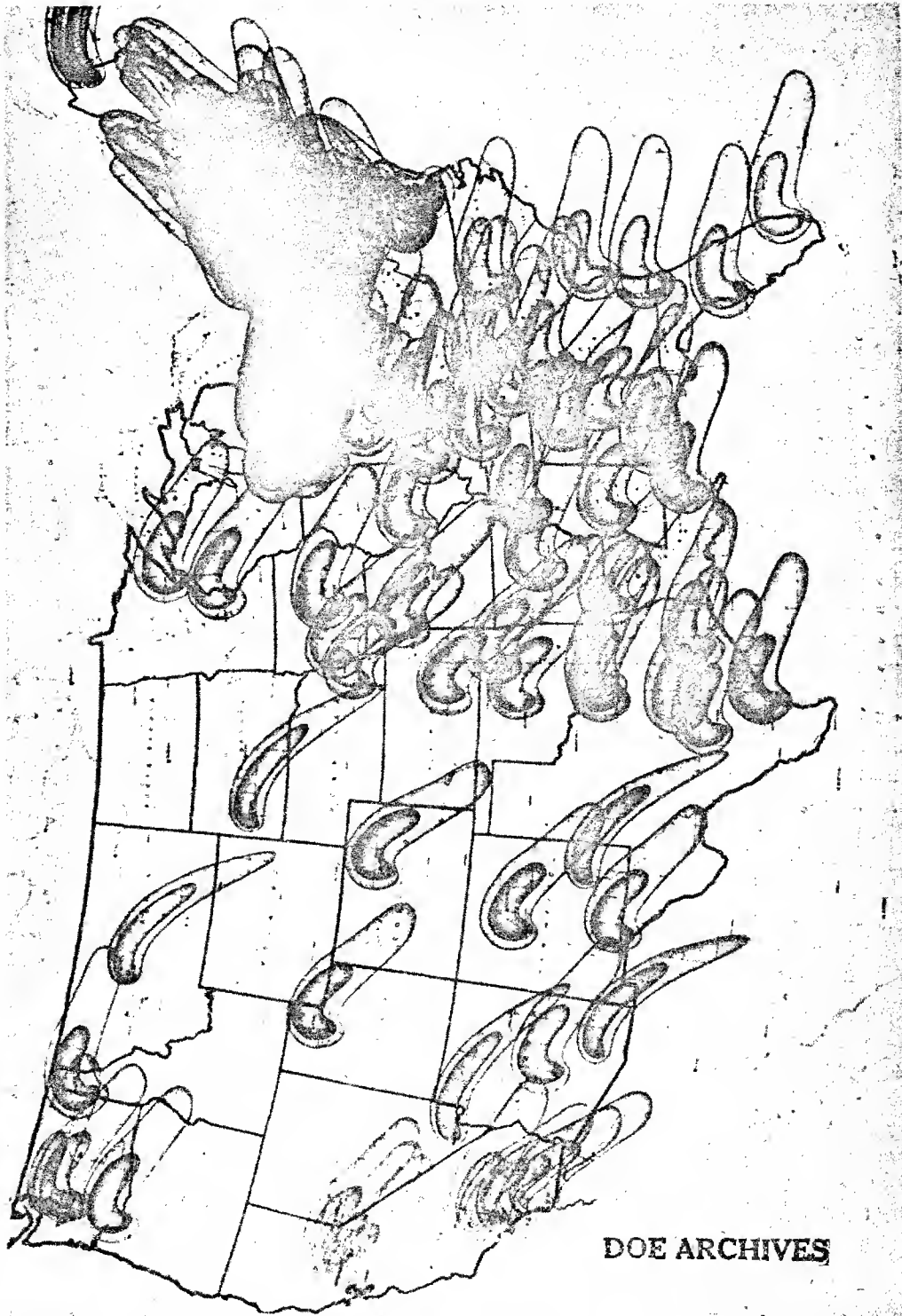


Figure 10
Fall-cut Pattern of 111 15MT Weapons

THIS PAGE IS BLANK

DOE ARCHIVES

288

ATOMIC ENERGY ACT-1954

SECRET

293

JLW

SURVEY OF FALLOUT AREA AT SEA FOLLOWING
YANKEE - NECTAR, OPERATION CASTLE

Mr. Merrill Eisenbud
U. S. Atomic Energy Commission
New York Operations Office
Health and Safety Laboratory

The fallout following Yankee and Nectar was estimated by means of aerial surveys. Evaluation of the data indicated that in the region of from 25 to 150 miles the estimated Yankee fallout of fission product, adjusted to H+1 days, was 1240 megacuries, the estimated Nectar fallout, at H+1 days, was 293 megacuries.

~~DELETED~~

Since it is possible to measure surface activity by aircraft, it is necessary only to know the law of height attenuation for the characteristic gamma radiations measured. In the case of fission product the height attenuation is shown in figure 1. Figure 2 illustrates also the correlation between the surface gamma activity as estimated from the aircraft, and measurements taken on shipboard. The estimate of total activity could be made since there was also correlation between surface activity levels and total fission product load in depth to the bottom of the thermocline, figure 3.

Figure 4 is the trace of activity taken on H+72 hours following Yankee, figure 5 is the related diagram of wind vectors, figure 6 represents the estimated isodose traces. Figures 7, 8, 9, 10, and 11 bear the same relationship to Nectar. It is interesting to note that the wind vector charts effectively display the probable path of fallout. In the case of Nectar the low level fallout, apparently stem debris, was found on H+24 hours but disappeared during the next 24 hour period.

DOE ARCHIVES

The method, beyond providing information on quantity of fallout, supplies data which will permit prediction of the direction of fallout paths, a means of determining safe areas for surface vessel operations and a general source of information for military and civilian defense planning for personnel protection.

Future planning should include the use of telemetering equipment plus automatic altitude compensation of readings to eliminate pilot error. The use of telemetering will permit a central plotting arrangement and is necessary since more than one plane will be required to provide a traverse of a 360° pattern. Sea water surface measurements should be related to depth measurements from the time immediately

~~SECRET~~

following the burst until the main body of activity disappears since no early data has been taken. With better equipment and adequate preparation it may be desirable also to survey beyond the 150 mile radius.

DOE ARCHIVES

290

~~SECRET~~
ATOMIC ENERGY ACT 1954

~~SECRET~~

295

~~SECRET~~

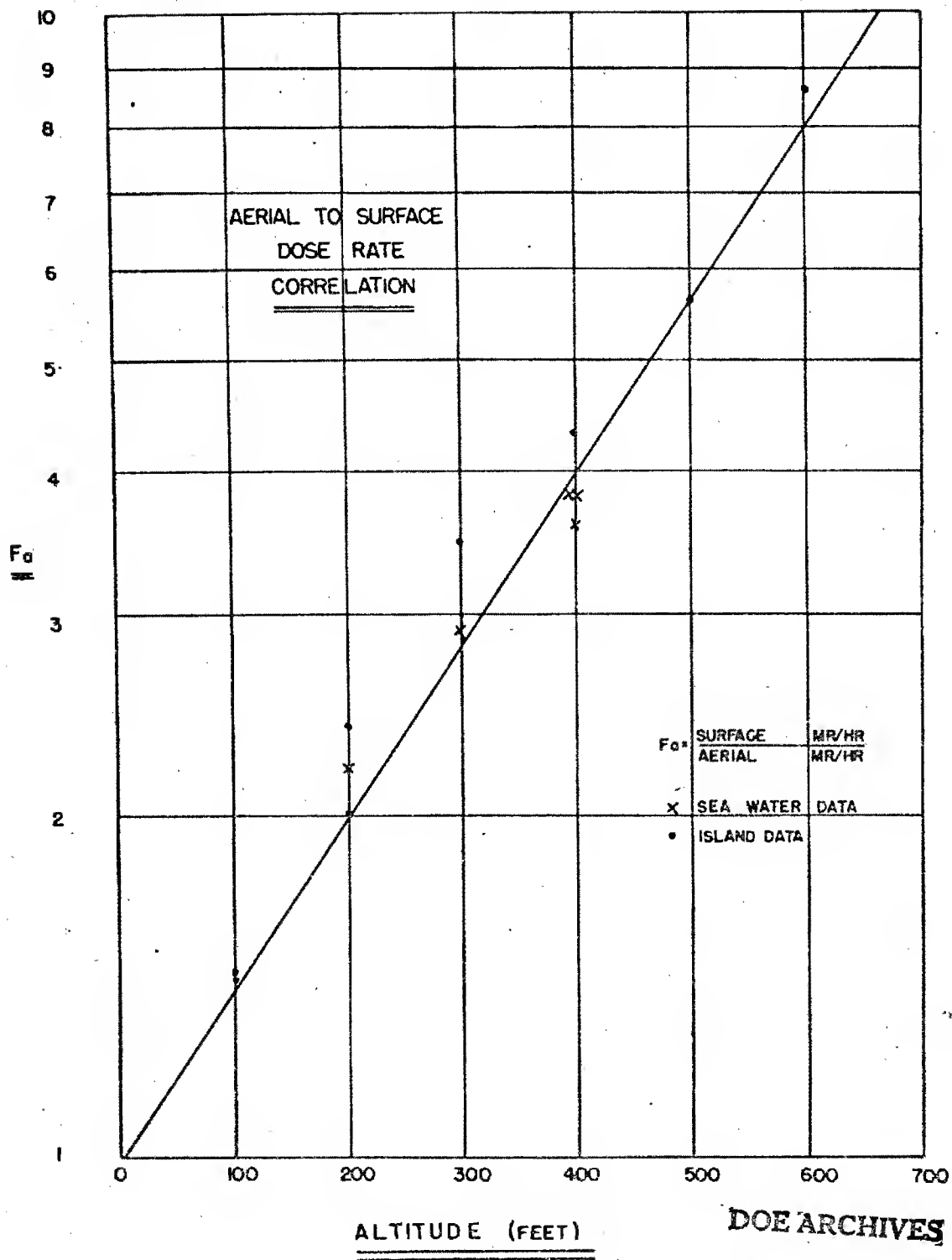


Figure 1
291

~~SECRET~~

~~SECRET~~
DATA
ATOMIC ENERGY ACT 1954
296

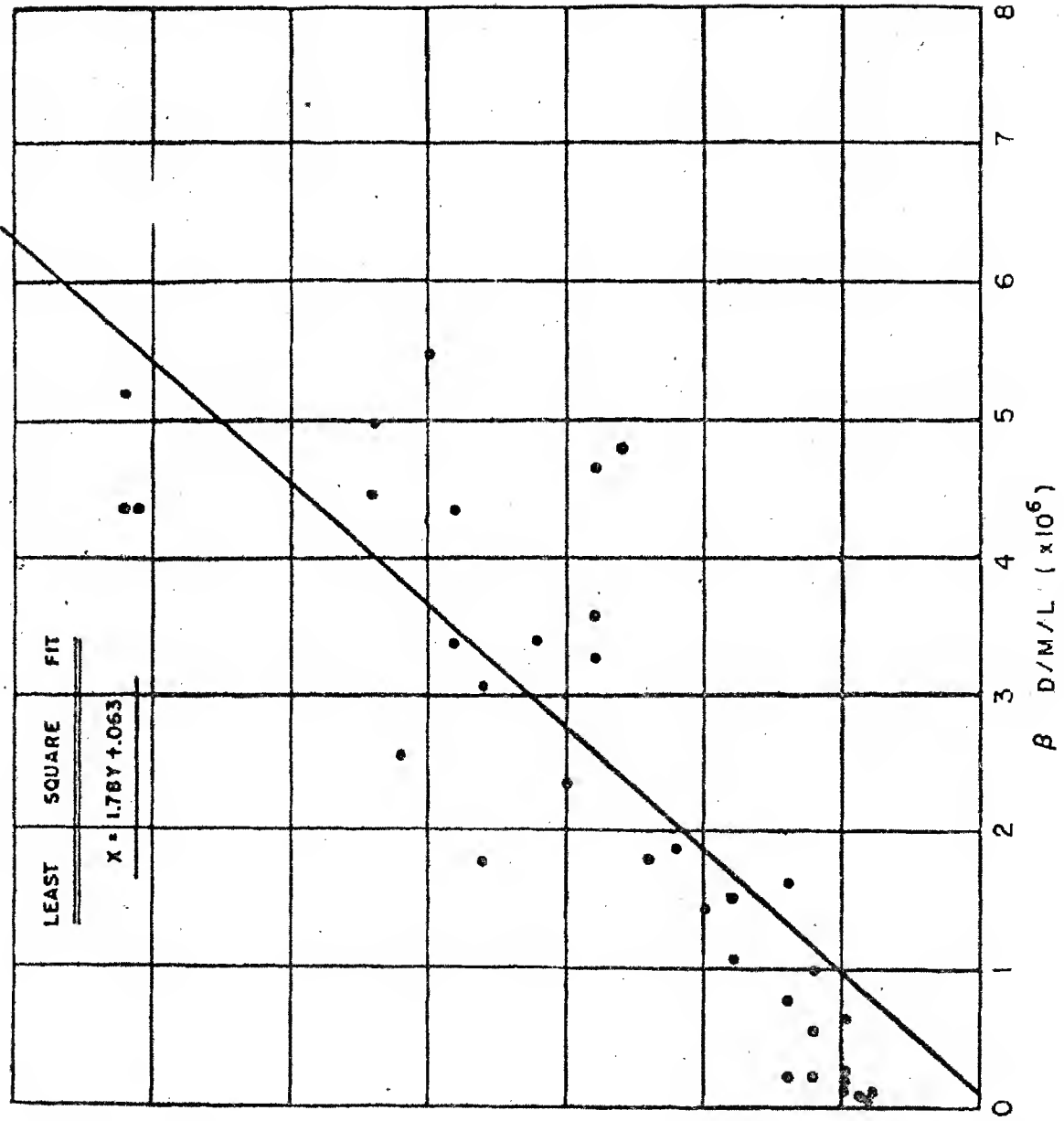


Figure 2

DOE ARCHIVES

SURFACE TO TOTAL ACTIVITY CORRELATION

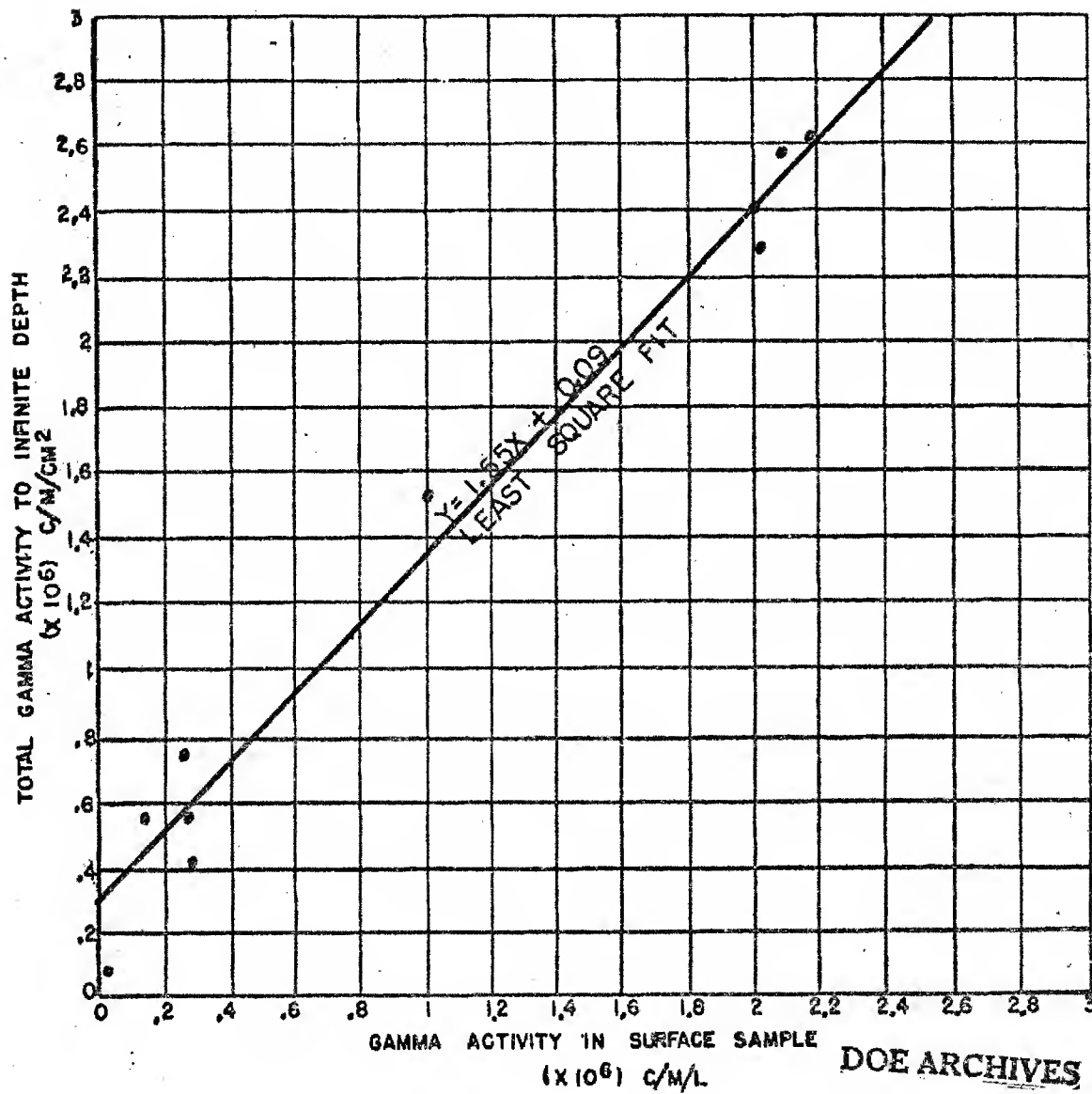
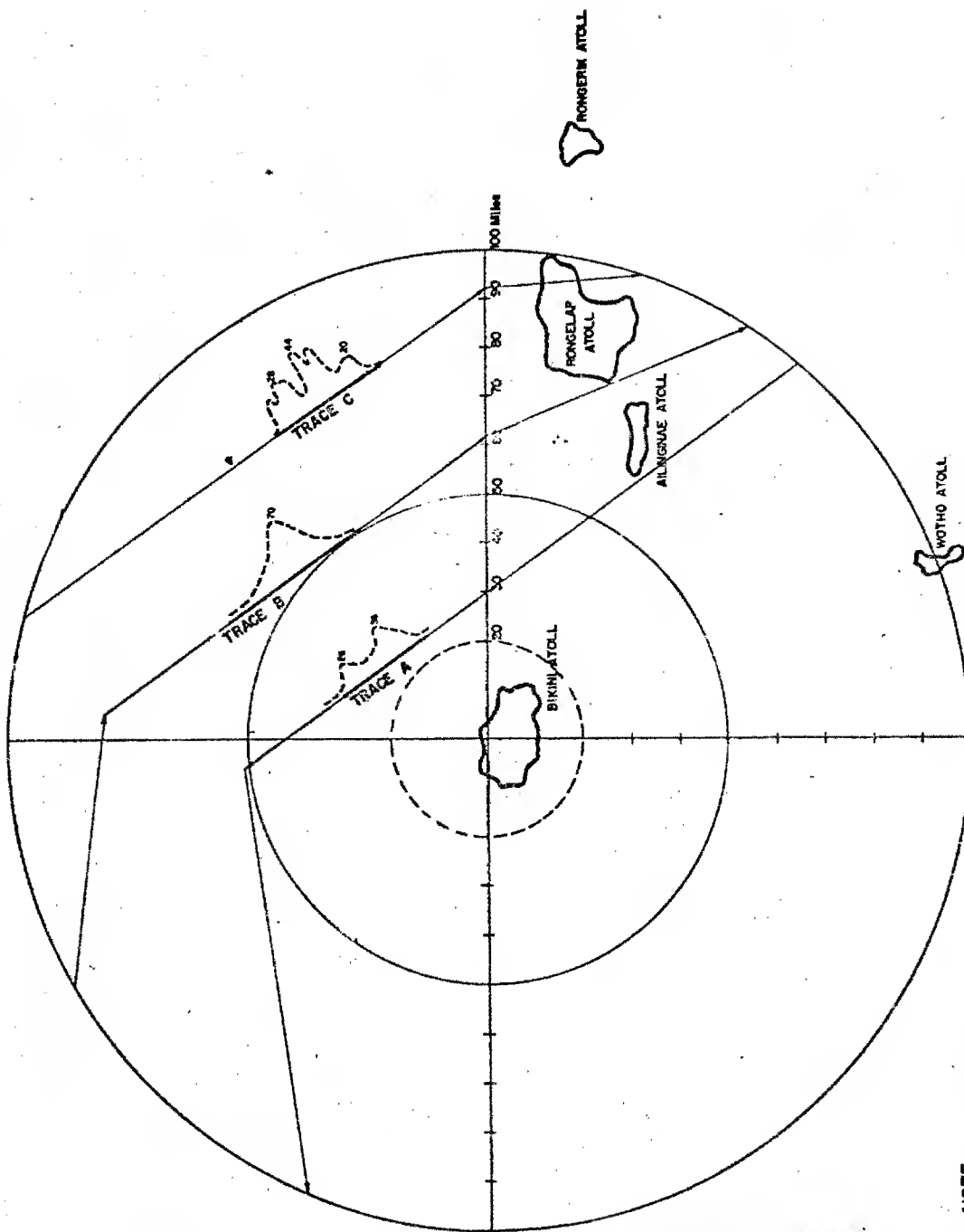


Figure 3

293

DOE ARCHIVES

ESTIMATED DATA

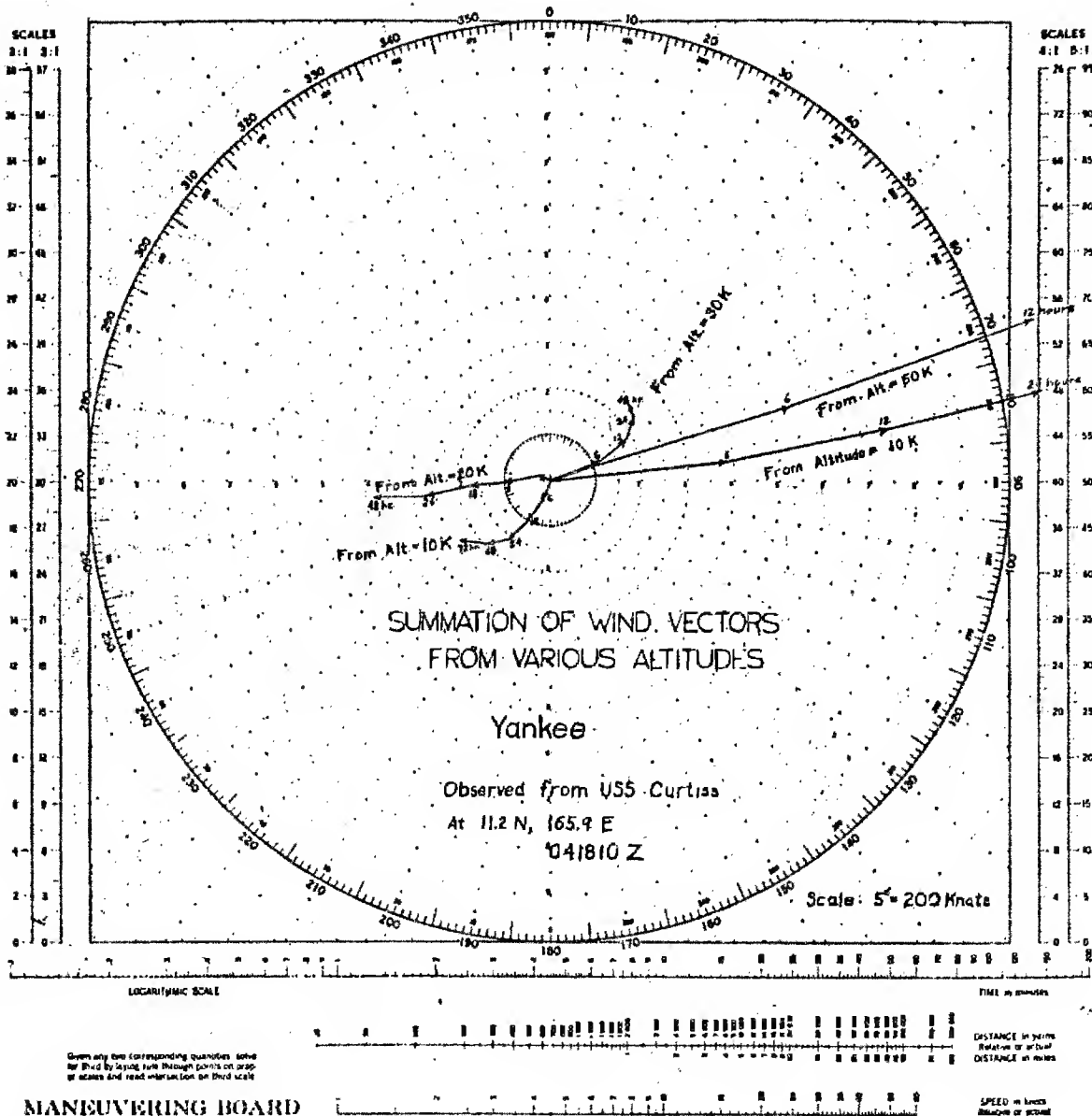


NOTE
 PROFILE READINGS IN MR/MR EXTRAPOLATED
 TO 3 FEET ABOVE SEA.

Figure 4

4473 to 4482
 hours

Y2445-01022 / 10-090343 Z

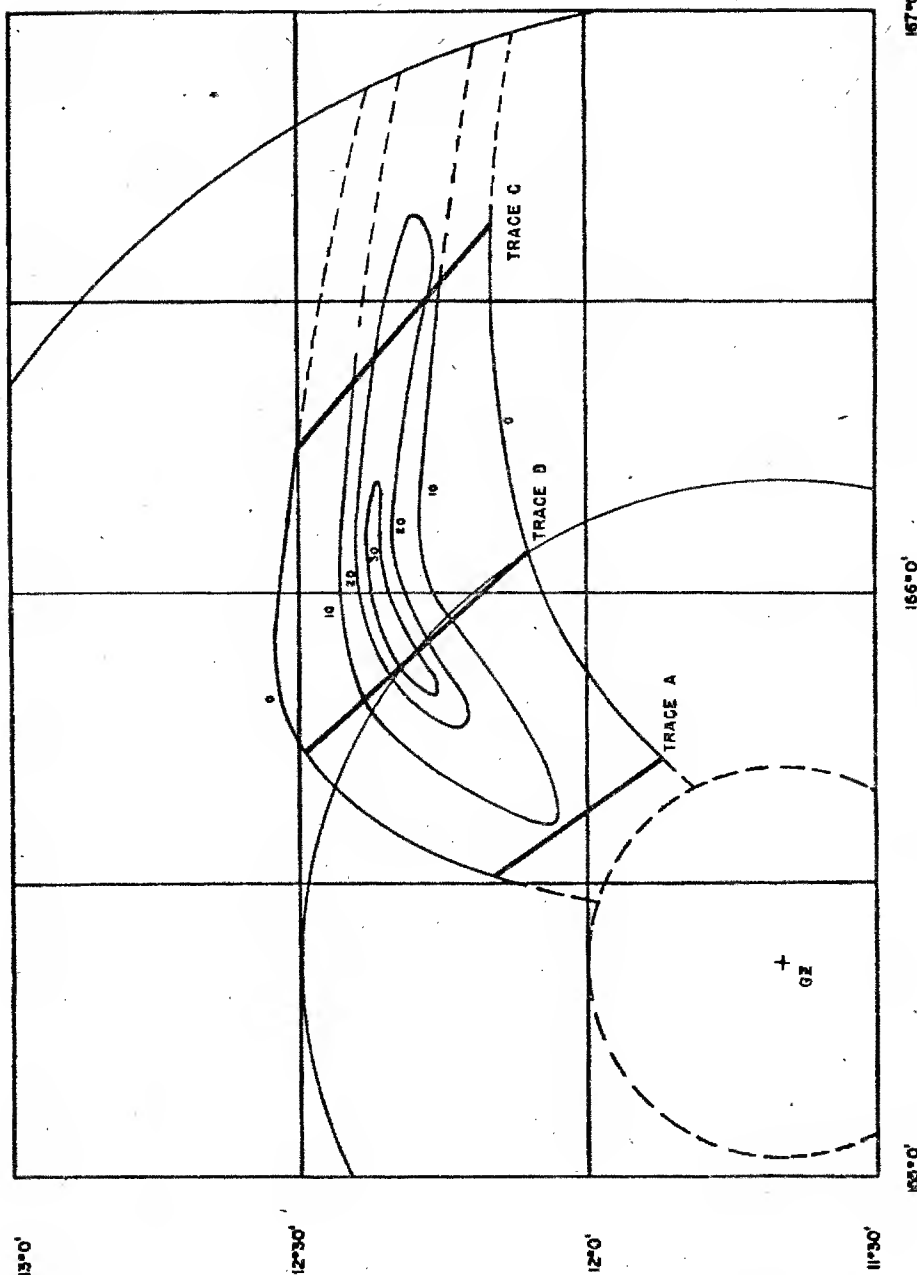


DOE ARCHIVES

Figure 5
295

~~DATA~~
ATOMIC ENERGY ACT 1954

YANKEE ISODOSE

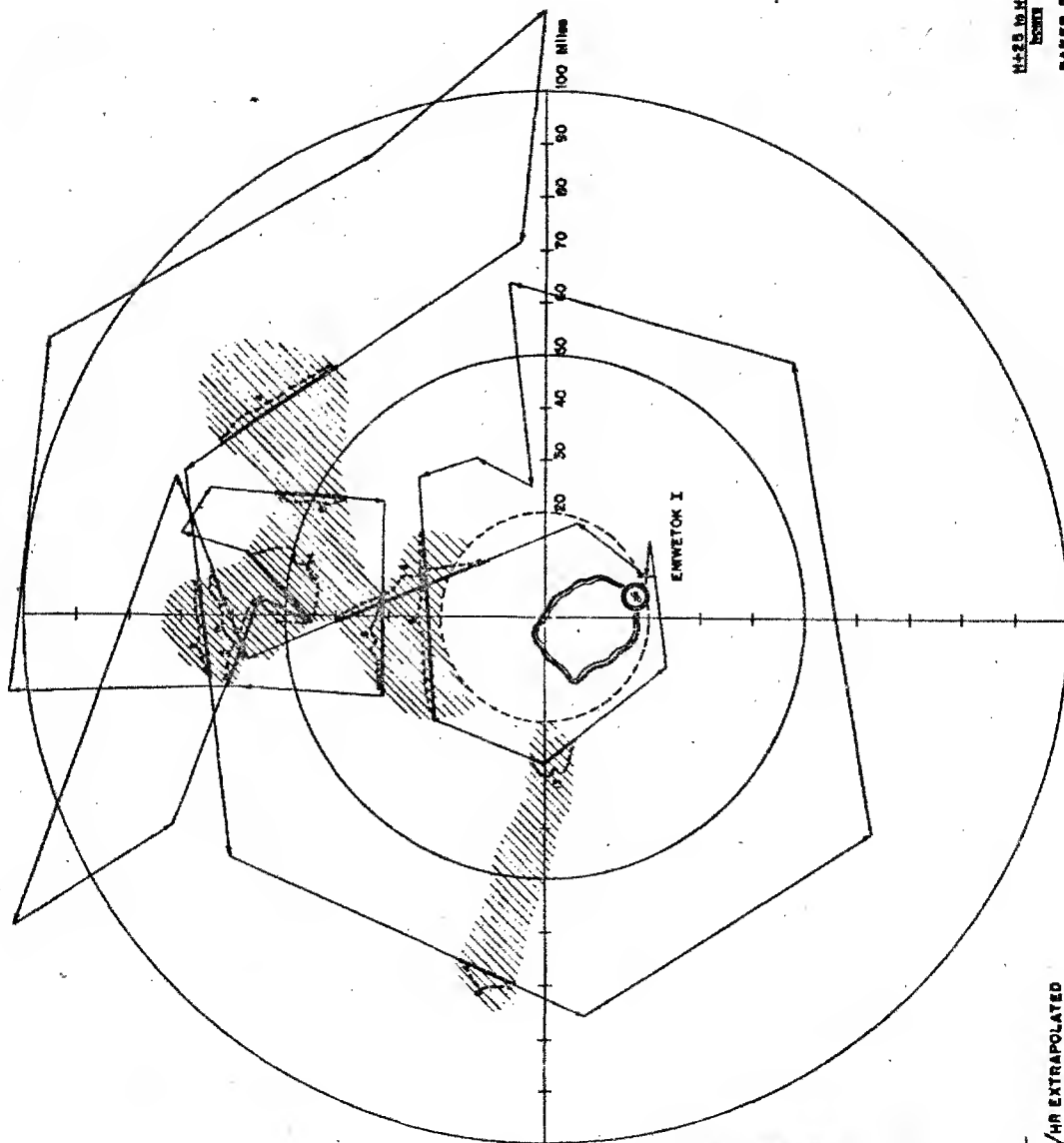


NOTE: READINGS IN MP/HR EXTRAPOLATED TO SURFACE AND CORRECTED TO H+2 DAYS

ISODOSE LINES BETWEEN TRACES ARE POSSIBLE CONDITIONS AND SHOULD BE CONSIDERED ILLUSTRATIVE ONLY

Figure 6

DOE ARCHIVES



DOE ARCHIVES

NOTE

PROFILE READINGS IN mSv/hr EXTRAPOLATED
TO 3 FEET ABOVE SEA, AND CONNECTED
TO H+48 HOURS

H+23 to H+32
DOWN

BAKER FLIGHT

MECHAN - 141913N to 150412E

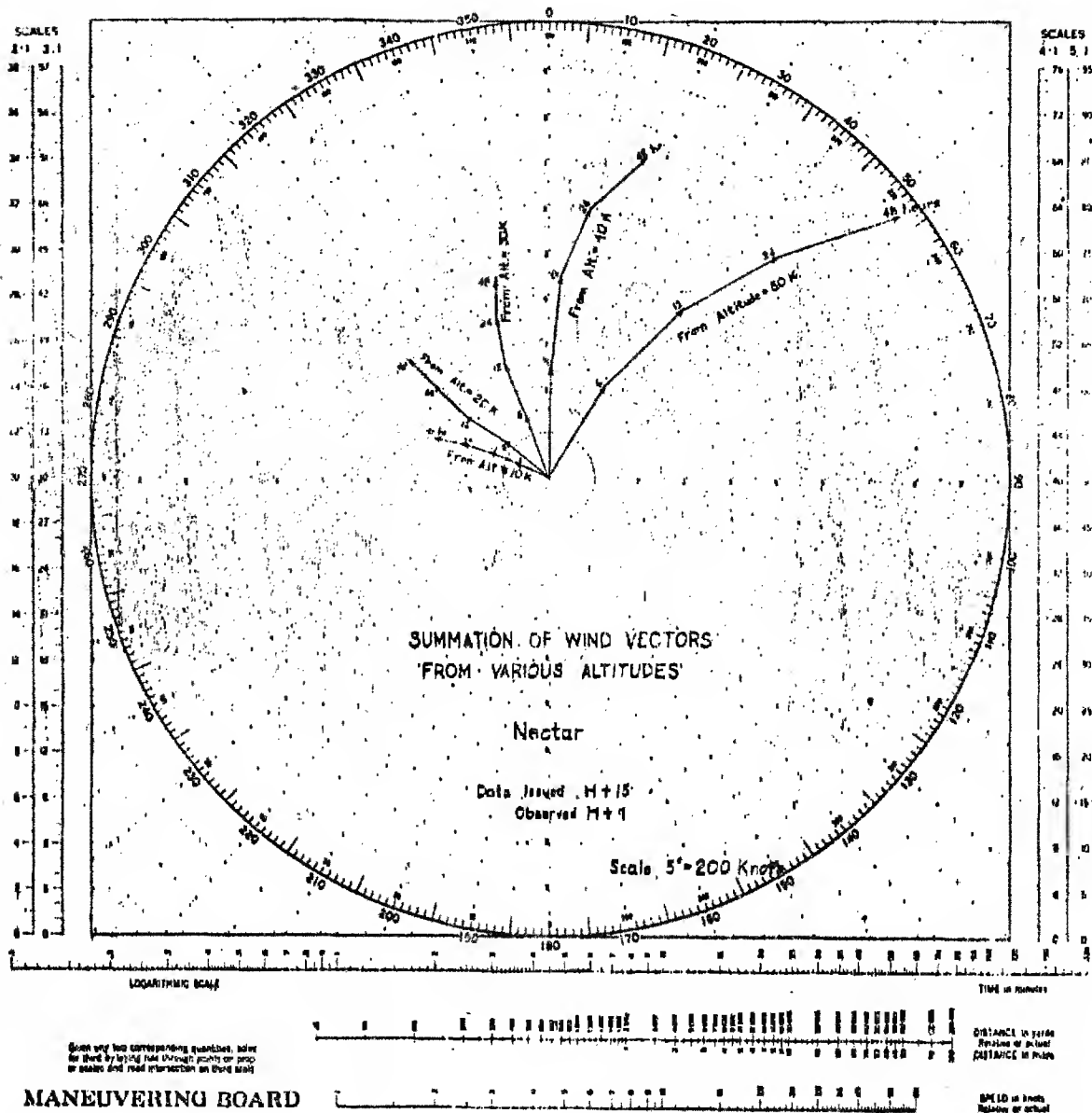
Figure 7

297

~~SECRET~~

~~RESTRICTED DATA~~
~~ATOMIC ENERGY ACT 1954~~

302

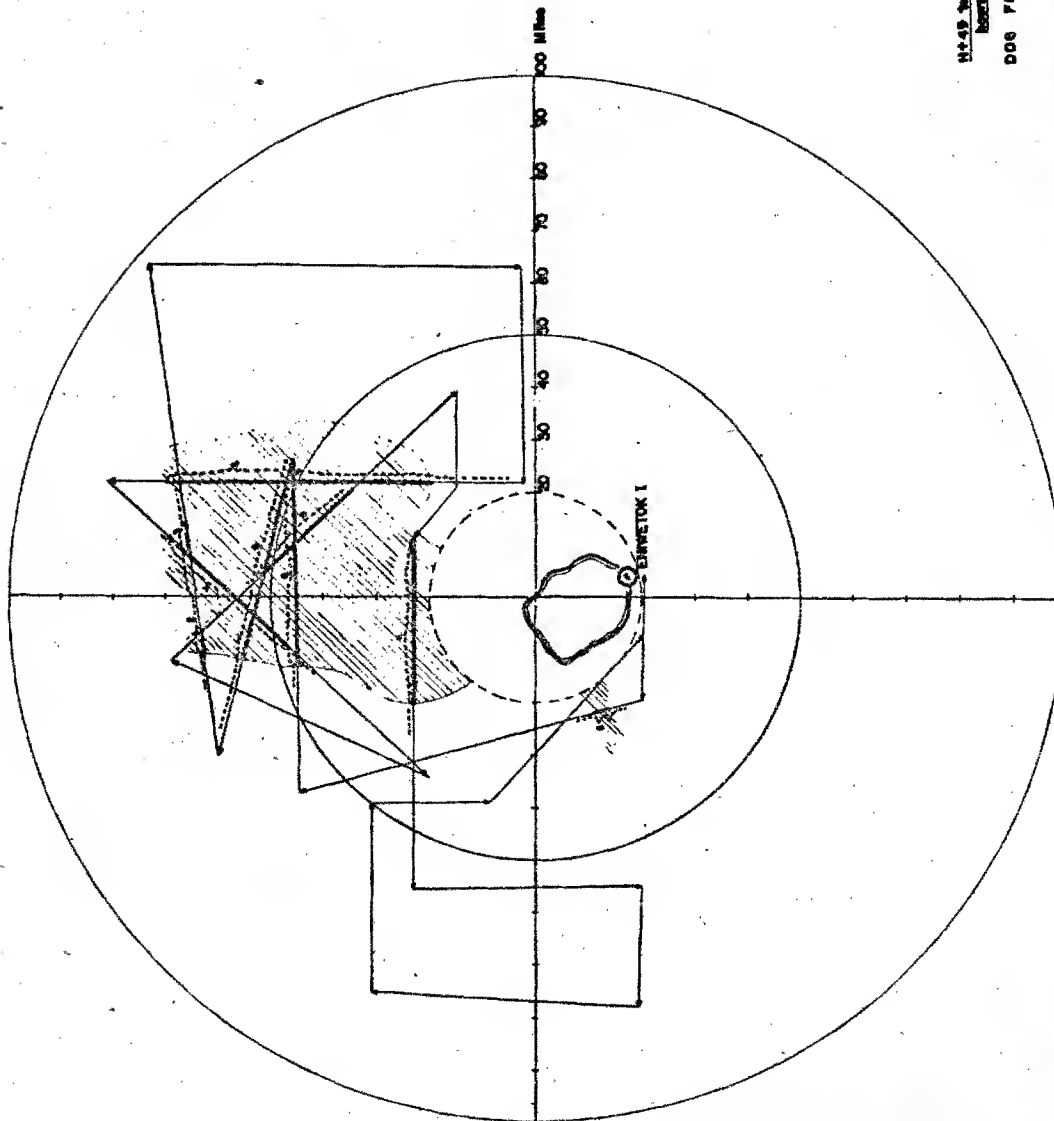


DOE ARCHIVES

Figure 8
298

~~CONFIDENTIAL~~
ENERGY ACT 1954

~~SECRET~~



H+48. 30 H+50
DOE FLIGHT

SECTION - PROFILE IN PROFILE

Figure 9

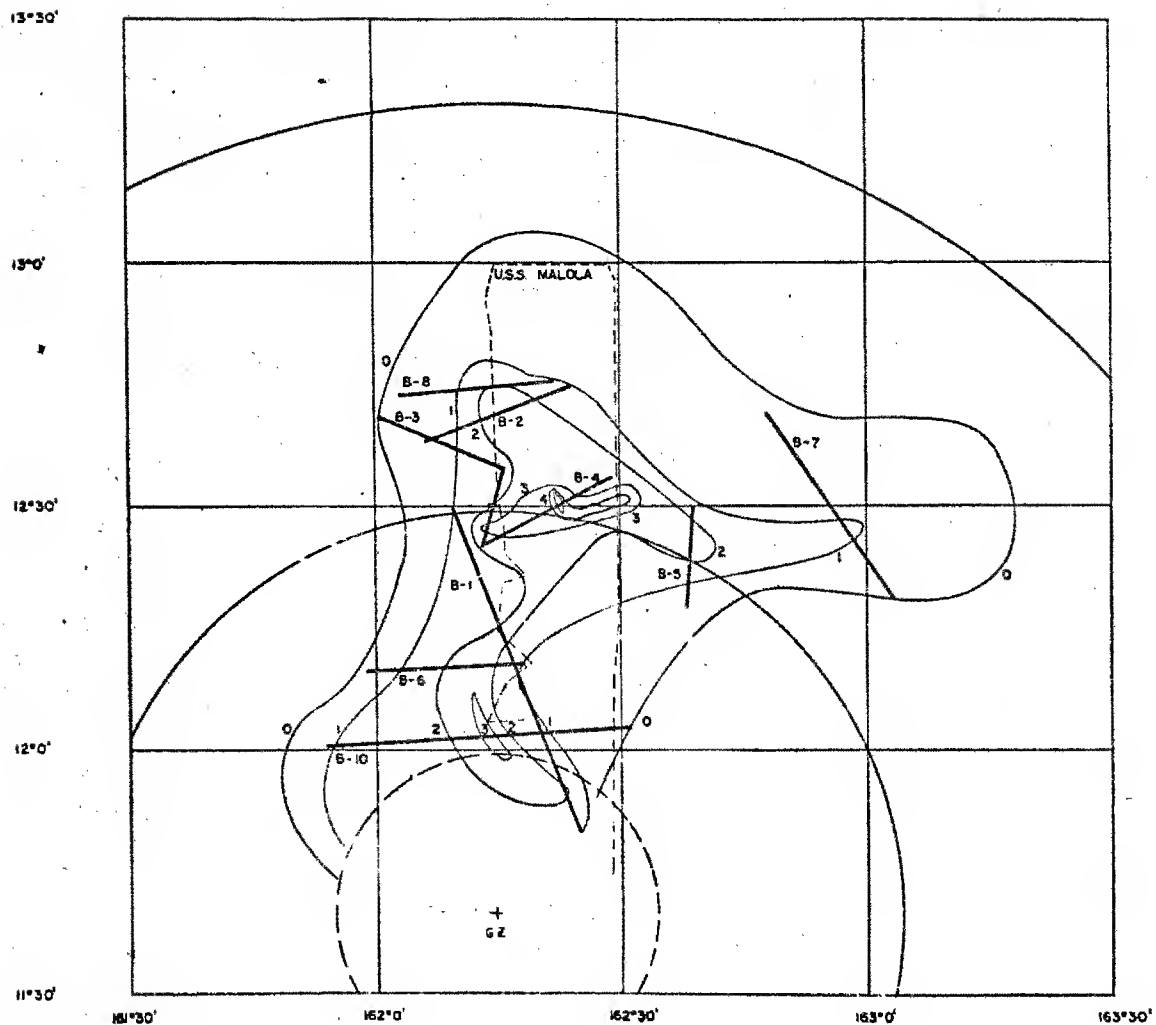
DOE ARCHIVES

NOTE

PROFILE READINGS IN METERS/HR EXTRAPOLATED
TO 3 FEET ABOVE SEA, AND CORRECTED
TO H+48 HOURS

SECRET

NECTAR ISODOSE



NOTE- READINGS IN MR/HR EXTRAPOLATED TO SURFACE AND CORRECTED TO H+2 DAYS

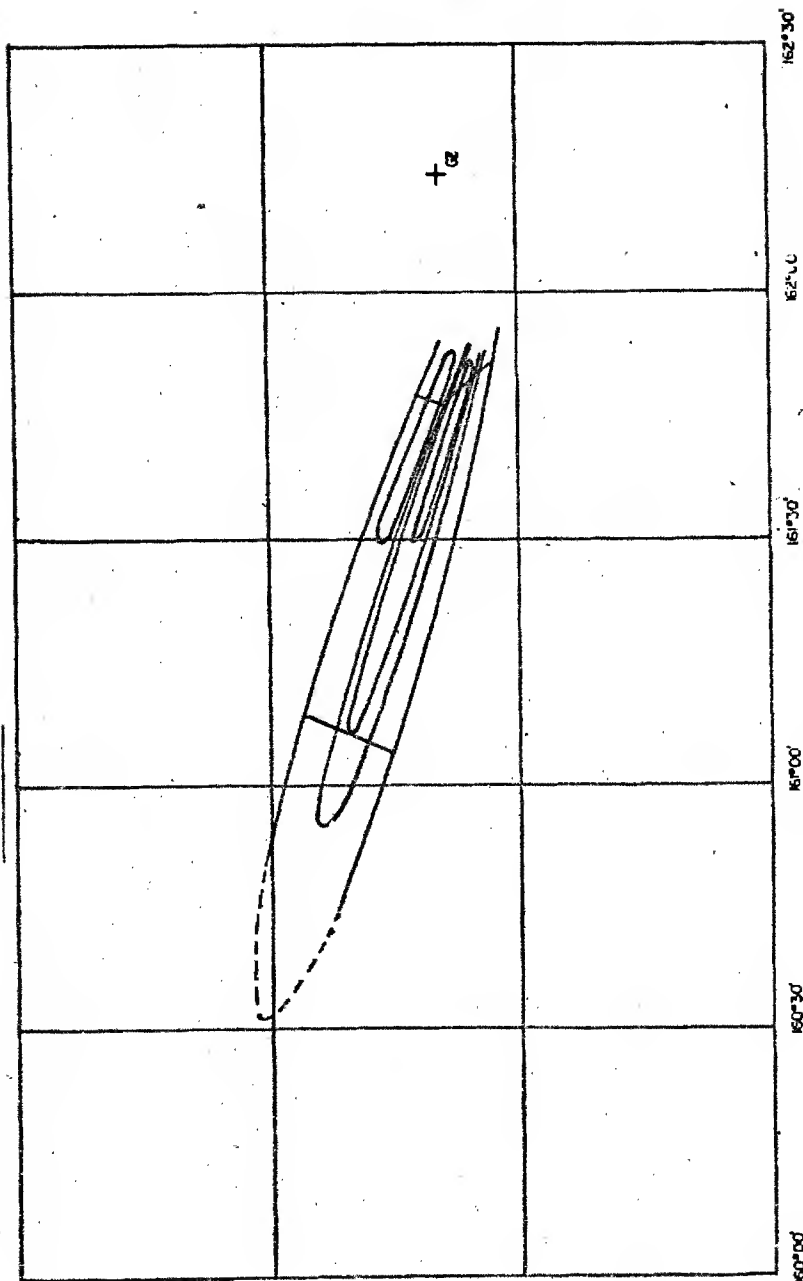
DOE ARCHIVES

ISODOSE LINES BETWEEN TRACES ARE POSSIBLE CONDITIONS AND SHOULD BE CONSIDERED ILLUSTRATIVE ONLY

Figure 10
300

NECTAR ISODOSE

WESTERN SECTOR



LONGITUDE (EAST)

NOTE - READINGS IN MB/HR EXTRAPOLATED TO SURFACE AND CORRECTED TO H+2 DAYS

ISODOSE LINES BETWEEN TRACES ARE POSSIBLE CONDITIONS AND SHOULD BE CONSIDERED ILLUSTRATIVE ONLY

Figure 11

LATITUDE (NORTH)

DOE ARCHIVES

THIS PAGE IS BLANK

DOE ARCHIVES

302

~~DOE ARCHIVES~~
NUCLEAR ENERGY

~~DOE ARCHIVES~~

151

307

[REDACTED]

PREDICTION OF DOSE-RATE AND DOSAGE CONTOURS AS
FUNCTIONS OF YIELD AND METEOROLOGICAL CONDITIONS,
LASL METHOD

PART I

FORECASTING OF THE 10 R ISODOSE LINE

Dr. Gaelen Felt
Los Alamos Scientific Laboratory

Introduction

The problem of long-range fall-out from very large devices (megatons) was first examined prior to Operation IVY. At that time the methods of analysis were based on a simple theoretical model devised to evaluate the hazards from the Jangle shots and on the empirical results from low-yield tests in Nevada. Neither source was truly applicable in detail to Mike, a fact well-known at the time, but the general result, as we know from [REDACTED] was correct; i.e., fall-out from Mike under adverse conditions could have been very severe at distances of 200 to 300 miles. The actual conditions on Mike-Day were, of course, favorable but at the same time rather unusual in that the location of the main fall-out was well clear of all populated areas.

The rare occurrence of ideal conditions, the length of the Castle operation, and the very evident hazards from the devices made necessary a re-examination of the problem of fall-out. In the field such a re-examination could be very crude at best, geared as it was to the immediately practical aim of operational forecasting. It was necessary to devise a system of forecasting simple enough to provide results based on the latest possible weather information, both observations and forecasts, conservative enough to guarantee no repetition of the unfortunate results of [REDACTED] and yet daring enough to enable one to take advantage of weather conditions different from those known to be ideal (no northern components from surface to 100,000 ft and axis of fall-out between about 315° and 045°).

DOE ARCHIVES

The treatment generally used in Nevada with moderate success was pretty clearly not well suited to fall-out forecasting at the Pacific Proving Grounds except possible under the condition of "deep easterlies", when all wind vectors from the surface up are easterly (an alternate "ideal" situation, incidentally for Eniwetok Atoll but not for Bikini). The basic difficulty with using the Nevada system for

[REDACTED]

analysis of the effects of large devices in the Pacific is that the wind structure in the Pacific is not primarily unidirectional in the pertinent altitude range. The usual fall-out pattern in Nevada is a narrow band, broadened at times by the presence of light and variable winds and by the occasional presence of abnormally great directional shear but still confined to a small sector. This general character is not often found in the Pacific, where the directional shear is almost always very great just above the east-northeast flow in the low altitudes and again at the tropopause (usually about 55,000 to 60,000 ft). In the Pacific the sector which includes all the distant fall-out is very frequently 180° and occasionally even greater.

While the sector is very large in the Pacific it is not true that the fall-out is uniformly distributed within it, and it therefore becomes necessary to look closely at the angular distribution of fall-out as well as the radial. It is this new factor in the analysis which makes the Castle system differ fundamentally from the Nevada system. It does not necessarily follow that the Nevada system should not also have this feature since there are evident failings there which may perhaps be removed in this way.

The Dose Index

The first step in the new system of analysis was to calculate the relative dose at various points about the origin for a given wind structure. The mechanics of preparing the isodose plots will be described in the following sections. Here we shall discuss the assumptions and general principles of the method. The assumptions used in the calculations are listed below:

The activity is uniformly distributed in height. This assumption is obviously a poor one and was subsequently altered to emphasize the middle region of the cloud and to depress the stem and the top. In the first plot this modification was applied at the plotting stage rather than at the calculational stage.

The distribution of particle sizes is uniform. This assumption also is not true but is justified by several arguments. From our point of view--distant fallout--the number of particles two feet in diameter relative to the number 100 microns in diameter makes not the slightest difference since the former all fall in the region of the crater anyway. On the other hand the relative number of very small particles is equally uninteresting since these do not fall quickly enough to affect the results significantly. What we have done in effect is to assume a "white" distribution for simplicity and to restrict the region of validity to distances between approximately fifteen miles and a couple

DOE ARCHIVES

of hundred miles from the origin. Again, in the absence of any detailed information on the real distribution, the assumption we have made is probably the safest.

The amount of activity deposited by an active particle is proportional to its area. One may fairly argue that in some cases the activity should be proportional to the particle volume. The choice of area dependence is based on the idea of plating on molten solids and on the idea of scavenging by water droplets.

The total activity is proportional to the total yield and decays as $t^{-1.2}$.

The particles settle by Stoke's law. This assumption is always challenged but no suitable substitute has yet been suggested. In the range of particle sizes of interest it is probably as good a law as any modification of it.

The area at the surface covered by particles falling from a given height is proportional to the square of the time of fall. This assumption expresses the fact of divergence which may arise from any number of reasons. No numerical value is assigned to the divergence.

The net radial distance that a particle travels is proportional to the time of fall.

With the above assumptions one obtains the dose index in the following inelegant way. At a given point "P" on the surface (Fig. 1) active particles can arrive from certain discrete altitudes of the cloud determined by the intersection with the hodograph of the radius vector from ground zero through the point. In the example these are the altitudes 79,000 ft at "A" and 39,000 ft at "B". The hodograph is customarily drawn for a fall rate of 5,000 ft per hour so that particles with that fall rate which start from 39,000 ft at nominally zero time will land at "B" in 7.8 hours. These particles will have a definite diameter "d". We have said that the activity brought down by any particle is proportional to its area; i.e., the dose index "D" contains a factor "d²".

DOE ARCHIVES

The remainder of the argument concerns the time. Two other assumptions contain time terms, the natural decay and the area of deposition. Now the dose rate is expressible in activity per unit area. For example, one megacurie per square mile is roughly equivalent to 3 r/hr about 3 ft above a fission fragment deposition. The dose rate is therefore expressible as

$$\text{rate} \sim \frac{a}{A} \sim \frac{t^{-1.2}}{t^2} \quad (1)$$

and the integrated dose, apart from other factors, is expressible as

$$\text{dose} \sim t^{-2.2}. \quad (2)$$

We chose to define the dose index as

$$D = \frac{d^2}{t^2} \quad (3)$$

where "d" is the particle diameter in microns and "t" is the time at which it arrives in hours. In the event that particles arrive from two heights as indicated for point "P" in Fig. 1, one merely adds the two indices arithmetically. We have felt, in view of the crudeness of these arguments, that very little would be achieved by keeping the power of "t" at -2.2 and have used -2.0 instead.

One will note that in this form the dose index does not yet contain Stoke's law but states merely that particles of size "d" arrive at time "t". The use of Stoke's law and some of the other assumptions permits the dose index to be written in a wide variety of alternate forms. Stoke's law states that the terminal rate of fall is proportional to the area of the particle. In our case the terminal rate is reached so quickly that one may write

$$\frac{h}{t} = K d^2 \quad (4)$$

where "h" is the starting height, "t" is the time of fall, "d" is the particle diameter and "K" is a constant of proportionality containing the density, the viscosity, and numerical factors. The viscosity, incidentally, is temperature dependent, but the variation is small compared to the other uncertainties in this system and we have chosen to keep the viscosity constant. Substitution of equation (4) permits one to write the dose index as

$$D = \frac{h}{K} \cdot \frac{1}{t^3} \quad (3a)$$

and further use of assumption (7) above permits the form

$$D = \frac{h}{K'} \cdot \frac{1}{R^3} \quad (3b)$$

DOE ARCHIVES

where "K" is some new constant and "R" is the radial distance along a bearing from ground zero.

Numerical values of the dose index can be computed from any of the forms of equation (3) with the proper selection of units.

We defined the numerical value of the dose index as the ratio of the square of the particle diameter in microns to the square of the time of fall in hours. In these units the dose index is of the same order as the dose in roentgens from a 10-megaton yield as determined by a rough match with [REDACTED] data. The adjustment to other yields in the megaton range is made by direct proportionality as indicated in assumption (4).

Preparation of the Plot: Static Case

We proceed now to describe the method of constructing the isodose contours for the simpler case of the static hodograph. The static hodograph presents a plan view of the vertical structure of the forecast winds at zero time and at the origin. Fig. 1 is a sample hodograph constructed from data in Table I. The criticisms against the static hodograph are that it should not be expected to persist unchanged even at the origin throughout the time of fall-out, and that it does not in principle apply at all to points displaced from the origin. These criticisms become more important as one attempts to forecast the low-level isodose lines which are established at considerable distances from the origin and many hours after shot time. The static hodograph does, however, provide a useful guide and has the virtue that a plot can be prepared from it very quickly indeed.

Using the sample hodograph of Fig. 1 let us compute the dose index for point "P" at 40° and 60 nautical miles from ground zero. There will be two components for "P" and all other points along the radius from "Z" through "P". From the hodograph the intercept heights and distances are 79,000 ft and 45 miles at "A", and 39,000 ft and 73 miles at "B". As mentioned above the total index for "P" is the sum of the indices computed from the two intercepts.

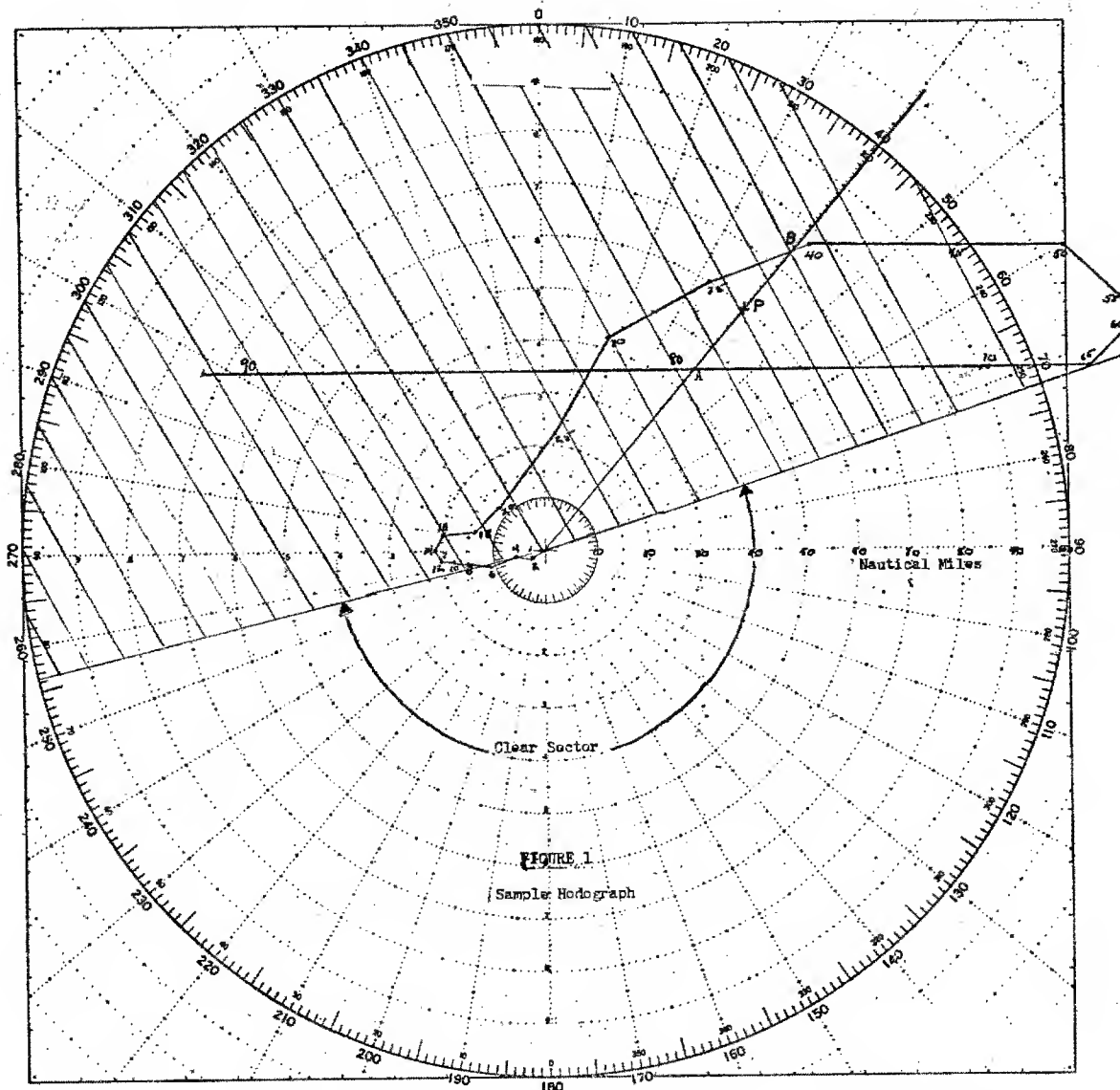
DOE ARCHIVES

Let us consider first the index from intercept "A". Particles which fall at "A" on the surface start at 79,000 ft above Zero. As they fall to 65,000 ft they travel westward approximately 75 miles. In falling the next 5,000 ft they travel approximately 10 miles southwest. Thereafter they swing around through the south, travel eastward between 50,000 and 40,000 ft, gradually turn to the northeast, and at about 15,000 ft settle into the surface trades for the last 20 miles of westward travel to point "A". Since the hodograph is drawn

Table I -- Sample Wind Forecast

Height in thousands of feet	Bearing in Degrees	Speed in Knots
2	080	08
4	080	10
6	070	10
8	090	10
10	090	08
12	110	05
14	160	05
16	200	08
18	260	13
20	230	15
25	220	18
30	210	20
35	240	23
40	250	20
45	270	28
50	270	20
55	310	15
60	350	05
65	040	10
70	090	20
80	090	30
90	090	40

DOE ARCHIVES



DOE ARCHIVES

Figure 1
Sample Hodograph

309

NIC ENERGY ACT 1954

314

for the convenient rate of 5,000 ft per hour the particles arrive at "A" 15.8 hours after zero. Particles arriving at "P" from 79,000 ft must spend a slightly longer time in each altitude layer; their trajectory is similar to that for the faster-falling particles but is expanded. The relative time for particles to arrive at "P" compared to "A" is given by the ratio of the vector sums or by the factor $60/45 = 1.33$. The time in hours is therefore 21.1 hours.

Now we have assumed a relationship between fall rate and particle diameter given by Stoke's law. Specifically, for land shots at the Pacific Proving Grounds, we assume that 75-micron particles settle at 4,000 ft per hour. Particles arriving at "P" from 79,000 ft settle at 3,740 ft per hour and are therefore slightly smaller than 75 microns. Stoke's law gives 72.4 microns. Using equation (3) with the numerical values 72.4 microns and 21.1 hours one obtains a dose index at "P" from the intercept "A" of approximately 12.

A similar computation for the dose index from intercept "B" gives the much higher value 208. The total index at "P" is therefore 220. This means that for 10 megatons one would expect an integrated lifetime dose of 220 roentgens in the vicinity of point "P".

It is obviously time-consuming to compute the index for a large number of points in the field in the way just described. In order to speed up the computation of dose indices the nomogram in Fig. 2 was constructed from an alternate form of the dose index equation. The most suitable form is

$$D(\theta, R) = \frac{v_o^3}{K_s h_o^2} \cdot \left[\frac{R_o}{R} \right]^3 \quad \text{DOE ARCHIVES} \quad (3c)$$

where " v_o " is the hodograph fall rate (5,000 ft per hour), " h_o " is the intercept height in feet, " K_s " is the Stoke's law constant (4,000/5625 in our units), " R_o " is the intercept radius in miles, and " R " is the distance in miles to a point on the bearing " θ ". One should note that for constant " θ " the intercept height and distance are also constant and that the dose index along this bearing decreases as " R^{-3} ". Consequently if one can determine the dose index at one point along the bearing the indices for other points can be read very quickly from a straight line of slope -3, on log-log graph paper. The obvious point to determine an index is at " R_o ". For all bearings the dose index at $R = R_o$ is determined by the intercept height alone. It becomes very simple therefore to make a suitable nomogram by drawing a line of slope -2 which gives the dose index " D_o " for $R = R_o$. The doses at any " R " are then obtained by placing a straightedge with slope -3 through the point " D_o, R_o ". For quick reading several arbitrarily

spaced lines of slope -3 have been drawn in Fig. 2.

Using again the sample wind structure of Fig. 1 one obtains the index for point "P" from the intercept "B" by entering the nomogram at $h_o = 39,000$ ft at the top of the page, coming down to the unweighted height line at index 110, moving left to a point above the distance $R_o = 73$ miles, then up a line of slope -3 to index 210 above $R = 60$ miles.

The nomogram in Fig. 2 has two height lines, the curved one corresponding to a weighted height distribution. This second curve is believed to be somewhat more realistic inasmuch as it reduces the weight of the very low and very high parts of the cloud and increases the weight of the middle cloud. This rather general weighting is based entirely on observation and experience and is not derived analytically.

With a very little experience in the use of the nomogram one can from the hodograph prepare the plot shown in Fig. 3 in approximately one-half hour. The weighted height line has been used in this plot.

Preparation of the Plot: Dynamic Case

For operational use a 10 R dose is a handy dividing point between "dangerous" and "harmless" levels. A dose index of the order of 10 is therefore perhaps the most important of the family of lines. An index of 10 is however established at rather late times -- it is completed for the 90,000 ft level at approximately 23 hours, and its extreme point may be a considerable distance from the origin. Consequently it is in general desirable to make appropriate corrections for time and space changes in the wind structure.

The method devised is based on the same general assumptions as for the static case and is again simple enough to permit the preparation of a plot in a short time. The complication here was that a complete weather analysis of the entire area could not be made every few hours by the limited crew at the Eniwetok Weather Central. Consequently it was necessary to have a forecaster present to make appropriate corrections as the plot developed.

Since in the dynamic case the trajectories of particles of different sizes falling from the same height are no longer similar, the terminal points do not fall along a straight line running out from the origin. The index falls off inversely as the cube of the distance along the line of terminal points instead of along a line of constant bearing.

DOE ARCHIVES

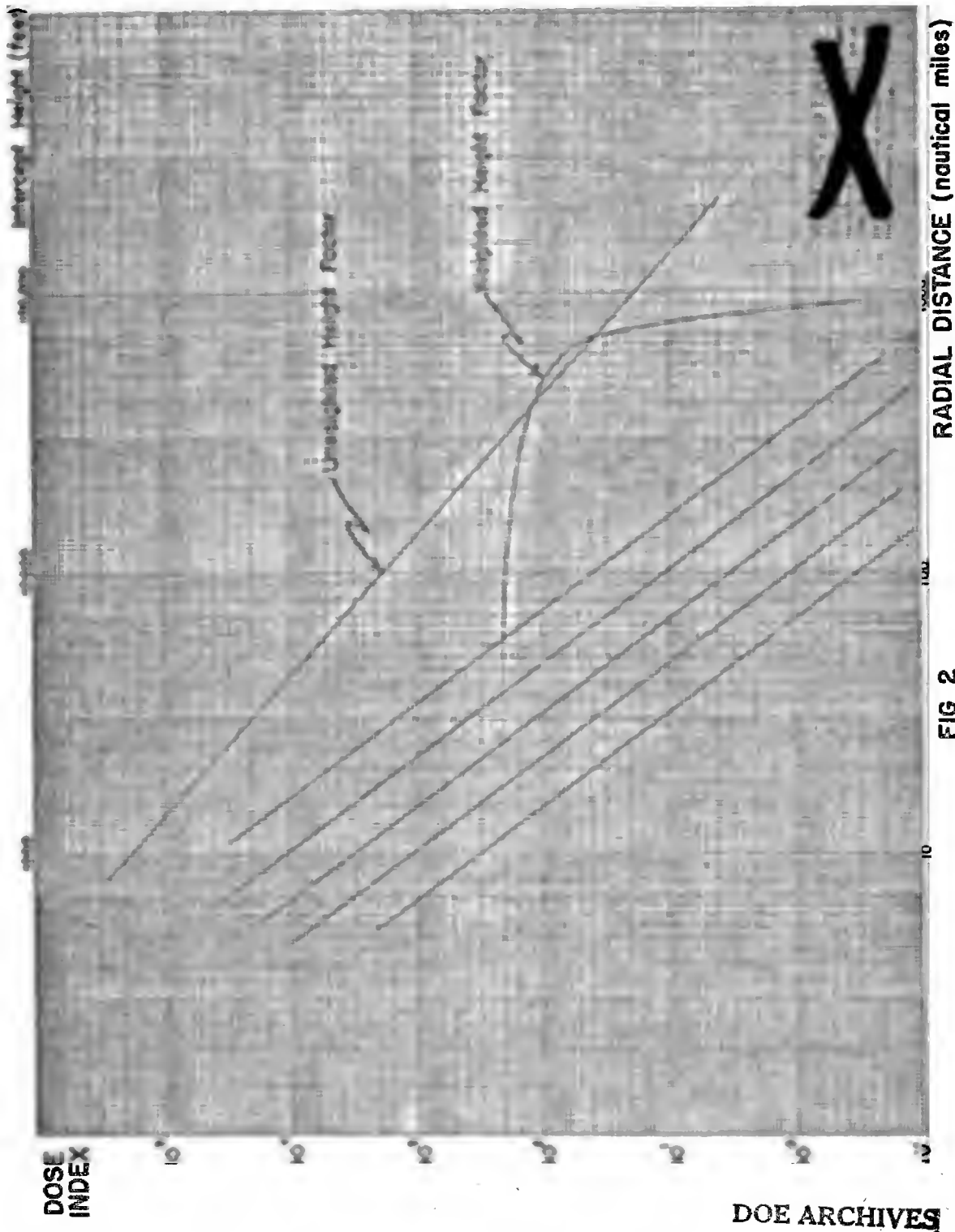


FIG 2

INDEX NOMOGRAM

Figure 2

It is possible but at present very time-consuming to compute the lines of terminal points for a set of altitudes complete enough for an adequate plot. The best that could be done in the time available was to locate the 10 R point for about a dozen altitudes and base the 10 R line on these points alone. A complication arises when the points fall at different distances on roughly the same angular bearing. This result corresponds to a contribution from two or more altitudes and means that the 10 R line must be drawn some distance beyond the outermost calculated point. The adjustment is easy to make approximately by simple application of the inverse R^3 relation to the inner points to find the contribution at the outermost and a second application of inverse R^3 to the sum. To take into account the height weighting one locates the terminal point and then contracts or expands radially, again by inverse R^3 . These approximate methods are an unhappy feature of the system but are necessary if the plot is to be completed in a reasonable time. We were unable to discover any quick, reliable analytic or graphical method of making these adjustments more precise.

The mechanics of locating the 10 R points (before any adjustments) are straightforward enough. The dose index equation (3) gives the dose in R for 10 megatons. For a predicted yield different from 10 megatons one may write a dose equation

$$I = \frac{W}{10} \cdot \frac{d^2}{t^2} \quad (5)$$

where "I" is the dose in roentgens, "W" is the yields in megatons, and "d" and "t" are defined as before. This equation follows, of course, from assumption (4). The form (5) is not convenient for calculations, since in the construction of a trajectory for a falling particle one is concerned only with the time the particle spends in a stratum characterized by a fixed mean wind. It is convenient then to introduce Stoke's law and to solve equation (5) for the fall rate "v". The result is

$$v = \sqrt[3]{\frac{10 I K_s h^2}{W}} \quad (5a)$$

where "K" is the constant 4000/5625, "h" is the starting height in feet and the unit of "v" is feet per hour. The time spent in a given stratum " Δh " is then

$$\Delta t = \frac{\Delta h}{v} \quad (6)$$

Equations (5a) and (6) were used to prepare a worksheet listing the strata, times in the strata, and accumulated times from the start to the strata. Forecast mean winds were then entered on the worksheet as the trajectory plots were made and the times and space

~~CONFIDENTIAL~~
DATA
ENERGY

locations became known. In the actual cases computed the changes in wind structure were never very significant and the resulting plots differed little from those made from the static hodograph. The dynamic system does, however, have the capability of handling a rapidly changing situation should it appear.

Conclusions

The fall-out forecasting systems described above have a large number of very obvious deficiencies which one would hope to remove by the next operation. For example one would hope to include a good representation of the particle size distribution for both land and water shots. The question whether area or volume of a particle is more significant for the deposition of activity should be investigated. A careful estimate of the height distribution of the activity should be made. Some attention should also be given to the effects of finite lateral cloud dimensions and to the spreading of the cloud. These are points which will refine the system.

Dr. Tom White of LASL began to make such refinements during Castle in an attempt to remove one outstanding defect of this system, its inherent inability to reveal any detail near the origin. His method is described in a separate report.

Two difficulties with the system cannot be removed at all. The case where the hodograph passes directly over the origin is not unlikely and gives embarrassing results, since $R_0 = 0$ and the dose index vanishes except at the origin. This result is at least circularly symmetric. The other awkward case is that in which one or more elemental wind vectors is radial, since one then has a continuous altitude range contributing to the dose index along a bearing in place of one or two discrete altitudes. This is in reality precisely the kind of wind structure which leads to very intense narrow bands, but the system as set up cannot estimate the magnitude of the dose index along such a bearing. One could perhaps handle this situation by revising the method such that each 5,000-ft altitude interval made a contribution as determined by the mean height of the interval along a bearing line through this mean height. Such a change would introduce difficulties in evaluating the contributions at one point from several heights since the bearing lines through the mean heights would not in general coincide.

One difficulty will continue to plague us even with any sort of refined system. At this time it is very difficult to obtain a weather forecast precise enough to justify the effort which must be put into a good fall-out forecast. Because of the inherent uncertainties in

weather forecasting one is tempted to conclude that a refined system of fall-out forecasting will for the time being be most useful for post-shot analysis and that a detailed fall-out forecast based on a normal weather forecast would be misleading. The weather forecasting presently available is of the highest quality but the cumulative errors resulting from small variations about the forecast mean winds can result in a pronounced change in the fall-out pattern. It appears desirable at this time to retain a crude system which is relatively insensitive to small variations in weather structure and which presents conservative upper limits to the fall-out hazard.

DOE ARCHIVES

[REDACTED]

PART II

A METHOD OF ESTIMATING RADIOACTIVE FALL-OUT

T. N. White
Los Alamos Scientific Laboratory

The method described herein is designed with an objective that is intermediate between operational requirements, and the requirements of a strictly scientific investigation. It is designed to include what are assumed to be the most important factors that determine a fall-out pattern, with the idea that we might find out enough about what is going on to produce a good simplified method for operational use. One simplified version that was used for local fall-out forecasting is described in Close-in Forecasting by New Techniques Developed after BRAVO, Tab D "Fall-out Forecasting Techniques" of the Task Force Castle Report. It seemed good enough to justify further investigation of the basic ideas as applicable to any range of distances over which a constant wind field could be assumed.

The basic assumptions of the method are as follows:

The whole cloud, up to its height of stabilization, is formed instantaneously at the time of detonation. This is what we call the "initial cloud".

In any height layer of the initial cloud, the concentration (radioactivity per unit volume) is distributed according to the Gaussian Law

$$c(h, r, a_0) = c_0(h) \exp(-r^2/a_0^2)$$

where $c(h)$ is the central concentration at height h , r is the radial horizontal distance, and a_0 is a "spread parameter" (analogous to standard deviation) that is also considered to be a function of height. From this assumption it follows that the total amount of radioactivity in a slice of unit vertical thickness is $\pi c_0(h) a_0^2$.

Throughout all of any such layer, the radioactivity is distributed normally with respect to the logarithm of the rate of fall of the particles. Thus at any distance r , the fraction of radioactivity that falls with speeds in the range f to $f + df$ is given by

$$\frac{1}{\sigma(h) \sqrt{2\pi}} \exp \left\{ -\frac{1}{2} \left[\ln \left[\frac{f}{\frac{f(h)}{\sigma(h)}} \right] \right]^2 \right\} \frac{df}{f}$$

where $f(h)$ is the fall-rate for particles of greatest radioactivity, and σ (also considered to be a function of height) is the standard deviation of the logarithm of fall-rates, weighted according to radioactivity; $f(h)$ and $\sigma(h)$ are constant throughout the layer.

The rate of fall of any particle remains constant until it reaches the ground.

Any particle that starts from the central axis will follow a path strictly in accordance with the wind pattern, while all other particles that fall at the same rate from the same level will diffuse laterally from the central particle in such a way that the gaussian distribution is maintained.

During this process, the increase in the spread parameter is described by

$$\frac{a}{a_0} = \left[1 + \frac{S}{\beta a_0} \right]^{\frac{m}{2}} = p^{\frac{m}{2}}$$

where S is the distance travelled by the central particle until it reaches the ground. (It is to be noted that S is not the straight-line distance from the origin to the landing point unless all winds at all levels are in the same direction. β and m are parametric quantities that may be used to describe the amount of diffusion. They are not at present regarded as functions of height. (The quantity p is merely an abbreviation for the quantity in brackets).

From these assumptions it follows that the dose rate on the ground is

$$\dot{I} = \frac{K}{\sqrt{2\pi}} \int_0^H \int_0^\infty \frac{C_0(h)}{\sigma(h)p^m} \exp \left[- \left[\left(\frac{\ln \left[\frac{f}{f_h} \right]}{\sigma(h)\sqrt{2}} \right)^2 + \frac{r^2}{a^2 p^m} \right] \right] dh \frac{df}{f}$$

where K is dose rate per unit of surface concentration, H is the height of the top of the cloud, and r is now the distance from the point at which the dose rate is estimated to each of the landing points of central particles. These landing points will depend on the wind pattern below the level from which the central particle originated, so that r is a function of h . The landing points also depend on the rate of fall, so that r is also a function of f . Changing from rate of fall to time of fall, one obtains

$$r^2 = [t \bar{u}(h) - X]^2 + [t \bar{v}(h) - Y]^2$$

where (X,Y) are the rectangular coordinates of the point where dose

DOE ARCHIVES

rate is estimated, and \bar{u} , \bar{v} are the wind components in the same coordinate system, averaged up to the height h .

We may also express

$$p = 1 + \frac{t\bar{w}(h)}{\beta a_0(h)}$$

noting that \bar{w} is the average speed regardless of direction. (\bar{u} and \bar{v} are not, in general, the components of \bar{w}). This expression is correct if one is satisfied that the diffusion depends on the total horizontal distance travelled by a central particle. If one wishes to assume that the vertical distance should be included, p becomes much more complicated.

The significance of β and m can now be visualized. If $m = 2$, then

$$\frac{a}{a_0} = \frac{\beta a_0 + t\bar{w}}{\beta a_0}$$

so that the lateral dimensions of any segment of the cloud will increase as if the segment had come from a point source located at a distance βa_0 upwind. The size increases linearly with distance travelled by the central particle. If m is greater than 2, the borders of the cloud will diverge more rapidly, and if m is less than 2 they will diverge less rapidly. One can prevent any increase in size either by making β infinite or by making m equal to zero. This method of describing the diffusive process is similar to that of Sutton, but not exactly the same.

If $m = 2$, then at sufficiently large values of t , the area covered by a segment of cloud is proportional to the square of the time, as in Felt's method. However, the proportionality factor varies, as \bar{w} varies with height, and further, the overall average proportionality factor changes with the overall strength of the wind field, and in these respects it differs from Felt's method.

Returning to the basic equation, the change of variable from f to t changes the argument of the logarithm to

$$\frac{t}{h} f(h)$$

DOE ARCHIVES

and $\frac{df}{f}$ becomes $\frac{dt}{t}$

One notes also that concentrations in the initial cloud must be

~~SECRET~~
DOE ARCHIVES
324

reduced to those that would have existed at that time for which the dose rate is being estimated.

The information that is needed for a calculation is then:

The winds pattern at heights up to H .

H , the height of the top of the cloud.

a_0 , the initial spread parameter, or radiological radius, as a function of height.

C_0 , the central concentration as a function of height in the initial cloud, adjusted to the time of dose-rate estimation.

f , the logarithmic mean rate fall (weighted according to radioactivity), as a function of height in the initial cloud.

σ , the logarithmic standard deviation of this distribution as a function of height in the initial cloud.

β , diffusion parameter, described above.

m , diffusion parameter, described above.

Testing of the method requires the use of high speed computing machinery. With such machinery one can make many changes in the quantities described above, proceeding on a trial and error basis. In order to achieve some degree of objectivity, the following approach is adopted.

The logarithm of the ratio of calculated to observed dose rate is estimated at a number of points for a given shot. This quantity is called γ (gamma). Then the mean gamma, and the statistical variance of the individual gamma about the mean gamma, are calculated. This process is repeated for a number of values of some parametric quantity, beta for example. One then plots the variance against beta, and selects as the best value the one that gives the least variance. One then moves on to other parametric quantities, and treats them in the same way, hoping that there is not too much correlation between the effects of the different types of parameters. It will be noted that this application of the "least squares" method discounts the overall ratio of calculation to observation. In principle it is possible to get zero variance (an exact fit) when each calculated value is, for example, exactly ten times the observed value. One would then suspect that 90% of the radioactivity had remained in the crater. If, however, one should obtain a good fit but with only 10% of the observed activity accounted for, one would have to consider other possibilities. One would first look to see whether any large fraction of the activity was excluded from the calculation. In numerical integration it is not practical to go all the way from zero to infinite time, and part of the activity might have fallen outside of the time range chosen. If this explanation fails, and if the fit is really good, one has to conclude

that the least squares criterion, as applied here, is not useful. We have not yet encountered this particular obstacle.

The method of approach is subject to a hackneyed old criticism running as follows: by subdividing the height of the cloud at will, you can obtain as many discrete parametric values of a_0 , c_0 , f , etc. as you wish, so that you should be able to fit any number of observations exactly. This is true, in principle. But if one can get a set of values that look reasonable, and can be scaled in a reasonable way with yield over a wide range, the method can serve a useful operational purpose even though the values might be scientifically unsound.

For machine integration, using the IBM Model 701 "Defense Calculator", those parametric quantities (a , c , σ and f) and the mean wind components (\bar{u} , \bar{v} , \bar{w}), which are functions of height, may be loaded as tables of data. The total height of the initial cloud, H , is subdivided into M equal layers, each identified by an integer $i = 0, 1, 2, \dots (m-1)$. The time variable is laid on a logarithmic scale, each time being identified by an integer $j = 1, 2, 3, \dots N$. Storage limits the maximum value of M to 32. N may be any value that doesn't take too much machine time, and the minimum and maximum limits of the time integration may be changed at will. The exponential factor in the formula is recorded as zero if the absolute value of the exponent exceeds a value A which may be as large as 10.

The coding is so arranged that the time integration is performed first and the height integration second. At each location, the fraction of the dose rate that comes from each initial cloud layer is computed and may be printed along with the calculated and observed dose rates and the co-ordinates of the location. Or one may by-pass this printing and obtain only the statistics: mean gamma and variance for a preselected series of locations.

The codes are not yet frozen, and additional features are being added from time to time. We have two codes (1) a fast "fixed-point" code as outlined above, and (2) a slower "floating-point" code that is more precise and which is more flexible in some respects.

Since starting on this problem about seven months ago, a considerable part of the time has been spent on coding and de-bugging, which we undertook ourselves in order to learn how to use the Model 701. Using Bravo fall-out data, we demonstrated that least squares solutions could be obtained for the various parametric quantities involved. However, the "best" values, as selected in this way, gave distant fall-out predictions that were only 20 to 30% of the observed values, and the

DOE ARCHIVES

~~SECRET~~

"fit" was not good. We then turned attention to Nevada data for a while, and became interested in an approximation that seemed to offer a hope of eliminating one of the two steps in the double integration. Before this possibility had been fully explored, Mr. Vay Shelton, Livermore Operations Division, joined forces with us, and we worked together for a week on UK-1 and UK-7. Mr. Shelton then took our codes to Livermore and continued working on the Nevada data, while we turned attention again to the Bravo shot. Mr. Shelton has reported recently that the method gives satisfactory results for UK-1 and UK-7, and he is continuing work on other shots. We have concentrated on the problem of predicting the Bravo fall-out on the assumption that practically all of the activity in the initial cloud was located above the tropopause. To date, our method of calculation has not been able to give satisfactory results, even when the winds were arbitrarily twisted to make the fall-out occur in more nearly the right place. At this point we feel, therefore, that we do not have any cloud model in which we have confidence. We have merely a mechanism of calculation, the value of which has not yet been proven as far as Bravo is concerned.

Lacking any satisfactory cloud model for Bravo, we tackled the "homework" predictions on a guess-work basis, which does not justify a description. The values that we used in the calculations are:

	<u>1 MT</u>	<u>50 MT</u>
Height of cloud (sea miles)	11.5	19.0
Height of stem (sea miles)	7.0	7.0
a for mushroom (sea miles)	0.94	4.58
for stem (sea miles)	0.41	1.49

Beta: 9.15

m: 1.0

Sigma: 1.0

DOE ARCHIVES

The values of c were taken as constant up to the tropopause, and thereafter decreased with air density. (The machine program requires only the entry of relative values, from which the actual values are adjusted so that the total radioactive content of the cloud is in accordance with the yield). Logarithmic mean rates of fall were assigned to the 16 layers of the cloud as follows, counting from the bottom. (Rates are in knots)

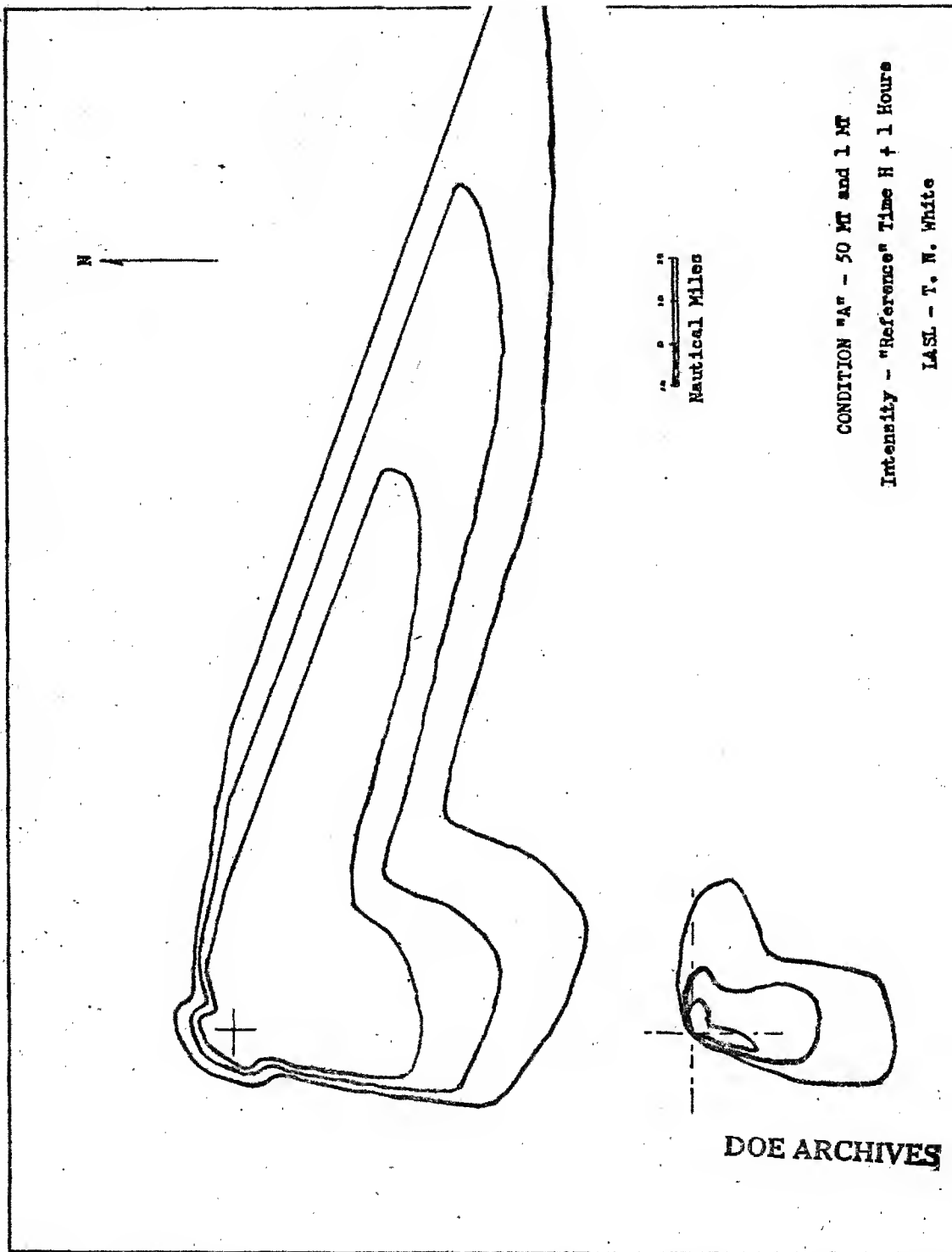
Layers 1 thru 4	20
Layers 5 thru 8	7.4
Layers 9 thru 12	2.7
Layers 13 thru 16	1

~~SECRET~~
ATOMIC ENERGY ACT 1954

SECRET

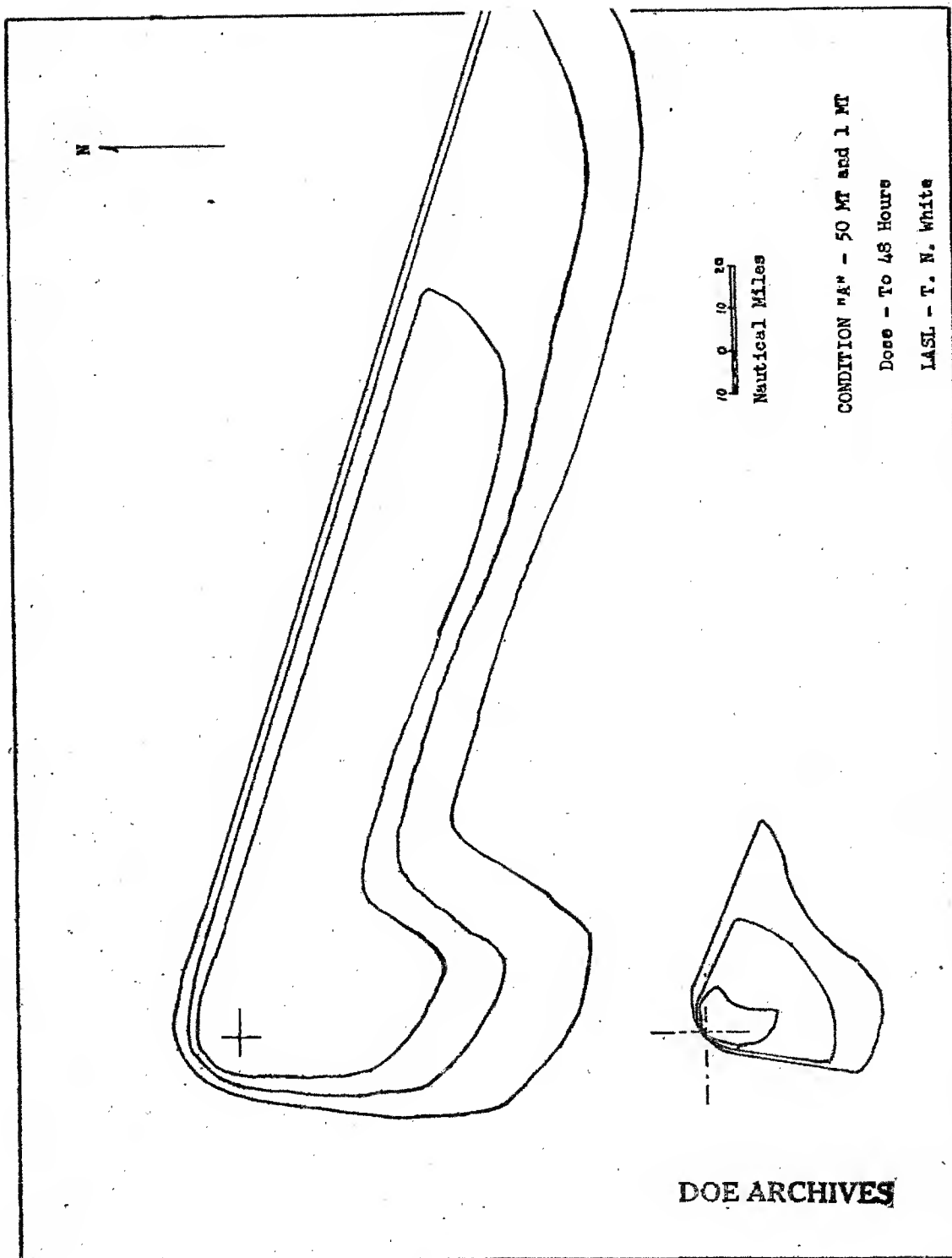
(Editor's note: The four contour figures which follow were received too late for inclusion in the comparison done by Cdr. Paine. The contours shown in that comparison for LASL were submitted prior to the symposium; and, being scaled by simple yield dependence, did not include allowance for different cloud dimensions as those presented here do.)

DOE ARCHIVES



324

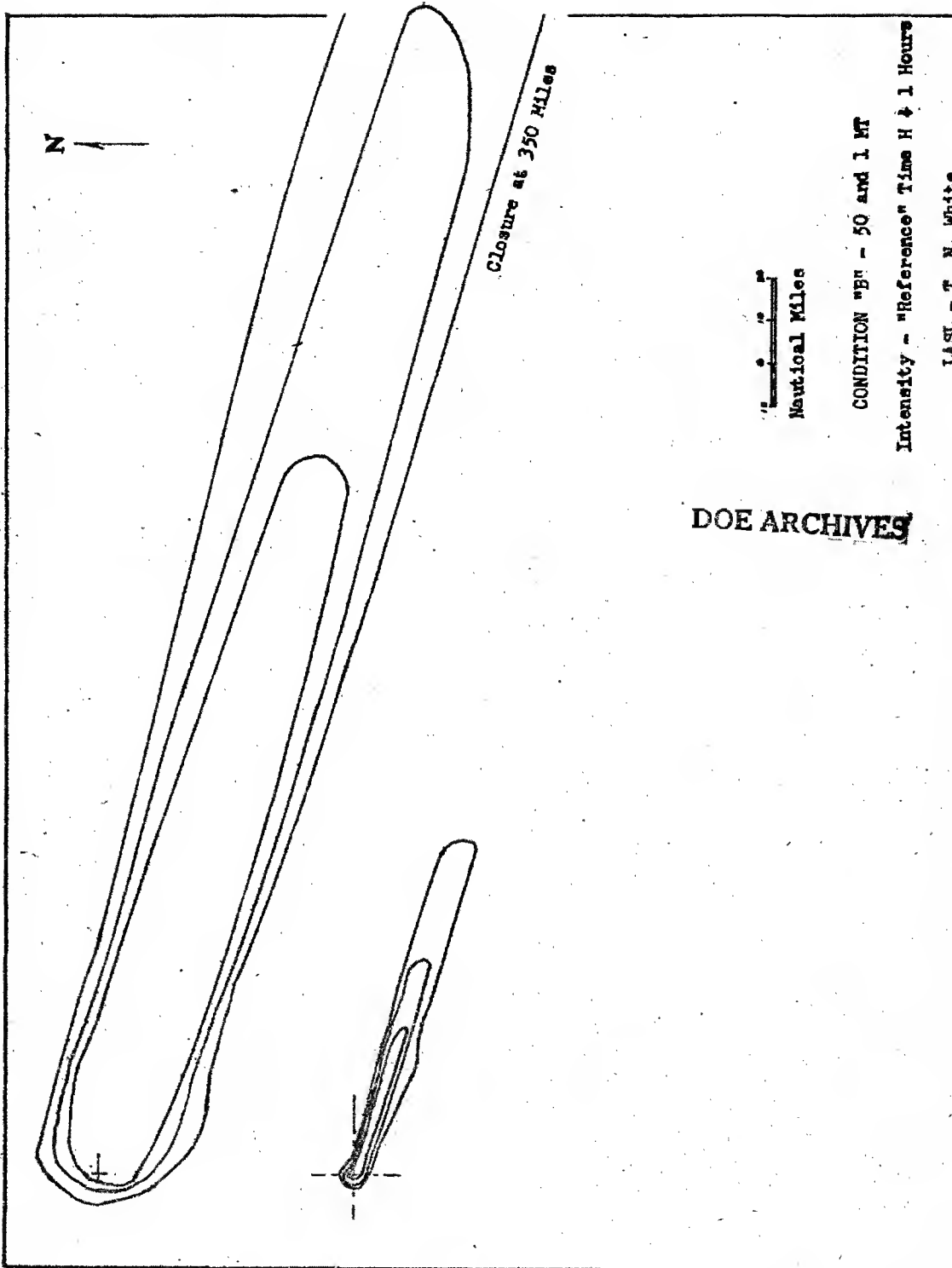
329



325

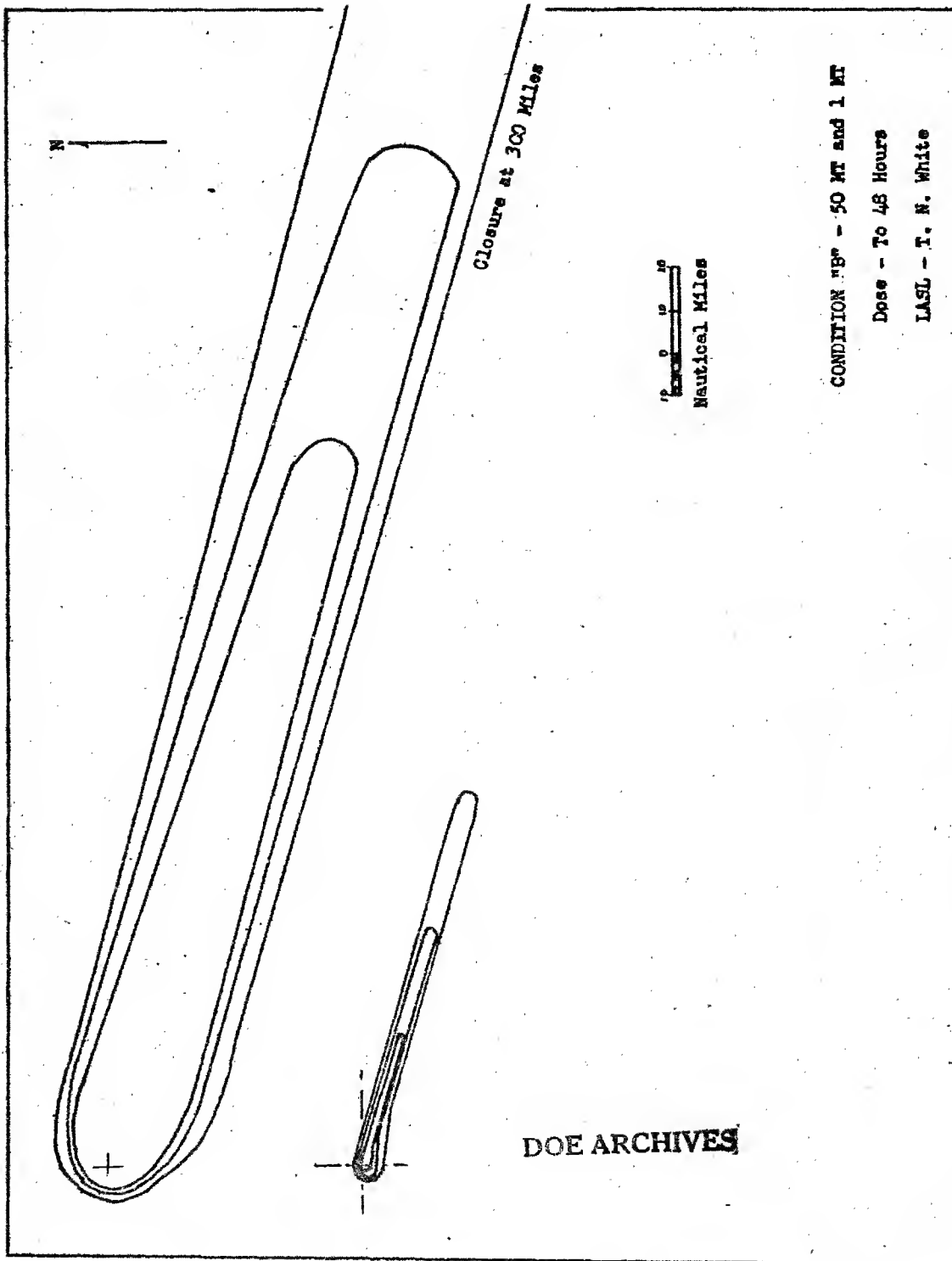
~~SECRET~~
ATOMIC ENERGY ACT

330



326

ATOMIC ENERGY ACT 1954



327

~~REDACTED~~
ATOMIC ENERGY ACT

332

THIS PAGE IS BLANK

DOE ARCHIVES

328

DATA
MIC ENERGY

333

[REDACTED]

PREDICTION OF DOSE-RATE AND DOSAGE CONTOURS AS FUNCTIONS
OF YIELD AND METEOROLOGICAL CONDITIONS, RAND METHOD

PART I

Dr. R. R. Rapp
Rand Corporation

The Formation of the Atomic Cloud

Dr. Kellogg has already presented the physical picture of the atomic cloud upon which the Rand model is posed. There are, however, a few points to stress. First, as shown by the first sketch in Figure 1, there are large amounts of earth taken into the fireball in the very early stages of formation. Next, as is indicated in the other sketches of Figure 1, a large amount of earth is carried aloft with the fission products by the extremely stable toroidal circulation. This toroidal circulation is caused by the intense thermal gradients of the fireball. Thus, large quantities of vaporized, liquified, and pulverized earth are in intimate contact with the newly formed fission products from a few milliseconds to a few minutes after detonation. By way of contrast, it is believed that the earth, which is seen to enter the fireball of an air burst, flows up through the "hole in the doughnut," circles around, and falls to the earth without actually encountering the radioactive material. For the surface burst, where there are large particles, after the cloud stops rising, there will be radioactivity present on particle sizes ranging from thousands of microns to about a very few microns spread through a region of the atmosphere. For a large yield burst, this region may look something like Figure 2. At this point, it is not necessary to quibble about the details of the configuration or the activity distribution with space and particle size, but simply to say that for a given bomb, there exists a space and particle size distribution of the activity produced. It is interesting to note, however, that on the basis of currently available data, there is marked disagreement on the distribution of activity in space. In the Rand model, as will be pointed out later, the size of the active cloud is smaller than the photographic observations of the CASTLE-Bravo cloud would indicate. Thus, although the figure indicates an active particle falling from the edge of the cloud, this is schematic and has no significance in the Rand model.

DOE ARCHIVES

The thermal and kinetic energy which produced the cloud and caused it to rise through the atmosphere has, by the time of stabilization, been dissipated and the particles will begin to fall under the force of gravity. If particles in the size range from 100 to 1000 are considered, it becomes necessary to consider the aerodynamics of the particle. No matter what value is used for a drag coefficient, the density of the air must enter the equations and the particle will fall more rapidly in the less dense atmosphere at high levels.

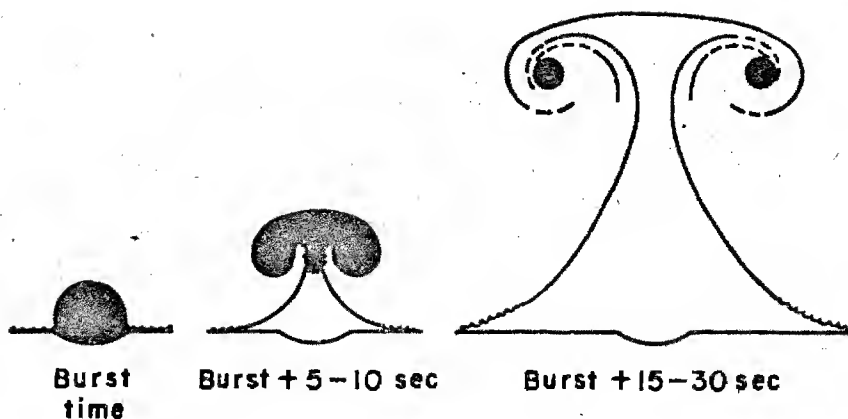


Figure 1
Surface Burst - Schematic Representation of the Manner in which Earth is mixed with Fission Products and carried to great Altitudes

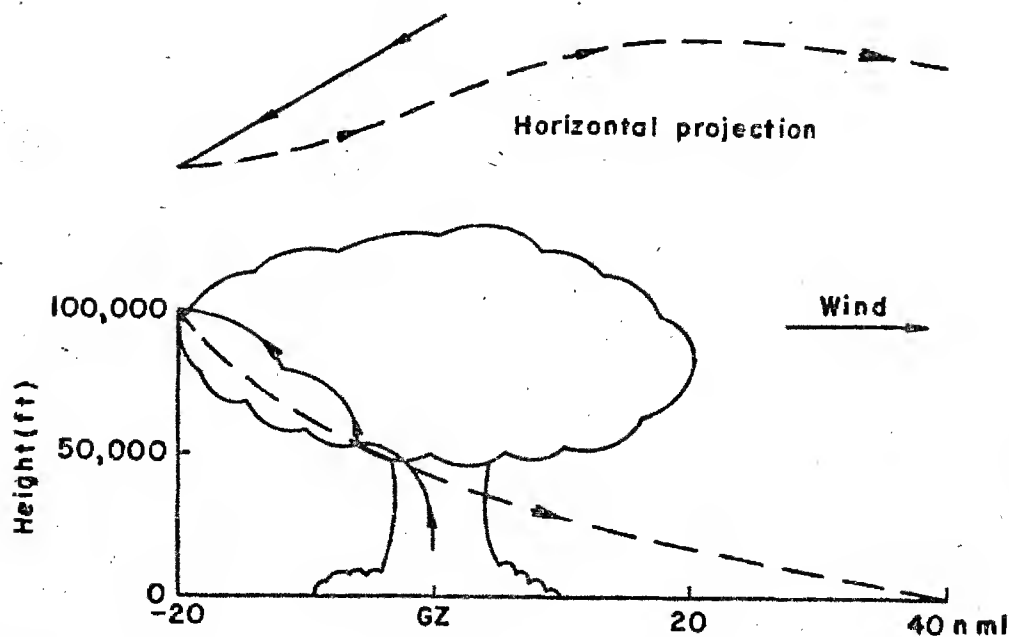


Figure 2
Path of a Particle - Schematic showing the Stabilized Cloud and the Idealized Path of One Particle

Figure 3 shows some possible assumptions about the fall velocities of the radioactive particles. The Rand curves are based on the aerodynamic fall of spherical particles as set forth in an article by Langmuir, whereas the NRDL curves are based on the formulae of Dalla Valla. The line labeled Stokes' Law is included mainly to show that it does not give the proper velocity variation with height and that it over-estimates the velocities of all except the very smallest particles. The variation of velocity with height is extremely important when computing the distance a particle will travel, since the more rapid fall through the upper layers means that the particle will spend a relatively shorter time in the upper wind flow than it will in the dense air near the surface. Referring back to Figure 2, it may be noted that the vertical section shows the particle falling faster in the high levels than it does in the low levels. The horizontal section of Figure 2 shows the erratic path a particle may take due to the action of the wind. It should be noted that the term wind implies all the components, scales and variations of the air movement. It may be informative to look at some of the wind factors which must be considered.

The picture of the motions of the atmosphere that one gets is very much a function of the sensitivity and spacing of the measuring instruments. The established weather networks, in which the instruments are spaced at large intervals, indicate a rather smooth flow of air with perturbations from the mean motion which are the size of cyclones and anticyclones. These perturbations change with time so that time and space variations must always be considered. For example, a steady change of a velocity component of 2 knots per hour could make a position error of 24 miles in 12 hours. If more sensitive instruments are used at a closer spacing, it is found that there are smaller perturbations imposed on the larger ones. There have been relatively few experiments with close networks, but the experiments which have been made show that perturbations may be found on almost any scale of measurements. The total motion of the atmosphere can, therefore, be represented by a spectrum of motions on different scales. Such a representation provides a useful mechanism for separating the motions into those which can be readily measured and those which must, for lack of observation, be treated statistically.

DOE ARCHIVES

An important feature of the spectrum of motions in the atmosphere is its variability in time and space. Large gaps in the spectrum apparently appear and disappear as the characteristics of a mass of air change with time because of mechanical and thermal effects. Sketch A, Figure 4, shows the effect of the large scale motions which move the cloud bodily. Sketch B shows the effect of motions on a scale comparable to the cloud dimensions. These motions tend to distort the cloud from its original shape and may cause an error up to 20 percent in the computed position of a particle on the ground. Sketch C indicates that motions on a scale, small compared with the horizontal cloud dimensions, tend to spread the cloud by drawing

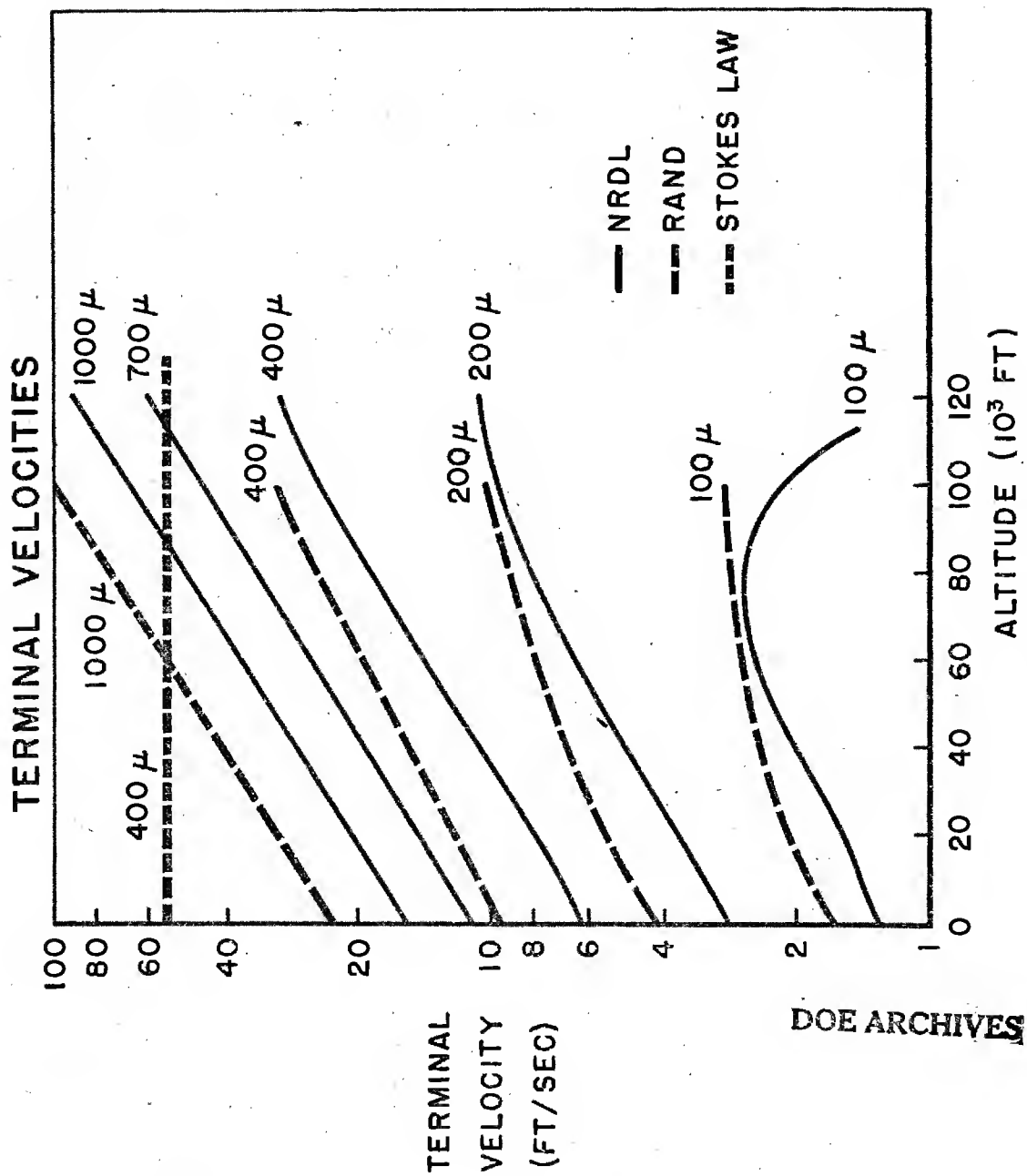
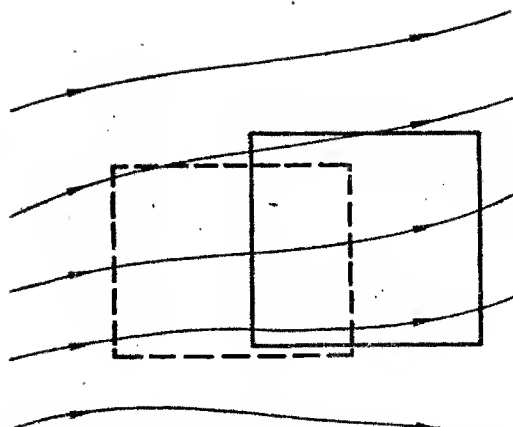
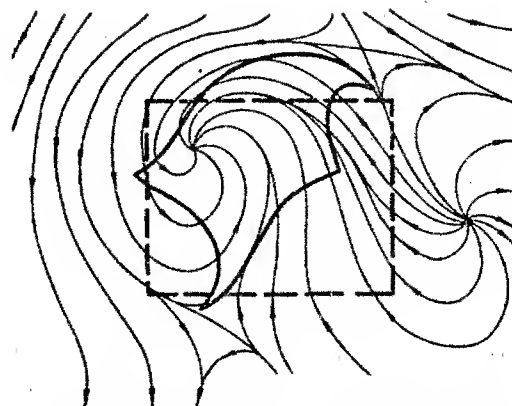


Figure 3
Comparison of the Fall Velocities under Several Assumptions
as a Function of Height

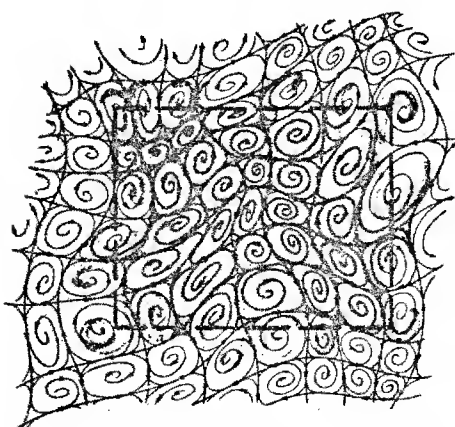
DOE ARCHIVES



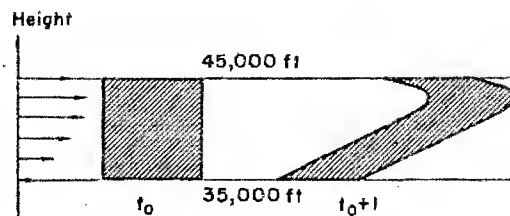
(A) Gross movement—atmospheric motions of a scale large compared with cloud dimensions



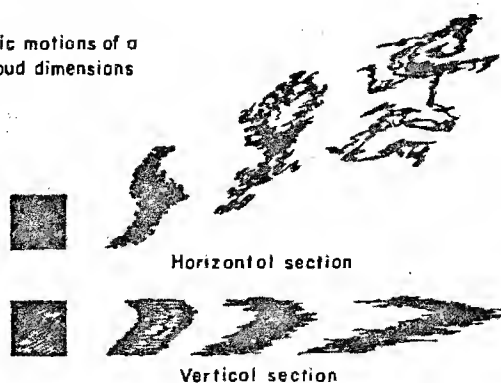
(B) Horizontal deformation—atmospheric motions of a scale comparable to cloud dimension



(C) Eddy diffusion—atmospheric motions of a scale small compared with cloud dimensions



(D) Vertical deformation—shear of horizontal wind in the vertical



(E) Total effect of gross movement, deformation, and eddy diffusion

Figure 4
Schematic Diagram showing Effect of Different Sized Eddies
on a Cloud of Material

333

DOE ARCHIVES

338

out small wisps of cloud matter from the edges and carrying clear air into the cloud; this type of phenomena is called eddy diffusion. Eddy diffusion spreads the cloud very slowly and may be neglected for short periods. Sketch D shows how the change of wind with elevation tends to shear the cloud into a long ribbon. The last sketch, E, is a schematic view of the integrated effects of these various motions on the cloud.

The breakdown of the atmospheric motion into different scales is, of course, highly artificial. Such a breakdown is dictated by the available measurements and by our ability to analyze them. The gross movement and the gross deformation in the vertical can be conveniently, if not accurately, handled by recourse to actual weather observations. The horizontal deformation and the eddy diffusion are, however, on much too small a scale to be observed by our present network of stations. With such a small scale of motion, it is necessary to resort to some type of eddy diffusion theory or to rely solely upon empirical evidence gathered from the tests that have been made. Since neither the empirical evidence nor the eddy diffusion theories show much spread, diffusion has been neglected.

A bit earlier, the distribution of activity with particle size was mentioned. There are two methods for arriving at such a distribution. One is to measure a large sample of collected particles, as is done by NRDL, and the other is to choose, by trial and error, a distribution which fits an observed case. At Rand, the latter method was applied to JANGLE S to derive a distribution. ARDC uses basically the same technique, but with different assumptions. Figure 5 shows a comparison of Rand, NRDL and ARDC distributions. The studies made by the Weather Bureau Group on reconstructing activity distribution with size and height for tower shots had found still another distribution. It is quite possible that there are changes in the distribution from shot to shot. Thus, in order to compute fall-out, it is necessary to know the space distribution of debris, which is known only by inference; the distribution of activity with particle size, for which no general law is known; the fall velocity of the active particles, which has not as yet been determined experimentally; and the wind in all its particulars, a requirement which is economically unfeasible. It is obvious that with the uncertainties inherent in the data now available, it would be unreasonable to expect any model to reproduce the observed fall-out with a great deal of accuracy. It might be possible to compute within five to ten percent of the relatively close observation where the heavy particles spend the least time in the wind field. For more distant observations, it may be possible to be within a factor of two for the highly significant observations, but on the fringes of an area, fall-out may be computed where none was observed and vice versa due to the unknown factors of the wind variation.

DOE ARCHIVES

FRACTION OF RADIOACTIVITY ON PARTICLE SIZES SMALLER THAN THAT GIVEN ON THE ABSCISSA

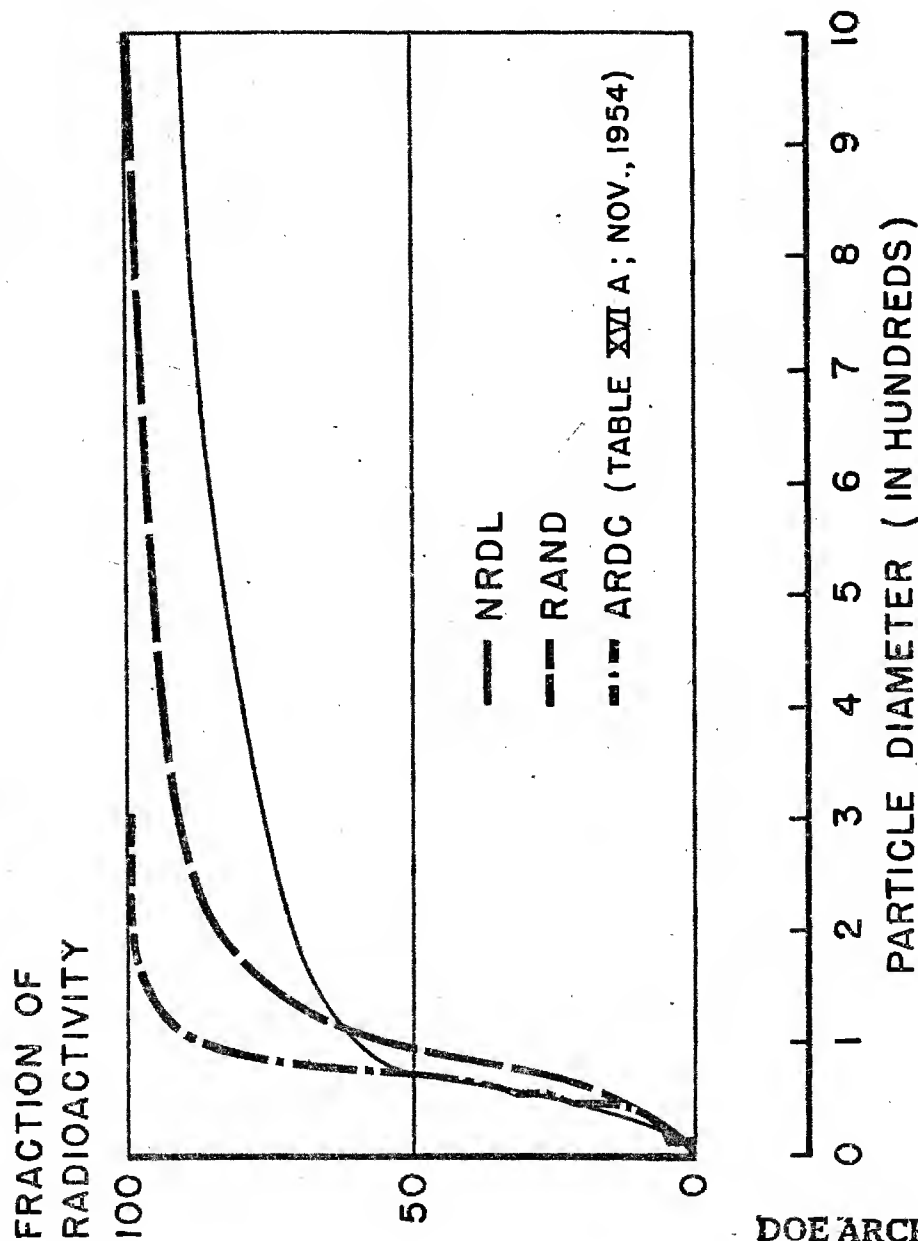


Figure 5
The Distribution of Gross Fission Activity with Particle
Size According to RAND, NRDL, and ARDC

DOE ARCHIVES

The Model

With all this uncertainty, it is still necessary to fix on some of the physical parameters in order to make computations. Therefore, a model appropriate to CASTLE-Bravo will be presented (see Figure 6). The assumptions used at Rand are, first, the distribution of activity with particle size deduced from the JANGLE surface shot data. We are currently of the opinion that the high temperature and large volumes of soil produce the characteristics of the activity distribution, but at present we have little to offer in support of our thesis. Our computations were based on early measurements of cloud diameters and heights, and have not been modified because the smaller sizes seem to fit the observation adequately. Our early model assumed homogeneous distribution of the material in the cloud and stem. We also assumed that the cloud and stem were cylinders. Recently, we have modified our concepts and adopted an exponential decrease in the activity within the cloud.

The assumption on the fall velocities is that the particles fall as though they were spheres.

For the winds, we have used two assumptions, both quite simple. First, we assumed that the winds at shot time apply to the entire descent of the particles. As the next more complex assumption, we have assumed that the time variation of the wind was more important than the space variation. These assumptions are shown for the Bravo shot in Figure 7.

We have neglected the effects of medium scale motions and turbulence simply because there is no simple way of including these effects. They would tend to spread the cloud, but they would not spread it in a uniform way. Thus, if a spread parameter were included and an even spread of the material were assumed, it would tend to cover a large area, but would smooth out the value of the hot spots. Without a spread parameter, the concentration of material is about right, but the clumps are not distributed over the proper area. Since we do not believe that we can place the debris accurately, we have decided to accept the position error and hope to keep the proper concentrations.

The Synthesis

DOE ARCHIVES

Having outlined the physical parameters of the Rand model, it is now necessary to go on to a method of computation. The machine method will be discussed later. This paper will be confined to the hand computational scheme.

Consider a section of the cylindrical cloud extending from h to $h + dh$ containing particles of a size range r to $r + dr$. Let $a_1(r, h)$ be the activity contained on these particles in this height interval over

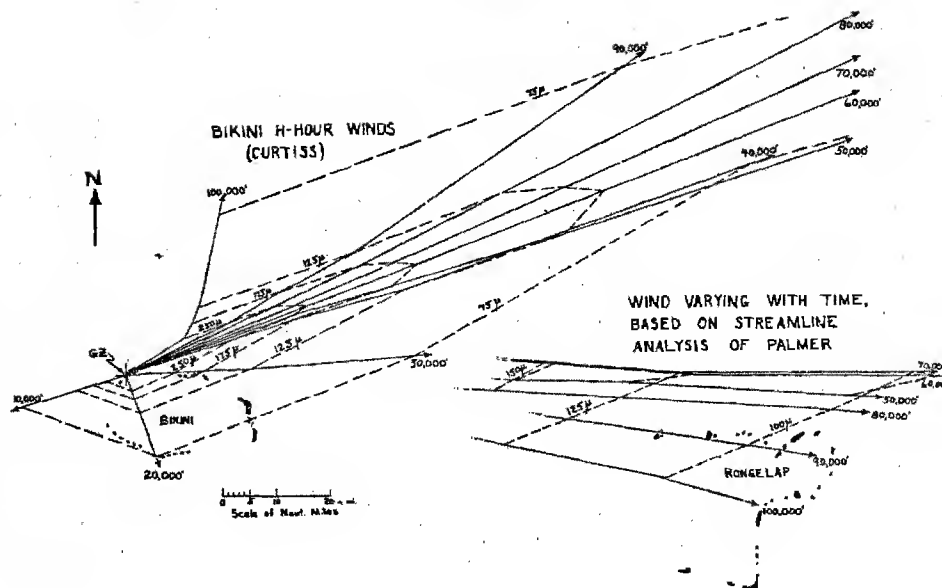


Figure 6
A schematic of the RAND Model showing the Spatial Dimensions of the Cloud, the Relative Distribution of Activity with Height, and the Distribution of Activity with Particle Size

MODEL FOR CASTLE "BRAVO"

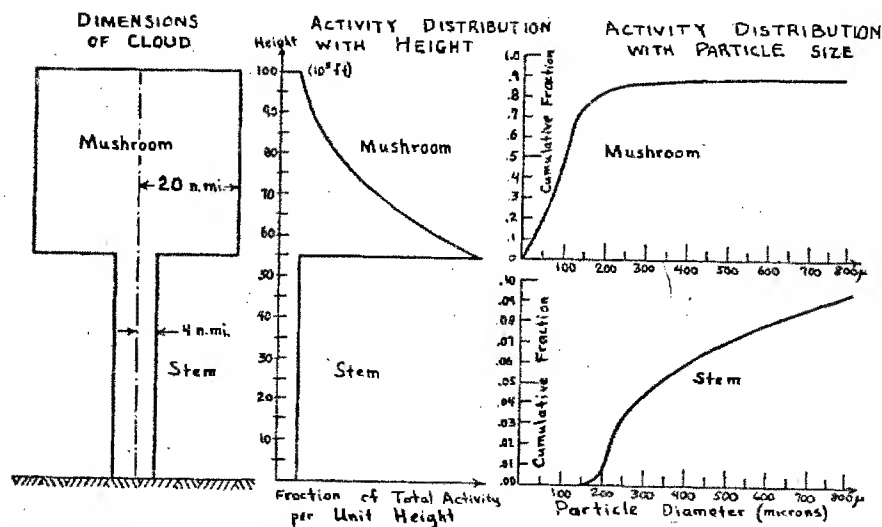


Figure 7
A Plot of the Position on the Ground of Particles of Size r , from Heights h for the CASTLE-Bravo Event. The Main Plot is Following the H Hour Winds. The added Sector Shows Time Variant Winds according to the Oahu Research Center Report.

a unit horizontal area of the cylindrical section. When all of these particles fall to the ground, the surface concentration will be simply

$$\sigma(r, h) = a_1(r, h)$$

Now it is necessary to determine $a_1(r, h)$ in the light of the assumptions of the model. First, it is assumed that, within the mushroom, the distributions in the height and particle size are independent. That is,

$$a_1(r, h) = K A(r) G(h) dr dh$$

Where K is the total activity per unit horizontal area of the cloud and A and G are distribution functions. Next, it is assumed that A(r) is the JANGLE distribution. This A(r) is now a density function and is the derivative of the curve, presented as the Rand curve in Figure 5. For G(h), it has been assumed that the distribution of particles follows the density distribution of air so that $G(h) = G_0 e^{-a(H - H_B)}$ where H is the height of a point in the mushroom and H_B is the height of the base of the mushroom.

Thus for the small cylindrical section

$$\sigma(r, h) = a_1(r, h) = K A(r) G_0 e^{-a(H - H_B)} dr dh$$

This is the surface density of activity for a point on the ground due to the particles of size r to r + dr from the height h to h + dh.

It is possible to find the coordinates of this point on the ground as follows: If $V_x(h)$ and $V_y(h)$ represent velocity components, then

$$dx = V_x(h) dt \quad \text{and} \quad dy = V_y(h) dt$$

But $W(r, h) = \frac{dh}{dt}$ thus $dt = \frac{dh}{W(r, h)}$ where W(r, h) is the vertical velocity. These are derived for all (r, h) from the aerodynamic fall of spheres, a sample of the variation was shown in Figure 3. Now

$$D_x = \int_h^0 \frac{V_x(h)}{W(r, h)} dh \quad D_y = \int_h^0 \frac{V_y(h)}{W(r, h)} dh \quad \text{DOE ARCHIVES}$$

D_x and D_y are distances traveled by a particle of radius r, from a height h. The actual position of a particle will depend on its initial position in the cloud. If the origin is placed at GZ and (x_1, y_1) is the initial displacement from GZ,

$$x = x_1 / D_x$$

$$y = y_1 / D_y$$

$$\approx x_1 / \sum_{J=1}^K \frac{V_x(h)}{W(r,h)} \Delta h$$

For any given point, say (x_0, y_0) , there will be many sets of r, h values which can reach the spot. If a grid is made of the x, y positions from the center of the cloud for a large number of r, h values, any r, h value from the center of a cloud which lies within a cloud radius will contribute to the activity at the point (x_0, y_0) , since the spread of the cloud has been neglected.

Since $\sigma(r, h)$ is the surface density of activity due to one particle size from one height, the total density at $x_0 y_0$ will be

$$\sigma_T = K \int_{r_1}^{r_2} \int_{h_1}^{h_2} A(r) dr G(h) dh$$

DOE ARCHIVES

If $R_1 = \int_0^{r_2} A(r) dr$

And $H_1 = \int_{H_B}^H G(h) dh$

Then $\sigma_T = K \int_{r_1}^{r_2} \int_{h_1}^{h_2} dR_1 dH_1$

Thus σ_T is equal to a constant, depending on the size of the cloud and the total activity in the mushroom, times the integral which is an area on an R_1, H_1 plot.

In order to compute the activity at a point, assuming all the activity has fallen out, the (x, y) positions of a set of (r, h) pairs starting over GZ are mapped onto the ground. A circle the size of the mushroom is

drawn about the point. The (x,y) positions of the edge of the circle are converted to (r,h) values. These (r,h) values are then converted to (R_1,H_1) values by means of appropriate graphs. These are then plotted on any convenient piece of rectangular graph paper and the enclosed area is measured. This area represents a fraction of a unit area column through the cloud which arrives at the point x_0,y_0 , multiplying this fraction by K gives the surface density of activity at this point.

CASTLE-Bravo

Referring again to Figure 7, the time variant winds were used to make the (r,h) plots shown across Rongelap. The 12-hour dose rate at the northern tip of Rongelap from the time variant winds computed by the method just outlined was 52 R/hr. The time of arrival of the debris was from 5 - 14 hours. By using the same system on the Bikini H hour winds, a 12-hour dose rate of 45 R/hr was computed at a point with similar (h,r) values. The observed 12-hour dosage at this island was reported to be 96 R/hr. Thus, with the best winds available, our computations are well within a factor of two of the observations. Using the Bikini winds, we are still nearly within a factor of two, but are about 55 miles off in position. The calculations, based on H hour winds which should be valid for this close-in fall-out, close to G-Z appear to be very accurate.

DOE ARCHIVES

340

~~RECEIVED~~
ATOMIC ENERGY ACT 1954

345

PART II

UTILIZING THE IBM 701 ELECTRONIC DIGITAL COMPUTER

S. M. Greenfield
Rand Corporation

The previous paper by Dr. R. R. Rapp has indicated that it is possible to construct a model which will adequately represent the physical phenomenon of fall-out. In working with the model he presented, we at Rand have found that it provides us with as much of the fine structure of the fall-out pattern as one might reasonably expect when considering the accuracy of the various parameters that go into it. By these parameters, I mean such things as the accuracy of the wind observations, the dimensions of the cloud at stabilization, etc.

As one might imagine, however, having once established what can be considered a representative model, it is not a simple task to use it for computing a fall-out pattern containing the fine structure that can be expected to result from the quality of the input data under normal conditions. One does not just sit down and, in a short half-hour or hour, construct a complete pattern. Rather, it may take as many as two people as much as a day to finish one of these. While a method requiring this many man-hours is certainly adequate if one were only interested in one or possibly two or three patterns, it falls far short of desirability when one enters into a general fallout study. This is true whether the study involves an investigation of the phenomenon of fall-out or an investigation of the implications of the phenomenon in an operational sense.

We at Rand are faced with both problems in our fall-out study. We would very much like to examine how the patterns change as one varies the wind structure with time and space, the distribution of activity with particle size, and the concentration of activity with altitude. Also, due to the peculiar nature of Rand's work, we have a very definite need for fall-out information as an input into an overall weapons employment study. As such, we have been painfully aware of the shortcomings of the hand computation of the fall-out pattern for many months. However, at Rand we are very fortunate in having available both an excellent digital electronic computer like the IBM 701 and a very capable staff of problem programmers for this machine. Working with two of these people, Miss Shirley Marks and Mr. Dave Langfield of our Numerical Analysis Division, it was recently found possible to place the model that has been described previously, or one with a slight modification, on the IBM 701 for computational purposes. As in the case of the hand computation method, the machine model recognizes the fact that the r,h

plot (that is, the positioning of particles, of different radii starting from different altitudes, on the x,y grid representative of the ground) is the basic bit of information necessary for the pattern calculation, and it is toward this end that the initial (and major) segment of the program calculation is slanted. However, it should be noted that, due to the computational speed of the 701, we have at our command the capability of making a much finer grid of (r,h) than was feasible by means of the tedious hand computations. Because of this advantage, we have chosen to subdivide the atmosphere into 1000 ft. intervals, this being a limit imposed on us as being about the smallest intervals at which winds are reported. In the case of radii of the particles, one-hundred intervals of particle size were chosen as being adequate to treat the problem. These intervals were chosen so as to contain equal fractions of the total activity in the cloud. It was initially assumed that within either the stem or the mushroom, the activity distribution with particle size was invariant with altitude. We then have, essentially, two matrices of particle size and altitude, one representing the stem and one the mushroom. Choosing the value at the center of both the particle size interval and the altitude interval as representative of both the intervals themselves, we can then tag each r,h combination with its appropriate fall velocity as described in the previous paper, assuming that this fall velocity taken for each r,h applies over the entire interval. Due to the fineness of the interval divisions, it is found that this assumption is true to within a maximum of one or two percent. These matrices provide us with the first part of our basic input for the machine. It should be noted that by choosing the particle size intervals so as to contain equal fractions of the activity, we have made these matrices independent of bomb yield. In other words, if we can fix on a distribution of activity with particle size, then each matrix can be constructed so as to include all necessary altitudes and then be included in the program as a semi-permanent part of the memory. For a specific case then, providing the machine with information as to the vertical dimensions of the cloud, and the variation of wind velocity and direction with altitude, will allow it to compute the position of the r,h grid on the ground.

DOE ARCHIVES

For this computation, it is assumed that all the particles are distributed along a line extending vertically upward from ground zero (the particles present at each altitude are fixed by the distribution assumed for the stem and mushroom). Under this assumption, the machine then proceeds to solve the following analytical equations:

$$x = \sum_h \frac{V_x(h)}{W(r,h)} \Delta h$$

$$y = \sum_h \frac{V_y(h)}{W(r,h)} \Delta h$$

Where $V_x(h)$ and $V_y(h)$ are the x and y components of the wind as a function of altitude, ΔH is the 1000 ft. altitude interval and $W(r,h)$ is the fall velocity applicable to a given particle size and altitude. Choosing an r and an altitude at which to start, the machine then holds the particle size constant and merely sums over the altitude to determine its x or y position on the ground. This process is presented schematically in Figure 1 where each dot represents the ground position of the r,h combination. At the same time, consideration is given to the expression $\frac{\Delta h}{W(r,h)}$ which is simply the time spent by a particle in each altitude interval. By summing this expression over altitude, we therefore have not only the ground position of each r,h combination, but also the time that it arrives at the ground.

As was stated previously, each r,h combination represents a given fraction of the total activity. Recognizing further that this fraction is contained in a slab whose thickness is 1000 feet and whose cross-sectional area is the cross-sectional area of the mushroom or stem, then the machine, having been given the yield of the bomb and the dimensions of the cloud can calculate the "infinite plane" gamma radiation effect of this slab when deposited on the ground. To do this, we utilize the well known relationships for gamma radiation from fission products

$$\text{Number of 1 hour megacuries/KT} = 300 \quad (3)$$

$$\frac{\text{Roentgen}}{\text{Per Hour}} \text{ at 1 hour} = r_1 = \frac{F(r,h) 300}{A} (3.09) \quad (4)$$

DOE ARCHIVES

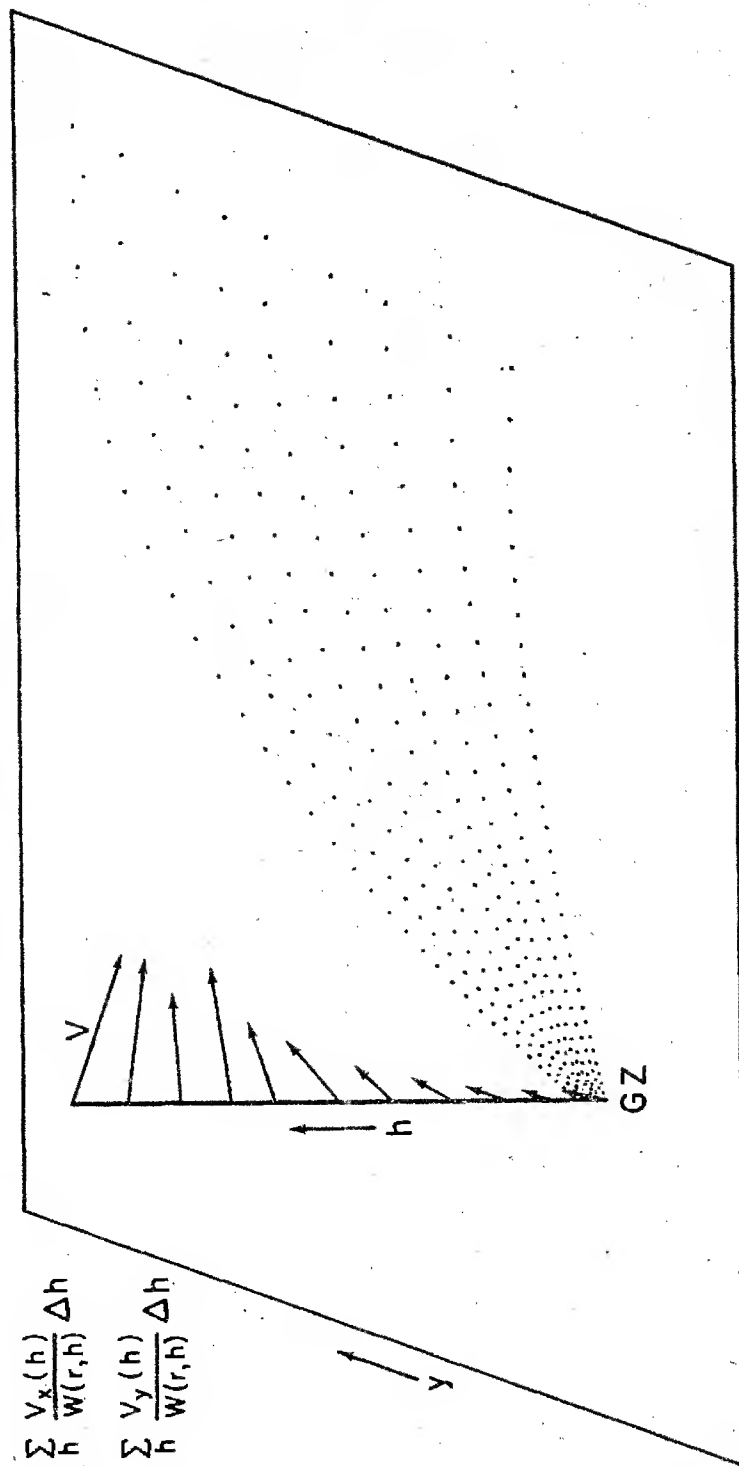
Where $F(r,h)$ is the fraction of the total activity associated with a given particle size at a given altitude, and A is a cross-sectional area of the mushroom or stem in square nautical miles, and 3.09 is the conversion factor for megacuries per square nautical mile to roentgens per hour at 1 hour.

$$r_t = r_1 t^{-1.2} \quad (5)$$

Where t is the time in hours, and r_t is the dose rate at any time t. And finally

$$R_{\Delta t} = \int_{t_1}^{t_2} r_1 t^{-1.2} dt$$

COMPUTED x, y POSITIONS OF PARTICLES FROM A LINE SOURCE



$$x = \sum \frac{V_x(h)}{h} \frac{\Delta h}{W(r, h)}$$

$$y = \sum \frac{V_y(h)}{h} \frac{\Delta h}{W(r, h)}$$

Figure 1

DOE ARCHIVES

344

349

[REDACTED]

where $R_{\Delta t}$ is the dosage accumulated over a time interval between t_1 and t_2 .

It was decided that the machine would calculate the dose rate at $t = 6, 12, 24$, and 48 hours after the bomb explodes, and the dosage accumulated between 0 - 6, 6 - 12, 12 - 24, and 24 - 48 hours. Implicit in this is the understanding that for any time or time interval occurring earlier than the computed time down for a particle, the dose rate and dosage that the machine will report will be equal to zero.

Having available many thousands of r, h combinations, positions on the ground and their radiation contribution as a function of the time, we can then proceed to calculate radiation levels at specific points within this pattern. Due to the fact that it has been found that about 100 points scattered representatively throughout the r, h grid are sufficient to determine the fall-out pattern, it is pointless to attempt to compute the radiation level at each of these many thousands of points and present them as a final output. What was done then was to choose 125 of these (r, h) combinations in such a way as to make them representative of the entire pattern. As illustrated schematically in Figure 2, this was accomplished in the following way. It is assumed that a representative set of grid points would have a density that was directly proportional to the gradient of density of radioactive material on the ground. Further, it is felt that the variation in time down for particles at the same altitude is a fair approximation to their relative positions on the ground. Under these assumptions, particle sizes were chosen at each 10,000 feet of altitude shot for the following times down:

Every .2 hour for the first hour.

Every .5 hour for the next four hours.

Every hour for the next five hours.

Every 2 hours for the next ten hours.

The r, h combinations resulting from this type of selection were taken as grid points with some degree of confidence that they truly are representative of the entire pattern. It should be noted that having once chosen our grid points, or r, h combination, we need not concern ourselves with the problem of how the pattern changes as a function of different wind inputs. This is due to the fact that grid points chosen in this manner will appropriately arrange themselves within the pattern with the wind so as to maintain their representativeness.

DOE ARCHIVES

It is in the final stage of this machine calculation that the dimensions of the cloud really come into play. It should be remembered,

SELECTED PATTERN OF GRID POINTS AT
WHICH RADIATION WILL BE COMPUTED

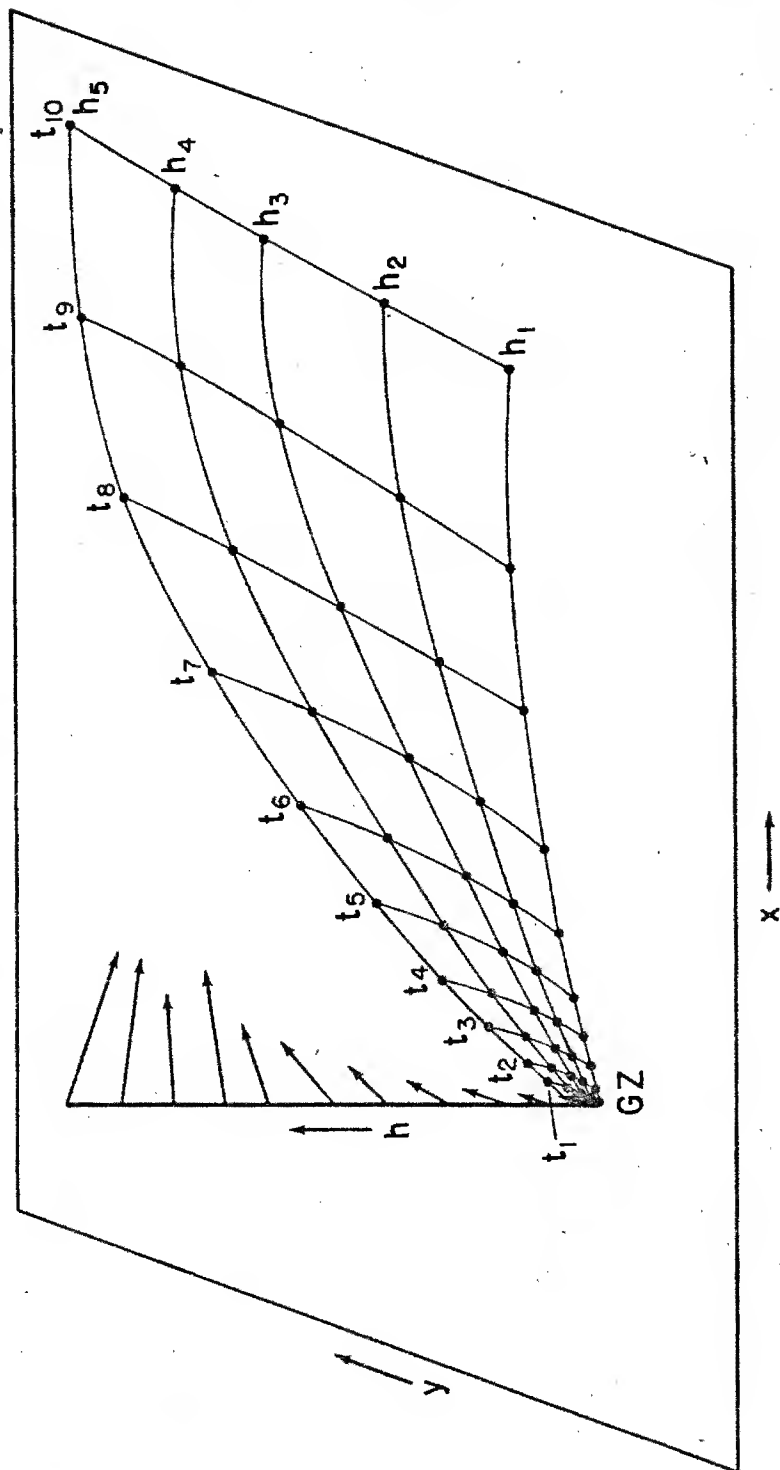


Figure 2

DOE ARCHIVES

SUMMATION OF THE RADIATION CONTRIBUTION FROM PARTICLES
IN THE STEM AND MUSHROOM TO A PARTICULAR GRID POINT

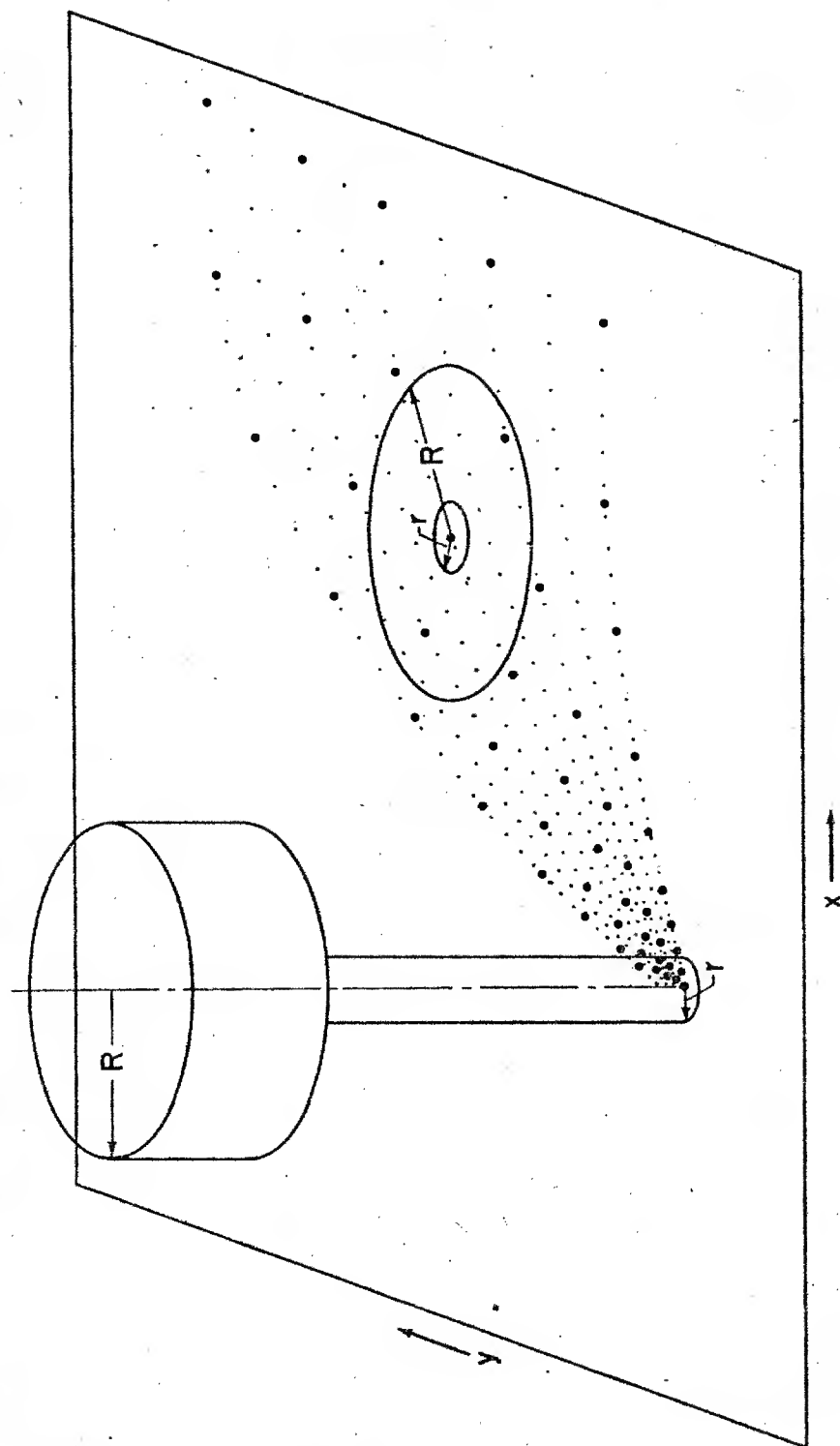


Figure 3

347

DOE ARCHIVES

352

as was stated previously, that each r,h point in the grid actually represents the center of a circle that is the projection of a slab of material onto the ground (slab 1000 ft. thick, cross-sectional area equal to the cross-sectional area of cloud). Furthermore, it is assumed that every ground point within this circle receives an equal radiation contribution from this r,h interval. Conversely, it can be seen that if a circle of radius equal to the radius of the stem or mushroom is drawn around any point on the ground, it will include all r,h combinations that will contribute to the radiation found at this point. This is illustrated in Figure 3. Figuratively, then, the machine draws a stem circle and a mushroom circle around each of the 125 grid points and simply sums the contributions from the appropriate r,h combinations. The final output from this machine calculation is, therefore, the coordinates of 125 points on an x,y grid (whose origin is ground zero), the dose rates found at these points at H / 6, H / 12, H / 24, and H / 48 hours, and the dosages accumulated from 0 - 6, 6 - 12, 12 - 24, and 24 - 48 hours after burst time. As a secondary output, we have available the many thousand of r,h combinations, their locations on the ground, and their associated radiation contributions. This means, in effect, that any other set of grid points can be utilized in conjunction with this data and their radiation levels calculated.

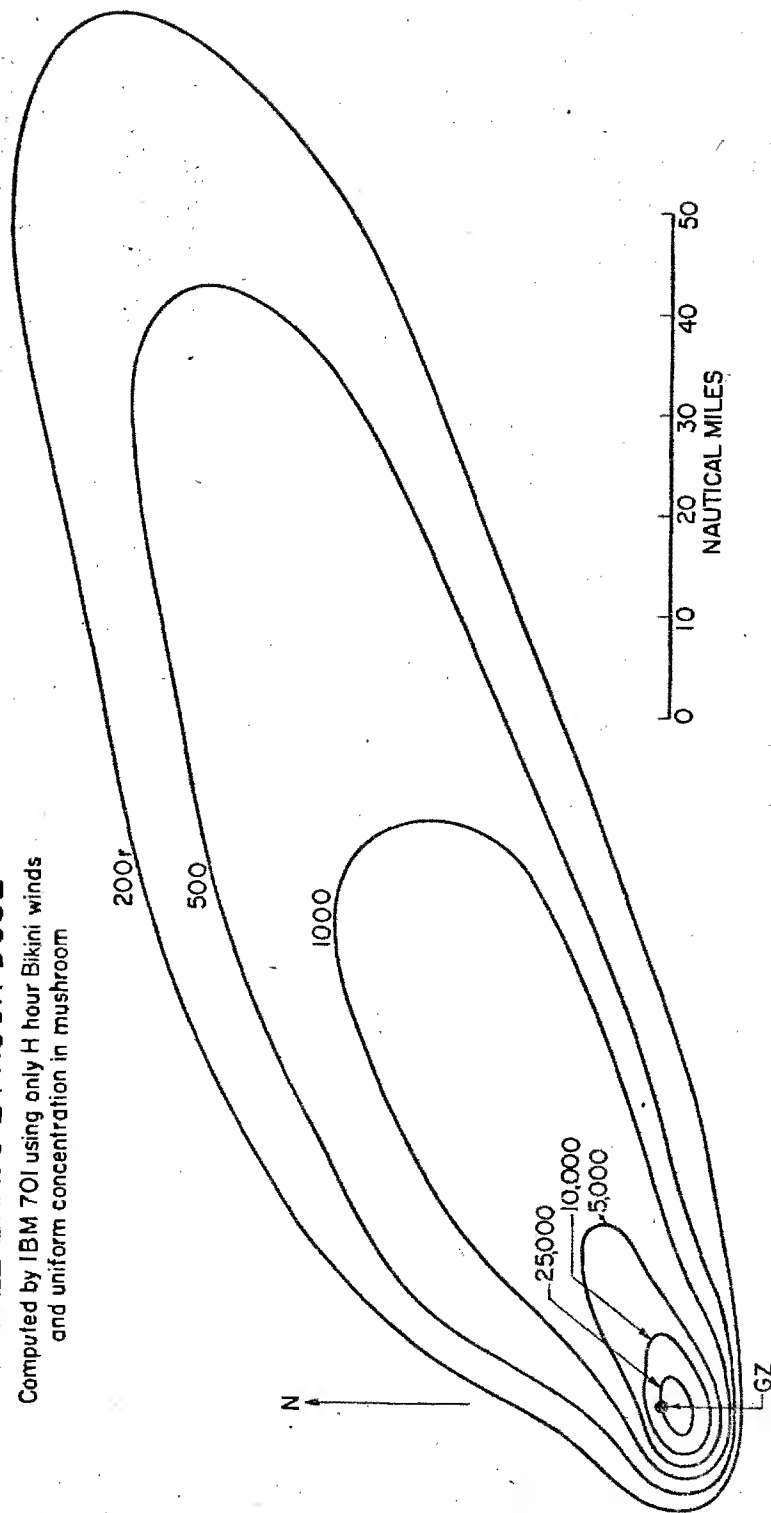
After the winds are fed into the computer, total machine time for a problem of this type is approximately one hour. Since plotting and analyzing the results takes about one-half hour, we can estimate that the total time from problem to pattern is something under two hours.

Let us now examine some results of these calculations. The first problem that was tried on the machine was the CASTLE-Bravo Shot. This was essentially our test of the machine program in that this particular case had been done by the original hand computing method reported in Rand Report R-265-AEC. An attempt was made, therefore, to duplicate the input data used in the initial calculation. In essence, then, the pattern computed by the machine was as wrong as the pattern in R-265-AEC in that it, too, used only the H-hour winds from the Curtiss (the ship near Bikini). This machine-computed pattern for integrated dosage to H / 24 hours is presented in Figure 4. As was hoped, the machine computation duplicated the hand computation surprisingly well. In fact, due to the greater accuracy of the fall velocities input into the electronic computer and the greater detail possible with the machine, the computed pattern duplicates very closely the observed pattern in the vicinity of Bikini where the H-hour Curtiss winds may be assumed to apply with some degree of confidence. This is illustrated in Figure 5 which presents the observed dose rates in the Bikini Lagoon and the pattern computed by the above method. It should be pointed out that the computed pattern does not fit the far out fall-out observed from CASTLE-Bravo. This is to be expected in that one should not hope to duplicate a pattern that

DOE ARCHIVES

CASTLE BRAVO 24 HOUR DOSE

Computed by IBM 701 using only H hour Bikini winds
and uniform concentration in mushroom



DOE ARCHIVES

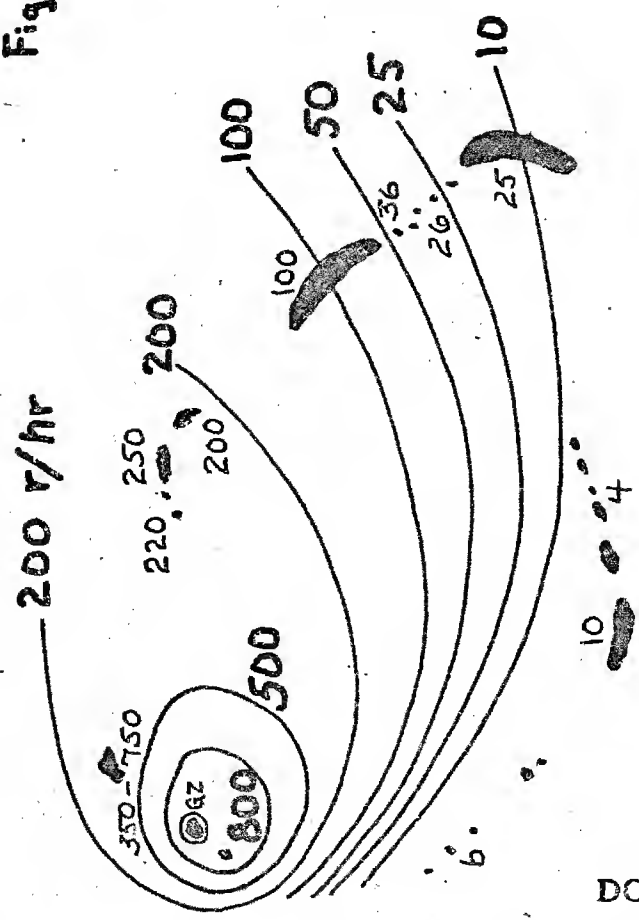
Figure 4

349

ATOMIC ENERGY ACT

354

Fig. 5- DOSE RATE
AT H+6 hours
FOR FALLOUT
OVER BIKINI
FROM CASTLE
"BRAVO"



— XX Computed
by IBM-701

XX Observed

Figure 5

DOE ARCHIVES

took 17 - 24 hours to deposit on the ground stretching over a distance 200 - 300 miles downwind from ground zero utilizing one set of winds for a particular time and place. As was pointed out in Dr. Rapp's paper, however, when this variation of wind in time and space is taken into account, the Rand model does, indeed, produce an adequate reproduction of the observed Bravo fall-out.

Figures 6 and 7 are the 48-hour dosage patterns for respectively a 50 MT bomb under condition "A" and a 1 MT bomb under condition "B". Conditions "A" and "B" are the wind conditions established by AFSWP for test purposes. Since these will be discussed later in this report, they are presented here just as a further illustration of machine computed patterns. It should be pointed out, that following the suggestion of Dr. F. Henriques of Technical Operations, we have gone over to the assumption that the concentration of activity in the mushroom decreases exponentially with altitude. This assumption has been used in all our calculations for conditions "A" and "B". One final point should be made. As was indicated above, to be truly representative, the computation must take into account the variation of wind in time and space. Although this capability has not been utilized in the past, the 701 program is flexible enough to take this into account with a very small modification. Very simply, sets of winds representative of the variation in time and space are placed in the machine memory (these variations being in terms of finite increments of time and x and y distance) in solving equations (1) and (2). Then, for a given r and h, the machine examines the step-wise buildup of x, y and t over the summation, and switches to the appropriate wind set at the proper time and distance. It is hoped that this added refinement will be utilized in the future wherever feasible.

DOE ARCHIVES

RAND MODEL
48-HOUR DOSE—50 MT—CONDITION "A"
COMPUTED BY IBM 701

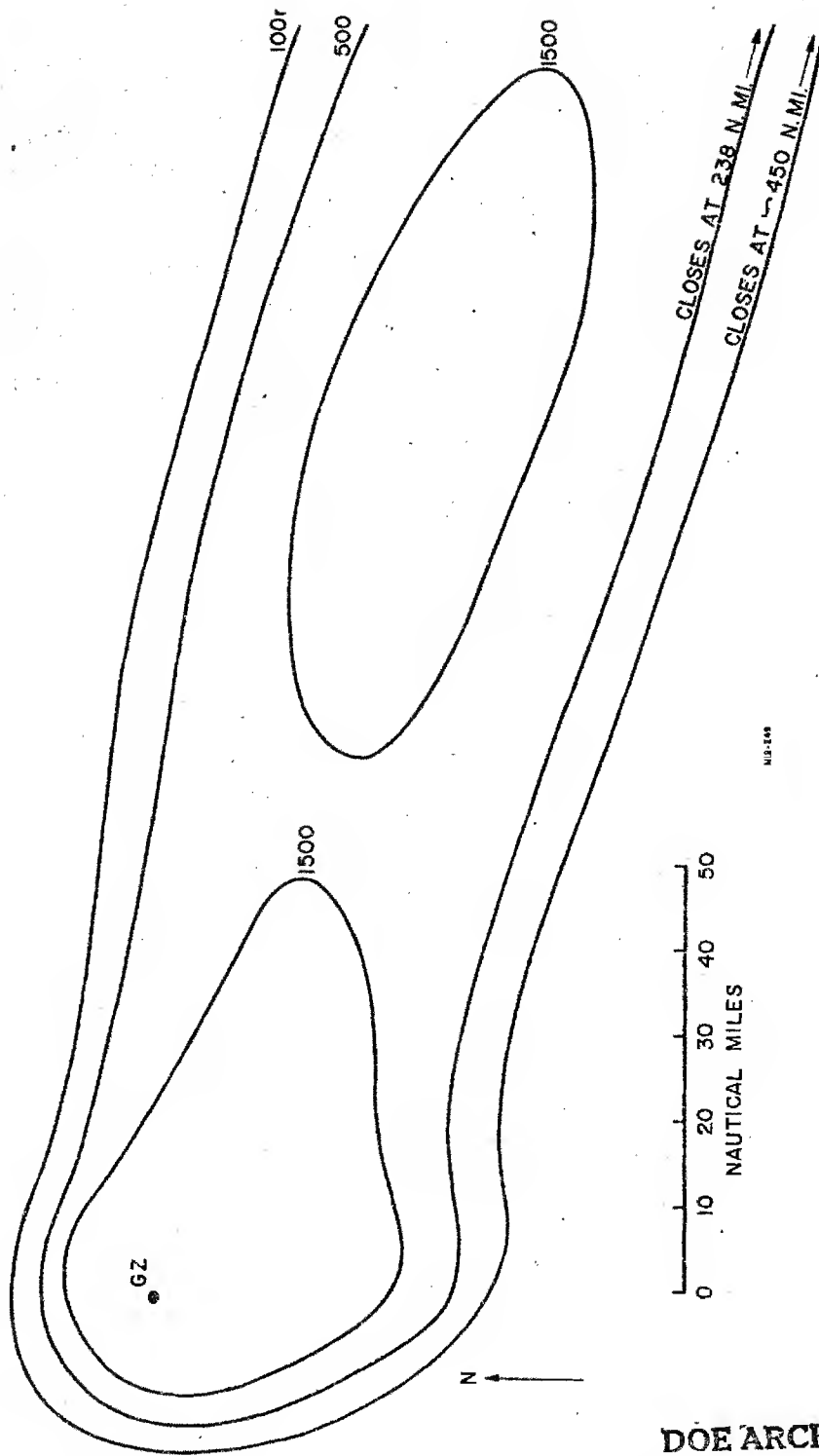


Figure 6

DOE ARCHIVES

RAND MODEL
48-HOUR DOSE — 1 MT — CONDITION "B"
COMPUTED BY IBM 701

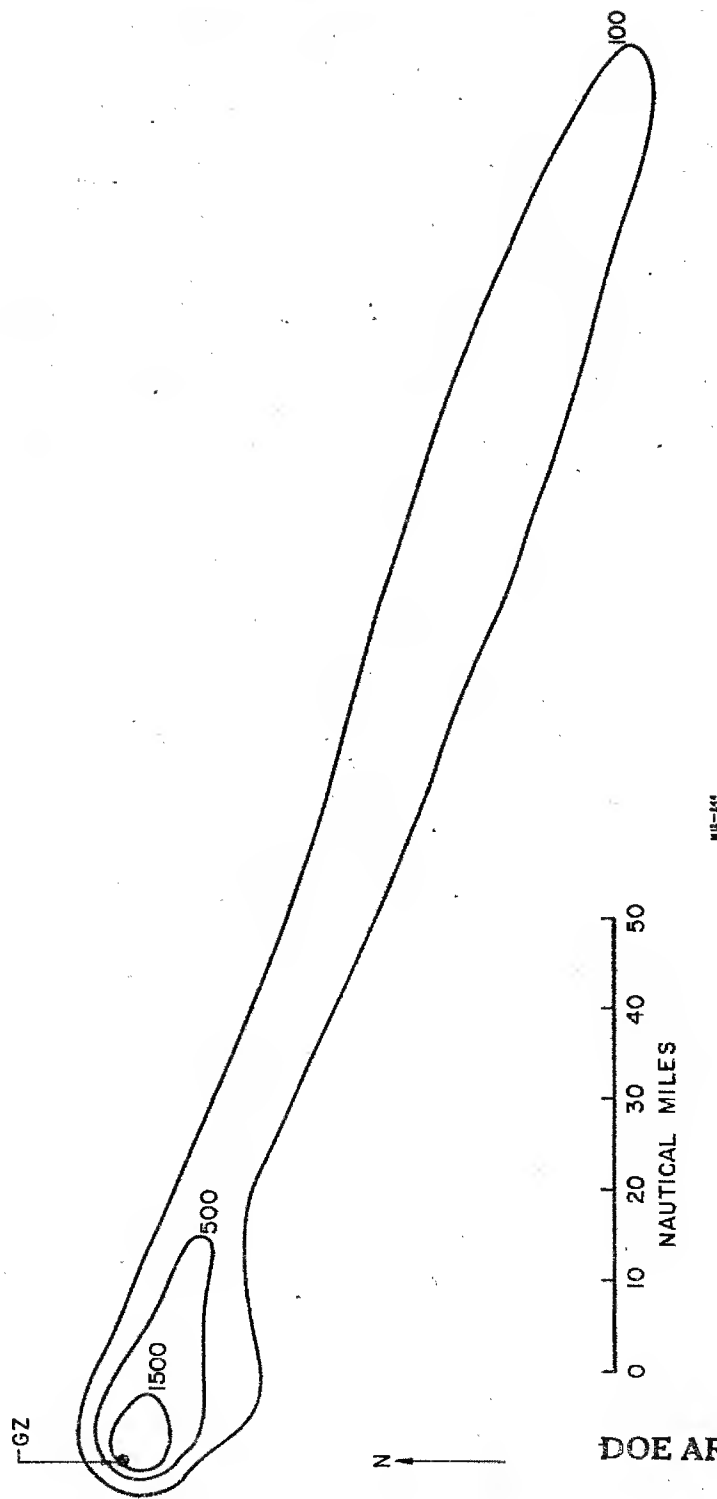


Figure 7

353

ATOMIC ENERGY ACT

358

THIS PAGE IS BLANK

DOE ARCHIVES

354

ATOMIC ENERGY ACT IS

359

[REDACTED]

PREDICTION OF DOSE-RATE AND DOSAGE CONTOURS AS FUNCTIONS OF YIELD
AND METEOROLOGICAL CONDITIONS, U.S. WEATHER BUREAU METHOD

Mr. K. M. Nagler
U.S. Weather Bureau

Introduction

Under contract to the Santa Fe Operations Office of the Atomic Energy Commission, the Special Projects Section of the Weather Bureau has attempted to devise a method of forecasting radioactive fall-out for tower bursts at the Nevada Test Site. In the past, fall-out forecasts have been made by various approximate empirical methods. It was felt, however, that enough data had accumulated during the TUMBLER-SNAPPER and UPSHOT-KNOTHOLE tests to provide a basis for a more logical forecasting scheme. Specifically, we had useable amounts of observational data from nine 300-foot tower shots, ranging from about 11 to about 52 kilotons in yield.

Observations of Deposited Activity

The first phase of our work involved the preparation of maps of the observed deposited radioactivity. We have used primarily the ground monitoring data and have considered the aircraft estimated of radioactivity at the ground merely as approximate information which can provide a rough independent check on our method of determining fall-out.

For most of the data outside the test site itself, the monitors drove along the roads taking readings at intervals of 1-5 miles. Where only a single monitoring run was made along a road, we accepted its reports; but for most roads, there were several runs by different monitors, and the concentrations which we used on the maps of observed radioactivity were a compromise - often a difficult one to make. The discrepancies between two or more monitoring runs along the same road may be due to several causes: redeposition of debris that originally landed elsewhere, removal of debris by wind, instrumental errors, a different rate of decay than that assumed, errors in positioning, or to various other human errors. Figure 1 shows the results of several monitor runs along one road, following the ninth UPSHOT-KNOTHOLE burst. This illustrates many of the uncertainties which are encountered in using the observational data. Two runs give similar peak values but differ markedly to the left of the peaks, probably because the fall-out was not complete when the one run was made. A third peak suggests much lower concentration and is displaced from the other two. The two partial runs obviously do not fit the others very well. One seemed to indicate that the reported positioning was wrong, perhaps due to a faulty speedometer on the monitoring automobile.

VARIATIONS IN OBSERVED ACTIVITY FROM MONITOR RUNS
ALONG ROUTE 93 FOR UPSHOT KNOTHOLE 9 (HARRY)

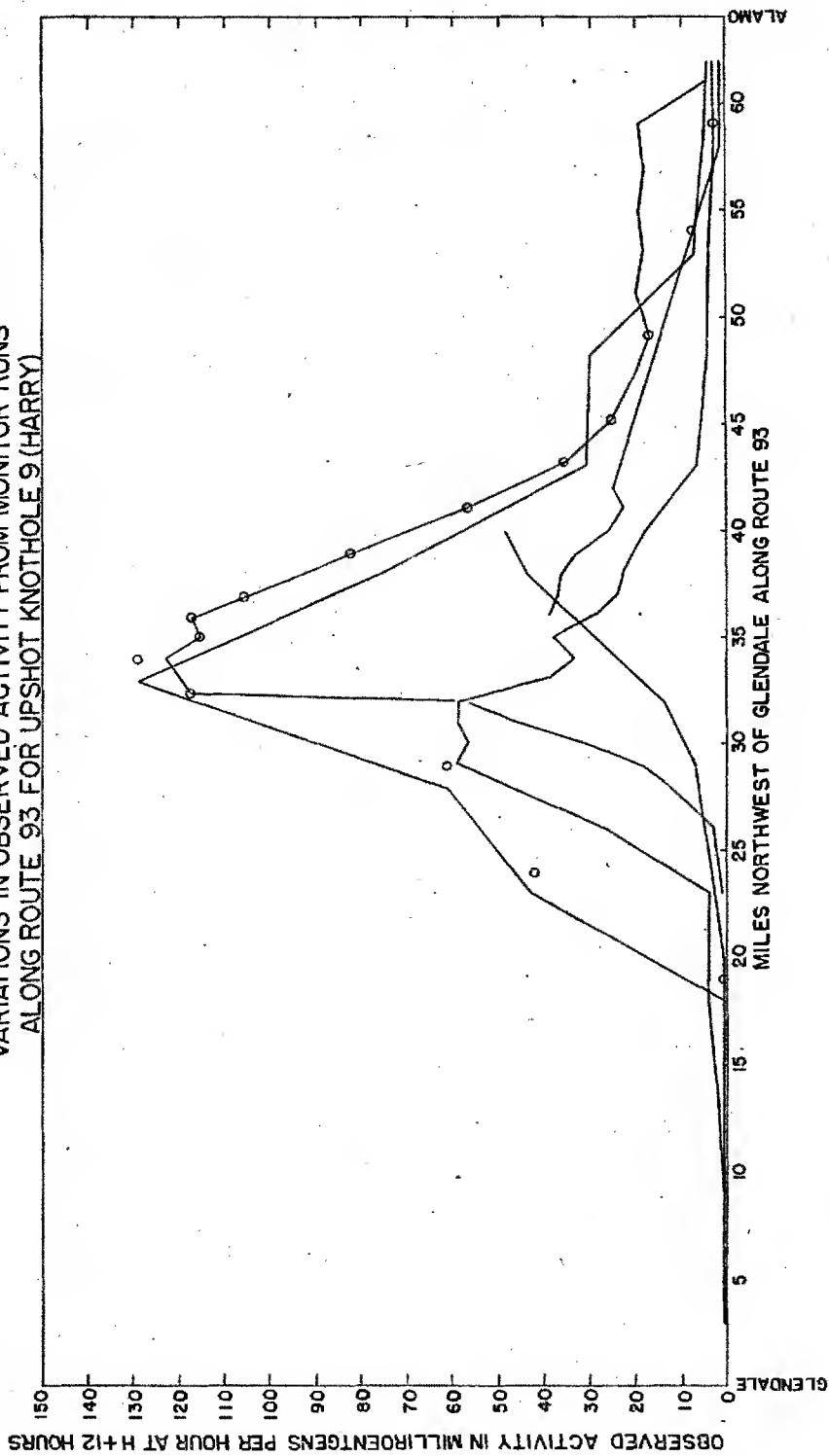


Figure 1

DOE ARCHIVES

356

361

[REDACTED]

This series of monitor runs is somewhat more confusing than most, but not as confusing as some. It must be remembered that these observations of deposited activity were not made with the care and accuracy desirable in a scientific experiment. They were made to determine whether there was any radiological hazard.

At any rate, for each tower burst in the TUMBLER-SNAPPER and UPSHOT-KNOTHOLE series, the observations we selected were extrapolated to a common time (12 hours after the burst) and were plotted on maps in units of milliroentgens per hour.

Fall-out Plots

The second phase of our work called for the preparation of fall-out plots. A fall-out plot or radex plot is an analysis which shows where particles of various sizes falling from various heights will reach the ground, based on the winds and on the assumed rates of fall of particles of the various sizes. A fall-out plot may also include an analysis of the times at which the different particles reach the ground.

Figure 2 gives an example of a fall-out plot for UPSHOT-KNOTHOLE-9. Each curving line shows the estimates of where particles of a certain size should fall, and each radial line indicates the line along which particles originating at a certain height in the atomic cloud are deposited. A line indicating constant time of reaching the ground would pass through large size, high altitude areas to small size, lower altitude areas.

Our fall-out plots differ from the type used previously at Nevada in two basic ways. In the first place, rather than a uniform rate of fall, we used an aerodynamic fall velocity, derived by means of the formulae given in the Rand report on Project Aureole. For the various altitudes, we used air temperatures and densities obtained from a mean sounding during the UPSHOT-KNOTHOLE series. As an example of the effect of the use of aerodynamic fall velocity, a particle in the 150-200 micron range falls only about 7/10 as fast at 10,000 feet as it does at 40,000 feet.

DOE ARCHIVES

The second basic difference from most earlier fall-out plots is that in computing the path of a falling particle, we used analyses of the space and time variability of the wind, not merely the wind reported at the time and place of the burst. In brief, we prepared maps showing the mean winds for each 5,000-foot layer for each three-hour time when observations were available. On the maps each individual wind observation (for a 5,000-foot layer) was plotted at the point over which the balloon actually was when it passed through that layer, rather than at

~~RESTRICTED DATA~~
ENERGY

FALLOUT PLOT
UPSHOT KNOTHOLE 9 (HARRY)

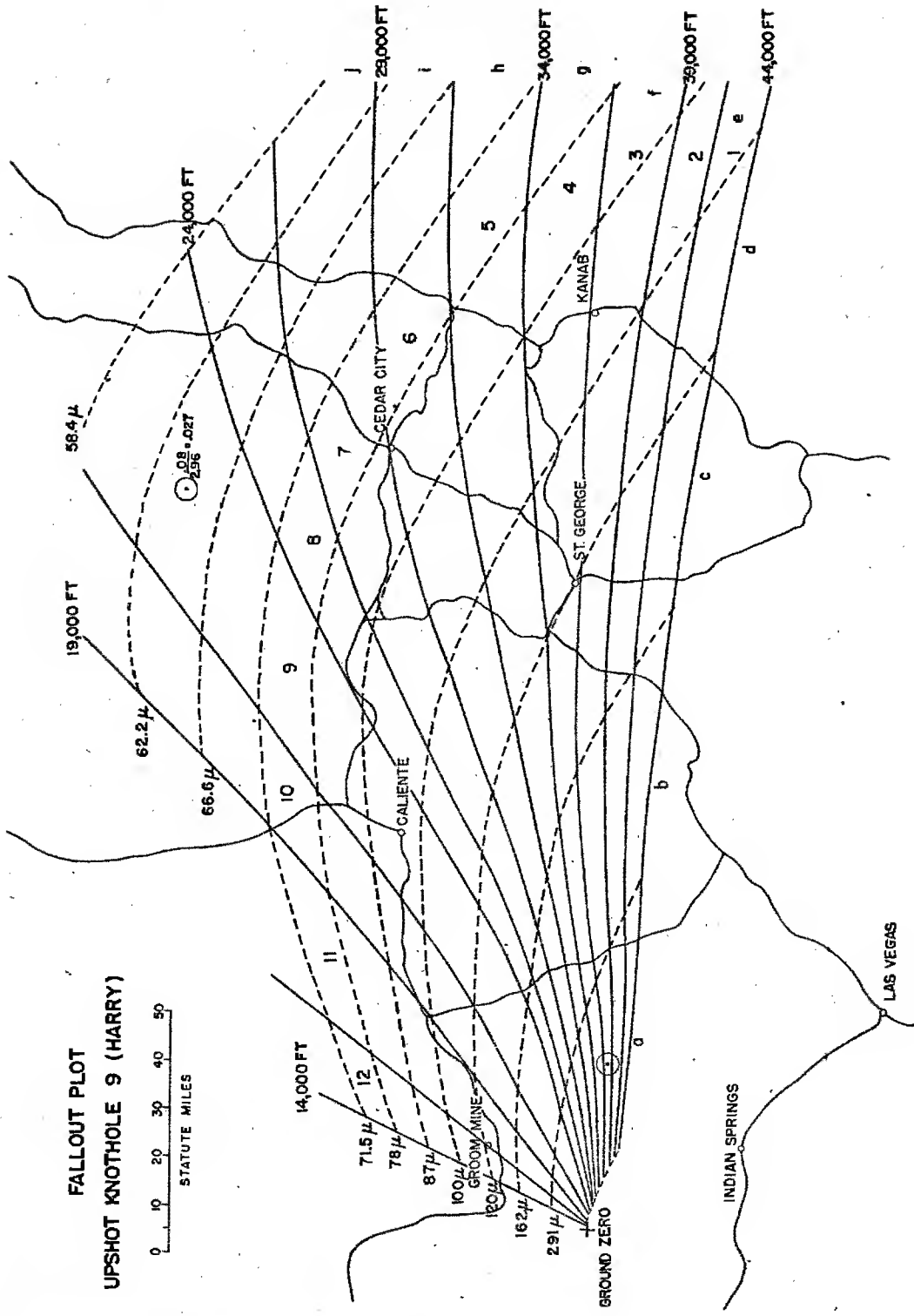
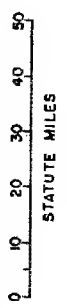


Figure 2

[REDACTED]

the station from which the balloon was launched. Also, the original drift of the rising atomic cloud was taken into account in determining the starting point for the various elevations.

Initially trajectories of particles of six sizes ranging from 60 to 833 microns were drawn, starting from each 5,000-foot level - 10,000, 15,000, 20,000 feet, etc. - and from the reported top of the cloud. Using the space and time changes in wind along the descending trajectory, particles of each size were tracked to the position on the ground or to the 5,000-foot surface (MSL), which with a few exceptions was close to the height of the terrain.

For this initial fall-out plot we interpolated to get convenient intervals of height and particle size, as shown in Figure 2. Our height lines are at 2500-foot intervals, starting with the height of the top of the cloud. The particle size interval was chosen such that the time of fall from 35,000 feet to 5,000 feet is in multiples of an hour. Thus, a particle 291 microns in diameter takes one hour to fall this distance, a 162 micron particle takes 2 hours, etc.

We took considerable care in preparing fall-out plots for the various tower bursts; nevertheless there are still several sources of error.

The trajectories of the falling particle may be in error, due to errors in the wind observations and the analysis. The error in the location of a point is probably less than 10% of the distance away from ground zero. However, the relative error between adjacent points on the fall-out plot is much less.

A further possible source of error is that the rate of fall may be incorrect because the particles are not spherical, have a density different from the 2.5 assumed, or follow a different settling law than the one assumed. However, as far as we have been able to determine, the radioactive particles produced by a tower burst are nearly spherical, particularly those smaller than 200 microns, which contribute mainly to the off-site fall-out. Moreover, data for the few cases for which times of arrival were available agreed with our fall-out calculations. Also, for the second UPSHOT-KNOTHOLE burst, there are particle size observations that seem to verify the aerodynamic law rather than Stoke's law, or uniform descent.

Construction of a Model

DOE ARCHIVES

Equipped with maps of the observed radioactivity along the roads and with fall-out plots for the various shots, we came to our basic

problem, namely to determine the distribution of the debris in the original clouds which would give rise to the ground radiological data.

An explanation of our procedures is in order, however, before we discuss our model of the distribution of debris in an atomic cloud. This fall-out plot, strictly speaking, represents the position where various sized particles from various heights would reach ground, if they originated along the central axis of the cloud or in other words, if the cloud were very narrow. We know, however, that the cloud does have a finite width. We have assumed a cloud to be cylindrical and five miles in diameter at all levels and that the diffusive spread of the cloud over the distances here being considered is negligible compared to the spread by wind shear. As will be pointed out later, the exact diameter chosen is not very important to our computations, so that our use of the same width for both stem and mushroom can be justified.

Let us examine the importance of using a cloud of finite cross-section. If the cloud were not of finite width but were a line source, then each height and particle size in the cloud would correspond uniquely to one point on the ground. With a finite cloud diameter, however, each point on the ground could be affected by a range of particle sizes and heights.

We take the finite dimensions of the cloud into account in a fashion similar to that of the Rand and other groups. We first center a circle of the diameter assumed for the cloud at the point on the fall-out plot for which the fall-out is to be computed. The particle sizes and initial heights which contribute to the activity at the point are those that lie within the circle.

In our model the amount of radioactivity is assumed to be uniform throughout each 2500-foot layer for each particle size range - a, b, c, etc. The mechanical computations of fall-out at a given point are of three types: first, where the circle lies entirely within one of the polygons; second, where the circle contains areas from several polygons; and third, where some or all of the polygons become squeezed into lines or nearly so - that is, the case of little or no directional shear.

DOE ARCHIVES

In the first case, if we know the concentration in appropriate units for each layer and size range, and if the circle lies within the sector, we merely need the ratio of the area of the initial cloud to the area of the sector, as shown by the upper point in Figure 2. This fraction multiplied by the amount of radioactivity assigned to the sector will give an estimate of the concentration at the point.

~~SECRET~~

In the second case, we must find the ratio of each part of the circle to the area in which it lies. Each of these ratios or fractions is multiplied by the amount of radioactivity assigned to the appropriate height and particle size range. The sum of these products gives the estimate of the radioactivity at the center of the circle. The third case - little or no directional shear - will be discussed later.

Here it should be pointed out that the assumed area of the cloud has no effect on the concentration as we would compute it at a point when the circle lies entirely within the bounds of one polygon. And, when the circle covers parts of several sectors, the assumed area is important only when the gradient of radioactivity from one sector to another is large.

The procedure I have just described is the one which would be used when the amount of radioactivity in each height layer and particle size range is known. However, it is this information which was sought.

To get this information, we first obtained the activities which would best fit individually the seven cases with best observational data. Each of these sets of numbers had to be a compromise, as no reasonable model could fit every observation well, and the various sets differed widely. Then, the main problem was to prepare a composite model which would give a best fit to all of the cases.

First, we considered all cases relative to the top of the cloud. Second, to scale for yield, we assumed that the amount of activity is proportional to the area of the ground intersected by the fireball. (This scaling method is a simple one and one which seemed to work reasonably well. Further tests will be made with other scaling methods which are physically more acceptable. Changes in the activity assigned to various ranges of height and particle size may result from changes in the scaling method. The revised values, together with any refinements or simplifications in our procedures, will be given in a forthcoming report.)

DOE ARCHIVES

When we completed our initial composite model, we used it to compute a grid of values - one for each sector on the fall-out plot, for each case. Then, considering how patterns and activities fitted the various cases, we continued to change the model to give a better fit. Figure 3 shows the resulting model, which gives the average activity in the various height and particle size ranges for a typical 20 kiloton bomb. In this connection, it should be pointed out that the total deposited radioactivity is not dependent solely on the yield, but also on the nature of the bomb itself. We have considered this effect only qualitatively, but feel that it may be an important one.

AVERAGE DISTRIBUTION OF RADIOACTIVITY FROM A 20-KT, 300 FOOT TOWER BURST,
 ASSUMING A CLOUD DIAMETER OF 5 MILES. UNITS ARE THOSE WHICH GIVE
 MILLIROENTGENS PER HOUR AT 12 HOURS AT THE GROUND.

Height in feet (MSL)	Particle size (microns)												Total activity for particle sizes greater than 58.3 microns
	a	b	c	d	e	f	g	h	i	j	k	l	
40,000	50	70	60	50	40	30	20	20	10	10	10	10	360
37,500	100	200	150	150	100	50	30	30	20	20	20	20	850
35,000	150	300	250	250	200	100	60	50	30	30	30	30	1420
32,500	200	350	300	300	250	150	70	60	40	40	30	30	1750
30,000	250	200	200	200	150	100	60	50	30	30	20	20	1260
27,500	300	200	150	100	100	70	50	40	20	20	10	10	1040
25,000	400	200	50	40	40	30	30	30	20	20	10	10	850
22,500	600	200	50	40	40	30	30	30	20	20	10	10	1050
20,000	700	300	70	40	40	30	30	30	20	20	20	20	1280
17,500	750	350	80	50	50	40	40	40	30	30	30	30	1460
15,000	800	400	80	50	50	40	40	40	30	30	30	30	1560
12,500	800	400	80	50	50	40	40	40	30	30	30	30	1560
10,000	800	400	80	50	50	40	40	40	30	30	30	30	1560

Average Mushroom

Figure 3

DOE ARCHIVES

[REDACTED]

The units are those which will yield milliroentgens per hour at 12 hours - if a cloud of 5 mile diameter is assumed. However, these units can be converted to units which will give the lifetime dosages (or dosages for any other period), since for each initial height and particle size the time of arrival at the ground can be calculated. In Figure 4 the units are for lifetime dose, in roentgens.

Figure 6 shows a similar diagram for UPSHOT-KNOTHOLE 2. In this case, the model, again scaled for the appropriate yield, overestimated the activity as given by the observations by about a factor of 2. Also, the axis of computed peak concentrations differs from the observed peak by about seven or eight miles. This could, of course, be due to meteorological errors in preparing our fall-out plot or to an anomalous distribution of radioactivity in the cloud, with very high concentrations existing near the very top of the mushroom.

DOE ARCHIVES

AVERAGE DISTRIBUTION OF RADIOACTIVITY FROM A 20-KT, 300 FOOT TOWER BURST,
 ASSUMING A CLOUD DIAMETER OF 5 MILES. UNITS ARE THOSE WHICH GIVE
 LIFETIME DOSE AT THE GROUND, IN ROENTGENS.

	Particle size (microns)												Average Mushroom
	a	b	c	d	e	f	g	h	i	j	k	l	
40,000	5.5	6.5	5.0	4.0	3.0	2.0	1.5	1.5	0.5	0.5	0.5	0.5	58.3
37,500	11.5	18.0	12.5	11.5	7.5	3.5	2.0	2.0	1.0	1.0	1.0	1.0	62.2
35,000	17.5	28.0	21.0	19.5	15.0	7.0	4.0	3.0	2.0	2.0	2.0	2.0	66.6
32,500	23.5	33.0	25.5	24.0	19.0	11.0	5.0	4.0	2.5	2.5	2.0	2.0	71.5
30,000	30.5	19.0	17.0	16.0	11.5	7.5	4.5	3.5	2.0	2.0	1.5	1.5	78
27,500	37.0	19.5	13.0	8.0	8.0	5.5	3.5	3.0	1.5	1.5	0.5	0.5	87
25,000	51.0	20.0	4.5	3.5	3.0	2.5	2.5	2.0	1.5	1.5	0.5	0.5	100
22,500	80.0	20.0	4.5	3.5	3.5	2.5	2.5	2.5	1.5	1.5	0.5	0.5	120
20,000	98.0	31.5	6.5	3.5	3.5	2.5	2.5	2.5	1.5	1.5	1.5	1.5	162
17,500	105.0	38.0	8.0	4.5	4.5	3.5	3.5	3.0	2.5	2.5	2.5	2.5	291
15,000	112.0	46.0	8.0	5.0	4.5	3.5	3.5	3.5	2.5	2.5	2.5	2.5	
12,500	112.0	50.0	9.0	5.0	5.0	4.0	3.5	3.5	2.5	2.5	2.5	2.5	
10,000													

Figure 4

Height in feet (MSL)

DOE ARCHIVES

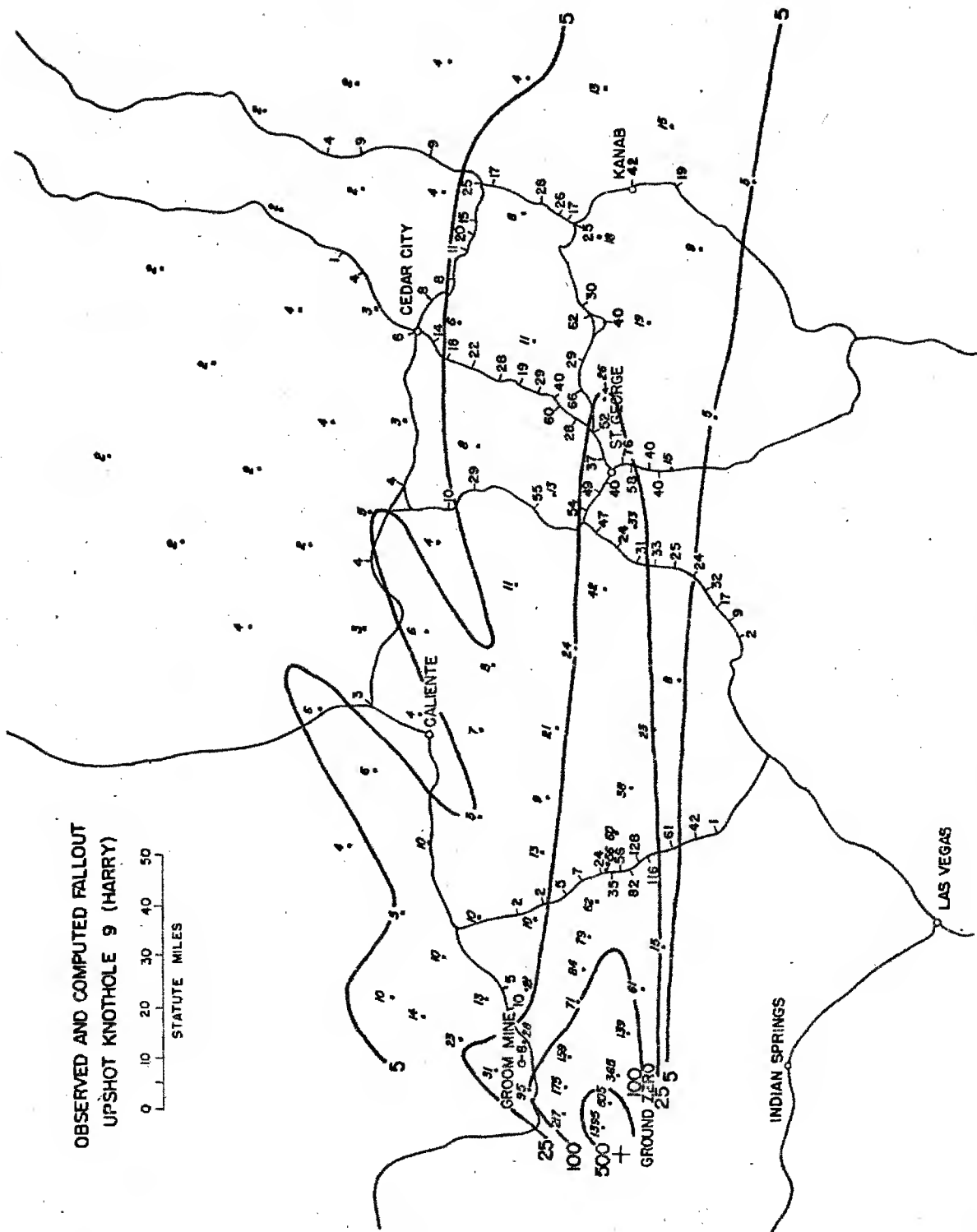


Figure 5

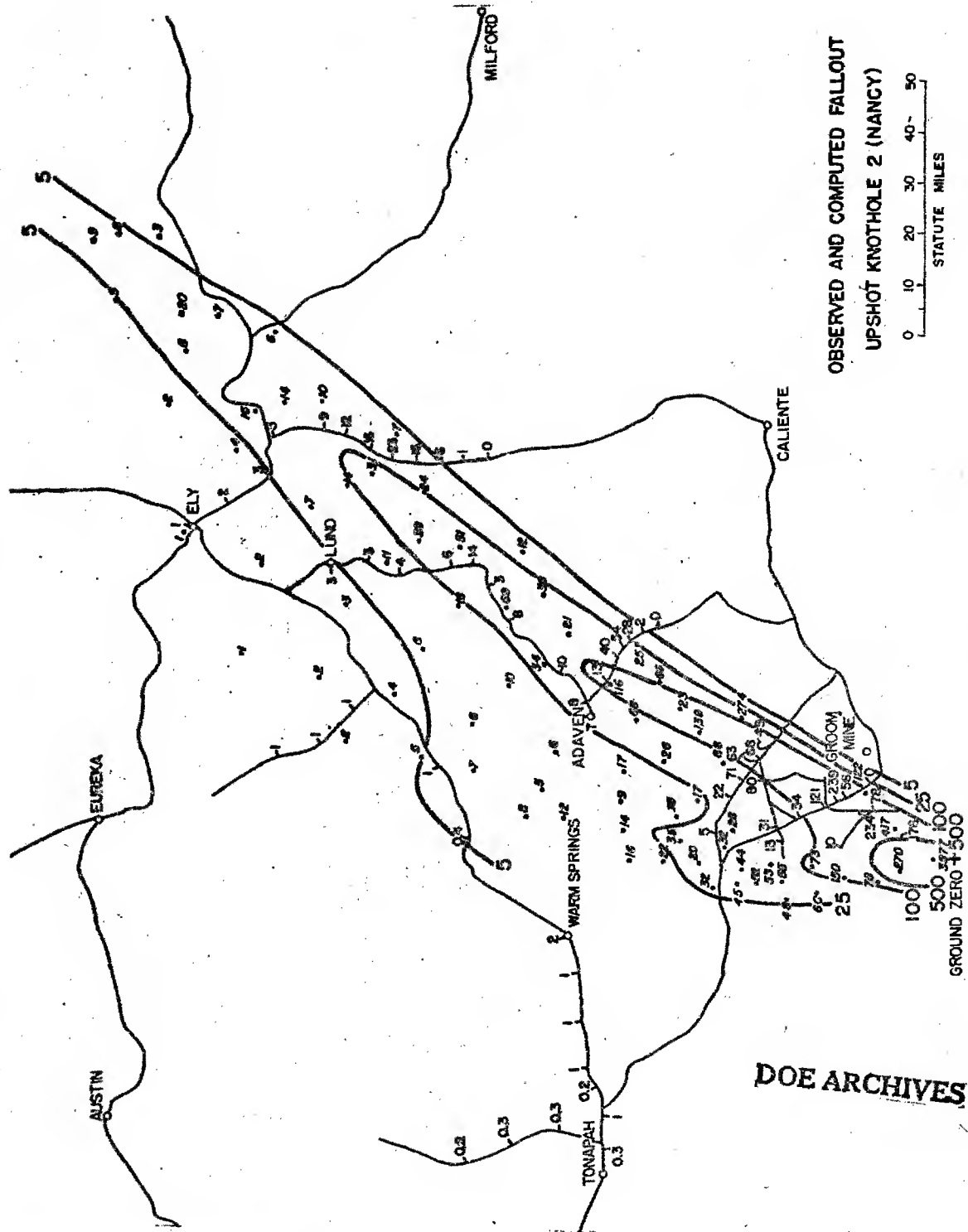


Figure 6

Cases with Little Lateral Wind Shear

I have described our physical approach to fall-out prediction only insofar as it applies to wind fields in which there is considerable lateral shear - that is, where the fall-out plot is spread out.

Figure 7 shows a partial fall-out plot for a case (UPSHOT-KNOTHOLE 7) with little lateral spread. A complete fall-out plot would be practically meaningless. The "X's" indicate the position of the 88 micron line and you can imagine the elongated shapes of the polygons. The first and sixth UPSHOT-KNOTHOLE bursts had similar fall-out plots with little lateral spread.

In order to utilize the observational data from these bursts, and to test our composite model, we had to devise an alternate method of treating these cases. What we have done is to assume that there was no directional shear at all. Then, from the distances to the various selected sizes, we prepared a working graph shown in Figure 8. In this graph, we have essentially compressed the fall-out plot into a line. One can see from this graph at what distance along this line a particle of a given size from any initial height will reach the ground. To determine the concentration at any point along the line, using our assumption of a cloud five miles in diameter, we first draw a vertical column five miles wide centered at the appropriate distance from ground zero. Then, to get the contribution, for example, of the top layer of the cloud and our "b" particle size range, we determine the fraction of the total area, (1, b) which lies within the column. In this case, it turns out to be about 17%. Thus, 17% of the radioactivity in the height range 40,500 to 43,000 feet and in the particle size range 162 to 291 microns in our model would contribute to the deposition at the selected point. To estimate the total deposition at the point, we have to compute similar percentages for each sector cut by the column, multiply each by the appropriate concentration from the model, and sum up the products. This resulting sum must, of course, be multiplied by a scaling factor based on the yield of the bomb. Now, what we get by this method is the deposition at the appropriate point on the ground which would exist if the cloud were five miles wide and if there really were no change in direction of the wind with height. We know that there is some directional shear. Therefore, we would normally expect the value computed by this method to be too high. There is one exception, namely that a narrower cloud than the assumed five mile one exists together with no directional shear. Figure 9 shows the observed fall-out from UPSHOT-KNOTHOLE 7 and shows the computations based on the method just described for several points where the fall-out line crossed roads along which observations were taken. The computed values are shown in italics and the observed values are plotted along the roads as before. In this case, it can be seen that the computed values in

~~SECRET~~

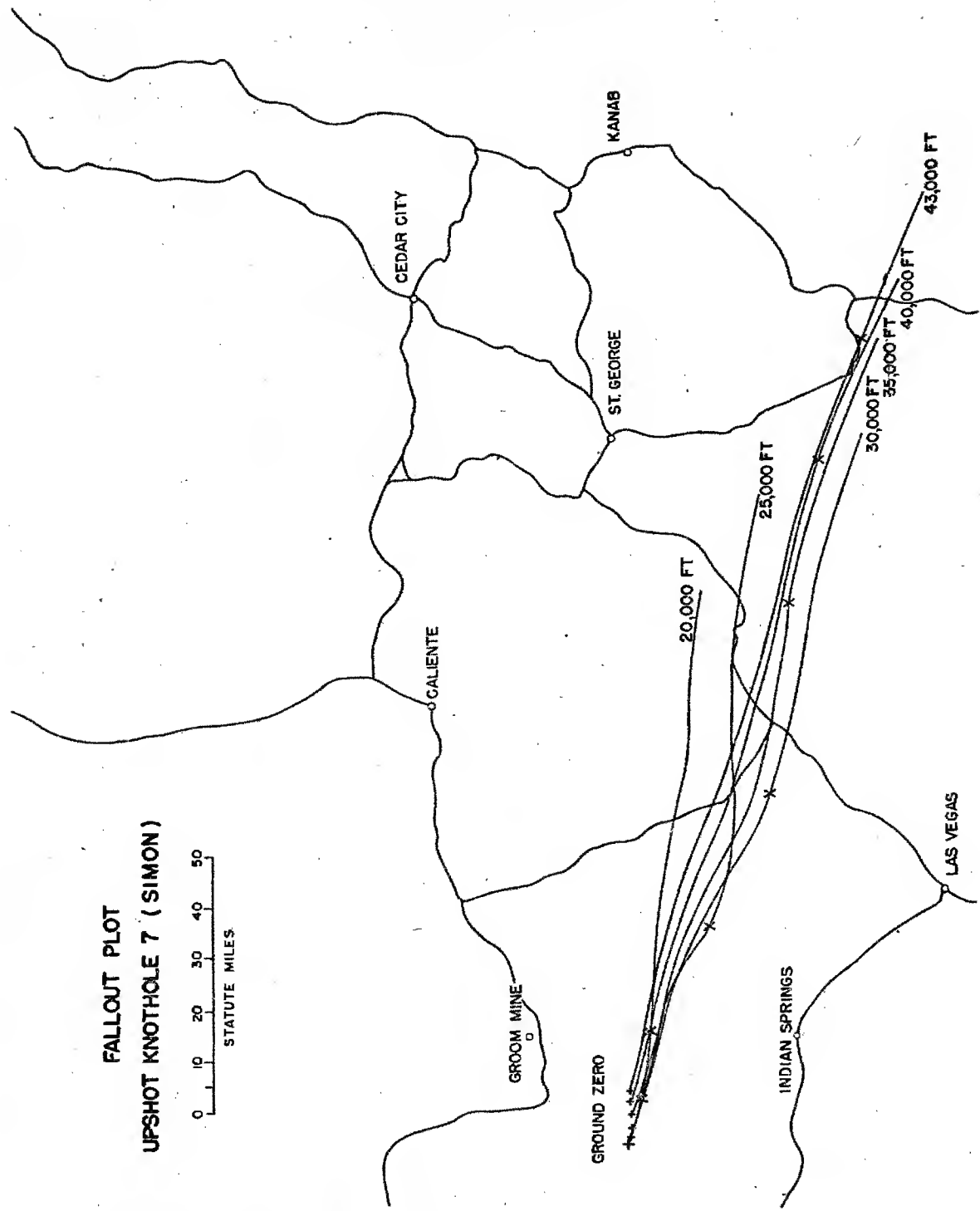


Figure 7

FALLOUT PLOT
UPSHOT KNOTHOLE 7 (SIMON)

0 10 20 30 40 50
STATUTE MILES

~~SECRET~~
ATOMIC ENERGY ACT

368

~~SECRET~~

DOE ARCHIVES

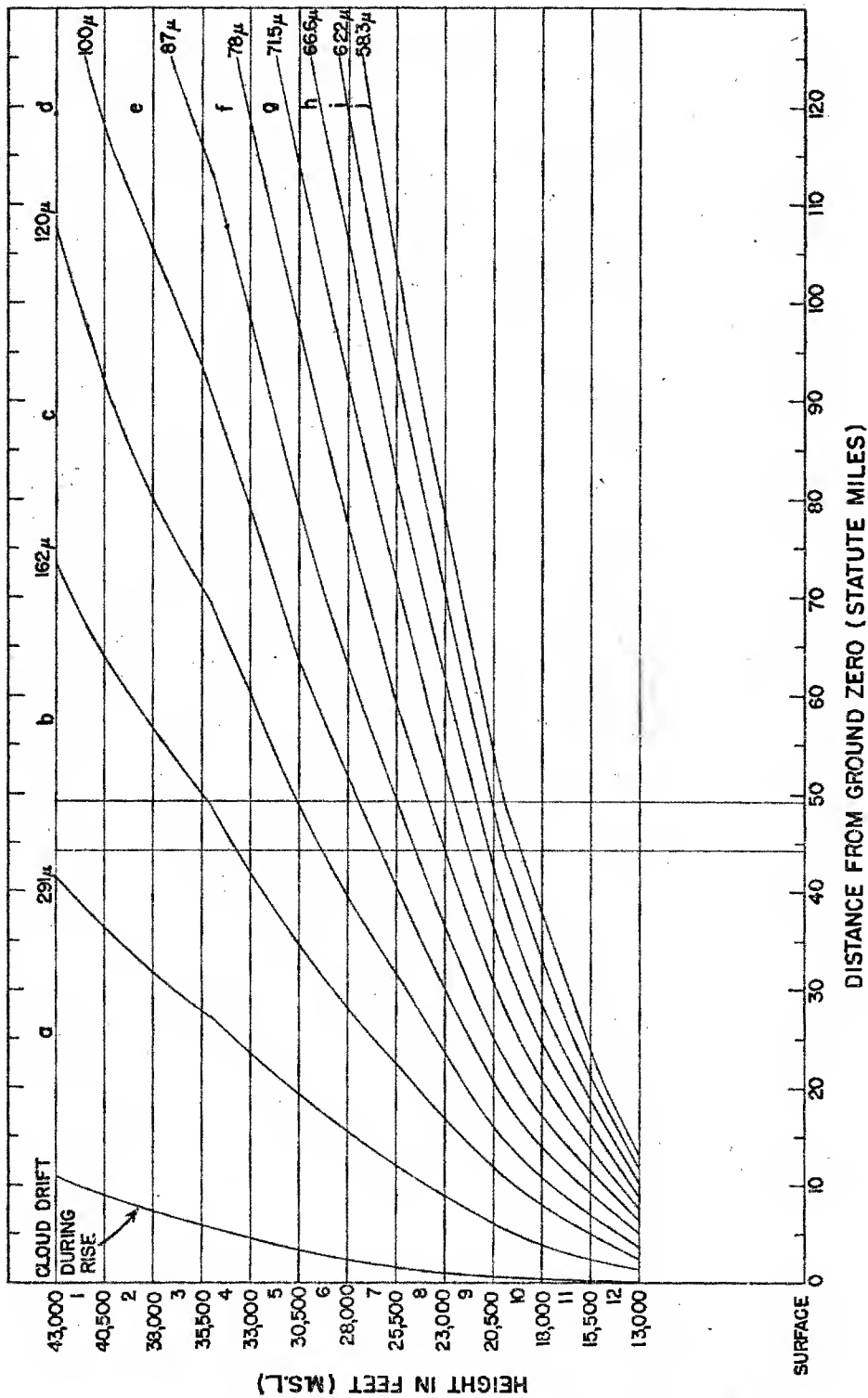


Figure 8

Working Graph for Computing Fall-out in a Case of Little Directional Shear, UPSHOT-KNOTHOLE-7

DOE ARCHIVES

369

SECRET

ATOMIC ENERGY ACT 1954

374

all cases exceed the observed peak values. As a test of our model, however, the observed peak values are not appropriate to use since we have assumed that the fall-out was compressed into a five mile band as shown in the figure. Accordingly, we have integrated the activity along the various roads and have converted to the concentration which would have existed if the cloud had been compressed to a five mile width. These fictitious peaks are shown in parentheses below the observations. It is apparent that in this case our model still gives excessive values but they are generally within a factor of 2 of the observed values. The position of the computed axis of high concentration fits the observed peak values very well.

Proposed Procedure for Future Tests

I have discussed the post mortem analysis of the fall-out from the 300-foot tower bursts in previous test series. Now, let us consider how we would use this information in forecasting for a future test.

First of all, unless we had a convincing forecast to the contrary, we would assume that the cloud would rise to 40,000 ft., and that the mushroom would be 15,000 ft. thick. We would assume the amount of debris available for close-in fall-out to be proportional to the area of the fireball intersecting the ground (or we might use some other scaling law if our present investigations indicate that it would work better). This can be estimated from the probable yield and from the tower height. Although in our post mortem investigation, we used trajectories and not merely the winds at the site, the time and effort to prepare such trajectories would not generally be warranted, considering the uncertainty which would occur in forecast winds. Thus, we would base the fall-out plot on the forecast winds at the site only and the height lines would then be straight lines.

Figure 10 presents a hypothetical fall-out plot showing considerable directional shear in lower levels, but little directional shear in upper levels. From the lower part of the cloud, where there is considerable lateral spreading by the wind, the fall-out would be determined by the method which we described for the UPSHOT-KNOTHOLE 9 shot. First, we would calculate the size of the various areas, possibly by planimetering, or by some more approximate but quicker method. Then where our assumed cloud lies entirely within a polygon, the ratio of the area of the 5-mile circle to the area of the polygon would yield the fraction of the activity which would fall at a point within the area. Multiplying this fraction by the proper contribution from the model, we get an estimate of the fall-out to be deposited at any point whose circle lies within that polygon. From a grid of these estimated depositions, generally one for the center of each sector, as isoline map should then be prepared.

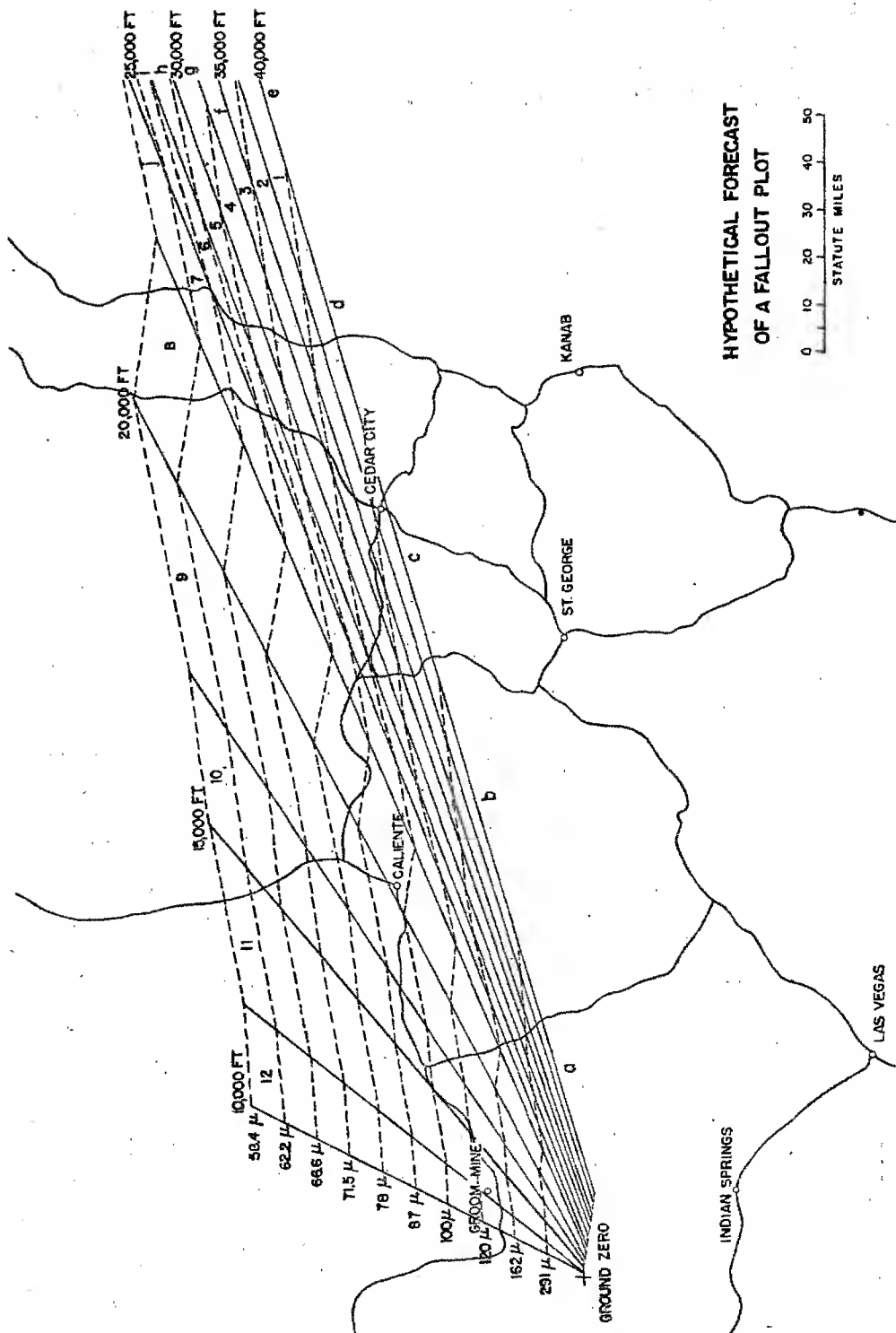


Figure 10

DOE ARCHIVES

From the higher altitudes of the cloud, where there is little lateral shear, the fall-out can more safely be predicted by the method assuming no directional shear, namely by assuming that the height lines are actually coincident. It must be remembered, of course, that the predicted values are apt to be on the high side unless the initial cloud has a diameter considerably less than five miles. At any rate, we would reduce the upper part of the fall-out plot to a graph similar to that previously shown, but only for the top 17,500 ft. (7 layers). On this graph, we would put columns five miles wide, centered at various distances from the burst site, and we would then determine the approximate fractions of the concentrations in the various layers and particle size ranges. Then, after multiplying the fractions by the appropriate numbers in the model, we would have a series of forecast concentrations in the area to be contaminated by the upper part of the cloud. Now, from the predicted concentrations for both parts of the cloud, an analysis of forecast activity can be made.

As with any forecast, the possibility of a shift in the wind from that forecast and hence a different area of peak concentration must be allowed for as a safety factor and there may also be errors due to incorrect estimates of the cloud height and yield and, of course, there are bound to be errors in the details of the fall-out.

Conclusions

If anyone expects to find a model which can predict the fall-out from Nevada shots to within a factor of two consistently, we feel he is bound to be disappointed. The errors in the radiological observations, meteorology and doubts about our various assumptions have already been dwelt upon at length.

Our attempt to fit a single model to all the fall-out data, however, uncovered certain interesting features. Two cases were very much different from all the others. Almost any reasonable composite model gives too much fall-out for TUMBLER-SNAPPER 8 and far too little fall-out from UPSHOT-KNOTHOLE 9. If it were not for an attempt to adjust the model to fit UPSHOT-KNOTHOLE 9, all the other cases would verify much better. While there was heavy cloudiness and possibly some rain following UPSHOT-KNOTHOLE 9, we did not feel justified in discarding this case.

DOE ARCHIVES

We have in rough form, maps of our computed and the observed fall-out, in the event that some of you would like to inspect them. The verification of our model by ground monitoring observations leads one to the conclusion that about half of the predictions verify by a factor of two and probably 80 or 90% verify within a factor of three.

THIS PAGE IS BLANK

DOE ARCHIVES

374

ATOMIC ENERGY ACT

379

PART I

levels would extend. The area concept is useful when one is considering a target region which is large compared to the fall-out contours. The downwind distance is useful when one wants to estimate the maximum radiation level which might be encountered at any distance from some assumed detonation.

While this kind of information has a number of uses, it was apparent that some kind of quantitative model of the fall-out process was needed, in order to predict dose rates and doses for a wide variety of situations. Some work was started on (the development of) such a model--which I will mentioned at the end of my talk. After that Mr. McCampbell will describe the recent development of a fall-out model.

Meanwhile, for planning purposes, we have been using the scaling methods--and since they still seem to be useful, I would like to give a brief review of their development.

Scaling Method

The general problem required extrapolating a very limited amount of fall-out data to other yields and to other detonation conditions--particularly wind velocities, soil types, and detonation depths. Scaling represents a limited solution; one starts with a known fall-out pattern and extrapolates to other yields.

The method of scaling fall-out contours from one yield to another was developed in the following way. Shortly after the detonation, we visualize a region in the air containing all the radioactive particles. They have just stopped rising, and this region we will call the radioactive cloud. In order to scale fall-out patterns from one yield to another, we make five basic assumptions about this cloud and the particles in it.

DOE ARCHIVES

First, for equivalent scaled depths of detonation, the radioactive clouds from different weapon yields are assumed to be geometrically similar. Both the dimensions and heights of corresponding volumes are assumed to vary as the yield to some power n .

Second, the total activity is assumed to vary directly with the yield.

Third, for a given soil, the size distribution of active particles is independent of yield.

Fourth, the relative spatial distribution of particles of any given size within the cloud is independent of yield.

~~SECRET~~

Fifth, the rate of fall, for particles of a given size, is independent of the yield.

These assumptions are undoubtedly idealizations of the actual facts. Later, some known departures of the facts from the assumptions will be mentioned. It appears, however, if the scaling is not done over too large a range of yields, these assumptions should lead to reasonable results.

One further assumption is made when field dose rate patterns are to be scaled, rather than activity concentrations on the ground—that the dose rate at any point is directly proportional to the activity per unit area (on the ground).

The scaling method follows directly from these assumptions. It can be stated in this way:

If all linear dimensions of a contour to be scaled are increased as the yield ratio to the power α , then the associated dose rate will vary as the yield ratio to the power $1 - 2\alpha$.

The best value to assign to the cloud scaling exponent α is somewhat questionable. However, the numerical results are not particularly sensitive to the exact value chosen; and in most calculations we have used a value of $1/3$. In this case, the scaling method simply requires that all linear dimensions of the contours, as well as the associated dose rates, be scaled as the cube root of the yield ratio.

The restrictions on this scaling method are that it applies only for: equal wind speeds—or if shear is appreciable, equal wind velocities at equivalent scaled heights; equivalent scaled depths of detonation; and the same soil.

We have tried to make some tentative estimates of the influence of detonation conditions on the fall-out patterns for a given yield.

DOE ARCHIVES

Wind: quantitatively, tends to elongate ideally-circular patterns for no wind. The data indicates areas of contours of given fall-out concentration quite insensitive to wind speeds; this generalization, together with an empirical estimate of the variation in downwind distance with wind speed, was used to control the wind correction.

Soil type: expected to influence size distribution of radioactive particles formed, and hence the resultant contamination patterns.

Examination of radioactive particles at JANGLE indicates they are formed from fused soil. It appears therefore that HE tests, where the dust fall-out consists of original soil particles, cannot be used to estimate influence of soil type.

Depth: provided cloud dimensions can be estimated as a function of depth of detonation, it is possible to make extrapolations by arguments similar to those used to develop the method for scaling with yield. The main difference is that in the basic assumptions, the total amount of activity is constant, and the cloud heights and dimensions are assumed to vary in some way with depth. If the ratio of cloud dimensions for two depths is denoted by μ , then it can be inferred that the dose rate will vary as $1/\mu^2$ at distances scaled as μ .

Departures from Idealized Scaling

The scaling method was first applied, for lack of any other data, to dust fall-out measurements from high explosive tests at Dugway Proving Grounds. Dust concentration contours from 320 pound charges were scaled to those from charges as great as 320,000 pounds—or over a charge weight ratio of one thousand. Generally the results were fairly good, the scaled areas being off in the worst case by a factor of less than three.

It is now possible to make a comparison between the JANGLE surface shot and CASTLE Bravo. In this case the yield ratio is about 10,000. The nature of the soil over which the detonations occurred is, of course, quite different, as were the meteorological conditions.

For the 2000 r/hr at 1 hour contour, the Bravo downwind distance is about twice the scaled JANGLE distance. For the 100 r/hr contour, the observed and scaled downwind distances are equal. In all cases, the Bravo contours are considerably broader than the scaled JANGLE contours—by an amount which depends on which estimate of the Bravo contours we look at. On the basis of AFSWP-507 and the preliminary report of Project 2.5a, the CASTLE contours are about 2 to 3 times as wide as the scaled JANGLE contours. The area enclosed by the contours are roughly 4 to 3 times as great as the scaled JANGLE areas. On the basis of the revised 2.5a contours, the discrepancy is considerably greater. The 2000 r/hr contour is about 9 times as wide as the scaled JANGLE value; and the 100 r/hr contour about 5 times as wide. DOE ARCHIVES

Two possible reasons for discrepancies between scaled JANGLE and Bravo results have already been mentioned: the difference in soil and in meteorological conditions, especially the wind structure. These differences really represent a failure of the tests of conform to the

necessary conditions. There are, however, two additional reasons (at least) where the basic assumptions used to derive the scaling method are not exactly correct. First, the rates of fall of the particles are not entirely independent of yield. The particles fall faster at higher elevations; hence as the yield is increased and the cloud height increases, the average rate of fall for a particle of given size increases somewhat. Second, the clouds are not geometrically similar. Empirical evidence shows a progressive flattening of the cloud with increasing yield. Thus the 1 KT JANGLE cloud was nearly spherical, while the width/thickness ratio of the Bravo cloud was close to 7:1. Scaling measurements as the cube root of the yield, the height of the center of the Bravo cloud corresponds almost exactly to the scaled JANGLE height. However, the depth of the Bravo cloud is only about one-half the scaled JANGLE value, while the width is about 3 times as great as the scaled JANGLE width.

Refined Model

Some approximate corrections could be made to account for the variation in cloud shape and rates of fall of particles, in order to improve the scaling method. But the only way to predict actual fall-out patterns for a variety of conditions is by way of a dynamic model of the fall-out process.

Exploratory work on such a model was begun nearly two years ago, to see what kind of agreement with the JANGLE data might be obtained. The first attempt assumed a spherical cloud, uniform wind velocity, and contained a very rough estimate of the distribution of activity with particle size. Somewhat surprisingly, the dose rates predicted from this model looked fairly much like the observed values.

Now it is apparent that any model of the kind that has been discussed here contains quite a few parameters, to which some numbers have been assigned. These parameters are closely related to the things which were mentioned earlier in the five basic assumptions used to develop the scaling method.

DOE ARCHIVES

First, the total activity released must be known—a relatively straightforward calculation.

Second, the cloud height and dimensions must be known. Generally these can be estimated from photographs and extrapolated with the help of some theories—although there is no guarantee that the radioactive cloud is actually coincident with the visible cloud.

Third, activity in the cloud must be known as a function of the particle size.

Fourth, distribution of the particles in space must be known.

Fifth, rates of fall of the particles must be known.

Regarding these last three points, there is some controversy.

Rates of fall depend on the properties of the atmosphere as well as those of the particles. Actually, particle properties vary considerably—those from Nevada being sometimes spherical, sometimes very irregular, and showing density variations of about a factor of 2, mainly because of varying amounts of included air bubbles. In our numerical work, we have assumed that all the particles are irregular and of uniform density.

Distribution in space is clearly not well known. Here we have assumed that practically all the activity is in the mushroom cloud and is uniformly distributed.

Finally, the relation of activity to particle size is not well known either. Rather than try to guess at this, or adjust the distribution to give the best agreement between the predictions of the model and experimental data, we tried to make an independent evaluation from some particle studies at JANGLE.

A fairly large number of fall-out samples were separated into various size fractions at NRDL, and the relative activity of each size fraction was measured. The data were not sufficient to draw activity concentration contours for each size fraction, which is what we would have liked, but it was possible, for the underground shot, to draw curves of activity concentration as a function of distance in the down-wind direction. By integrating these curves, it was then possible to estimate the percentage of activity in each size range which was initially present in a unit width slice of the cloud.

This distribution turned out to be a normal distribution with respect to the logarithm of the particle diameters--and this is the distribution we are using in our numerical calculations.

This gives some of the background of the development of our fall-out model, which Mr. McCampbell will describe.

DOE ARCHIVES

PART II

Mr. James M. McCampbell
U. S. Naval Radiological Defense Laboratory

During this Symposium, it has been amply demonstrated that the problem of devising a mathematical model of fall-out consists of two major parts; first, tracing the trajectories of the fall-out particles to determine where they land, and second, summing all the activity that lands at any given point on the ground. These two basic ideas will be developed in their mathematical form.

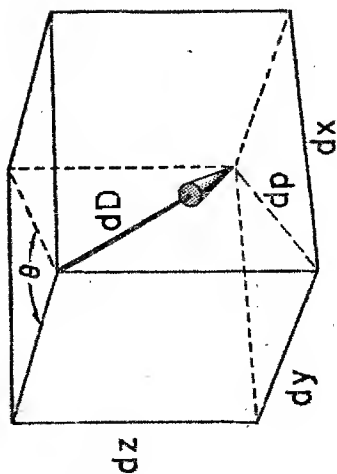
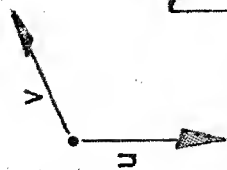
Concerning the first part of the problem, we consider a particle falling through the atmosphere with a velocity u and drifting in a wind of velocity v as shown in Figure 1. During a small interval of time the particle drifts along the vector dD whose components dx, dy , and dz refer to a convenient coordinate system. The magnitude of the time interval equals the distance the particle travels divided by its rate.

In the vertical direction, $dt = \frac{dz}{u}$. The distance traveled in the direction of the wind is $d\rho = v dt$ and by substitution, equals $v \frac{dz}{u}$. But dx is a component of $d\rho$, hence $dx = d\rho \sin \theta$ where θ is the angle between the y -axis and the direction toward which the wind is blowing. θ is 180° from the conventional wind angle.

As the particle traverses successive layers of the atmosphere, its path is defined by the sum of the vectors dD . Therefore, the total drift in the x direction is the sum of the x components; that is, D_x equals the integral from the surface to the altitude of origin of $v \sin \theta$ divided by u . A similar expression involving $\cos \theta$ will of course give the y component of the total drift. The parentheses indicate that the wind speed and direction vary with altitude and that the particle falling rate is also a function of the altitude. In addition, the falling speed of the particle is a function of its size, l .

A convenient coordinate system is the one with the origin at ground zero and the y -axis directed north as in Figure 2. Consider particles of a given size originating in the infinitesimal volume dV at the point (x, y, z) . These particles drift along some irregular path indicated by the heavy dotted line, and land at the point (A, B) . The final displacement of the particles from the origin is the sum of their initial displacement in the cloud and the displacement they experience while drifting with the wind. The x -component of the final displacement is A , and it equals x plus D_x . Transposing the terms gives

$$x = A - D_x \text{ and by a similar derivation } y = B - D_y$$



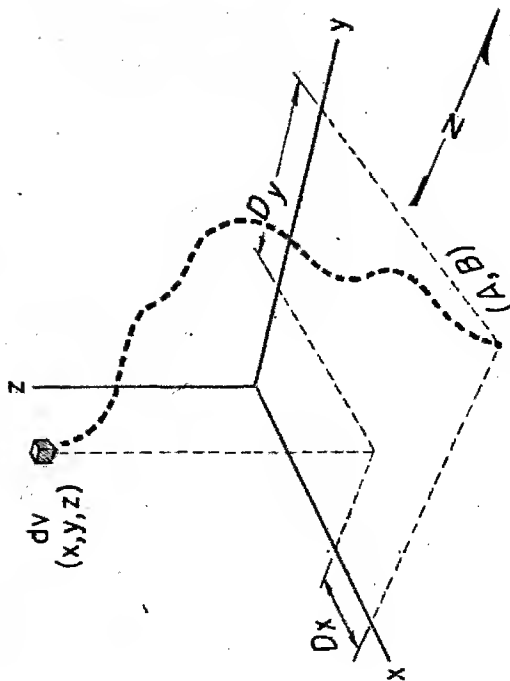
$$dt = \frac{dz}{u}$$

$$dp = v dt = v \frac{dz}{u}$$

$$dx = dp \sin \theta = v \frac{dz}{u} \sin \theta$$

$$D_X(z, l) = \int_0^z \frac{v(z) \sin \theta(z)}{u(z, l)} dz$$

Figure 1



$$A = X + D_X$$

$$X = A - D_X$$

$$Y = B - D_Y$$

Figure 2

DOE ARCHIVES

Now what is the meaning of these two equations? For a given point (A,B) and a given wind structure, any value of z determines Dx and Dy, and in turn determines a corresponding x and y. Thus, these equations are the parametric expression of a curve in space. It is along this curve that particles of a given size can possibly originate, traverse the wind structure, and land at the point (A,B). Mathematically, this locus of origins has an infinite extent, but physically, only a segment has significance; that is, that segment which lies within the cloud. We must therefore define the boundary of the cloud.

As shown in Figure 3, an ellipsoidal cloud is assumed. Its semi-axes are a and b and its center is directly above the origin at the altitude H. Such a model will accommodate the very flat clouds from high yield weapons, and will degenerate into a sphere for clouds from low yield weapons. The locus of origins is shown penetrating the cloud at the altitudes z₁ and z₂. The values for z₁ and z₂ are different for each particle size. The points of intersection are found by the simultaneous solution of the equation of the curve and the equation of the cloud boundary. For a spheroid, the latter is

$$\left[\frac{Z-H}{a}\right]^2 + \left[\frac{X}{b}\right]^2 + \left[\frac{Y}{b}\right]^2 = 1$$

Our equations for the curve were in terms of x and y, so substitution gives

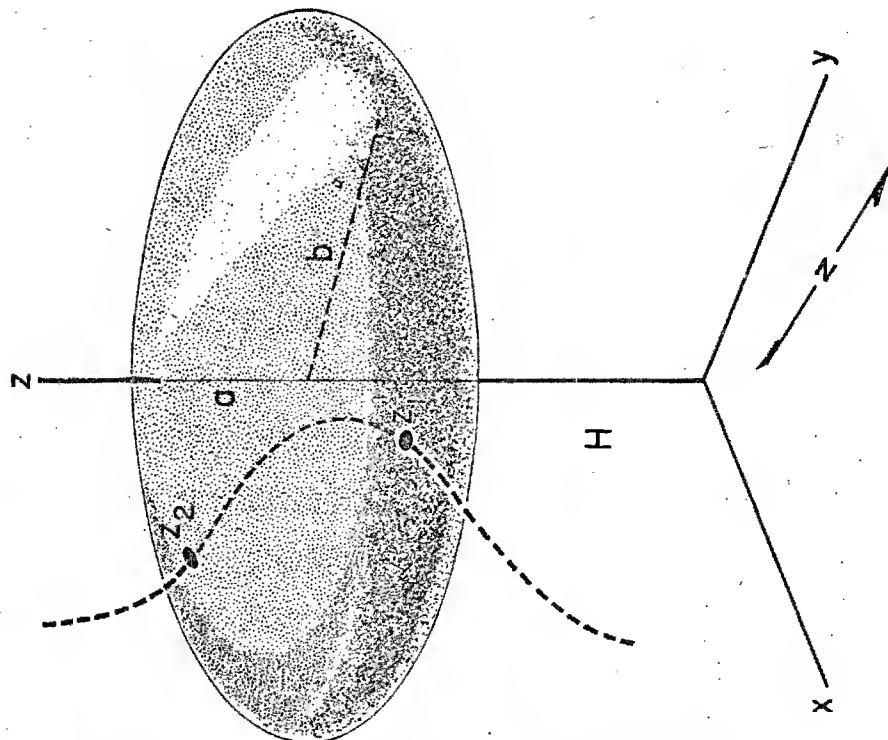
$$\left[\frac{Z-H}{a}\right]^2 + \left[\frac{A-Dx}{b}\right]^2 + \left[\frac{B-Dy}{b}\right]^2 = 1$$

DOE ARCHIVES

The values of z₁ and z₂ are implicitly given by the last equation. Any point in space which satisfies this equation must lie on the curve and also on the cloud surface; it is therefore a point of intersection. These points may occur in real pairs, imaginary pairs, or singly. Real pairs indicate penetration of the cloud, imaginary pairs indicate that the curve does not touch the cloud, and single points indicate that the curve is tangent to the cloud. The physical meaning of the imaginary case is that particles corresponding to that curve can not reach the point in question. The curve may penetrate the cloud, fold back and penetrate it again; and perhaps again. However, for most wind conditions, the simple case as shown in the figure will probably prevail. Whether or not it does is immaterial—as will be shown later.

Because the cloud height, shape, and size vary with the yield, the cloud parameters H, a, and b will take on values depending upon the yield. Therefore, substituting empirical or theoretical relations between these parameters and the yield would make the last equation applicable for all yields.

~~CONFIDENTIAL~~
~~NUCLEAR ENERGY ACT~~



$$\left(\frac{z-H}{a}\right)^2 + \left(\frac{x}{b}\right)^2 + \left(\frac{y}{b}\right)^2 = 1$$

$$\left(\frac{z-H}{a}\right)^2 + \left(\frac{A-D_x}{b}\right)^2 + \left(\frac{B-D_y}{b}\right)^2 = 1$$

Figure 3

DOE ARCHIVES

$$n = P\phi(I) dI \, dx dy dz$$

$$a = P\phi(I) dI \, dx dy dz \, \xi(I)$$

$$da_I = \frac{P\phi(I) dI \, dx dy dz \, \xi(I)}{dx dy}$$

Figure 4

$$a_I = P\phi(I) dI \, \xi(I) \int_{z_1}^{z_2} dz$$

$$A(A,B) = \int_{-\infty}^{\infty} a_I = \int_{-\infty}^{\infty} P\phi(I) \xi(I) [z_2(I) - z_1(I)] dI$$

$$R(x,y) = K \int_{-\infty}^{\infty} P\phi(I) \xi(I) [z_2(I) - z_1(I)] dI$$

Figure 5

SECRET

We must now turn our attention to the second part of the problem, that is, to summing the activity that lands at a given point. In Figure 4, P is the number of particles per unit volume in the cloud. If $\phi(l)$ is the size distribution of the particles then $P\phi(l)dl$ is the number of particles per unit volume of sizes l to l plus dl . Multiplying by $dx dy dz$ gives the number of particles of that size in the volume dV .

Let $\xi(l)$ denote the radioactivity of a particle of size l , assuming that the radioactivity of particles is in some way related to their size. Then multiplying by $\xi(l)$ gives the radioactivity of the particles of size l in dV . But it was previously shown that these particles were deposited at the point (A,B) . Assuming that there is no dispersion of the particles in their flight, they will be spread over an infinitesimal area $dx dy$. Therefore, the activity per unit area is found by dividing by $dx dy$ as in the last equation in the figure. It must be pointed out that da_1 is a second order infinitesimal; the two remaining differentials are dl and dz . It is apparent that subsequent integration must be performed over the altitudes and the particle sizes.

For particles of each size, the integration with respect to z must be confined to the applicable altitudes. In Figure 5 we see that a_1 , the activity due to particles of size l , is found by summing over the range z_1 to z_2 . If our curve of origins had penetrated the cloud twice, we would add another term with limits z_3 and z_4 . Having integrated with respect to altitude, we must now sum over the particle sizes as shown in the middle equation, where the previous integration has been carried out.

Finally, the radiation field produced above a contaminated surface is proportional to the activity on the surface. Therefore, the radiation field R is obtained by multiplying the activity per unit area by the proportionality factor K . The value of K includes the effect of shielding by rough terrain, the mean energy of the gamma rays, and the height above the surface that the radiation intensity is desired. It should be pointed out that the product $\phi(l)\xi(l)$ is the activity distribution. It is sufficient to know the product of the two functions; they need not be known separately.

DOE ARCHIVES

It turns out that solving the problem in this form is virtually impossible. However, it can be readily solved by taking finite increments of particle size and altitude. When formulated in terms of finite intervals, it is ideally suited to machine computation. A computational scheme based on this theory is currently being used in computing fall-out patterns on a Univac. The machine work is being done by the Applied Mathematics Laboratory of the Bureau of Ships.

SECRET

NUCLEAR ENERGY

~~SECRET~~

You will notice that no mention has been made of a very important variable, namely, the time elapsed since the explosion. This variable enters the problem in four specific ways:

In the decay of radioactivity,

In the build-up of the activity at any point and the consequent growth of the fall-out pattern,

In the changes of wind structure that occur during the fall-out process, and finally,

In the change of the mean gamma energy with time.

Recent extensions of the present theory permit a machine solution including the variable time in all four aspects. The output table from the machine could provide the following information:

The coordinates of the point in question,

The radiation intensity at the point at any time,

The dosage accumulated at the point up to any time,

The time in question,

The time that fall-out began to arrive at the point, and,

The time that fall-out ceased at the point.

If the preliminary computations now being made confirm the model, there will then be available a useful tool for studying fall-out problems. In particular, investigations could be carried out in such subjects as the:

Scaling of radiation fields,

The effect of different wind shears, and,

The effect of different particle and activity distributions.

DOE ARCHIVES

~~SECRET~~
ENERGY

~~SECRET~~

[REDACTED]

PREDICTION OF DOSE-RATE AND DOSAGE CONTOURS AS
FUNCTIONS OF YIELD AND METEOROLOGICAL CONDITIONS;
PREDICTED CONTOURS FOR THE CASTLE DETONATIONS

E. A. Schuert

U. S. Naval Radiological Defense Laboratory

At Operation CASTLE Project 2.5a had as a primary responsibility the definition of the fall-out patterns resulting from the 6 detonations. A great deal of analytical work has been expended in the reconstruction of the contours that defined the primary fall-out pattern resulting from Shot 1. Since the analysis that was employed combined experimental data with particle trajectory evaluations, much of the work is similar to the model developments presented here this week. I will discuss the assumptions made and the techniques employed in this development as well as the relevant experimental data obtained and how this data fits the resulting fall-out contours.

The data available after Shot 1 included the measured fall-out in and about the Bikini lagoon, the negative data from the free floating sea stations west of the atoll, the outer island survey measurements made by Dr. Scoville's team, the observed time of arrival of fall-out at Bikini and on the outer atolls, as well as the measured radioactive particle size, particle density, and particle configuration data for both the Bikini area and the outer islands. There was also data obtained on the time of arrival of fall-out particulate at Bikini.

An attempt to reconstruct the fall-out contours solely from the measured gamma field data offered the analyst a great deal of latitude, for there existed no information that would control the lateral width of the fall-out pattern. Because of this problem an attempt was made to define the area of fall-out by use of particle trajectory analysis. Since we were primarily interested in singularly defining the Shot 1 pattern, data from this detonation was used in defining the trajectory parameters. The parameters necessary to apply the trajectory analysis were:

- A source of activity.
- The initial spacial distribution of the source material.
- A mechanism for distributing the source material.

DOE ARCHIVES

Some of the above parameters were supported by experimental data; others required basic assumptions. The assumed parameters were:

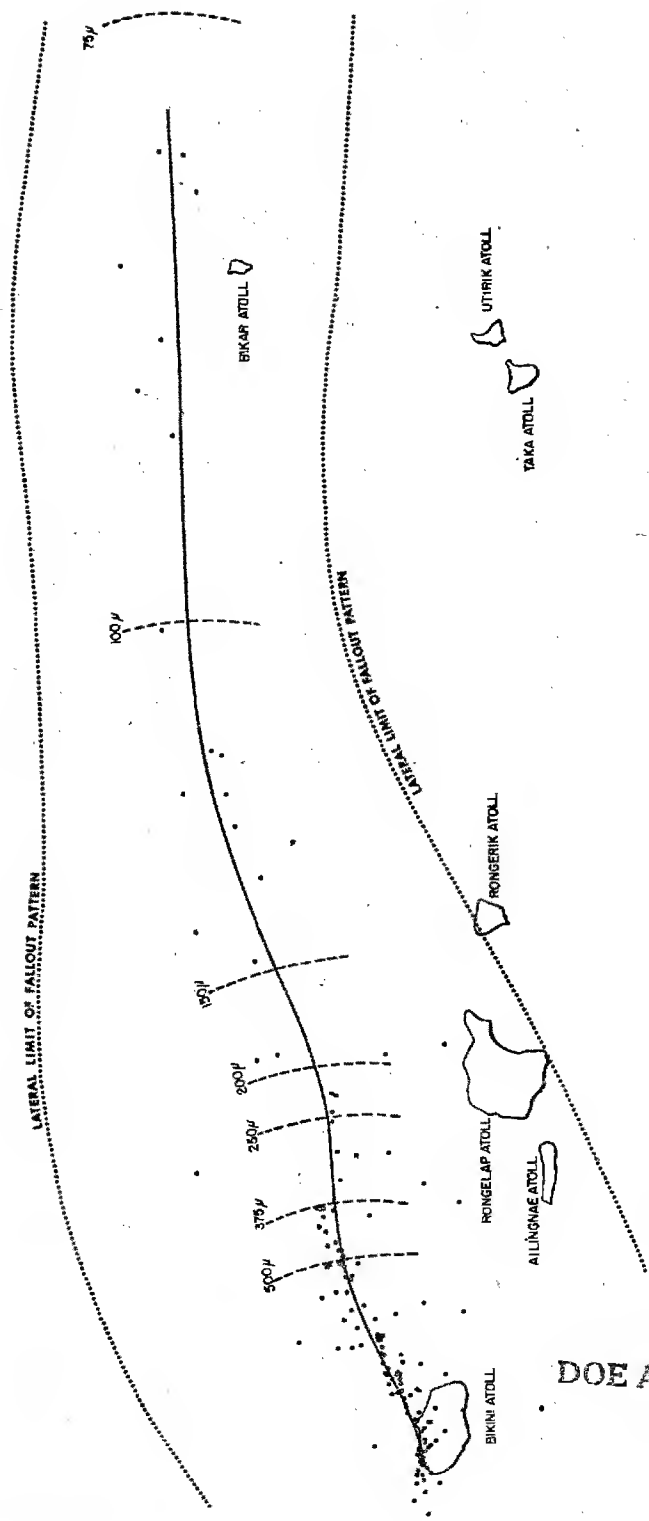


Figure 1
General Area of Fall-out, CASTLE-Bravo

DOE ARCHIVES

The spacial distribution of the source material was described by the visible dimensions of the cloud and stem at time 0 + 10 minutes. This assumption was further simplified by describing the Shot 1 stem and cloud as cylinders.

The distribution of the source material was homogeneous throughout the cloud and stem with all particle sizes at all locations.

The particle trajectories could be defined by their rate of fall under the influence of the existing wind speeds and directions.

The experimental data obtained from analysis of the fall-out material as well as other physical measurements was used as follows:

The measured physical characteristics of the particles were used to determine their rate of fall and to describe the particle size distribution that was actively contributing to the primary fall-out.

The cloud dimensions as measured by cloud photography were used to describe the physical dimensions of the source.

The observed meteorological data both on windspeed and direction and temperature distribution as obtained by the Task Force weather central were used to calculate the particle trajectories.

The trajectory analysis was then defined on both assumed and measured parameters.

In determining the rate of fall of the particles, a size range of from 2000 μ to 25 μ diameter was used. The shape of the particles had been experimentally determined to be almost entirely irregular in shape. The apparent density of 70 particles was measured resulting in a mean density of 2.36 g/cm³ with a standard deviation of 9 per cent. The air temperature used in determining the viscosity of the atmosphere with respect to height was taken from that measured at Bikini just prior to shot time. After determining the falling speeds of the particles over the stated size range using the above experimentally determined parameters and applying aerodynamic particle settling rates, a table of average falling speeds was constructed for each 5000 foot increment of altitude to a height of 100,000 feet.

DOE ARCHIVES

With the above falling rates, 231 particle trajectories were computed. These computations were done manually, for at that time application to machine analysis was not available. Particle sizes of 2000, 1500, 1000, 750, 500, 375, 250, 200, 150, 100, 75, 50, and 25 μ in diameter were placed at 5000 foot intervals to an elevation of 100,000 feet and their intersections with the surface of the earth were determined by following each particle as affected by the wind structure. In constructing these trajectories the changes in the wind pattern both with respect to time and location of the particles were

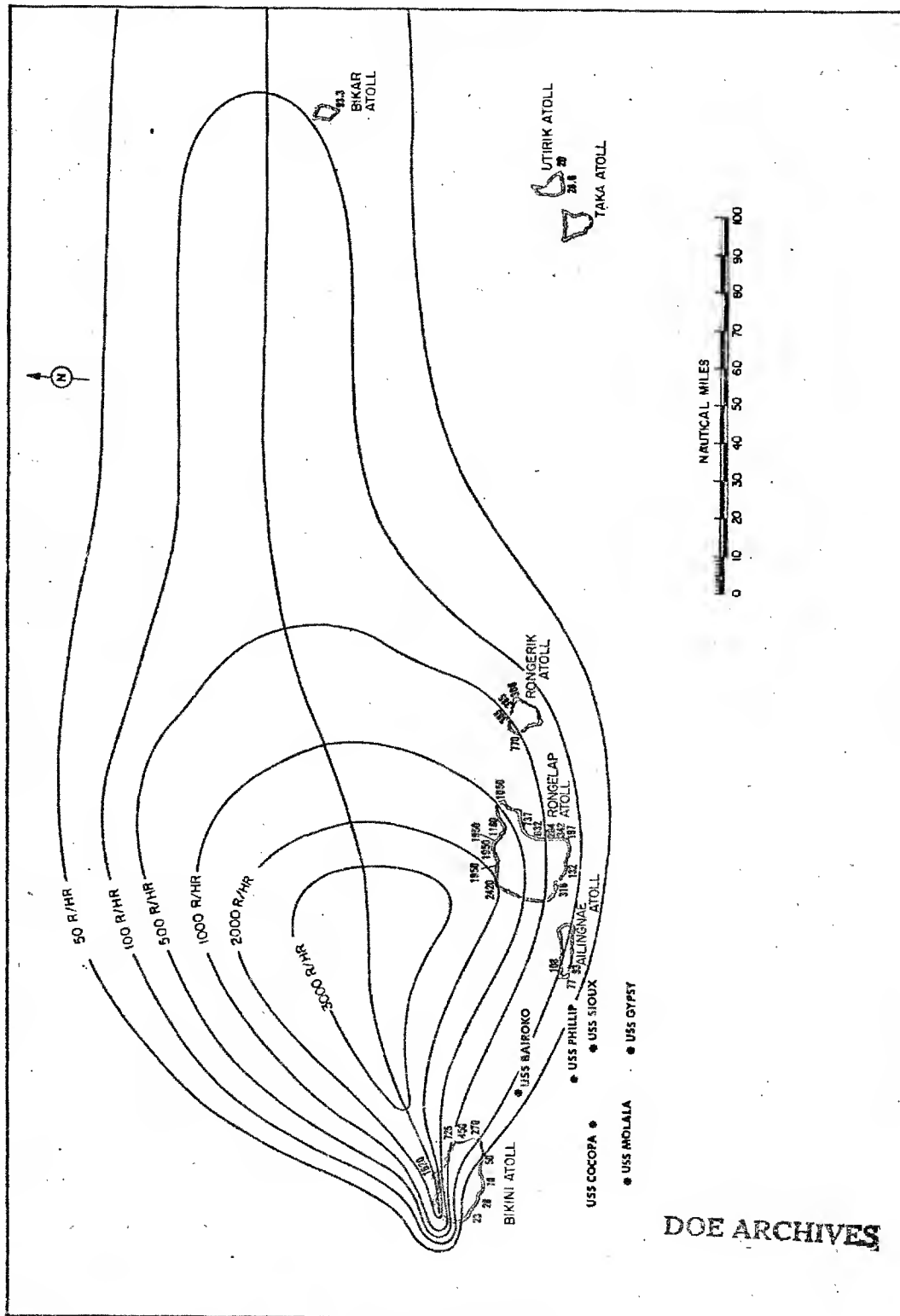


Figure 2
Fall-out Contours, CASTLE-Bravo

considered. This analysis resulted in the plot shown in Figure 1. Here there is a picture of the general area of fall-out based on the stated assumptions. The outer dashed line was constructed by expanding each point by the cloud or stem radius from which the particle originated. The dimensions used were 66 nautical miles cloud diameter and 6.6 nautical miles stem diameter, with the cloud base at 60,000 feet. The dashed arcs show the maximum distance the stated particle size could travel. Because of the wind structure existing at shot time the area of fall-out had a rather well defined axis along which the larger particles were closely grouped. This axis is shown by the heavy solid line in the figure. Because this axis did not change noticeably by varying the particle size distribution, it was reasonable to represent it as an axis of symmetry of the fall-out pattern.

The reconstruction of the fall-out contours for Shot 1 were then made, based solely on the directive axis of fall-out as determined above and the measured gamma field readings. The analysis resulted in the fall-out contours as shown in Figure 2. These contours show gamma activity in r/hr at 1 hr.

The most significant result of this analysis was the unusual width of the fall-out pattern. For comparison, the surface Jangle fall-out pattern was scaled to 15 megatons using the cube root relationship. The most significant observation was again the great difference in the configuration of the two patterns. A reason for this discrepancy was discussed by Mr. McCampbell earlier this morning.

This analysis based on a fall-out axis and the measured gamma fields, created a pattern that fits well with the lateral limit of the pattern as defined by the expansion of the trajectory points as previously shown in Figure 1.

Two material balances were made on the reconstructed pattern. The first material balance based on calculated parameters as described by Dr. Werner earlier this week resulted in from 50 to 70 per cent of the device accounted for within the 100 r/hr at 1 hr. contour. The second analysis based on extrapolation of a radio-chemical analysis of the fall-out material collected at one location, indicated 30 per cent of the device accounted for within the 100 r/hr at 1 hr. contour.

In order to show pictorially the growth of the fall-out pattern with time and the actual existing levels of activity, I have prepared five figures (Figures 3-7), showing the existing gamma field at 1, 3, 6, 12 and 18 hours.

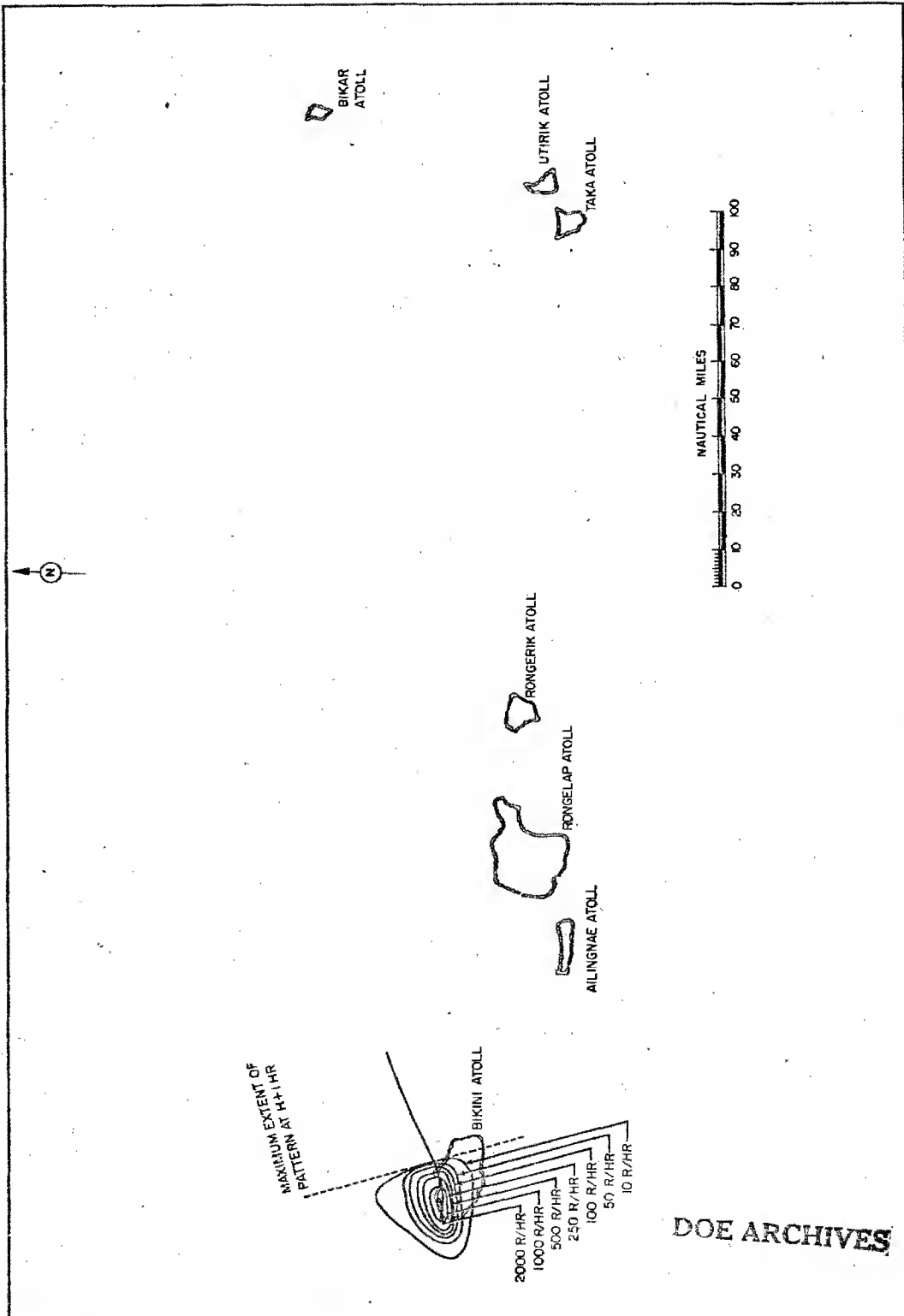
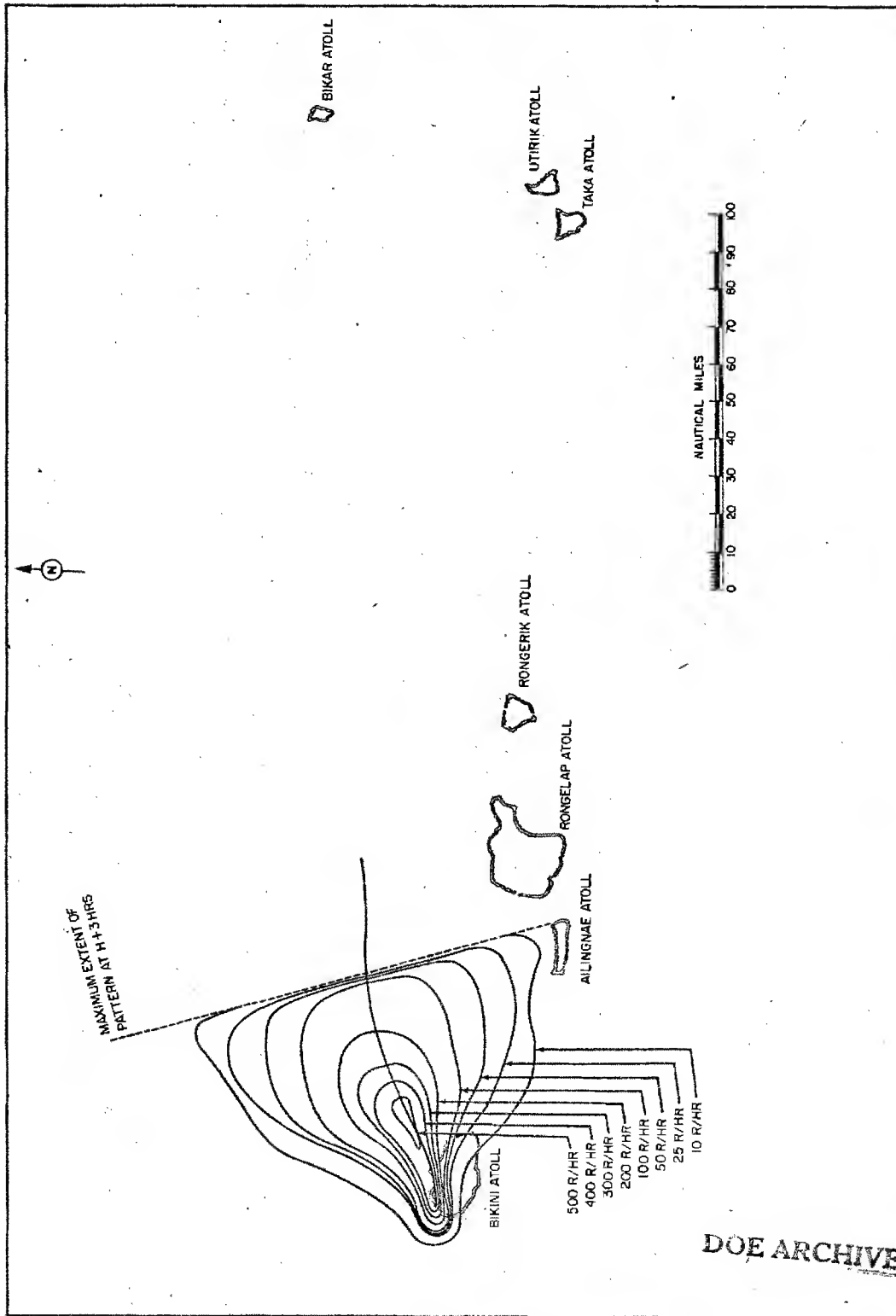


Figure 3
H+1 Hour Fall-out Contours, CASTLE-Bravo



DOE ARCHIVES

Figure 4
H+3 Hours Fall-out Contours, CASTLE-Bravo

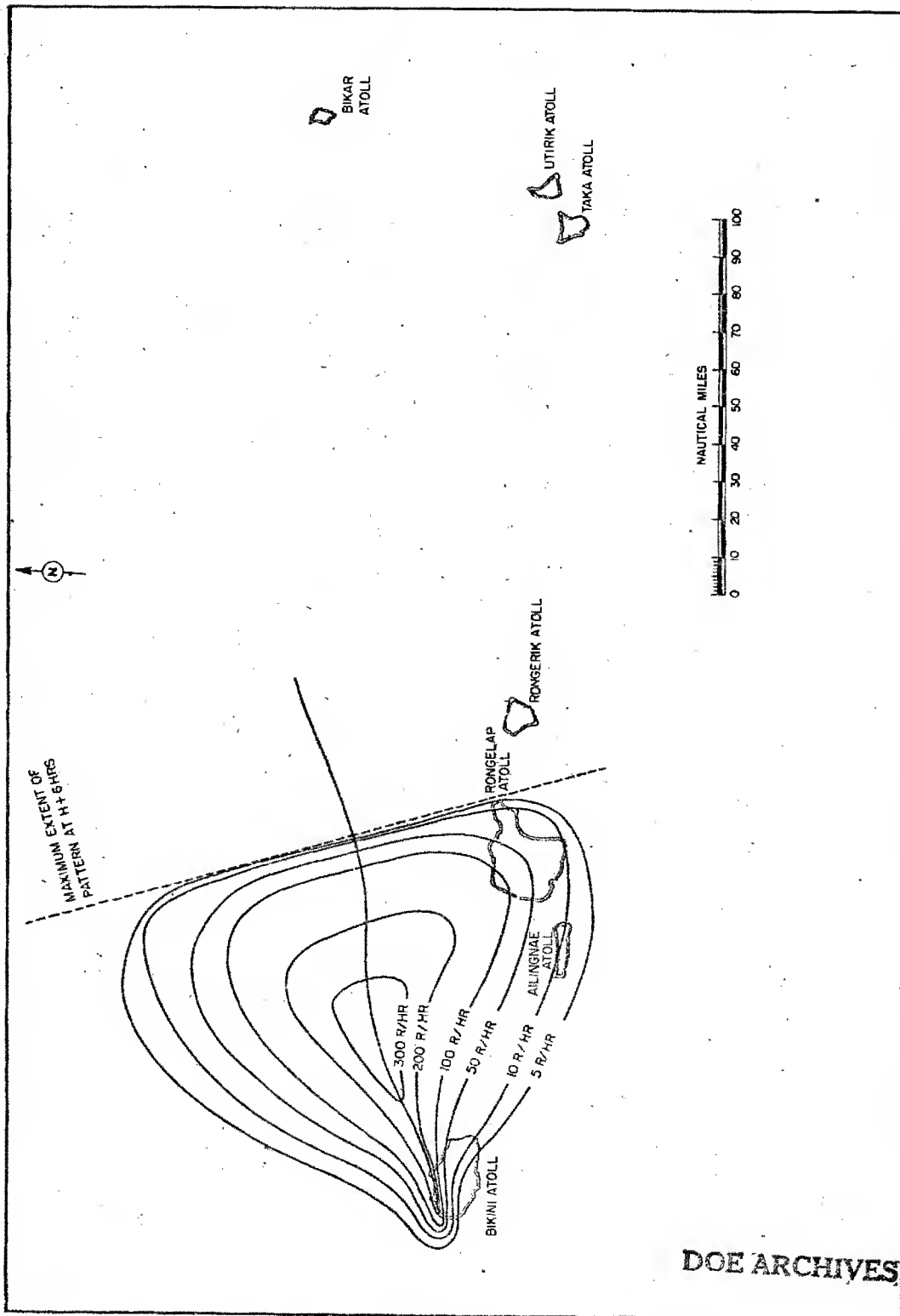


Figure 5
H+6 Hours Fall-out Contours, CASTLE-Bravo

394

RESTRICTED
NUCLEAR ENERGY

399

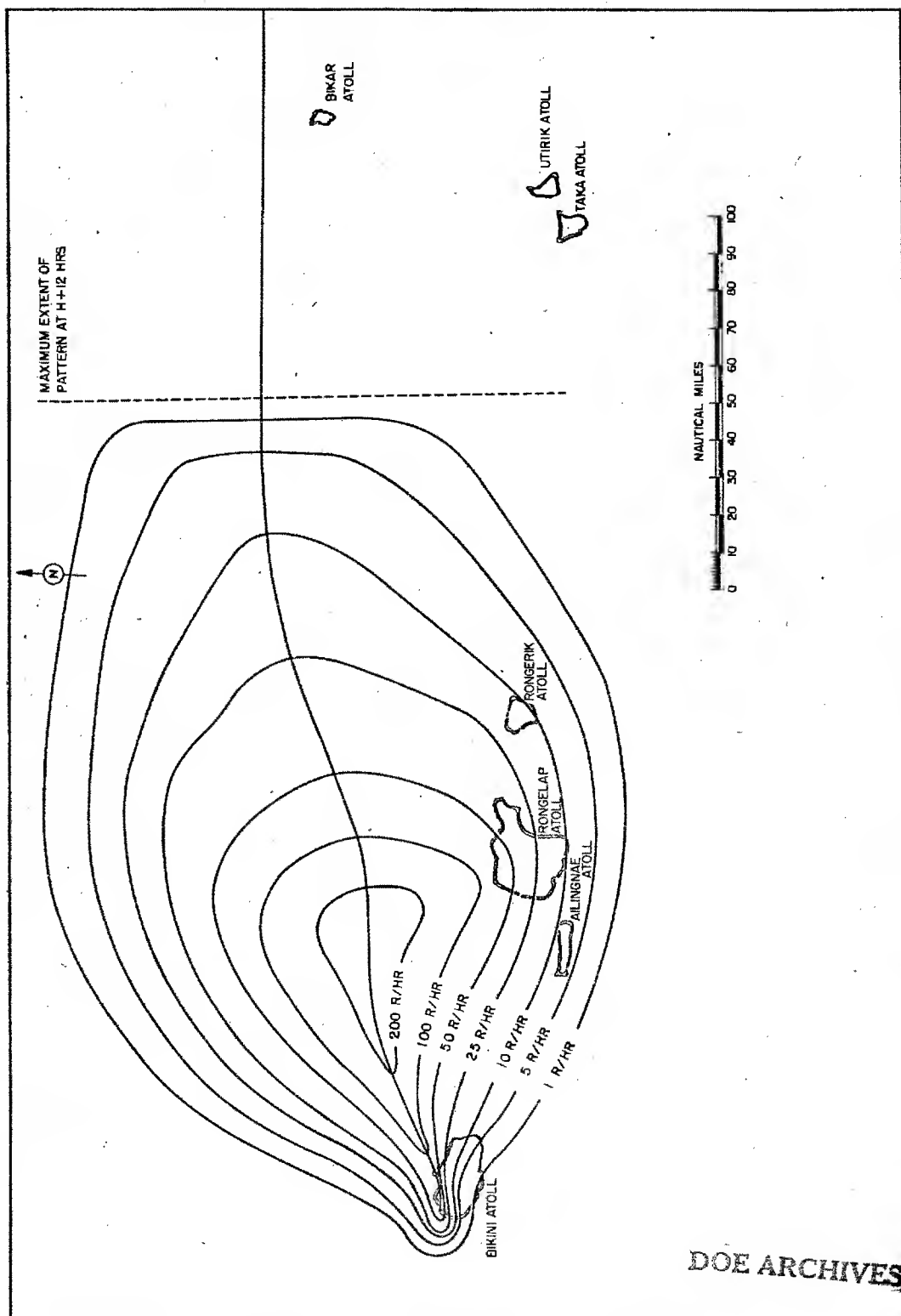


Figure 6
H+12 Hours Fall-out Contours, CASTLE-Bravo

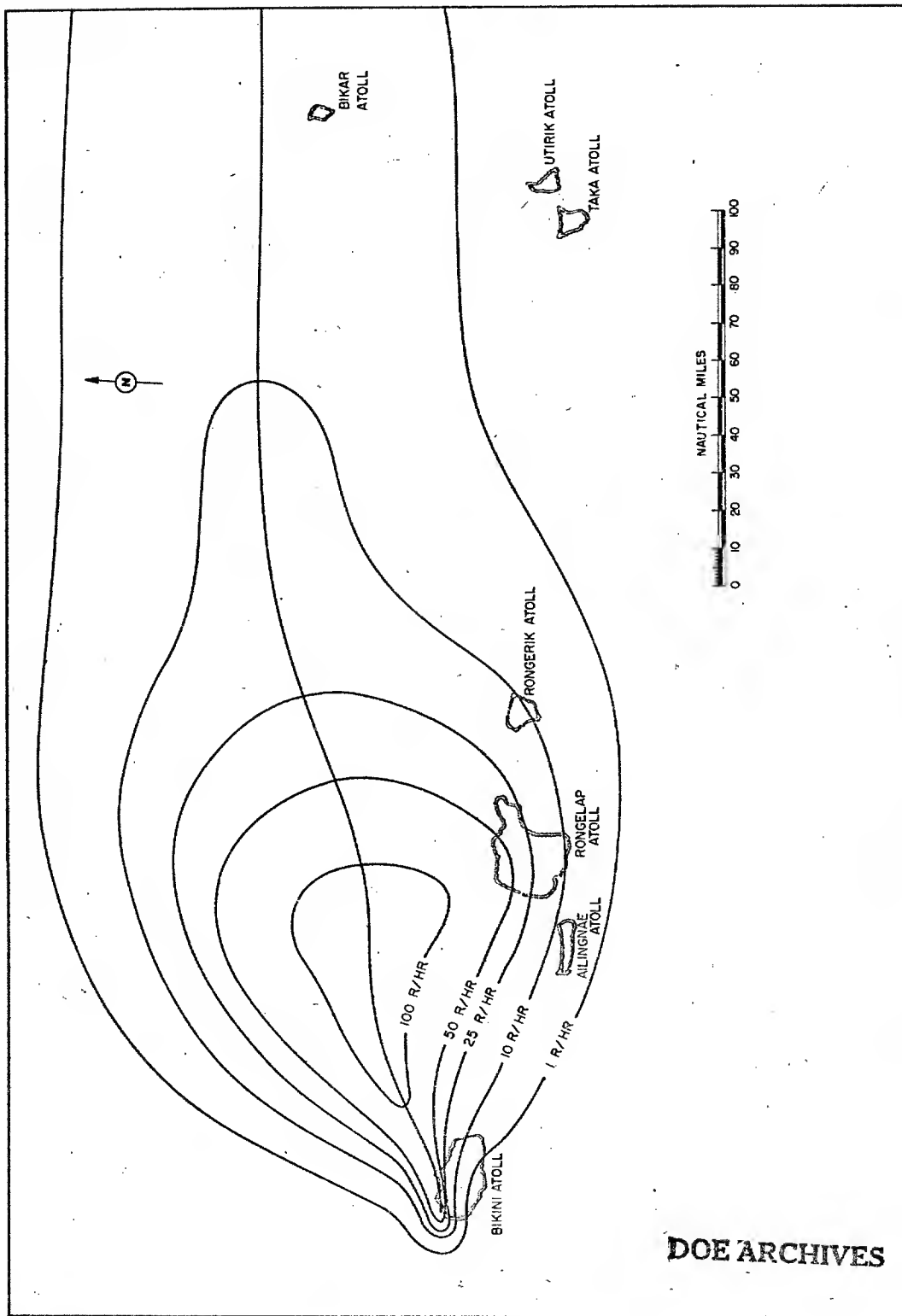


Figure 7
H418 Hours Fall-out Contours, CASTLE-Bravo

396

~~RESTRICTED~~
ENERGY ACT

~~SECRET~~

401

I would like to discuss the experimental data collected that is relevant to the analysis of the fall-out based on trajectory evaluations. Figure 8 shows the computed time of arrival of fall-out based on the 231 trajectories evaluated. It indicates an arrival time of 8.25 hours at Rogerik where the measured time of arrival was 8 hours. It shows an arrival time of 15.4 hours at a distance of 302 nautical miles when the observed time was 18 hours. The analysis appears to satisfy the time of arrival parameter very well.

Figure 9 shows the particle size distribution obtained experimentally from fall-out at Bikini atoll. This is a histogram of some 7000 radioactive particles. The trajectory analysis agrees well with deposition over this size range at Bikini atoll. The data on these particles analyzed with respect to their time of arrival shows positive evidence that of the particles over 500μ in diameter 50 to 90 per cent had to come from above 60,000 feet.

Figure 10 shows the measured particle size distribution of the fall-out that arrived at the outer islands of Alinginais, Rongelap and Utirik. The computed size distribution at Rongelap atoll based on the trajectory analysis indicates that particles from 50 to 150μ diameter would arrive at this location and the 250μ particles would fall just 10 nautical miles north of the atoll. The measured distribution shows that only 4 particles arrived at Rongelap with diameters larger than 200μ .

The analysis also indicates no particles above 75μ diameter could arrive at a distance of 302 nautical miles from ground zero where the measured distribution at Utirik had a geometric mean diameter of 45μ with only 3 particles being over 100μ in diameter.

The agreement here is surprisingly good and certainly suggestive of continuation of work along these lines. The major discrepancy in the analysis is the inability to account for fall-out at Utirik. This may be resolved by the use of Dr. Palmers analysis of the wind data existing at and after shot time.

In conclusion, it may be well worth discussing the fields in which serious work should be added both from an experimental as well as theoretical viewpoint. A portion of this work necessary to a more complete understanding of the phenomenology may be listed as follows:

The relation of activity to particle size appears necessary to most model evaluations. At this time data is seriously lacking in this field.

DOE ARCHIVES

397

SECRET

ATOMIC ENERGY ACT

402

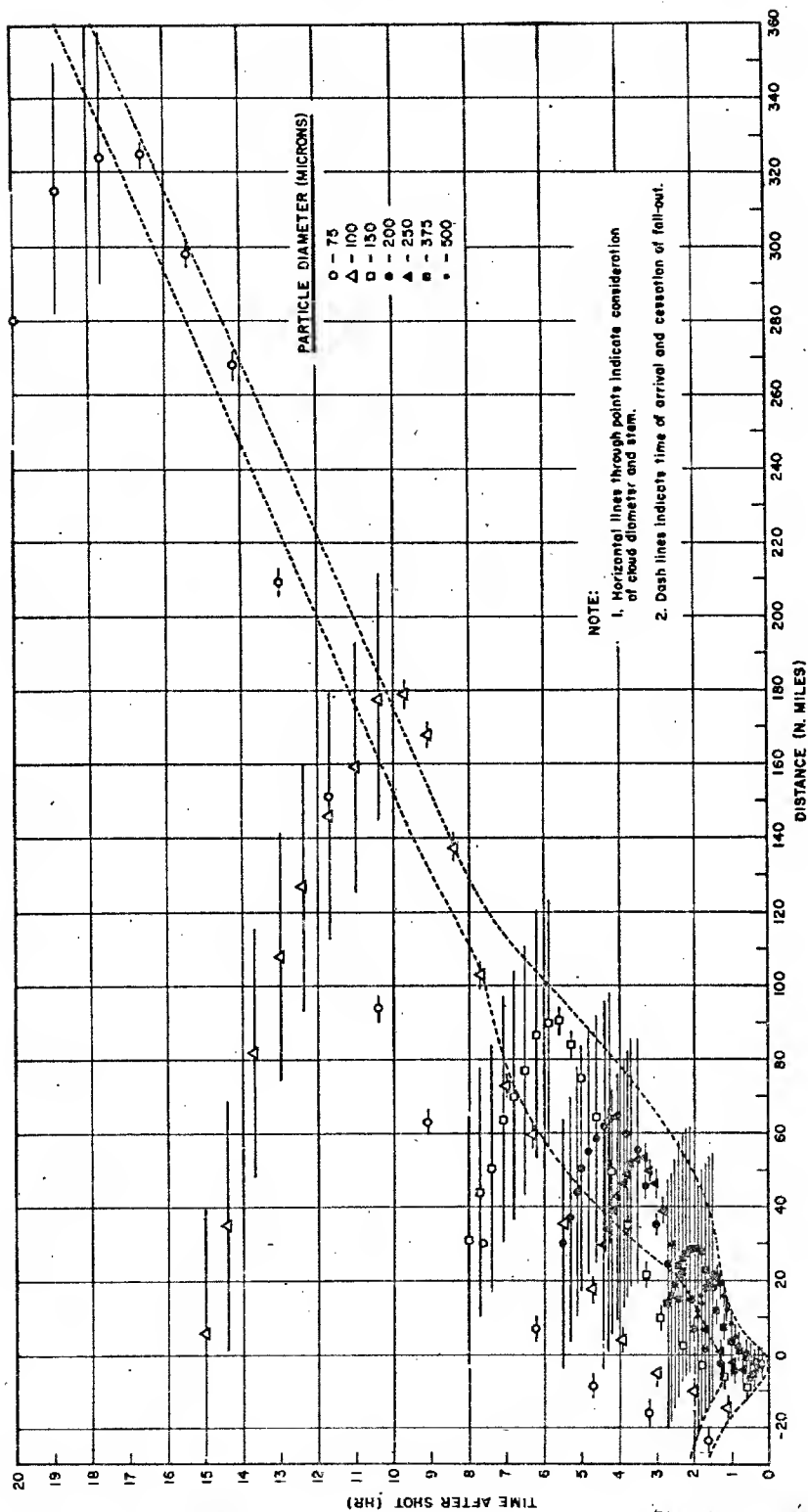


Figure 8
Computed Time of Arrival of Fall-out

DOE ARCHIVES

398

RESTRICTED
ENERGY ACT

403

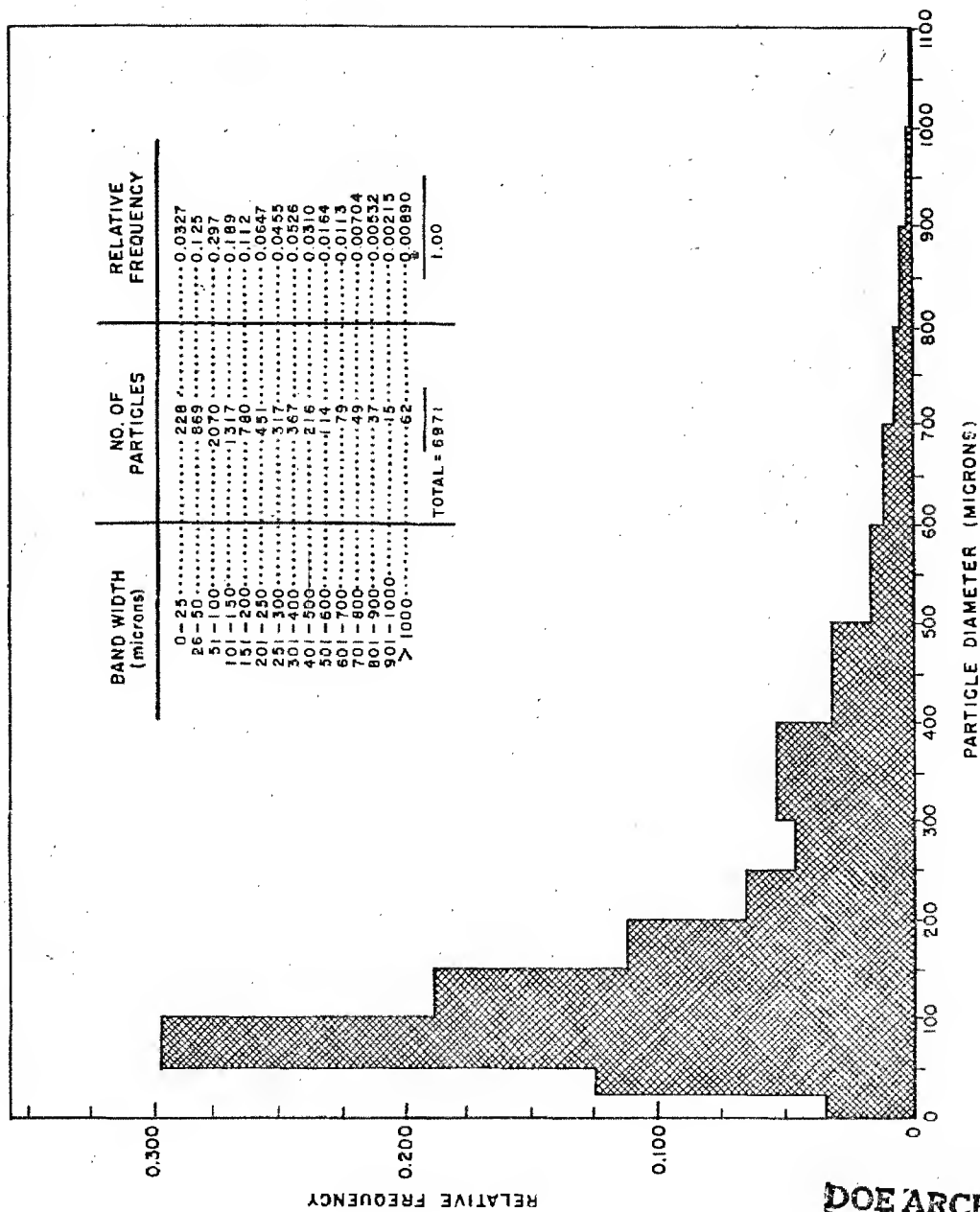


Figure 9
Particle Size Distribution at Bikini

DOE ARCHIVES

399

SECRET

DATA

404

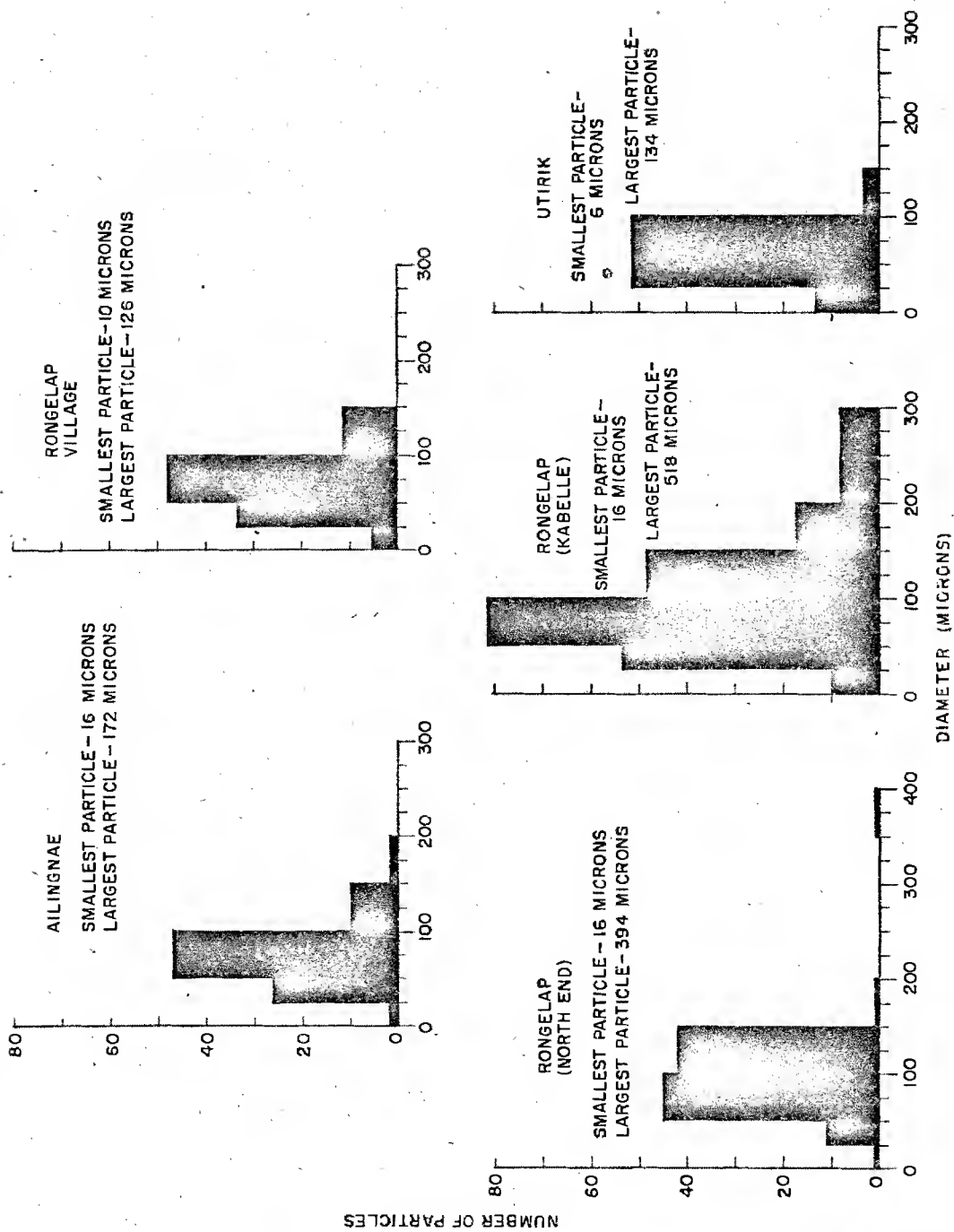


Figure 10
 Particle Size Distribution at Outer Islands

DOE ARCHIVES

[REDACTED]

Little is known at this time on particle formation phenomena. Certainly more thought should be given to this field, especially with respect to understanding the complete mechanism of fall-out.

The configuration of the radioactive cloud source as well as the particle size distribution within the source are at this time unknown. This knowledge seems paramount to any resolution of the basic concepts of the models presented at this symposium.

There still remains the small particle anomaly where measured fall-out with respect to time indicates the very small particles arriving at times much too early to account for their trajectory by any falling rate equation.

DOE ARCHIVES

THIS PAGE IS BLANK

DOE ARCHIVES

402

ATOMIC ENERGY ACT 1954

411

407

PREDICTION OF DOSE-RATE AND DOSAGE CONTOURS AS
FUNCTIONS OF YIELD AND METEOROLOGICAL CONDITIONS,
ORO AND TECHNICAL OPERATIONS, INC. METHOD

F. C. Henriques
Technical Operations, Incorporated

Introduction

Three months ago Technical Operations was requested by the Operations Research Office of the Johns Hopkins University (ORO) to provide 1 Hr-R/hr dose rate and two-day dose contamination patterns which would result from the surface detonation of a 15 MT thermonuclear weapon. These patterns were computed for the thirty wind conditions which resulted from considering wind conditions at six different locations along the Eastern Seaboard during five different but "typical" meteorological situations. Previous to initiation of these computations, conferences were held with those groups at Sandia, NRDL and Rand that are developing fallout models and prediction procedures. Based upon these discussions, a "fallout" model was evolved and a "hand" computational procedure was developed which enabled the calculation of sixty fallout patterns in a one-calendar month with a reasonable number of man months.

The same fallout model and procedural method were used to compute in a two-week period the thirty-six radiological contamination patterns given in this report. These thirty-six patterns result from the calculation of dose rate and two-day dose contours for 1, 15 and 50 MT surface detonations for the six AFSWP wind conditions.

The underlying constraints required for these computations are markedly similar to those which have been described in the Symposium Report by Rand, the Signal Corps, and NRDL. The details of the computational methods employed by the various groups do differ; those recently developed by Rand and NRDL are well suited to machine computations, while those developed by the Signal Corps and Technical Operations have been specifically tailored to "hand" calculation procedures. It is not the purpose of this report to detail our computational procedure; this is reported elsewhere.

DOE ARCHIVES

If the input assumptions used by the above-mentioned groups were identical, identical fallout prediction patterns should result. Unfortunately, since there is a lack of experimental data, assumptions must be made to: (1) the radioactive cloud spacial dimensions; (2) the size distribution and fall times of entrained particles; (3) the fraction of activity associated with a given particle size; and (4) all the conversion factors which ultimately convert this activity once it reaches the ground to roentgen dose rate and biologically effective cumulative dose. Each

SECRET

of the four above-mentioned groups use different sets of assumptions.

In Section I we outline the constraints which are believed to be common to each of these four methods and list the assumptions inherent in the Technical Operations model. We then discuss the areas and shapes of the 100, 500 and 1500 fission product 1 hr-R/hr dose rate and two-day cumulative dose contours which result from the surface detonation of 1, 15 and 50 MT weapons for the six AFSWP wind conditions. This is followed by an analysis of the similarities and scaling relationships of both the areas and shapes of these contours. Finally we propose a rapid scaling procedure that is believed to be reasonably valid.

In Section II we assume that the 1 hr-R/hr and 2-day dose roentgen readings at any ground location are known input data. We then derive the equations required to compute the biological effective dose from fission products and the contribution of U-239 and Np-239 thereto. The utility of the graphs and tables generated by these equations is illustrated by solving three typical practical problems.

The detailed justification of the information stated in Sections I and II is available elsewhere (ORO report in press).

Radioactive Fall-out Constraints, Assumptions and Results

To avoid duplication, it is assumed that the Rand and Signal Corps papers which comprise a portion of the Symposium Report have been read. The constraints inherent to their procedures as well as our approach may first be listed. Some of these could be dropped but only at cost of more complicated calculation procedures.

- A. There is some instant ("instant of stabilization") at which the distribution of activity vs particle size and the spatial distribution of such particles is known.
- B. The range of particle sizes is such that pure diffusion of particles can be neglected and yet the particles as they fall will follow wind currents at each pertinent altitude with no important lag.
- C. The range of particle size is also such that for any two given particles the ratio of their fall times from various altitudes is constant (independent of altitude) to sufficient approximation.
- D. At the instant mentioned in A, the distribution of activity vs particle size is independent of spatial position.
- E. At the instant mentioned in A, the spatial distribution of total activity is laterally uniform (within some area) at any one altitude.
- F. There are no vertical winds, and the horizontal wind pattern vs altitude remains constant over a time sufficiently

DOE ARCHIVES

long for all those particles destined to arrive at locations of interest to complete their fall.

These list only those constraints required to yield a rapid "hand" calculation technique. Before discussing these, it is perhaps worth pointing out several items that need not be assumed to achieve computation rapidity. The vertical distribution of activity in the cloud at the instant of stabilization can be arbitrary, and the cloud can have an arbitrary physical shape. Likewise, the distribution of activity vs particle size can have any shape; the only restrictions here are on the range of sizes, which must satisfy B and C.

Constraint A merely states that the problem is restricted to falling-particle calculations and does not concern the processes which establish the radioactive cloud.

An inertial lag and diffusion analyses show that particles at least in the range 10 microns to 2000 microns satisfy Constraint B. The lower limit is certainly unnecessarily high, but appreciable raising of the upper limit would require more careful investigation. However, the effects of large particles in the model are rather insensitive to this constraint since they all fall close to ground zero in any case.

The rather surprising property postulated in Constraint C is actually satisfied quite well over the same range, 10 to 2000 microns. This is subject to direct calculation. The results of these calculations are given in Tables 1 and 2.

Constraint D is rather ad-hoc; it enables the problem to be broken into independent components. Until actual measurements at the "instant of stabilization" are available, it must rest entirely on the argument that continual mixing occurs during the relatively brief period (10 min) when the "boiling" cloud is rising and that in this way the chances of a given particle being located at a given position are independent of its size and of the activity which it carries. It is doubtful that this is literally true, but the argument seems intuitively reasonable enough to justify its use until data can be shown to seriously refute it.

DOE ARCHIVES

Constraint E simplifies calculation to the extent that only geometric coincidence data need be taken off the plots used in calculation. It could be lifted at the cost of considerably more data-handling during calculation, but it does not affect the over-all scheme of calculation. Very little data seem available on this point, but the few measurements which have been made with drone airplanes at Greenhouse tend to give confirmation.

CLOUD PROPERTIES "AT STABILIZATION"

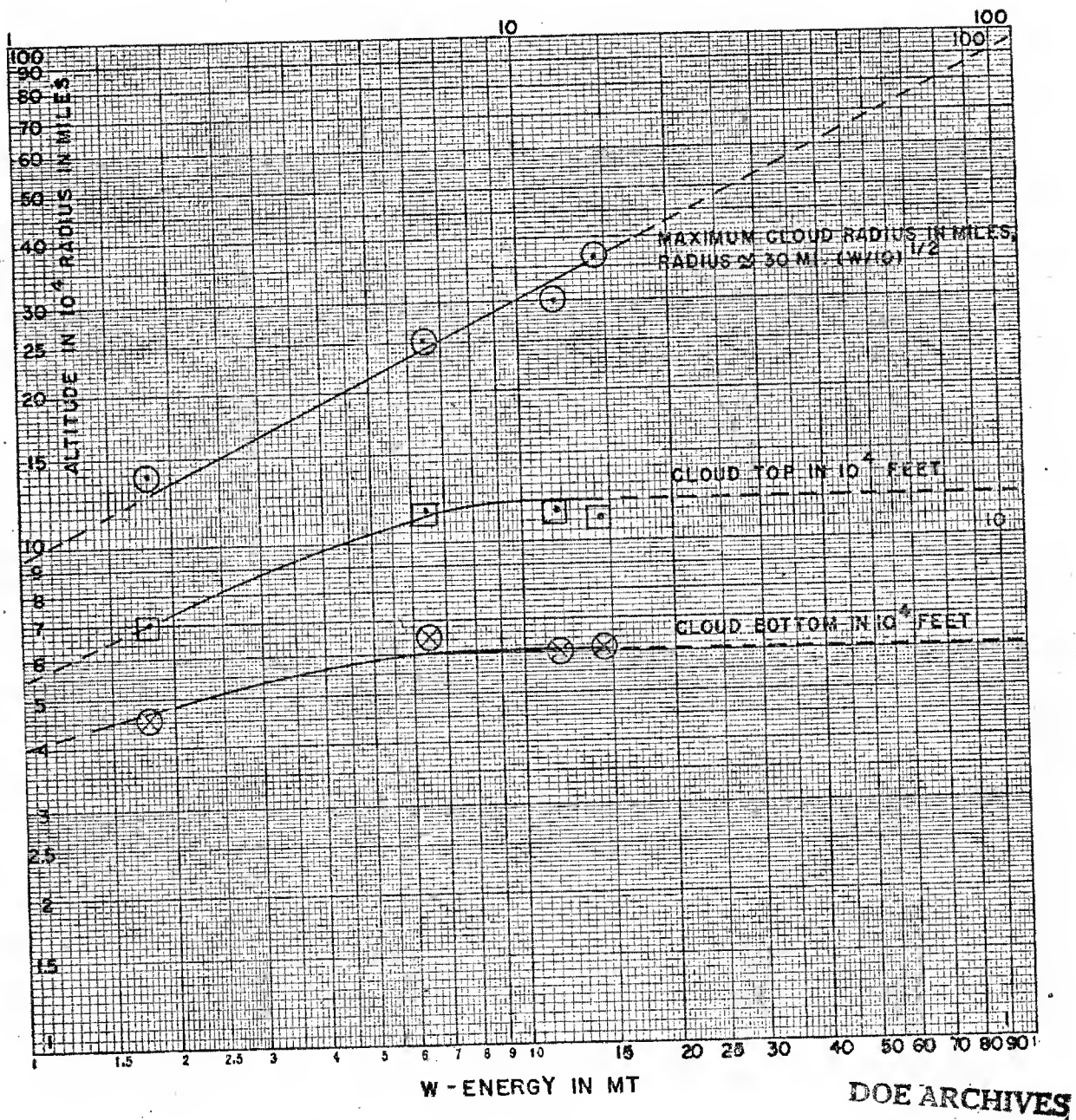


Figure 1

406

RESTRICTED

Constraint F is required to avoid plotting the map position of more than one particle size. Vertical winds are probably negligible in a great many cases. Constancy of the horizontal winds over long time periods is probably not too realistic. Provided that the meteorological data were sufficiently well known, Constraint F could be lifted at the cost of plotting in detail the final positions of all particle sizes from all altitudes. Subsequent calculation would not be affected however.

We now proceed to discuss the Technical Operations data assumptions which result in our specific fall-out patterns. These assumptions are not specific to the method of calculation but must, of course, be given before a calculation can be performed.

The cloud properties are shown in Figure 1. The plotted points are experimental surface shots where the radius is the maximum radius of each cloud. The experimental points have been connected by rough curves which have been extrapolated in both directions. These extrapolations are based on the following arguments.

For larger weapon yields, in lieu of data, it seems reasonable to assume that the radius will continue to grow at about the same rate as before; thus the radius is extrapolated as $W^{1/2}$. A positive steep atmospheric temperature gradient starting at about 120,000 ft (the "ozone absorption layer") can be expected to limit the cloud top to about this altitude. This is because the cloud must expand as it rises in order to maintain pressure balance with the surrounding air. Because of the expansion, it cools more or less adiabatically. At lower altitudes, however, the surrounding air temperature also drops with pressure approximately adiabatically and the cloud, once much hotter than its surrounding air, remains hotter as it rises and thus continues to have bouyancy. This process reverses, however, at about 120,000 ft and the cloud should very rapidly lose bouyancy and come to thermal equilibrium with the atmosphere. The atmosphere exhibits another positive temperature gradient in the neighborhood of 40,000 - 60,000 feet (the tropopause). However, clouds resulting from nuclear detonations in excess of 1 MT still have sufficient internal energy when they reach the tropopause to punch through it. The cloud top has therefore been assumed to have a ceiling of 120,000 ft. The data for the cloud bottom also appear to indicate a leveling off. This would be expected on the basis of the other two curves, for the mass of the original fireball is known to be nearly proportional to W . If this is true also of the cloud, the cloud bottom must level off as shown at 60,000 ft. The data seem to support this conclusion.

DOE ARCHIVES

The extrapolation toward lower energies is based on data for the



Figure 2
Photograph of IVY-Mike Shot taken at the "Instant of Stabilization"

DOE ARCHIVES

408

413

surface shot of 1.2 KT which nearly fall on the straight-line extrapolations shown. In addition, these extrapolations yield a total cloud mass very nearly proportional to yield - assuming the mass-distribution within the cloud is the same as that in the atmosphere it replaces.

An additional property of clouds which is required is their shape. Here data are quite sparse for the "late times" (about 10 min) when the cloud finally stabilizes.

Early calculations were done assuming a cylindrical shape but this leads to rather low peaks of contamination* and does not agree with photographs and descriptions scattered through the classified literature. The shape finally used was taken from a written description of the Castle-Bravo shot and is substantiated by Figure 2 which is a photograph** of Ivy-Mike shot (11.2 MT) taken essentially at the "instant of stabilization". The result (illustrated in Figure 4) is an inverted cone truncated so that the cloud bottom has a diameter 40% of top diameter given by Figure 1. There is nothing at all sacred about this particular shape; any shape could be used in the calculations but a truncated cone seems to be the best possible assumption at the present state of knowledge, especially since the limiting action of the "ozone ceiling" must enlarge the cloud top with respect to the bottom.

Another piece of required data is the distribution of radioactivity vs. particle size. Such measurements have been made only*** for the Jangle surface and underground shots of about 1 KT. These data (NRDL, private communication) are plotted in Figure 3 which shows for each particle size, plotted vertically on a logarithmic scale, the fraction of activity associated with particles of that size or less, plotted

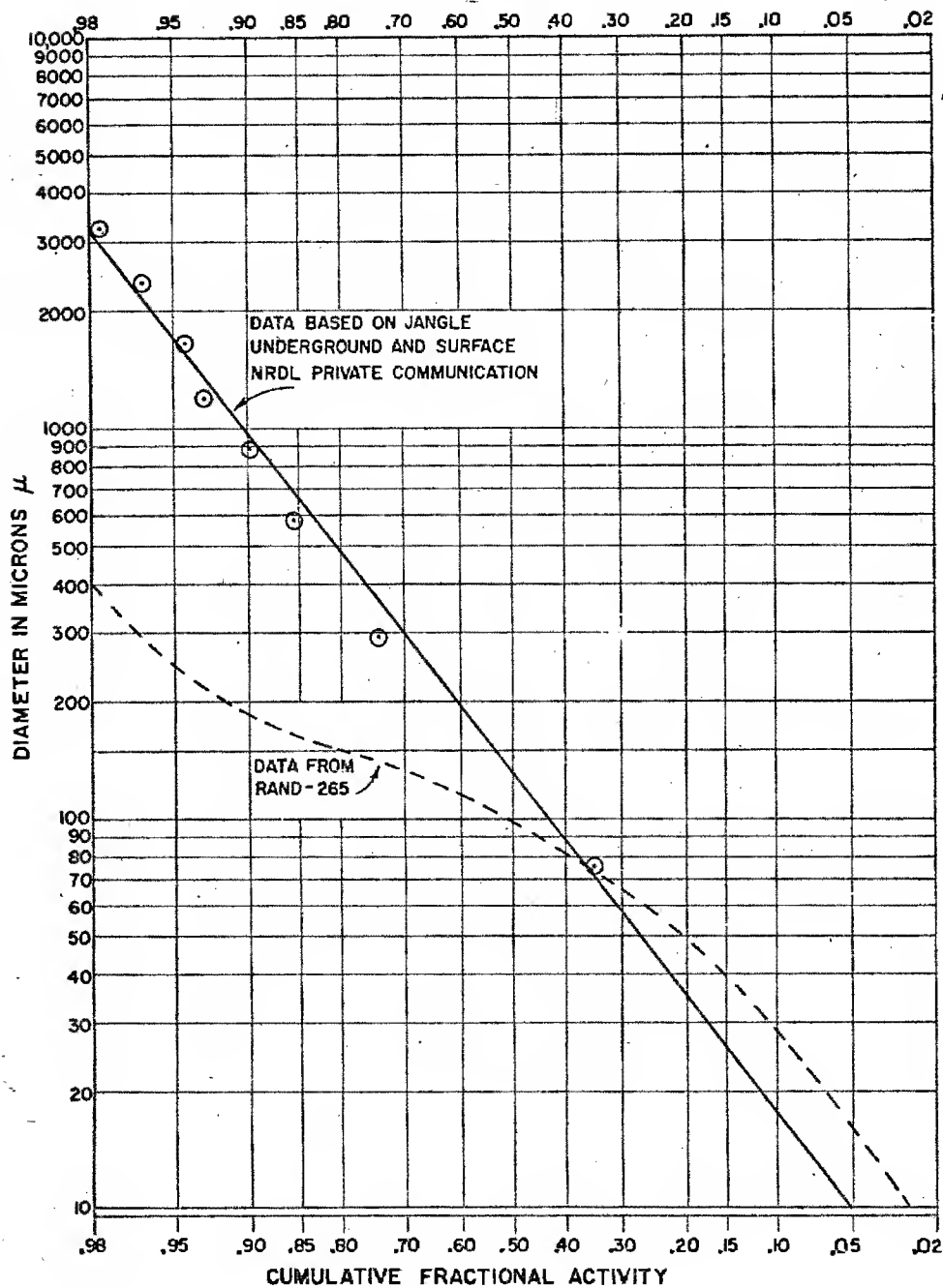
* This fact has also been recognized by the Rand group. For their calculations they are apparently now using artificial cloud radii which are about 60% of the reported cloud radii.

** Observation of the motion picture of the 15 MT Castle-Bravo shot indicates the same shape at this late time. A still photograph is not available at this writing.

*** Other measurements have given the size-distribution of particles with some activity, while still other measurements have yielded activity versus particle size but unfortunately for different weapon tests. Neither alone is sufficient. The combination of these is what is required.

DOE ARCHIVES

~~NUCLEAR ENERGY A~~



PROBIT PLOT OF CUMULATIVE PARTICULATE ACTIVITY
FRACTION OF ACTIVITY IN PARTICLES OF SIZE $\leq \mu$

Figure 3

410

DOE ARCHIVES

[REDACTED]

horizontally on a probit scale. The straight line plot means that the activity has a Gaussian normal distribution in the logarithm of particle diameter. The data in Figure 3 may be expected to hold for surface shots over most land areas since the intrinsic particle sizes of various soil-particles and concrete are not greatly different. The data may also be expected to hold for a wide range of weapon energies for the following reason. Within the fireball the conditions of formation of radioactive particles must be quite localized and thus depend only upon the energy density per unit mass of debris. The mass of soil blown out of the crater which becomes part of the fireball in a surface shot is proportional to weapon energy. Therefore the energy density per unit mass of soil within the fireball is independent of yield. This leads one to expect that the conditions of formation of the radioactive particles are independent of the weapon energy.

It must be realized, however, that the distribution curve of Figure 3 does not necessarily hold for all other soils. In particular, the coral found in the Pacific area is very different; it is very likely decomposed under the intense heat with CaCO_3 giving off CO_2 to become CaO which may then be converted to hydroxide by moisture in the air. These processes should still lead to a distribution relatively independent of weapon energy but the curve may be vastly different from the Nevada results. Also shown in Figure 3 is the curve which Rand found necessary to duplicate the results of Castle shot Bravo. Our calculations lead to a similar result.

The distribution of total concentration in the cloud must also be known. (Figure 3 has only specified the breakdown of this total into particles of various sizes.) For reasons discussed under Constraint E, we have assumed the total activity density to be constant within the cloud at any one altitude, but the vertical distribution has not yet been specified.

DOE ARCHIVES

The first assumption that generally springs to mind when this question is asked is that the activity is probably uniformly distributed in the vertical direction as well. Consider, however, the fact that a cloud from a large weapon extends from altitude 60,000 to 120,000 ft. Over this range the air density and pressure change by a factor of 8. Now the pressure in the cloud must equal the external air pressure if motion is to cease and the temperature cannot long stay very different from that of the surrounding air. If this is so and if the cloud maintains a stable shape, then the (mass) density must (by the universal gas law) also be near that of the surrounding air. This also balances the buoyancy forces due to gravity.

RESTRICTED

412

DOE ARCHIVES

417

TABLE I
Time for Particle to Fall 10,000 Feet from Altitude, H
Tabulated Values in Hours

Altitude in Thousand Feet, H	Particle Diameter, μ , in Microns											
	10	20	30	50	70	100	150	200	300	500	1000	2000
0	---	---	---	---	---	---	---	---	---	---	---	---
10	157	39	17.4	6.05	4.05	2.24	1.20	0.84	0.50	0.30	.170	.094
20	149	36	16.6	5.80	3.72	2.15	1.11	0.75	0.45	0.27	.149	.090
30	139	34	15.5	5.43	3.28	1.96	0.99	0.67	0.40	0.23	.127	.077
40	131	32	14.8	5.25	2.99	1.80	0.90	0.60	0.35	0.20	.107	.064
50	125	32	14.3	5.14	2.72	1.65	0.82	0.54	0.31	0.17	.092	.052
60	120	31	14.3	5.04	2.64	1.50	0.77	0.49	0.27	0.15	.084	.043
70	115	30	13.9	5.04	2.62	1.46	0.72	0.45	0.25	0.13	.063	.035
80	109	30	13.5	4.93	2.62	1.39	0.70	0.42	0.23	0.11	.054	.029
90	100	28	13.1	4.78	2.56	1.29	0.69	0.41	0.21	0.10	.045	.024
100	89	26	12.3	4.60	2.44	1.23	0.66	0.39	0.20	0.09	.039	.020
110	73	23	11.2	4.37	2.34	1.18	0.62	0.37	0.18	0.08	.034	.017
120	58	20	10.0	4.09	2.23	1.13	0.59	0.33	0.17	0.08	.030	.014

~~SECRET~~

Thus, the mass of the whole cloud must be distributed in the same way as that in the surrounding atmosphere. (As already mentioned, this checks the expected proportionality of total cloud mass to yield, given the data of Figure 1.) If the further assumption of violent mixing during the short (10 min) cloud rise is invoked, the cloud debris must also be distributed in the same way as the density of the atmosphere.

In lieu of detailed data, then, it would appear that the most reasonable assumption is that total activity density is proportional to air density. There is an indication from early drone flights at Greenhouse that ion chamber readings were independent of altitude within the cloud. This is precisely what would be expected on the above assumption since the gamma ray path lengths would vary with air density in such a way as to exactly cancel the variation of activity concentration; in other words, an ion chamber measures activity per unit air-mass which is what we have assumed to be constant. Further data on this point would, however, be most desirable.

In order to compute the fall times of the radioactive particles from various altitudes, they were treated as irregular spheres subjected to the standard aerodynamic fall equation. For very small velocities this equation reduces to Stokes Law and for very high velocities to the law for the turbulent region. At very low air densities, when the mean free path of the air molecules becomes comparable to the particle diameter, the fall velocity must be increased according to a slip-page equation. The fall velocities presented as the time in hours to fall 10,000 ft as a function of particle size and altitude are given in Table I. The computational details are presented elsewhere. Table II has been prepared from Table I. It demonstrates that the relative time for irregular spheres of various sizes to fall to ground is markedly invariant to the originating altitude. Thus Constraint C is satisfied and it is this fact properly exploited which results in the tremendous simplification of the Technical Operations computational method.

Finally, we present the conversion factors used to obtain the fission product dose-rates expressed in roentgen units. These are shown in Table III. In comparing the fallout contour predictions of the various groups, due consideration must be given to the numerical values used by these groups which correspond to those presented in Table III. For example, Rand at this writing uses 1200 in column (A) and unity in column (C).

DOE ARCHIVES

All of the constraints, assumptions and data required to predict fallout patterns have been enumerated above. At this point we will in-

~~SECRET~~

~~DATA~~
~~NUCLEAR ENERGY~~

TABLE II

Relative Particle Fall Time to Ground from Altitude, H
Normalized to 100 Units for 70 μ Particles

Altitude in Thousand Feet, H	Particle Diameter, μ , in Microns											
	10	20	30	50	70	100	150	200	300	500	1000	2000
10	3880	963	430	149	100	55.3	29.6	20.7	12.4	7.41	4.20	2.32
20	3940	965	436	153	100	56.5	29.7	20.5	12.2	7.34	4.11	2.37
30	4030	986	447	156	100	57.5	29.9	20.5	12.2	7.24	4.04	2.36
40	4100	1000	457	161	100	58.0	29.9	20.4	12.1	7.12	3.94	2.31
50	4180	1030	468	165	100	58.5	30.0	20.3	12.0	6.98	3.85	2.25
60	4230	1050	478	169	100	58.2	29.8	20.0	11.8	6.80	3.76	2.16
70	4250	1060	485	171	100	57.9	29.6	19.7	11.5	6.58	3.60	2.07
80	4240	1070	487	173	100	57.4	29.2	19.3	11.2	6.32	3.44	1.96
90	4210	1070	490	175	100	56.8	29.0	19.0	10.9	6.10	3.28	1.87
100	4160	1070	491	175	100	56.2	28.8	18.7	10.7	5.90	3.14	1.78
110	4090	1070	490	177	100	55.8	28.7	18.5	10.5	5.72	3.02	1.70
120	3990	1050	488	177	100	55.5	31.5	18.3	10.3	5.58	2.91	1.63
40-120 Average	4160	1050	482	171	100	57.1	29.6	19.4	11.2	6.34	3.44	1.98

icate how this information is employed through reference to Figure 4.

In Figure 4 the cloud sizes containing the radioactive debris at the instant of stabilization for the three sizes of weapons are drawn to scale with the top and bottom altitudes and top-radius given by Figure 1. This shape is then divided into horizontal slabs having equal activity per unit area. (Ten slabs suffice for 15 and 50 MT weapons, and five slabs for the 1 MT.) Due to the assumption that activity density varies as air density, the pressure drops across all slabs are the same. This results in the slabs having the radii and mean altitudes depicted

TABLE III

Roentgen Contour Constants
(Fission Products Only)

	Flat Ground 1 hr-R/hr per sq mi/fission products on Ground per KT of Thermonuclear Explosion	Radioactive Decay Law (ii)
DELETED	(AxBxC)	
	550	$t^{-1.2}$

(ii) This $t^{-1.2}$ law is a good approximation for moderate t but is known to be inaccurate for times beyond 200 days; however, until better data are available this law seems to be adequate for purposes at hand

in the lower portion of Figure 4. In the "zero wind case" all of the activity from each of the slabs must ultimately fall upon the ground with zero lateral displacement. The conversion factors listed in Table III and shown in Figure 4 result in the 1 hr-R/hr dose rates for various

DOSE RATE PATTERNS FROM THERMO-NUCLEAR WEAPONS

ZERO WIND CASE

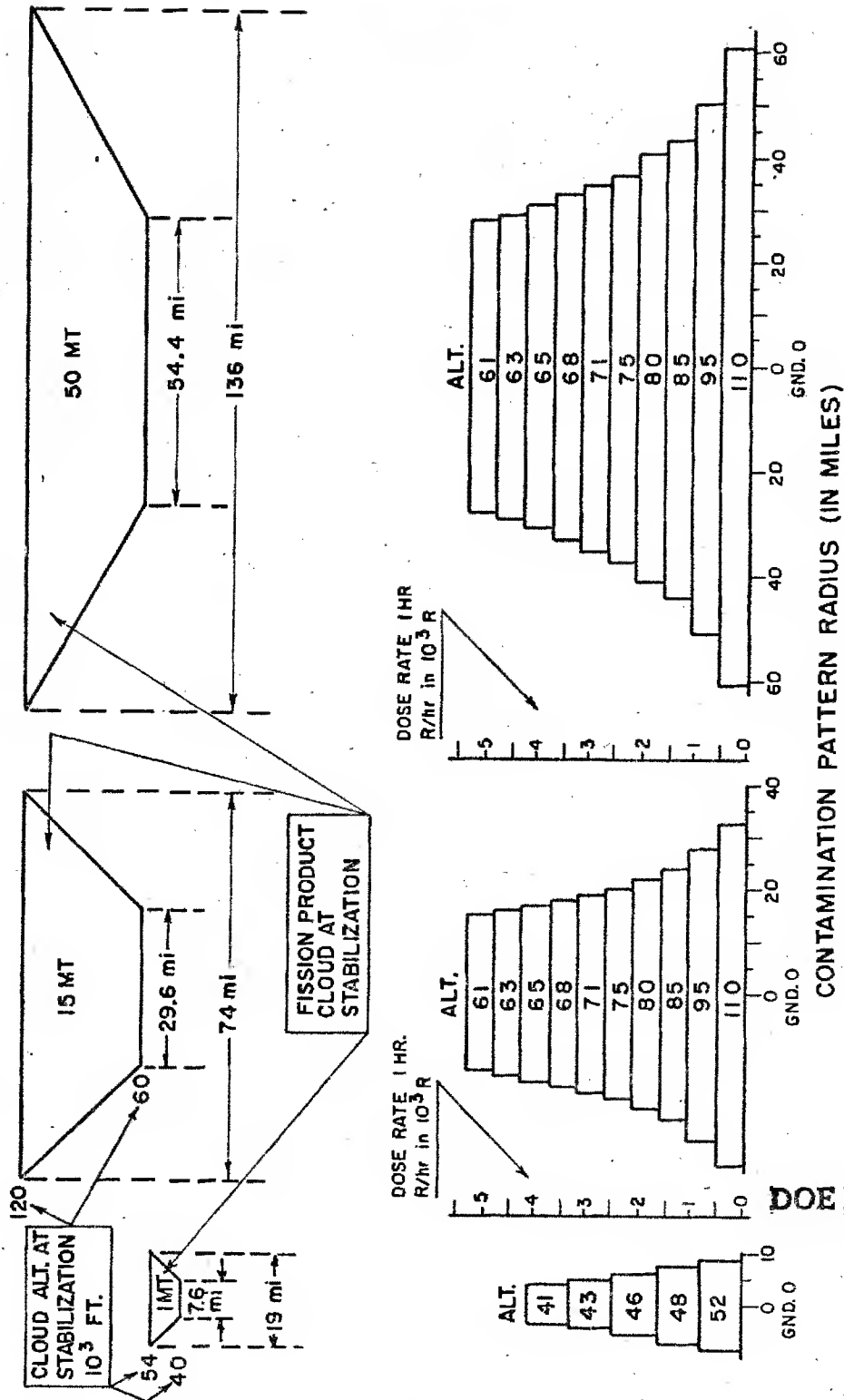


Figure 4

DOE ARCHIVES

~~SECRET~~

distances from ground zero. Thus the highest possible effective 1 hr-R/hr dose rates which can result from this model under any wind conditions is 5700 for the 15 MT and 50 MT weapons and 4200 for the 1 MT weapon. The additional contamination near ground zero due to the small amount of radioactive debris in the stem is not treated in this model. Although the two-day cumulative dose for the zero wind case is not shown, it is readily calculable since: (a) the fall times to ground of the various size particles from each horizontal cloud slice is predetermined by Table I; (b) the portion of activity associated with the various size particles is given in Figure 3; and (c) radioactive decay is assumed to obey the $t^{-1.2}$ law.

The effect of wind on zero wind patterns is to change the ground coordinates but not the fall times of the particles contained in each horizontal cloud slice. This distorts the shape and alters the area of the roentgen contours. The degree of distortion and alteration depends upon the meteorological conditions and is calculable from assumptions and constraints discussed above by a method similar in principle to that described by Rand in this Symposium Report. The results of these calculations are the eighteen 1 hr-R/hr and two-day roentgen cumulative dose contours compiled in another section of the Symposium Report. To facilitate comparison, our contours have been renormalized to a terrain factor of unity. We are of the opinion that a terrain factor of 0.55 for flat land is far more realistic. Thus with respect to what would actually be measured with a roentgen dose-rate meter 3 ft above ground, the roentgen levels of our contours as depicted (as well as those shown for the other groups) should be reduced twofold. Table IV tabulates the contaminated ground areas enclosed by fission product roentgen level contours for 1, 15 and 50 thermonuclear surface bursts for all six AFSWP winds.

From the data contained in Table IV, we can draw the following conclusions, some of which in view of the complexity of fallout phenomena could not have been anticipated:

These contour patterns were computed for a variety of rather widely varying wind conditions. Therefore, for a given burst energy, the contaminated area enclosed by any 1 hr-R/hr contour is not strongly dependent upon the meteorology; this is also true for each two-day cumulative dose contour.

DOE ARCHIVES

For each wind condition, except for some of the 1500 R contours resulting from the 15 and 50 MT surface bursts, the areas enclosed by the same numerical value of the 1 hr-R/hr and two-day dose do not differ greatly.

TABLE IV

Areas of Contaminated Ground Enclosed by the Roentgen Levels Noted for the Six AFSWP Wind Conditions
(Areas Tabulated in 103 sq. mi.)

Fission* Product Roentgen Level	Burst Energy MT	R is 1 hr-R/hr Dose Rate						D is two-day Cumulative Dose					
		Dodge City, Ia. 28 December Condition A		Washington, D.C. 28 September Condition B		Carribou, Maine 18 March Condition C		Boise, Idaho 14 May Condition D		Washington, D.C. 9 February Condition E		Washington, D.C. 8 July Condition F	
		R	D	R	D	R	D	R	D	R	D	R	D
100	1	0.7	0.9	1.0	1.3	0.8	1.8	0.7	0.8	0.5	1.9	0.8	0.7
	15	10.7	10.2	12.6	11.4	13.1	13.0	10.0	5.6	11.0	15.5	8.7	5.2
	50	32.3	29.0	42.4	28.0	46.0	36.0	27.6	14.4	40.0	43.0	27.3	15.6
500	1	0.2	0.3	0.0	0.4	0.0	0.3	0.2	0.4	0.0	0.0	0.2	0.3
	15	2.6	3.7	2.8	3.7	2.0	4.3	2.4	3.2	0.3	4.0	2.7	3.2
	50	9.3	12.8	10.5	12.1	9.6	14.7	10.3	9.6	5.2	15.0	9.0	8.7
1500	1	0.0	0.1	0.0	0.0	0.0	0.0	0.0	0.1	0.0	0.0	0.0	0.1
	15	0.0	1.4	0.0	1.6	0.0	0.0	1.1	1.6	0.0	0.0	0.6	1.3
	50	1.3	6.2	1.8	6.2	1.0	6.0	5.0	6.0	0.0	3.6	4.0	4.0

Condition A - Winter. - Wintertime situation of an abrupt approximately 90° shear at a height of approximately 40,000 ft. 30 to 50 knot winds.

Condition B - Fall. - Gradual shear of approximately 90 per cent, 20 to 30 knot winds.

Condition C - Winter. - Winds at all levels from approximately the same direction, 30 to 60 knot winds.

Condition D - Spring. - Relatively low wind speeds at all levels, 0 to 15 knot winds.

Condition E - Winter. - Relatively high wind speeds above 10,000 ft, 50 to 130 knot winds.

Condition F - Summer. - Gradual shear of approximately 180°, 10 to 30 knot winds.

* Increasing the roentgen level twofold yields contaminated areas for a terrain factor of unity.

A similar table has been tabulated elsewhere in the Symposium Report for comparative purposes. This latter table gives roentgen levels for our predicted areas based upon a unity terrain factor.

DOE ARCHIVES

~~SECRET~~

A Castle-Bravo type weapon (15 MT) detonated on land areas similar to that of the Eastern Seaboard would result in 1 hr-R/hr dose rate and two-day cumulative roentgen dose contours of 100, 500 and 1500 whose contamination areas would encompass about 10,000, 3,000 and 600 square miles, respectively.

For any given wind condition the area encompassed by any dose rate or two-day dose, respectively, appears to be nearly proportional to the weapon size.

Note that Conditions A, B and C are all moderate wind cases with varying degrees of shear; Conditions D and E are of low wind velocity; and Condition F is a high wind case. Thus, if meteorological conditions are classed solely according to wind velocity, namely as low, moderate and high, the phrase, effectively independent of, can be substituted for the phrase, not strongly dependent upon, contained in the first Conclusion.

The last two Conclusions enable Table IV to be reduced to Table V.

TABLE V
The Effect of Low, Moderate and High Wind Velocities on the Amount of Area
Enclosed by the Roentgen Levels Noted
(Tabulated values are average ground area in 10^3 sq. mi/MT)

Fission Product Roentgen Level	Wind Velocities					
	Low		Moderate		High	
	R	D	R	D	R	D
100	0.6	0.35	0.8	0.7	0.7	1.0
500	0.2	0.2	0.2	0.3	0.1	0.3
1500	0.08	0.1	0.025	0.1	0.0	0.06

R is 1 hr-R/hr dose rate; D is two day cumulative roentgen dose.

DOE ARCHIVES

IDEALIZED CONTOUR SHAPES

APPLICABLE TO BOTH 2 DAY DOSE AND 1 hr. - R/hr.

100 TO 1500 ROENTGEN LEVELS

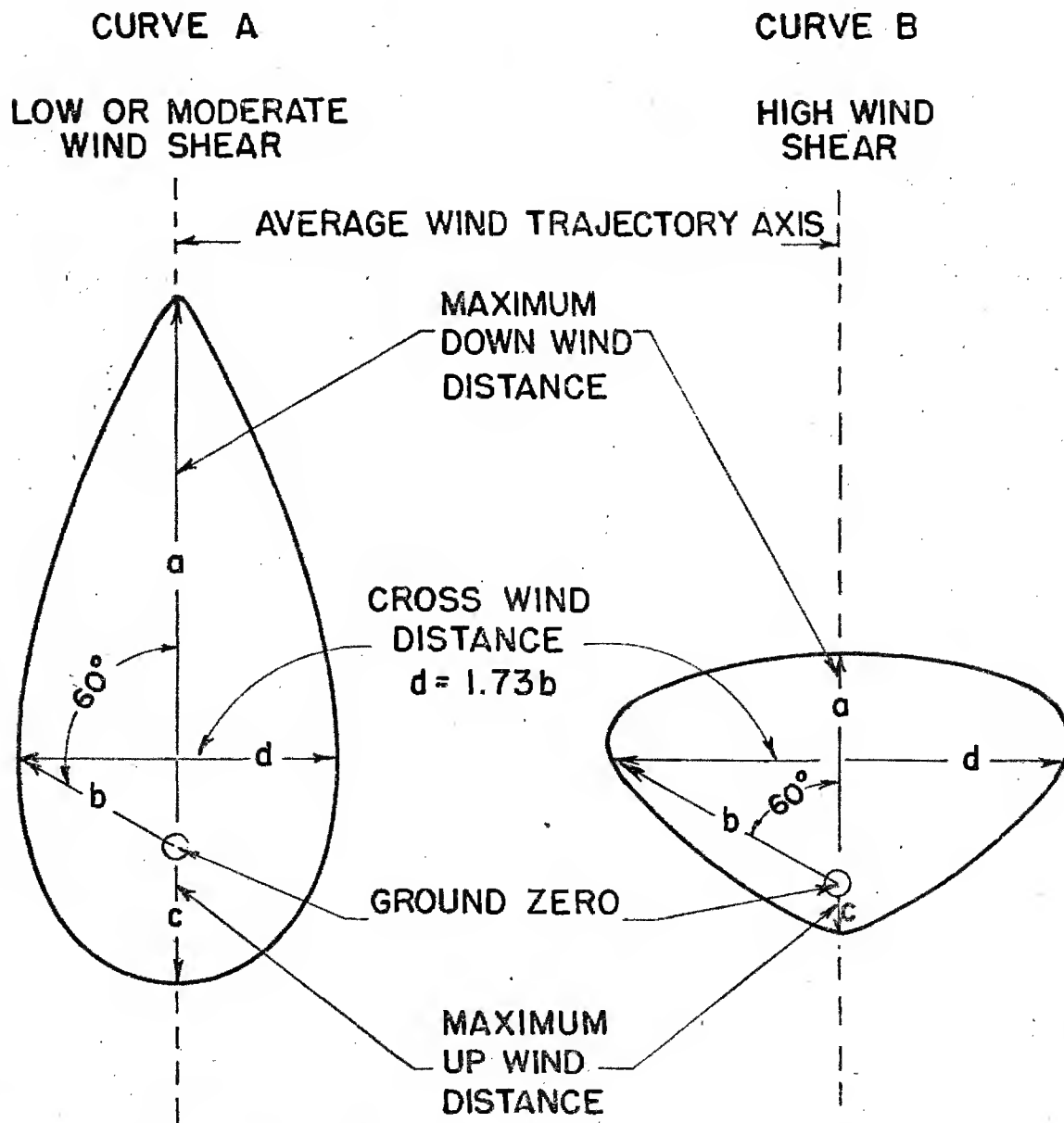


Figure 5

420

DOE ARCHIVES

425

Table V should be a fairly good guide to the roentgen level flat ground area coverage to be expected from the surface detonation of all thermonuclear weapons under most meteorological conditions, provided that the land area is not comprised of coral.

The fact that the contaminated contour areas seem to scale almost directly as the thermonuclear burst energy means that any known contamination pattern for a given energy can be transformed at once into a pattern for another energy if the meteorological condition remains unchanged. Draw vectors from ground zero to various points along the periphery of the contour in question, and scale the length of these vectors by the square root of the ratio of the weapon energies. This working rule is subject to direct verification by measurement of our contour plots for each of the six AFSWP winds. This has been done with excellent agreement between the 15 and 50 MT weapons and fair agreement between the 1 MT and the 15 or 50 MT weapons. Further inspection shows that all of the dose and dose rate contours (somewhat idealized) are lemniscatic in shape, as depicted in Figure 5. Figure 5 shows two curves. Curve A is typical of contours when the wind shear is low or moderate (Conditions A to E). Curve B typifies the contour shape for high wind shear (Condition F). For contour curves both A and B, the terminus of maximum cross-wind dimension, d, is the end of a polar vector which makes an angle of about 60° with the average downwind trajectory line. The relative ratios and scaled lengths of polar vectors a, b and c depend, of course, upon the wind velocity, but appear to be relatively independent of wind shear. The numerical values of these three polar vectors for low, moderate and high winds (see Conclusion (e)) are tabulated in Table VI.

In view of the data on the contour areas (Table V), the R and D polar vector numerical values for each case should be nearly identical, except for the 1500 R contours under high winds. This is borne out by Table VI. Table VI indicates that a CASTLE-Bravo type weapon (15 MT) detonated on land areas along the Eastern Seaboard under a moderate wind condition would result in both a 1 hr-R/hr dose rate and a two-day cumulative dose 500 R contour which would extend about 100 miles downwind, 10 miles upwind, and have a maximum cross-wind extent of about 40 miles; the total area encompassed would be about 3000 square miles. (See Table V).

DOE ARCHIVES

TABLE VI

The Effect of Low, Moderate and High Wind Velocities
on Figure 5 Polar Vector Distances for the Roentgen Levels Noted
(Tabulated Values are Polar Vectors in $\text{mi}/(\text{MT})^{\frac{1}{2}}$)

Fission Product Roentgen Level	Polar Vector	Wind Velocities					
		Low		Moderate		High	
		R	D	R	D	R	D
100	a	27	15	80	58	69	70
	b	17	13	8	9	5	8
	c	7	8	4	6	2	4
500	a	11	10	25	25	21	36
	b	8	9	5	7	2	4
	c	5	12	1	4	-7	-2
1500	a	8	8	9	13	0	17
	b	6	6	2	5	0	1
	c	4	4	-1	2	0	-3

R is 1 hr-R/hr dose rate. D is 2-day cumulative roentgen dose.

(-) sign for polar vector c denotes that c is above ground zero in Fig. 5.

a is maximum downwind distance to contour.

b is 60° polar vector; $1.73b$ is maximum crosswind distance.

c is maximum upwind distance to contour.

DOE ARCHIVES

Figure 5 and Tables V and VI can be used as a rapid method to estimate 2-day dose and 1-hour dose rate contour patterns over contaminated land areas as follows:

Use Figure 1 to determine altitudes of bottom and top of initial cloud resulting from a surface thermonuclear burst of energy in MT.

To characterize wind shear, qualitatively examine wind vector data for only those altitudes which are bounded by cloud bottom and top. If wind shear is high, contour patterns will be similar to Curve B, Figure 5; otherwise it will be like Curve A. Since for altitudes above 40,000 ft, high wind shear is rare, most contour patterns will be like Curve A.

Use an air density table to determine a mean altitude, H, which corresponds to the center of mass of an arbitrary cylinder bounded by the cloud top and bottom altitudes. If the burst energy is 1 MT, H is 45,000 ft; if the energy exceeds 10 MT, H is 70,000 ft.

Consider a 100 μ particle that was originally located H feet directly above zero ground. Use fall times given in Table I together with the wind data to ascertain the location of this 100 μ particle when it reaches the ground.

Draw a line through ground zero and the location of this particle. This is the average wind trajectory axis. Measure distance in miles from ground zero to this particle location. If this distance is less than 150 miles, classify as low wind; if distance is between 150 and 750 miles, call moderate; and if distance exceeds 750 miles, it is a high wind case.

Now draw polar vector distances for the 100, 500 and 1500 roentgen levels as given in Table VI for appropriate wind velocity case and burst energy. Sketch in contour lines as depicted in Figure 5 for appropriate wind shear case. Keep in mind that enclosed areas must satisfy Table V.

DOE ARCHIVES

Roentgen levels of these contour lines are valid for the conversion factors listed in Table III. If you are using other values for these factors, alter roentgen levels accordingly.

**Fission Product Biological Damage Dose and Contribution of U-Np
Activity Thereto**

Introduction

Biological damage from exposure to radioactivity is complicated by the tendency of the body to repair itself. Thus the maximum effect from a given total dose depends upon the length of time over which the dose was received. If the duration of the dose is less than two or three days, the effect of self-repair on the danger level is slight, but times longer than this are of current interest.

Data on this subject are still rather sparse. However two studies have been made which give two estimates of the effect. The results differ principally at periods of the order of six months or more, where data do not yet exist in sufficient quantity to support either theory. The mathematical forms which summarize the two studies differ considerably, and both will be considered in what follows.

Method I

A British study states that exposure to a constant dose rate d per day for t days is equivalent, at the end of that period, to a one-day dose ("Damage Dose") given by

$$D = d t^{0.64} \quad (t \geq 1 \text{ day}) \quad (1a)$$

Manifestly the restriction " $t \geq 1$ " day is required since for very short times, the effective dose must be more nearly

$$D = d t \quad (t \leq 1 \text{ day}) \quad (1b)$$

Equations (1a) and (1b) fit data taken with a constant dose rate d per day. To get relations for dose rates which vary in time due to radioactive decay, consider the effect of extending t by a small amount Δt which is added at the beginning of the interval t . The additional damage dose due to this increment is easily seen to be:

$$\Delta D = \begin{cases} d\Delta t & \text{if } t \leq 1 \text{ day} \\ 0.64 t^{-0.36} d\Delta t & \text{if } t \geq 1 \text{ day} \end{cases} \quad \text{DOE ARCHIVES}$$

This relation says that the effect of a pulse ($d\Delta t$) of radiation is (a) unreduced for times less than 1 day, and (b) reduced by a factor ($0.64 t^{-0.36}$) after times, t , longer than one day. If then, exposure

occurs from time t_1 to t_2 at variable fission product dose rate of $c/t^{1.2}$, the final damage dose will be (provided $t_2 \geq t_1 + 1$ day):

$$D = \int_{t_2-1}^{t_2} \frac{cdt}{t^{1.2}} + \int_{t_1}^{t_2-1} \frac{0.64 cdt}{(t_2-t)^{0.36} t^{1.2}} \quad (2)$$

If $t_2 \leq t_1 + 1$ day:

$$D = \int_{t_1}^{t_2} \frac{cdt}{t^{1.2}} \quad (3)$$

Therefore if $t_2 \leq t_1 + 1$ day

$$D = 5 c(t_1^{-0.2} - t_2^{-0.2}) \quad (4)$$

In equations (2) and (4) time is in days and the dose rate from decaying fission products is taken as $c/t^{1.2}$. The constant c is therefore in roentgens per day at one day. To convert to more usual units let R_0 be the dose rate due to fission products in roentgens per hour at one hour. It is then easily seen that

$$c = R_0 / (24)^{0.2} = (0.530 R_0) \quad (5)$$

In equations (2) and (4), time is still measured in days.

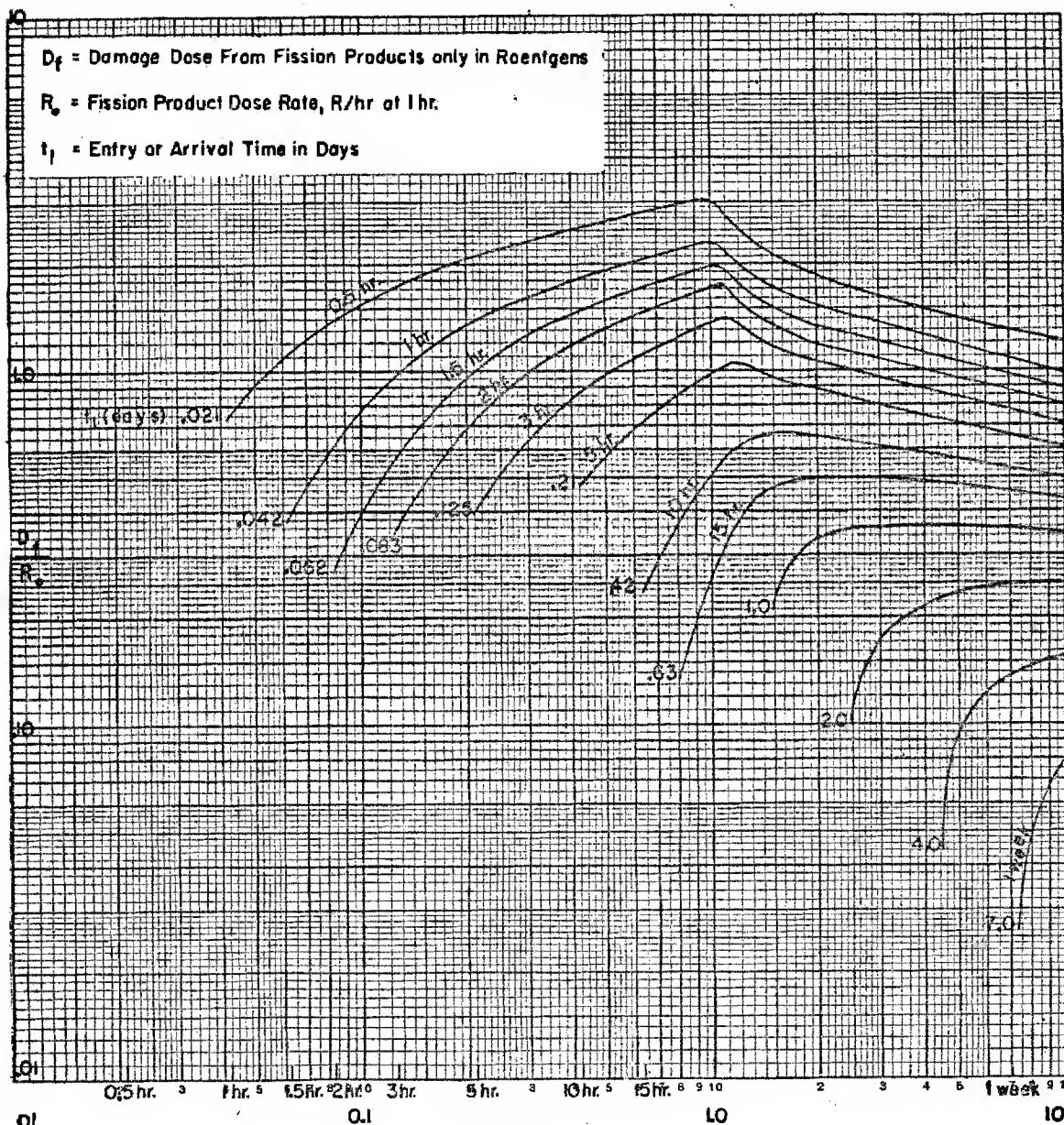
The second integral of equation (2) has been computed numerically. The results along with those from equation (4) have been plotted in Figures 6a and 6b which give directly the ratio D_p/R_0 , for fission products alone and various entry and exit times, as implied by the British results, equations (1a) and (1b). An example will be given after discussing other approaches and refinements.

Method II

DOE ARCHIVES

An American investigation of the same questions has yielded a different expression. The concepts used here are those of a "permanent

BIOLOGICAL EFFECTIVE DOSE FROM FISSION PRODUCT DECAY (BRITISH DATA)



Abscissa: Exit Time in t_2 (days)

Ordinate: D_f/R_o

DOE ARCHIVES

Figure 6a

426

ATOMIC ENERGY DATA

431

The graph is a log-log plot with the following features:

- Y-axis:** Labeled D_f and R_f , ranging from 0.01 to 10.
- X-axis:** Labeled t_1 (days), ranging from 10 to 10,000.
- Curves:** A series of curves representing different half-lives ($T_{1/2}$): 2 weeks, 1 mo, 2 mo, 3 mo, 1 yr, 2 yr, 3 yr, 5 yr, 10 yr.
- Diagonal Lines:** A set of lines sloping downwards from left to right, labeled with values: 0.21, 0.25, 0.3, 0.4, 0.5, 0.6, 0.8, 1.0, 2.0, 4.0, 7.0.
- Legend:**
 - D_f = Damage Dose From Fission Products only in Roentgens
 - R_f = Fission Product Dose Rate, R/hr at 1 hr.
 - t_1 = Entry or Arrival Time in Days

Ordinate: D/R_0

Figure 6b

427

ATOMIC ENERGY AC

432

injury" and a "recoverable injury". The former is empirically 20% of the "instantaneous injury" while the latter decays exponentially with an apparent recovery half-life of about 2.4 days. In symbols, if I_p is the permanent injury dose, I_r the reparable injury dose, and R the dose rate then

$$\frac{dI_p}{dt} = 0.2 R \text{ and } \frac{dI_r}{dt} = 0.8 R - k I_r \quad (6)$$

where $k = \frac{0.693}{2.4} = 0.29$ per day.

The damage dose at time, t , is then

$$D(t) = I_p(t) + I_r(t) \quad (7)$$

For the case of fission product decay $R = c/t^{1.2}$ and exposure from t_1 to t_2 , equations (6) and (7) may be integrated. The result is

$$D = (0.2) c \int_{t_1}^{t_2} \frac{dt}{t^{1.2}} + (0.8) c \int_{t_1}^{t_2} \frac{e^{k(t-t_2)}}{t^{1.2}} dt \quad (8)$$

Here time may also be measured in days and equation (5) again applies:

$$c = (0.530)R_0 \quad (5)$$

where R_0 is the dose rate in R/hr at one hour due to fission products.

Equation (8) has also been computed numerically. The results are given in Figures 7a and 7b which are completely analogous to Figures 6a and 6b.

Integral Dose Without Recovery (Fission Product Cumulative Dose)

To emphasize the effect of biological recovery, there is displayed in Figures 8a and 8b the integral dose, which would correspond to the case of no self repair. The equation for the integral or cumulative dose is simply equation (4) without the restriction that $t_2 \leq t_1 + 1$ day. It will be noted that such a computation is in error in two respects. First the time of maximum danger would always appear to be the exit time.

Secondly, the maximum dose may be much too high. These points are illustrated in Figure 9 which shows the integral and damage doses versus time for an entry or fallout arrival time of 10 hours. For long times, the integral dose is at least a factor of 5 above the actual biological damage dose. The spread between the "American" and "British" curves in Figure 9 gives some idea of the accuracy (or rather, paucity) of the original data as a function of exposure time.

Neptunium Activity

Before discussing further the application of results obtained above, it is necessary to consider an additional factor. The curves developed above concern only the gamma activity from fission products. There is in addition another activity which has a different decay law. This arises from capture of neutrons by U-238 to yield U-239 which decays to Np-239. Both give off biologically significant radiation. U-239 gammas have a mean energy of 0.074 MEV while that of Np-239 (including the effect of internal conversion) is 0.225 MEV per disintegration. The half lives are 23.5 min. and 2.36 days, respectively.

Calculations lead to the following results. If R_0 is the dose rate in R/hr at one hour for fission product activity, the integral dose from U and Np assuming unity capture to fission ratio is

$$\frac{I_{Np}}{R_0} = 0.315 \left[e^{-42.5 t_1} - e^{-42.5 t_2} \right] + e^{-0.29 t_1} - e^{-0.29 t_2} \quad (9)$$

The units for I_{Np} are R/day and t_1 and t_2 are the entry (or arrival) and exit times in days. The biologically effective dose (damage dose) is

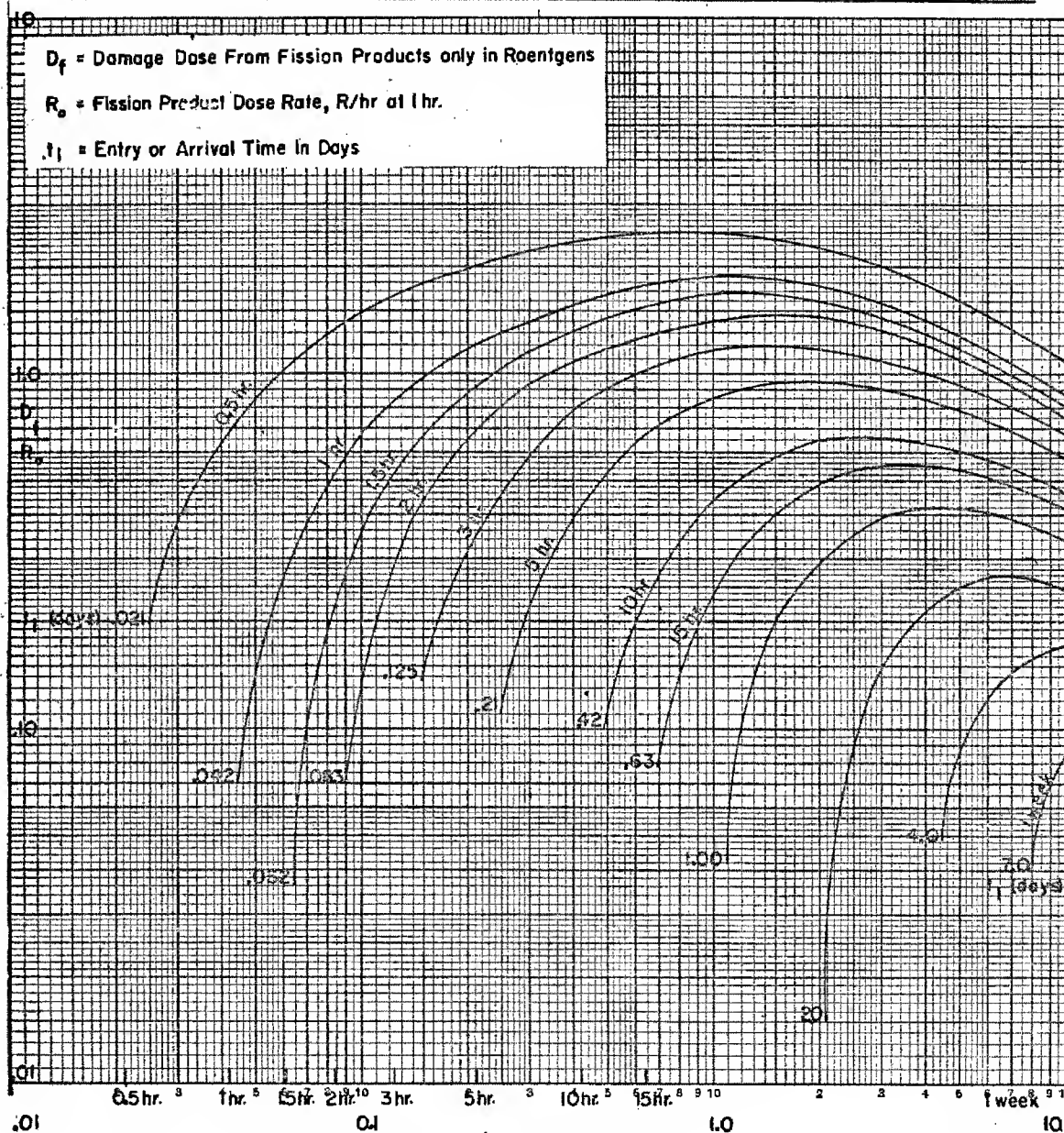
(10)

$$\frac{D_{Np}}{R_0} = 0.2 \frac{I_{Np}}{R_0} + 0.254 e^{-0.29 t_2} \left\{ e^{-42.2 t_2} - e^{-42.2 t_1} \right\} + 0.232 e^{-0.29 t_2} (t_2 - t_1)$$

where the units are the same and I_{Np}/R_0 is given by (9). DOE ARCHIVES

The damage dose (10) is to be added to that previously computed for fission product gamma rays. To give an indication of the relative importance of the two terms (for unity capture to fission ratio), Table VII gives the relative dose rates from the two processes as a function of time for a unity capture to fission ratio. Table VII shows that from 1 to 10 days after shot time, U-Np-239 make a significant contribution to the dose rate.

BIOLOGICAL EFFECTIVE DOSE FROM FISSION PRODUCT DECAY (AMERICAN DATA)



Abscissa: Exit Time in t_2 (days)

Ordinate: D_f/R_o

DOE ARCHIVES

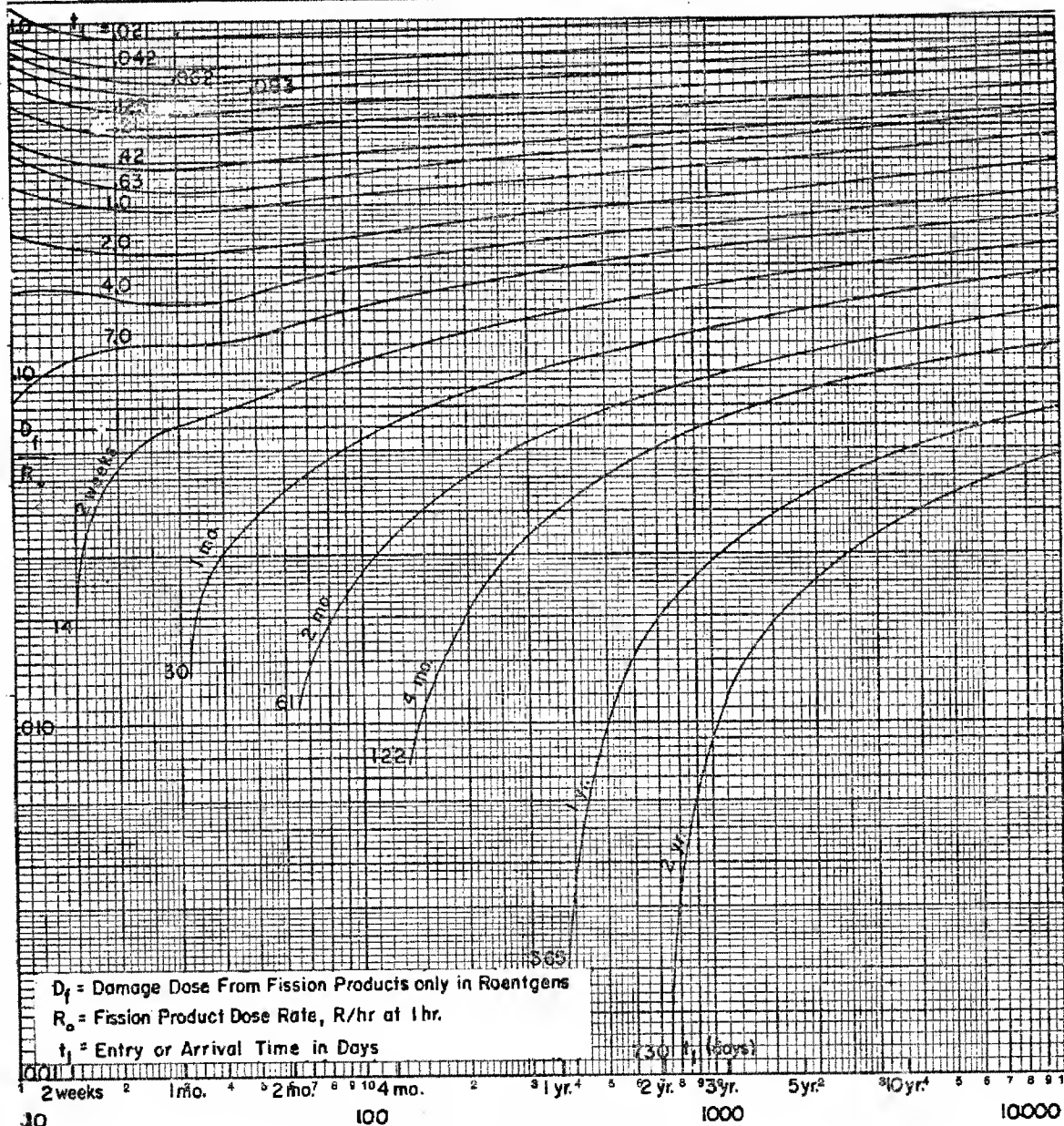
Figure 7a

430

ATOMIC DATA

435

BIOLOGICAL EFFECTIVE DOSE FROM FISSION PRODUCT DECAY (AMERICAN DATA)



Abscissa: Exit Time in t_2 (days)

Ordinate: D_f/R_o

DOE ARCHIVES

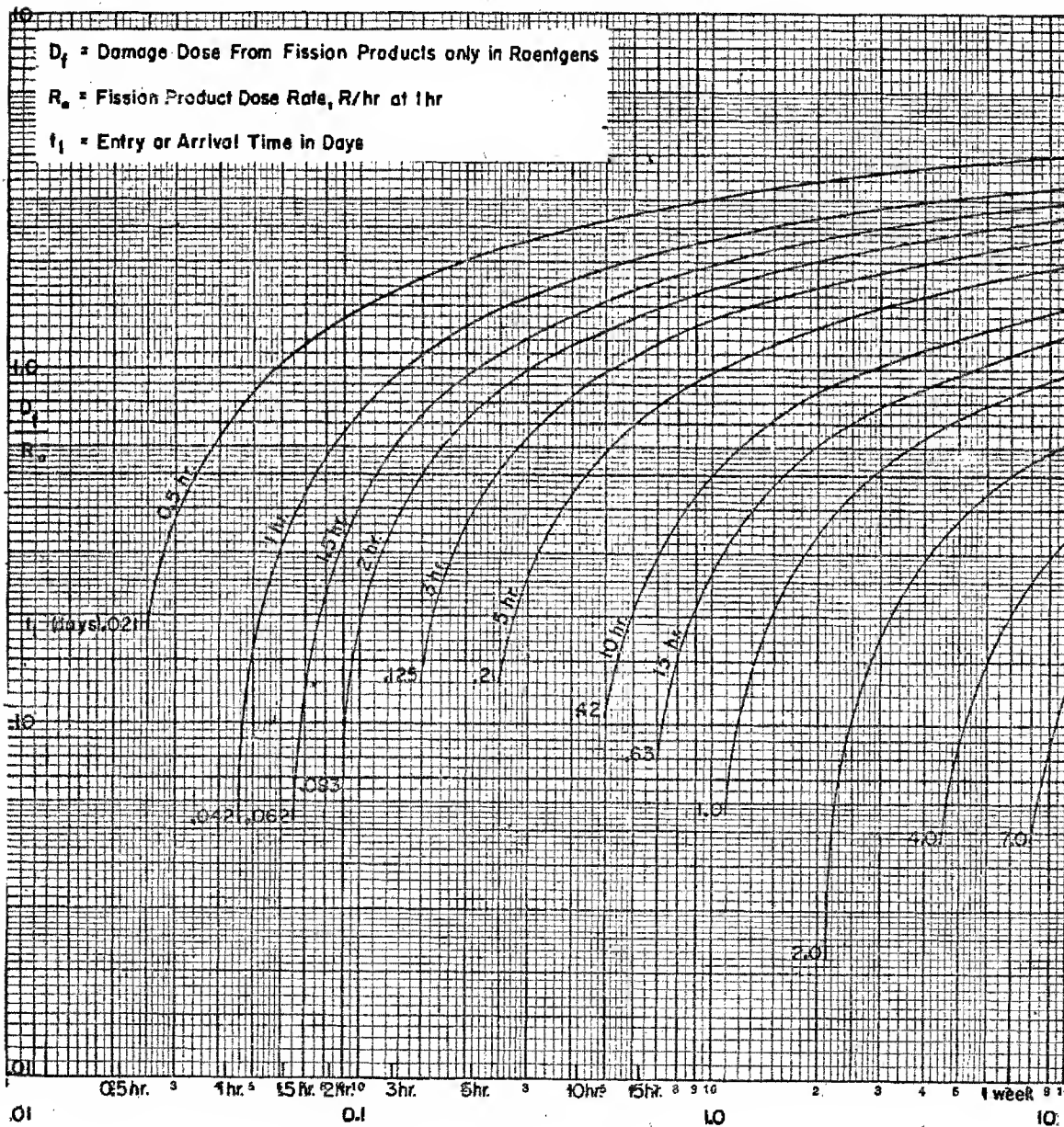
Figure 7b

431

NUCLEAR ENERGY ACT 4

436

INTEGRAL DOSE FROM FISSION PRODUCT DECAY



Abscissa: Exit Time in t_2 (days)

Ordinate: D_1/R_0

DOE ARCHIVES

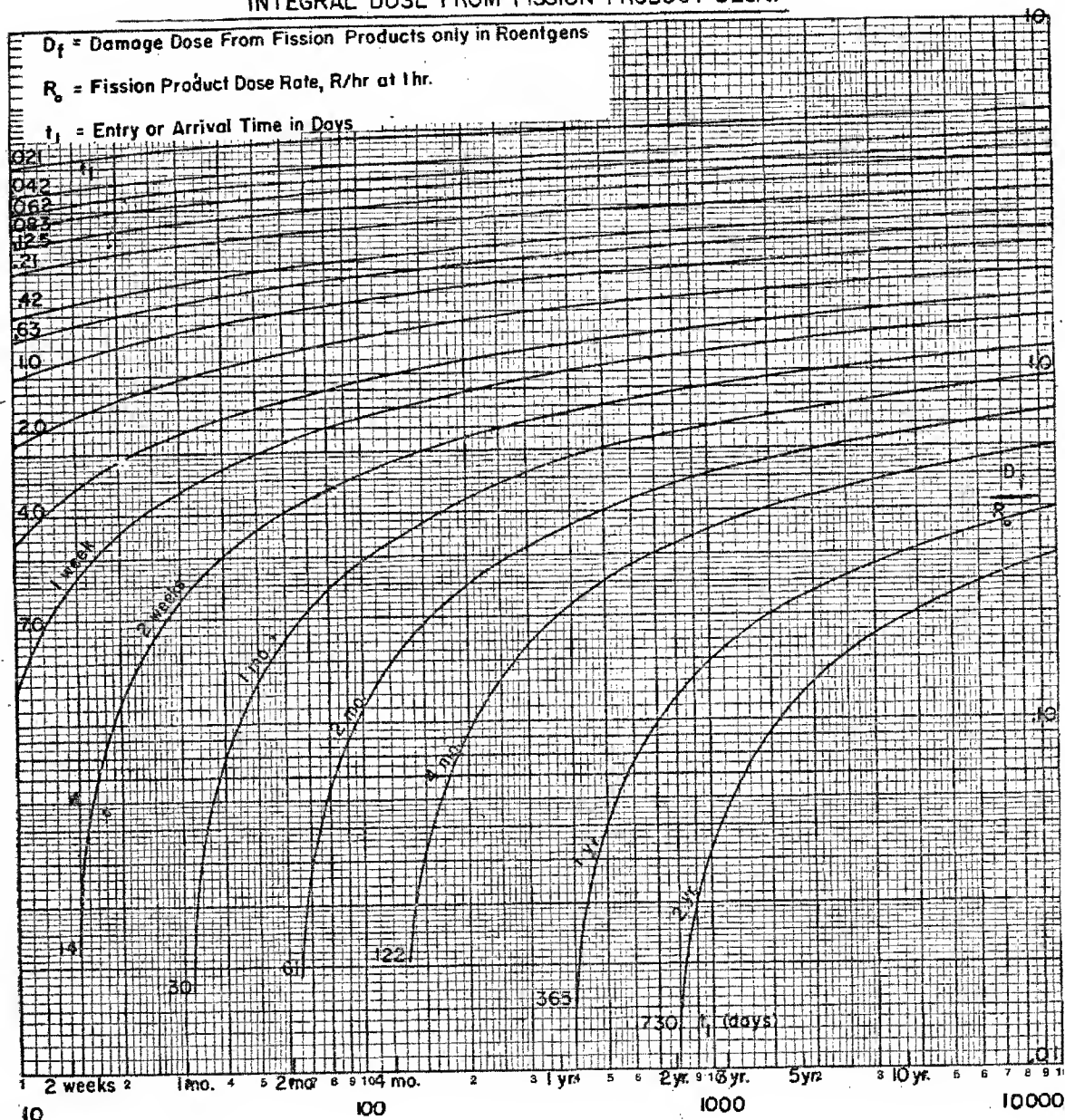
Figure 8a

432



437

INTEGRAL DOSE FROM FISSION PRODUCT DECAY



Abscissa: Exit Time in t_2 (days)

Ordinate: D_f/R_0

DOE ARCHIVES

Figure 8b

433

ATOMIC ENERGY ACT

438

COMPARISON OF PREDICTED DOSES FROM FISSION PRODUCTS
ONLY, FOR 10 HOUR ENTRY OR ARRIVAL TIME.

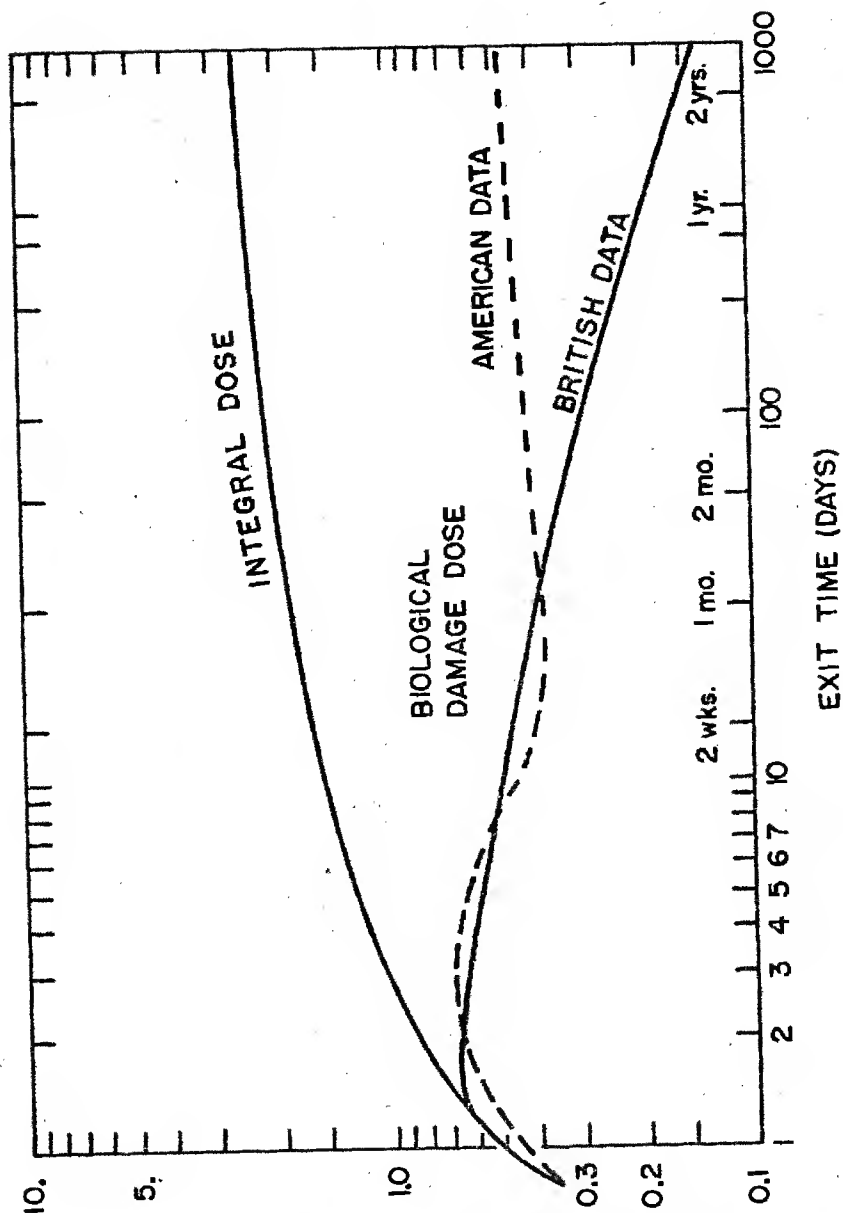


Figure 9

$\frac{D_t}{R_0}$

DOE ARCHIVES

434

439

TABLE VII

Dose Rate Ratio of Np-239 and U-239 to Fission Products
at Various Times Following Detonation
(Unity Capture to Fission Ratio)

Time	Hours							Days				
	0.1	0.3	0.5	2	5	10	24	2	4	7	14	30
Dose Rate Ratio Np and U/F. P.	0.03	0.14	0.11	0.06	0.08	0.17	0.41	0.66	0.84	0.71	0.20	0.04

In order to simplify the addition of this extra activity to that of the fission products, there is presented in Figure 10, α , the ratio of the biological damage dose due to Np and U to that due to fission products alone (for unity capture to fission ratio):

$$\alpha = \frac{D_{NP}}{D_f} \quad (\text{Ratio of equation (10) to equation (8)} \quad (11)$$

Figure 10 presents calculations for α for various entry and exit times, where D_{NP} is given by (10) and D_f is the ("American") damage dose given in Figures 7a and 7b.

To use the information in Figure 10 the damage dose D_f due to fission products alone is first determined from Figures 7a or 7b for given values of t_1 and t_2 . These same times are then used to obtain a value of α from Figure 10. The complete damage dose D is then found by

$$D = D_f(1 + F\alpha) \quad (12)$$

where F is the capture to fission ratio for the weapon in question. (F = number of neutrons captured in U-238 for each fission which takes place at the instant of detonation.)

To complete the presentation, Figure 11 shows the analogous ratio, β , for integral doses as computed from (9) and the standard integral-dose formula (Figures 8a and 8b).

DOE ARCHIVES

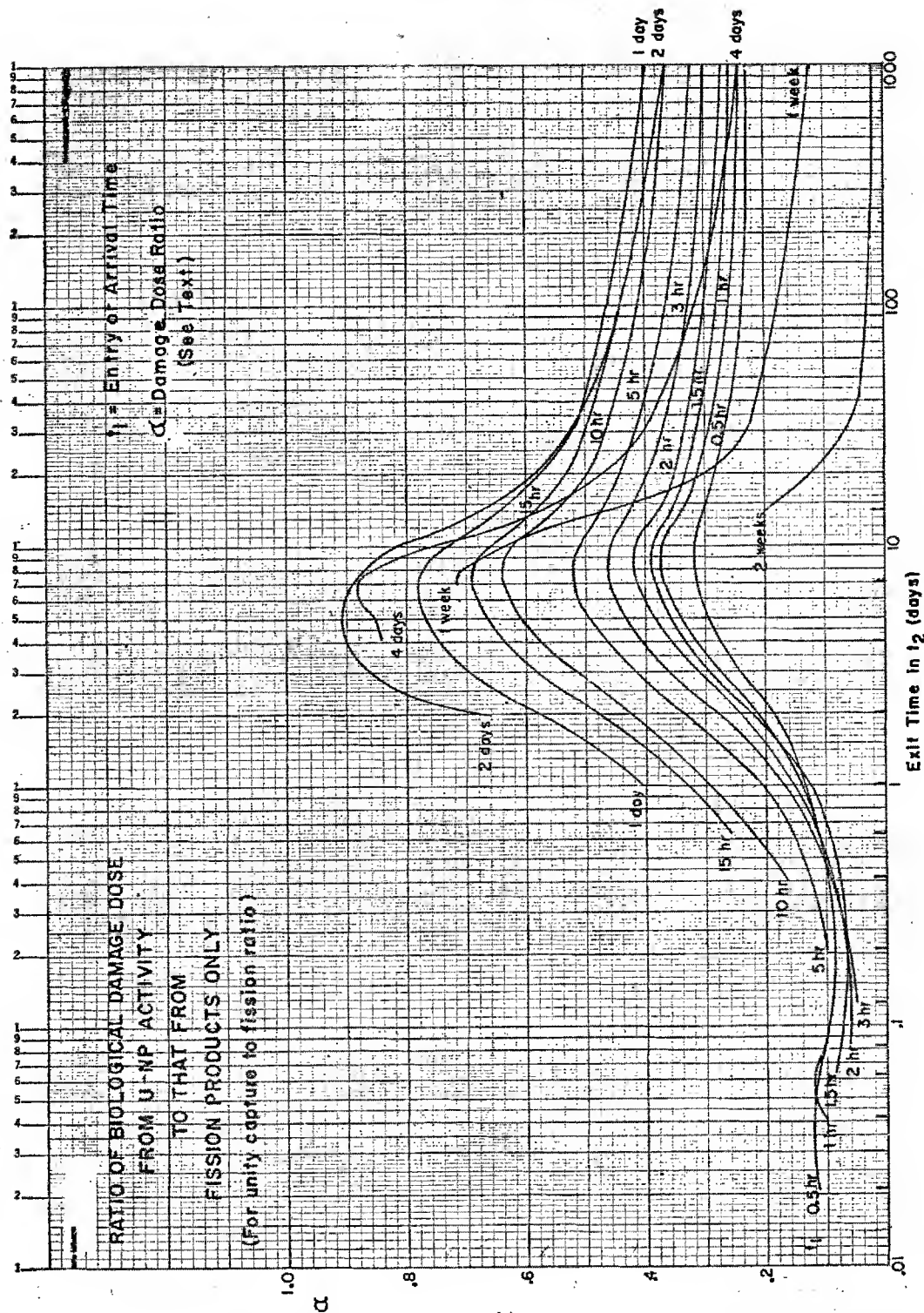


Figure 10

DOE ARCHIVES

436

441

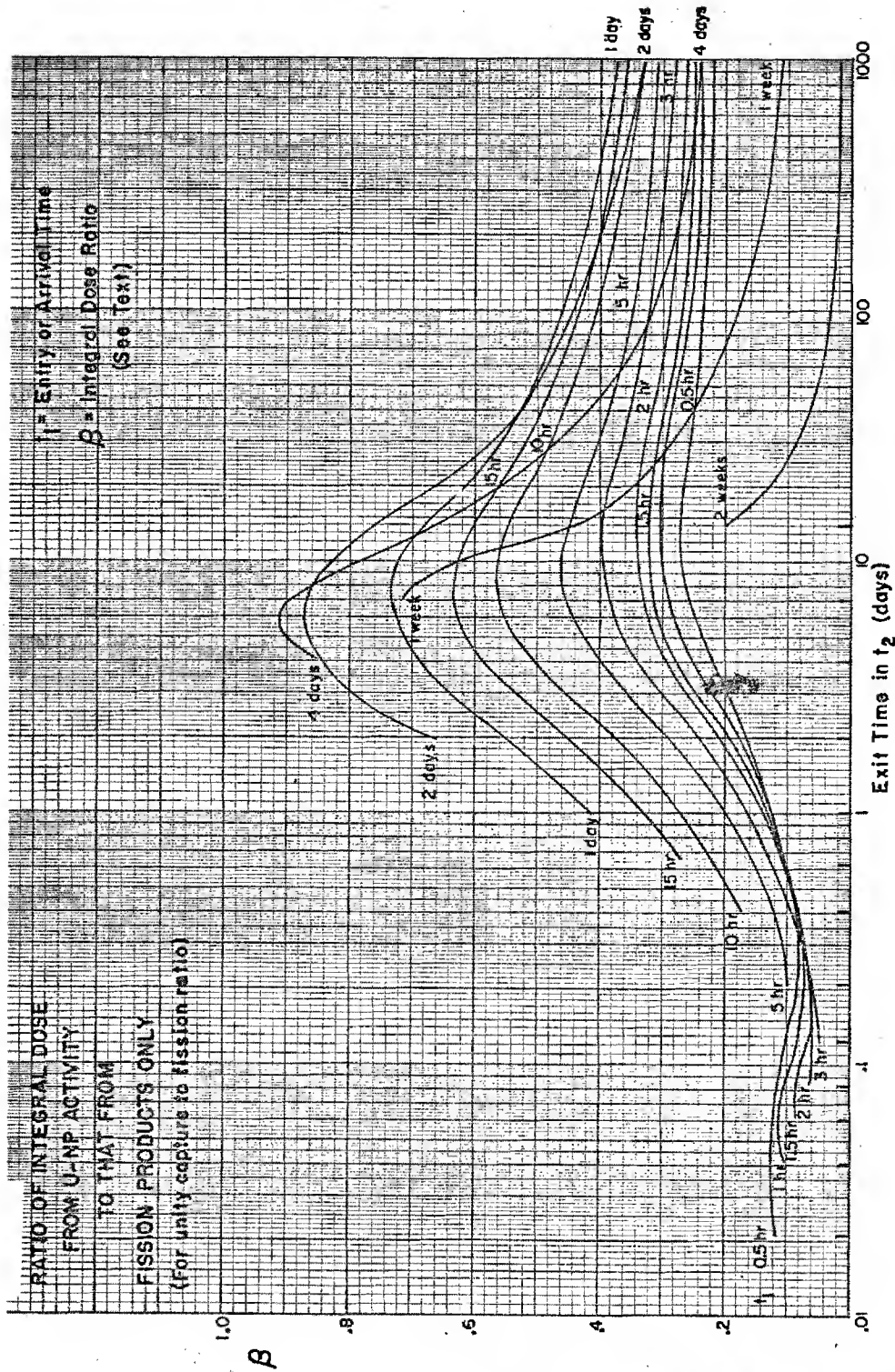


Figure 11

DOE ARCHIVES

437

ATOMIC ENERGY ACT 1954

442

Use of the Data in Fallout Calculations

In calculations such as discussed in Section I, the final results are presented in the form of 1 hr-dose-rates and 2-day integral (cumulative) dose. The employment of the data presented in this section to modify dose rate patterns is straightforward but the effect on integral dose is more complicated. We will first consider the effect on dose rate.

Dose Rate. - The 1-hr dose rate contour cannot be used to predict actual dose rates on the ground until most of the radioactive debris contributing to the roentgen rate has reached the ground location of interest; depending upon the distance from ground zero, this may be as long as twenty hours following shot time. Thus the dose rate contours should not be used to predict dose rates as would be measured on the ground by a roentgen dose-rate meter for times less than twenty hours after explosion. The following example illustrates the use of these contours to predict the dose rates at a given location:

Example. -

Surface detonation of 15 MT weapon with capture to fission ratio of unity.

Contour predicts 1500 1 hr-r/hr due to fission products, 70 miles NW of ground zero.

What is dose rate as measured by roentgen dose meter 24 hours after detonation?

$$\text{fission product dose rate} = \frac{1500}{24^{1.2}} = \frac{1500}{46} = 33 \text{ R/hr}$$

$$\text{From Table VII, (U-Np/F. P.)}_{24 \text{ hr}} = 0.41$$

$$\text{U-Np dose rate} = 0.41 \times 33 = 14 \text{ R/hr}$$

$$\text{Total roentgen dose rate at 24 hrs} = 47 \text{ R/hr}$$

Integral Dose. - It must first be emphasized that all graphs in Figures 6 through 11 are plotted on the assumption that the amount of contamination is constant. No further fallout particles are considered to arrive during the time of exposure. The modifications due to arrival during exposure will be discussed below; for simplicity we shall first suppose that, as predicted in Figures 6 through 11, all contamination is already present at time t_1 .

DOE ARCHIVES

With this proviso, consider first a simple example: Exposure occurs at a location where the fission product dose rate is 500 R/hr at 1 hr. Exposure starts at $t_1 = 10 \text{ hr} = 0.42 \text{ days}$ and exit occurs at $t_2 = 2 \text{ weeks} = 14 \text{ days}$.

From Figure 6b we find that the "British" curve for $t_1 = 0.42$ has the value $D_f/R_0 = 0.47$ when $t_2 = 14 \text{ days}$. Thus the damage dose due to fission products only is $0.47 R_0 = 235 \text{ roentgens}$ at the exit time of 2 weeks. The American data predicts approximately the same biological effect; from Figure 7b the damage dose is $0.42 R_0 = 210 \text{ roentgens}$ at 2 weeks.

Note, however, that both curves have an earlier maximum. From Figure 7a, for example, the damage dose (from fission products only) at 2.6 days was $0.66 R_0 = 330 \text{ roentgens}$. In effect, the mechanism of biological repair was unable to "keep up" with the damage at early times when the radioactivity level was high. After 2.6 days, however, the activity decayed to the point where repair mechanisms could somewhat more than make up for the damage.

Consequently, the danger is measured not by the final damage dose but by its maximum value during the time of exposure. The (possibly delayed) manifestations of injury will in general correspond to this maximum and not to the final value.

So far, we have considered only the damage dose due to fission products alone. This must be further increased by the effect of U-Np activity. From Figure 10, for example, the $t_1 = 10 \text{ hr}$ curve shows that $\alpha = 0.56$ at $t_2 = 2 \text{ weeks}$. The total damage dose at the exit time is thus $210(1 + 0.56F) = 322 \text{ roentgens}$ if the capture to fission ratio F of the weapon was unity.

Recall, however, that it is the maximum dose which represents the actual danger. We must therefore maximize $D_f(1 + \alpha)$ (if $F = 1$) where D_f is obtained from Figure 7a and α from Figure 10. Calculating this quantity for the 10 hr curve in the two figures, one soon finds that the maximum is very flat and occurs at about 3 days where $(D_f/R_0)(1 + \alpha) = 0.99$. Thus the maximum danger in this exposure occurs at 3 days and the total damage dose is then 500 roentgens. (Assuming $F = 1$)

This result is to be contrasted with integral dose which may be determined from Figures 8b and 11. The former gives a fission product dose of $1.6 R_0$ for the same times while the latter leads to a correction factor of $(1 + 0.55F)$. If $F = 1$, the total integral dose is therefore

DOE ARCHIVES

1240 roentgens. Not only is this 250% too high in terms of actual biological damage but the maximum always occurs at the exit time, thereby leading to the false conclusion that earlier evacuation would be helpful. We saw above, that unless evacuation occurs before 3 days, there is no reduction of the danger.

At this point, it may be noted that even moderate shielding can provide considerable protection. The maxima which measure the danger of biological damage all occur earlier than about one week and their high values are due almost entirely to the very high dose rates occurring at times earlier than this. Protection during these early times is therefore very important and helpful. Thus retreat to a shelter for a period of one week under the circumstances already used in the above example changes all calculations to the curves for $t_1 = 1$ week. Suppose the shielding reduces the earlier 3-day maximum by a mere factor of 10 leading to a dose of 50 roentgens while in a shelter. The one week curves in Figures 7 and 10 then show that the quantity $(D_e/R_0)(1 + F\alpha)$ has a maximum (assuming $F = 1$) of 0.16 at the exit time, 2 weeks. The maximum damage dose is then 80 roentgens due to exposure after leaving the shelter plus $(0.42)(1 + 0.56)(R_0/10) = 33$ roentgens lingering damage dose from that received while in shelter. The net result is thus a dose of 113 roentgens instead of 500. If the arrival time is smaller than 10 hrs, the effect of even moderate shielding is even greater.

Finally, we consider the result of lifting the restriction stated earlier on the arrival of contamination. All of the above discussion assumed that fallout was complete before exposure started.

We will consider the contribution to the 2-day biological effective dose from radioactive debris that arrives at a ground location five hours after shot time. It will be comprised of two parts, that due to fission products alone and that due to U-Np. We will again assume a unity capture to fission ratio. If the fission-product-only 1 hr-R/hr dose rate of this debris is R_0 then from Figure 7a,

the fission product contribution to the

$$\text{2-day biological effective dose} = 0.95 R_0$$

while from Figure 11 the Np-U contribution

$$\text{is given by } 0.34 \times 0.95 R_0 = 0.32 R_0$$

Hence the total 2-day biological effective dose

$$= 1.27 R_0$$

We will now compare this total value with the fission product only 2-day integral dose from 5 hrs arrival time debris whose 1 hr-R/hr dose rate is also R_0 . We refer to Figure 8a and find this to be $1.3 R_0$, and note that this is identical to the value for the 2-day biological effective dose. If we repeat these calculations for any other arrival time between 0.5 and 15 hrs and again make the above comparison, we reach the same conclusion. Now it can be proved that the location of the perimeter of any two-day dose contour equal to or greater than 100 R is determined solely by radioactive particles which arrive at a ground location in 15 hours or less.

In view of the above, the following conclusion can be stated, namely:

Conclusion (A). -

Irrespective of arrival times of the radioactive debris, for all thermonuclear surface detonations where the capture to fission ratio is about unity, the fission product two-day contour is the two-day damage (biological effective) dose contour, provided that the contour in question is at least 100 roentgens.

We will now consider damage dose for periods greater than two days.

Biological damage is apparently additive. The effects of self-repair require one to successively "down-grade" earlier doses before adding them to obtain the total effect, but the addition otherwise appears to reproduce the data on damage. (This additivity is implicit in both the British and American damage dose relations, equations (1a, 1b, 6 and 7).) Further, two days after shot time, the 1 hr-R/hr dose rate is a real measure of the actual dose rate at any ground location within the two-day dose 100 R contour, since by this time all radioactive particles have arrived.

The information in the preceding paragraph plus Conclusion (A) means that the biological effective (damage) dose at a non-shielded reasonably flat location at any time, t , is given by the following equation:

For $t \geq 2$ days, $D_{2d} \geq 100$ roentgens and capture to fission = 1; then the damage dose at the time, t , is

$$D_t = D_{2d} \left\{ 0.2 + 0.8 e^{-0.29(t-2)} \right\} + R_0 \left(\frac{D_f}{R_0} \right) (1 + \alpha) \quad (13)$$

where t is time in days. D_{2d} and R_0 are the respective fission product

two-day dose and 1 hr-R/hr dose rate levels in roentgens at the ground location in question. The right hand term is the "down-grading" of the 2-day damage dose with time and comes from equation (6). The left hand term is the damage dose which results from an exposure starting at 2 days and ending at t . It comes from equation (12) where D_f/R_0 and α at the time, t , can be found from the curves labeled two-day entry time on Figures (7) and (10), respectively.

Equation (13) can be rearranged to read:

$$D_t = D_{2d} M(t) + R_0 Q(t) \quad (14)$$

where the functions $M(t)$ and $Q(t)$ are obvious by comparison with equation (13). For convenience they are tabulated in Table VIII.

TABLE VIII

Values of $M(t)$ and $Q(t)$ of Equation (14)

	Time after Shot in Days						
	2	3	4	5	7	10	20
$M(t)$	1.00	0.80	0.65	0.54	0.39	0.28	0.20
$Q(t)$	0.00	0.28	0.40	0.50	0.51	0.45	0.35

These values are based upon continuous exposure to radioactive fallout for time periods of at least two days duration where time period is measured from shot time. See equation (13) for other restrictions.

From Table VIII we see that the time after shot at which maximum damage dose due to continuous exposure to radioactive fallout can never exceed 7 days. The time at which the maximum damage dose takes place and its numerical value depend only upon the 2-day dose and the 1 hr-R/hr fission product roentgen contour values of the ground location in question. To illustrate the use of equation (14), we will now give two numerical examples; Example (i) leads to a practical working rule, while Example (ii) illustrates the use of equation (14) to solve a problem which involves protective shielding.

Example (i).-

Surface detonation of 50 MT weapon with capture to fission ratio of unity.

Contours predict 300 R 2-day dose and 350 1 hr-R/hr due to fission products 270 miles NW of ground zero.

What is maximum biological effective (damage) dose due to continuous exposure and when after shot time will it occur?

From equation (14) and Table VIII we obtain

<u>Days after Shot</u>	<u>Damage Dose</u>
2	$300 \times 1.00 + 350 \times 0.00 = 300 \text{ R}$
3	$300 \times 0.80 + 350 \times 0.28 = 340 \text{ R}$
4	$300 \times 0.65 + 350 \times 0.40 = 335 \text{ R}$
5	$300 \times 0.54 + 350 \times 0.50 = 335 \text{ R}$
7	$300 \times 0.39 + 350 \times 0.51 = 295 \text{ R}$

Thus maximum damage dose is 340 R and will occur 3 days after shot time.

In Example (i), where ratio of R_0/D_{2d} is 1.2, the maximum damage dose is only 10% greater than D_{2d} . Examination of all of the contour patterns for roentgen values of interest for all of the AFSWP winds shows that R_0/D_{2d} is usually of the order of unity, and essentially never exceeds 1.2. This fact results in the following working rule:

Conclusion B.-

For a surface burst thermonuclear weapon with a capture to fission ratio of about unity, the maximum biological damage dose that can ever be received at any geographic location (with no shielding) is essentially the 2-day fission product integral dose and hence can be read directly from a 2-day fission product dose prediction contour map.

We now proceed to Example (ii).-

Example (ii).-

Surface detonation of 15 MT weapon with capture to fission ratio of unity.

Contour predicts 1500 l hr-R/hr and 2000 R 2-day dose due to fission products, 70 miles NW of ground zero.

A person is in shelter of shielding factor 10, for the first two days after shot. After first two days he leaves shelter and is exposed in open flat area for 8 hours each day; remaining 16 hours spent in shelter.

What is maximum biological dose received by the person and when will it occur?

$$\text{Effective } D_{2d} = \frac{2000}{10} = 200 \text{ R}$$

$$\text{Effective } R_o = \frac{1500 \times 8}{24} + \frac{1500 \times 16}{10 \times 24} = 600 \text{ l hr-R/hr}$$

From equation (14) and Table VIII we obtain

<u>Days after shot</u>	<u>Damage Dose</u>
2	$200 \times 1.00 + 600 \times 0.00 = 200 \text{ R}$
4	$200 \times 0.65 + 600 \times 0.40 = 370 \text{ R}$
5	$200 \times 0.54 + 600 \times 0.50 = 410 \text{ R}$
7	$200 \times 0.39 + 600 \times 0.51 = 380 \text{ R}$

Thus the person will receive a maximum damage dose of 410 roentgens and this will occur 5 days after shot time.

DOE ARCHIVES

444

~~DATA~~
ATOMIC ENERGY ACT

449

QUESTIONS AND ANSWERS FOLLOWING DR. HENRIQUES' PRESENTATION

Question: Dr. Kellogg, Rand Corp.

This last slide Dr. Henriques showed brought up a question. Would you include the attenuation factor for the terrain or are they based on the infinite flat plain?

Answer: Dr. Henriques, TOI

Mine include both the ~~DELETED~~ terrain factors.

Question: Dr. Genevese, AFOIN

~~DELETED~~

Answer: Dr. Henriques, TOI

When you have a nuclear explosion, two main things happen. One is you get fission products that fall to the ground; and you get some U-239 which goes into Neptunium-239 and these are normally not considered with the fission products. These curves provide a means to do it if you know what fraction of the bomb goes to fission products and what goes to U-239. It makes no contribution to the fission products dose rate early but it does in time, because of the difference between the 1.2 law and the exponential decay.

Question: (Unknown)

Could you amplify your remarks about the degrading effects of terrain? How much does it vary with different types of terrain? What is the cause of it and so forth?

Answer: Dr. Henriques, TOI

There are magic numbers you can use and they are all available in reports and all roughly the same. I just don't know how to answer it. It depends on whether you are in the city and it comes down on buildings or if you are on the ground. The reason for using .55 instead of .7 is not basically important. Any open terrain or open field will not be as flat as the Salt Lake flats.

~~SECRET~~

Question: Dr. Krey, CRL

You think the different types of soil around ground zero will have an effect?

Answer: Dr. Henriques, TOI

Yes. Two different things, coral and Nevada dirt, there is a real basic difference. If you use the NRDL curve, it is impossible to duplicate Bravo with the NRDL particle.

Comment: Dr. Kellogg, Rand Corp.

There was one point you mentioned - the geometry of the cloud and that altitude is an important point. The height of the cloud as being constant through a rather large range of yields - this seems not to be borne out when you plot the CASTLE results with IVY results. The entrainment at each altitude is relatively insensitive to yield. When you put in more energy, the cloud would become higher. The difference might not be very large, but I think it would be incorrect to assume that the altitude is not a function of yield.

Question: Dr. Scoville, AFSWP

Isn't the bottom of the cloud likely to be at the bottom of the tropopause?

Answer: Dr. Kellogg, Rand Corp.

I don't know.

Comment: Dr. Felt, LASL

The Chemical or physical nature of the soil are more important to the fall-out. Dr. Henriques mentioned coral and I think I was talking mainly about soil. Some have proposed that the physical nature is more important.

Comment: Dr. Rapp, Rand Corp.

I would like to clarify our position. Our way of looking at it is the earth that will eventually become active must get into the fireball almost instantaneously.

DOE ARCHIVES

Comment: Dr. Krey, CRL

At CASTLE, we found quite a lot of particles over 100 microns to have activity principally on their surface. It was hard to see how they could get into the fireball and have activity strongly on their surface. These were actually found at CASTLE.

Comment: Dr. Rapp, Rand Corp.

I will quote some work that was done at Rand. They investigated this condensation principle. According to this model, the silicates come out and then some of the fission products are condensed at a later time, so this model definitely accounts for not having the fission products evenly distributed throughout the fall-out particle. Most of it is from the condensation particles.

Comment: LTCOL Lulejian, ARDC

I think I remember reading in a GREENHOUSE report where they found a small piece of chlorophyll which had fission products on it. Apparently everything is happening. Condensation, vaporization, and other things. Hence, a leaf coming down with a lot of activity on it.

DOE ARCHIVES

447.

~~RESTRICTED~~
ATOMIC ENERGY ACT

452

[REDACTED]

THIS PAGE IS BLANK

DOE ARCHIVES

448

[REDACTED]
[REDACTED] ENERGY [REDACTED]

[REDACTED]

453

PREDICTION OF DOSE-RATE AND DOSAGE CONTOURS AS FUNCTIONS
OF YIELD AND METEOROLOGICAL CONDITIONS; RECENT DEVELOPMENTS
IN WEATHER FORECASTING TECHNIQUES FOR THE PACIFIC PROVING GROUND

PART I

LTCOL C. D. Bonnot, USAF
Joint Task Force SEVEN

Introduction

We have been talking the last few days about fall-out, and now we will talk about weather. We know we can only have as good fall-out analysis as we have weather forecasts. We have discussed that pretty thoroughly. From the various fall-out models given, I thought it would be well to go back and discuss the Bravo weather situation. I want to give credit for this work to the Oahu Research Center in Hawaii. The work was not done by me personally, but by Ohmstead and Dean under Dr. C. E. Palmer's direction. The report is unclassified and it was deliberately made that way; there is no reference to Bravo or to shot times. They selected this date because there is a lot of good weather data, so the report states. The Oahu Research Center is part of the Institute of Geophysics, UCLA, and operates under contract to the Air Force Cambridge Research Center. They have both military and civilian personnel assigned and the Task Force works with them. They assist during the test period and then we give them all the raw weather data. They now have data from all the Pacific tests. They are a storehouse of all the raw data and weather information for the tropical Pacific. It might be well for everyone interested in Bravo to get this report. It has now been published in its final form as Special Report No. 1, Oahu Research Center. The report is unclassified and available to anyone who wants it. Just ask AFCRC at Boston, or contact me and I'll see that you get a copy.

This presentation will be in three sections. I am going to talk about just the horizontal field, or streamline analysis, for Bravo day. Commander Rex will speak of the vertical motions for Bravo day, which are also analyzed in the report mentioned above. He also will discuss five other situations which he has analyzed for vertical motions, and then I will close with a short discussion of the proposed rawinsonde observing net for the Southwest Pacific which we feel is necessary if adequate analyses and forecasts of the weather and wind fields are to be furnished to the Commander, Joint Task Force SEVEN.

Horizontal Fields

The synoptic situation changed very little during the three day period between February 28 and March 2, 1954. At any given level, the wind directions and speeds did change slowly but these changes were due to systematic internal developments within the cyclones and anticyclones

[REDACTED]

in situ. No synoptic systems moved through the area; no new synoptic systems developed in the area during this three day period.

In the vertical, two transition levels (shear levels) happened to intersect various parts of the analysis levels. The transition levels occurred near 10,000 and 60,000 feet. The apparent synoptic changes at these analysis levels are due to small height changes in the shear levels together with some slow internal synoptic intensifications.

During the three day period, at 10,000 feet, there was a gradual intensification of two cyclonic vortices that lay in a trough oriented east-west between Wake and Rongerik. (Figures 1, 2, 3. Note: These maps have been analyzed by the isogon-isotach method on a 1:7,500,000 scale. All time changes of the winds in the horizontal as well as in the vertical have been incorporated into the isogon-isotach analysis.) Only one cyclonic vortex appears on the analyses. It is located north of Rongerik; the other lies in the area covered by the legend box. These vortices slowly intensify during the period, but do not descend to the surface. They are reasonably well fixed by reconnaissance reports (10,000 feet only) on February 28, March 1, and later again on March 3. The gradual intensification of the trough in which they are imbedded is apparent by the westward movement of the neutral point from Eniwetok on February 28 to the Guam area by March 2. In other words, the higher level westerlies have descended into the analysis level.

An anticyclone at 10,000 feet is located near Kwajalein on February 28 (Figure 1), and during the period it moves slowly southwestward to Kusaie. At the same time another anticyclone appears to the north of Ponape (based on off-time reconnaissance reports). It also moves slowly southwestward towards Truk during the three days. Both systems descend further into the 10,000 foot surface during the period. The combined effect of the slow intensification of the cyclones and the equatorial anticyclones at 10,000 feet over the Marshall Islands is to maintain northerly wind components over the Rongerik area below 20,000 feet.

The subtropical anticyclones are located north of 20°N at 10,000 feet (just off the map). (Figures 2 and 3.) They weaken vertically north of Wake, completely disappearing as wind singularities above 10,000 feet, and cannot be found in the speed field above 20,000 feet. The systems have very little effect on the weather of the Marshall Islands.

DOE ARCHIVES

At 30,000 and 40,000 feet the flow pattern around the equatorial anticyclones is the same with height and with time, giving southwesterly

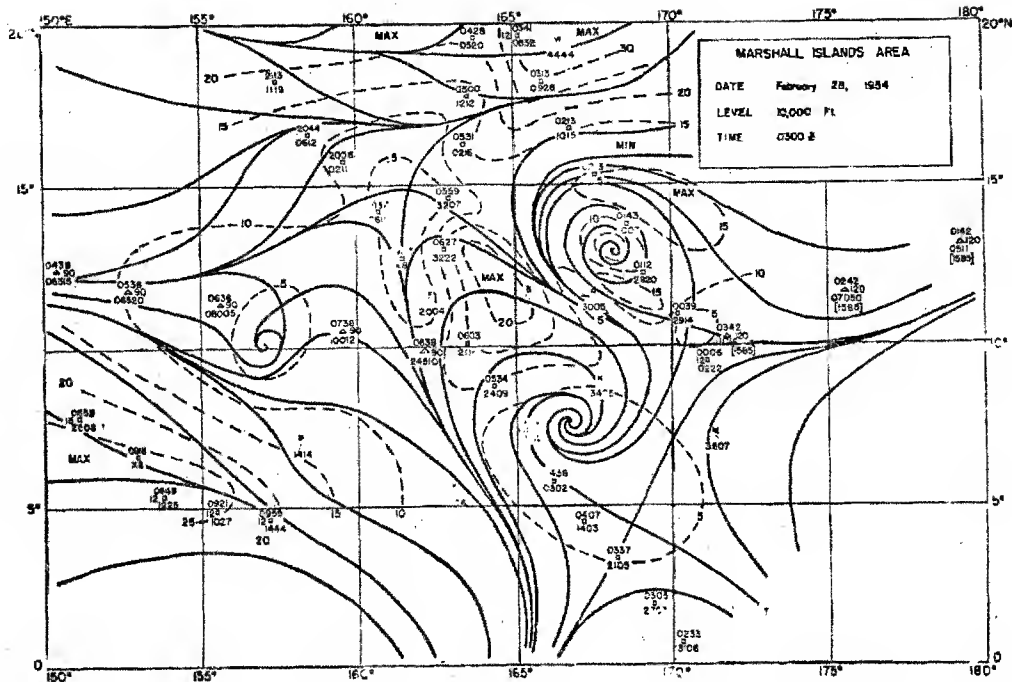


Figure 1

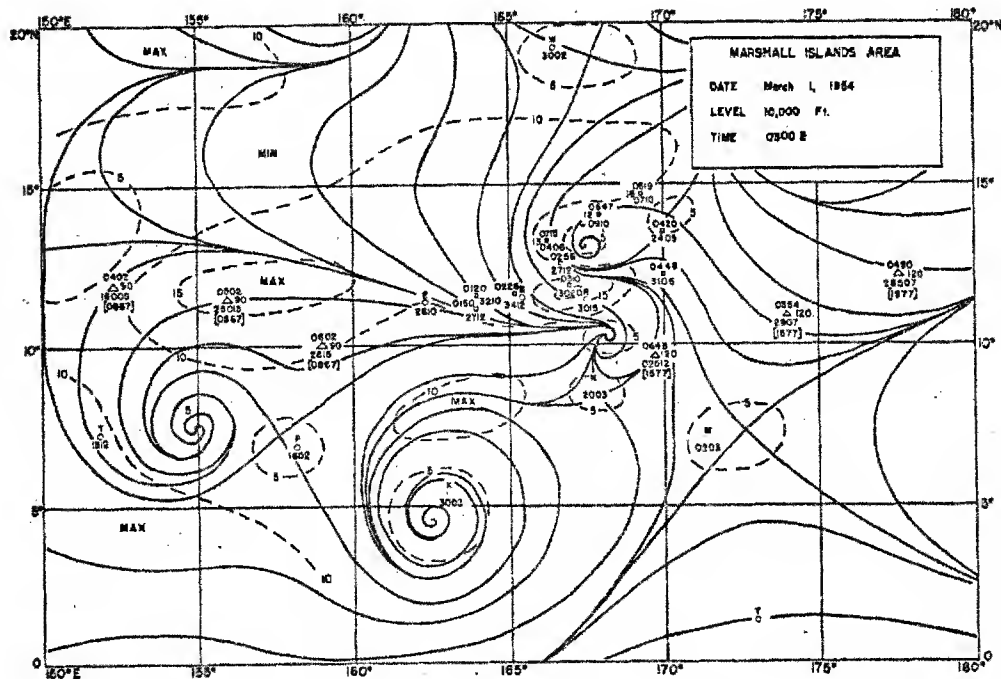


Figure 2

DOE ARCHIVES

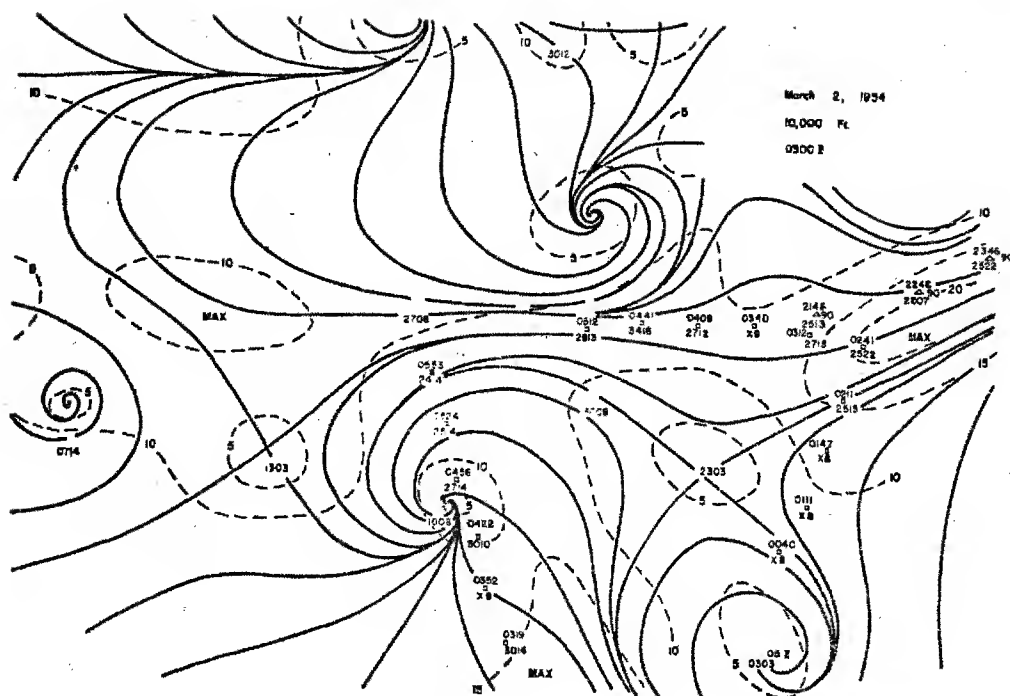


Figure 3

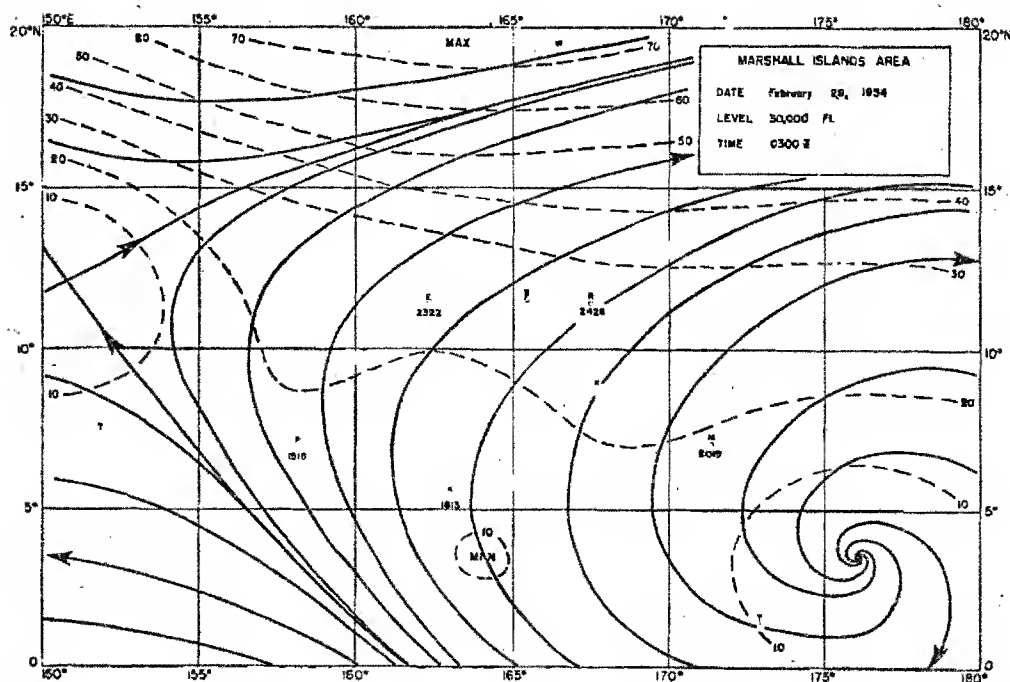


Figure 4

DOE ARCHIVES

452

457

[REDACTED]

components over the Bikini area. (Figures 4, 5, 6, 7) A gradual southwestward shift of this belt occurs with time, in agreement with the southwestward displacement of the anticyclones at 10,000 feet.

At 50,000 feet southwesterly flow appears on February 28. (Figure 8) On March 1 an anticyclone descends into the analysis level at map time, but ascends again after a 6 hour period, and is not evident at 50,000 feet on 2 March. (Figures 9 and 10)

The horizontal picture of the wind flow at 60,000 and 70,000 feet is complicated by the presence of the tropopause and the low level stratospheric easterlies. (Figures 11 and 12) Any horizontal analysis in these layers represents only the height changes in all of these shear levels, and therefore has not been performed except for March 1. (Figures 13, 14, 15) Wind speeds at these levels are light.

Steady and strong easterly winds persist at 80,000 feet throughout the period.

In conclusion, analyses for all levels from the surface through 80,000 feet for 1 March 1954 are shown (Figures 16, 17, 2, 18, 5, 6, 9, 11, 12, 14).

DOE ARCHIVES

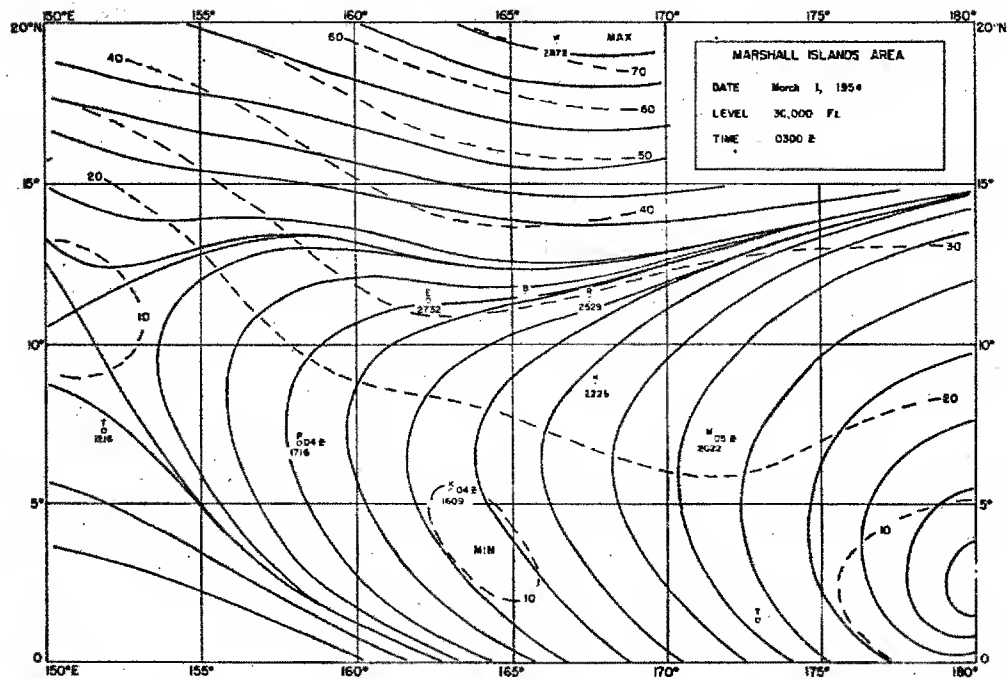


Figure 5

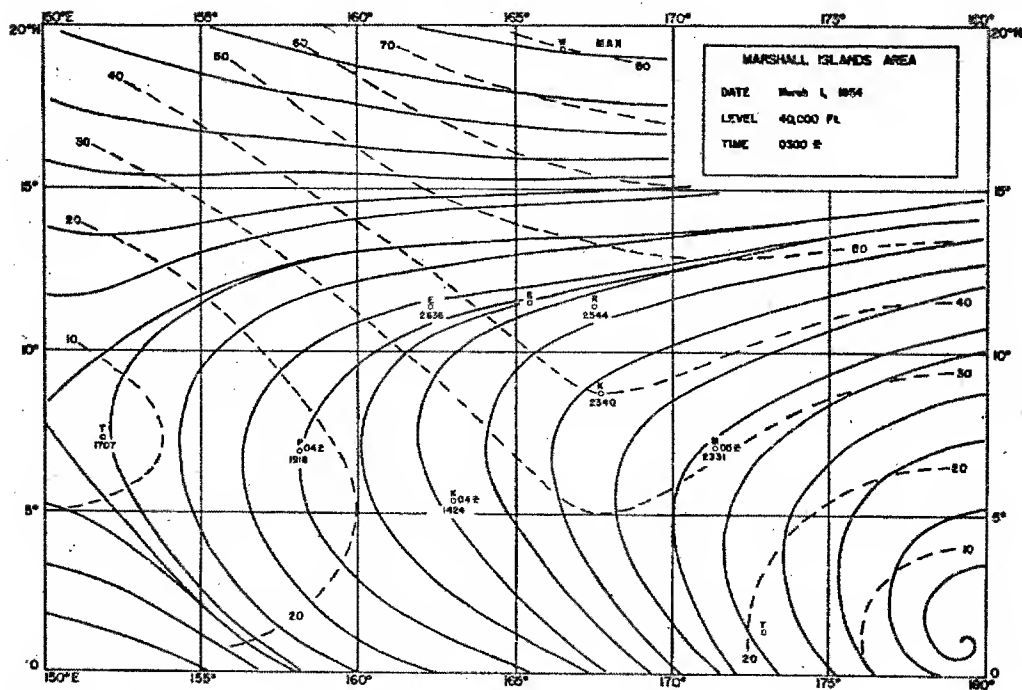


Figure 6

DOE ARCHIVES

454

ATOMIC ENERGY ACT 1954

459

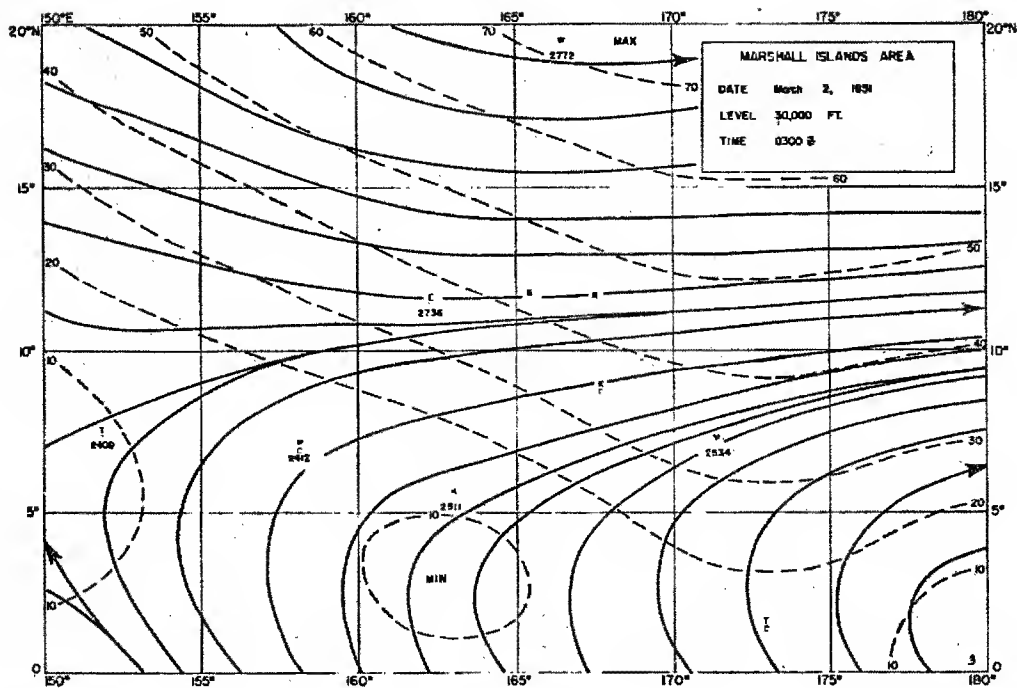


Figure 7

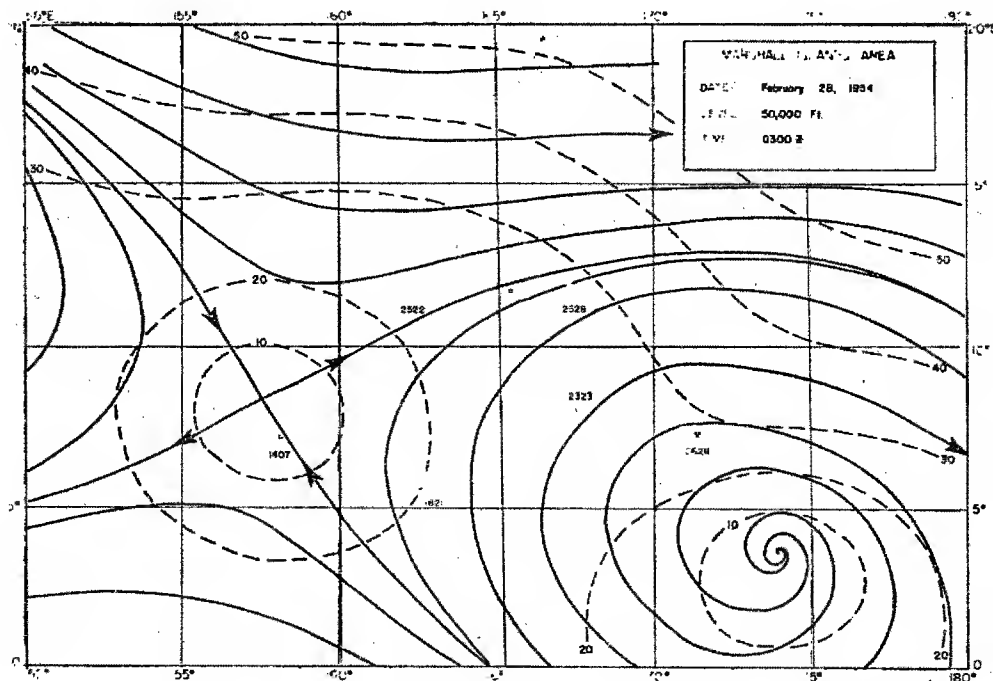


Figure 8

DOE ARCHIVES

455

460

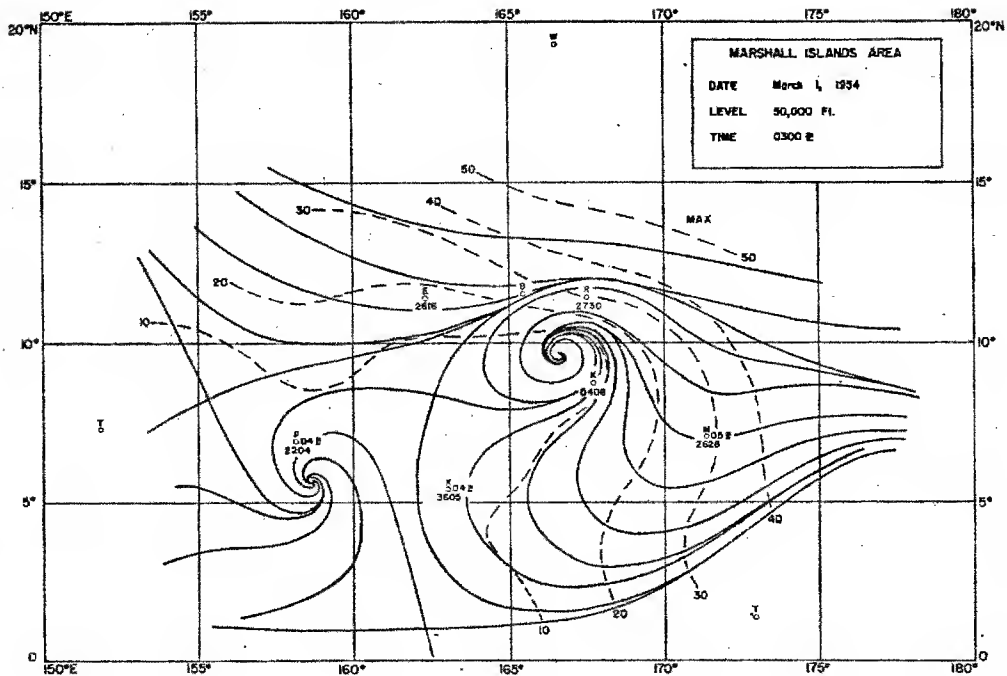


Figure 9

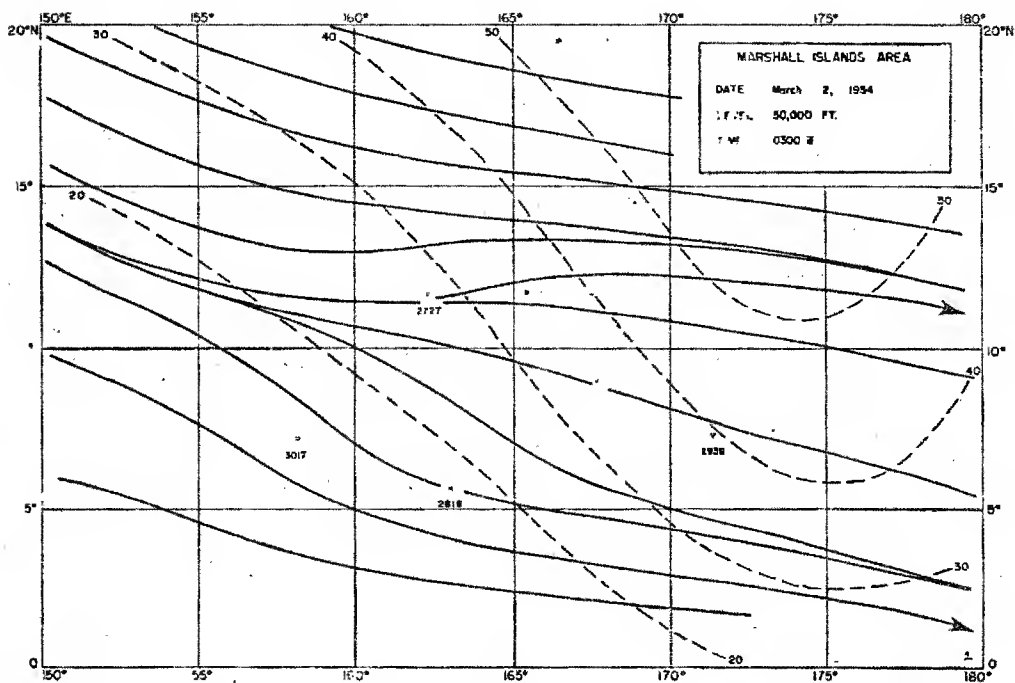


Figure 10

DOE ARCHIVES

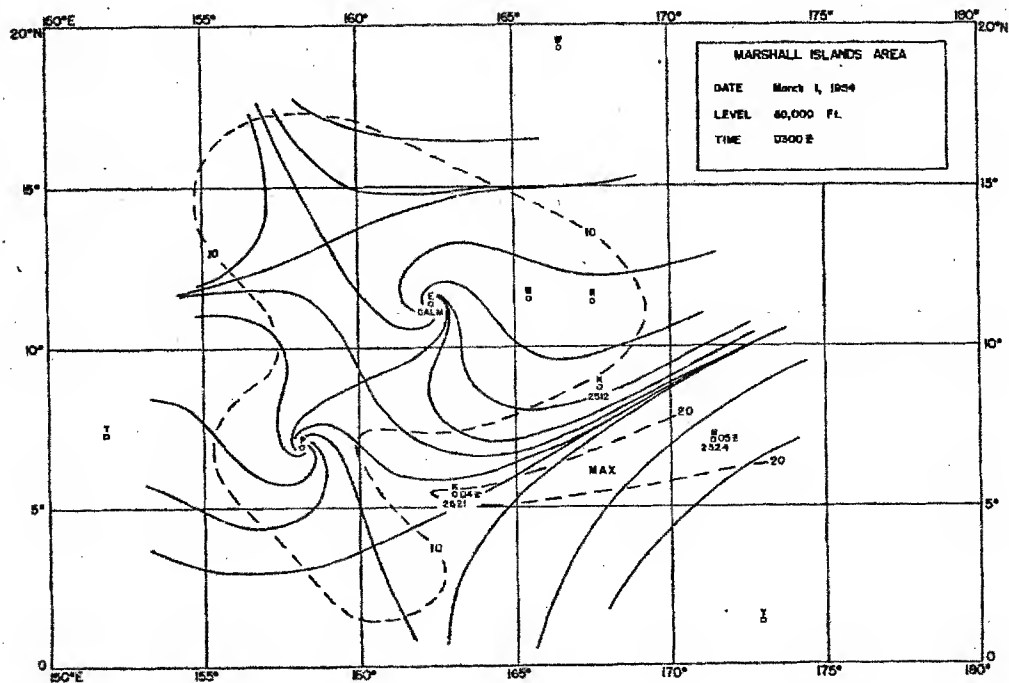


Figure 11

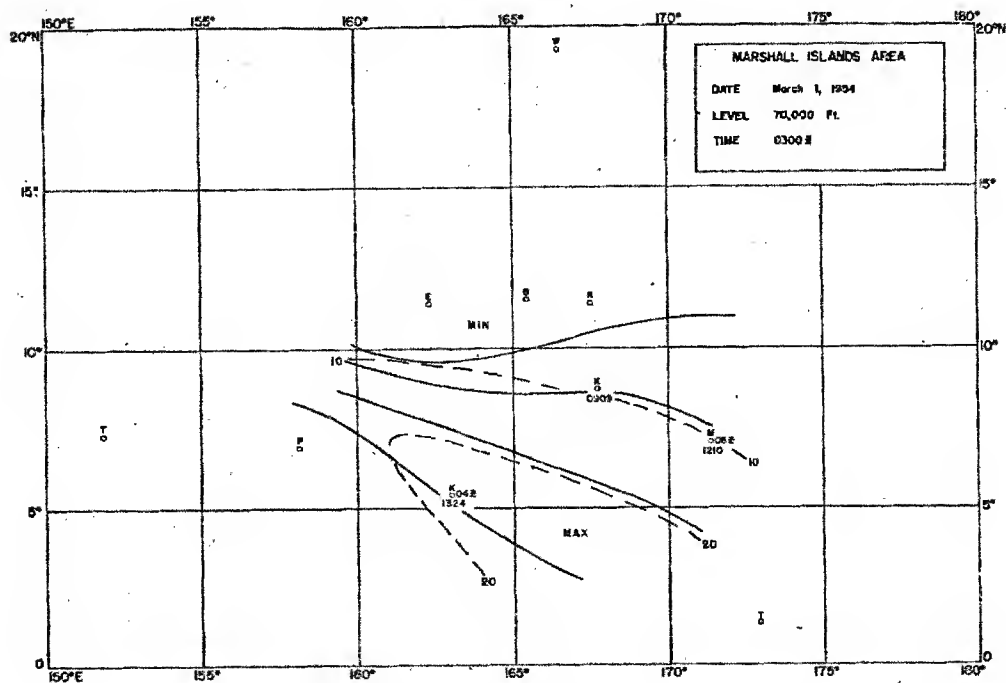


Figure 12

DOE ARCHIVES

457

ENERGY ACT 1954

462

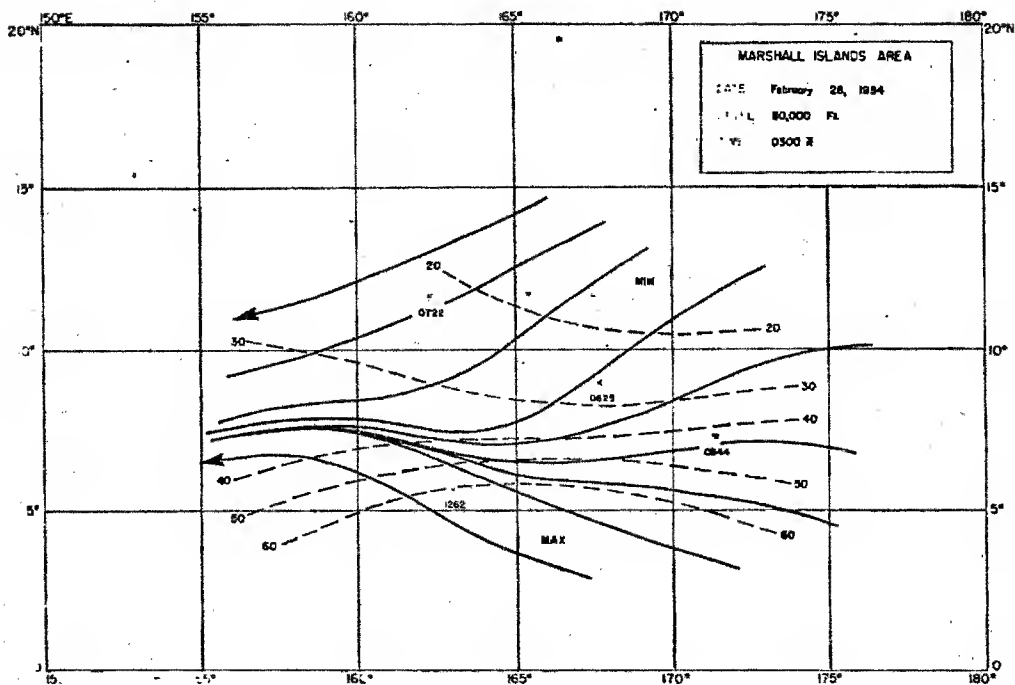


Figure 13

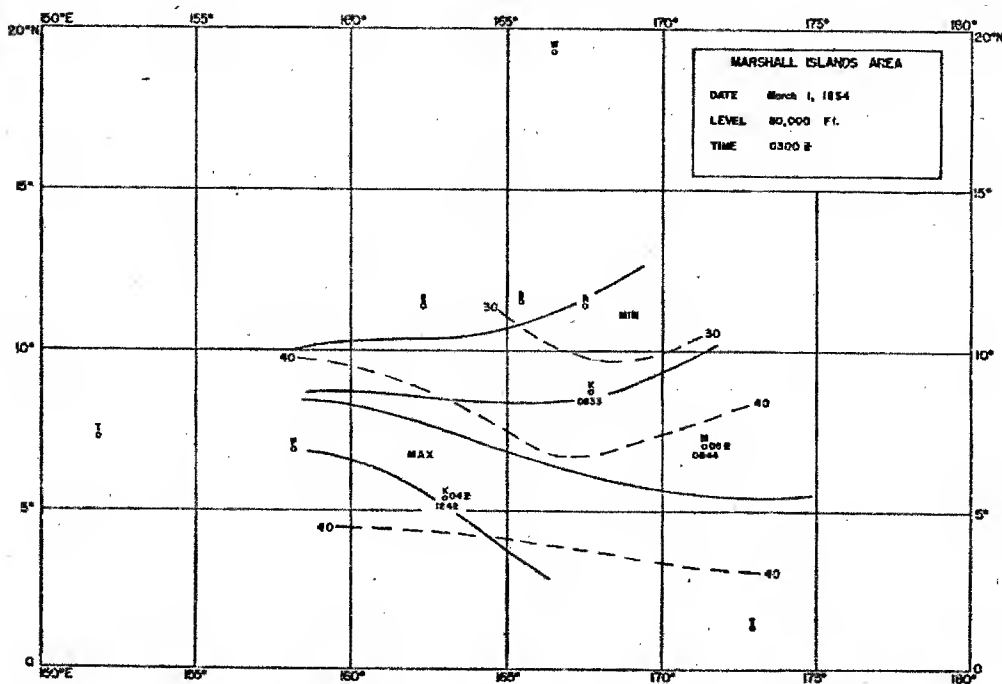


Figure 14

DOE ARCHIVES

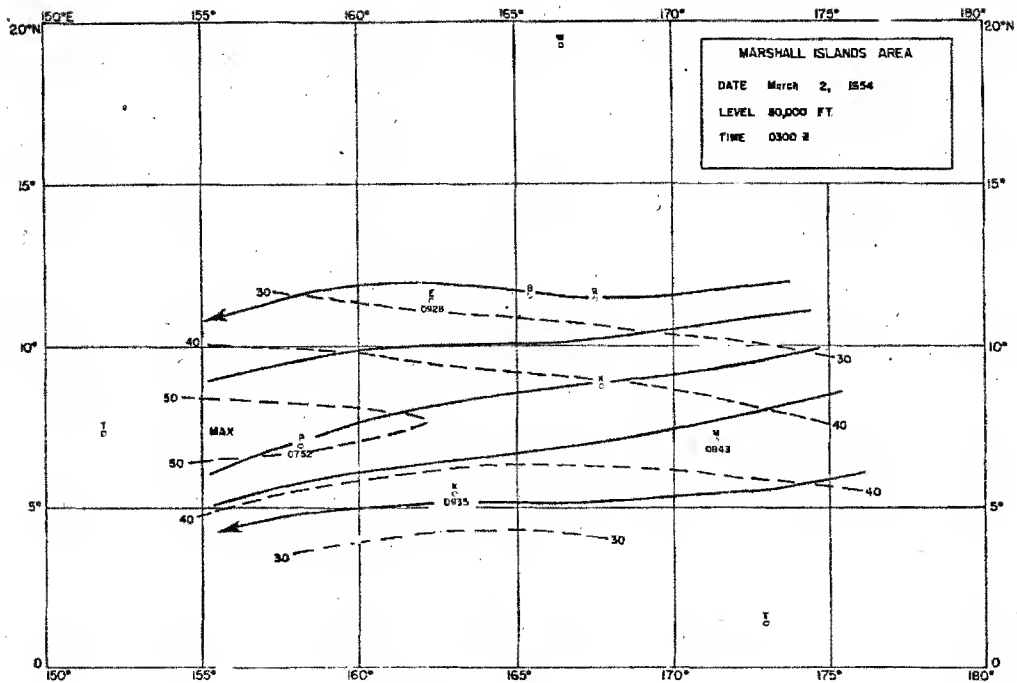


Figure 15

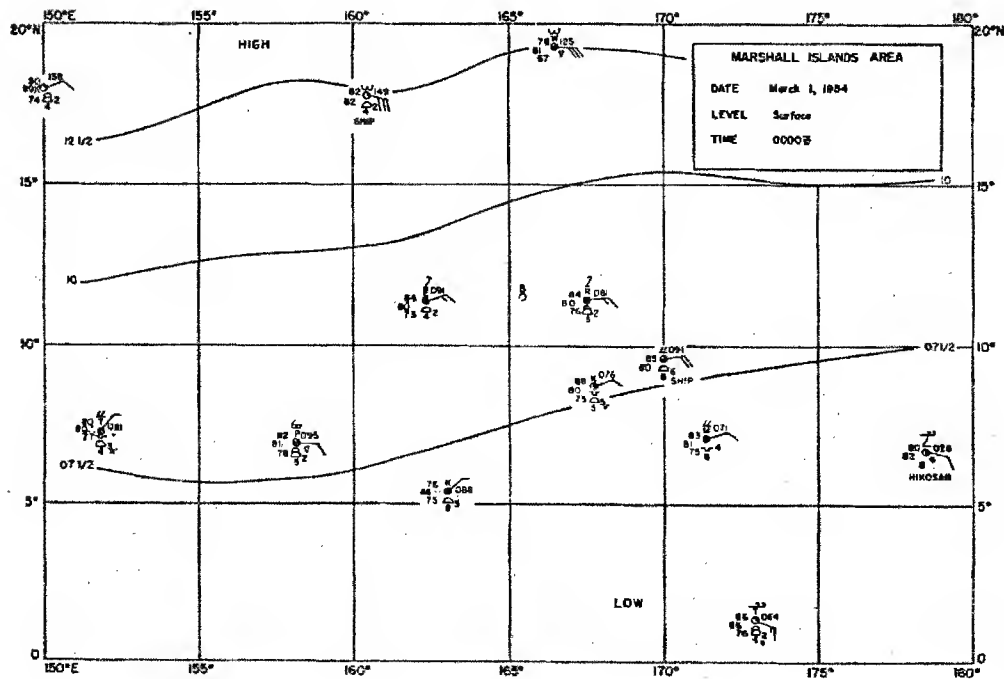


Figure 16

DOE ARCHIVES

459

464

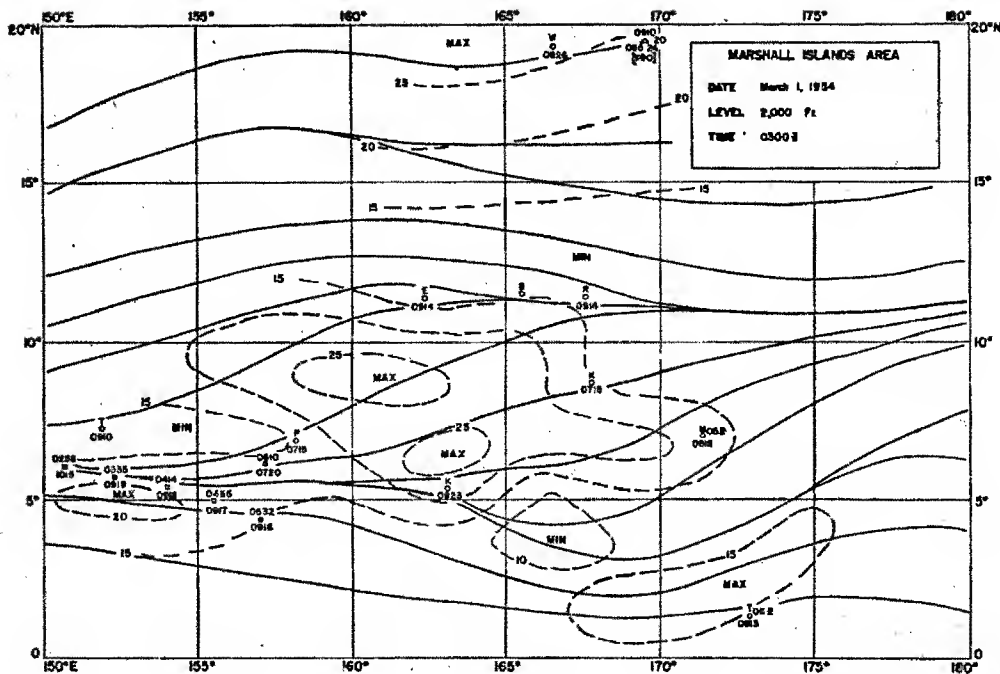


Figure 17

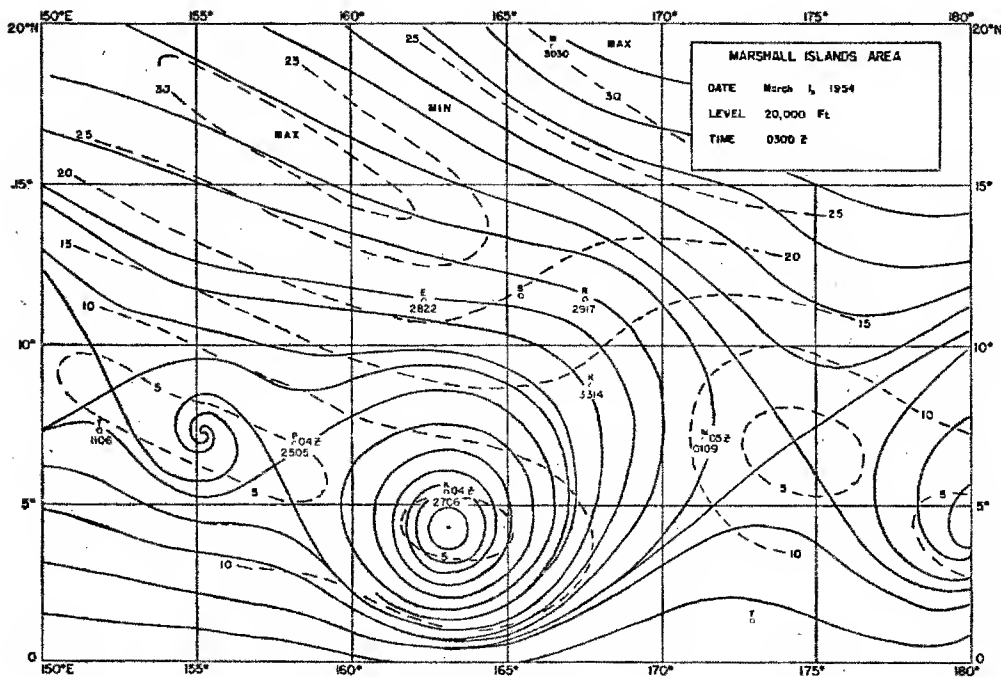


Figure 18

DOE ARCHIVES

~~SECRET~~

PART II
VERTICAL MOTION IN THE MARSHALL ISLANDS AREA

CDR Daniel F. Rex, USN
Joint Task Force SEVEN

In the Task Force we are interested in the field of vertical motion for two reasons; first of all, through an analysis of vertical motions we may be able to gain a better understanding of the circulation in the tropical atmosphere and secondly, if the vertical components are sizeable they will certainly affect the fall-out pattern produced following an atomic explosion. G. A. Dean and W. D. Ohmstead, in Oahu Research Center Special Report No. 1 under Air Force Contract No. AF 19(604)-546, have computed the vertical motion at various levels for 1 March 1954 at 0300Z from streamline analyses of the horizontal wind field. In order to extend their interesting results it was decided to compute the same and other cases using a different technique. So my purpose is first, to describe the vertical motions "typically" observed in the Marshall Islands area and second, to demonstrate the computational method which was used--a method which is perhaps simple and objective enough to be applied successfully under operational conditions.

We have available six cases in which the vertical motion in the area of interest has been computed; 0300Z 1 March 1954 by Dean and Ohmstead; 2100Z 28 February 1954, 0300Z and 1500Z 1 March 1954, and 0300Z 2 March 1954 by Rex; and one case during GREENHOUSE computed by Dr. C. E. Palmer and published in the GREENHOUSE meteorological report. It is obvious that no general conclusions may be drawn from such a meager statistical sample. Nevertheless, one can perhaps obtain a gross, qualitative picture of vertical fields common in the Marshall area. Figures 1 through 6 illustrate the fields of vertical motion obtained at the 2000, 10000, 20000, 30000, 40000 and 50000 foot levels by Dean and Ohmstead and are generally typical of the computational results for all cases both with respect to the magnitude of the values and to the geometry of the patterns obtained. A comparison between the vertical wind speeds drawn in Figures 1 through 6 with those obtained in each of the other cases computed, gives a maximum variability of $\pm 25\%$ of the values illustrated for any particular level. It may be seen from the figures that the vertical motions are organized into upward and downward moving currents or cells having horizontal dimensions of many hundreds of miles. It is also apparent that the magnitude of the vertical component increases with increasing altitude, and there is a tendency toward larger cell dimensions at the higher levels. In a very brief way this summarizes the computational results. For comparison purposes it should perhaps be noted that all vertical speeds in Figures 1 through 6 are given in centimeters per second; one centimeter per second is equal to one hundred and twenty feet per hour or thirty centimeters per second is equal to 3,600 feet per hour.

DOE ARCHIVES

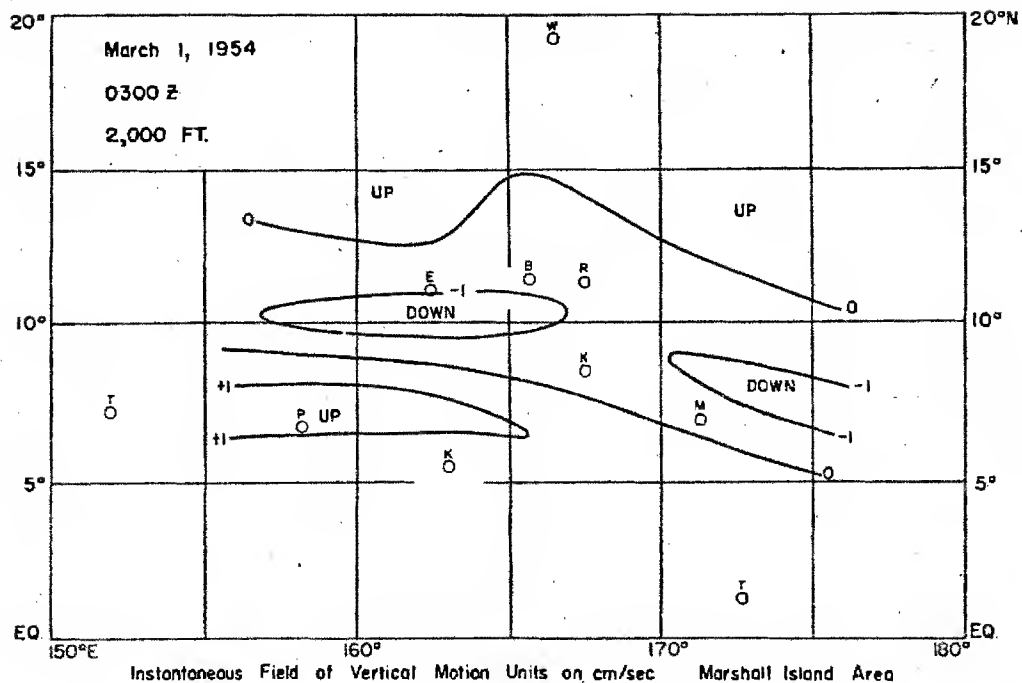


Figure 1

DOE ARCHIVES

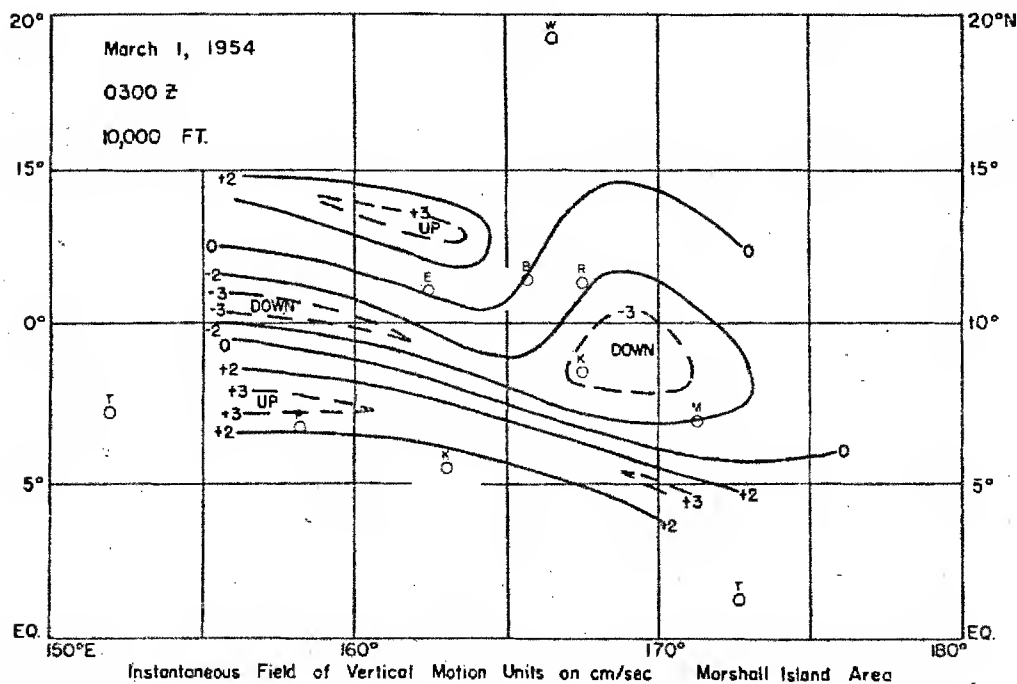


Figure 2

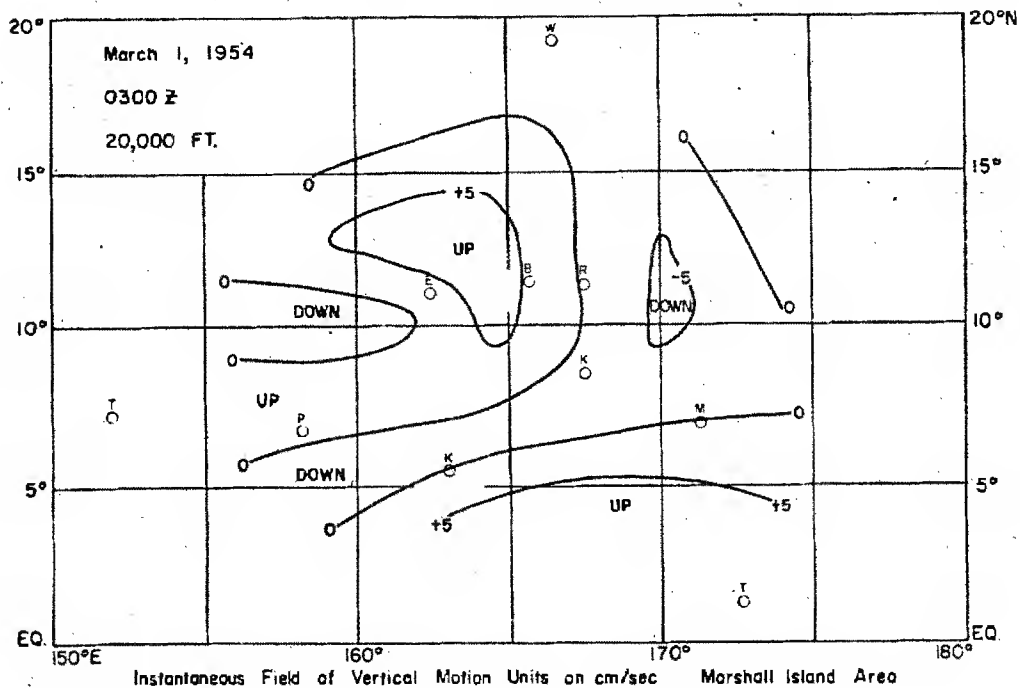


Figure 3

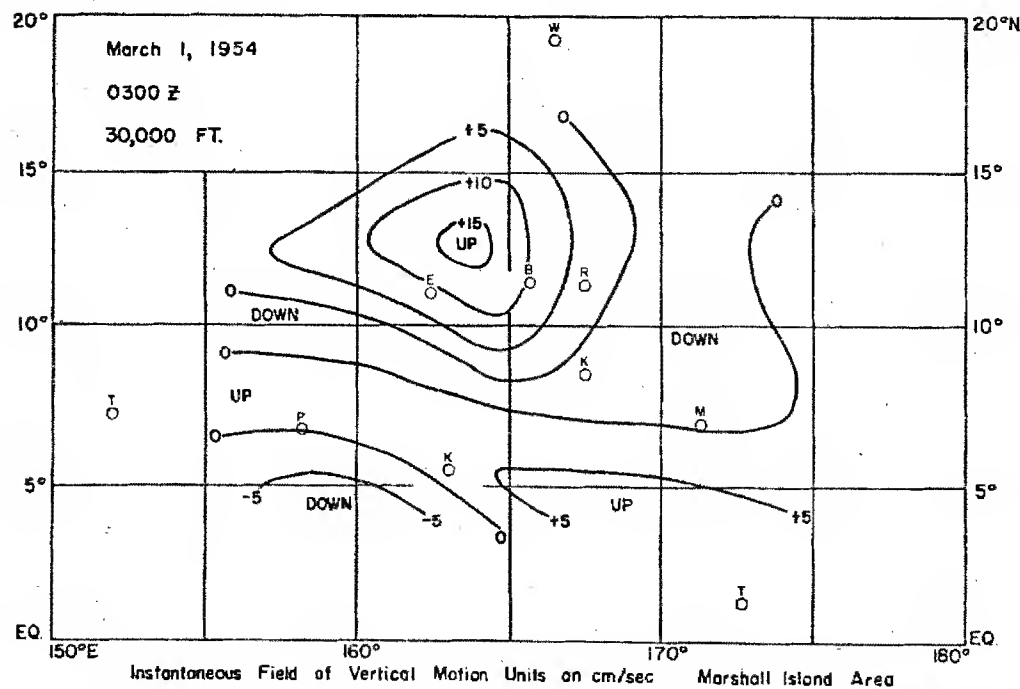


Figure 4

463

DOE ARCHIVES

465

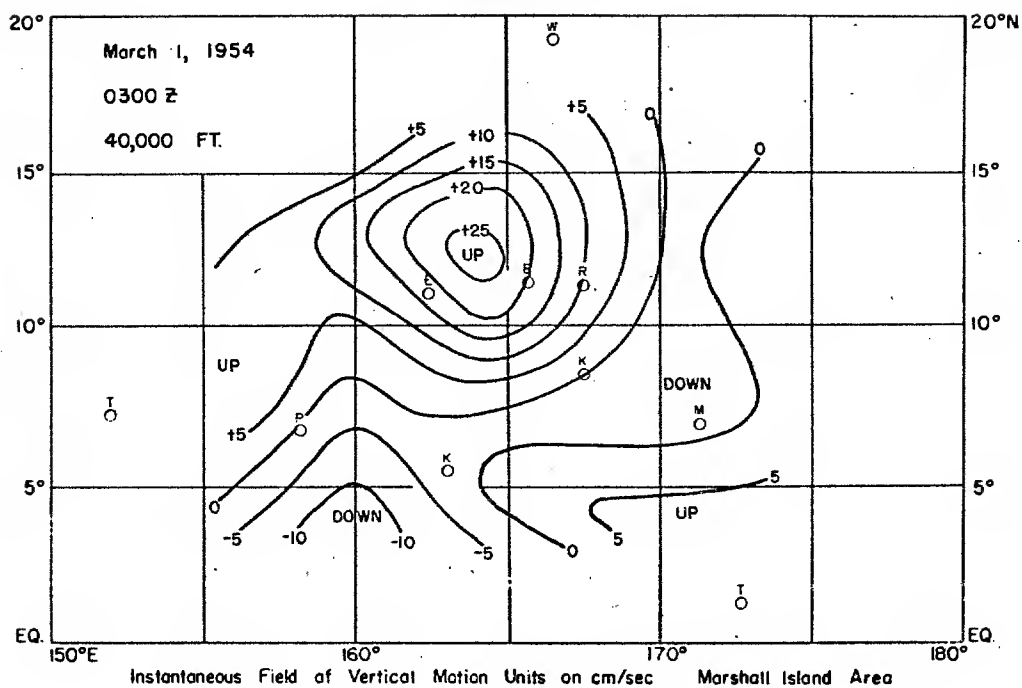


Figure 5

DOE ARCHIVES

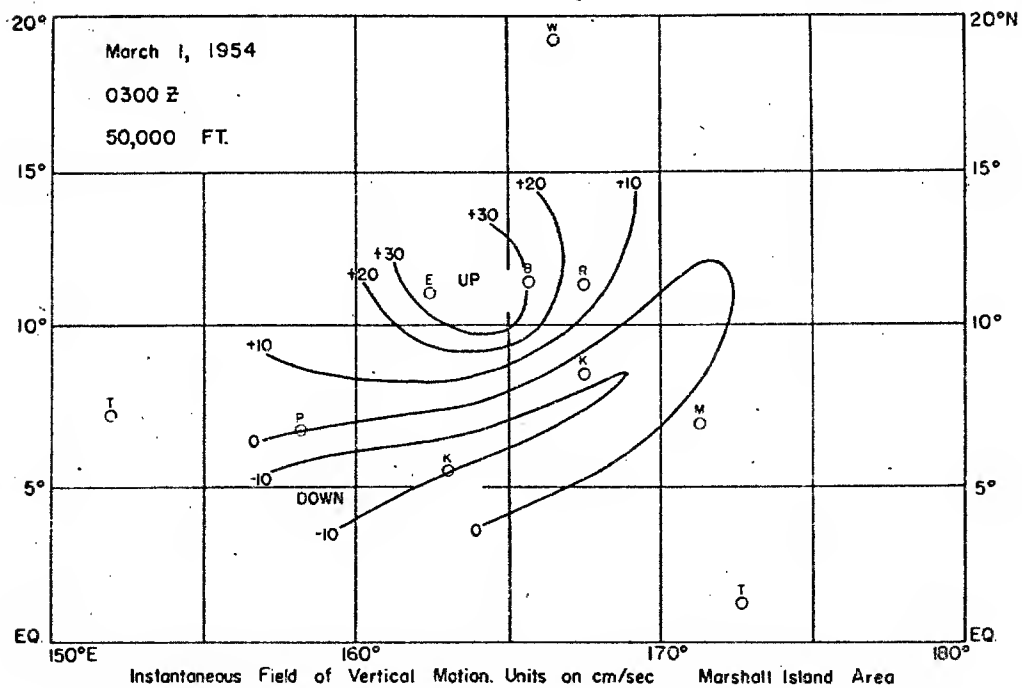














Figure 6

464

DATA

469

Because the fields of vertical motion are obtained indirectly through computation of the horizontal divergence it is important to investigate the reality of the computed patterns. For this purpose two checks were used: the distribution of observed weather was compared with the computed motion; and vertical motions, computed for the same time by two different methods, were compared. In Figure 7 is shown the distribution of weather in the Marshall Islands area at 2300Z on 28 February 1954; the observed cloud amounts and types and the location of precipitation elements are indicated by the following symbols:

- RAIN
 - - Rain
- SHWRS
 - - Showers
- TSTMS
 - - Thunderstorms
-  - - Cumulonimbus
-  - - $\frac{1}{8}$ to $\frac{3}{8}$ Cumulus (low cloud)
-  - - $\frac{4}{8}$ to $\frac{6}{8}$ Cumulus (low cloud)
-  - - $\frac{7}{8}$ to $\frac{8}{8}$ Cumulus (low cloud)
-  - - $\frac{1}{8}$ to $\frac{3}{8}$ Stratus or Stratocumulus (low cloud)
-  - - $\frac{4}{8}$ to $\frac{6}{8}$ Stratus or Stratocumulus (low cloud)
-  - - $\frac{7}{8}$ to $\frac{8}{8}$ Stratus or Stratocumulus (low cloud)
-  - - $\frac{1}{8}$ to $\frac{4}{8}$ Cirrus, Cirrostratus or Cirrocumulus (high cloud)
-  - - $\frac{4}{8}$ to $\frac{8}{8}$ Cirrus, Cirrostratus or Cirrocumulus (high cloud)

Blank areas are cloud and precipitation free

DOE ARCHIVES

Figure 7 was taken without modification from the original weather briefing chart used just prior to the Bravo event; it is simply a reproduced section of the original and was constructed many months before the vertical field computations were begun. Figure 8 shows the field of vertical motion computed for the 2,000 foot level (Figure 9 for the 30,000 foot level) at 2100Z on 28 February 1954 or just two hours prior to the time of Figure 7. Comparing Figures 7 and 8 we find the greatest

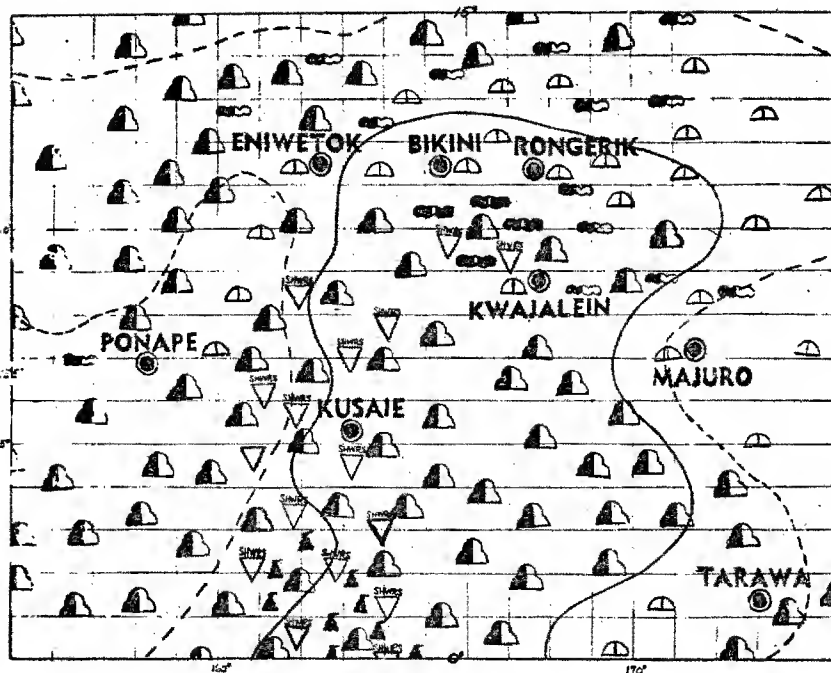


Figure 7
Weather Chart, Marshall Islands Area, 2300Z 28 Feb 54

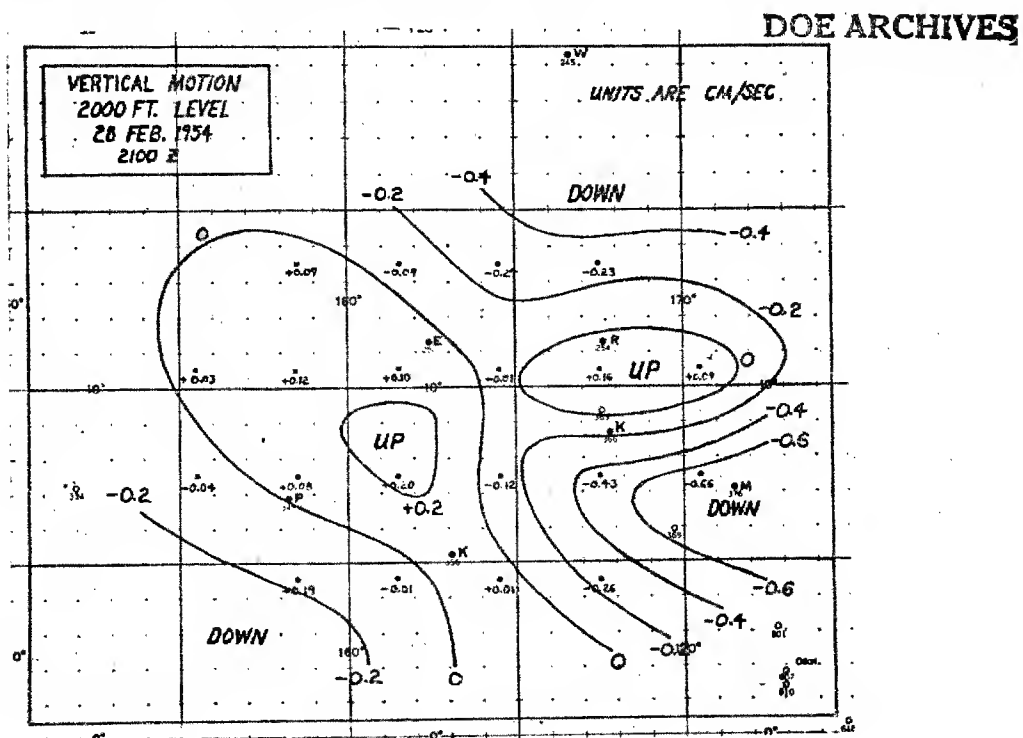


Figure 8

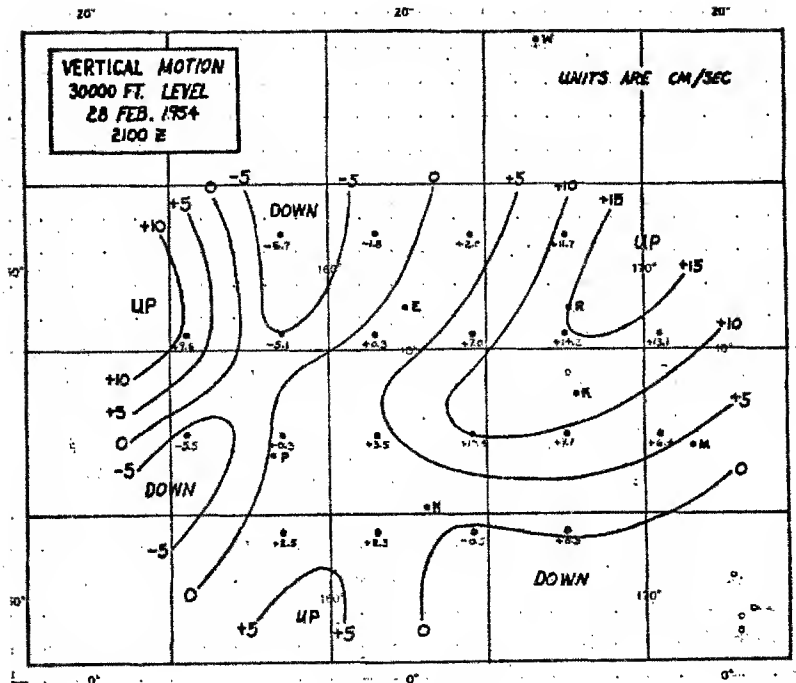


Figure 9

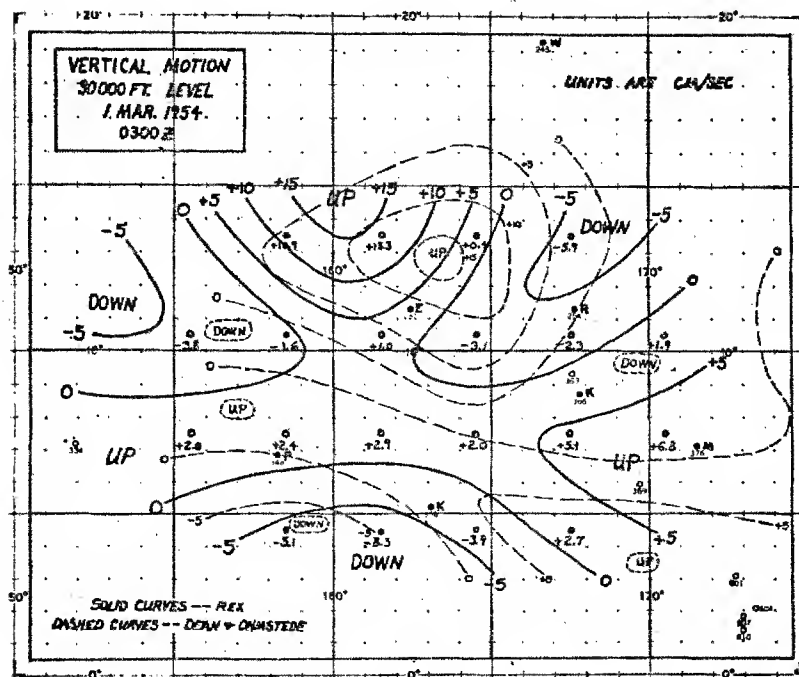


Figure 10

DOE ARCHIVES

467

472

convective activity (showers, thunderstorms and cumulonimbus) in the areas of upward motion. The similarity between the two patterns is quite striking. In a similar fashion comparing Figures 7 and 9 we find high cloud amounts greatest in the areas of upward motion at the 30,000 foot level. Figure 10 shows the field of vertical motion at the 30,000 foot level at 0300Z on 1 March 1954 as computed by two independent methods, that of Dean and Ohmstead which is described in their report mentioned earlier and is based upon the calculation of horizontal divergence from streamline analyses and a method, suggested by Dr. C. E. Palmer, which I have used and which will be described later. Inspection of Figure 10 will show that the vertical wind speeds obtained by the two methods are of the same order of magnitude and further, that the geometry of the two patterns is quite similar. From the studies which have been completed and were briefed in the preceding paragraphs, it appears to be possible to compute fields of vertical motion which are at least qualitatively representative of the actual atmospheric motions.

Now I should like to discuss briefly the method of computation which we have used. There are in general two approaches to the computation of vertical velocity; the thermodynamic and the kinematic. Thermodynamic methods are derived from the fact that changes in the vertical temperature and humidity structure are largely the result of vertical motions. Such changes as may be produced by non-adiabatic processes such as radiative effects, the release of precipitation, etc., are either neglected or treated empirically. It is for this reason that the thermodynamic approach is not especially useful in tropical areas where non-adiabatic processes are maximized. Kinematic methods are derived from the continuity equation; they involve the computation of the divergence of the horizontal wind field at various levels and a vertical integration to determine the vertical velocities. The simplest kinematic methods involve the calculation of horizontal divergence within a polygon (usually a triangle) having observation stations at its vertices; the observed winds being averaged along each side of the polygon. This method produces good results in an area of dense observations where the sides of the figure are not long but cannot be applied in the Marshall Islands area with any assurance of success because of the extremely sparse observing network. The method used by Dean and Ohmstead, as has been mentioned before, required a streamline (isogon-isotach) analysis at various, rather closely-spaced, levels. Divergence fields are computed from the streamline charts and the vertical velocities computed over a set of grid points from smoothed values of the divergence at each point.

DOE ARCHIVES

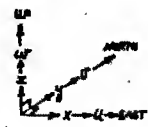
The method which I have used was originally suggested by V. Bjerknes in Dynamic Meteorology and Hydrology, Part II and was further

~~RESTRICTED DATA~~
~~NO FORN DISSEM~~

developed by C. E. Palmer during GREENHOUSE. In Figure 11 is shown the derivation of the computational function as I have used it. Using standard nomenclature the of continuity (1) is integrated in the vertical direction and by substitution the variable is changed to pressure resulting in equation (4). Defining the vector components \bar{u} and \bar{v} as indicated in equation (5) we may write the vertical velocity at the level of interest, w_i is equal to the horizontal divergence of the vector field \bar{V} divided by the product of density times gravity. The computational procedure used was developed from this relationship, equation (6). The two assumptions made in the derivation of equation (6), i.e., that the local rate of change of density and the vertical velocity at the surface are both negligible, have been shown to be essentially valid over low oceanic stations in the tropics.

To determine the \bar{u} and \bar{v} values for any particular case, the u and v components of the observed winds at each station available within the area of interest are plotted as a function of pressure as illustrated in Figure 12. In the figure, which is for Eniwetok at 2100Z on 28 February 1954, the heavier curves represent the u and v values. These curves are then graphically integrated with respect to pressure by the method of equal areas to determine the corresponding \bar{u} and \bar{v} values; a pressure interval of 5 centibars was used in the computation. The \bar{u} and \bar{v} values are then plotted as a function of pressure; the lighter curves in Figure 12 represent these graphs. Finally the value of \bar{u} and \bar{v} at any particular height can be read from the graphs by means of the pressure-height relationship. In Figure 12 the average values of the wind components u and v in each 5 centibar pressure interval are denoted as $\overline{[u]}$ and $\overline{[v]}$ respectively. In order to interpolate between the few stations available in the Marshall Islands area it has been found best to plot and analyze the \bar{u} and \bar{v} fields. This step is illustrated in Figure 13 showing the \bar{v} field as solid isolines and the \bar{u} field as broken isolines. An analysis must be made for each level at which it is desired to compute the field of vertical motion, but it should be emphasized that the \bar{u} and \bar{v} fields may be analyzed as scalar fields thus greatly simplifying the labor involved. From the charts of the \bar{u} and \bar{v} fields the field of vertical motion at any level can be computed as indicated in Figure 14. A square grid was drawn on a transparent overlay in order to facilitate reading off the required \bar{u} and \bar{v} values; values were read off at each solid black dot shown in Figure 14. The average value of \bar{u} along the east side of square 3 is denoted as \bar{u}_{3E} ; other averages are indicated by a similar nomenclature. Also shown in Figure 14 are the locations of the nine observing stations which were available in the Marshall Islands area for the cases investigated.

From the preceding discussion we conclude that if any appreciable percentage of the active material producing radioactive fall-out is



$$\textcircled{1} \frac{\partial p}{\partial t} + \frac{\partial p u}{\partial x} + \frac{\partial p v}{\partial y} + \frac{\partial p w}{\partial z} = 0$$

Assume $\frac{\partial p}{\partial t} = 0$ (essentially true over tropical ocean areas)

$$\textcircled{2} \int_z^{z_i} \left(\frac{\partial p u}{\partial x} + \frac{\partial p v}{\partial y} \right) dz = - \int_z^{z_i} \left(\frac{\partial p w}{\partial z} \right) dz = - (p w_i - p w_z)$$

Assume $w_z = 0$ (since all stations are low oceanic)

$$\textcircled{3} \int_z^{z_i} \left(\frac{\partial p u}{\partial x} + \frac{\partial p v}{\partial y} \right) dz = - p w_i = - \frac{\partial}{\partial x} \int_z^{z_i} p u dz + \frac{\partial}{\partial y} \int_z^{z_i} p v dz$$

Multiply by $-g$ and substitute $dp = -g \rho dz$

$$\textcircled{4} \frac{\partial}{\partial x} \int_p^{p_i} u dp + \frac{\partial}{\partial y} \int_p^{p_i} v dp = \rho g w_i$$

Define the functions \bar{u} and \bar{v} as follows:

$$\textcircled{5} \bar{u} = \int_p^{p_i} u dp \quad \text{and} \quad \bar{v} = \int_p^{p_i} v dp$$

Then

$$\textcircled{6} \frac{\partial \bar{u}}{\partial x} + \frac{\partial \bar{v}}{\partial y} = \rho g w_i = \nabla \cdot \bar{w} ; \text{ where } \bar{w} = \bar{u} + \bar{v}$$

VERTICAL MOTION
COMPUTATION

Figure 11

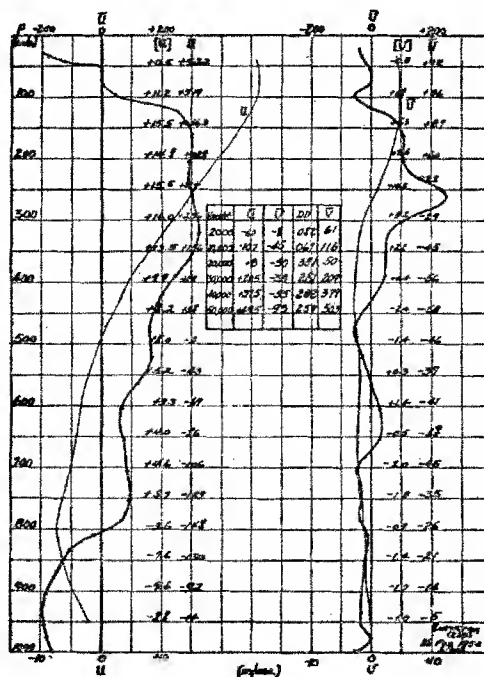


Figure 12
Vertical Motion Computations

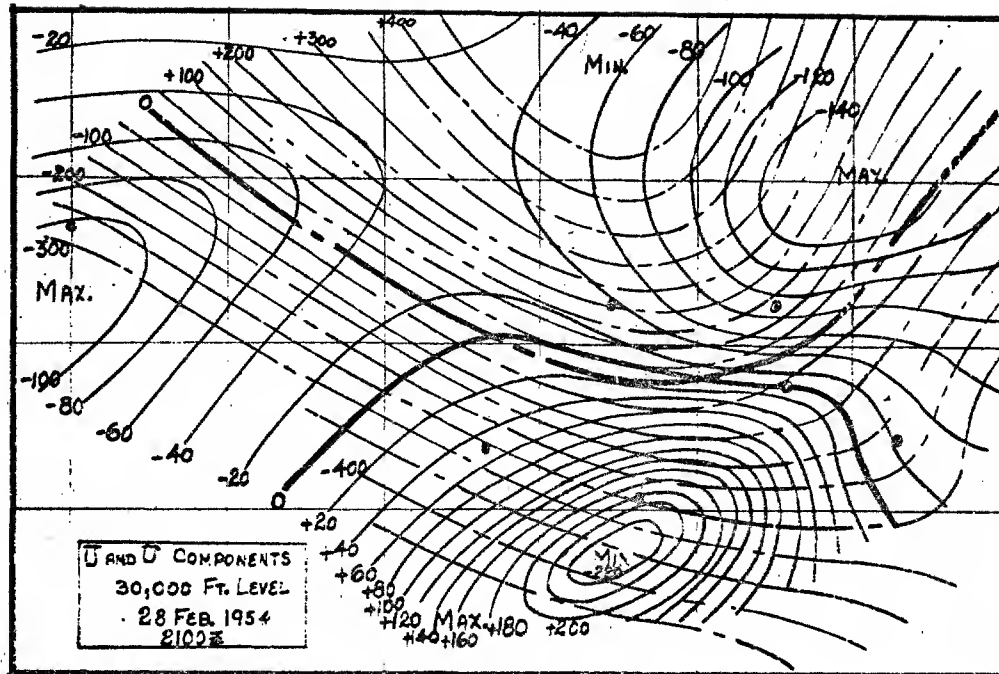


Figure 13

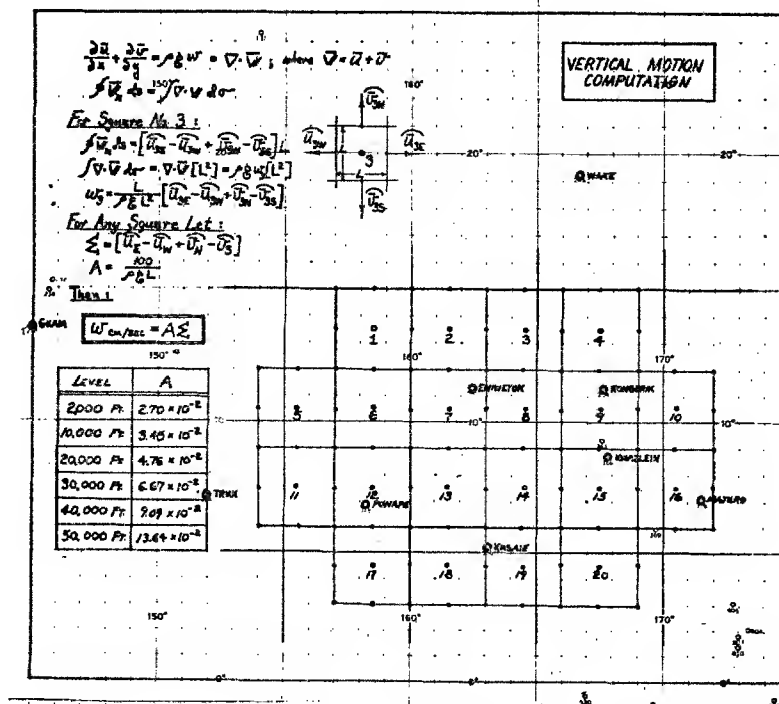


Figure 14

DOE ARCHIVES

carried above the 30,000 to 40,000 foot level in the atomic cloud and if such material, or any large part of it, is carried on particles having a falling velocity less than about 5,000 feet per hour, then any quantitative calculation of the fall-out pattern geometry and activity will certainly have to take into account the existing field of vertical motion within the area in question. Furthermore, if computations of the vertical field are required in connection with future test operations, it would appear to be feasible to compute them on a routine basis by means of the technique described in the preceding paragraphs.

DOE ARCHIVES

[REDACTED]

PART III
CONCLUDING REMARKS

LTCOL C. D. Bonnot, USAF
Joint Task Force SEVEN

Figure 1 is a map of the Southwest Pacific area, centered on Eniwetok. This map presents the presently operational rawinsonde stations, as well as several new sites which we are proposing. You will note that Yap, Koror, Truk, Ponape, and Majuro are to give us additional information; this was obtained through contract with the Weather Bureau by the Task Force. There are several sites south of the equator which we are asking the British Commonwealth to establish. Also, there are two ocean station weather ships we are requesting the Coast Guard to operate for us on a continuing year-round basis. Lastly, you will note that we plan to establish temporary stations during test periods at Kapingamarangi, Kusaie, Bikati, and Taongi. This net will give us what we feel is an absolutely minimum observing net to support the Task Force.

If such a weather observing net is operating, we feel that adequate information will be available to those required to predict the fall-out and radiation hazards at the Pacific Proving Ground. Work is being continued at the Oahu Research Center by Dr. Palmer toward improving our weather forecasting procedures for this area.

DOE ARCHIVES

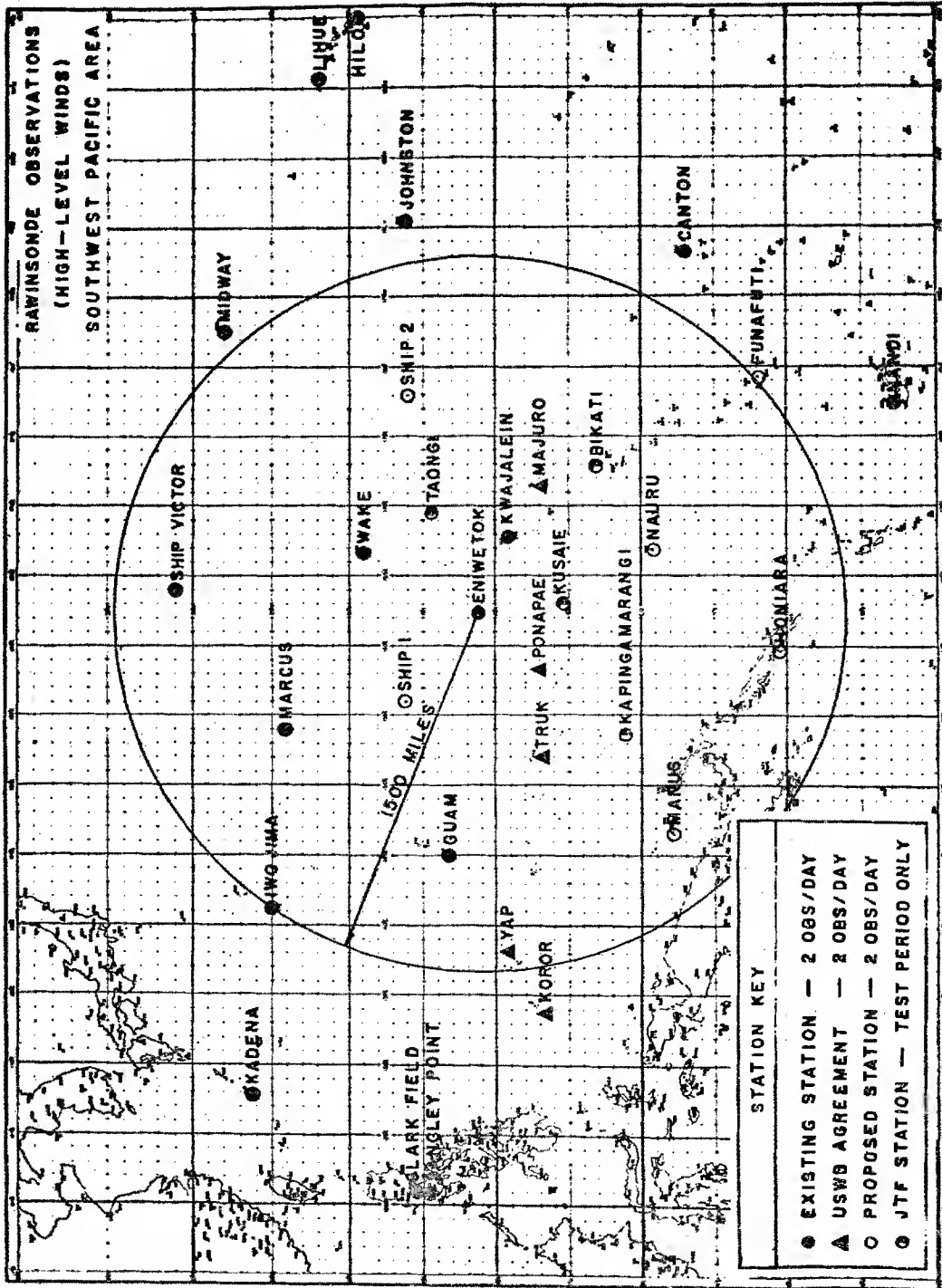


Figure 1

DOE ARCHIVES

474

ATOMIC ENERGY

479

[REDACTED]

PREDICTION OF DOSE-RATE AND DOSAGE CONTOURS AS
FUNCTIONS OF YIELD AND METEOROLOGICAL CONDITIONS;
EFFECTS OF SPECIFIC WIND STRUCTURES USING THE ARMY
SIGNAL CORPS METHOD

Kenneth Barnett
Office Chief Signal Officer

Dr. Swingle has explained to you the Signal Corps procedure for making forecasts of the radiological fall-out patterns that result from 15 megaton explosions in the tropics. I would like to show you three things. First, how this forecast procedure was calibrated by comparison with CASTLE Bravo observations. Second, the forecast made by using this procedure with different wind conditions, and third, some suggestions for making better fall-out forecasts in the future. In Figure 1, we have the trajectory of the 68 micron particles which fall out from the center of the cloud. These winds are the winds taken at shot time at CASTLE Bravo with some changes in the higher altitudes to account for the changes that occurred eight hours after the shot time. Since it required about one hour for the 68 microns particles to fall through 5,000 feet, this trajectory is very similar to a hodograph. In Figure 2, we have the iso-chrones of the arrival time of the first particles and the ending times of the particles. Both are in hours, and using the predicted data from CASTLE Bravo. In the upper part we have two points where the fall-out time, the arrival time of the first particles, was observed. We have one point at 5.7 hours; it is right on the 5 hour predicted line. We have another point at 7.8 hours that is almost exactly correct. The comparison of these few pieces of observed data fit quite well and give us confidence in the dimensions of our model. It is interesting to point out that somewhere between 30 and 35 hours the particles begin to drift backwards, as would be indicated by the 180 degree wind shift around 55,000 feet. Likewise in the lower curve, the ending time of particles, we also see how the ending time begins to change. In Figure 3, we have at the top the predicted dose rate, and this requires a calibration. As you will recall, we determine our dose rate by bringing out each of the disks or slices from our model according to the wind velocity and according to the rate of fall of the median particle size for that particular disk. We let these fall over a square, cross-sectional grid. We make a tally of the total number of cylinders that fall on each grid and then we draw lines for total numbers of each of these tallies. In order that these total numbers for each square will be in roentgens per hour, we have compared the top figure of Figure 3 with the bottom figure, which is the observed data from AFSWP Report 507. You will notice that in the top figure, our predicted figure, as drawn here, our 100 line encloses an area a little larger than the area enclosed

CASTLE BRAVO COMPOSITE WINDS

LEVEL	DEG.	KNOTS	FACTOR	VECTOR LENGTH (N.M.)	MB HEIGHT
SFC.	060	12	.98	11.8	1006
1,000'	097	10	1.14	11.4	845
10	307	11	1.15	12.4	709
15	296	12	1.12	13.4	584
20	283	13	1.11	20.0	495
25	251	24	1.10	27.5	336
30	241	31	1.09	33.8	323
35	246	38	1.08	40.1	260
40	251	45	1.07	48.1	209
45	257	44	1.06	46.7	163
50	260	30	1.05	31.5	132
55	008	18	1.04	16.7	104
60	350	04	1.03	4.1	88
65	090	03	1.02	3.1	70
70	090	18	1.01	16.2	55
75	090	20	1.00	20.0	45
80	080	22	.99	21.8	37
85	090	37	.98	36.2	26
90	090	39	.97	37.6	20

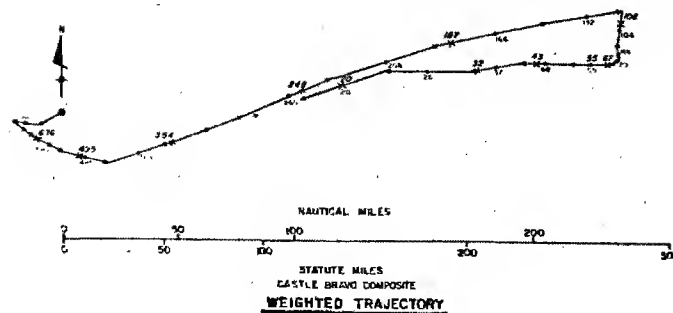
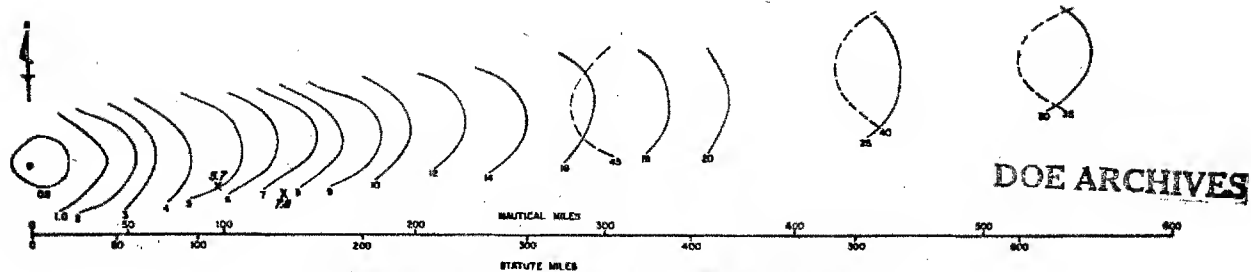


Figure 1



SECRET

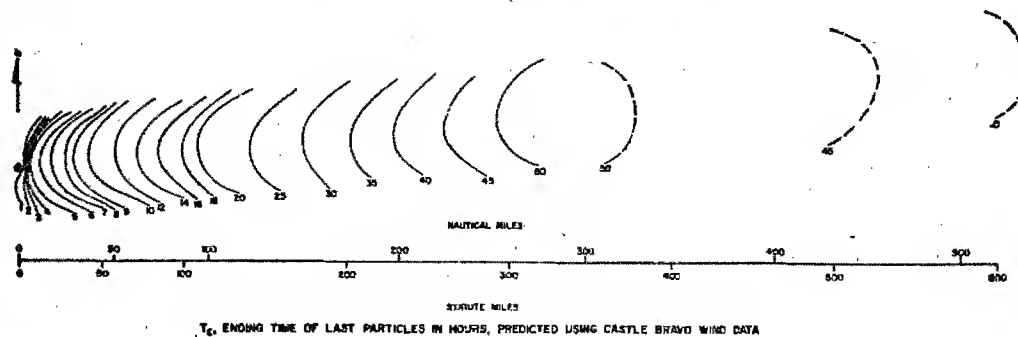
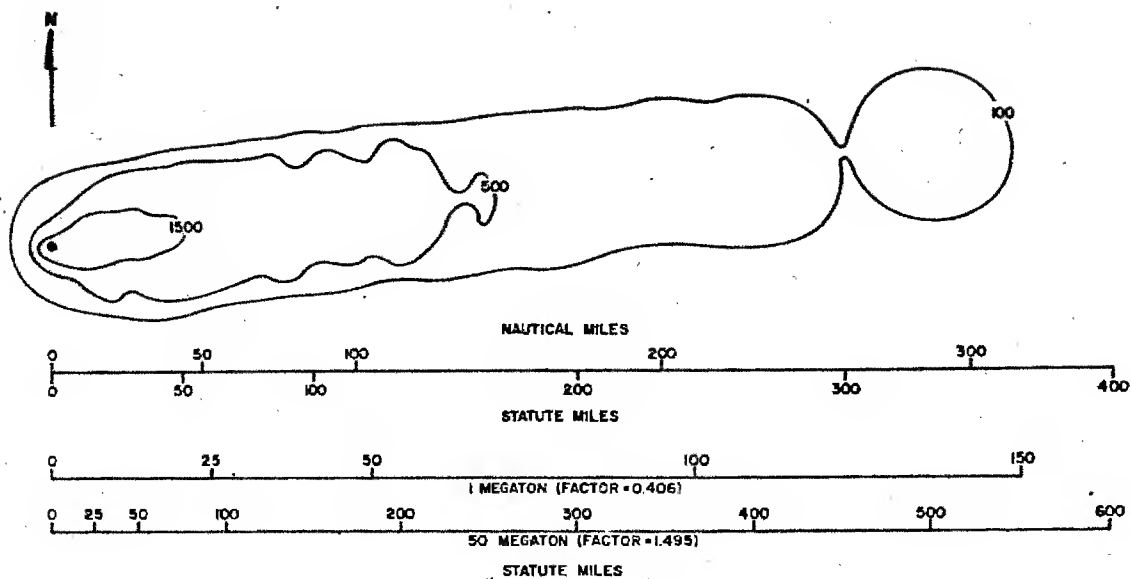


Figure 2

476

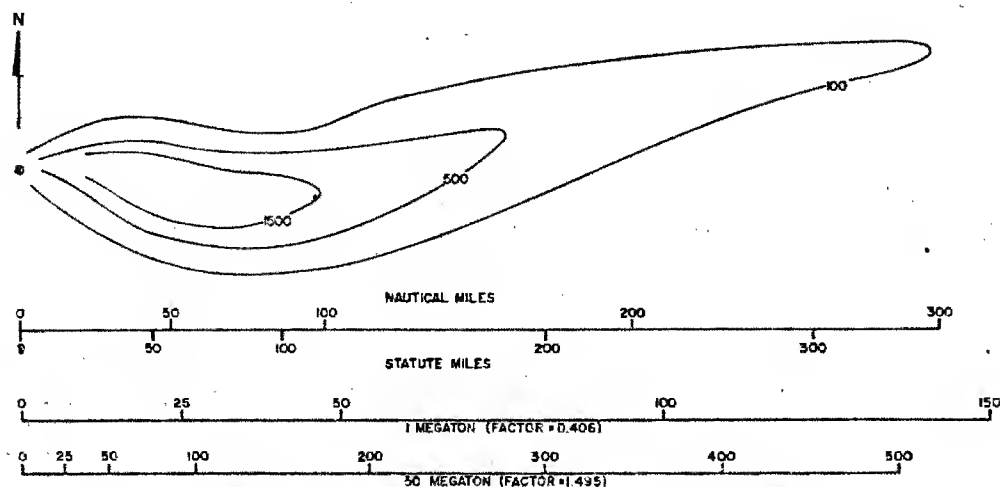
ENERGY

481



SCALING FACTORS, USING RATIO OF CUBE ROOTS OF YIELDS (AFTER AFSWP 507)

PREDICTED DOSE RATE, R/HR, USING CASTLE BRAVO WIND DATA



SCALING FACTORS, USING RATIO OF CUBE ROOTS OF YIELDS (AFTER AFSWP 507)

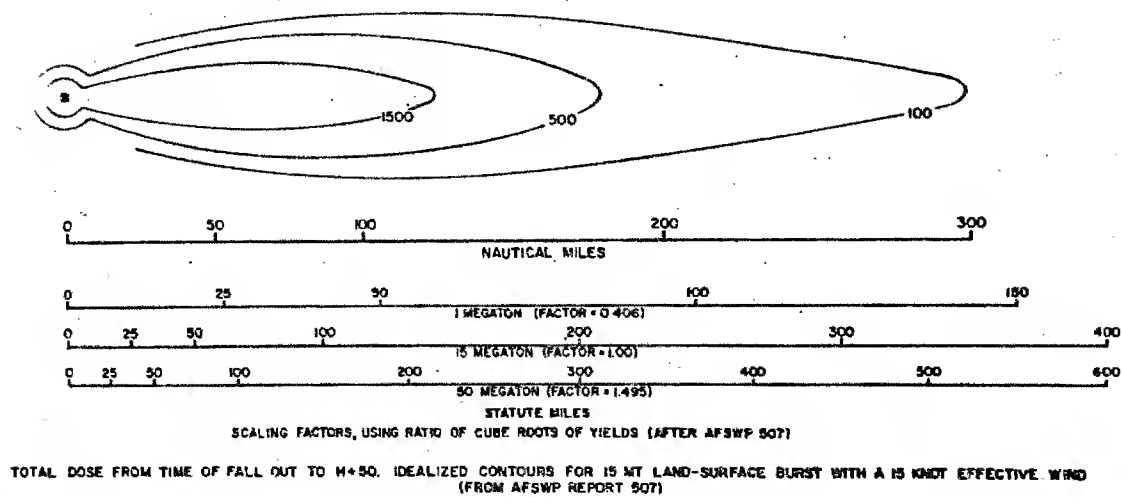
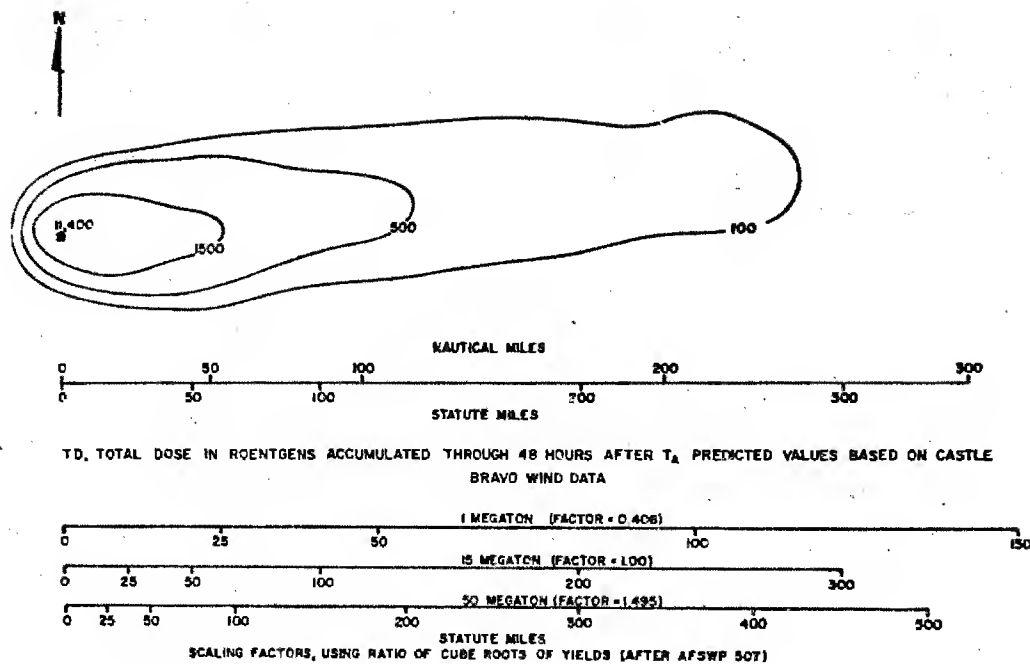
CONTOURS FROM CASTLE BRAVO DOSE RATE, ROENTGENS PER HOUR AT H+1 (FROM AFSWP REPORT 507)

DOE ARCHIVES

Figure 3

477

482



DOE ARCHIVES

Figure 4
478

by the 100 line in the bottom or observed figure. Likewise in our predicted pattern, the area enclosed by the 1500 r/hr line is slightly smaller than the observed area enclosed by the 1500 r/hr line. We used a calibration factor of 100 to obtain this tip figure and somewhere, probably around the 600 roentgen per hour line, the areas are the same in the predicted model and in the observed areas. Looking at our predicted dose rate, you will see that there is one problem rather obvious, that is the lumping of it. For example, out towards the end of the 100 line there's almost a perfect circle which indicates that one disc alone fell at that point. And right next to it, to the left, are the other circles. Later on I'll discuss some ways we have we hope will improve this. All of our calculations have been for the 15 megaton model and we did not have the time to make models for one and 50 megatons for this symposium. So we used a simple scaling factor to give some idea of what this procedure should give for a one megaton and 50 megaton yield. You'll see the two scales here in Figure 3 and in later Figures. In Figure 4 we have a comparison of our predicted total dose pattern with the idealized observed total dose pattern from CASTLE Bravo. The total area included by our predicted 100 total dose line and the idealized observed 100 total dose line is almost the same. However, the area included by our 1500 total dose line is a little smaller than the observed area. We think we have some procedures that will improve this, that is, that will make our 1500 total dose line a little larger relative to our 100 predicted total dose line. Again here in Figure 4 we have these scaling factors to go from 15 megatons to either one megaton or 50 megatons. I would now like to go on to the examples that were furnished to us by AFSWP. You know their example 1 was the condition of an approximately 90 degree shear at a height of about 40,000 feet at Dodge City, Kansas. In the lower 40,000 feet, the mean vector is generally towards the south, from the ground zero; above that the vector goes out toward the east, and I think in our resulting patterns we should see some indications of these two vectors. In Figure 5, we have the isochrones for the arrival times and the ending times. The arrival time curves are quite symmetrical and go out steadily. This suggests that we might develop a short-cut method in which we extend one vector out along one azimuth and then space the isochrones at equal spaces there and draw them off, more or less, as circles. I think we could use that to get an approximation that would be very close to this and would save us a great deal of time. Looking at the predicted ending values we see that at one hour, there is a little irregularity which I think is the lower vector which points toward the south. In Figure 6, we have our predicted dose rates and our predicted total dose. You will see that in both of those there is a little extension of the 1500 area toward the south, which is a reflection of the fall-out in the lower 40,000 feet which is extended toward the south. And again we have our scaling factors here to give

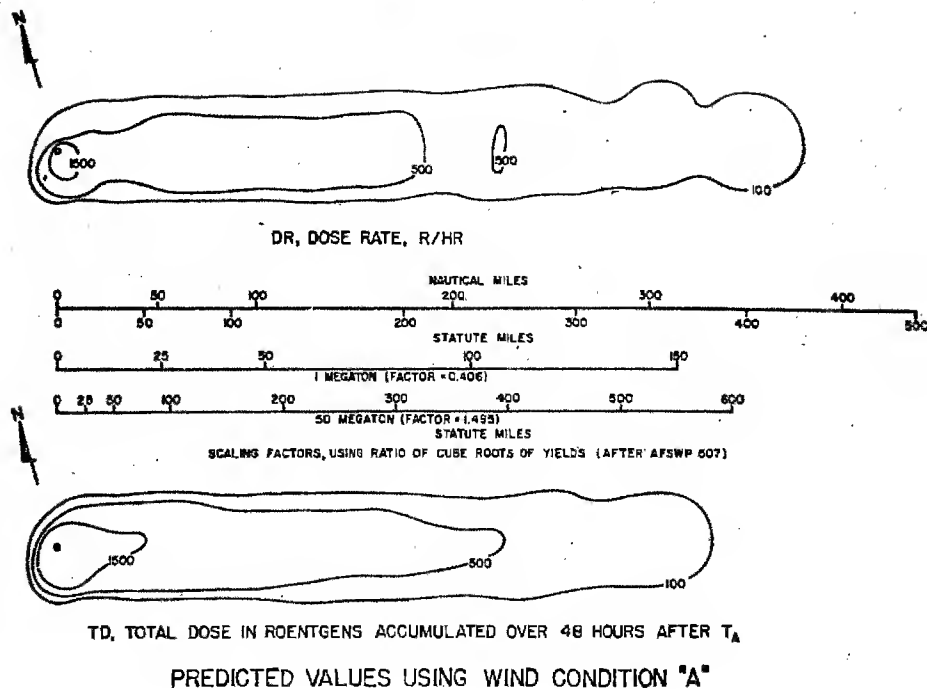


Figure 5

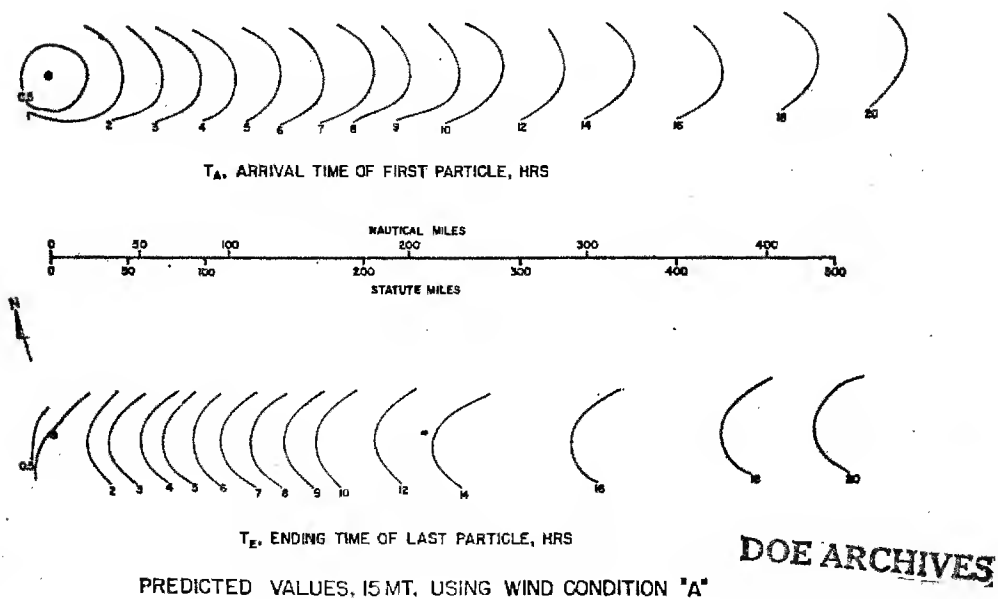


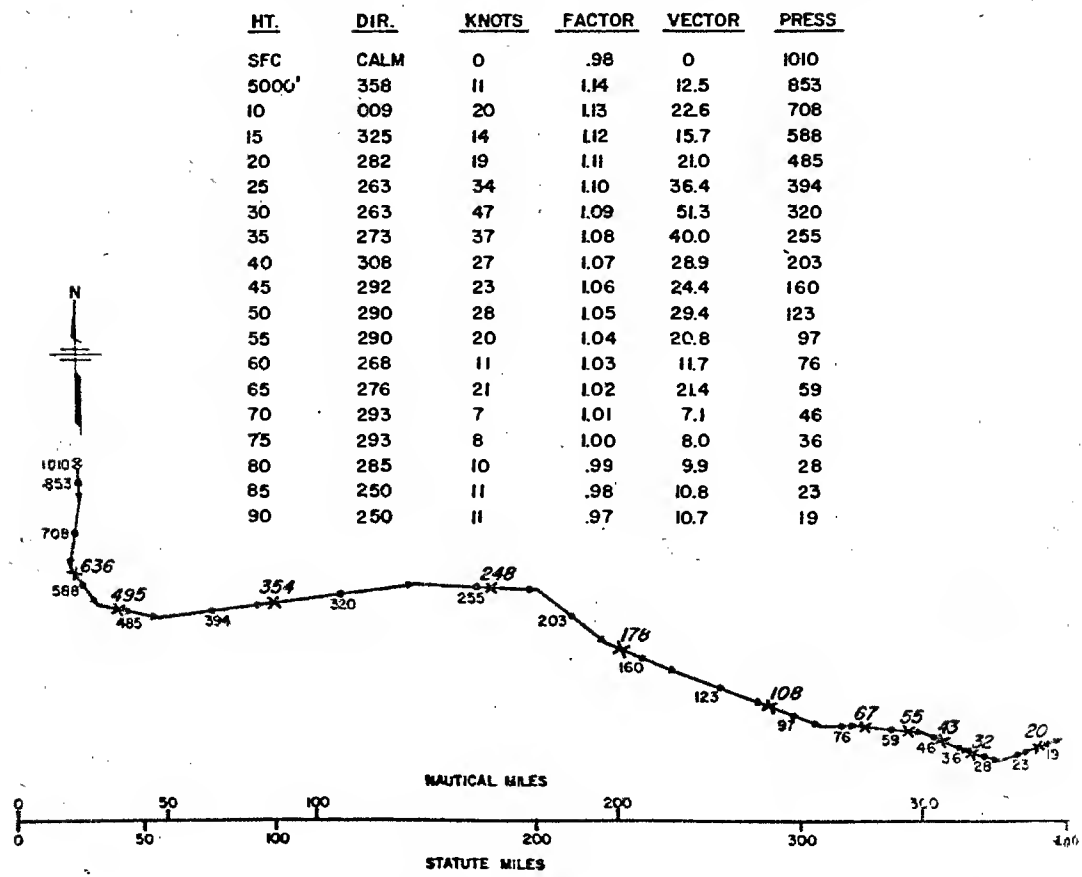
Figure 6
480

~~SECRET~~
ENERGY ACT 1954

the approximate dimensions for a one megaton and a 50 megaton yield. Going on to Case B, which is a gradual wind shear of approximately 90 degrees (Figure 7), I think we should find a fairly symmetrical pattern because the mean wind vector from the surface up to various altitudes is almost constantly towards the east-southeast. In our Figure 8, we see that the arrival time of the first particles, the isochrones for those and the ending time are quite symmetrical and extend out towards the east-southeast. Likewise, in Figure 9, the dose rate contours and total dose contours were quite symmetrical and point straight out towards the east-southeast. Case C should give us very symmetrical results too, since the winds are from almost the same direction at all levels. And Figures 11 and 12 give the isochrones for ending and arrival times for dose rates and total dose. Case D, in my opinion, is the most interesting one, and that is the condition of relatively low wind speeds at all levels. In fact, the effective wind from the base of the fireball on down to the ground is only about six miles per hour. Figure 14 shows the arrival time of the first particles and you notice that up to about 25 or 30 hours it is quite regular and then due to an almost 180 degree wind shift, the lines bunch up together and begin to go down towards the south. We likewise have a pattern for the ending time (Figure 15), which might be the super-position of two symmetrical patterns, one on the other. Figure 16 shows by the dose rate contours that, at least the 1500 contour is almost a circle, with a long piece sticking up towards the northeast where the winds had begun to shift around and there was an unusually large amount of fall-out at that distance out in this particular case. Figure 17 shows us the total dose and the contours here are nearly circles and up towards the northeast those we have are very small, much smaller than the dose rate values in that area. This is due to the deterioration factor because it is further out from the source. Figures 19 and 20 show the results of condition E, which is a case of relatively high wind speed above 10,000 feet. (Figure 18) As would be expected, it is a long, thin pattern in the dose rate and total dose. Condition F is a case of a gradual shear of approximately 180 degrees (Figure 21), and again this might be broken down into two major vectors; the lower half and the top half. Then we see that reflected in Figures 22, the isochrones of arrival time that are fairly symmetrical out to about 10 or 12 hours and after that the upper shear which goes down toward the south and makes itself apparent. In Figure 23 we have the dose rate and the total dose. Notice that on the right hand side there is quite a big lump out by itself in both cases. This is due partly to the wind shift at high levels going down towards the south. It is also the result, partly, of the lumpiness problem that we have in this model. In Figure 24 we have a summary of the dose rate and total dose areas for all of the conditions as well as for the observed CASTLE Bravo results and our predicted results. One interesting thing that should

SECRET

GRADUAL WIND SHEAR OF APPROXIMATELY 90°



CONDITION "B"
WEIGHTED TRAJECTORY

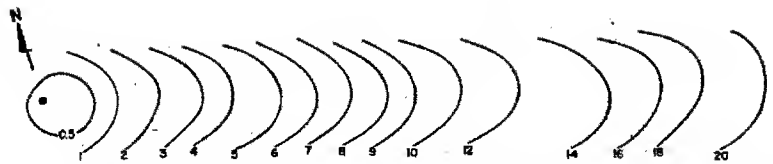
DOE ARCHIVES

Figure 7

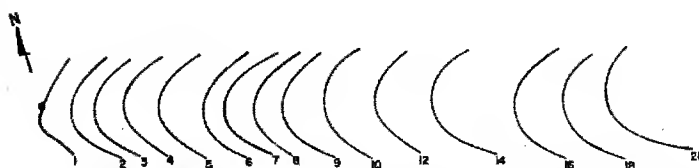
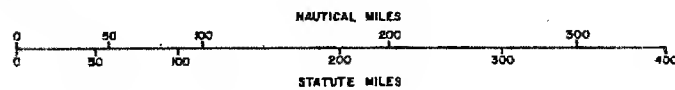
482

RESTRICTED
ENERGY ACT 1954

491 487



T_A , ARRIVAL TIME OF FIRST PARTICLE, HRS, PREDICTED USING WIND CONDITION "B"

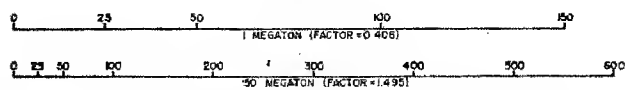
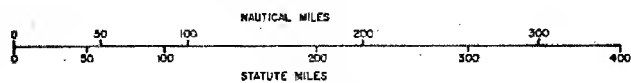


T_E , ENDING TIME OF LAST PARTICLE, HRS, PREDICTED USING WIND CONDITION "B"

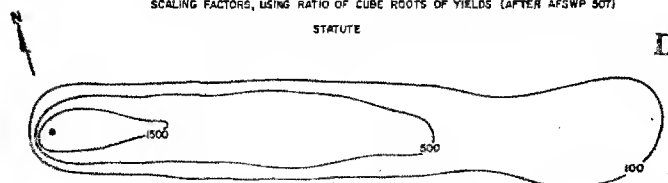
Figure 8



DR, DOSE RATE, R/HR.



SCALING FACTORS, USING RATIO OF CUBE ROOTS OF YIELDS (AFTER AFSWP 507)
STATUTE



TD, TOTAL DOSE IN ROENTGENS ACCUMULATED OVER 48 HOURS AFTER T_A
PREDICTED VALUES, 15 MT, USING WIND CONDITION "B"

Figure 9

483

DOE ARCHIVES

ATOMIC ENERGY ACT

488

SECRET

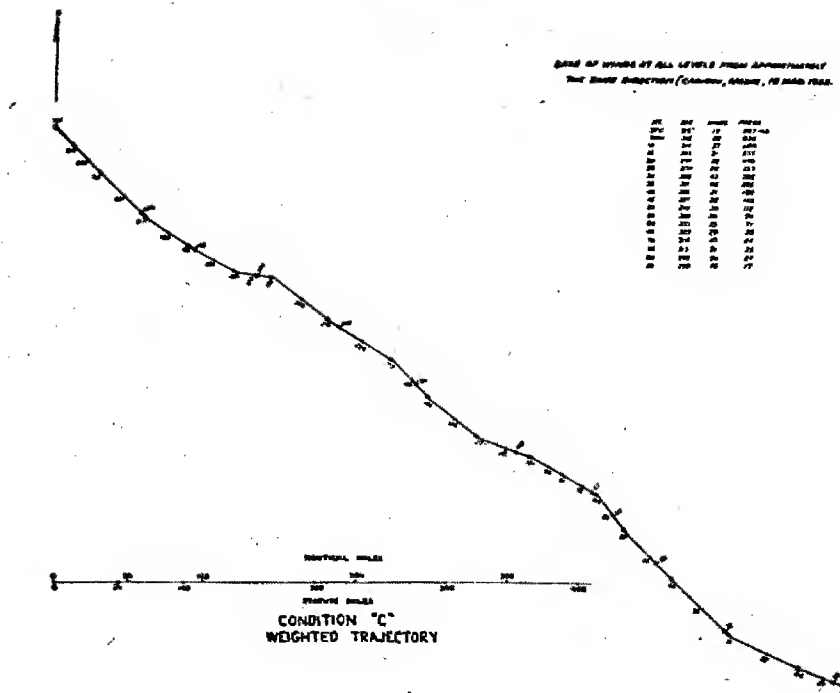


Figure 10

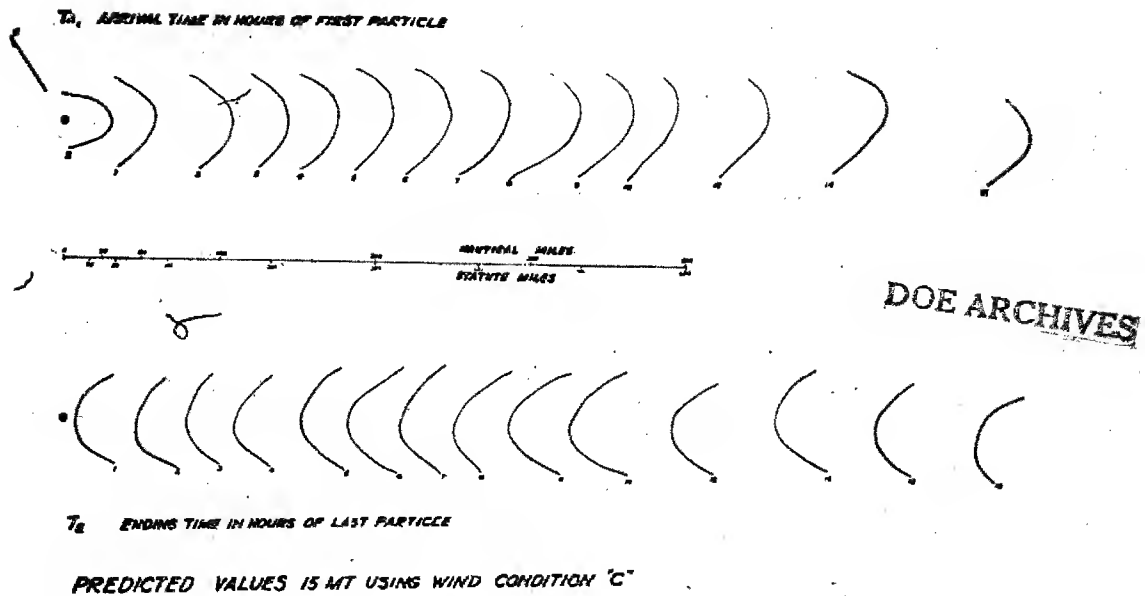


Figure 11

484

SECRET

489

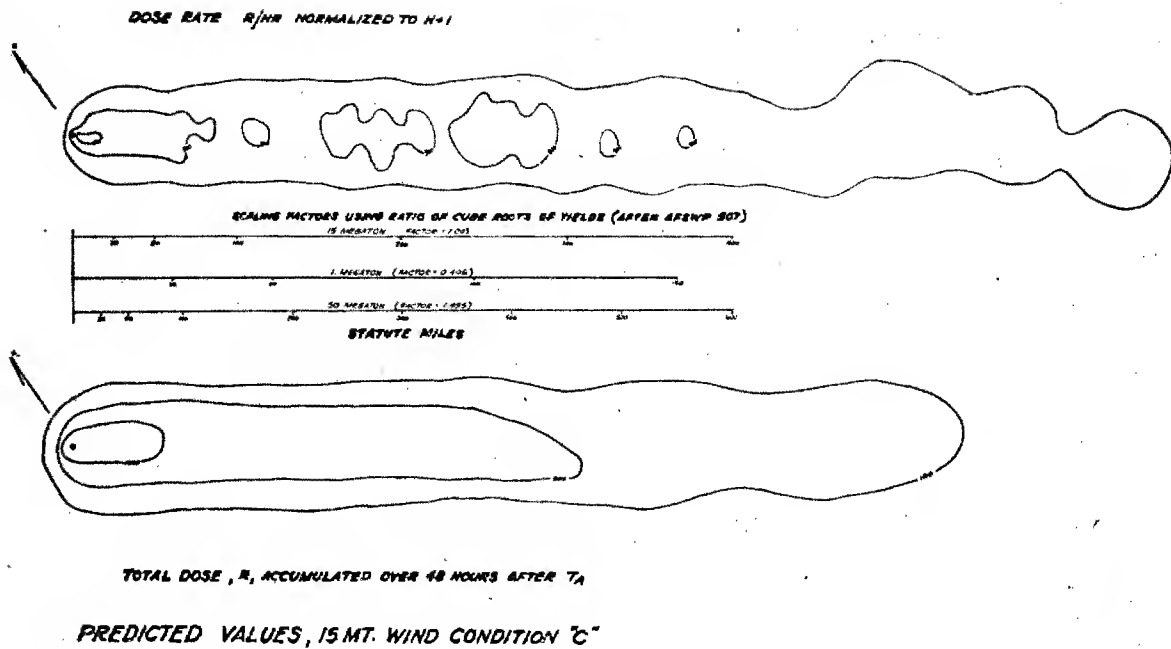
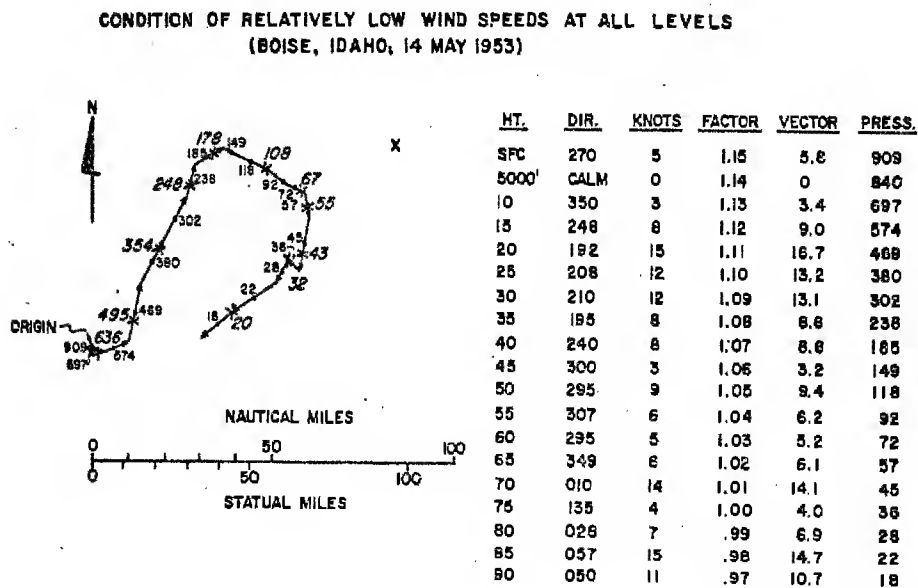


Figure 12



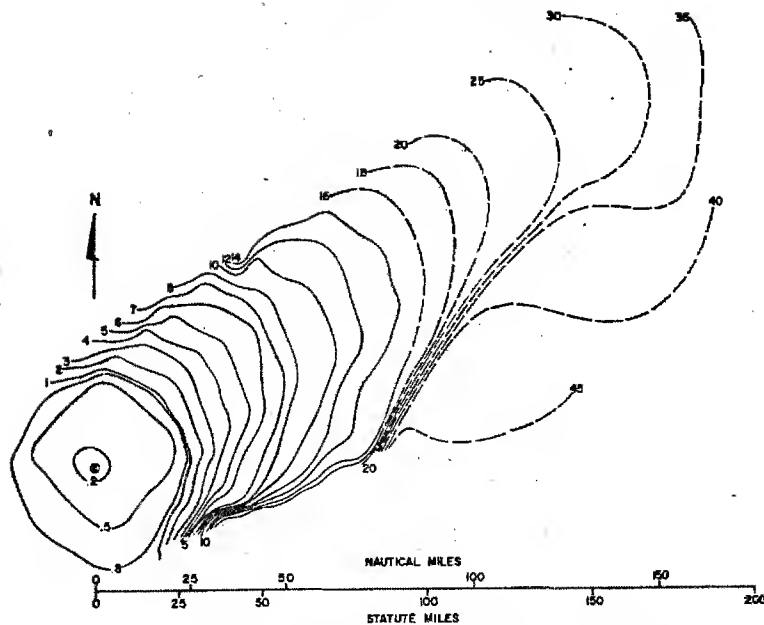
CONDITION "D"
WEIGHTED TRAJECTORY

DOE ARCHIVES

Figure 13

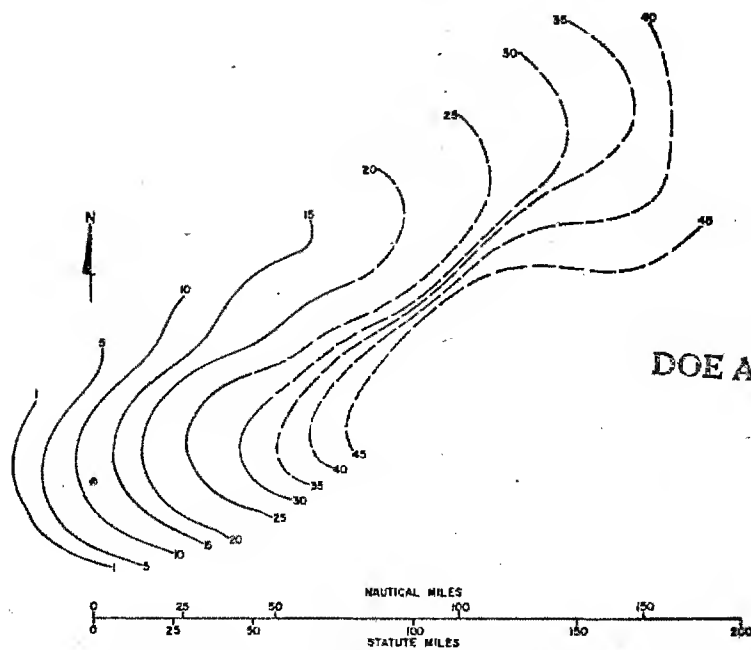
485

490



T_A , ARRIVAL TIME OF FIRST PARTICLE, IN HOURS, PREDICTED USING WIND CONDITION "D"

Figure 14



T_E , ENDING TIME OF LAST PARTICLE, IN HOURS, PREDICTED USING WIND CONDITION "D"

Figure 15

486

DOE ARCHIVES

RENEWABLE ENERGY ACT 1954

491

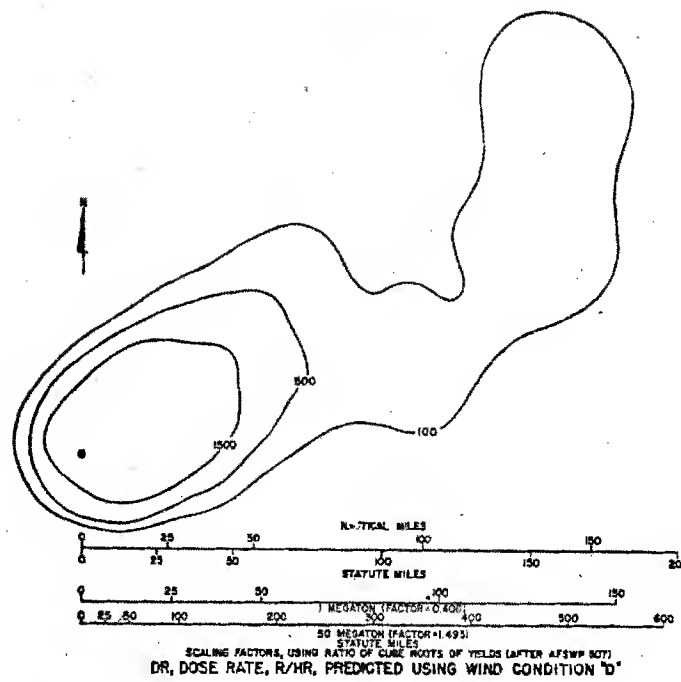


Figure 16

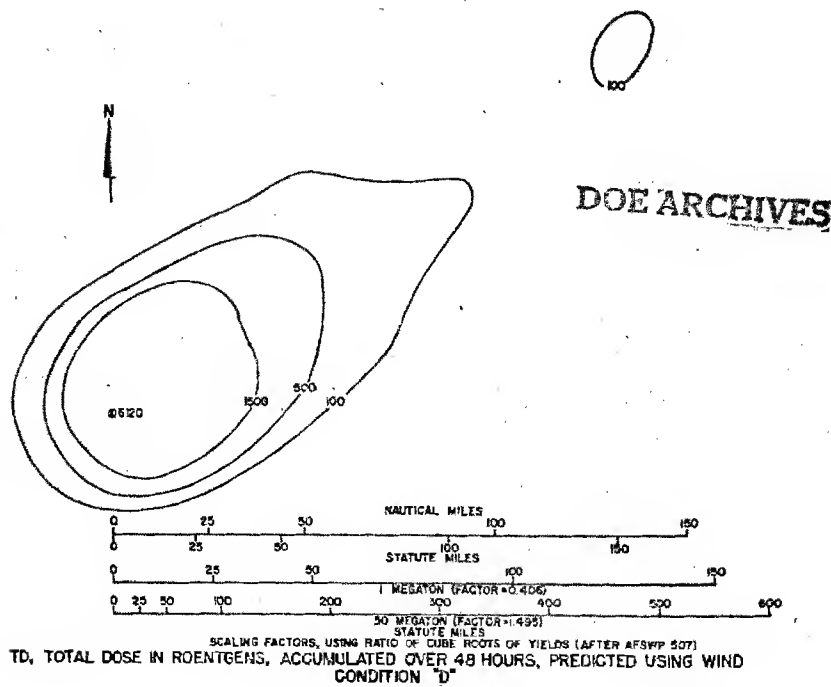
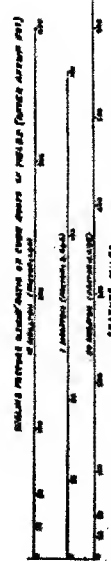
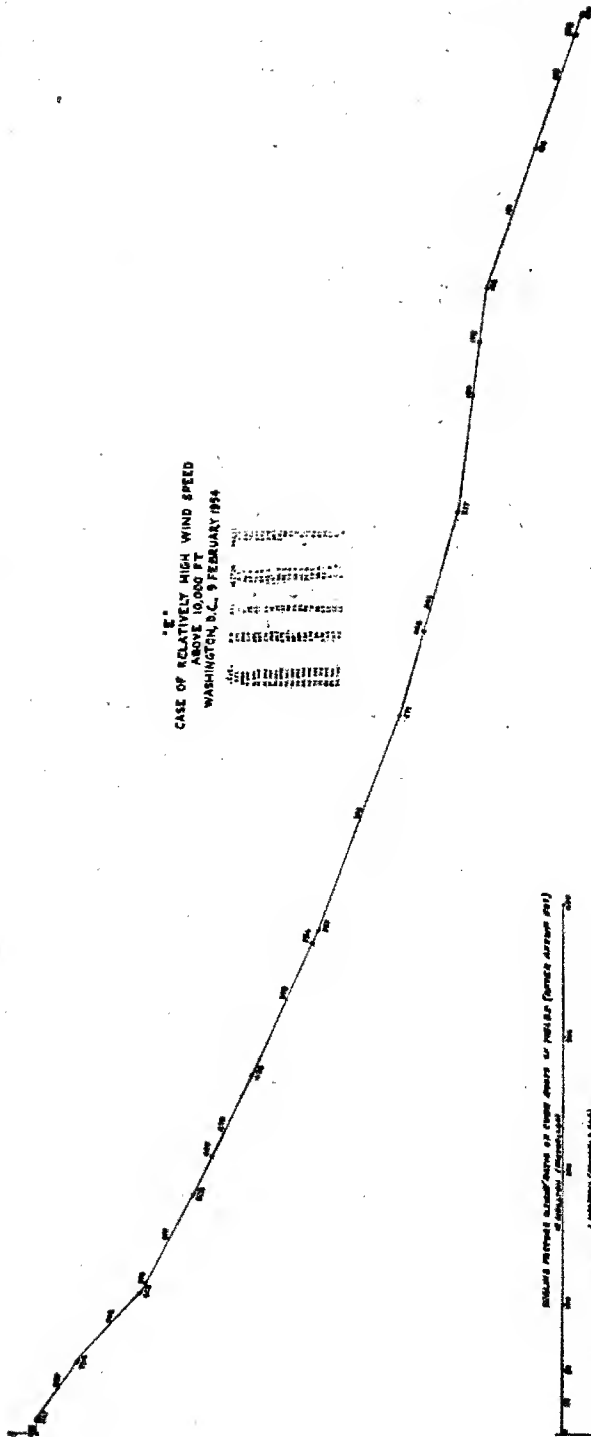


Figure 17

487

492

"E"
CASE OF RELATIVELY HIGH WIND SPEED
ABOVE 10,000 FT
WASHINGTON, D.C. 9 FEBRUARY 1994



WEIGHTED TRAJECTORY
CONDITION "E"

DOE ARCHIVES

Figure 18



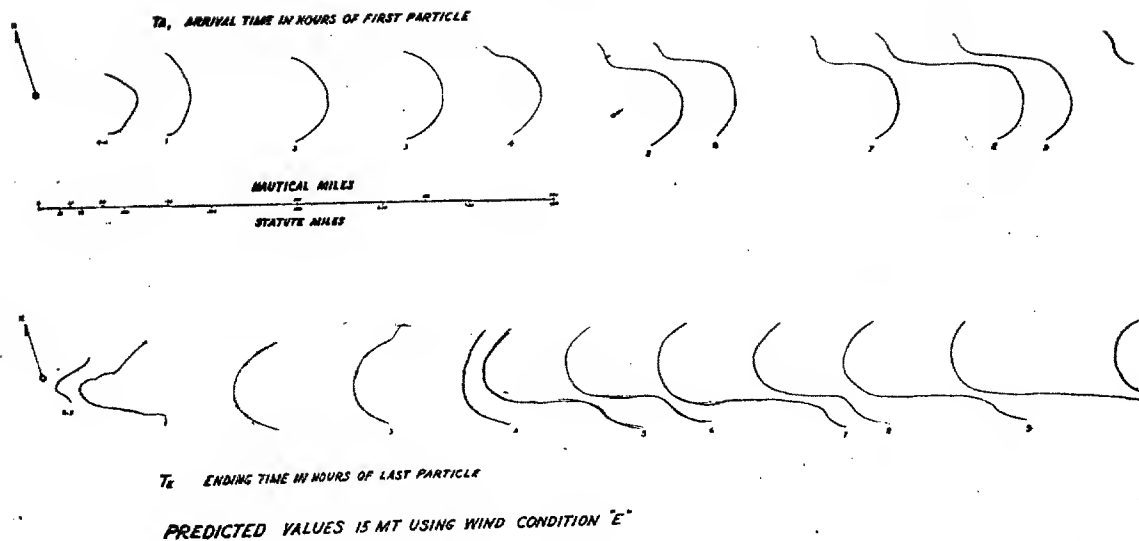


Figure 19

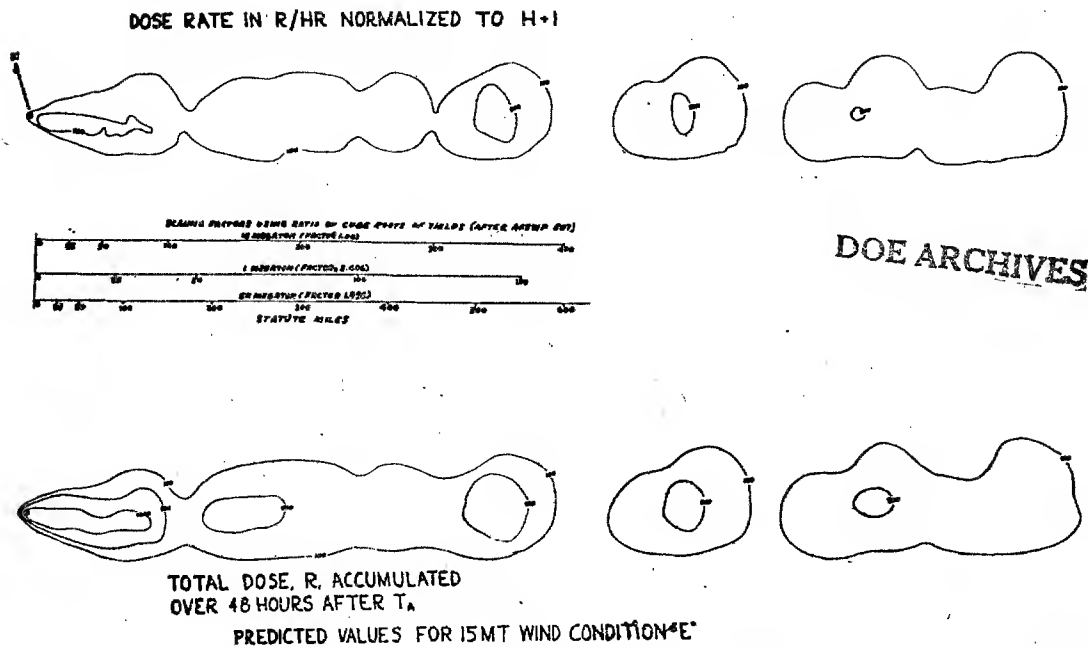


Figure 20

489

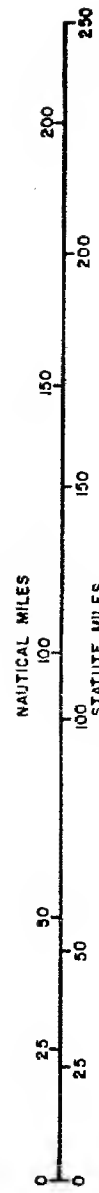
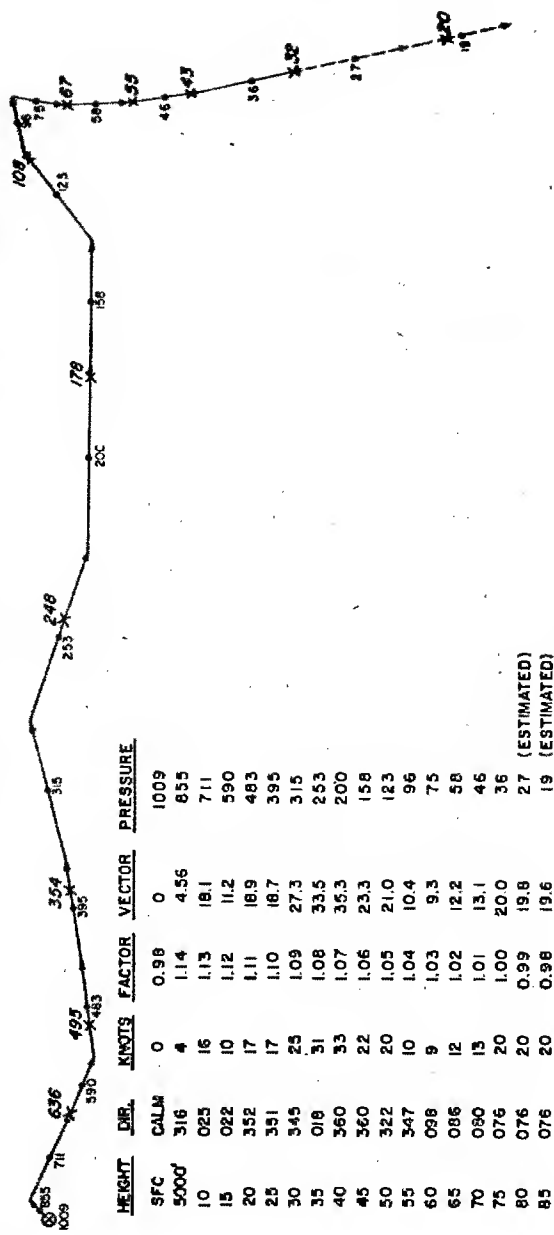
~~SECRET~~

~~ATOMIC ENERGY~~

494

490

GRADUAL SHEER OF APPROXIMATELY 180° (WASHINGTON DC, 8 JULY 1951)

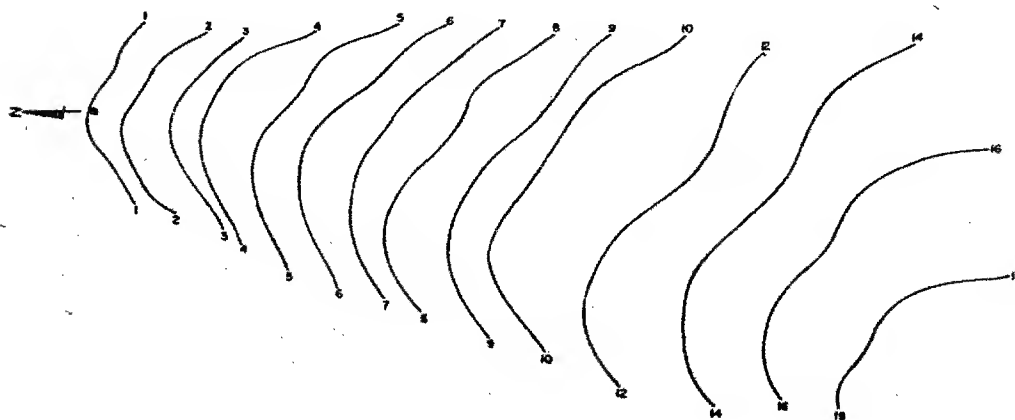
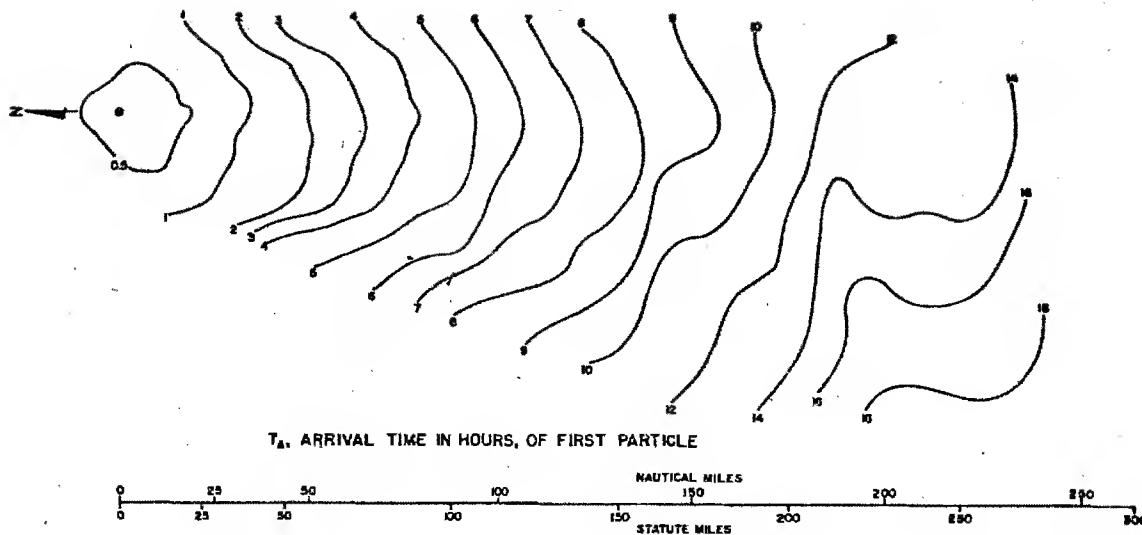


DOE ARCHIVES

CONDITION "F" WEIGHTED TRAJECTORY

Figure 21

495



T_E , ENDING TIME IN HOURS, OF LAST PARTICLE
 PREDICTED VALUES FOR 15 MT USING CONDITION "F"

DOE ARCHIVES

Figure 22
 491

DOE ENERGY ACT 1954

496

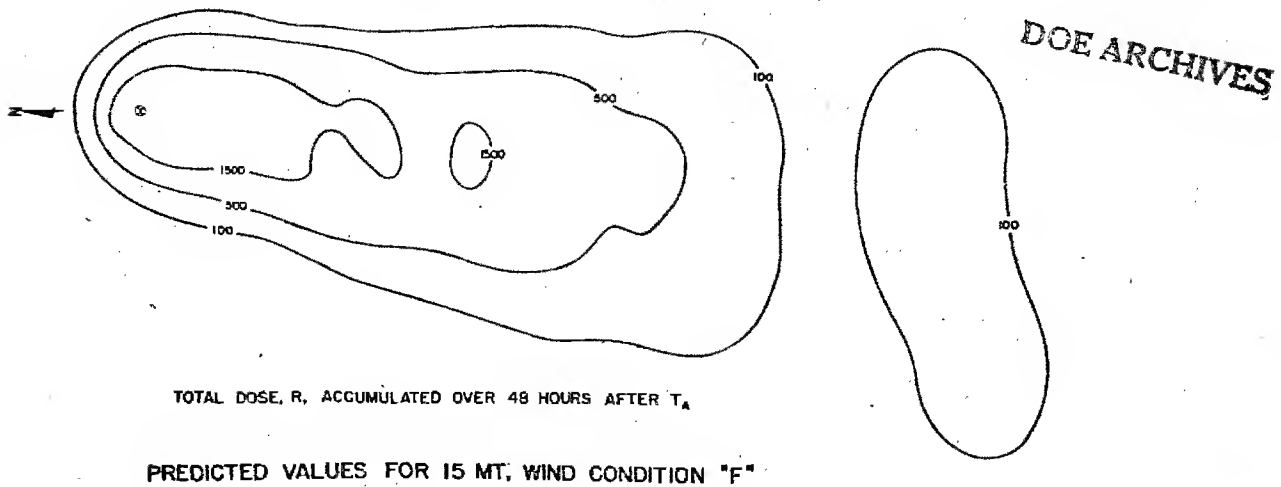
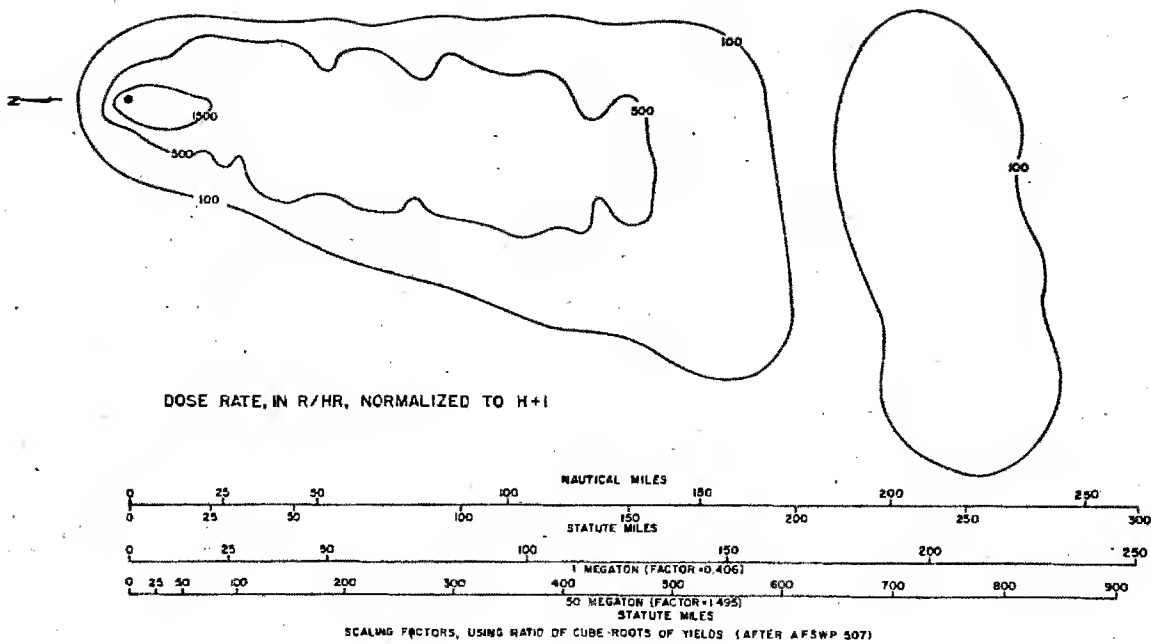


Figure 23

492

501 497

SUMMARY OF DOSE RATE AND TOTAL DOSE AREAS, 15 MT

Wind Condition and Method	Value of Dose Rate (DR) and Total Dose (TD)					
	100		500		1,500	
	DR	TD	DR	TD	DR	TD
Castle Bravo Observed Or Idealized Results. (Approx. Wind Surface To Base of Mushroom 19.4 mph)	13,240 sq mi	17,200	4,520	7,600	1,300	3,240
Castle Bravo Predicted Results, Using Composite Winds and Signal Corps Procedure	20,800	16,200	5,950	5,870	540	1,890
Predicted Results, Using The following Wind Conditions & Signal Corps Procedure:						
"A" Abrupt 90° Shear At 40,000 Ft. Wind 19.0)	35,000	23,000	9,000	10,600	250	1,440
"B" Gradual 90° Shear Wind 23 mph)	35,300	24,800	9,900	10,900	100	1,690
"C" Constant Wind Direction Wind 36 mph)	39,000	37,800	6,180	13,000	60	1,330
"D" Low Wind Speeds Wind 6 mph)	15,750	8,780	4,850	4,730	2,700	2,480
"E" High Wind Speeds Wind 94 mph)	46,600	50,800	2,400	7,860	None	1,240
"F" Gradual 180° Shear Wind 17 mph)	23,400	21,900	6,750	9,100	280	2,620

NOTE: Dose Rates Are In Roentgens Per Hour Normalized To $H \neq 1$
 Total Dose in Roentgens Accumulated Over forty-eight (48) hours After First
 Particle With No Biological Recovery Factor
 Areas Are In Square Statute Miles.

DOE ARCHIVES

Figure 24

493

ATOMIC ENERGY ACT

498

be noticed is that for very high wind speeds, the area enclosed by the 100 roentgen total dose line is much larger than in the low wind speeds. However, in very high wind speed cases the area enclosed by the higher roentgen values, such as 1500, are much smaller than those enclosed in the low wind speeds. I mentioned to you earlier that we had some suggestions for improving this forecast procedure and we have two. The first one is to get rid of the lumpiness by increasing the total number of discs in particle size categories. To make any significant correction in this direction is going to require a great deal more work. For example, in working up the example of this type, if we use a 15 mile grid for tallying the dose rate, it requires three or four hours for an example. If we use a smaller grid, such as the $3\frac{1}{2}$ mile grid which we employed for these examples, it requires from 15 to 20 man-hours. Now if we were to increase the disc and particle size categories, say ten times, it would increase our work ten times which is beginning to get unreasonable. The obvious answer to this is to apply it to machine methods which we hope to do. The second improvement we would like to make to our procedure applies to the case of the CASTLE Bravo where we made predicted values using the composite winds in that test. Our results would have been better if the area enclosed by the 1500 roentgen total dose lines had been better and larger relative to the area enclosed by the 100 roentgen total dose line. I believe that this is partially the result of the assumption we made in developing our total dose formula. This assumption was that between the arrival time of the first particle and the ending time, at any one point, the accumulation of particles is constantly timed. Now, this does not hold, and particularly near ground zero in the first few hours. I believe that our total dose values near ground zero would be significantly larger if we integrated instead of once, if we integrated several times, and particularly with each particle disc as it came down. Naturally this is going to be a great deal more work and again it implies the necessity for machine methods. One additional advantage that might come from a procedure like that is that we can use a different deterioration rate with time; that is, in the first few hours we might use a $t^{-0.8}$ or -1 , and later on, after 8 to 10 hours, we might use values $t^{-1.5}$ or something of that nature. In any case, we are attempting to do this and see if we can compute the CASTLE Bravo pattern by electronic calculating machines employing the improvements that I have just discussed. There are several obvious advantages to electronic calculations; first it is much faster and this allows one to compute a great many cases of fall-out patterns which are necessary if we are to determine realistic probabilities. For example, suppose we wanted to know what the probability was of a lethal dose occurring 50 miles west of a certain town. The only really reliable way to do that is to compute daily patterns for several years and then add up these patterns and see what the probabilities are of having the lethal

[REDACTED]

dose 50 miles to the west. At the present we can make some approximations to this by using statistical wind data but this can lead to misunderstandings, if not used very carefully. Another advantage of computing these faster is that it admits the possibility of very detailed forecasts for tactical purposes; that is, ones that can be made in perhaps an hour or two. A last advantage to electronic computations is that it will make it practical for us to consider more factors in our procedure. For example, we should take more accurate account of the time space variations of wind during fall-out. We should take more accurate account of the stability of the atmosphere, dispersion, the terrain effects, and perhaps even precipitation. All of these things will greatly complicate the calculations and would only be practical with electronic computations.

If we can look into the crystal ball for a few minutes here I would like to make some suggestions on something that might develop as a result of the electronic calculations. Suppose we develop a series of wiring panels, each of which contains a different model; another series which contains a number of particle size distributions. Once we have those and have tested them to the point where we feel they are reliable then it would be possible to get a prediction of the fall-out pattern for any yield bomb for a wide variety of soil types and for any part of the world. For example, the yield of the explosion and the atmospheric stability would indicate the model size, so that the appropriate wiring panel for that model size could be chosen. Likewise, if we knew the soil type, we could choose the particle size distribution for that soil type, we could choose the particle size distribution for that soil type and put that into the machine. Then our dose rate calibration factor, which you recall in our CASTLE Bravo prediction was 100, could be varied with the condition of the soil and the height of the explosion. That is, if the soil were frozen, there certainly would be much less soil sucked up in the explosion than if the soil were not frozen. Likewise, if the explosion were 500 or 1,000 feet above the surface, it probably would suck up much less dirt. The dose rate calibration factors take account of these things.

DOE ARCHIVES

One final point comes up and that is the question: Are we trying to do something that is more accurate than the data we are working with? I think perhaps we are. The data we have of the actual resulting fall-out patterns, some of the wind conditions, are not as accurate as we are trying to do. However, we can surely expect that this data will be more accurate in the future and ultimately we are going to need the most accurate prediction procedures possible. So I think we are justified in going ahead in trying to develop a fall-out prediction procedure as accurate as possible.

[REDACTED]

In closing I would like to say that I believe that we have a procedure that gives relatively good results and we have immediate prospects of some improvement. However, there are problems that need to be solved along with problems of this procedure. We need more information about soil types, particle size distribution, biological factors. We need more information about the winds to high levels. We need more accurate forecasts of winds. Last but not least, we need more observed data of fall-out patterns to thoroughly test forecast procedures.

DOE ARCHIVES

496

~~RESTRICTED~~
ATOMIC ENERGY ACT 1954

~~SECRET~~

501

[REDACTED]

COUNTERMEASURES; AN ANALYSIS OF NEW WEAPONS EFFECTS
INFORMATION REQUIRED FOR FALL-OUT COUNTERMEASURES

Paul C. Tompkins
U. S. Naval Radiological Defense Laboratory

A symposium on fall-out would not be complete if the need for information were not analyzed in the light of countermeasures needed to offset the effects. It is the purpose of this paper to consider that type of information which will lead to reliable countermeasures systems.

The general conclusions derivable qualitatively from an analysis of existing information may be summarized as follows:

Radioactively contaminated areas can be expected to be encountered with sufficient frequency and at sufficient gamma intensity levels to demand direct countermeasures.

Existing facilities and equipment are not adequate to provide the necessary protection.

Areas which can be affected are too large to permit use of evacuation or avoidance of a radiological area as the predominant control measure.

Protection of both personnel and installations from the initial and subsequent effects supersedes recovery as a primary objective. Alternatives to protection and recovery from the effects of the event decrease as areas affected increase.

The primary countermeasures system must be based on provision of sheltered living areas with shielding for protection against the gamma radiation, and recovery through pre-protection of an installation or its subsequent decontamination.

The objective of countermeasures studies is to arrive at a determination of the provisions that must be made to permit people to live through a contaminating event, and still perform essential functions. This implies that not only must one deal with the effects of radioactive contamination under emergency conditions, but one must also know how to live with radioactive contamination under long-term exposure conditions.

Let us now turn to a consideration of the essential elements of countermeasures systems. These elements are:

Reduction of gamma radiation intensities by shielding.

DOE ARCHIVES

TABLE 1
 Comparison of Fall-out vs Non-fall-out Conditions on Radiological Practice
 Peacetime (non-fall-out conditions)

Fall-out Area	
1. Environment Clean. Radioactive materials restricted to limited areas and/or conditions. Objective. Keep activity greater than background confined to sharply limited regions.	1. Environment Contaminated. Clean areas restricted to those protected in advance. Objective. Keep activity out of critical localities.
2. Shielding around the source.	2. Shielding around the person.
3. Control points at entry to confined area. Time in restricted area limited.	3. Control points at exit from confined area. Time in environment limited.
4. Contamination monitoring done under low and constant background conditions.	4. Contamination monitoring done under high and variable background conditions.
5. Food supply unlimited and generally not exposed to contamination.	5. Food supply sharply limited and generally exposed to contamination.
6. Clean water supply not limited.	6. Clean water supply very limited.
7. Material control requirements increase with increasing specific activity and total activity.	7. Personnel contamination protective measures increase with increasing specific activity and total activity.
8. Requirement for exposure limited to few people under good administrative control.	8. Requirement for exposure affects many people not under administrative control.
9. Assume things in contaminated area are affected until proved clean.	9. Same.
10. Acceptable dosage/unit time decreases with increasing frequency and duration of exposure.	10. Same.

DOE ARCHIVES

[REDACTED]

Reduction of gamma radiation fields caused by loose radioactive weapon debris by removal of such debris. This includes both post event reclamation methods and protective measures such as the "washdown" system employed by the Navy.

Reduction of ingestion, inhalation, and beta radiation burn hazards by the use of proper doctrines, clothing, respirators and effective decontamination.

Reduction of dosage by control of exposure time. This requires an intimate knowledge of time and motion involved on the part of personnel, and an equally intimate knowledge of the radiation intensity and radiological conditions under which these personnel must operate.

Exclusion of contaminated material from critical areas such as those designed for occupancy, food and water sources, etc.

The first requirement of countermeasures is to provide enough protection to permit survival during the acute phase immediately following a detonation. This must be done primarily through an adequate shelter program. Such shelters must provide a shielding factor of the order of 1000, if military forces are to retain the capability of operating despite the presence of fall-out.

DOE ARCHIVES

The second requirement is to establish the capability of recovering and occupying the affected regions as normally as possible. To do this it is necessary that "living areas" be designated. These areas must have maximum shielding available and provisions for excluding the entry of radioactively contaminated material. This requirement must be met if dosage control is to be possible. It is from these centers that personnel would then emerge into the surrounding contaminated area to discharge their assigned duties. The decontamination of "work areas" will be a requirement in many cases. The provision of clean food and water supplies will be the predominant practical problem encountered in this phase. The acceptance of a single, sub-lethal acute dose as the criterion of acceptable dosage is not sound practice. It is required that a new set of medical standards be developed to cover continued exposures at various rates, comparable to the 30 roentgens per two years which is the current standard for peacetime operations permitted by the Navy. Criteria for properly prorating the revised acceptance doses are needed.

Unlike industrial practices, fall-out influences the environment. Although this fact does not affect the currently practiced principles of radiological procedure, there are drastic practical influences on the conditions to which these principles are applied. Table I illustrates some of the more obvious differences brought about by the radiological effect on environmental conditions. Notice that only items 9 and 10 stay the same under the two situations.

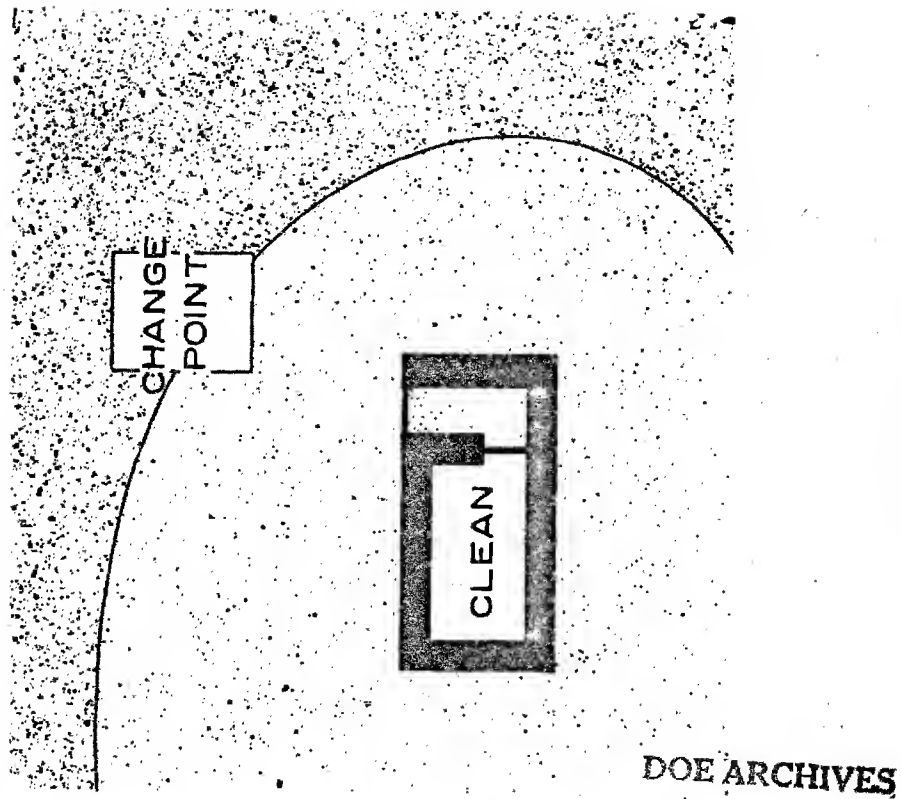


Figure 2
Contamination Pattern

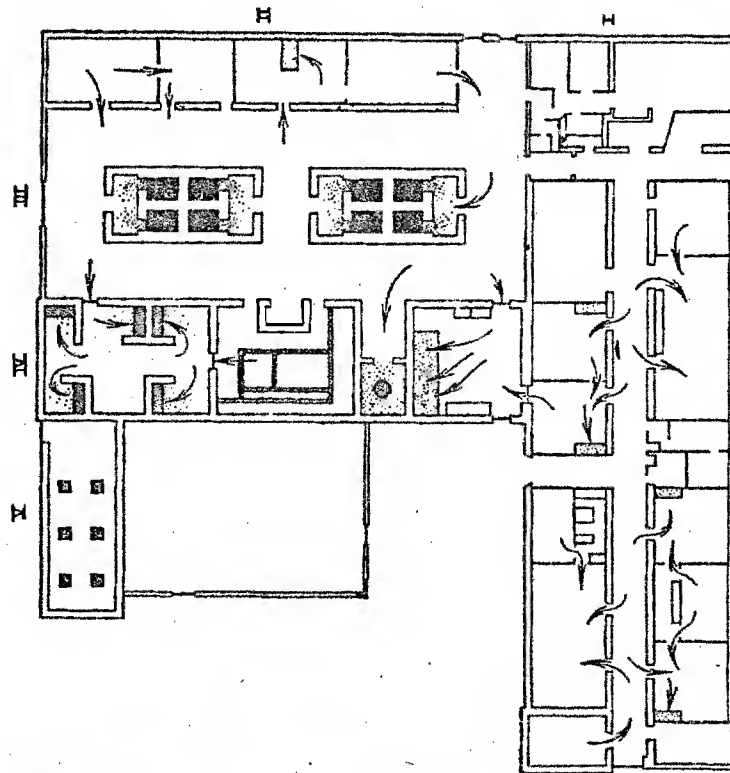


Figure 1
Floor Plan

~~RESTRICTED~~
ENERGY ACT 1954

500

505

These differences are further illustrated by Figures 1 and 2. Note particularly the relationships between areas and contamination density. Figure 1 shows the lay-out of a building designed to conduct research work with multicurie quantities of radioactive materials. The highest activity area marked by the heavy stippling is the interior of the cells which are surrounded with 3-foot concrete walls for shielding, maze entrances to further reduce radiation levels when the cell doors are open, doors to confine activity to the interior, and air flow (shown by the arrows) for regions of low contamination to those of higher contamination. In Figure 2, the principles employed are identical, but the pressure is in the opposite direction. The situation in Figure 2 is that which one encounters when one is required first to survive and subsequently live with the effects of a major fall-out event without evacuation. The same principles of ventilation control would lead to positive pressure ventilation in the shelter.

Three types of protection are required: from whole-body gamma radiation; from skin burns arising predominately through direct contamination of the person; and internal deposition of radionuclides from all methods of entry into the body.

For gamma exposure, DOE AR
 Not over 500 r accumulated over 5 years,
 Not over 200 r in any one year,
 Not over 20 r in any event under maximum protection.

For beta exposure,
 Not over 5,000 rep in 5 years,
 Not over 2,000 rep in any one year,
 Not over 200 rep in any single exposure.

TABLE II (a)

Reference Contours Related to Delivery of 1000 Rep
or 10,000 Rep in One Week

Time After Burst of Start of Initial Exposure	Reference Contour (b) Leading to 1000 rep in 1 week (r/hr at 1 hr)	Reference Contour Leading to 10,000 rep in 1 week (r/hr at 1 hr)
1 hr	7.8	78
1 wk	107	1,070
1 mo	455	4,550
1 yr	7,500	75,000

(a) Calculations by Broido, A., and Teresi, J.

(b) The calculations assume the applicability of the $t^{-1.2}$ decay law, and uniform contamination over the whole body. Whole-body beta exposure LD_{50} assumed to be about 5000 rep. The 10,000 rep column applies to small particles only.

DOE ARCHIVES

For internal deposition,

The accumulation of $5 \mu\text{C Sr}^{89-90}$ as the body burden should be considered the absolute upper limit.

It must be stressed that these criteria have a limited biological safety factor and those personnel getting the maximum of any one of these might be expected to show a high incidence of delayed effects. Further, a quantitative basis for reduction in allowable whole-body exposure in the presence of radionuclides deposited in the bone is not available.

The problem of controlling gamma exposure has been dealt with many times. Suffice it to say that exposure time control is the essential ingredient and that design appears to call for a shielding factor of the order of 1000 or more.

The probable scope of the beta burn problem is shown in Table II. Here one sees an estimate of the reference contour lines expressed in r/hr at 1 hr which would be expected to give 1000 rep and 10,000 rep in one week. The selection of these two levels was based on the assumptions that:

The burns would come largely from weapon debris in direct contact with the skin.

No immediate burn would be developed with less than 1000 rep.

A local burn would be certain above 10,000 rep from a small particle (point source). The current effects table (AFSWP) states that incapacitation will occur in 3 to 6 hours from 3000 to 5000 rep over a relatively small area (a few square centimeters) of the body.

Health habits will insure that no contamination stays in one particular locality on the body for more than 1 week.

No subsequent contaminating material will expose exactly the same area of the skin by depositing in exactly the same place.

Note that the reference value shifts upward as the initial time of exposure increases from T_0 .

DOE ARCHIVES

The internal deposition problem can be assessed from the Sunshine project which reached the conclusion that the Sr^{90} tolerance level in soil would be reached at about the 120 r/hr at 1 hour reference line. During the first 18 months, the activity of Ba^{140} - La^{140} and Sr^{89} is about 10 times this amount or more. Allowing for build-up from detonations occurring over a period of time and the possible addition of inhalation as a source of internal deposition, reference contour of 1 r/hr at 1 hour can be taken as defining the point at which one must start becoming concerned.

[REDACTED]

The general character of the applicable countermeasures systems as related to the reference contour lines from a single detonation are summarized in Table III.

Summary of Effects Data Needed to Guide Countermeasures Development

Biological:

Maximum "acceptable" dosages prorated over 5 years. Particular attention should be paid to late biological effects occurring between 5-10 years.

Medical Effects Table for skin effects as functions of time and area. Particular emphasis should be paid to burns from small "hot" particles.

Instruments:

Contamination meters for clothing, water, air, food, etc. must be able to cancel out surrounding radiation field between ~ 0.1 mr/hr to 1 r/hr.

Dosimetry should distinguish between deep dose and surface dose.

Calibrations with a point source appear to be inadequate. Calibrations should reflect the distributed geometry which is actually encountered.

Characteristics of radionuclides:

Beta energy and amount as function of time up to 2 years.

Gamma energy and amount as function of time up to 2 years.

Fission Yields.

Solubility in the range of 10^{-3} to 10^{-6} .

Exchange properties with soil and other surfaces, particularly Sr and Pu.

Uptake of radioelements into growing foods.

DOE ARCHIVES

Radiation Fields characteristics:

Radiation fields from contamination distribution other than the infinite flat plane. Knowledge of important variations in either the spectrum or air ionization are needed.

A "simulated" or "synthetic" gamma spectrum as a function of time is needed for both dosimetry and shielding development work.

Typical radiation fields from basic geometric models should be developed schematically so that actual situations can be analyzed by a summation of parts.

Shielding:

Basic types of construction geometry should be schematized.

Build-up factors should be measured for energies of about 0.4 Mev, 0.7 Mev, and 1.5 to 2.0 Mev.

Build-up factors should be based on data for slab, edge, and corner orientations.

Fall-out:

Mathematical model should cover region to the 1 r/hr at 1 hr. reference contour line.

Meteorological conditions leading to deposition of "hot" spots in lower activity areas should be identified possibly through refinement of the model. Probable number and size but not location should be statistically predictable.

Chemical composition of the weapon debris is extremely important in relation to contamination density and solubility.

Countermeasures:

Reduction in the radive field without shielding by removal of the weapon debris should aim at 90 to 99 per cent reduction.

Water treatment should aim at a reduction of $\sim 10^3$ in total activity and $\sim 10^3$ for Sr.

Contaminability of clothing and skin from the environment must be quantitated at least roughly.

DOE ARCHIVES

TABLE III
Comparison of Countermeasures Requirements as Related to Initial Contamination Level

Reference Contour Line	Ingestion	Surface Burn	Whole-body Gamma
Less than 1 r/hr at 1 hr	No severe problems. Good hygiene required. Radioactive decay will prevent serious consequences.	No severe problems. Good hygiene required. Radioactive decay will prevent serious consequences.	No severe problems. Good hygiene required. Radioactive decay will prevent serious consequences. Probable total body dose less than 20 r for the total event.
1 r/hr at 1 hr to 10 r/hr at 1 hr	Upper limit controllable by procedural methods alone. Availability of clean water essential. Fresh vegetables grown and consumed within the 6 mo. period following fall-out may cause some trouble. Methods for assessing level of contamination in food and water predominant requirement.	Probably no problem if reasonable precautions against unnecessary exposure are observed. Upper limit for reasonably normal behavior.	Protection at a factor of 2 to 10 required. Can still operate uninhibited at a total dosage of less than 100 r for the whole event.
10 r/hr at 1 hr to 100 r/hr at 1 hr hr (Approaching Rongelap region)	Intermediate level of protection. Food & water definitely affected, but area may be recoverable by biological scavenging plus decay within ~ 1 year.	Protective covering and controlled procedures should be employed. Burns will definitely develop in a few people unless good hygiene and precautions are used.	Upper limit is approaching the LD ₅₀ unless shielding or evacuation can cut the dose by at least a factor of 5 to 10.

DOE ARCHIVES

TABLE III (continued)
Comparison of Countermeasures Requirements as Related to Initial Contamination Level

Reference Contour Line	Ingestion	Surface Burn	Whole-body Gamma
More than 100 r/hr at 1 hr. (a)	Protection of food and wa- ter supplies essential. Hy- droponics best technique for growing new crops. Soil scavenging essential if agriculture is to be resumed within 5 years.	Full protective covering essential. Buffer zones between contaminated areas and living areas must be in- troduced. Contamination control is predominant problem.	Minimal shielding of 10 to 100 required on lower side. Between 100 to 1000 required for higher contours. Operations must be planned on basis of limited ex- posure in unshielded condition.

(a) Since contours of ~ 10,000 r/hr at 1 hr can be encountered, this region covers approximately a factor of 100 in severity. Doses as high as 50,000 r can be received and beta burns can be initiated with contact times of minutes.

(b) Rongelap region is probably between the 100 r/hr at 1 hour and the 200 r/hr at 1 hour reference line.

507

DOE ARCHIVES

ATOMIC ENERGY

512

[REDACTED]

THIS PAGE IS BLANK

DOE ARCHIVES

508

[REDACTED]

[REDACTED]

ENERGY ACT 1954

513

PREDICTION OF DOSE RATE AND DOSAGE CONTOURS AS FUNCTIONS
OF YIELD AND METEOROLOGICAL CONDITIONS; COMPARISON OF
PROBLEM SOLUTIONS

CDR Roger W Paine, Jr., USN
Headquarters, Armed Forces Special Weapons Project

Early in the planning phase of the fall-out symposium, it was decided that a ready means of comparing the various methods of generating fall-out contours would be a desirable addition to the symposium summary report, and to the symposium itself if such a means of comparison could be made ready in time. In the last analysis, the contours generated by a model for a specific weapon yield and for a specific weather situation probably form the best means of comparison with other models. Accordingly, speakers who had consented to present their methods at the symposium under Topic F were sent six actual weather soundings taken at various localities in the United States in recent years and asked, time permitting, to work out a series of contour solutions for two or more of these weather situations. In order to make a distinct break with the CASTLE BRAVO event, against which most of the methods had already been calibrated, yields of 1 MT and 50 MT were chosen. The participants were asked to generate by their methods for surface bursts of each of these yields, contours of 100, 500, and 1500 r/hr referred back to H-1 hour, and contours of 100, 500, and 1500 r total dose accumulated up to 48 hours after burst time.

DOE ARCHIVES

This "homework", as the participants chose to call it, represents a considerable amount of hard work by the agencies involved, some of whose methods are not easily adaptable to generate the particular contours asked for. It is therefore very gratifying that complete problem solutions by each method were turned in for one of the weather situations, and at least partial solutions by each method for a second. Particular thanks are due the Army Signal Corps, the Air Weather Service, and Technical Operations Incorporated for completing work on all six weather situations.

Owing to the great volume of material involved, only problem solutions for the two situations for which almost complete returns are available will be compared in detail in this report. Solutions for these situations are sufficient to point out the

[REDACTED]

more important conclusions which can be drawn from the comparisons, which are:

For situations which do not involve abrupt wind shears, the contours generated by the several methods, although differing in detail, do not differ greatly in the direction of fall-out nor in the order of magnitude of the area covered.

Because of the basically different assumptions as to the location of radioactive materials in the stabilized cloud, the presence of an abrupt wind shear between 15,000 and 50,000 feet is apt to cause considerable differences in the predicted direction of fall-out for certain contours, although predictions of the magnitudes of the areas covered do not differ greatly.

None of the methods predict very high intensity dose or dose rate contours, even for the hypothetical 50 MT yield. A maximum dose rate of the order of 10,000 r/hr or less at H+1 hour appears to be indicated, and this is likely to occur only in a very small area at or near surface zero.

In comparing the problem solutions, it is well to keep in mind the basic assumptions and limitations of the methods being compared. Some of these account directly for the differences observed. Examples are:

AFSWP Method

This method is based on ground surveys at JANGLE-S and CASTLE BRAVO, and consists of "idealized" contours, which follow a single scaling wind direction. Abrupt wind shears and unusual weather conditions are not easily handled. The method is suitable for planning purposes only; not for post-shot analysis. An order-of-magnitude contour can be drawn for any weapon yield between 0.1 KT and 100 MT in two or three minutes by untrained personnel.

ARDC Method

DOE ARCHIVES

The model assumes that 90% of the bomb debris activity is in the stem of the stabilized cloud, and 10% is in the mushroom. Mean effective particle sizes are assumed for the cloud and parts of the stem, and Stokes Law fall rates for spherical particles are used. Wind and weather conditions are allowed for. The method is calibrated to CASTLE BRAVO, but is adaptable over a wide range of yields. A problem solution requires several hours by trained personnel.

Army Signal Corps Method

The model divides a hypothetical stabilized bomb cloud consisting of super-posed cylinders into disc or cylindrical wafers or compartments, each associated with a particular particle size category and fall rate. Each disc is then brought to the ground according to the winds acting on it, and ground values are then summed over all the discs to obtain contours. A different model must be generated for each weapon yield, and for different localities (tropical, polar, etc). Wind and weather conditions are allowed for. A particle size distribution hypothesized by the Rand Corporation is used. Aerodynamic particle fall rates are used. The method is calibrated to the AFSWP-507 reported survey of CASTLE BRAVO. Because of the finite number of discs in the model, contours are often lumpy and may involve artifact "hot spots". A problem solution requires several hours by trained personnel. (The dose contours presented are for 48 hours after arrival time, rather than for H+48 hours).

Air Weather Service Method

The method is essentially a radex plot resulting in rough sectors within which fall-out may be expected, together with estimated times of arrival along vectors from ground zero for particular altitudes from which it is assumed particles start their fall. The method does not generate contours, and thus is not directly comparable to methods that do. The plot can be drawn in about 15 minutes by trained personnel.

Los Alamos Method

The method was devised for use during CASTLE in forecasting the gross results to be expected from surface bursts of about 10 MT fired in the northern Marshalls. The plots submitted are modified only by direct yield dependence. The effect of yield on initial cloud geometry is not included, nor is the effect of the different tropopause height of the middle latitudes from that in the Marshalls. The method gives very little detail anywhere and none at all near the origin. It is not intended for use in detailed post-shot analyses, but rather for radSAFE planning. A problem solution probably requires about an hour for an individual familiar with the method.

Navy Method

DOE ARCHIVES

This method, which is based largely upon a radex wind plot, is a system of weighting incremental square areas according to the degree of fall-out expected, relative one to another. It results in wind-sensitive contours which have only relative values. Actual values may be fitted to the contours as a result of one or more post-shot survey

~~SECRET~~

readings taken in the contaminated area. For purposes of this comparison, the contours submitted have been roughly normalized in area to the corresponding contours of another method or methods (e.g., LASL) in order to show agreement in shape. A problem solution requires something more than an hour for personnel familiar with the method.

NRDL Method

This is a wind and weather dependent system which assumes the bulk of the radioactive material originates in the lower portion of the mushroom, and utilizes an aerodynamic particle fall rate which varies considerably with the altitude of the particle. A problem solution requires several hours by personnel familiar with the method.

Rand Corporation Method

The method gives wind and weather-sensitive contours, based on an assumed particle size distribution and the hypothesis that 90% of the fission product radioactivity falls out from the mushroom cloud and 10% from the stem. An aerodynamic rate of fall is used which is somewhat different from that used by NRDL, but which also varies markedly with altitude. A problem solution requires a great amount of hand calculation. The method has also been programmed for machine solution, and the machine method was used for the solutions presented here.

Technical Operations, Incorporated, Method

The method utilizes an inverted cone cloud model, the NRDL assumption of particle size distribution, and fall rates which increase with increase in altitude.

~~DELETED~~

A problem solution requires somewhat more than an hour, utilizing trained personnel.

DOE ARCHIVES

The problem situations presented for comparative solutions were as follows:

CONDITION "A"

Wintertime situation of an abrupt, approximately 90° shear at a height of approximately 40,000 feet.

Dodge City, Kansas

1500 GMT 28 Dec 1953

37° 46' N, 99° 58' W.

Elevation: 2625 feet

Height ft, msl	Wind Direc- tion Degrees	Wind Speed Knots	Pressure Millibars	Temperature Degrees C	Relative Humidity -%
Surface	260	7	925	-7.4	84
5,000	247	12	842	-3.0	36
10,000	273	19	695	-8.7	30
15,000	307	13	570	-13.2	MB
20,000	008	16	463	-24.0	
25,000	045	41	373	-34.2	
30,000	036	52	300	-45.5	
35,000	357	29	238	-53.5	
40,000	243	47	187	-55.5	
45,000	255	43	148	-58.0	
50,000	255	55	115	-60.2	
55,000	260	47	90	-60.6	
60,000	272	54	71	-61.0	
65,000	289	40	55	-58.8	
70,000	285	36	43	-59.3	
75,000	285	38	34	-56.5	
80,000	285	45	27	-56.0	

DOE ARCHIVES

CONDITION "B"

Gradual Shear of Approximately 90°

Washington, D. C. (Silver Hill)

0300 GMT 28 Sept 1952

38° 50' N, 76° 57' W.

Elevation: 289 feet

Height Ft, msl	Wind Direc- tion Degrees	Wind Speed Knots	Pressure Millibars	Temperature Degrees C	Relative Humidity-%
Surface	Calm	0	1010	9.7	85
5,000	358	11	853	11.8	16
10,000	009	20	708	5.8	39
15,000	325	11	688	-0.2	MB
20,000	282	19	485	-10.9	
25,000	263	34	394	-21.4	
30,000	263	47	320	-34.0	
35,000	273	37	255	-44.0	
40,000	308	27	203	-51.5	
45,000	292	23	160	-60.2	
50,000	290	28	123	-66.5	
55,000	290	20	97	-65.4	
60,000	268	11	76	-64.0	
65,000	276	21	58	-61.5	
70,000	293	7	46	-59.0	
75,000	293	8	36	-55.5	
80,000	285	10	28	-54.3	
85,000	250	11	23	-52.0	

The salient features to note about Condition "A" are that the winds are generally from the west, except for a band between 15,000 and 35,000 feet, wherein the winds are from the north and the north-east. The mean wind is about 40 knots.

DOE ARCHIVES

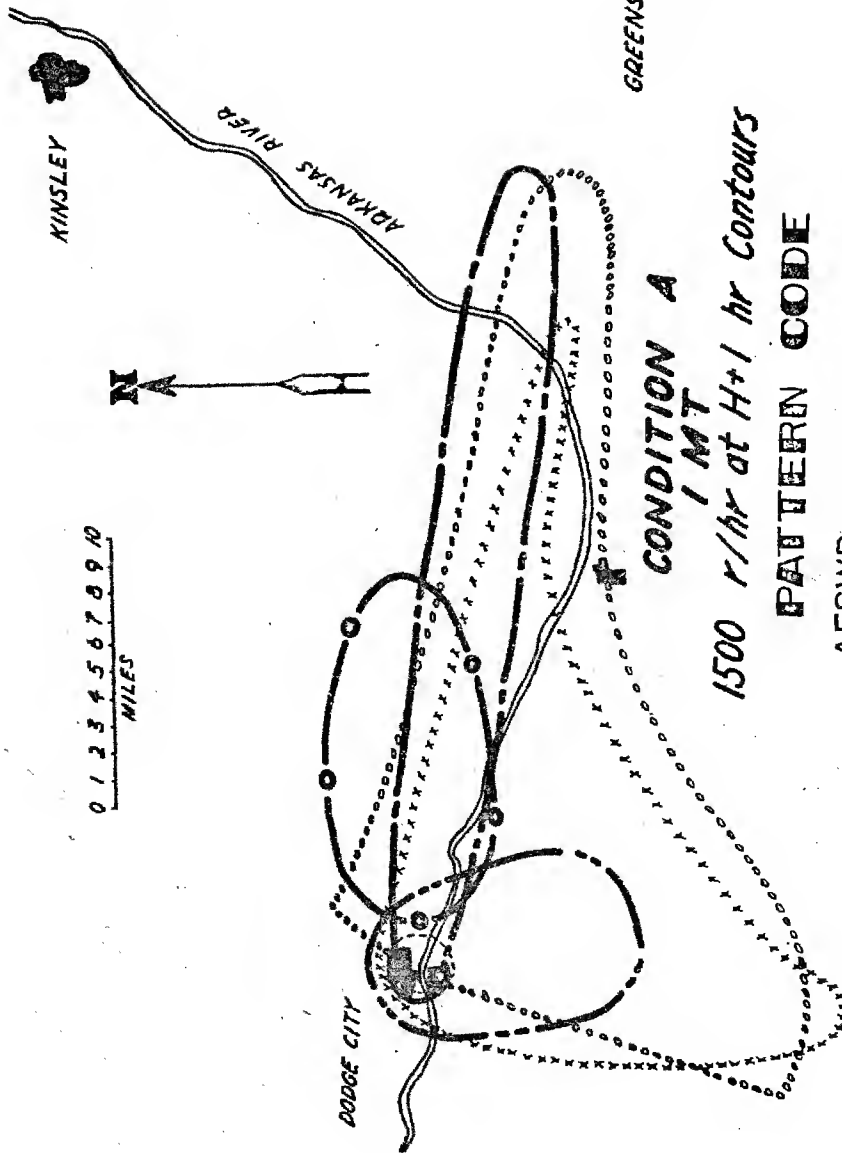
For Condition "B", the winds are again generally from the west, except for the region between the surface and about 15,000 feet, within which the winds are northerly. The mean wind is about 20 knots.

The problem solutions are compared by superposition on the charts which follow, using coded overlays as indicated on each chart. Missing solutions either had not been received in Headquarters, AFSWP, at time of press make-up (1 February 1955), or the material received was not readily adaptable for comparison. Tables giving numerical comparisons of contour areas and downwind and crosswind extents follow the charts.

514

RE
ENERGY ACT 1954

519



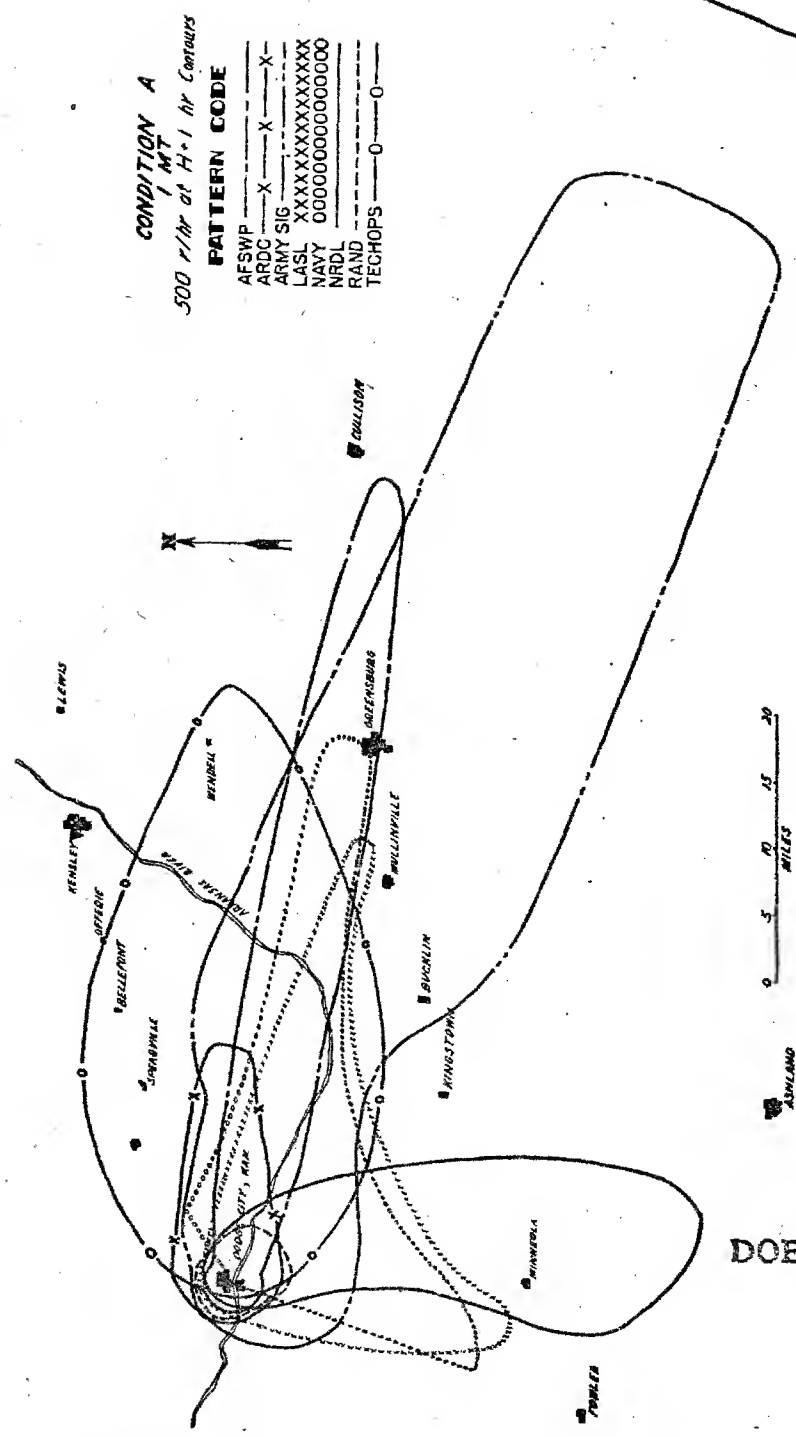
CONDITION A
1 MT
 1500 r/hr at H+1 hr Contours

PATTERN CODE

AFSWP	---	---	---
ARDC	---	X---	X---
ARMY SIG	---	---	---
LASL	XXXXXX	XXXXXX	XXXXXX
NAVY	000000	000000	000000
NRDL	---	---	---
RAND	---	---	---
TECHOPS	---	0---	0---

DOE ARCHIVES

ATOMIC ENERGY ACT 1954

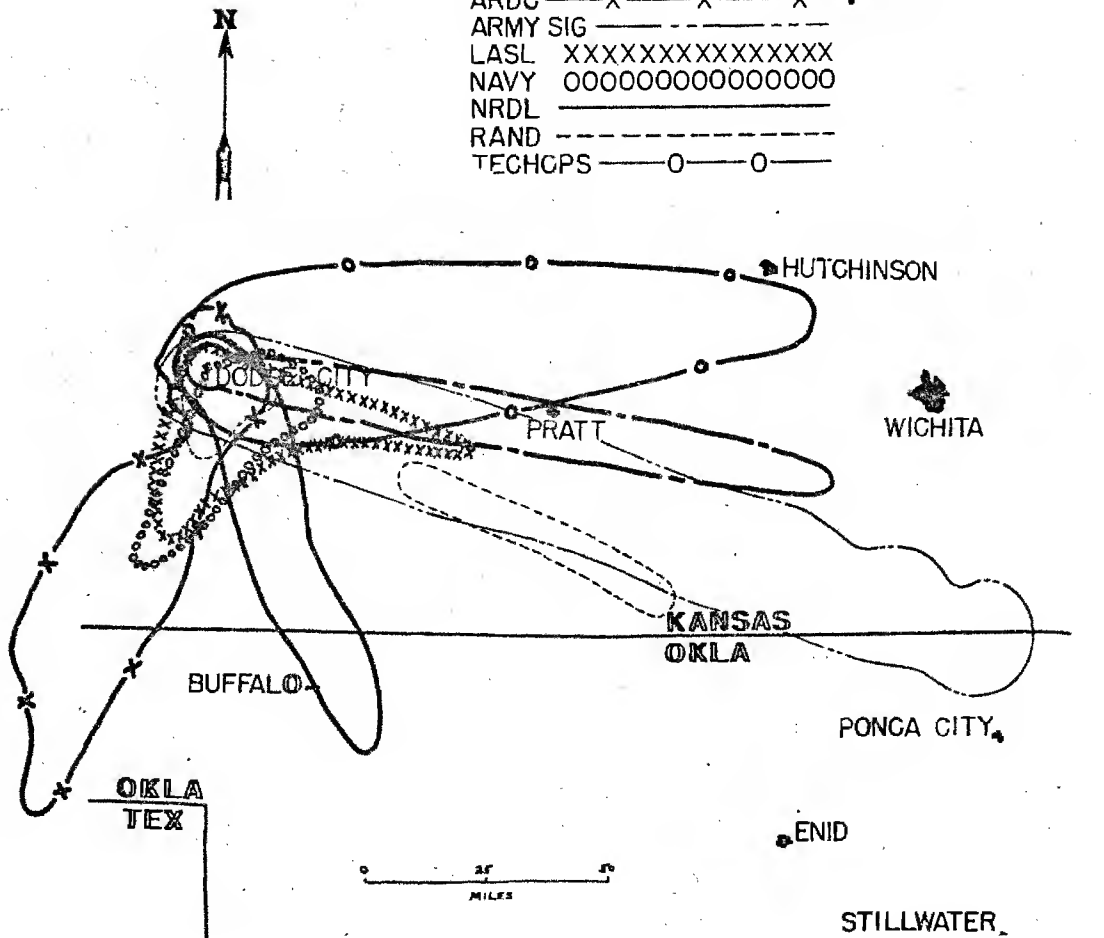


DOE ARCHIVES

CONDITION A
I MT
 100 r/hr at H+1 Contours

PATTERN CODE

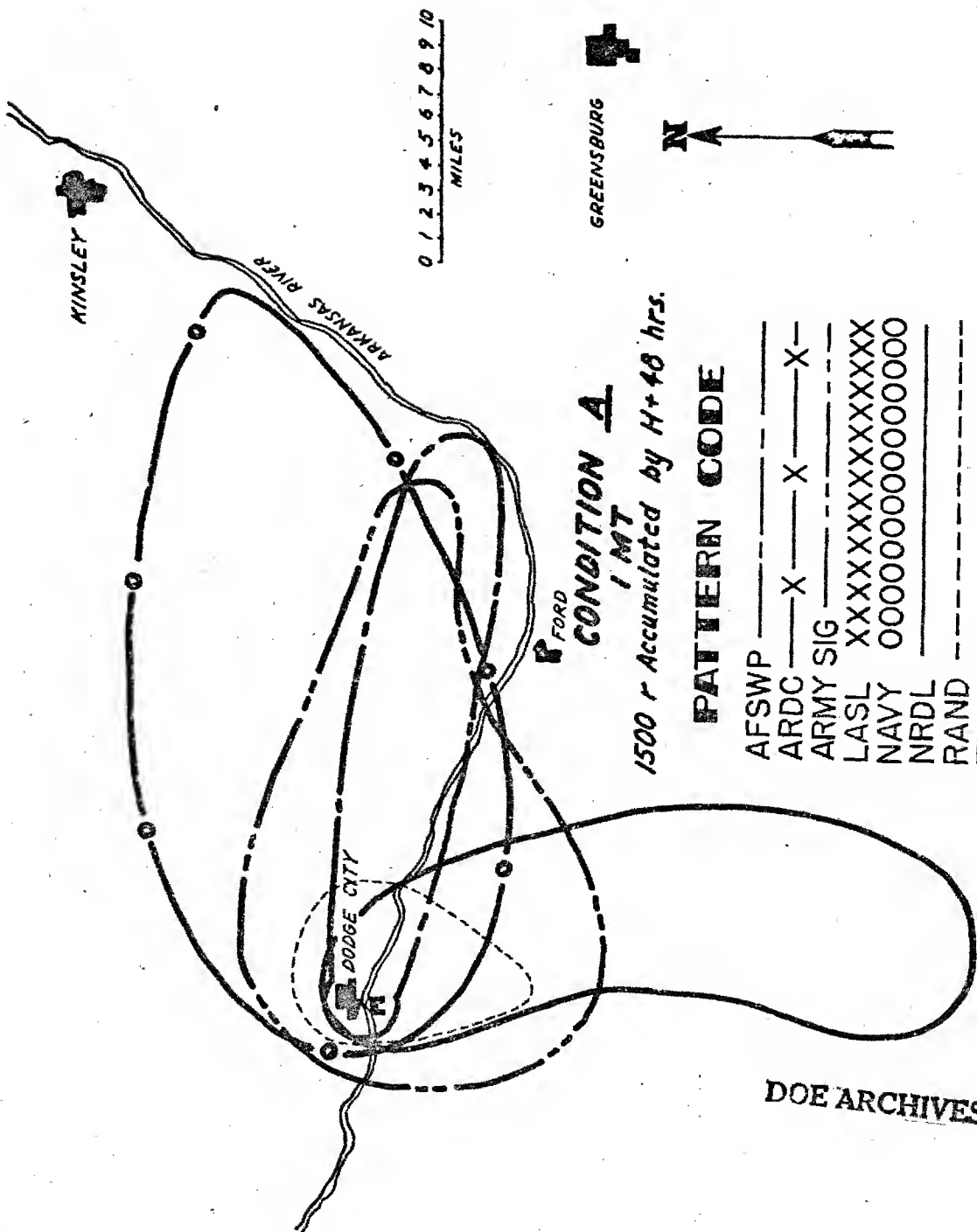
AFSWP	-----	
ARDC	—X—X—X—	† SALINA
ARMY SIG	-----	
LASL	XXXXXXXXXXXXXXXXXX	
NAVY	0000000000000000	
NRDL	-----	
RAND	-----	
TECHCPS	—O—O—	



DOE ARCHIVES

~~ATOMIC ENERGY ACT 1954~~

518



CONDITION A
1 MT
1500 r Accumulated by H+48 hrs.

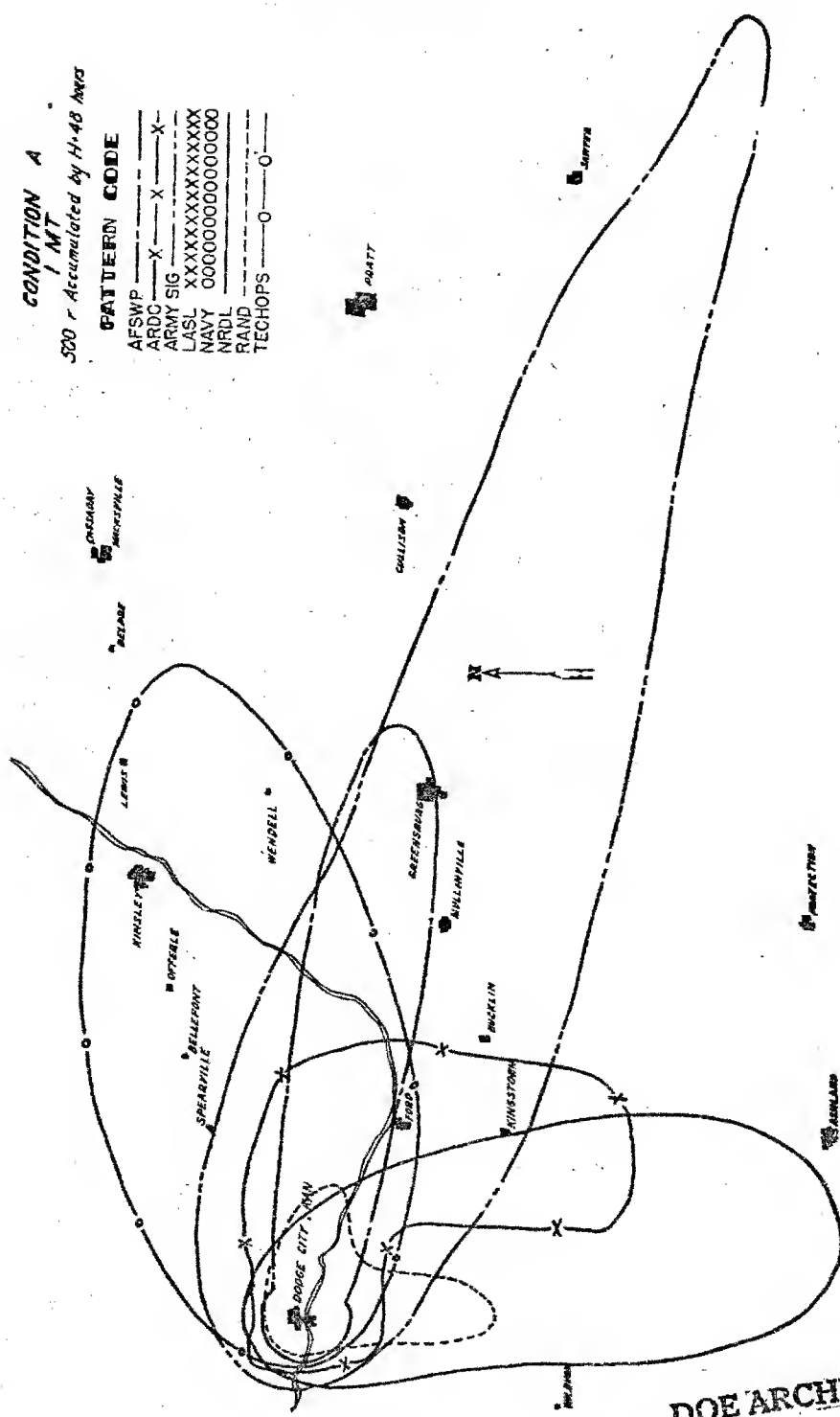
PATTERN CODE

AFSWP	---	---	---
ARDC	X	X	X
ARMY SIG	---	---	---
LASL	XXXXXXXXXXXX	---	---
NAVY	000000000000	---	---
NRDL	---	---	---
RAND	---	---	---
TECHOPS	0	0	0

DOE ARCHIVES

CONDITION A
1 MT
500 r Accumulated by H-48 hrs

PATTERN CODE
AFSWP ---X---X---X---
ARDC ---X---X---X---
ARMY SIG ---X---X---X---
LASL XXXXXXXXXXXXXXXX
NAVY 0000000000000000
NRDL ---X---X---X---
RAND ---X---X---X---
TECHOPS ---0---0---

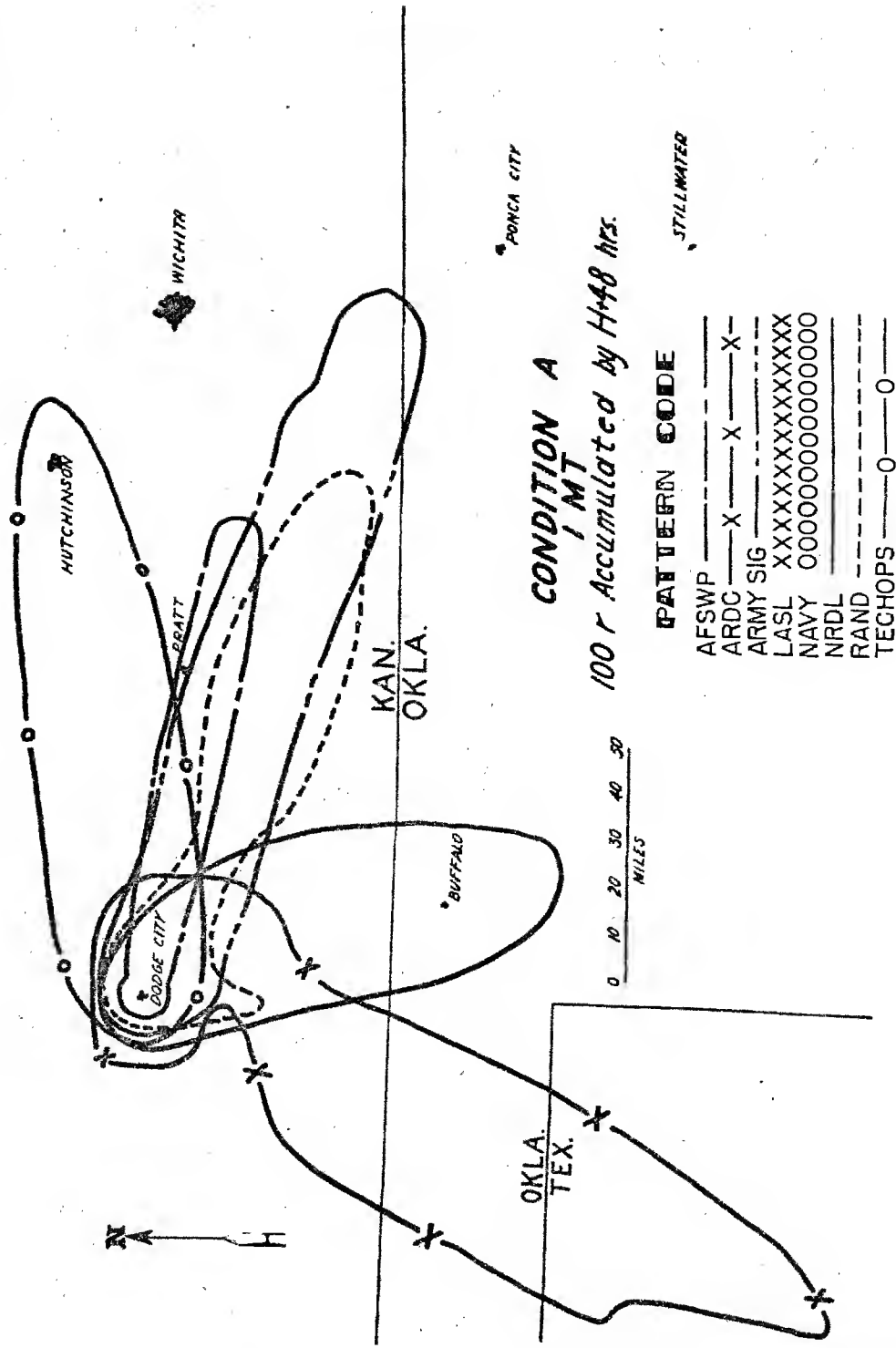


DOE ARCHIVES

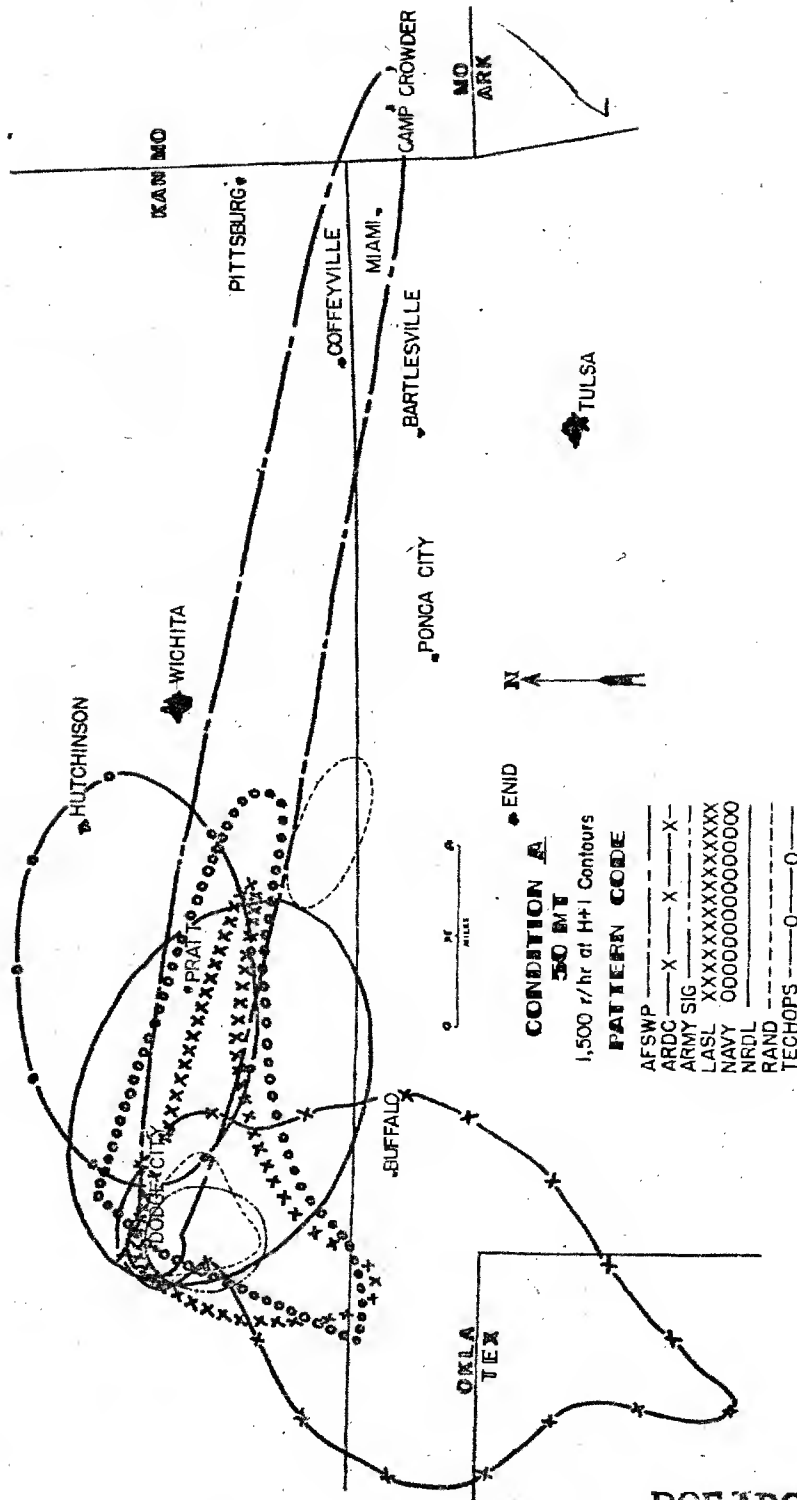
~~SECRET~~

~~ATOMIC ENERGY ACT~~

EMPORIA



DOE ARCHIVES



DOE ARCHIVES

521

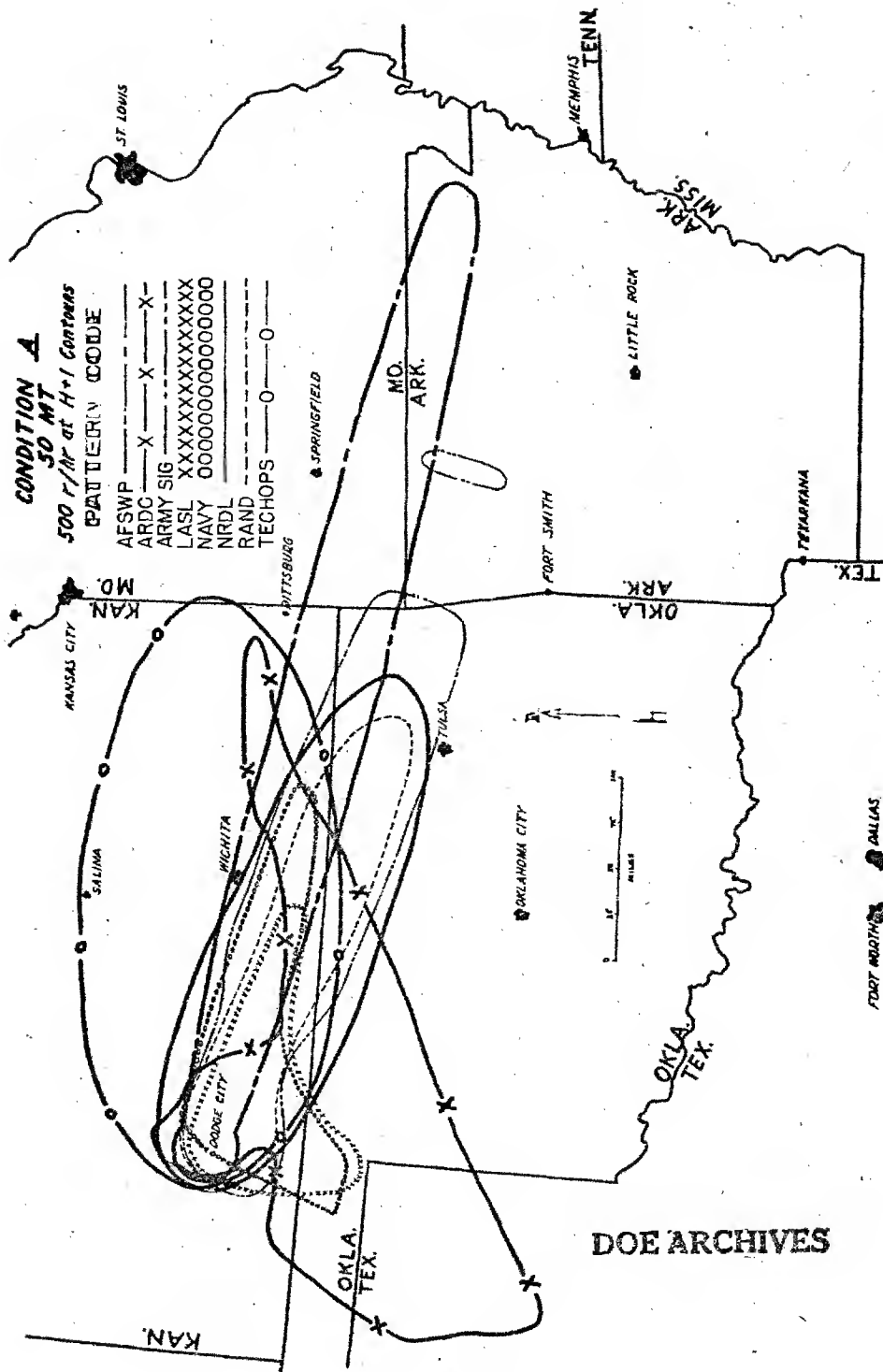
ATOMIC ENERGY ACT 1954

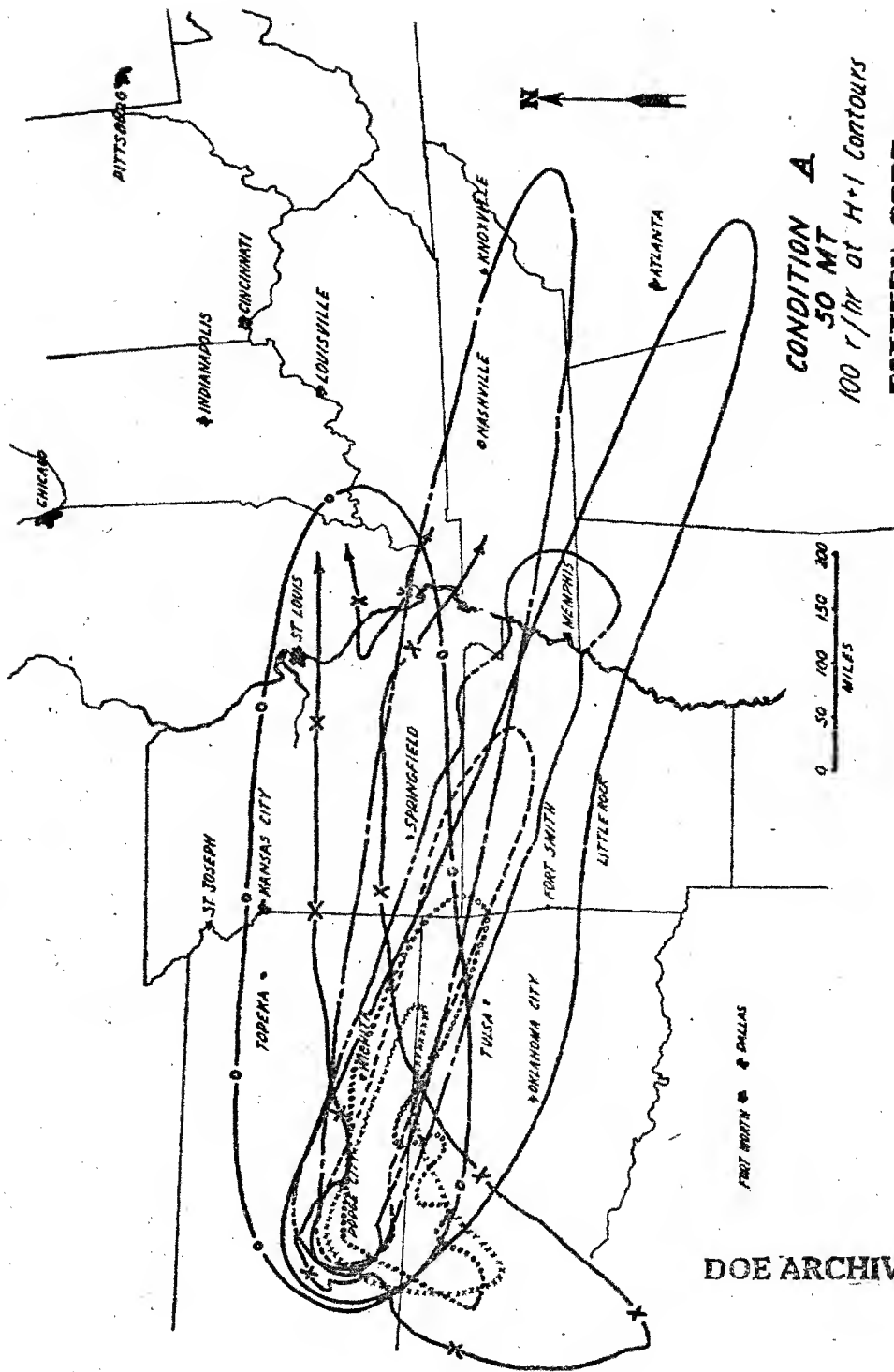
526

CONDITION A
50 MT
500 r/hr at H+1 CONTINUES

PATTERN CODE

AFSWP	---	---
ARDC	X	X
ARMY SIG	---	---
LASL	XXXXXXXXXXXX	---
NAVY	00000000000000	---
NRDL	---	---
RAND	---	---
TECHOPS	0	0



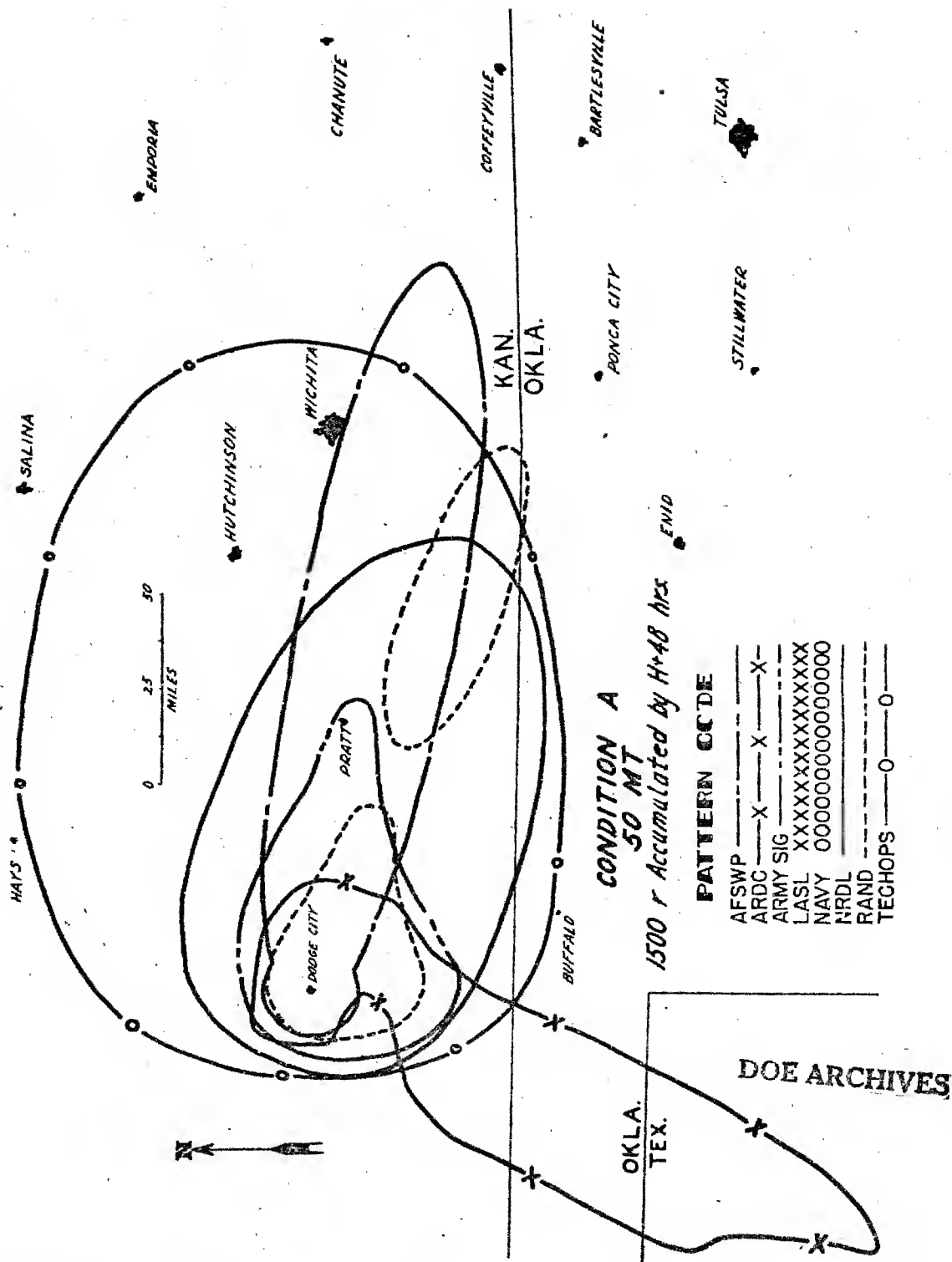


CONDITION A
 50 MT
 100 r/hr at H+1 Contours

PATTERN CODE

AFSWP	---	---	---	---
ARDC	X	X	X	X
ARMY SIG	---	---	---	---
LASL	XXXXXXXXXXXXXX	---	---	---
NAVY	00000000000000	---	---	---
NRDL	---	---	---	---
RAND	---	---	---	---
TECHOPS	0	0	0	0

DOE ARCHIVES



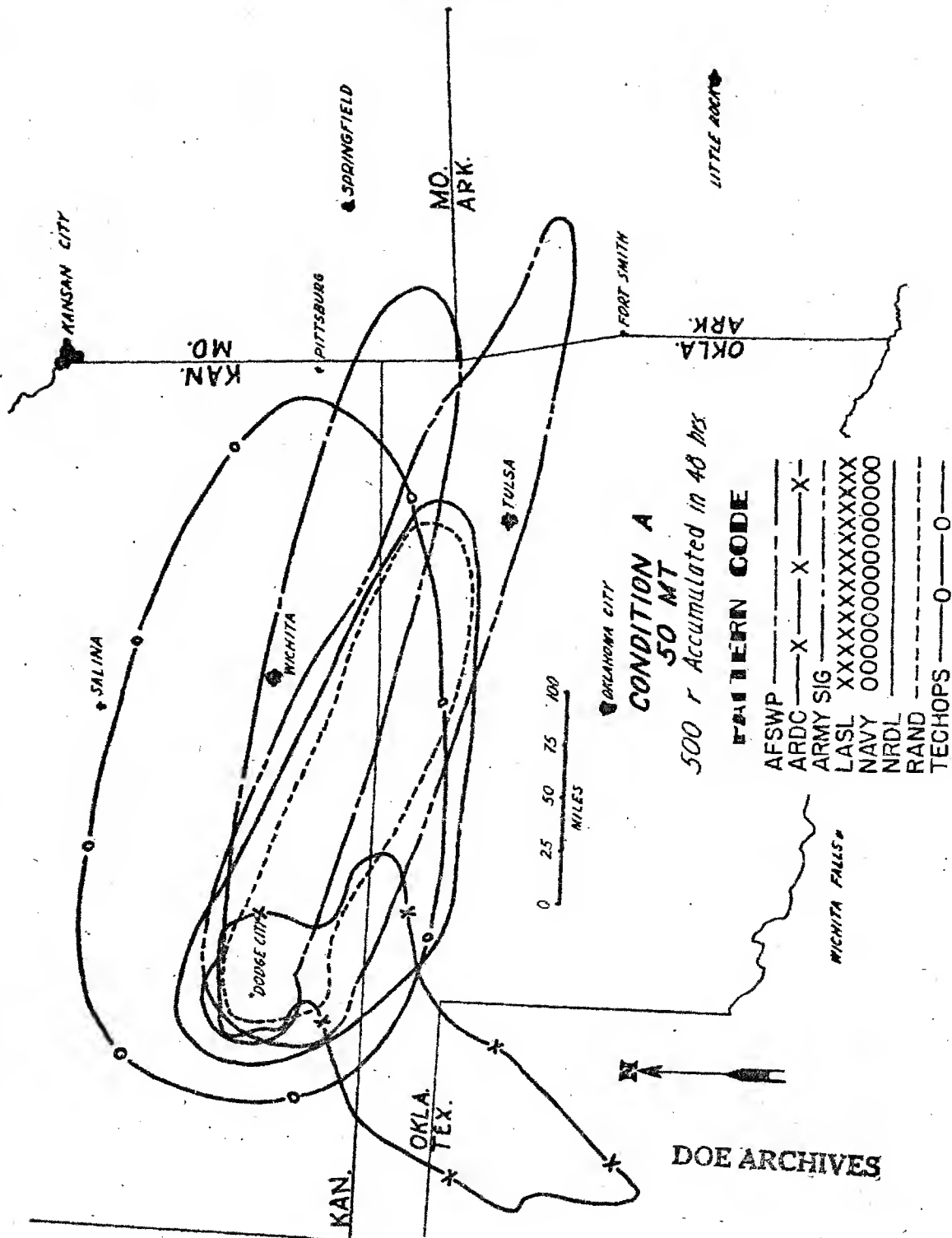
CONDITION A
50 MT
1500 r Accumulated by H-48 hrs

PATTERN CODE

AFSWP	---	X	---	X	---
ARDC	---	X	---	X	---
ARMY SIG	---	X	---	X	---
LASL	XXXXXX	XXXXXX	XXXXXX	XXXXXX	XXXXXX
NAVY	000000	000000	000000	000000	000000
NRDL	---	---	---	---	---
RAND	---	---	---	---	---
TECHOPS	---	0	---	0	---

DOE ARCHIVES

OKLA.
TEX.



CONDITION A

50 MT

500 r Accumulated in 48 hrs

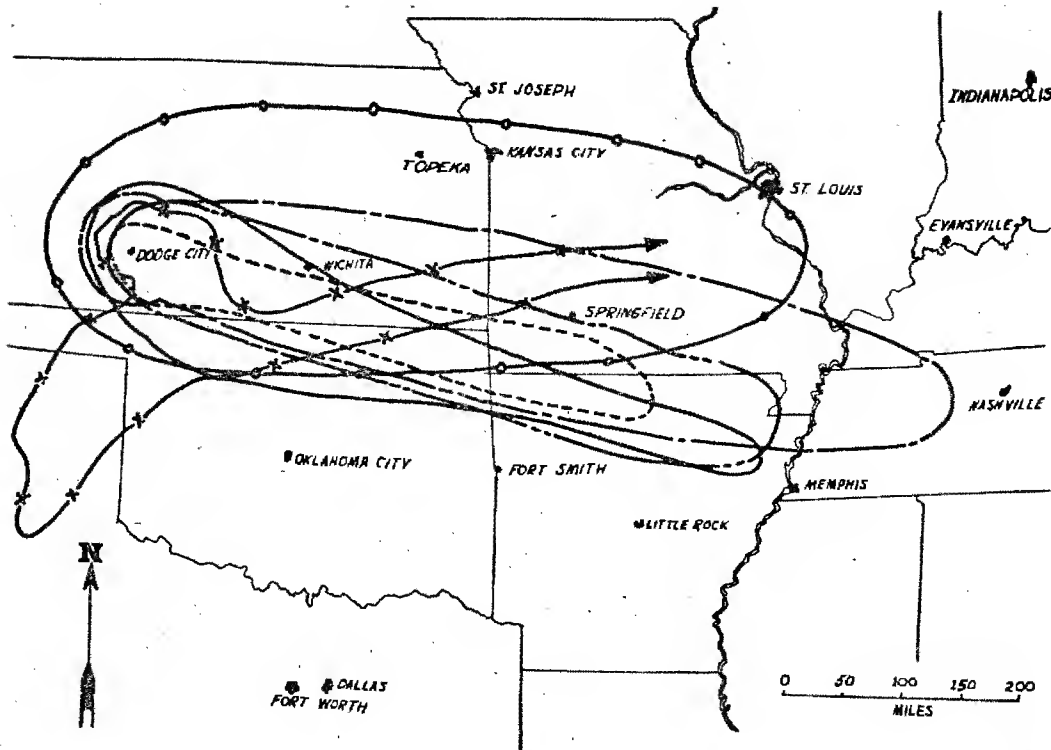
PATTERN CODE

AFSWP	---	---	---
ARDC	X	X	X
ARMY SIG	---	---	---
LASL	XXXXXXXXXXXX	---	---
NAVY	000000000000	---	---
NRDL	---	---	---
RAND	---	---	---
TECHOPS	0	0	0

525

DOE ARCHIVES

ATOMIC ENERGY ACT



CONDITION A
50 MT

100 r Accumulated in 48 hrs.

PATTERN CODE

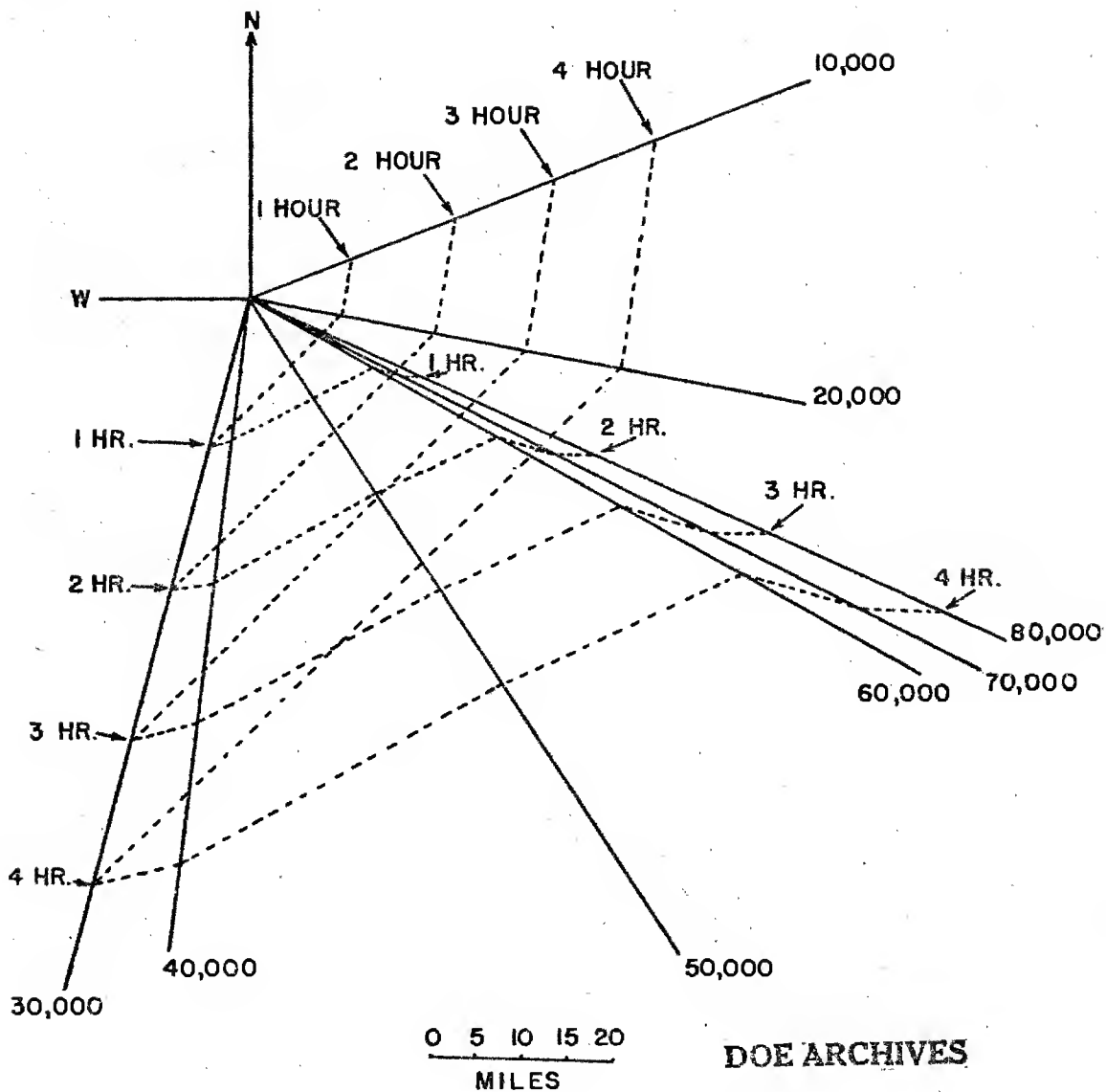
AFSWP _____
 ARDC —X—X—X—
 ARMY SIG _____
 LASL XXXXXXXXXXXXXXXX
 NAVY 0000000000000000
 NRDL _____
 RAND _____
 TECHOPS —0—0—

DOE ARCHIVES

526

531

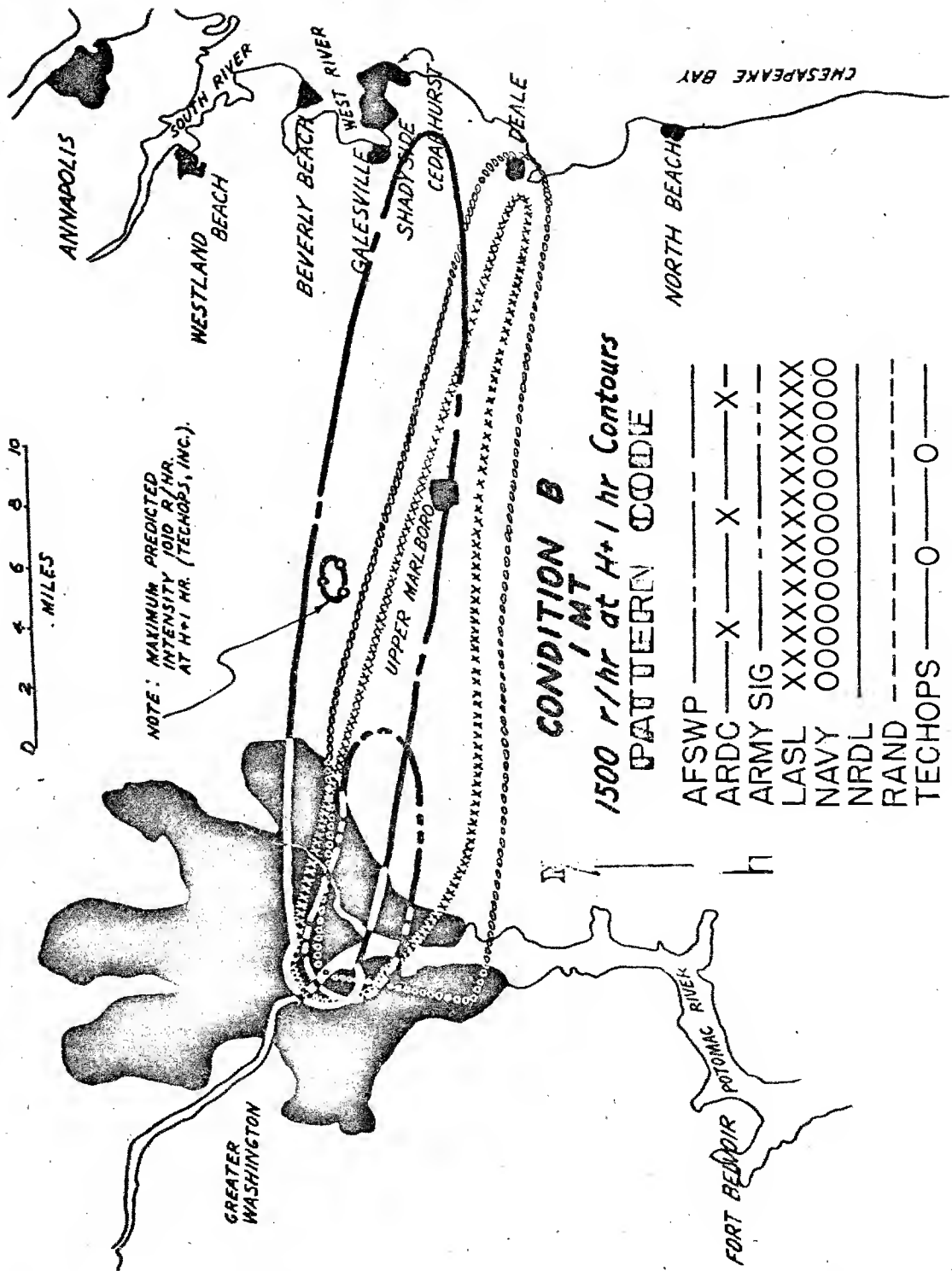
FALL-OUT PREDICTION
AIR WEATHER SERVICE METHOD
CONDITION "A"



DOE ARCHIVES

0 2 4 6 8 10
MILES

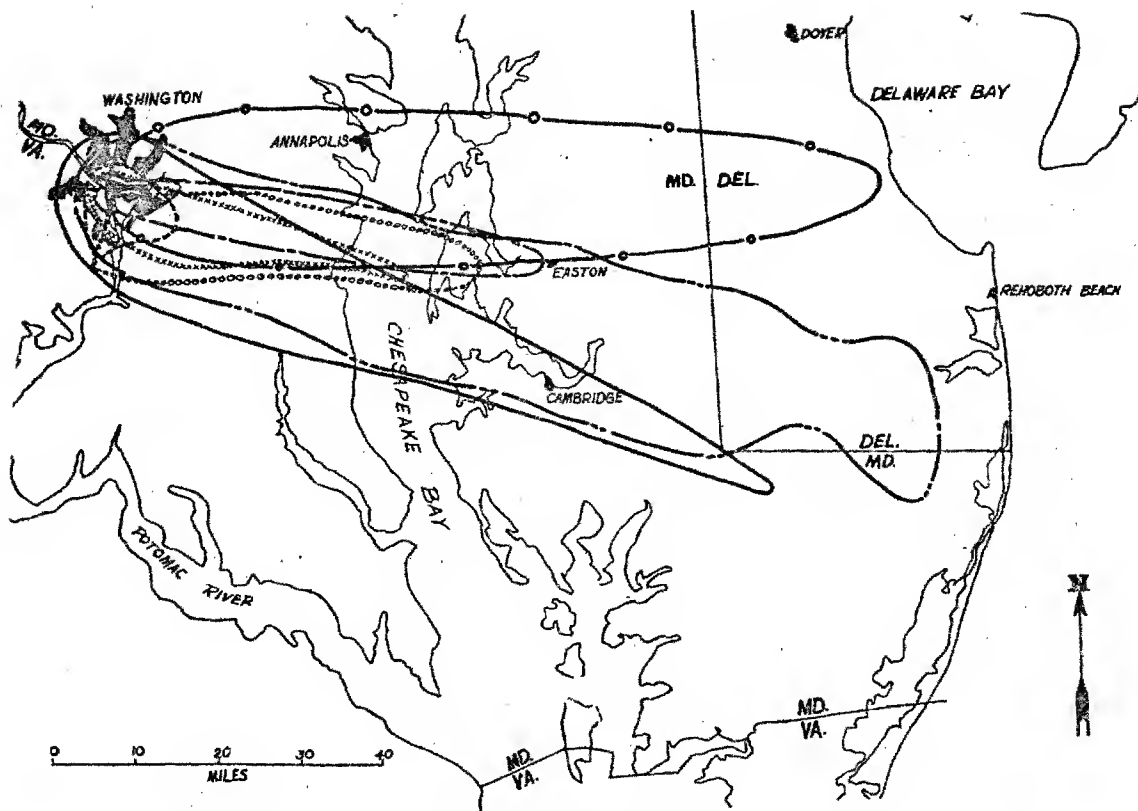
NOTE: MAXIMUM PREDICTED
INTENSITY 1010 R/HR.
AT H+1 HR. (TECHOPS, INC.)



CONDITION B
1500 r/hr at H+1 hr Contours
PATTERN CODE

AFSWP	---	---	---
ARDC	X	X	X
ARMY SIG	---	---	---
LASL	XXXXXXXXXXXXXX	---	---
NAVY	OOOOOOOOOOOO	---	---
NRDL	---	---	---
RAND	---	---	---
TECHOPS	O	O	O

DOE ARCHIVES



CONDITION B

1 MT

500r/hr At H+1 Hour Contours

PATTERN CODE

AFSWP _____
 ARDC —X—X—X—
 ARMY SIG _____
 LASL XXXXXXXXXXXXXXXX
 NAVY 000000C000000000
 NRDL _____
 RAND _____
 TECHOPS —0—0—

DOE ARCHIVES

529

NUCLEAR ENERGY ACT 4

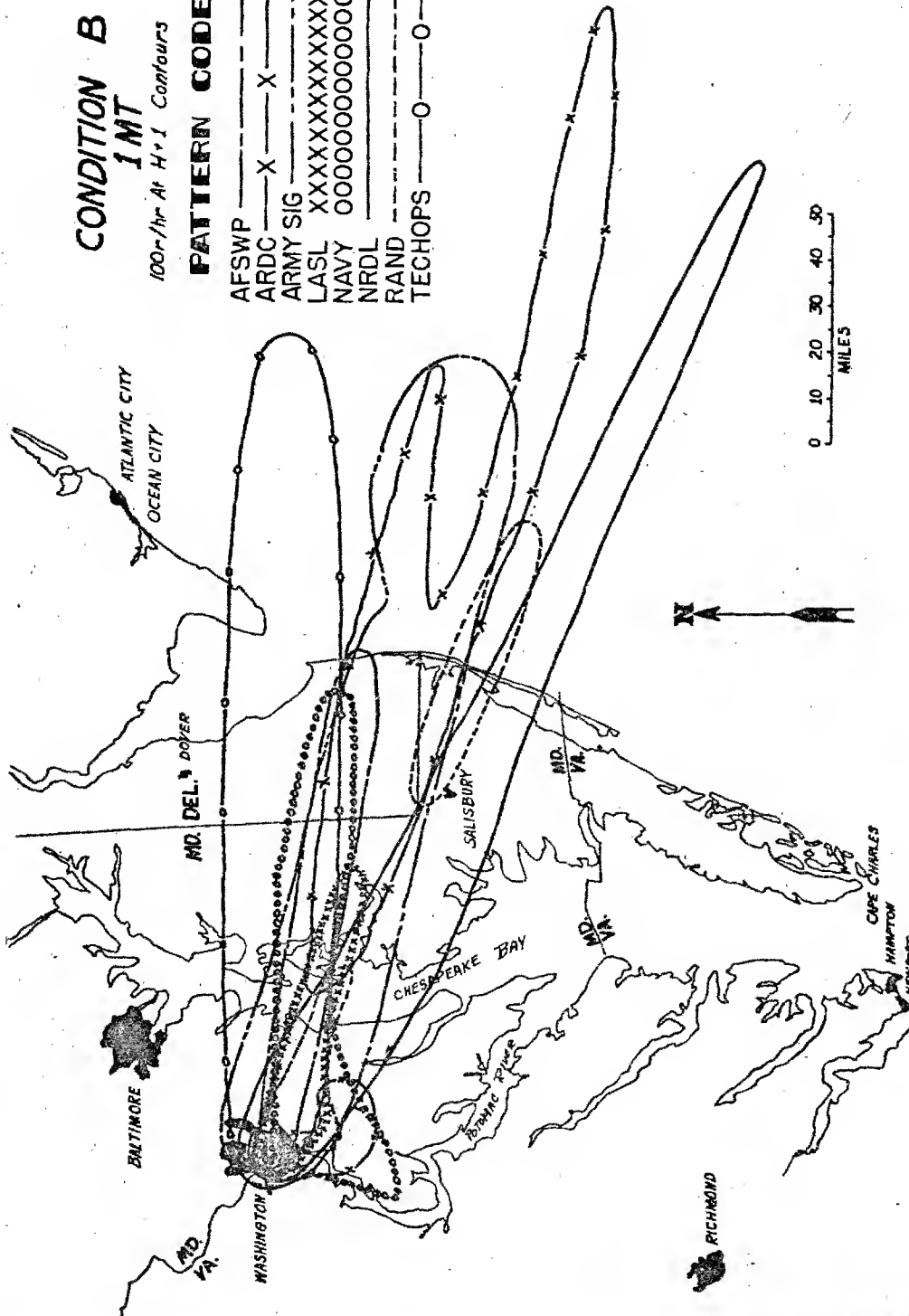
534

CONDITION B 1MT

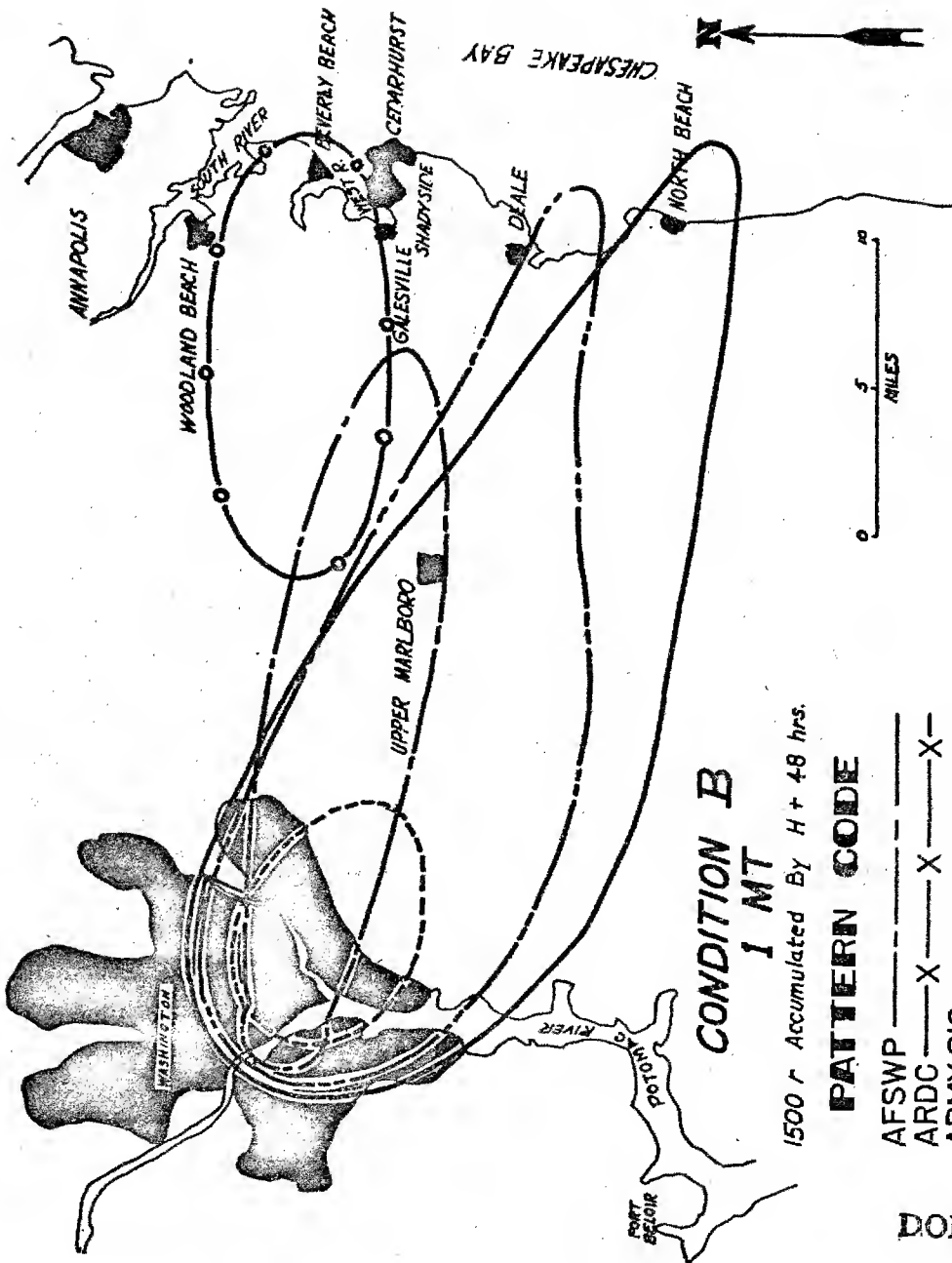
100-1hr At H+1 Contours

PATTERN CODE

AFSWP	---	---	---
ARDC	X	X	X
ARMY SIG	---	---	---
LASL	XXXXXXXXXXXXXXX	---	---
NAVY	000000000000000	---	---
NRDL	---	---	---
RAND	---	---	---
TECHOPS	0	0	0



DOE ARCHIVES



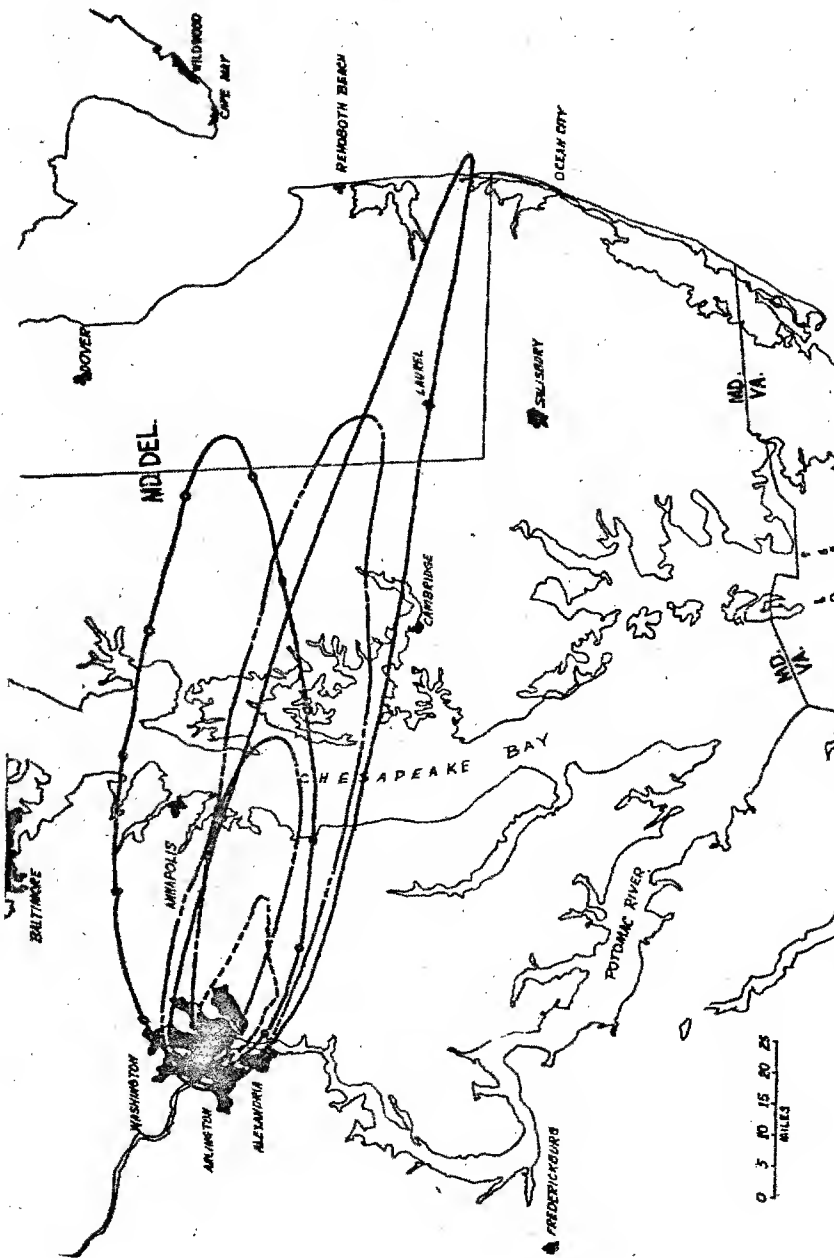
CONDITION B 1 MT

1500 r Accumulated By H + 48 hrs.

PATTERN CODE

AFSWP	---	---	---
ARDC	X	X	X
ARMY SIG	---	---	---
LASL	XXXXXXXXXXXX	---	---
NAVY	000000000000	---	---
NRDL	---	---	---
RAND	---	---	---
TECHOPS	0	0	0

DOE ARCHIVES



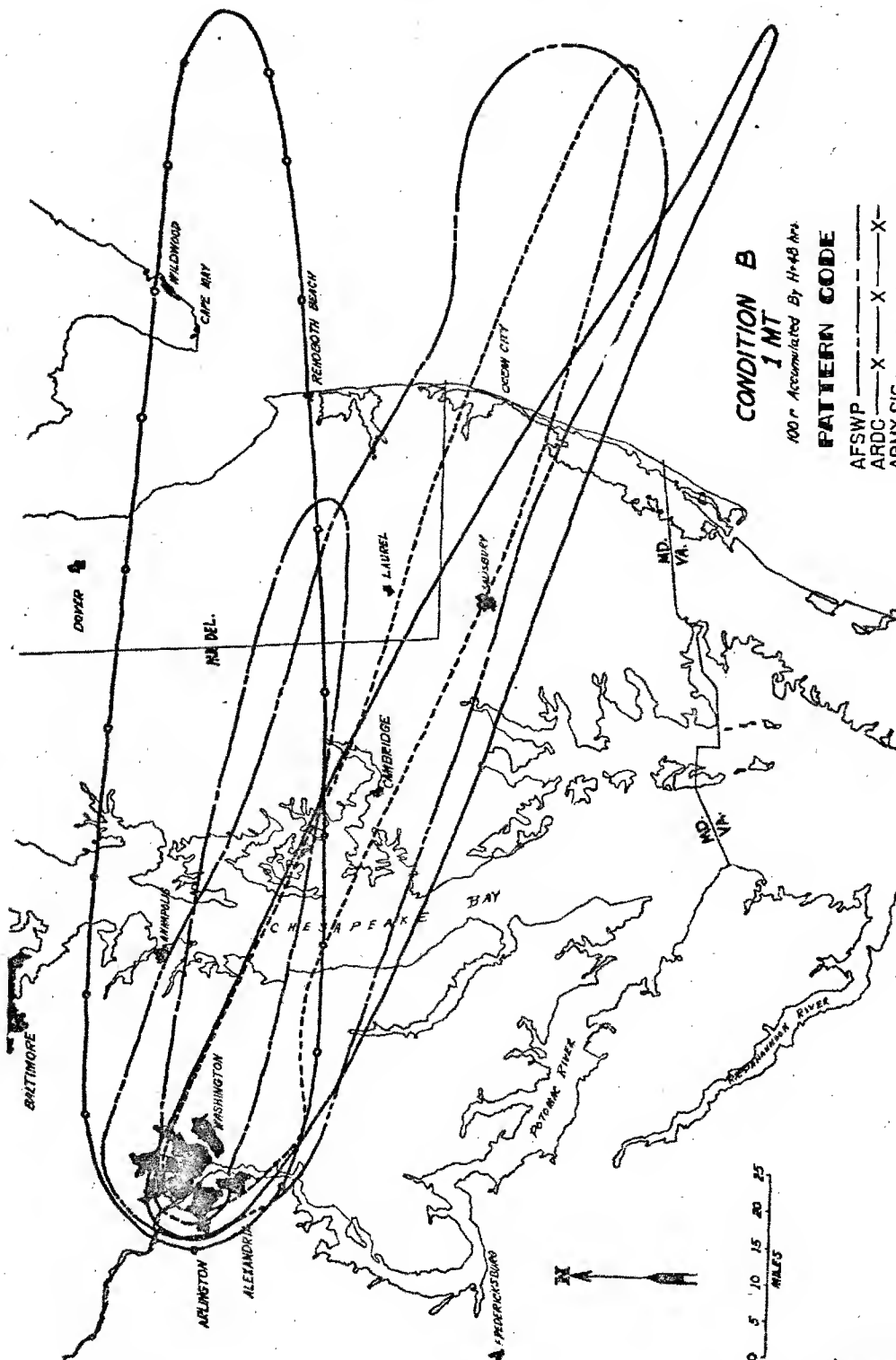
CONDITION B
1 MT

500 r Accumulated By H-48 hrs.

PATTERN CODE

AFSWP	---	X	---	X	---	X
ARDC	---	X	---	X	---	X
ARMY SIG	---	X	---	X	---	X
LASL	---	XXXXXXXXXXXX	---	XXXXXX	---	XXXXXX
NAVY	---	XXXXXXXXXXXX	---	XXXXXX	---	XXXXXX
NRDL	---	XXXXXXXXXXXX	---	XXXXXX	---	XXXXXX
RAND	---	XXXXXXXXXXXX	---	XXXXXX	---	XXXXXX
TECHOPS	---	XXXXXX	---	XXXXXX	---	XXXXXX

DOE ARCHIVES



CONDITION B 1 MT

100 r Accumulated By H-48 Arx

PATTERN CODE

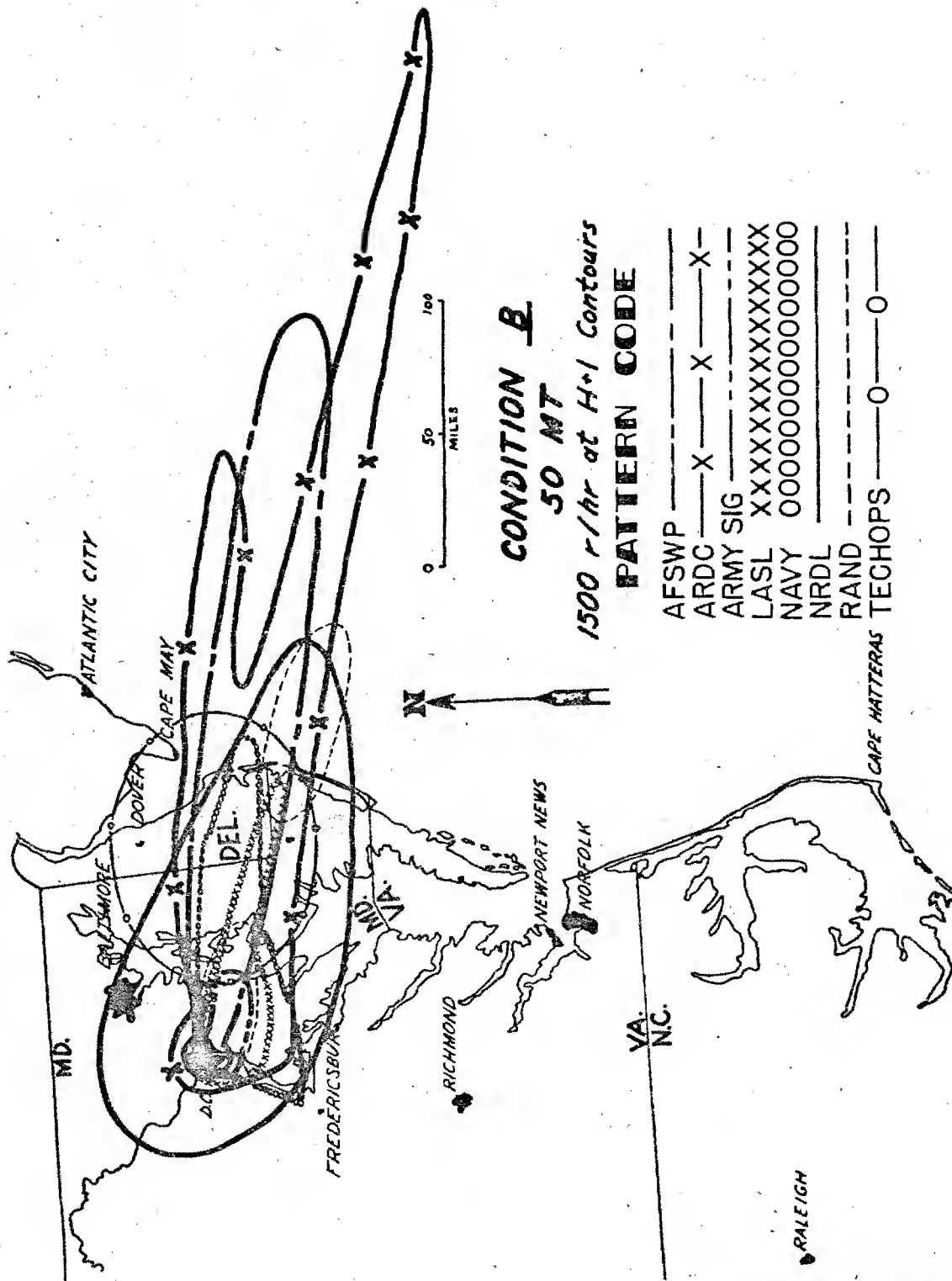
AFSWP	---	---	---
ARDC	X	X	X
ARMY SIG	---	---	---
LASL	XXXXXXXXXXXXXXX	---	---
NAVY	000000000000000	---	---
NRDL	---	---	---
RAND	---	---	---
TECHOPS	---	0	0

DOE ARCHIVES

533

ATOMIC ENERGY ACT 1954

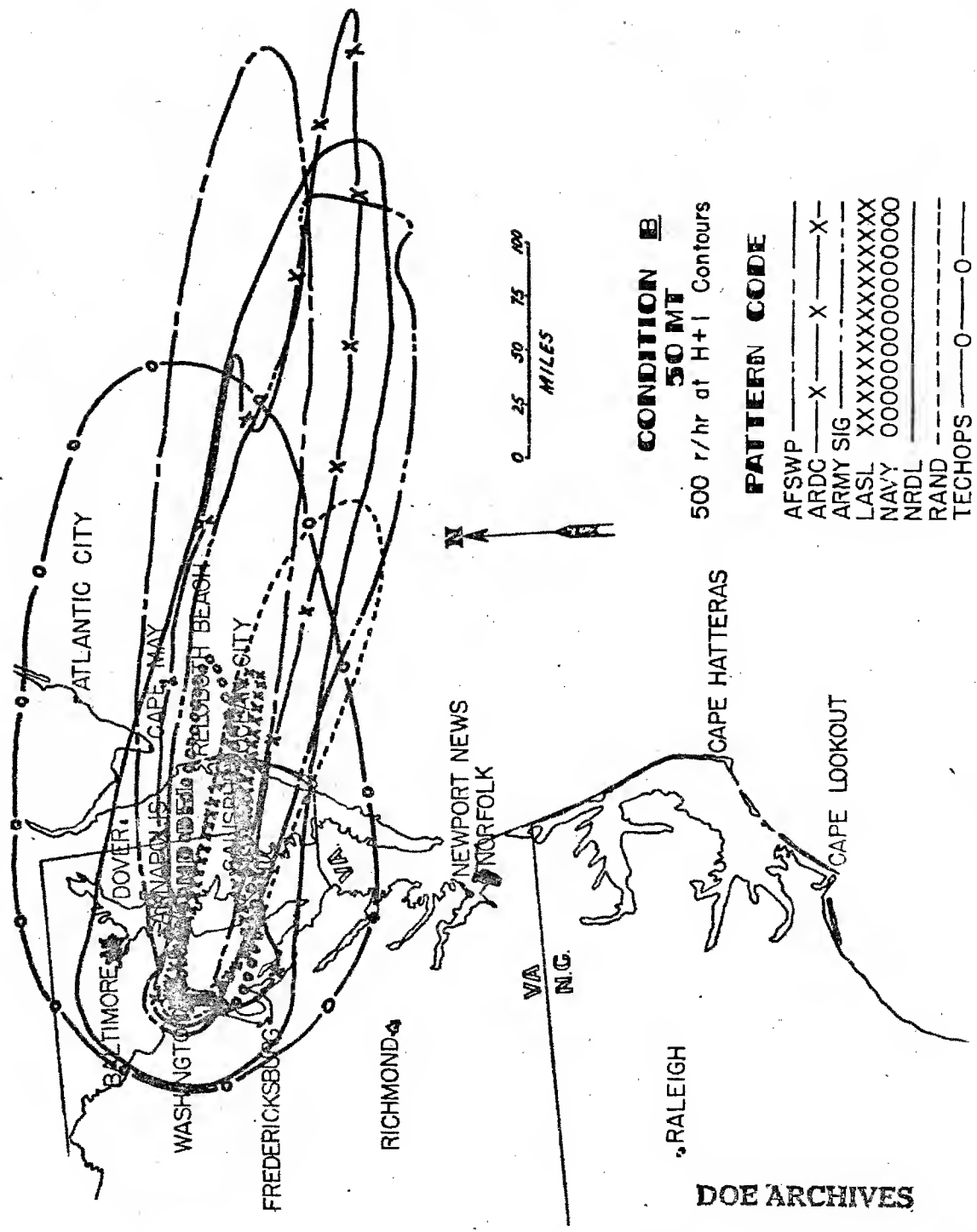
538



DOE ARCHIVES

534

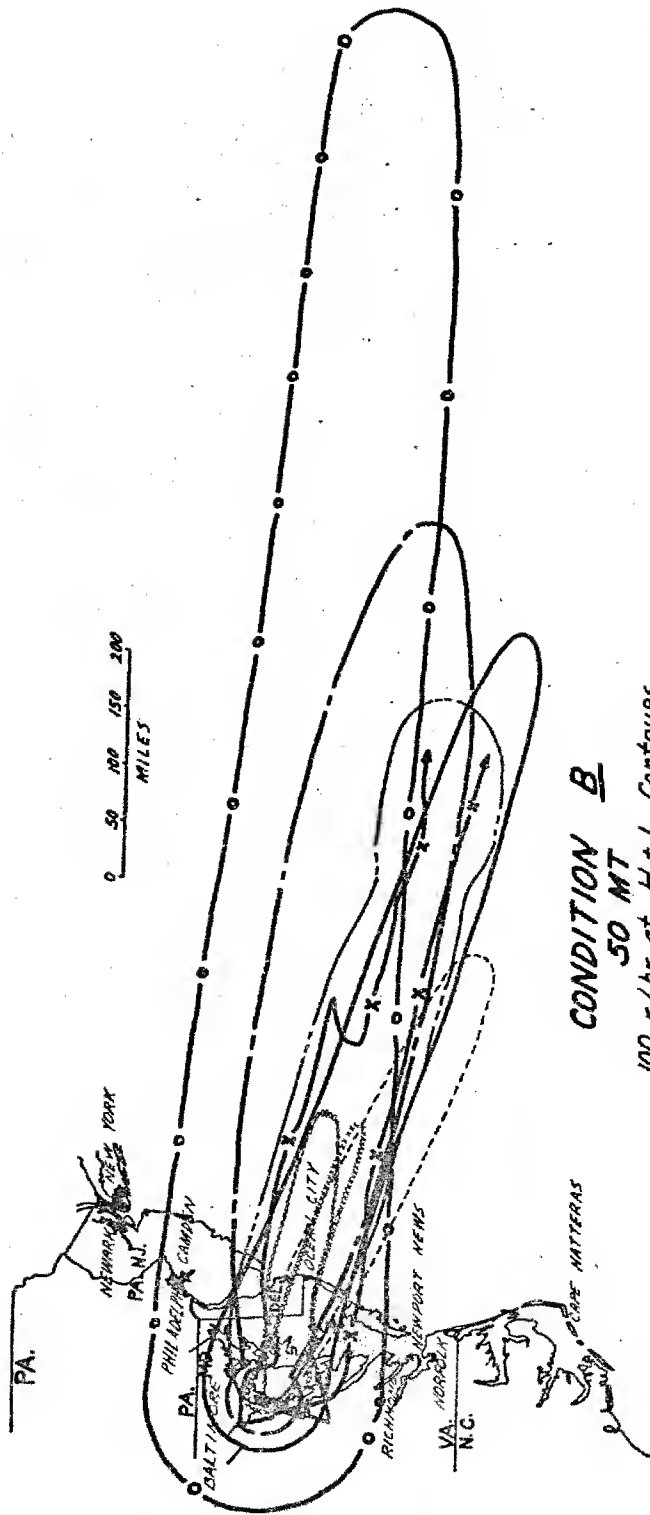
539



535

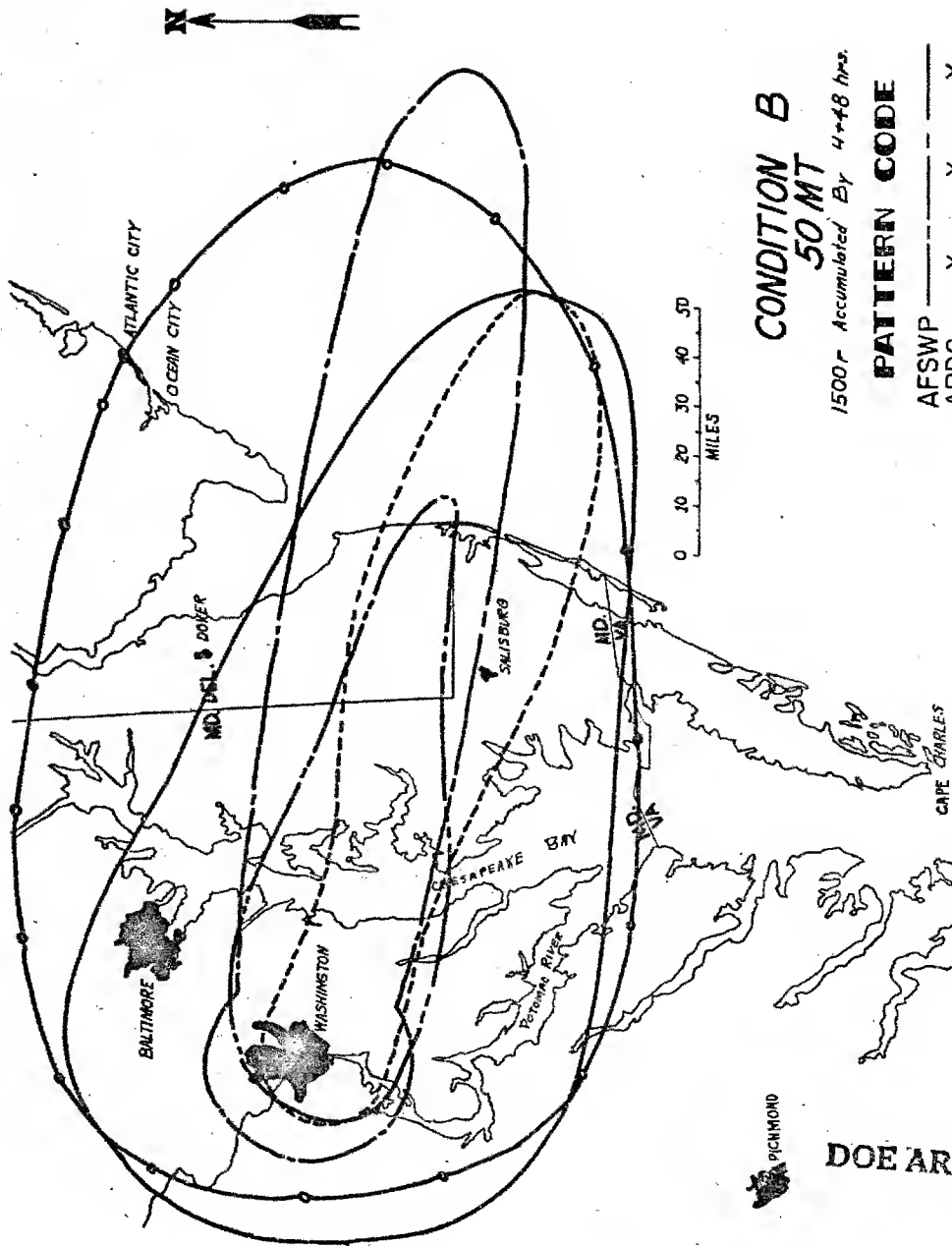
DOE ARCHIVES

540



536

DOE ARCHIVES



CONDITION B **50 MT**

1500r Accumulated By 4+48 hrs.

PATTERN CODE

AFSWP	---
ARDC	X --- X --- X ---
ARMY SIG	---
LASL	XXXXXXXXXXXXXXXXXX
NAVY	0000000000000000
NRDL	---
RAND	---
TECHOPS	0 --- 0 ---

PICHMOND

DOE ARCHIVES

537

ATOMIC ENERGY

542

7/18/88

INCOMPLETE DOCUMENT REFERENCE SHEET

The archive copy of this document is incomplete.

Pages missing 538

Enclosures missing _____

Attachments missing _____

Other _____

CR8
signature

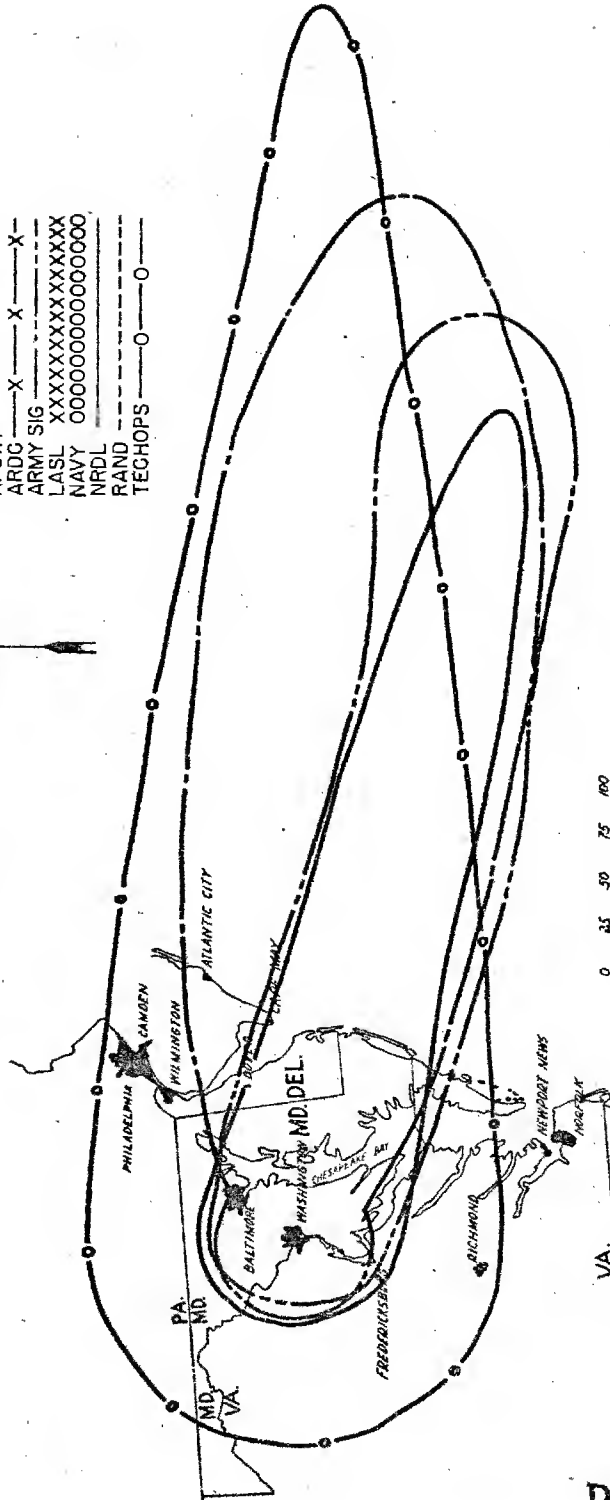
2-11-92
date

542 A

CONDITION B
50 MT
 100 r Accumulated by H-48 hrs

PATTERN CODE

AFSWP	---	X	---	X
ARDG	---	X	---	X
ARMY SIG	---		---	
LASL	XXXXXX	XXXXXX	XXXXXX	XXXXXX
NAVY	000000	000000	000000	000000
NRDL	---		---	
RAND	---		---	
TECHOPS	---	0	---	0



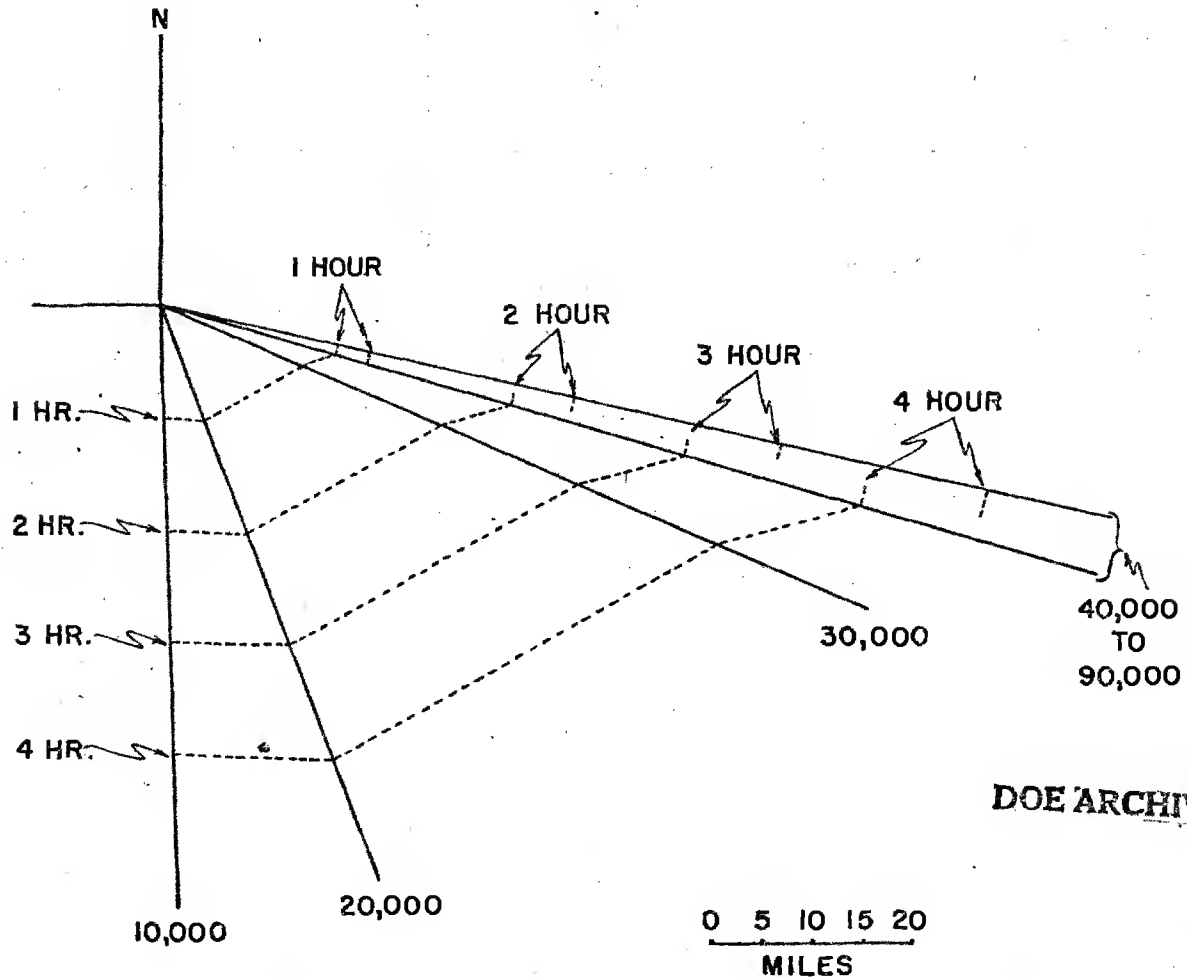
DOE ARCHIVES

539

ATOMIC ENERGY

543

FALL-OUT PREDICTION
AIR WEATHER SERVICE METHOD
CONDITION "B"



DOE ARCHIVES

540

ATOMIC ENERGY

544

Comparison of Certain Contour Parameters

CONDITION "A"
1 MT Surface Burst

	AFSWP	Army Sig	ARDC	LASL	NAVY	NRDL	RAND Tech Ops
1500 r/hr at H+1	92	52		180	260		3 61
	30	9	(**)	25	30	(**)	2 13
	4	7		20	22		2 6
500 r/hr at H+1	330	1590	115	350	350	330	(33) 680
	60	107	18	33	40	34	(4) 14
	(6)	20	9	25	30	13	7 24
100 r/hr at H+1	1,200	3,900	1,850	(950)	650	1,150	(950) 3,300
	130	180	95	(55)	70	83	110 124
	(10)	26	20	35	40	29	14 32
1500 r/48 hrs	75	240				190	(40) 350
	25	22	(**)	*	*	26	(7) 30
	(5)	15				10	7 16
500 r/48 hrs	350	1620	450			670	(120) 950
	45	105	26	*	*	40	(14) 50
	(9)	22	(9)			22	12 30
100 r/48 hrs	(1,300)	3,600	5,350			3,150	2,500 3,750
	105	158	160	*	*	(92)	120 130
	(13)	26	38			40	24 32

The first figure given is the contour area in square miles; the second is the greatest downwind extent of the contour from ground zero in miles; and the third is the greatest crosswind extent of the contour in miles.

* Indicates contours not received for this condition at time of press make-up.

** Indicates method does not predict a significant contour for the conditions specified.

() Indicates smallest value predicted.

Underlining indicates largest value predicted. (Navy and Tech Ops values not included in this comparison, since the contours had to be normalized from data furnished.)

Comparison of Certain Contour Parameters

CONDITION "A"

50 MT Surface Burst

	AFSWP	ARMY SIG	AFDC	LASL	NAVY	NRDL	RAND	TECH OPS
1500 r/hr at H+1	7,500 330 27	(650) (30) (25)	2,700 180 50	2,850 100 65	4,500 125 75	6,200 100 80	1,100 113 (25)	5,600 130 64
500 r/hr at H+1	23,000 550 50	20,000 400 65	27,000 280 80	(6,800) (134) 100	8,800 200 130	20,500 275 108	7,000 260 (47)	34,000 300 140
100 r/hr at H+1	92,000 1,000 110	57,000 660 98	> 76,000 > 600 270	(18,000) 215 120	24,000 250 150	119,000 1,000 152	28,000 500 (65)	126,000 690 200
1500 r/48 hrs	6,700 210 10	(2,900) (76) 56	5,700 160 38	* * *	* * *	9,000 125 80	3,000 153 (39)	22,000 170 150
500 r/48 hrs	18,000 340 60	22,000 395 75	12,200 (200) 70	* * *	* * *	20,000 246 110	(10,500) 238 (50)	42,000 280 168
100 r/48 hrs	84,000 700 135	55,000 580 96	> 39,000 (> 380) 95	* * *	* * *	44,000 550 152	(24,000) 450 (62)	111,000 560 216

The first figure given is the contour area in square miles; the second is the greatest downwind extent of the contour from ground zero in miles; and the third is the greatest crosswind extent of the contour in miles.

* Indicates contours not received for this condition at time of press make-up.

** Indicates method does not predict a significant contour for the conditions specified.

() Indicates smallest value predicted.

Underlining indicates largest value predicted. (Navy and Tech Ops values not included in this comparison, since the contours had to be normalized from data furnished.)

Comparison of Certain Contour Parameters

CONDITION "B"

1 MT Surface Burst

	AFSWP	ARMY SIG	ARDC	LASL	NAVY	NRDL	RAND	TECH OPS
1500 r/hr at H+1	97 28 <u>1</u>	15 8 2	(**)	72 26 <u>6</u>	116 27 5	(**)	6 2 3	**
500 r/hr at H+1	300 52 7	1,800 <u>105</u> <u>22</u>	(**)	200 36 8	375 40 8	950 86 16	114 6 8	1,350 92 18
100 r/hr at H+1	2,100 110 (11)	4,100 <u>172</u> 27	3,500 250 <u>28</u>	(600) (61) 14	2,750 100 14	3,250 235 26	2,500 115 (11)	4,000 176 24
1500 r/48 hrs	110 23 (5)	220 30 11	*	*	*	290 <u>33</u> <u>14</u>	(38) (8) 6	73 30 6
500 r/48 hrs	325 40 (10)	1,900 <u>105</u> 22	*	*	*	1,200 115 <u>20</u>	(110) (26) 12	1,300 76 24
100 r/48 hrs	(1,100) (95) (11)	4,000 <u>165</u> 28	*	*	*	2,100 176 <u>26</u>	1,500 165 17	3,900 160 30

The first figure given is the contour area in square miles; the second is the greatest downwind extent of the contour from ground zero in miles; and the third is the greatest crosswind extent of the contour in miles.

* Indicates contours not received for this condition at time of press make-up.

** Indicates method does not predict a significant contour for the conditions specified.

() Indicates smallest value predicted.

Underlining indicates largest value predicted. (Navy and Tech Ops values not included in this comparison since the contours had to be normalized from data furnished.)

Comparison of Certain Contour Parameters

CONDITION "B"
50 Ft Surface Burst

	AFSMP	ARMY SIG	ARDC	LASL	NAVY	NRDL	RAND	TECH OPS
1500 r/hr at H+1	7,500 260 32	(350) (33) (12)	11,600 410 46	1,500 106 22	3,000 120 25	11,000 160 80	1,700 168 22	5,800 130 76
500 r/hr at H+1	27,000 435 62	24,000 380 76	17,500 450 56	(2,600) (152) (30)	3,700 155 35	31,000 400 96	8,500 240 52	40,000 290 160
100 r/hr at H+1	92,000 775 110	56,000 630 100	>34,000 >500 70	(6,000) (250) (50)	10,000 250 50	54,000 700 100	22,000 425 63	190,000 1,200 200
1500 r/L8 hrs	7,500 200 110	(3,100) (115) 42	* * *	* * *	* * *	14,000 160 98	4,500 160 (32)	19,500 180 110
500 r/L8 hrs	21,000 300 80	25,000 380 75	* * *	* * *	* * *	20,500 250 100	(9,000) (225) (50)	28,000 280 180
100 r/L8 hrs	76,000 550 170	47,000 600 100	* * *	* * *	* * *	35,000 450 100	(18,000) (350) (63)	102,000 650 210

The first figure given is the contour area in square miles; the second is the greatest downwind extent of the contour from ground zero in miles; and the third is the greatest crosswind extent of the contour in miles.

* Indicates contours not received for this condition at time of press make-up.

** Indicates method does not predict a significant contour for the conditions specified.

() Indicates smallest value predicted.

Underlining indicates largest value predicted. (Navy and Tech Ops values not included in this comparison since the contours had to be normalized from data furnished.)

DOE ARCHIVES

[REDACTED]

CLOSING REMARKS

Dr. Herbert Scoville, Jr.
Armed Forces Special Weapons Project

Before opening the general discussion of the conference, I should like to summarize briefly my own impressions of what has been accomplished. First, we should remember that the prime objectives of this symposium were to make all the data on fallout available to everyone who has been making studies in the field. The second objective was to put forth the various theories and fallout models so that their assumptions and methods could be compared. Obviously, it is not possible to reach any decision as to a best method at a meeting of this sort. Actually, there is probably no such thing as a best method since different groups have different requirements for information.

I believe this symposium has rather graphically shown, in case anyone had previously doubted it, that the radiological fallout involves very complex phenomena. The initial stages in the process depend upon reactions occurring in the fireball and the properties of the atomic cloud. Later stages include atmospheric transport problems, particularly those related to the settling velocity of particulate matter. Finally, one has the radiological phenomena which determine the radiation fields in actual locations and which are effected by the radiochemical properties of the bomb debris. The entire fallout process is moreover strongly dependent on such external variables as the nature of the soil at the point of detonation and the meteorological conditions. It is, therefore, no wonder that all the data are not self-consistent and that a variety of models can be developed to explain the test observations.

With respect to the data, I believe that it is important to remember that to a large extent it derives from one or two actual test shots. For example, the data from the BRAVO shot has been used for calibration of all theories. Other shots have produced bits and pieces of data which are very useful in checking parts of the theories but with the exception of the JANGLE surface shot, all others have certain basic differences from the situation of greatest operational interest; i.e., surface land detonations of high yield weapons. Furthermore, as Lt Colonel Lulejian has pointed out, the weather conditions which actually existed at the BRAVO shot were not good for differentiating between some of the proposed models. In particular it was not satisfactory for determining what fractions of the active material are in the cloud and stem. I think it is also important to remember that obtaining data on fallout at the Pacific Proving Grounds is an extremely difficult process. A great deal of credit is due to those who have

[REDACTED]

actual wind conditions with those which had been previously used in a machine solution. This approach would be similar to that described by Dr. Felt, who indicated that at the Nevada Test Site it is possible to predict with considerable confidence, based on previous experience, the fallout levels which will occur.

In summary, I believe that we can conclude that: (a) the general scale of the fallout problem under various detonation conditions can be reasonably well defined, (b) a number of models are now available which will provide reasonable estimates of the specific fallout patterns which are likely to occur under different meteorological conditions, and finally, (c) there is a real need for further experimental data to check the various theories. In this connection, the oceanographic techniques offer considerable promise in the Pacific, but truly satisfactory results will be obtained when it is possible to detonate large yield weapons on the surface of a large land mass.

DOE ARCHIVES

[REDACTED]

THIS PAGE IS BLANK

DOE ARCHIVES

548

[REDACTED]
[REDACTED] NUCLEAR ENERGY ACT [REDACTED]

[REDACTED]

552

~~SECRET~~

GENERAL DISCUSSION

Question: Dr. Kellogg, Rand Corp.

Is there any initial dosage rate at which it would be advisable to evacuate a contaminated area? It would seem that there must be a limit somewhere.

Answer: Dr. P. C. Tompkins, USNRDL

No. In my opinion, it is completely feasible to reduce the radiological effects at any location down to a safe value so that the limiting factor will be blast or fire. I am equally sure that one can design shelters to provide blast protection quite close to the limits of the crater, but here the problem may become economic.

Question: (Unknown)

Does this hold for civilian populations too?

Answer: Dr. P. C. Tompkins, USNRDL

In principle yes; however, practically there may be situations where evacuation is the best.

Question: Dr. Langer, FCDA

When you said you rule out evacuation, does this mean you rule out permanent evacuation also?

Answer: Dr. P. C. Tompkins, USNRDL

DOE ARCHIVES

In general, yes. I do not believe that we are going to run off and leave 5,000, 10,000, or 15,000 square miles deserted. If a single weapon were going to be dropped, then evacuation might be more practical but in a situation where many weapons may be released then this measure does not appear too useful.

Comment: LTCOL Lulejian, ARDC

I should like to show this slide of 111 bombs exploded over this country, 106 on cities of 100,000 or more. This points out that in such a situation there are very few locations to which it is safe to evacuate. Furthermore, it points out that when you have large numbers of bombs, meteorology becomes less important since the over-lap tends to blanket such large areas.

549

~~SECRET~~
ENERGY ACT

553

Comment: Dr. Knapp, OEG

This last chart certainly makes evacuation not look very good, up in the north, anyway. However, I would like to point out that people living within 5 or 6 miles of the center of a city might be killed by blast. The only solution for these people if they have an hour or two warning time might be to go upwind and take shelter.

Comment: Dr. Felt, IASL

In the event that we find ourselves forced to live in a contaminated area following an attack, I might point out that about twenty-five of us lived almost two months in such an area and after the first week people adjusted to it quite readily. After a couple of mistakes, it never occurred to us to go outside without taking necessary precautions.

Comment: LCDR Miller, BuAer

If one is planning to measure fall-out by surveying wide areas with aircraft, I believe that the accuracy of the method should be checked more thoroughly. My experience at CASTLE indicated considerable variation in the correction factors to reduce aerial readings to surface values.

Comment: Dr. Werner, USNRDL

DOE ARCHIVES

I believe that the aerial techniques for obtaining the intensity over the water are reasonably well established. However, care should be exercised to avoid the impression that these can give you the total amount of material in the water without additional information on the distribution of activity with depth. Perhaps the apparent correlation which was observed at CASTLE resulted from a constant distribution with depth which can not be relied on in all cases.

Comment: Mr. LeVine, NYOO, AEC

We too had difficulty initially in correlating aerial data with ground surveys but by the last shot the techniques had been sufficiently well developed so that we obtained a constant correction factor in almost every case. It should be noted that the aerial surveys picked up activity which went off to the northeast and which was not detected by other

means. This activity disappeared on the second day indicating that particles had settled below the surface. There is, of course, considerable question as to how much activity had disappeared before the first survey was made. This observation may give some clue as to the presence of activity in the stem since the fall-out pattern from the stem was to the northeast in contrast to the pattern from the cloud which was to the west.

Comment: Dr. Scoville, AFSWP

One of the reasons for the discrepancies in aerial survey measurements results from the non-uniformity of the source. When a large area is uniformly contaminated, the altitude correction factors should be constant. However, for the Eniwetok situation, where the contamination is heavy on a small land mass and low over the water, it is quite natural to expect big variations from one location to the other. I do believe, however, that it will always be necessary to calibrate the aerial surveys over the ocean with oceanographic measurements in order to obtain depth distribution.

Comment: LTCOL Lulejian, ARDC

We did lots of aerial measurements at Nevada and these show the importance of the geometric factors. If the contamination is not uniform or if there is shielding, then the altitude relationships will vary.

Question: MAJ Hord, AFSWP

DOE ARCHIVES

What is there about the thermocline which traps the fission products?

Answer: Mr. Isaacs, Scripps

In the ocean there is a layer, about 100 meters thick, in which there is considerable mixing; but there is very little mixing between this layer with the water below it. Therefore, diffusion of fission products through this boundary, i.e., the thermocline, is very slow.

Question: Dr. Scoville, AFSWP

Both the shots at which oceanographic measurements were made were lagoon shots where the fall-out was primarily associated with very small particles. In a surface land shot where the

particles are 100 micron or larger, would they be expected to have an appreciable settling velocity through the thermocline?

Answer: Dr. Folsom, Scripps

We do not know. In order to check this at an actual shot it will be necessary to collect water samples below the thermocline and, where possible, even on the bottom.

Comment: Dr. Kellogg, Rand Corp.

With respect to fall-out model construction, it is interesting to note that a great many agencies have started by using a simple model, finding that it does not satisfy the experimental results and finally going to more and more complex models, including eventually machine calculations. It should be pointed out that the machine calculations, once they are developed, will again reverse the trend and decrease the time required to solve a specific fall-out problem.

Comment: Dr. Graves, IASL

I think what Dr. Kellogg said is true. It is possible that complicated calculations may now be made by machine. On the other hand, we have seen examples of various computations here and they do not disagree enough to be able to evaluate them with the available data. I wonder whether we are yet at the stage where these more complicated calculations are justified until we have more input data.

Question: Mr. Isaacs, Scripps

DOE ARCHIVES

In this connection, one matter worries me. This is the type of material over which the bomb is exploded. We have talked about particles produced from soil but soil does not enter into it if one has a surface burst in New York City. In such a case, what would be the particle size? I also question how realistic a very careful model would be.

Answer: Mr. Tompkins, CRL

As far as cities are concerned the Chemical Corps is looking into this now. I think this problem can be approached by trying to develop a better understanding of the mechanism of the formation of the original particles in the cooling

[REDACTED]

fireball. If we understand this mechanism, we should be better able to predict what will happen for different types of surfaces.

Comment: Dr. Felt, LASL

I think that Dr. Scoville mistakenly gave the impression that it is not worthwhile for people to consider data resulting from other types of shots, particularly those at Nevada. These produced lots of information, some good, some poor. The models should be able to say something about the Nevada shots if they are good models, and these shots provide a lot more data for checking the various systems.

Comment: Dr. Scoville, AFSWP

I agree. I only meant to imply that the only test which approaches the situation which one is most interested in operationally was the Bravo shot, but certainly other shots can be useful in providing checks on various steps in the different fall-out models.

Question: Dr. Tompkins, USNRDL

I wonder if Mr. Young of NOL would be willing to discuss some of his work on mass subsidence which might explain some of the other fall-out observations.

Answer: Mr. Young, NOL

DOE ARCHIVES

We have observed mass subsidence from HE tests and underwater shots. A few pictures we have seen at CASTLE indicated that this may have occurred during the first five minutes but unfortunately there was insufficient light to get good pictures. This effect might have contributed to the early spreading out of the active material along the surface.

THIS PAGE IS BLANK

DOE ARCHIVES

554

ENERGY ACT 1954

558

ATTENDANCE LIST

<u>NAME</u>	<u>RANK</u>	<u>ORGANIZATION</u>
ADAMS, Charles E.	Civ	USNRDL
ADKINS, W. H.	LtCol	AFMPC-AE
AITKEN, Harold L.	Civ	FCDA
ALLEN, Philip W.	Civ	Weather Bureau
ANDREWS, Howard	Dr	Health, Education & Welfare
ANDREWS, Thomas J.	LtCol	OASD (R&D)
ARMSTRONG, W. W.	Civ	BuShips
BALLINGER, Edwin R.	Capt	Hq, ARDC
BALLOU, Nathan E.	Dr	USNRDL
BARNETT, Benjamin	Dr	Chem & Radiological Lab
BARNETT, Kenneth M.	Civ	Sig Corps
BASCOM, Williard	Civ	Nat'l Academy of Science
BEERS, B. W.	Col	OSD
BEHNKE, A. R.	CAPT	USNRDL
BENNETT, B. F.	CAPT	BuShips
BENNETT, W. F. V.	CDR	CNO OP-36
BIRD, D. C.	LtCol	Hq, AFSWP
BLIFFORD, Irving H. Jr.	Civ	NRL
BODINGER, Norman B.	Maj	CONAD
BONNOT, Carlos D.	LtCol	JTF-7
BOGHER, Arnold	LtCol	AFMLP
BOUSE, Therman	LtCol	DA, Research & Development
BOWMAN, Donald	Civ	OSD
BRENNAN, John W.	Capt	Army Map Service
BRENNAN, James T.	Col	Walter Reed
BRETTLER, Benjamin J.	Civ	EG&G Inc
BRICE, Charles S.	LtCol	DA, Research & Development
BRILL, Heber C.	Maj	DA, Research & Development
BROOKS, W. K.	CIR	CNO OP-34LE1
BROWN, B. F.	CAPT	Hq, AFSWP
BROWNING, L. E.	LtCol	Hq, AFSWP
BROWNIARD, Theodore L.	Dr	BuOrd
BURRISS, Richard C.	Capt	Air Weather Service
BYARS, David O. Jr.	Col	JTF-7
CADLE, Richard D.	Dr	Stanford Research Inst
CALLAHAN, Cornelius J.	Civ	Air Weather Service
CARP, Gerald	Civ	Evans Sig Lab
CHAPMAN, Rupert D.	LtCol	DA, Research & Development
CHUBBUCH, James B.	LtCol	OCE
CLARK, Francis	Civ	Nuclear Dev Assoc
CLARK, Fred J. Jr.	Maj	DA, Research & Development

CLARK, Joseph T.	Col	OSD
CLAUS, Walter D.	Dr	B&M, AEC
COATES, J. K.	LCDR	BuShips
CONANT, Frank D.	Capt.	DA, Research & Development
CONDIT, Richard I.	Dr	G3
COOK, Clarence S.	Dr	USNRDL
COOK, Thomas B.	Civ	Sandia Corp
COONS, Richard David	Civ	Hq, ARDC
COWAN, Maynard	Civ	Sandia Corp
CRISTADORO, M. A.	LtCol	AFDAP
CURTIN, G. P.	LtCol	G3
CRUMLEY, Harold J.	Civ	ARDC
DALE, C. R.	CDR	OP-533
DAVIDSON, Harold O.	Dr	ORO
DAVIDSON, Glenn M.	Civ	BuOrd
DAVIES, John M.	Civ	DA, Research & Development
DHEIN, Ernest H.	Civ	Corps of Engineers
DUDLEY, Robert A.	Civ	AEC
DUNNING, Gordon	Dr	B&M, AEC
DURHAM, A. C.	Civ	BuShips
EDDY, Leonard A.	LtCol	Hq, AFSWP
EISENBUD, Merrill	Civ	NYOO
ELY, Strode L.	Civ	AFCIE
ERICKSON, Kenneth Warne	Dr	WSEG
ERNST, Martin L.	Civ	CNO Oper Eval Grp
ETTER, Harry S.	CDR	Med Corps USN
FACCI, Hugo A.	Civ	AFCIE
FAIR, William R.	Civ	Stanford Research Inst
FANO, Ugo	Civ	Nat'l Bureau of Standards
FAVORITE, W. M.	Maj	AFDRQ
FELDMAN, David	Civ	DA, Research & Development
FELT, Gaelen	Civ	LASL
FIESTER, Irving	Civ	AFOOA
FINE, Paul C.	Dr	DMA-AEC
FLETCHER, Robert Dawson	Civ	Air Weather Service
FOLSOM, Theodore R.	Civ	ONR
FRENCH, Joseph E.	Maj	Air Weather Service
GAGGE, Adolph Pharo	Col	AFDRD-HF
GALE, Donald I.	Civ	NRL
GARCIA, Luis F.	Civ	NRL
GARDNER, J. H.	Dr	OCAFF
GAYER, H. Kenneth	Dr	AFOOA
GENEVESE, Frank	Dr	AFOIN

DOE ARCHIVES

GETZINGER, P. L.	LtCol	OCAFF
GIBSON, Thomas A. Jr.	Maj	Hq, AFSWP
GILFILLIAM, Edward S.	Dr	Tech Operations
GILLER, Edward B.	Col	AFSWC
GOLDTHWAITE, Robert	RAIM	JTF-7
GRAVES, Alvin C.	Civ	LASL
GREENBERG, Norman D.	LtCol	DMA-AEC
GREENE, Jack C.	Civ	FCDA
GREENFIELD, Stanley M.	Civ	Rand Corp
GROSSMAN, Bertram H.	Civ	AFCRC
GUILD, Walter A.	Col	Health, Education & Welfare
GUTHRIE, William L.	Capt	DMA-AEC
HAFSTAD, Katherine	Civ	ORO
HALLOCK, H. E.	Civ	Sig Corps
HANSEN, Carl L., Jr.	Maj	Hq, AFSWP
HARDIN, Luther M.	Civ	Chem & Rad. Lab
HARMAN, Leo V.	Col	AFDDC-ND
HARRIS, D. Lee	Civ	Weather Bureau
HARTMANN, Gregory K.	Dr	BuOrd
HAYES, George T.	Civ	Stanford Research Inst
HENRIQUES, F. C.	Dr	Tech Operations
HILCKEN, John A.	Maj	MSC
HILL, Jerald Everett	Dr	Rand Corp
HINNERS, Robert A.	CAPT	USNRDL
HODGES, Charles T.	LtCol	USMC JCS
HOLLAND, Willis D.	Capt	Army Med Service Grad School
HOLZMAN, Benjamin G.	Col	AFSWC
HOME, William M.	Capt	Chem & Radio. Lab
HOOKS, D. E.	BrigG	AFOAT-1
HORD, John d'H	Maj	Hq, AFSWP
HORTON, H. Burke	Civ	Office of Defense Mobilization
HUGHES, James Henry	Civ	ONR
IRVINE, James Jr.	Maj	Corps of Engineers
ISAACS, John Dove III	Civ	Scripps Inst Oceanog.
JACKSON, John Early	Civ	OASD (R&D)
JAMES, Jack G.	LtCol	Field Command, AFSWP
JENNINGS, Feenan Dee	Civ	Scripps Inst Oceanog.
JOHNSON, Robert F.	LTJG	USNRDL
JOHNSON, William S.	Civ	LASL
JONES, John Junior	Col	Air Weather Service
JONES, William L.	Maj	OSD

DOE ARCHIVES

KAESSER, Herman H.	LtCol	Hq, AFSWP
KANE, John Joseph	Civ	ONR
KELLOGG, William Welch	Civ	Rand Corp
KENNEDY, William R.	Civ	LASL
KESLING, Earl W.	Col	AFOAT
KESSLER, Irving J.	Civ	AFOOA
KNAPP, Harold A.	Dr	CNO Oper Eval Grp
KORTY, Vernon M.	Civ	BuOrd
KOTSCH, W. J.	CDR	OP-533
KREY, Philip W.	Civ	Chem & Radiological Lab
KRIEGER, Firmin Joseph	Civ	Rand Corp
KSANDA, Charles F.	Civ	USNRDL
LANGER, Rudolph	Civ	FCDA
LANGEVIN, R. A.	Civ	Tech Operations
LaRIVIERE, Philip D.	Civ	USNRDL
LA VIER, Eugene C.	LtCol	Hq, AFSWP
LAURINO, Richard K.	Civ	USNRDL
LAWTON, Alfred H.	Dr	AFLRD-HF
LAY, Dent L.	Col	Hq, AFSWP
LE VINE, Harris D.	Civ	NYOO, AEC
LIFTON, S. E.	Maj	USAF(MC)
LIST, Robert J.	Civ	Weather Bureau
LOCKHART, Luther B. Jr.	Civ	NRL
LOWRY, Philip	Dr	ORO
LUKES, George D.	Civ	OSD
LULEJIAN, Norair M.	LtCol	Hq, ARDC
McCAMPBELL, James M.	Civ	USNRDL
McCOWN, Dean A.	LtCol	AFOAT
McGINLEY, Eugene	MajG	JTF-7
McLAUGHLIN, Earl W.	CDR	BuAir
MACHTA, Lester	Civ	Weather Bureau
MAHAFFEY, George W.	Civ	USNRDL
MARCIANO, Joseph J.	Civ	NEL
MARFING, T. E.	LtCol	OCAFF
MARGENAC, Henry	Civ	ONR
MARTELL, Edward A.	Dr	Inst of Nuclear Studies
		Univ. of Chicago
		JTF-7
MASSEY, Donnell	Col	ONR
MASTERSON, John E.	LCDR	Field Command, AFSWP
MAUPIN, Clinton S.	Civ	Tech Operations
MAXWELL, Richard	Civ	Hq, AFSWP
MAXWELL, Roy D.	Col	DOE ARCHIVES
MEYER, George R.	LCDR	Field Command, AFSWP

MILLER, Carl F.	Dr	USNRDL
MILLER, Charles A.	Col	CONAD
MITCHELL, Harold H.	Lt	Hq, AFSWP
MITCHELL, James P.	Civ	Chem & Radiological Lab
MITTLEMAN, Don I.	Civ	DA, Research & Development
MOMSEN, Charles B.	RA DM	JTF-7
MORGAN, Bruce H.	Civ	OM Food & Cont (Chi)
MORRIS, Wilford E.	Dr	BuOrd
MULLER, Ragnwald (NMI)	LCDR	BuAir
MURDEN, Charles H.	LtCol	School of Aviation Med
		Hq, Cmd, Bolling AFB
MURPHY, Howard L.	CDR	BuDocks
MUTCH, William W.	Civ	NRL
NAGLER, Kenneth M.	Civ	Weather Bureau
NASH, Russell J.	Maj	AFOAT-1
NELSON, Robert K.	LtCol	SGO
NEUNDORFFER, J. D.	Dr	CNO Oper Eval Grp
NEWELL, John F.	Civ	AEC
NIEMAN, A. S.	Civ	AFCIE
NORTHROP, Doyle L.	Civ	AFOAT-1
O'DONOGHUE, John A.	CIR	Med Corps, USN
O'KEEFE, Bernard J.	Civ	EG&G Inc
OWNBY, Frederick D.	Maj	AFIRD-HF
OYSTER, Dale E.	Civ	USAF OPN
PACK, Donald H.	Civ	Weather Bureau
PAINE, Roger W.	CDR.	Hq, AFSWP
PARSONS, Edgar L.	Dr	FCDA
PARTHUM, Alfred H. Jr.	LtCol	Hq, AFSWP
PENLAND, J. R.	Capt	JCS
PENNINGTON, Ralph W.	Civ	SWD Ft Bliss, Tex
PERLEY, R. H.	CDR	JTF-7
PFEIFFER, Edward G.	Capt	Air Weather Service
PICKLER, D. A.	CDR	JTF-7
PINSON, Ernest A.	Col	AFSWC
POOLER, Francis Jr.	Civ	Weather Bureau DOE ARCHIVES
POSEY, James T.	Col	JCS
POWELL, Clinton C.	Dr	Health, Education & Welfare
FRITCHARD, William C.	Col	OSD
PURCELL, W. P.	LtCol	G3
RAPP, Ralph Robert	Civ	Rand Corp
REEVES, James E.	Civ	SFOO
REX, Daniel F.	CDR	JTF-7

RICHIE, Frank G.	Maj	JTF-7
ROBERTS, William K.	Maj	Field Command, AFSWP
ROCK, Donald H.	Civ	AFOAT-1
ROSE, Howard C.	Maj	Hq, AFSWP
SCHORR, Marvin	Dr	Tech Operations
SCHUERT, Edward A.	Civ	USNRDL
SCHUYLER, Garrett L.	Civ	FCDA
SCOVILLE, Herbert Jr.	Dr	Hq, AFSWP
SHAPIRO, Maurice M.	Civ	NRL
SHIELDS, Buren R.	Capt	Hq, RECOM
SINGER, S. E.	Maj	AFSWC
SINGLEVICH, Walter	Civ	AFOAT-1
SMITH, James W.	Civ	ONR
SMITH, Scott W.	Civ	Bureau of Standards
SMITH, Sherwood B.	Civ	Hq, AFSWP
SPOHN, Clifford A.	LtCol	Air Weather Service
SPREEN, William C.	Civ	Air Weather Service
STEEL, Charles L.	Maj	Army Map Service
STETSON, Robert L.	Civ	USNRDL
STOPINSKI, Orin W.	Civ	LASL
STROCK, Alan M.	LtCol	USA JCS
STUDER, Robert	LtCol	G3
SUNDSTROM, Harold J.	Civ	Corps of Eng
SVENDSON, E. C.	CDR	BuShips Code 850
SWOMLEY, Neely M.	Maj	Sig Corps
SWINGLE, Donald M.	Dr	Evans Sig Lab
TARRANT, Legare K.	BrigG	Hq, AFSWP
TAYLOR, P. H.	LtCol	AFCIE
TAYLOR, Robert L.	Capt	AFOOP
TERRILL, James G.	Civ	Health, Education & Welfare
TEST, Herbert H.	Civ	AFDRQ
THOMAS, Norman C.	Civ	DA, Research & Development
THOMSON, Warren	Civ	OSD
TOMPKINS, Edward R.	Dr	USNRDL
TOMPKINS, Paul C.	Dr	USNRDL
TOMPKINS, Robert C.	Civ	Chem & Rad Lab
TORBETT, Oscar C.	Capt	Army Map Service
TYLER, George W.	Civ	AFOOA
UNDERWOOD, Warren N.	Col	Corps of Eng
UNGAR, Stanley H.	Civ	Evans Sig Lab
VAN HORN, William H.	Civ	Corps of Eng
VAN STRATEN, F. W.	Dr	OP-533
VANN, James O.	LtCol	AFSWC

DOE ARCHIVES

VINE, Allyn C.	Dr	BuShips
WALLACE, Duane G.	Maj	AFOPD
WALSH, Thomas	Civ	Corps of Engineers
WATSON, William W.	Dr	ONR
WEIDLER, Roy C. Jr.	Maj	Hq, AFSWP
WERNER, Louis B.	Dr	USNRDL
WHEDON, Frances	Civ	OC Sig O
WEXLER, Harry	Civ	Weather Bureau
WHITE, Fred D.	Civ	Weather Bureau
WHITE, Thomas N.	Civ	LASL
WHITE, William L.	Civ	Stanford Research Inst
WIENER, Martin	Civ	AFOIN
WILKINS, James Jr.	Civ	Nuclear Dev Assoc
WILLIAMS, Edwin G.	Civ	FCDA
WILSEY, Edward F.	Civ	Chem Radiological Lab
WYCKOFF, Harold L.	Civ	Bureau of Standards
YOUNG, George A.	Civ	BuOrd
ZIGMAN, Paul E.	Civ	USNRDL
ZIRKIND, Ralph A.	Civ	BuAir

DOE ARCHIVES

~~SECRET~~

THIS PAGE IS BLANK

DOE ARCHIVES

562

~~RESTRICTED DATA~~
ENERGY ACT

~~SECRET~~

566
571